

Dissertation zur Erlangung des Doktorgrades  
der Fakultät für Chemie und Pharmazie  
der Ludwig-Maximilians-Universität München

**Kinetic and Mechanistic Studies on Reactions of Quinones:  
SET vs. Polar Reactions**

Xingwei Guo

aus

Qinhuangdao, Hebei, China

2014

## Erklärung

Diese Dissertation wurde im Sinne von § 7 der Promotionsordnung vom 28. November 2011 von Herrn Prof. Dr. Herbert Mayr betreut.

## Eidesstattliche Versicherung

Diese Dissertation wurde eigenständig und ohne unerlaubte Hilfe erarbeitet.

München, 14.03.2014

---

Xingwei Guo

Dissertation eingereicht am 14.03.2014

1. Gutachter: Prof. Dr. Herbert Mayr
2. Gutachter: Prof. Dr. Hendrik Zipse

Mündliche Prüfung am 24.04.2014

*...dedicated to my family*

## Acknowledgements

First, I would like to express my deepest gratitude to Professor Dr. Herbert Mayr for offering me the opportunity to work and perform this thesis in his group. I have really appreciated many valuable discussions with him, his endless support, and his broad knowledge very much. I really enjoyed working under these excellent conditions and I really appreciated the freedom he gave to me for exploring chemistry. I cannot overemphasize my gratitude for all the things I learned from him.

Furthermore, I would like to thank Prof. Dr. Hendrik Zipse for reviewing my thesis and also the board of examiners for their participation in my defense examination.

The financial support by the China Scholarship Council is gratefully acknowledged and special thanks to the Consulate General of China in München for their kind help.

I would like to thank all my colleagues within the group of Professor Dr. Mayr for the pleasant working atmosphere, especially Dr. Sami Lakhdar, Dr. Guillaume Berionni, Dr. Biplab Maji, Dr. Saloua Chelli, Follet Elsa, Varvara Morozova, Dr. Wei Han, Dr. Xi Chen, Feng An, Prof. Shinjiro Kobayashi, Dr. Haruyasu Asahara, Shanshan He, Artem Leonov. I will never forget the great time with you. Special thanks to Dr. Sami Lakhdar for good suggestions and useful discussions since the very beginning of my work. I would also like to thank Francisco Corral, Dr. Ángel R. Puente G., Dr. Hans Laub, Alexander Wagner, Elija Wiedemann, Anna Antipova, Dr. Johannes Ammer, Dr. Dominik Allgäuer. It has been a pleasure to work with you.

Many thanks to Dr. Armin R. Ofial for the excellent advices, suggestions, and critical comments for improving my manuscripts. I am also grateful to Frau Hildegard Lipfert for all her kind help.

I am fully indebted to my whole family for their unconditional support over the years. I cannot overemphasize my most sincere gratitude to my wife, Lu Pei, who accompanied me all the way. Her encouragement, patience, and considerate always kept me going forward. I keep my final gratitude for my son Yize, I wish you growing up healthy and always fighting for your dreams!



**Parts of this Ph.D. thesis have been published or submitted:**

“Manifestation of Polar Reaction Pathways of 2,3-Dichloro-5,6-dicyano-p-benzoquinone (DDQ)”

Guo, X.; Mayr, H. *J. Am. Chem. Soc.* **2013**, *135*, 12377-12387.

“Quantification of the Ambident Electrophilicities of Halogen-Substituted Quinones”

Guo, X.; Mayr, H. *J. Am. Chem. Soc.* **2014**, *submitted*

“Mechanisms of Hydride Abstractions by Quinones”

Guo, X.; Zipse, H.; Mayr, H. *J. Am. Chem. Soc.* **2014**, *submitted*



## **Table of Contents**

Chapter 0	Summary	1
Chapter 1	Introduction	9
Chapter 2	Manifestation of Polar Pathways of DDQ	31
Chapter 3	Quantification of the Ambident Electrophilicities of Halogen-Substituted Quinones	101
Chapter 4	Mechanisms of Hydride Abstractions by Quinones	169



## Chapter 0: Summary

### 0.1 General

Most organic reactions are polar reactions of electrophiles with nucleophiles, the rates of which can be described by eq.1,

$$\log k(20\text{ }^{\circ}\text{C}) = s_N(E + N) \quad (1)$$

where  $s_N$  and  $N$  are nucleophile-specific, solvent-dependent parameters and  $E$  is an electrophilicity parameter.

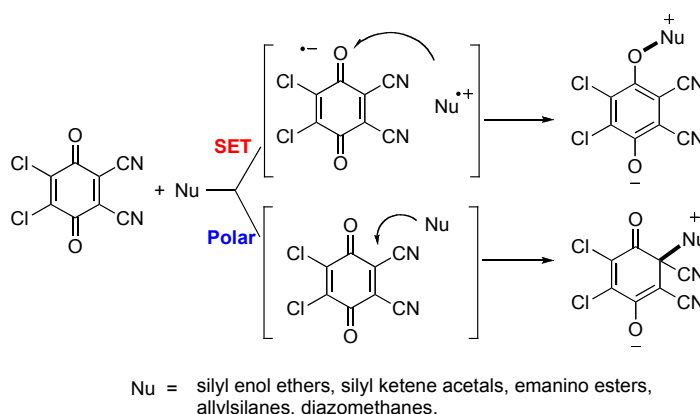
Numerous electrophilicity parameters  $E$  for different types of carbocations, cationic transition-metal  $\pi$ -complexes, typical Michael acceptors, and electron-deficient arenes have been derived from eq. 1. However,  $E$  parameters for quinones, which are common oxidants, have never been studied.

This thesis was designed to examine the applicability of eq.1 to the reactions of quinones nucleophiles.

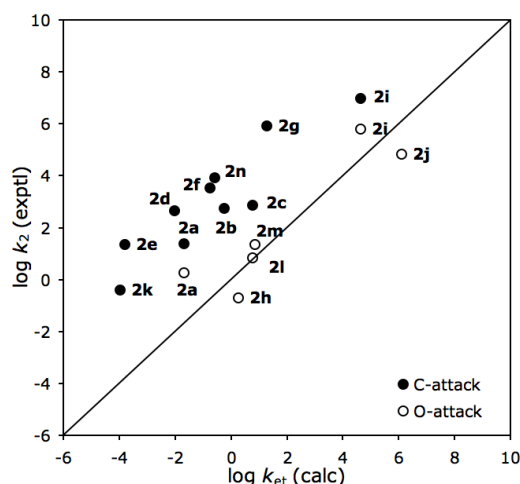
### 0.2 Manifestation of Polar Reaction Pathways of DDQ

Reactions of 2,3-Dichloro-5,6-dicyano-*p*-benzoquinone (DDQ) with silyl enol ethers, silyl ketene acetals, allylsilanes, enamino esters, and diazomethanes have been studied in  $\text{CH}_3\text{CN}$  or  $\text{CH}_2\text{Cl}_2$  solutions.  $\pi$ -Nucleophiles attack DDQ either at C-2 to give 4-hydroxycyclohexadienones or at oxygen to give O-substituted hydroquinones (Scheme 1).

**Scheme 1.** C- and O-Attack Pathways of DDQ

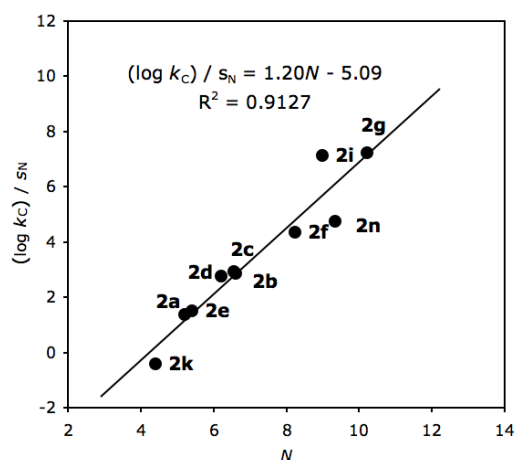


The second order rate constants for C-attack at DDQ are 2 to 7 orders of magnitude larger than those expected for SET processes, which strongly supports the polar mechanism for C-C bond formation.



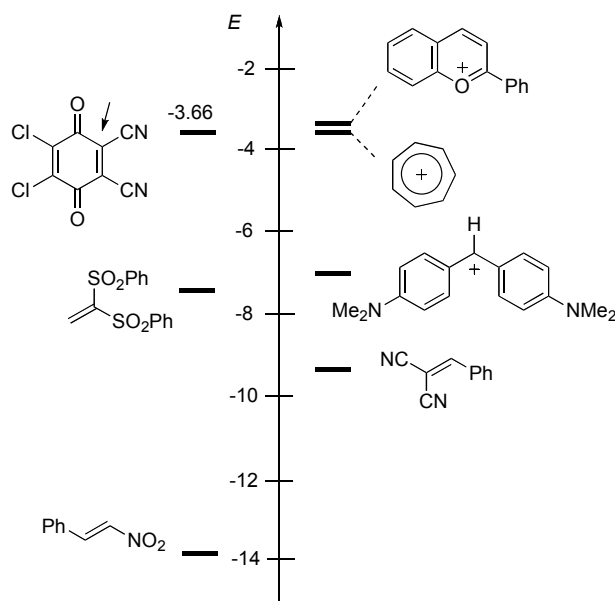
**Figure 1.** Correlation of experimental rate constants ( $\log k_2$ , in  $\text{CH}_3\text{CN}$ ) with calculated rate constants for SET ( $\log k_{\text{et}}$ ).

On the other hand, the second-order rate constants of O-attack agree well with the calculated rate constants for SET mechanism. As a radical clock experiment ruled out outer sphere electron transfer, an inner sphere electron transfer mechanism is suggested for O-attack.



**Figure 2.** Plot of  $(\log k_{\text{C}})/s_{\text{N}}$  vs  $N$  for the reactions of DDQ (C-attack) with  $\pi$ -nucleophiles in  $\text{CH}_3\text{CN}$  at  $20^\circ\text{C}$

For the reactions of DDQ (C-attack) with  $\pi$ -nucleophiles, it was found that the rate constants  $k_{\text{C}}$  for the attack of the  $\pi$ -nucleophiles **2** at C-2 of DDQ can be described by the linear free energy relationship (1), which allowed us to derive the electrophilicity parameter  $E = -3.66$  for the C-2 position of DDQ. It thus possesses an electrophilic reactivity comparable to the flavylium and tropylium ion, considerably more reactive than the bis(dimethylamino)-substituted benzhydrylium ion or other highly reactive Michael acceptors (Figure 3)

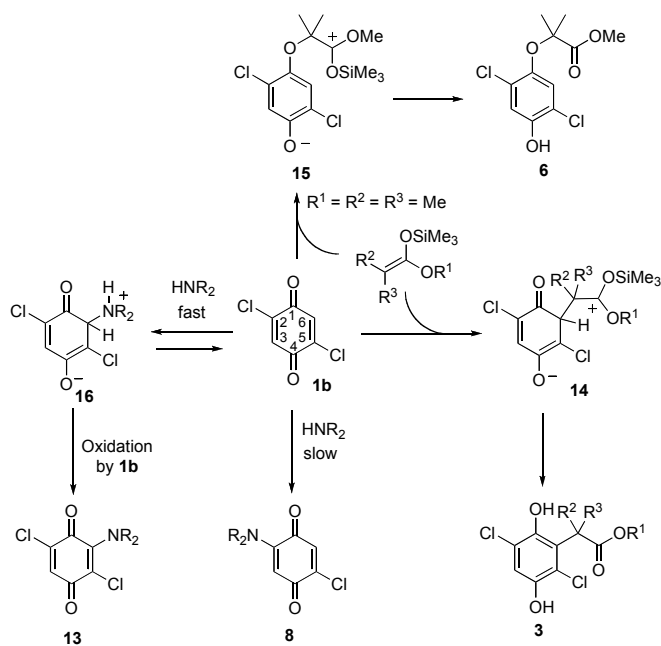


**Figure 3.** Comparison of the electrophilic reactivity of DDQ with that of other electrophiles.

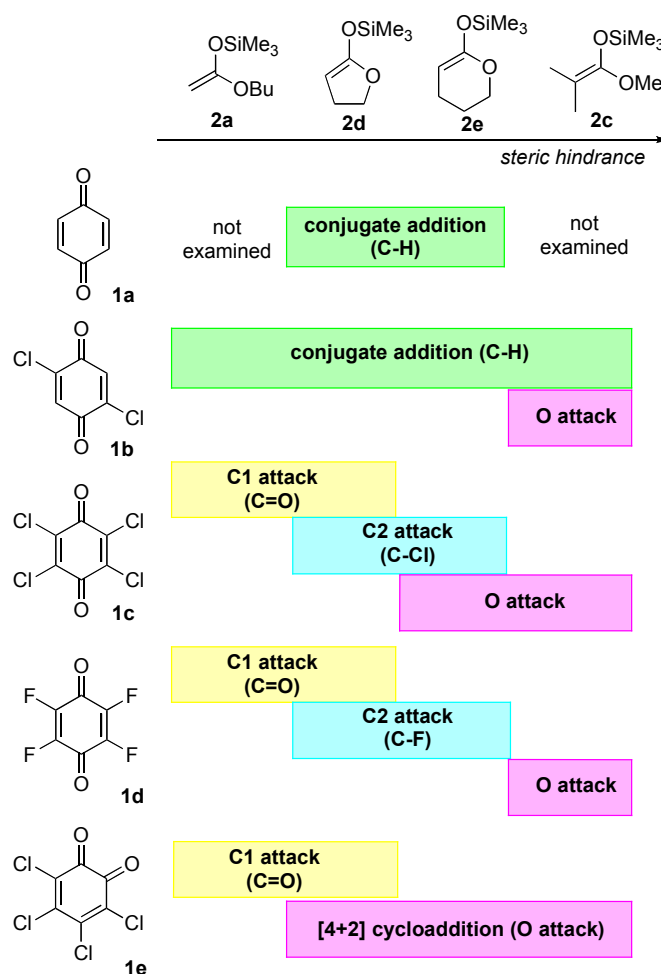
### 0.3 Quantification of the Ambident Electrophilicities of Halogen-Substituted Quinones

Reactions of halogen-substituted quinones with silyl enol ethers, silyl ketene acetals, enamines, and amines have been studied in  $\text{CH}_3\text{CN}$  or  $\text{CH}_2\text{Cl}_2$  solutions. Silyl ketene acetals and silyl enol ethers attack quinones either at C-1 to give 1,2-addition products, at C-2/3 to give conjugate addition (substitution) products, or at oxygen to give O-substituted hydroquinones. Scheme 2 shows the reaction pathways of 2,5-dichloro-benzoquinone.

**Scheme 2.** Reaction Pathways of 2,5-Dichloro-benzoquinone



The changes of selectivity due to increasing steric hindrance of silyl ketene acetals are shown in Figure 4. In the reactions of **1a** and **1b** conjugate additions at the C(-H) position are always favored. Both tetrahalogen-substituted quinones **1c,d** react with **2a** at the carbonyl carbon, but increasing steric hindrance of the nucleophiles shifts the reactions to C-2 attack (substitution) and further increase of steric hindrance results in attack at O, which is the least shielded position and gives the thermodynamically most stable product. Like the para-quinones **1c,d**, the ortho-quinone **1e** also reacts exclusively at C-1 with the terminal ketene acetal **2a**, but increasing steric shielding now leads to a Diels-Alder reaction.

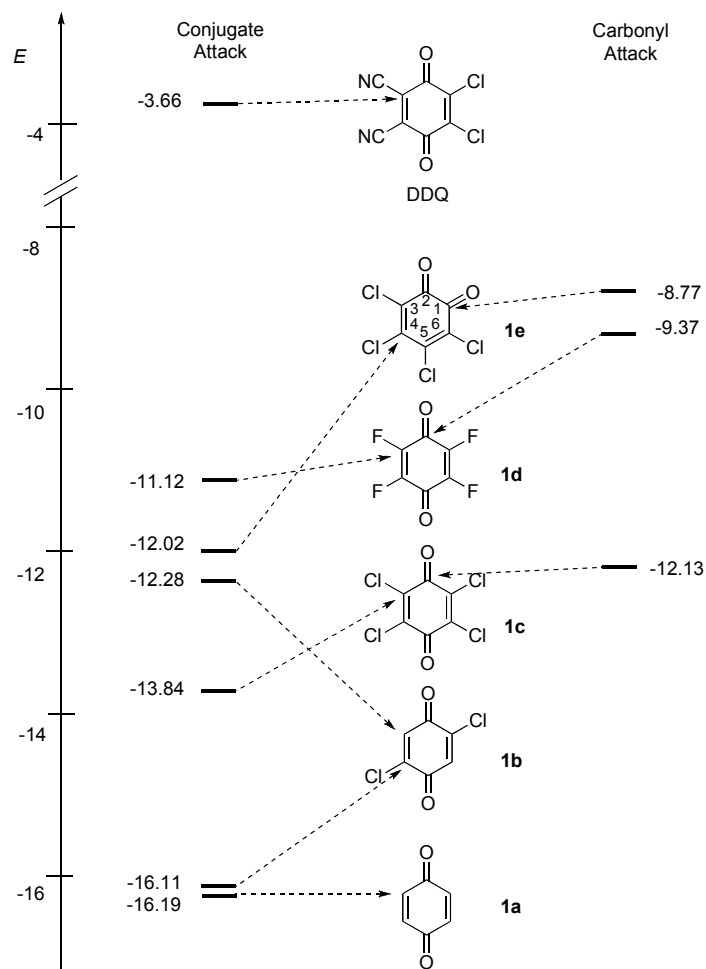


**Figure 4.** Steric effect on the product selectivities of quinones with silyl ketene acetals.

Amines attack halogen-substituted quinones to give conjugate substitution products. Computational studies reveal that the substitution reaction proceeds through a concerted process rather than via a stepwise addition-elimination mechanism. Kinetics for the reactions of quinones with  $\pi$ -systems as well as with amines have been determined photometrically, and it was found that the rate constants for the C attack of the  $\pi$ -systems and amines can be



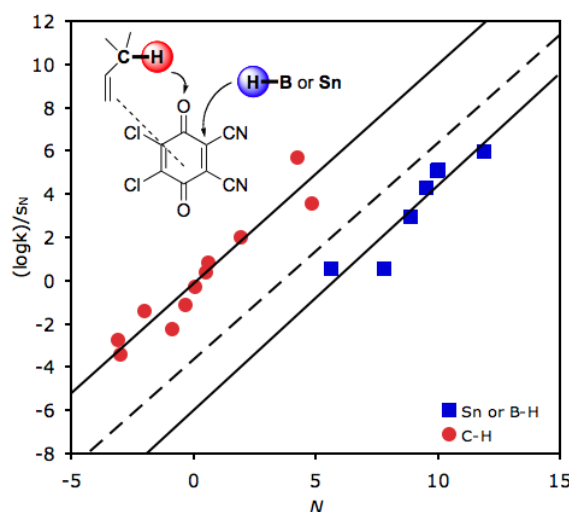
described by the linear free energy relationship (1), which allowed us to quantify the ambident electrophilicities of quinones (Figure 5).



**Figure 5.** The ambident electrophilicities of halogen-substituted quinones.

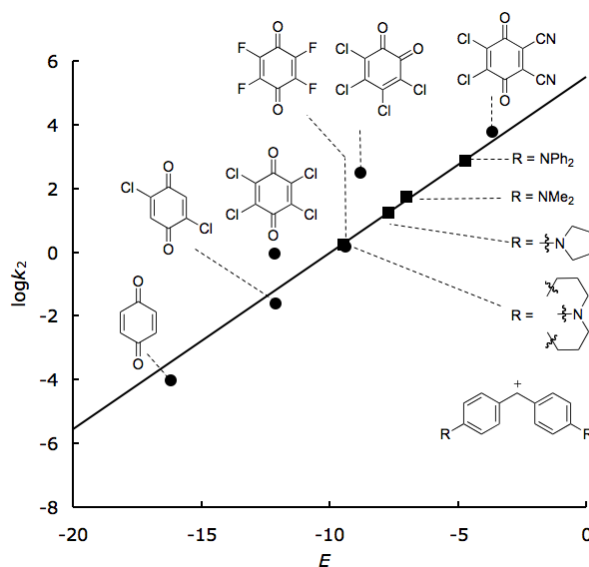
## 0.4 Hydride Transfer Mechanisms of Quinones

Kinetics of the reactions of DDQ with C-H, B-H, and Sn-H hydride donors have been studied photometrically in  $\text{CH}_2\text{Cl}_2$  solution at 20 °C. As shown in Figure 6, plots of  $(\log k)/s_N$  vs nucleophilicity parameters  $N$  gave separate correlation lines for C-H hydride donors (red circles) and B-H and Sn-H hydride donors (blue squares). The C-H hydride donors react 3-5 orders of magnitude faster than calculated by eq. (1) from the  $N$  and  $s_N$  parameters of the hydride donors (which were derived from their reactions with benzhydrylium ions) and the  $E$ -parameter for the 2-position of DDQ (which was derived from its reactions with  $\pi$ -nucleophiles). In contrast, B-H or Sn-H hydride donors react somewhat more slowly than calculated by eq. (1).



**Figure 6.** Correlation of  $\log k/s_N$  vs  $N$  for the reactions of DDQ with C-H, B-H, and Sn-H hydride donors, the broken line represents the calculated line according to eq. 1 and  $E = -3.66$ .

Figure 7 shows that the rate constants for the reactions of  $\text{Bu}_3\text{SnH}$  with a variety of quinones and benzhydrylium ions follow the same correlation with their electrophilicity parameters. As the reactions of stannanes with benzhydrylium ions have previously been shown to proceed by a polar mechanism, Figure 7 supports a polar reaction mechanism via C attack for the reactions of Sn-H hydride donors with quinones

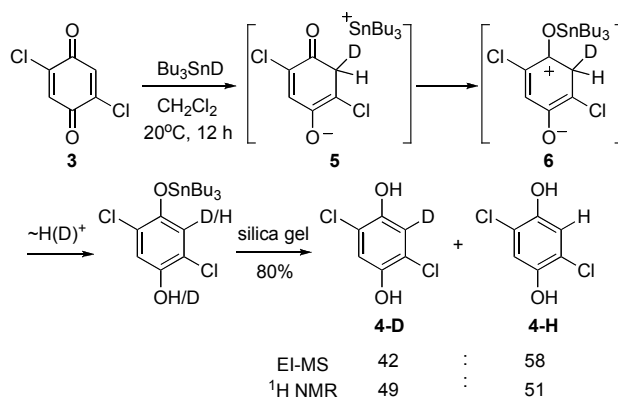


**Figure 7.** Correlation of  $\log k$  vs  $E$  for the reactions of  $\text{Bu}_3\text{SnH}$  with quinones and benzhydrylium ions.

Furthermore, the deuterium labeling experiments for the reactions of 2,5-dichlorobenzoquinone with deuterated 1,4-cyclohexadiene, tributylstannane (Scheme 3) and

borane pyridine complex further confirm the O-attack pathway for C-H hydride donors and C-attack pathway for borane hydrides and tin hydrides.

**Scheme 3.** Reaction of 2,5-Dichloro-p-benzoquinone with  $\text{Bu}_3\text{SnD}$



In agreement with the experimental results, computational studies of the reactions of DDQ with the hydride donors provide further evidence for this hypothesis.

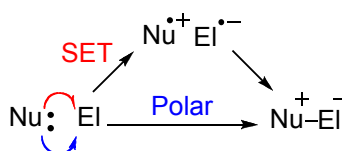


## Chapter 1: Introduction

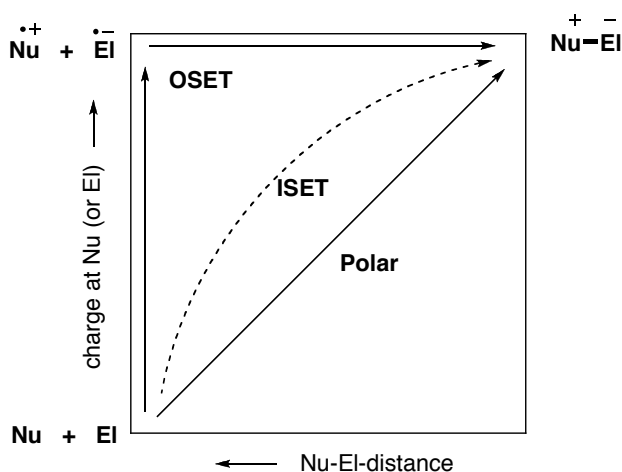
### 1.1 SET vs. Polar

Pushing electrons is a common practice to describe organic reaction mechanisms. Ingold's "curved arrow" mechanisms deeply influenced the thinking of organic chemists in the last century.<sup>1</sup> However, since the pioneering work of Kornblum,<sup>2</sup> Russell,<sup>3</sup> and Bunnett,<sup>4</sup> the importance of single electron transfer (SET) processes has been recognized in various areas of organic chemistry.<sup>5</sup> For the reactions of electrophiles with nucleophiles, two different mechanisms have to be considered, as shown in Scheme 1.

**Scheme 1.** Electron Transfer vs Polar Reaction



In the polar pathway, the transfer of electrons is accompanied by the movement of the nuclei, i.e., the formation of a chemical bond. In the alternative SET pathway, the transfer of a single electron from a nucleophile to an electrophile generates a radical pair, which may combine to give the same product as the polar pathway.



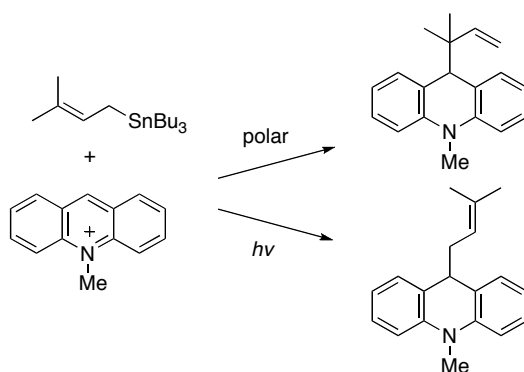
**Figure 1.** Potential energy surface diagram illustrating the relationship between polar and SET processes. The possible inner sphere mechanism is indicated by the broken line.

As illustrated in Figure 1, in a polar reaction, bond formation and electron transfer are tightly coupled (as indicated by the diagonal solid line), while in the outer sphere electron transfer (OSET) mechanism, the two processes are fully uncoupled, i.e., the movement of the

electrons precedes the movement of the nuclei. Between these two extremes, inner sphere electron transfer (ISET) processes may exist. As indicated by the broken line in Figure 1, in this process both events are weakly coupled.

The differentiation between SET processes and polar reactions is a fundamental question in mechanistic studies of organic reactions. Sometimes, the two mechanisms may give two different products. Thus, Fukuzumi, Fujita and Otera have reported that photoinduced electron transfer between *N*-methylacridinium ion and prenyl tributylstannane gave the  $\alpha$ -adduct predominantly, while the  $\gamma$ -adduct was obtained by the polar thermal reaction,<sup>6</sup> which is a clear indication of a change in mechanism. However, analysis becomes complicated when the two processes are not selective or the selectivities are unknown.

**Scheme 2.** Two Reaction Pathways of the Reaction of *N*-Methylacridinium Ion with Prenyl Tributylstannane<sup>6</sup>



Several techniques have been applied to identify SET processes. The most direct observation of the radical intermediates might be the use of ESR spectroscopy.<sup>7</sup> this approach can be used for the reactions where relatively stable long-lived radical intermediates are generated. Another method is cyclization or ring-opening of an intermediate radical, known as radical clock.<sup>8</sup> However, in some cases, the validity of the probe has been criticized.<sup>9</sup> A loss of stereochemistry in bimolecular nucleophilic substitutions has also been considered to be indicative for radical formation, when the radical intermediates are not detectable by cyclization, trapping, or direct observation by ESR.<sup>10</sup> Kinetic isotope effects<sup>11</sup> and formation of radical-derived secondary products (i.e., dimerization)<sup>12</sup> were also applied to support SET processes.

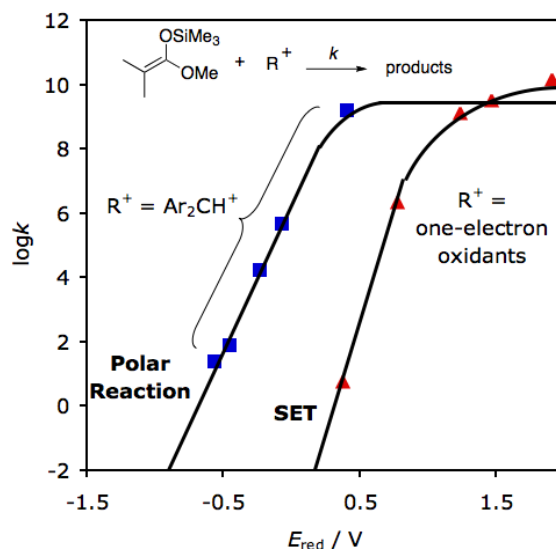
The differentiation of OSET and polar mechanisms can also be based on comparison of experimental rate constants with the predicted values for OSET processes,<sup>13</sup> as the activation free energy  $\Delta G^\ddagger$  of an OSET reaction, which is linked with the rate constants by the Eyring equation (1), can be calculated using the Marcus (eq. 2)<sup>14</sup> or the Weller (eq. 3)<sup>15</sup> equations.

$$k_{\text{et}} = k_{\text{b}} T / h \exp(-\Delta G^\ddagger / RT) \quad (1)$$

$$\Delta G^\ddagger = \Delta G^\circ/2 + \Delta G_0^\ddagger + (\Delta G^\circ)^2/(16\Delta G_0^\ddagger) \quad (2)$$

$$\Delta G^\ddagger = \Delta G^\circ/2 + [(\Delta G^\circ/2)^2 + (\Delta G_0^\ddagger)^2]^{1/2} \quad (3)$$

When a measured reaction rate is in agreement with the calculated rate for electron transfer, an SET mechanism appears feasible. When the reaction is substantially faster than the calculated rate for the electron transfer, a polar mechanism can be assigned.



**Figure 2.** Comparison of the rate constants for the reactions of 1-methoxy-2-methyl- 1-trimethylsiloxyprene with carbenium ions and one-electron oxidants vs. their reduction potentials.<sup>16</sup>

We have previously reported that the reactions of carbenium ions with CC double bonds usually do not occur via SET processes but through one-step polar reactions.<sup>16</sup> Figure 2 shows the comparison between the rates of reactions of carbenium ions and one-electron oxidants with 1-methoxy-2-methyl- 1-trimethylsiloxyprene. The reactions of the benzhydrylium ions are 10 orders of magnitude faster than the OSET reactions, which clearly indicates the operation of a polar mechanism.

However, often either the oxidation potential of the nucleophile or the reduction potential of the electrophile are not known. Often it is also difficult to obtain the value of the intrinsic barrier. Even if the rate constant for OSET can be calculated, the interpretation is problematic when the reaction is not substantially faster than the calculated rate constants for OSET.

In recent years, we have developed a linear free energy relationship based model to predict rates and selectivities for polar organic reactions.<sup>17</sup> The rate constants of these reactions can be described by eq 4:

$$\log k(20\text{ }^\circ\text{C}) = s_N(E + N) \quad (4)$$

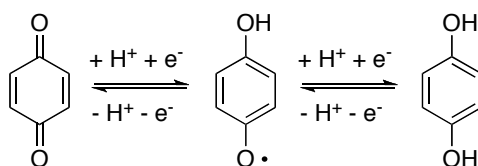
In equation (4) the second-order rate constant ( $\log k$ ) is calculated by two nucleophile-specific parameters  $s_N$ ,  $N$  and one electrophile-specific parameter  $E$ . A comprehensive nucleophilicity scale covering more than 30 orders of magnitude<sup>18</sup> has been created by using a series of benzhydrylium ions and structurally related quinone methides as reference electrophiles.<sup>19</sup> This thesis was designed to examine the applicability of eq. 4 for the reactions of nucleophiles with quinones, which will be shown to be in the border area between electron transfer and polar mechanisms.

## 1.2 Quinone Chemistry

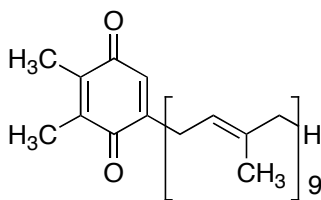
### 1.2.1 Quinones in Biology

The oxidizing properties of quinones have been known since the early 20th century.<sup>20</sup> The most important reaction of quinones especially in view of biology is their reversible reduction to the corresponding hydroquinone.

**Scheme 3.** Benzoquinone/Hydroquinone Redox Couple



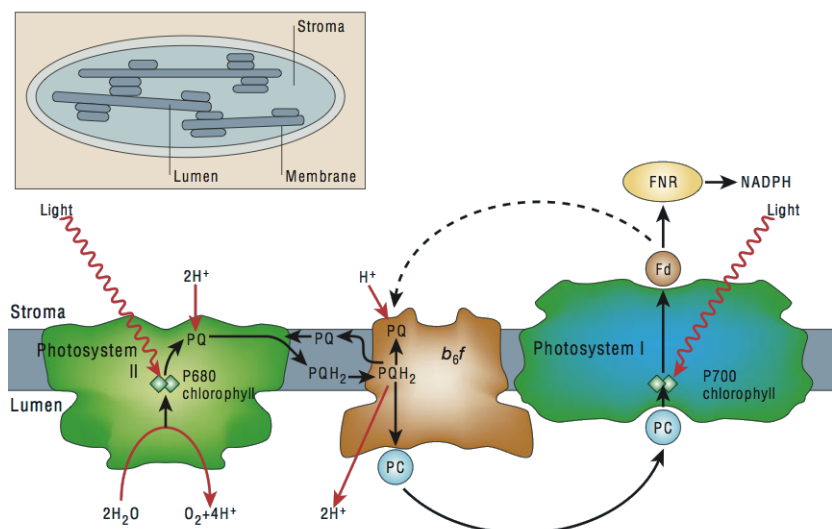
Derivatives of benzoquinone/hydroquinone (Q/QH<sub>2</sub>) play essential roles in biology.<sup>21</sup> The redox reaction, quinone-hydroquinone, constitutes one of the elements of the electron transport chain. An important example appears in photosynthesis, in the reduction of plastoquinone (PQ, Figure 3) to the mobile redox carrier plastoquinol (PQH<sub>2</sub>).



**Figure 3.** The structure of plastoquinone (PQ).

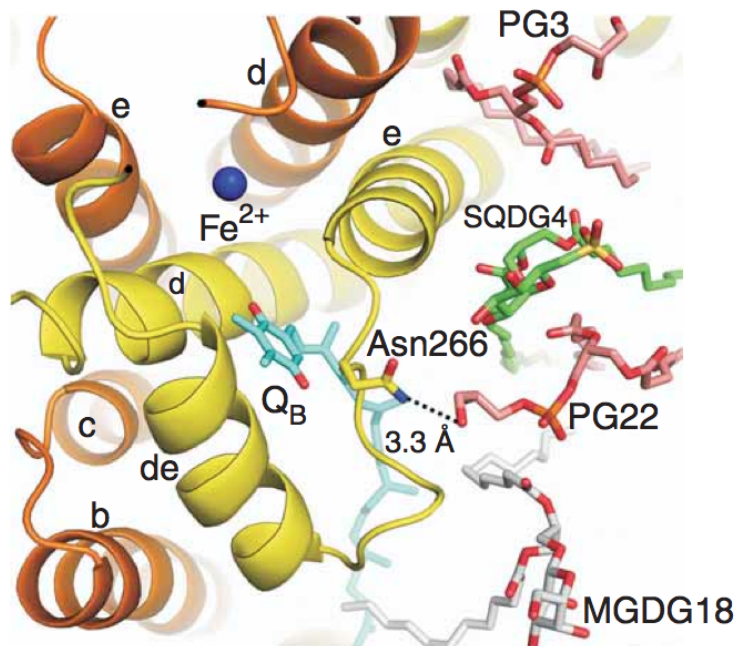
Plastoquinone is one of the electron acceptors associated with photosystem II (PSII) in photosynthesis. As shown in Figure 4, it accepts two electrons from PSII and  $2H^+$  from the stroma and is reduced to plastoquinol PQH<sub>2</sub>, which is transported through the thylakoid membrane to cytochrome b<sub>6</sub>f, where it is oxidized to PQ with proton release to the lumen.<sup>22</sup> Figure 5 shows the electron transfer channel for plastoquinone in the crystal structure of PSII.<sup>23</sup>





**Figure 4.** The electron transport chain in photosynthesis.

The redox couple PQ/PQH<sub>2</sub> has the dual functions of transferring excited electrons from PSII to the cytochrome b<sub>6</sub>f complex as part of the ETC, and of shuttling protons from the stroma to the thylakoid lumen as part of the generation of a protonmotive force. This latter function is important for the generation of ATP.

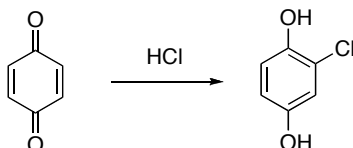


**Figure 5.** The X-ray structure illustrating the electron transfer channel for plastoquinone in photosystem II (PSII) from *Thermosynechococcus elongatus* at 2.9-Å resolution.<sup>23</sup>

### 1.2.2 Quinones in Organic Synthesis

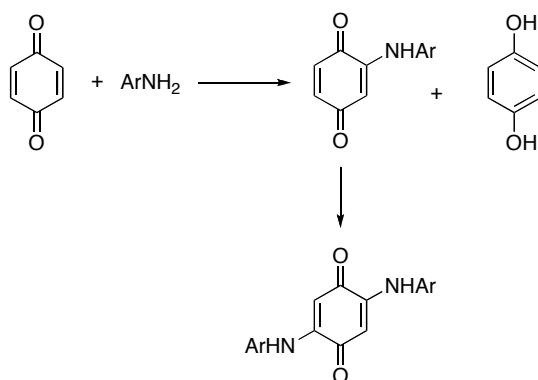
From the very beginnings of modern organic chemistry quinone chemistry has continuously attracted the attention of organic chemists.<sup>24</sup> In 1844, Wöhler reported the first addition reaction of hydrogen chloride to benzoquinone,<sup>25</sup> which has already been cited as one of the earliest reported quinone addition reactions.<sup>24c,d</sup>

**Scheme 4.** Addition of HCl to Benzoquinone First Reported by Wöhler<sup>25</sup>



In the late 19th and early 20th century, nitrogen-containing compounds were found to undergo Michael addition with a variety of quinones. Suida reported the preparation and characterization of 50 addition products of 1,4-benzoquinone and various substituted anilines.<sup>24b</sup> The usual product is the result of a sequence of two additions each followed by oxidation. The competition between addition and substitution was recognized in the case of several chloroquinones.

**Scheme 5.** Reactions of Quinones with Anilines Reported by Suida<sup>24b</sup>

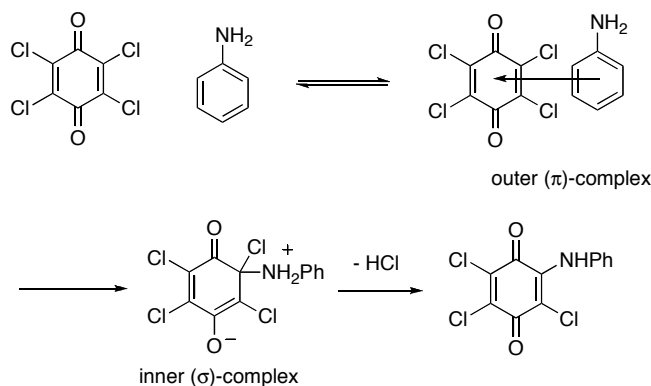


Since Mulliken presented the well-known theory of the charge-transfer interaction between electron donors and electron acceptors, it has been successfully and widely applied to many interesting research subjects.<sup>26</sup> One of them is the possible role of CT complexes in chemical reactions. The nitrogen substitution of halogen-substituted quinones had attracted the attention of physical organic chemists. The question of the importance of charge transfer complexes as intermediates in such substitution reactions is a central concern.

Nagakura and coworkers reported on the reactions of chloranil with various substituted anilines.<sup>27</sup> They confirmed the existence of the charge transfer complex ( $\pi$ -complex) in this system and postulated an  $\sigma$ -adduct (inner-complex) as the reaction intermediate between the

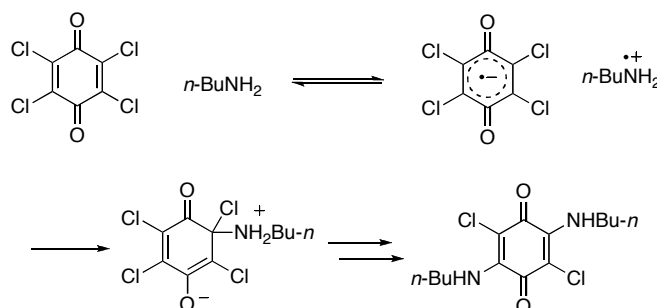
charge transfer complex and the final product (anilino-quinone). However, It was not possible to prove that the outer-complex actually takes part in the reaction.

**Scheme 6.** Mechanism of the Substitution Reaction of Chloranil with Aniline Proposed by Nagakura<sup>27</sup>



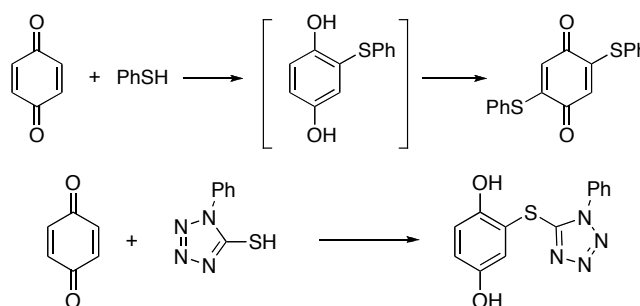
In a later study, Tamaoka and Nagakura claimed that electron transfer, prior to the substitution, takes place.<sup>28</sup> Spectra of the chloranil-butylamine system and related kinetics suggest the sequence of steps depicted in Scheme 7. However, the monoaminated intermediate was not detected.

**Scheme 7.** Electron Transfer Mechanism of the Reaction of Chloranil with Butylamine Reported by Tamaoka and Nagakura<sup>28</sup>



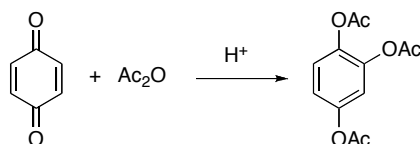
Besides the reactions of amines with quinones, the addition of sulphur nucleophiles had also been extensively studied, which either lead to oxidized or reduced products under appropriate conditions.<sup>29</sup>

**Scheme 8.** Reactions of Quinone with Sulphur Nucleophiles<sup>29</sup>



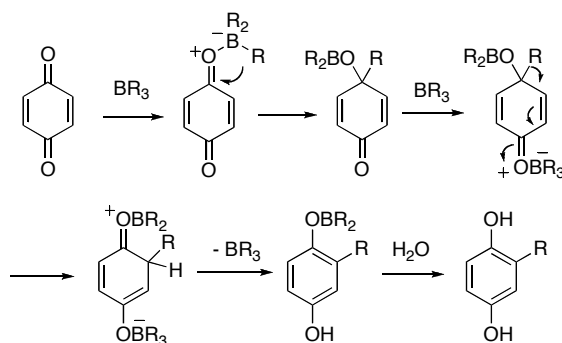
Another widely used and extensively studied addition reaction is the Thiele acetylation.<sup>30</sup> The treatment of quinones with acetic anhydride under acidic conditions produces a product of addition and esterification. The reaction has been very widely used for the synthesis of new quinones and hydroquinones.

**Scheme 9.** Thiele Acetylation Reaction<sup>30</sup>



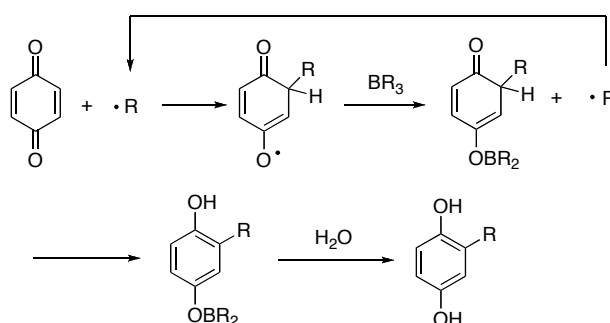
In view of the extensive use of alkylboranes in organic synthesis, it is not surprising that they have also been applied for the alkylation of quinones. Trialkylboranes undergo a facile reaction with p-benzoquinone producing quantitative yields of the corresponding 2-alkyl hydroquinones after hydrolysis.<sup>31</sup> It had been postulated that the reaction proceeds via a reductive alkylation, direct 1,2-addition of trialkylboranes to carbonyl group followed by acid catalyzed migration of the alkyl group from carbonyl carbon to the adjacent carbon.

**Scheme 10.** Reaction Mechanism for Alkylation of Quinone with Boranes Proposed by Hawthorne and Reintjes<sup>31</sup>



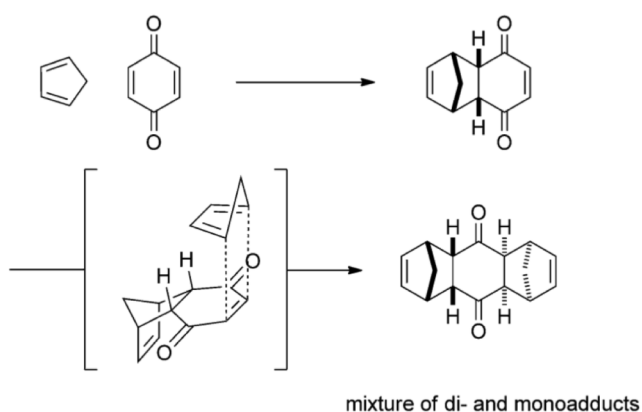
However, a later study by Kabalka suggested a free radical chain mechanism for the alkylation of quinones with trialkylboranes, because iodine, and to a smaller extent galvinoxyl, inhibits the addition of triethylborane to 1,4-benzoquinone.<sup>32</sup> In light of previous findings, which demonstrate that the 1,4-addition of trialkylboranes to  $\alpha,\beta$ -unsaturated carbonyl systems is a free radical process,<sup>33</sup> he postulated the mechanism as a radical addition to the carbon-carbon double bond of quinone.

**Scheme 11.** Radical Chain Mechanism for Alkylation of Quinone with Boranes Suggested by Kabalka<sup>32</sup>



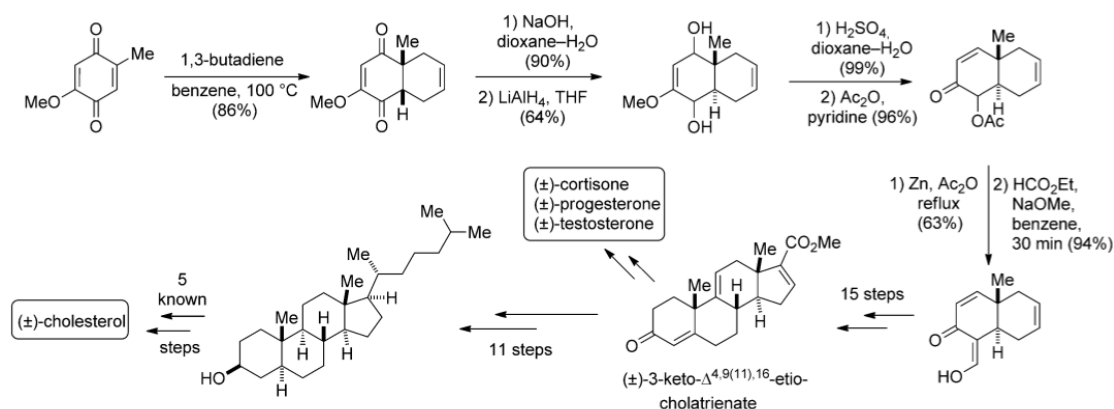
The most important applications of quinones in organic synthesis are undoubtedly the [4+2] cycloadditions. Since Diels and Alder first reported the [4+2] cycloaddition reaction of benzoquinone and cyclopentadiene,<sup>34</sup> a wide variety of quinones have been used in the diene synthesis through [4+2] cycloadditions. Although the [4+2] cycloaddition reaction now bears the names of Professor Otto Diels and his student Kurt Alder for their seminal publication in 1928, in fact, a quinone Diels-Alder reaction had been carried out more than twenty years before Diels and Alder's paper was published. Walther Albrecht (a student of Johannes Thiele) had performed the same reaction as that shown in Scheme 12 some two decades earlier,<sup>35</sup> but had misassigned the structures of the products and thus missed the significance of the chemistry he had performed. The reaction had undoubtedly inspired some of the greatest organic chemists of that time. Woodward had been fascinated by the Diels–Alder paper since a young age,<sup>36</sup> as described by Todd in the Royal Society Biographical Memoir of Robert Burns Woodward.<sup>37</sup> Todd wrote “*it is certain that his reading of that original paper in Annalen was the start of a lifelong interest, both practical and theoretical, in the Diels–Alder reaction, and so played an important role in the train of events leading finally to the development of the Woodward–Hoffmann rules on orbital symmetry relations.*”

**Scheme 12.** [4+2] Cycloaddition Reaction of Benzoquinone with Cyclopentadiene.



Early reports on the synthetic aspects of quinone cycloaddition reactions had been reviewed by Butz and Rytina in 1949.<sup>38</sup> The history and applications of quinones as dienophiles in the Diels-Alder reaction in total synthesis have recently been reviewed by Moody.<sup>39</sup> Scheme 13 shows an example by Woodward in his syntheses of racemic cortisone, progesterone, testosterone, and cholesterol in 1951 and 1952.<sup>40</sup>

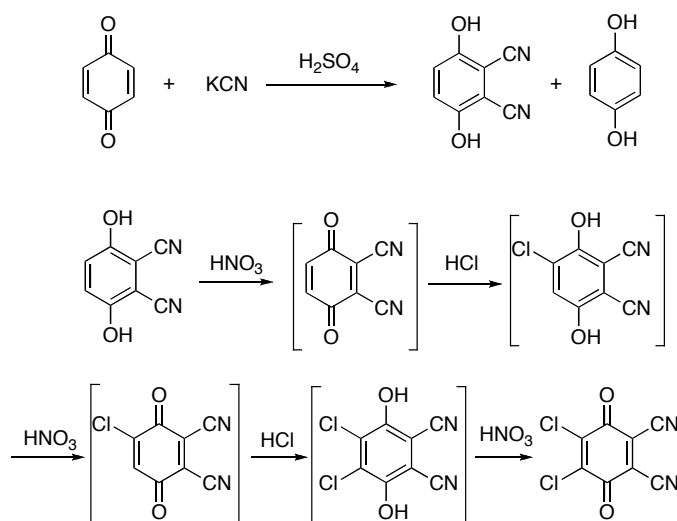
**Scheme 13.** Woodward's Syntheses of Racemic Cortisone, Progesterone, Testosterone, and Cholesterol<sup>40</sup>



### 1.2.3 Quinones as Dehydrogenating Agents

Quinone is one of the most important oxidizing reagents in organic chemistry.<sup>41</sup> 2,3-Dichloro-5,6-dicyano-*p*-benzoquinone (DDQ) has a particularly high redox potential (0.54 V / vs. SCE)<sup>42</sup> and is one of the most frequently used oxidants in organic synthesis.<sup>43</sup> The first synthesis was described by Thiele and Gunther using the following steps.<sup>44</sup>

**Scheme 13.** The First Synthesis of DDQ by Thiele and Günther<sup>44</sup>



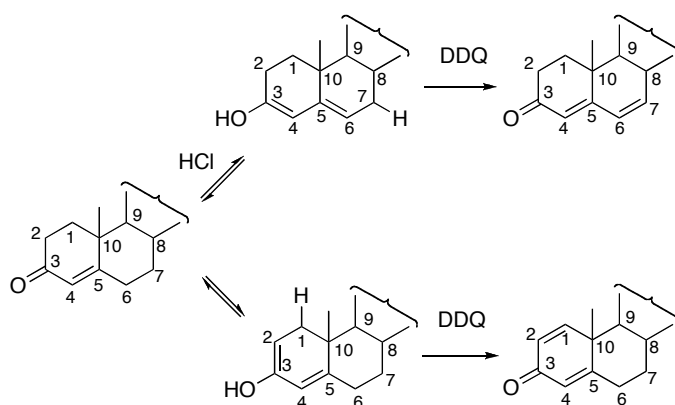
2,3-Dicyano-hydroquinone was obtained from the reaction of benzoquinone with potassium

cyanide in the presence of sulfuric acid. Further oxidations and HCl additions by a mixture of  $\text{HNO}_3$  and HCl gave 2,3-dichloro-5,6-dicyano-p-benzoquinone (DDQ) as the final product.

However, little interest was shown in the compound at that time. Although the dehydrogenation of hydroaromatic compounds by quinones was first reported by Clar and John in 1930,<sup>45</sup> it failed to gain general acceptance until the extensive investigations of Braude, Jackman, Linstead, and co-workers more than 20 years later.<sup>46</sup> They found it to be a very superior reagent for the dehydrogenation of hydroaromatic compounds. These studies established the advantage of quinone dehydrogenation as a method of selective abstraction of hydrogen from hydroaromatic compounds under mild conditions. During later decades, the scope of quinone dehydrogenation, which was previously largely limited to hydroaromatic compounds, had been extended to various other area of organic chemistry.

Since 1960, DDQ and other high redox potential quinones (e.g. o-chloranil) have found considerable applications in the steroid field. A comprehensive list of dehydrogenation reactions of steroidal compounds by DDQ had been reviewed by Walker and Hiebert in 1967<sup>43a</sup> and Becker in 1974 and 1988.<sup>41</sup> Steroids, especially  $\Delta^4$ -3-keto steroids, have been the subject of most studies from a mechanistic viewpoint. Interestingly,  $\Delta^4$ -3-keto steroids react with DDQ to give  $\Delta^{1,4}$ -3-keto steroids,<sup>47</sup> while the same reaction with chloranil leads to  $\Delta^{4,6}$ -3-keto steroids. In the presence of anhydrous hydrogen chloride as catalyst, DDQ also gives the  $\Delta^{4,6}$ -3-keto steroids. This has been explained in the terms of the scheme depicted in Scheme 14.

**Scheme 14.** Two Reaction Pathways for the Oxidations of  $\Delta^4$ -3-Keto Steroids with DDQ<sup>43a, 47</sup>

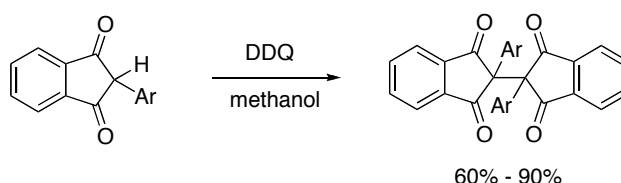


In the absence of a catalyst, the kinetically determined enol is predominantly the  $\Delta^{2,4}$ -enol. Hydride ion abstraction by DDQ leads to the preferred formation of  $\Delta^{1,4}$ -3-ketones. In the presence of a catalyst, such as anhydrous hydrogen chloride, formation of the thermodynamically more stable  $\Delta^{3,5}$ -enol occurs, and hydride ion abstraction from this enol

gives a  $\Delta^{4,6}$ -3-ketones.

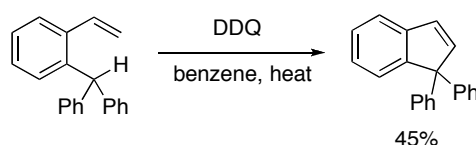
An intermolecular dehydrogenative homo-coupling of 2-arylidane-1,3-diones using DDQ had been described by Becker in 1965.<sup>48</sup>

**Scheme 15.** Homo-Coupling Reactions of 2-Arylidane-1,3-diones Using DDQ as the Oxidant<sup>48</sup>



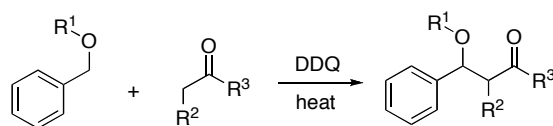
Jackman had reported intramolecular dehydrogenative coupling reaction of 2-benzhydryl-styrene using DDQ as the oxidant.<sup>49</sup>

**Scheme 16.** DDQ Mediated Intramolecular Dehydrogenative Coupling Reaction of 2-Benzhydryl-Styrene<sup>49</sup>



More recent developments on the use of DDQ as dehydrogenating agent for C-H functionalizations have attracted great attention. In 2006, Li reported intermolecular dehydrogenative cross coupling reactions between benzyl ethers and simple ketones under mild condition by using DDQ as an oxidant.<sup>50</sup>

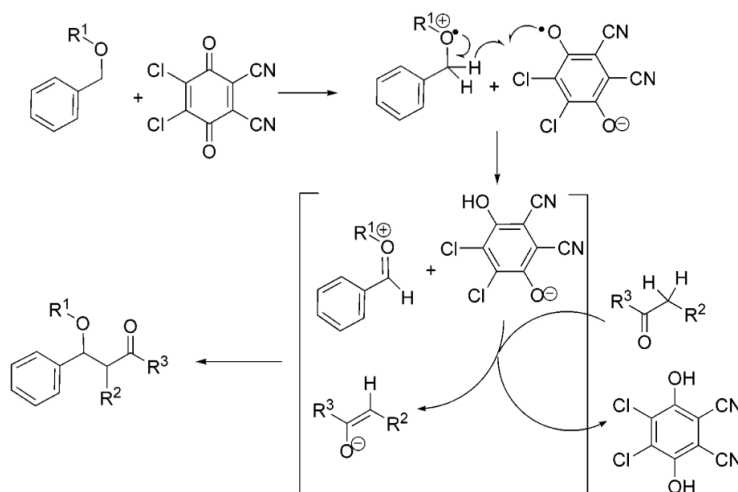
**Scheme 17.** Intermolecular Dehydrogenative Cross Coupling Reactions Between Benzyl Ethers and Simple Ketones Using DDQ as the Oxidant<sup>50</sup>



An electron-transfer initiated dehydrogenation mechanism was proposed. A single electron transfer from the benzyl ether to DDQ generates a radical cation and a DDQ radical anion. The radical oxygen of the DDQ radical anion then abstracts a H-atom from the radical cation and generates an alkoxybenzyl cation, and the anionic oxygen of DDQH<sup>-</sup> anion then abstracts an R-hydrogen from the ketone to generate an enolate. Finally, the attack of the enolate on the benzyloxy cation generates the coupling product and the hydroquinone derivative.

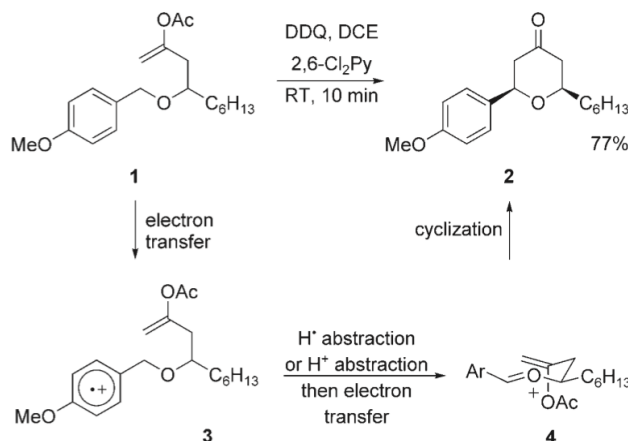


**Scheme 18.** Proposed Reaction Mechanism for the Dehydrogenative Cross Coupling Reactions by Li<sup>50</sup>



A later study on the oxidative cyclization reactions of benzylic or allylic ethers containing enol acetate nucleophiles to give diastereoselective tetrahydropyrone have been reported by Floreancig.<sup>51</sup>

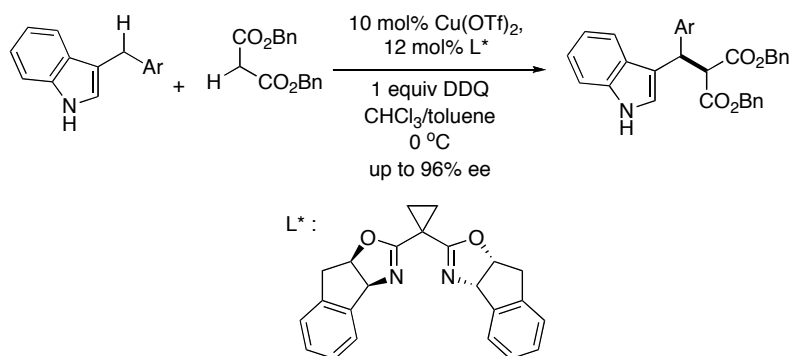
**Scheme 19.** Diastereoselective Oxidative Cyclization Reactions of Benzylic Ethers<sup>51</sup>



This reaction proceeds by electron transfer from **1** to DDQ to form radical-ion pair **3**. Because of the substantially weakened carbon–hydrogen bonds in alkylarene radical cations, the formation of benzylic cation **4**, shown in the chair conformation that is relevant to cyclization, either undergoes subsequent direct hydrogen atom transfer, or a sequence including proton transfer and rapid benzylic radical oxidation. Cyclization and cleavage of the acetyl group yields **2**.

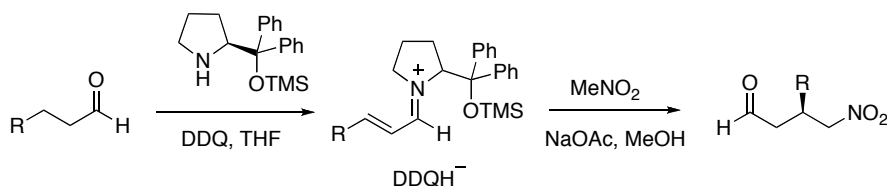
The combination of chiral Lewis acid and DDQ as dehydrogenating reagent was proved to be an efficient method to achieve enantioselective oxidative couplings. Recently Gong reported the oxidative coupling reactions of 3-benzylindole derivatives with dibenzyl malonate by using chiral Lewis-acid-bonded nucleophiles to provide an approach to indole derivatives.<sup>52</sup>

**Scheme 20.** DDQ-Mediated Enantioselective Cross-Coupling of 3-Benzylindole Derivatives and Dibenzyl Malonate Catalyzed by Chiral Lewis Acid<sup>52</sup>



In a recent study, an organo-catalyzed asymmetric and oxidative coupling of aldehydes with nitromethane using DDQ as the oxidant was established by Hayashi.<sup>53</sup>

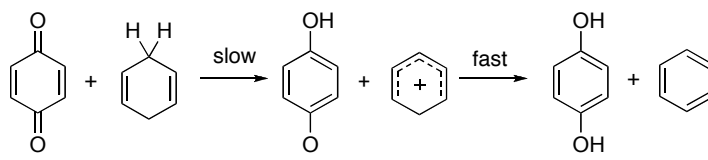
**Scheme 21.** Enantioselective Oxidative Cross-Coupling of Aldehydes with Nitromethane Catalyzed by Diphenylprolinol Silyl Ether<sup>53</sup>



### 1.2.4 Dehydrogenation Mechanisms of Quinones

As suggested by Linstead, Jackman, and coworkers,<sup>46</sup> the oxidation of hydrocarbons by quinone often occurs via a rate-determining hydride transfer, leading to a delocalized carbocation, which rapidly loses a proton or undergoes nucleophilic attack in a subsequent step. However, the seemingly simple two-step mechanism was a subject of recurring investigation in the late 20th century.<sup>54</sup>

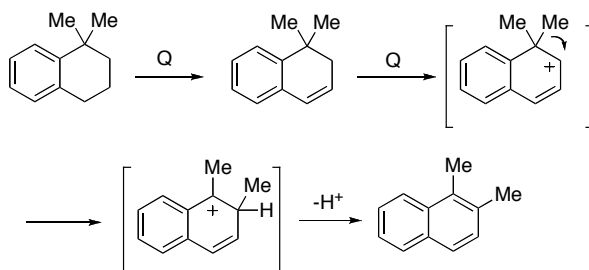
**Scheme 22.** Dehydrogenation Mechanism Proposed by Linstead, Jackman, and Coworkers<sup>46</sup>



Consistent with this mechanism, the reactions studied were found to be (1) first order in both reactants; (2) faster in polar solvents, such as dimethylformamide, than in nonpolar solvents, such as benzene; (3) unaffected by radical initiators; (4) faster with quinones of higher oxidation potential; and (5) acid catalyzed in the case of quinones of low potential. Moreover, large isotope effects are observed.<sup>54b,e,j</sup>

In line with the ionic mechanism, a Meerwein-Wagner rearrangement was observed in the oxidations of 1,1-dimethyl-tetrahydronaphthalene by quinones.<sup>46g</sup>

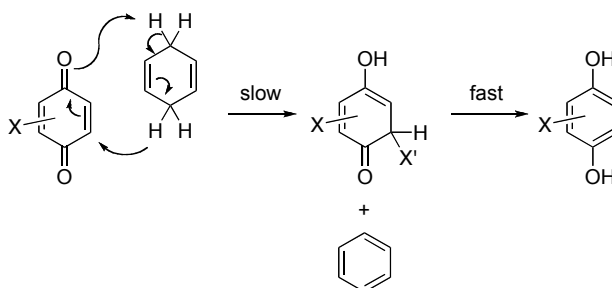
**Scheme 23.** Oxidation of 1,1-Dimethyl-tetrahydronaphthalene Involves a Meerwein-Wagner Rearrangement<sup>46g</sup>



Further mechanistic details are provided by the observation that the dehydrogenation of *cis*-1,2-dideuterioacenaphthene by DDQ proceeds with predominant *cis*-elimination.<sup>54a</sup> Initial ion-pair formation and partial collapse of the ion pairs to product before dissociation accounts for the net *cis* elimination. The amount of *cis* elimination decreases as solvent polarity increases, in agreement with the ion-pair hypothesis.

A later study suggests that reaction of 1,4-cyclohexadiene with DDQ may involve concerted rather than stepwise hydrogen transfer (Scheme 24).<sup>54c</sup>

**Scheme 24.** Concerted Mechanism for Synchronous Transfer of Two Hydrogen Atoms in the Reaction of 1,4-Cyclohexadiene with DDQ<sup>54c</sup>

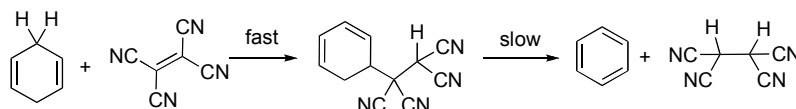


As the reactivity of 1,4-cyclohexadiene toward DDQ is much higher than that of 1,4-pentadiene, which were expected to have similar reactivities (although now it appears to be incorrect according to their nucleophilicity parameters<sup>19a</sup>), Roček proposed a concerted mechanism for the transfer of two hydrogen atoms at the same time.

Based on the observation of an intermediate which may be formed by an ene-reaction of 1,4-cyclohexadiene with tetracyanoethylene, Jacobson suggested a similar ene-mechanism for the dehydrogenation by quinones.<sup>55</sup> However, no evidence was obtained for the appearance of an intermediate. As pointed out by Müller, spectroscopic monitoring of the reaction shows that disappearance of the substrate proceeds at the same rate as the formation of the product.

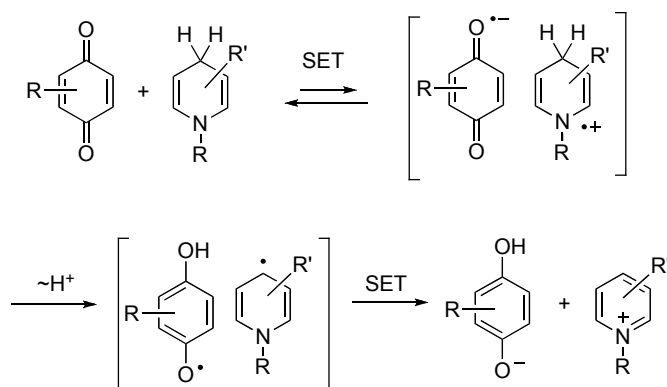
Therefore, fast formation, followed by slow decomposition of an intermediate can be ruled out.<sup>54f</sup>

**Scheme 25.** Ene-reaction of 1,4-Cyclohexadiene with Tetracyanoethylene<sup>55</sup>



The hydride abstractions from nicotinamide adenine dinucleoside (NADH) and its model compounds by quinones had triggered numerous mechanistic studies because of the biological importance of these processes. It has been the subject of considerable controversy whether hydride transfer occurs in one-step<sup>56</sup> or via an SET mechanism as depicted in Scheme 26.<sup>57</sup>

**Scheme 26.** Electron Transfer Mechanism for the Hydride Transfer Reactions of NADH Model Compounds with Quinones Proposed by Tanaka and Co-workers<sup>57</sup>



### 1.3 Objectives

As described in Chapter 1.2 quinones have often used as one-electron oxidants, but there have also been many reports about reactions which are indicative of the operation of polar reactions. It was the goal of this work, whether the correlation equation  $\log k(20\text{ }^{\circ}\text{C}) = s_N(E + N)$  can be used to differentiate these cases and make predictions of the potential use of differently substituted quinones as electrophiles. Particular attention should be paid to their ambident electrophilic character as nucleophiles may attack either at C or O of the carbonyl group or at conjugate positions, which may even be different in the case of unsymmetrical systems.

As different chapters of this thesis have been published or prepared for publication, parts of the introductions of the individual chapters are repetitive.

## 1.4 References

- (1) Ingold, C. K. *Structure and Mechanism in Organic Chemistry*; Cornell University Press: Ithaca, NY, 1953.
- (2) Kornblum, N.; Michel, R. E.; Kerber, R. C. *J. Am. Chem. Soc.* **1966**, 88, 5660.
- (3) Russell, G. A.; Danen, W. C. *J. Am. Chem. Soc.* **1966**, 88, 5663.
- (4) Kim, J. K.; Bunnett, J. F. *J. Am. Chem. Soc.* **1970**, 928, 7463.
- (5) (a) Ashby, E. C. *Acc. Chem. Res.* **1988**, 21, 414. (b) Pros, A. *ibid.* **1985**, 18, 212. (c) Saveant, J.-M. *Adv. Phys. Org. Chem.* **1990**, 26, 1. (d) Chanon, M.; Tobe, M. L. *Angew. Chem. Int. Ed.* **1982**, 21, 1. (e) Bordwell, F. G.; Harrelson Jr., J. A. *J. Org. Chem.* **1989**, 54, 4893. (f) Ebersson, L. E. *Electron transfer reactions in organic chemistry: Reactivity und structure*, Vol. 25, Springer, Heidelberg. 1987. (g) Kochi, J. K. *Angew. Chem. Int. Ed.* **1988**, 27, 1227. (h) Fukuzumi, S.; Kochi, J. K. *J. Am. Chem. Soc.* **1981**, 103, 7240. (i) Arnett, E. M.; Whitesell Jr., L. G.; Amarnath, K.; Cheng, J. P.; Marchot, E. *Makromol. Chem. Macromol. Symp.* **1988**, 13/14, 21. (j) Lund, T.; Lund, H. *Acta Chem. Scand. B* **1986**, 40, 470.
- (6) Fukuzumi, S.; Fujita, M. and Otera, J. *J. Chem. Soc., Chem. Commun.* **1993**, 1536–1537.
- (7) Ashby, E. C.; Goel, A. B.; DePriest, R. *J. Am. Chem. Soc.* **1980**, 102, 7779.
- (8) (a) Griller, D.; Ingold, K. U. *Acc. Chem. Res.* **1980**, 13, 317. (b) Newcomb, M.; Curran, D. P. *Acc. Chem. Res.* **1988**, 21, 206–214. (c) Tolbert, L. M.; Sun, X.-J.; Ashby, E. C. *J. Am. Chem. Soc.* **1995**, 117, 2681–2685. (d) Zard, S. Z. *Radical Reactions in Organic Synthesis*; Oxford University Press, New York, **2003**.
- (9) (a) Newcomb, M. and Curran, D. P. *Acc. Chem. Res.* **1988**, 21, 206–215; (b) Tanko, J. M. and Drumright, R. E. *J. Am. Chem. Soc.* **1990**, 112, 5362–5363.
- (10) Todres, Z. V. *Russ. Chem. Rev.* **1974**, 43, 1099.
- (11) Pryor, W. A.; Hendrickson, W. H. *J. Am. Chem. Soc.* **1983**, 105, 7114.
- (12) Singh, P. R.; Kumar, R. *Aust. J. Chem.* **1972**, 25, 2133.
- (13) (a) Ebersson, L. *Adv. Phys. Org. Chem.* **1982**, 18, 79. (b) Saveant, J.-M. *J. Am. Chem. Soc.* **1987**, 109, 6788.
- (14) (a) Marcus, R. A. *Angew. Chem.* **1993**, 105, 1161–1180; (b) Marcus, R. A. *Annu. Rev. Phys. Chem.* **1964**, 15, 155–196.
- (15) (a) Rehm, D. and Weller, A. *Ber. Bunsenges. Phys. Chem.* **1969**, 73, 834–839; (b) Rehm, D. and Weller, A. *Isr. J. Chem.* **1970**, 8, 259.

- (16) (a) Patz, M.; Mayr, H.; Maruta, J.; Fukuzumi, S. *Angew. Chem. Int. Ed. Engl.* **1995**, *34*, 1225-1227. (b) Ofial, A. R.; Ohkubo, K.; Fukuzumi, S.; Lucius, R.; Mayr, H. *J. Am. Chem. Soc.* **2003**, *125*, 10906-10912.
- (17) (a) Mayr, H.; Patz, M. *Angew. Chem., Int. Ed. Engl.* **1994**, *33*, 938-957. (b) Mayr, H.; Ofial, A. R. *Pure Appl. Chem.* **2005**, *77*, 1807-1821. (c) Mayr, H.; Ofial, A. R. *J. Phys. Org. Chem.* **2008**, *21*, 584-595. (d) Mayr, H.; Kempf, B.; Ofial, A. R. *Acc. Chem. Res.* **2003**, *36*, 66-77.
- (18) For a comprehensive database of nucleophilicity parameters  $N$  and  $s_N$  as well as electrophilicity parameters  $E$ , see <http://www.cup.lmu.de/oc/mayr/DBintro.html>.
- (19) (a) Mayr, H.; Bug, T.; Gotta, M. F.; Hering, N.; Irrgang, B.; Janker, B.; Kempf, B.; Loos, R.; Ofial, A. R.; Remennikov, G.; Schimmel, H. *J. Am. Chem. Soc.* **2001**, *123*, 9500-9512. (b) Lucius, R.; Loos, R.; Mayr, H. *Angew. Chem., Int. Ed.* **2002**, *41*, 91-95. (c) Richter, D.; Hampel, N.; Singer, T.; Ofial, A. R.; Mayr, H. *Eur. J. Org. Chem.* **2009**, 3203-3211. (d) Ammer, J.; Nolte, C.; Mayr, H. *J. Am. Chem. Soc.* **2012**, *134*, 13902-13911.
- (20) (a) Conant, J. B.; Fieser, L. F. *J. Am. Chem. Soc.* **1923**, *45*, 2194-2218. (b) Conant, J. B.; Fieser, L. F. *J. Am. Chem. Soc.* **1923**, *46*, 1858-1881. (c) Peover, M. E. *J. Chem. Soc.* **1962**, 4540-4549.
- (21) (a) Müh, F.; Glöckner, C.; Hellmich, J.; Zouni, A. *BBA-Bioenergetics* **2012**, *1817*, 44. (b) Nohl, H.; Jordan, W.; Youngman, R. J. *Adv. Free Radical Biol.* **1986**, *2*, 211. (c) Efremov, R. G.; Baradaran, R.; Sazanov, L. A. *Nature* **2010**, *465*, 441.
- (22) (a) Weinberg, D. R.; Gagliardi, C. J.; Hull, J. F.; Murphy, C. F.; Kent, C. A.; Westlake, B. C.; Paul, A.; Ess, D. H.; McCafferty, D. G.; Meyer, T. *J. Chem. Rev.* **2012**, *112*, 4016. (b) Huynh, M. H. V.; Meyer, T. *J. Chem. Rev.* **2007**, *107*, 5004. (c) Meyer, T. J.; Huynh, M. H. V.; Thorp, H. H. *Angew. Chem., Int. Ed.* **2007**, *46*, 5284. (d) Stubbe, J.; van der Donk, W. A. *Chem. Rev.* **1998**, *98*, 705. (e) Reece, S. Y.; Hodgkiss, J. M.; Stubbe, J.; Nocera, D. G. *Philos. Trans. R. Soc. B* **2006**, *361*, 1351.
- (23) Guskov, A.; Kern, J.; Gabdulkhakov, A.; Broser, M.; Zouni, A.; Seanger, W. *Nat. Struct. Mol. Biol.* **2009**, *16*, 334-342.
- (24) (a) Thiele, J. *Ber.* **1898**, *31*, 1247. (b) Suida, H. and Suida, W. *Justus Liebigs Ann. Chem.* **1918**, *416*, 113-163. (c) *The Chemistry of the Quinoid Compounds, Part I*; Patai, S., Ed.; Wiley: Chichester, UK, 1974. (d) *The Chemistry of the Quinoid Compounds Vol. 2*; Patai, S., Rappoport, Z., Eds.; Wiley: Chichester, UK, 1988.
- (25) Wöhler, F. *Justus Liebigs Ann. Chem.* **1844**, *51*, 145-163.

- (26) (a) Mulliken, R. S.; Person, W. B. *Molecular Complexes, a Lecture and Reprint Volume*; Wiley-Interscience: New York, 1969. (b) Mataga, N.; Kubota, T. *Molecular Interactions and Electronic Spectra*; Marcel Dekker: New York, 1970.
- (27) Nogami, T.; Yoshihara, K.; Hosoya, H. and Nagakura, S. *J. Phys. Chem.* **1969**, *73*, 2670.
- (28) Yamaoka, T. and Nagakura, S. *Bull. Chem. Soc. Japan* **1971**, *44*, 2971.
- (29) (a) Snell, J. M.; Weissberger, A. *J. Am. Chem. Soc.* **1939**, *61*, 450-453. (b) Porter, R. F.; Rees, W. W.; Frauenglass, E.; Wilgus III, H. S.; Nawn, G. H.; Chiesa, P. P.; Gates Jr., J. W. *J. Org. Chem.* **1964**, *29*, 588-594.
- (30) Thiele, J. *Ber.* **1898**, *31*, 1247.
- (31) Hawthorne, F. M. and Reintjes, M. *J. Am. Chem. Soc.* **1965**, *87*, 4585-4587.
- (32) Kabalka, G. W. *J. Organometal. Chem.* **1971**, *33*, C25.
- (33) (a) Kabalka, G. W.; Brown, H. C.; Suzuki, A.; Honma, S.; Arase, A. and Itoh, M. *J. Am. Chem. Soc.* **1970**, *92*, 710. (b) Brown, H. C. and Kabalka, G. W. *J. Am. Chem. Soc.* **1970**, *92*, 712. (c) Suzuki, A.; Nozawa, S.; Itoh, M.; Brown, H. C.; Kabalka, G. W. and Holland, G. W. *J. Am. Chem. Soc.* **1970**, *92*, 3503.
- (34) (a) Diels, O. and Alder, K. *Justus Liebigs Ann. Chem.* **1928**, *460*, 98. (b) Diels, O.; Alder, K.; Stein, G.; Pries, P.; and Winckler, H. *Ber.* **1929**, *62*, 2337.
- (35) Albrecht, W. *Justus Liebigs Ann. Chem.* **1906**, *348*, 31.
- (36) Woodward, R. B. *J. Am. Chem. Soc.* **1942**, *64*, 3058-3059
- (37) Todd, A. R.; Cornforth, J. W. *Biogr. Mem. Fellows R. Soc.* **1981**, *27*, 628-695.
- (38) Rutz, L. W. and Rytina, A. W. in *Organic Reactions*, Vol. V, John Wiley, New York, 1949, pp. 136-192.
- (39) Moody, C. J. and Nawrat, C. C. *Angew. Chem. Int. Ed.* **2014**, *53*, 2-24.
- (40) Woodward, R. B.; Sondheimer, F.; Taub, D.; Heusler, K.; McLamore, W. M. *J. Am. Chem. Soc.* **1952**, *74*, 4223-4251.
- (41) (a) Becker, H.-D. in *The Chemistry of the Quinoid Compounds*, Part I (Ed: Patai, S.), Wiley: Chichester, UK, 1974; pp 335-423; b) Becker, H.-D.; Turner, A. B. in *The Chemistry of the Quinoid Compounds*, Vol. 2 (Eds: Patai, S.; Rappoport, Z.), Wiley: Chichester, UK, 1988; pp 1351-1384;
- (42) Andrieux, C. P.; Merz, A.; Saveant, J.-M.; Tomahogh, R. *J. Am. Chem. Soc.* **1984**, *106*, 1957-1962.
- (43) (a) Walker, D.; Hiebert, J. D. *Chem. Rev.* **1967**, *67*, 153-195. (b) Buckle, D. R. In *Encyclopedia of Reagents for Organic Synthesis Vol. 3*; Paquette, L. A., Ed.; Wiley: Chichester, UK, 1995; p 1699.

- (44) Thiele, J.; Günther, F. *Liebigs Ann. Chem.* **1906**, 349, 45–66.
- (45) Clar, E. and John, F. *Ber.* **1930**, 63, 2967.
- (46) For the series of papers, see: (a) Braude, E. A.; Jackman, L. M. and Linstead, R. P. *J. Chem. Soc.* **1954**, 3548-3563. (b) Braude, E. A.; Jackman, L. M. and Linstead, R. P. *J. Chem. Soc.* **1954**, 3564-3568. (c) Braude, E. A.; Brook, A. G. and Linstead, R. P. *J. Chem. Soc.* **1954**, 3569-3574. (d) Braude, E. A.; Linstead, R. P. and Wooldridge, K. R. *J. Chem. Soc.* **1956**, 3070-3074. (e) Barnard, J. R. and Jackman, L. M. *J. Chem. Soc.* **1960**, 3110-3115. (f) Braude, E. A.; Jackman, L. M.; Linstead, R. P. and Shannon, J. S. *J. Chem. Soc.* **1960**, 3116-3122. (g) Braude, E. A.; Jackman, L. M.; Linstead, R. P. and Lowe, G. J. *J. Chem. Soc.* **1960**, 3123-3132. (h) Braude, E. A.; Jackman, L. M.; Linstead, R. P. and Lowe, G. J. *J. Chem. Soc.* **1960**, 3133-3138. For a review, see: (i) Jackman, L. M. in *Advances in Organic Chemistry, Methods and Results*, Vol. 2 (Eds: Raphael, R. A.; Taylor, E. C. and Wynberg, H.), Interscience Publishers, Inc., New York, N. Y., 1960.
- (47) (a) Ringold, H. J.; Gut, M.; Hayano, M. and Turner, A. *Tetrahedron Lett.* **1962**, 835. (b) Ringold, H. J.; Hayano, M. and Stefanovic, V. *J. Biol. Chem.* **1963**, 238, 1960. (c) Ringold, H. J. and Turner, A. *Chem. Ind.* **1962**, 211.
- (48) Becker, H.-D. *J. Org. Chem.* **1965**, 30, 989.
- (49) Brown, R. F. and Jackman, L. M. *J. Chem. Soc.* **1960**, 3144.
- (50) Zhang, Y.; Li, C.-J. *J. Am. Chem. Soc.* **2006**, 128, 4242-4243
- (51) Tu, W.; Liu, L.; Floreancig, P. E. *Angew. Chem.* **2008**, 120, 4252; *Angew. Chem. Int. Ed.* **2008**, 47, 4184.
- (52) Guo, C.; Song, J.; Luo, S.-W.; Gong, L.-Z. *Angew. Chem., Int. Ed.* **2010**, 49, 5558-5562.
- (53) Hayashi, Y.; Itoh, T.; Ishikawa, H. *Angew. Chem., Int. Ed.* **2011**, 50, 3920-3924
- (54) (a) Trost, B. M. *J. Am. Chem. Soc.* **1967**, 89, 1847-1851; (b) Müller, P. and Roček, J. *J. Am. Chem. Soc.* **1972**, 94, 2716-2719; (c) Stoos, F. and Roček, J. *J. Am. Chem. Soc.* **1972**, 94, 2719-2723; (d) Thummel, R. P.; Cravey, W. E. and Cantu, D. B. *J. Org. Chem.* **1980**, 45, 1633-1637; (e) Müller, P. *Helv. Chim. Acta.* **1973**, 56, 1243-1251; (f) Müller, P. and Joly, D. *Helv. Chim. Acta.* **1983**, 66, 1110-1118; (g) Carlson, B. W. and Miller, L. L. *J. Am. Chem. Soc.* **1985**, 107, 479-485; (h) Fukuzumi, S.; Koumitsu, S.; Hironaka, K. and Tanaka, T. *J. Am. Chem. Soc.* **1987**, 109, 305-316; (i) Zaman, K. M.; Yamamoto, S.; Nishimura, N.; Maruta, J. and Fukuzumi, S. *J. Am. Chem. Soc.* **1994**, 116, 12099-12100; (j) Batista, V. S.; Crabtree, R. H.; Konezny, S. J.; Luca, O. R. and Praetorius, J. M. *New J. Chem.* **2012**, 36, 1141-1144;
- (55) Jacobson, J. M. *J. Am. Chem. Soc.* **1980**, 102, 886-887.



- (56) (a) Abeles, R. H.; Hutton, R. F.; Westheimer, F. H. *J. Am. Chem. Soc.* **1957**, *79*, 712. (b) Bunting, J. W.; Sindhuatmadja, S. *J. Org. Chem.* **1981**, *46*, 4211. (c) Srinivasan, R.; Medary, R. T.; Fisher, H. F.; Korris, D. J.; Stewart, R. *J. Am. Chem. Soc.* **1982**, *104*, 807. (d) Powell, M. F.; Bruice, T. C. *J. Am. Chem. Soc.* **1983**, *105*, 1014, 7139. (e) Donkersloot, M. C. A.; Buck, H. M. *J. Am. Chem. Soc.* **1981**, *103*, 6549-6554. (f) Kurtz, L. C.; Frieden, C. *J. Am. Chem. Soc.* **1975**, *97*, 677. (g) Kurtz, L. C.; Frieden, C. *J. Am. Chem. Soc.* **1980**, *102*, 4198.
- (57) (a) Steffens, J. J.; Chipman, D. M. *J. Am. Chem. Soc.* **1971**, *93*, 6694. (b) Ohno, A.; Yamamoto, H.; Oka, S. *J. Am. Chem. Soc.* **1981**, *203*, 2041. (c) Shinkai, S.; Tsuno, T.; Asatani, Y.; Manabe, O. *J. Chem. Soc., Perkin Trans. 2* **1983**, 1533. (d) Fukuzumi, S.; Kondo, Y.; Tanaka, T. *J. Chem. Soc., Perkin Trans. 2* **1984**, 673. (e) Lai, C. C.; Colter, A. K. *J. Chem. Soc., Chem. Commun.* **1980**, 1115. (f) Jarvis, W. F.; Dittmer, D. C. *J. Org. Chem.* **1983**, *48*, 2784. (g) van Eikeren, P.; Kenney, P.; Tokmakian, R. *J. Am. Chem. Soc.* **1979**, *101*, 7402. (h) Fukuzumi, S.; Nishizawa, N.; Tanaka, T. *J. Org. Chem.* **1984**, *49*, 3571. (i) Fukuzumi, S.; Tanaka, T. *Chem. Lett.* **1982**, 1513. (j) Fukuzumi, S.; Koumitsu, S.; Hironaka, K.; Tanaka, T. *J. Am. Chem. Soc.* **1987**, *109*, 305-316.



## Chapter 2: Manifestation of Polar Reaction Pathways of DDQ

Xingwei Guo and Herbert Mayr\*

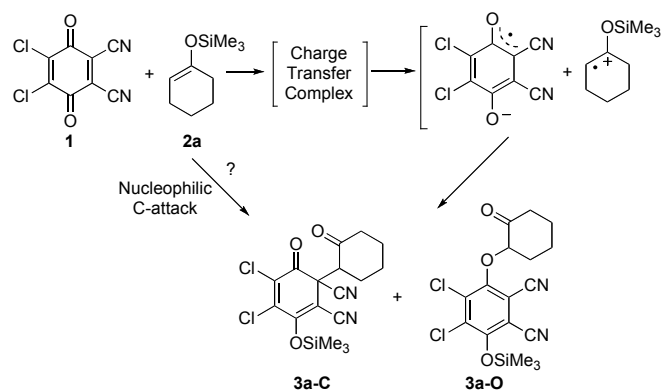
*J. Am. Chem. Soc.* **2013**, *135*, 12377-12387

### 2.1 Introduction

2,3-Dichloro-5,6-dicyano-*p*-benzoquinone (DDQ), first synthesized by Thiele and Günther in 1906,<sup>1</sup> has a high redox potential (0.54 V vs. SCE in acetonitrile)<sup>2</sup> and is one of the most important oxidizing reagents in organic chemistry. It usually reacts as a one-electron acceptor to give a radical anion in the first step, and has been used for the oxidation of steroid ketones, hydroaromatic compounds, alcohols, phenols, and heterocycles.<sup>3</sup> Recently, DDQ was used as an oxidant for several oxidative coupling reactions.<sup>4</sup>

Triggered by the observation of DDQ-substrate adducts during the oxidation of 4-aza-3-ketosteroids by DDQ,<sup>5</sup> Bhattacharya and coworkers investigated the reactions of cyclic silyl enol ethers with DDQ and found the formation of adducts **3a-C** and **3a-O** (Scheme 1).<sup>6</sup>

**Scheme 1.** The Reaction of DDQ(**1**) with the Silyl Enol Ether **2a** as Suggested by Bhattacharya.<sup>6</sup>




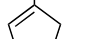
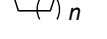

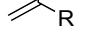



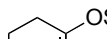
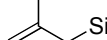
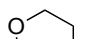
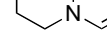
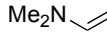
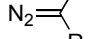
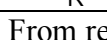
The dramatic solvent and temperature effects on the product ratios were considered to be indicative of the operation of two distinctly different pathways for the formation of **3a-C** and **3a-O**. Though both products were suggested to be formed via a radical ion pair, the possibility of a nucleophilic attack of the silyl enol ether on DDQ to form the carbon-carbon adduct **3a-C** was explicitly mentioned as an alternative.<sup>6</sup> We now report kinetic investigations of the reactions of DDQ with  $\pi$ -nucleophiles, which clearly show that polar mechanisms are rather the rule than the exception for these reactions.

In recent years, we have developed a linear free energy relationship based model for polar organic reactions,<sup>7</sup> which uses eq. (1) to predict rates and selectivities for these reactions:

$$\log k(20\text{ }^{\circ}\text{C}) = s_{\text{N}}(E + N)$$

In equation (1) the second-order rate constant ( $\log k$ ) is calculated by two nucleophile-specific parameters  $s_{\text{N}}$ ,  $N$  and one electrophile-specific parameter  $E$ . A comprehensive nucleophilicity scale covering more than 30 orders of magnitude<sup>8</sup> has been created by using a series of benzhydrylium ions and structurally related quinone methides as reference electrophiles.<sup>9</sup> We have now used the linear free energy relationship (1) to elucidate the mechanisms of the reactions of DDQ with  $\pi$ -systems (Table 1).

**Table 1.** Nucleophiles **2a-o** and their Reactivity Parameters  $N$  and  $s_{\text{N}}$  in  $\text{CH}_2\text{Cl}_2$

Nucleophile			$N (s_{\text{N}})^a$
	<b>2a</b>	$n = 2$	5.21 (1.00)
	<b>2b</b>	$n = 1$	6.57 (0.93)
	<b>2c</b>	$n = 3$	6.62 (1.00)
	<b>2d</b>	R = Ph	6.22 (0.96)
	<b>2e</b>	R = Me	5.41 (0.91)
	<b>2f</b>	R = OPh	8.23 (0.81)
	<b>2g</b>	R = OBu	10.21 (0.82)
	<b>2h</b>	R = H	3.94 (1.00)
	<b>2i</b>	R = OMe	9.00 (0.98)
	<b>2j</b>		4.61 (1.19) <sup>b</sup>
	<b>2k</b>		4.41 (0.96)
	<b>2l</b>		8.52 (0.80)
	<b>2m</b>		9.43 (0.80)
	<b>2n</b>	R = Ph	9.35 (0.83)
	<b>2o</b>	R = COOEt	4.91 (0.95)

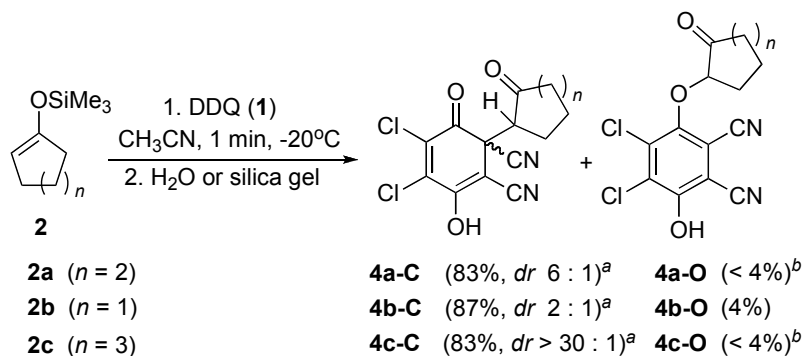
<sup>a</sup> From ref. 8. <sup>b</sup> This work.

## 2.2 Results

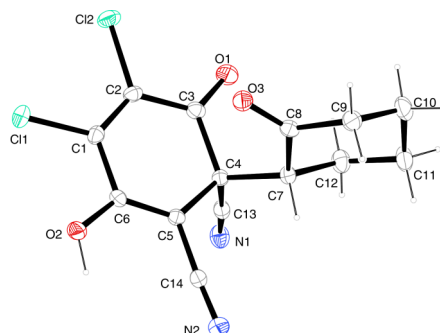
**Product Studies in Acetonitrile.** In line with earlier investigations,<sup>6</sup> the cyclic silyl enol ethers **2a-c** were found to give predominantly **4(a-c)-C**, the products of C-attack in

acetonitrile, and only a trace ( $\approx 4\%$ ) of **4b-O**, the product of O-attack, was detected by  $^1\text{H}$  NMR spectroscopy (Scheme 2). Compounds **4(a-c)-C** were isolated as mixtures of diastereomers after column chromatography. The major diastereomers of **4(a,c)-C** were obtained and characterized as pure compounds by recrystallization from a mixture of dichloromethane and pentane. Additionally, the major diastereoisomer of **4a-C** was characterized by X-ray crystallography (Figure 1).

**Scheme 2.** Reactions of DDQ with Cyclic Silyl Enol Ethers **2a-c**



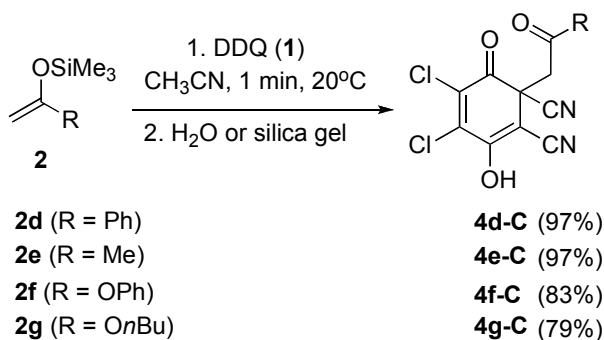
<sup>a</sup> Isolated yield. <sup>b</sup> Not observed by  $^1\text{H}$  NMR in the crude material.



**Figure 1.** Crystal structure of **4a-C** (major diastereomer, thermal ellipsoids are drawn at the 50% probability level).

The reactions of the terminal silyl enol ethers **2d**, **2e** and silyl ketene acetals **2f**, **2g** with DDQ yielded the products of C-attack (**4(d-g)-C**) quantitatively (Scheme 3), which were purified by column chromatography.

**Scheme 3.** Reactions of DDQ with Terminal Silyl Enol Ethers and Ketene Acetals

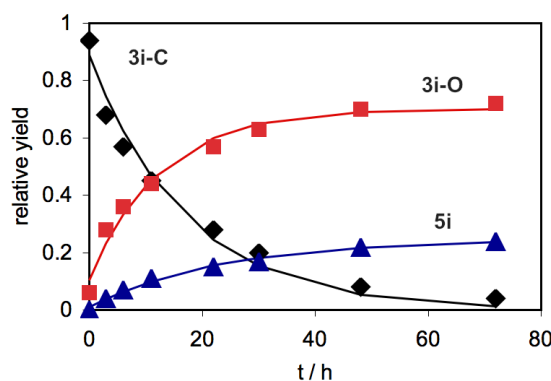


While the isobutyraldehyde-derived silyl enol ether **2h** reacted via O-attack to give 68% of **3h-O** and 32% of the dehydrogenated product **5h** (Scheme 4), according to  $^1\text{H}$  NMR analysis of the crude reaction product, the structurally analogous silyl ketene acetal **2i** reacted with DDQ preferentially at carbon to give 94% of **3i-C** and 6% of **3i-O**. At elongated reaction times **3i-C** slowly transformed into a mixture of **3i-O** and **5i** (Scheme 4). The parallel increase of **3i-O** and **5i** (Figure 2) shows that both products are formed in parallel reactions from **3i-C** and excludes the generation of **5i** by elimination from **3i-O**. In view of the slow conversion of **3i-C** into **3i-O** (after 10 min, only 7% of **3i-O** are present), the observation of a small amount of **3i-O** even after one minute indicates that 6% of **3i-O** is directly formed from DDQ and **2i** (kinetic product control). The desilylated products **4h-O** and **4i-O** were obtained by column chromatography on silica gel in 45 and 63% yield, respectively (see Supporting Information).

**Scheme 4.** Relative Yields ( $^1\text{H}$  NMR) of the Reactions of DDQ with **2h** and **2i** in  $\text{CD}_3\text{CN}$

Starting Material	Time	3h-C	3h-O	5h
<b>2h</b> (R = H)	1 min	<i>n.d.</i> <sup>a</sup>	68 %	32 %
	1 h	<i>n.d.</i> <sup>a</sup>	68 %	32 %
<b>2i</b> (R = OMe)	1 min	94 %	6 %	<i>n.d.</i> <sup>a</sup>
	10 min	93 %	7 %	<i>n.d.</i> <sup>a</sup>
	1 h	82 %	16 %	2 %
	22 h	28 %	57 %	15 %
	48 h	8 %	70 %	22 %
	72 h	4 %	72 %	24 %

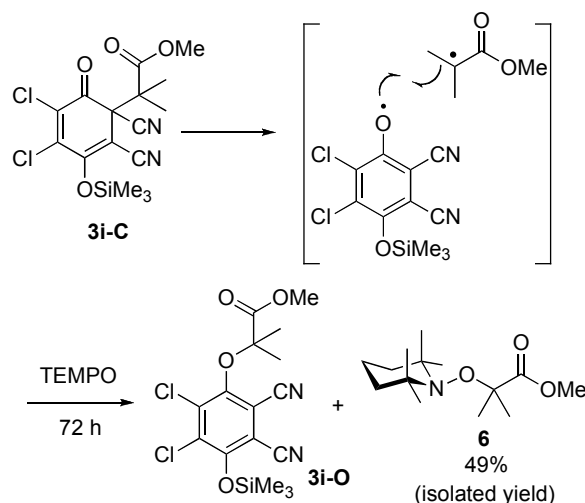
<sup>a</sup> *n.d.* = not detected.



**Figure 2.** Time resolved relative  $^1\text{H}$  NMR yields of **3i-C**, **3i-O**, and **5i** during the reaction of DDQ with **2i** (in  $\text{CD}_3\text{CN}$ , at  $20^\circ\text{C}$ ).

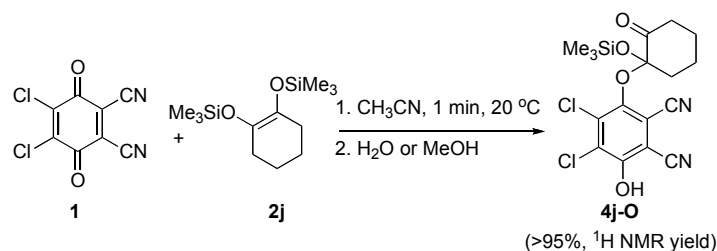
The rearrangement of **3i-C** to **3i-O** can be assumed to proceed via a radical pathway, as shown in Scheme 5. When (2,2,6,6-tetramethylpiperidin-1-yl)oxyl (TEMPO) was added to crude **3i-C**, which was formed from **1** and **2i** in  $\text{CH}_3\text{CN}$  within 1 minute (Scheme 4), a 45 : 55 mixture of **3i-O** and **6** was formed within 72 h at room temperature ( $^1\text{H}$  NMR). Methyl methacrylate **5i** probably was lost during evaporation of the solvent. Column chromatography of the mixture provided pure **6** in 49% yield, which was fully characterized.

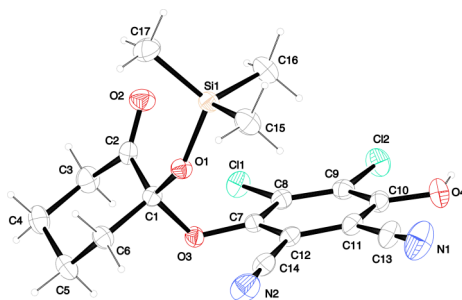
**Scheme 5.** Trapping of the Intermediate of the Rearrangement of **3i-C** to **3i-O**



The reaction of 1,2-disiloxycyclohexene **2j** with DDQ gave exclusively the product of O-attack (Scheme 6). The partially desilylated product **4j-O** crystallized from  $\text{CH}_2\text{Cl}_2$ /pentane solution and was analyzed by X-ray crystallography (Figure 3).

**Scheme 6.** Reaction of DDQ with **2j**

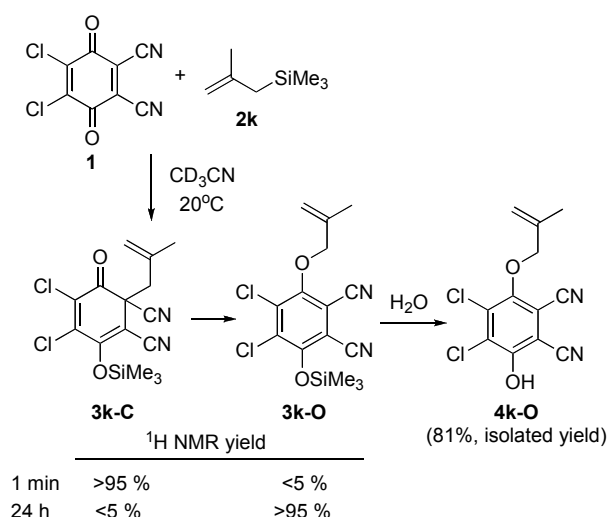




**Figure 3.** Crystal structure of **4j-O** (thermal ellipsoids are drawn at the 50% probability level).

The reaction of allylsilane **2k** with DDQ initially gave **3k-C**, the product of C-attack, that slowly rearranged into the allyl phenyl ether **3k-O** (Scheme 7). After hydrolysis, the desilylated derivative **4k-O** was obtained by crystallization in 81% yield (see Supporting Information).

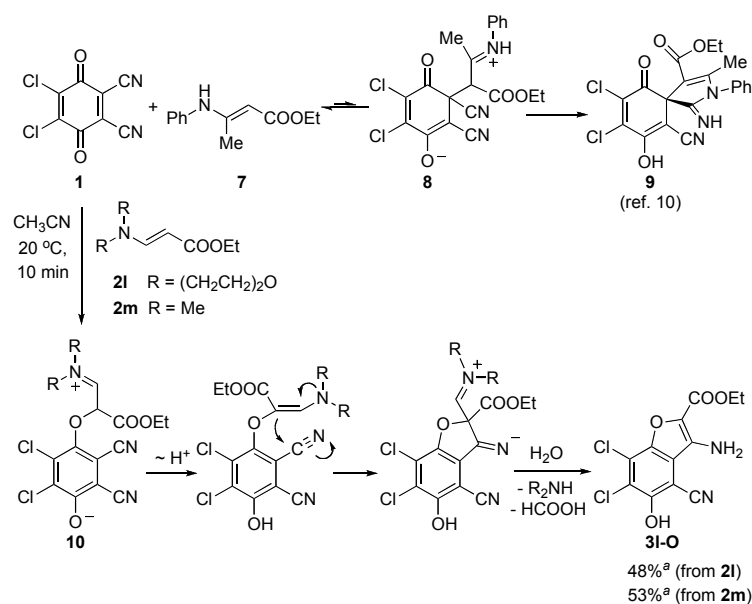
**Scheme 7.** Reaction of DDQ with **2k**



Previous investigations have shown that DDQ reacts with the secondary enaminoester **7** to give the spirane **9** (Scheme 8), indicating that **7** attacks at C-2 of DDQ.<sup>10</sup> In this work, we observed the exclusive formation of **3l-O** from **1** and the tertiary enaminoesters **2l** or **2m** after aqueous workup, which can be explained through O-attack and formation of **10** as illustrated in Scheme 8. Proton migration, cyclization, hydrolysis, and decarbonylation eventually yield benzofuran **3l-O** as the final product. Possibly, **2l** and **2m** initially also attack **1** at carbon, to give a zwitterion analogous to **8**, which cannot cyclize to a spirane because of the absence of an NH proton. Therefore, it may revert to reactants and subsequently react via O-attack to give **3l-O** as the final product.

**Scheme 8.** Reactions of DDQ with Enamino Esters

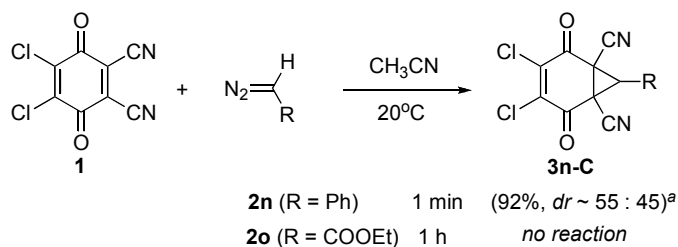




<sup>a</sup> Yield isolated after crystallization from AcOH/CH<sub>3</sub>CN

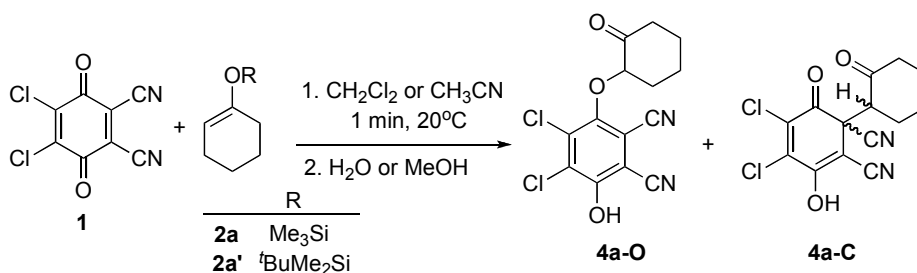
While the reaction of phenyldiazomethane with DDQ gave 92% of the bicyclic diketone **3n-C** (diastereomer ratio: ca. 55/45), no reaction between ethyl diazoacetate and DDQ was observed at room temperature within one hour (Scheme 9).

**Scheme 9.** Reactions of DDQ with Diazoalkanes



<sup>a</sup> Yield and  $dr$  (<sup>1</sup>H NMR) correspond to the crude product; only the major isomer was isolated and characterized.

**Scheme 10.** Solvent Effect on the Reaction of DDQ with **2a** and **2a'**

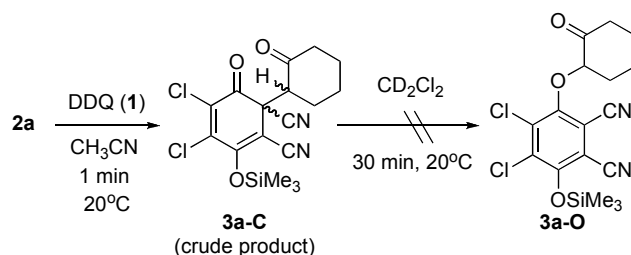


entry	nucleophile	solvent	[ <b>2a</b> or <b>2a'</b> ] <sup>a</sup> / mol L <sup>-1</sup>	relative yield <sup>b</sup> /%	
				<b>4a-O</b>	<b>4a-C</b>
1	<b>2a</b>	CH <sub>2</sub> Cl <sub>2</sub>	0.1	40	60 (58:42)
2		CH <sub>2</sub> Cl <sub>2</sub>	0.02	92	8 (50:50)
3		CH <sub>2</sub> Cl <sub>2</sub> (1% MeOH)	0.02	39	61 (74:26)
4		CH <sub>2</sub> Cl <sub>2</sub> (4% MeOH)	0.02	22	78 (41:59)
5		CH <sub>2</sub> Cl <sub>2</sub> (10% MeOH)	0.02	14	86 (36:64)
6		CH <sub>2</sub> Cl <sub>2</sub> (20% MeOH)	0.02	9	91 (29:71)
7		CH <sub>3</sub> CN	0.02	7	93 (25:75)
8		CH <sub>3</sub> CN	0.1	7	93 (25:75)
9		CH <sub>3</sub> CN (1% MeOH)	0.1	7	93 (25:75)
10		CH <sub>3</sub> CN (10% MeOH)	0.1	6	94 (22:78)
11	<b>2a'</b>	CH <sub>2</sub> Cl <sub>2</sub>	0.02	>95	<4
12		CH <sub>3</sub> CN	0.02	30	70 (50:50)
13		CH <sub>3</sub> CN	0.1	33	67 (51:49)
14		CH <sub>3</sub> CN (1% MeOH)	0.1	25	75 (51:49)
15		CH <sub>3</sub> CN (5% MeOH)	0.1	11	89 (45:55)
16		CH <sub>3</sub> CN (10% MeOH)	0.1	7	93 (41:59)
17		CH <sub>3</sub> CN (20% MeOH)	0.1	7	93 (34:66)

<sup>a</sup> In all cases, 10 equiv of **2a** or **2a'** were used [**2a** or **2a'**]/[**1**] = 10. <sup>b</sup> Quantitative product formation, ratios of diastereoisomers were determined by <sup>1</sup>H NMR of the crude product mixture and are given in parentheses (see Supporting Information for details).

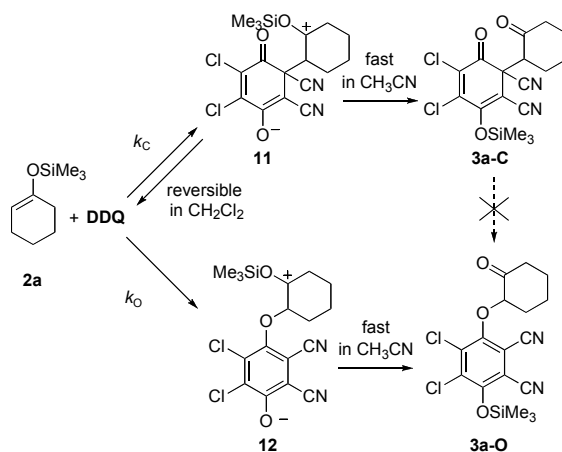
**Solvent Effect.** Scheme 10 shows that the **4a-O**/**4a-C** ratio generated by the reaction of DDQ with **2a** depends strongly on the concentration of the reactants and on the solvent. According to entries 1 and 2, the **4a-O**/**4a-C** ratio increases from 40/60 to 92/8 when reducing the concentration of **2a** from 0.1 to 0.02 mol L<sup>-1</sup> in CH<sub>2</sub>Cl<sub>2</sub>. In the dilute solution (0.02 mol L<sup>-1</sup>), the **4a-O**/**4a-C** ratio decreases dramatically from 92/8 to 7/93 when the solvent is changed from CH<sub>2</sub>Cl<sub>2</sub> to CH<sub>2</sub>Cl<sub>2</sub>/MeOH, and CH<sub>3</sub>CN (entries 2–7, Scheme 10). In acetonitrile solution, the product ratio is neither affected by the concentration of **2a** nor by the presence of methanol (entries 7–10, Scheme 10). As **3a-C** does not rearrange into the thermodynamically more stable isomer **3a-O** when dissolved in CD<sub>2</sub>Cl<sub>2</sub> (Scheme 11), we can rule out isomerization at the product stage.

**Scheme 11.** Examination of Product Stability of **3a-C** in CD<sub>2</sub>Cl<sub>2</sub>

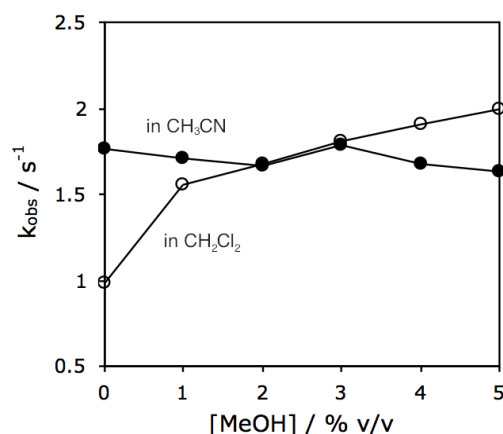


When the *tert*-butyldimethylsilyl substituted enol ether **2a'** was used, more product of O-attack was observed than in the corresponding reactions with the trimethylsilyl substituted compound **2a** in both  $\text{CH}_2\text{Cl}_2$  and  $\text{CH}_3\text{CN}$  (entries 2/11 and 7/12, Scheme 10). In the reactions of DDQ with **2a'**, the **4a-O**/**4a-C** ratio decreases when methanol is added to acetonitrile and reaches a constant value of 7/93 for >10% of MeOH (entries 13–17, Scheme 10).

**Scheme 12.** Possible Mechanism of the Reaction of DDQ with **2a**



A rationalization for these observations is given in Scheme 12. Attack of **2a** at a carbon of DDQ to give **11** is faster than O-attack to give **12**. As silyl shifts to convert **11** into **3a-C** and **12** into **3a-O** cannot occur intramolecularly, silyl-carriers are needed. Such a carrier may be the solvent when the reaction is carried out in acetonitrile solution ( $\rightarrow$  N-trimethylsilyl-nitrilium ions). As the product ratio  $[\text{4a-O}]/[\text{4a-C}]$  obtained from **2a** is not affected by addition of the stronger nucleophile methanol in acetonitrile, we conclude that **11** and **12** are formed irreversibly in acetonitrile solution due to the fast subsequent silyl shift, and that the product ratio  $[\text{4a-O}]/[\text{4a-C}] = 7/93$  corresponds to  $k_O/k_C$ . The independence of the observed rate constants  $k_{\text{obs}}$  (for measurements see below) of methanol additives (Figure 4) and  $\text{NBu}_4\text{OTf}$  additives (Table S2, S14, see Supporting Information) are in line with this interpretation.



**Figure 4.** Effect of methanol on the rate of the reaction of DDQ ( $5.0 \times 10^{-3} \text{ mol L}^{-1}$ ) with **2a** ( $5.0 \times 10^{-2} \text{ mol L}^{-1}$ ) in  $\text{CH}_2\text{Cl}_2$  and in  $\text{CH}_3\text{CN}$  (monitoring the CT complex at 570 nm).

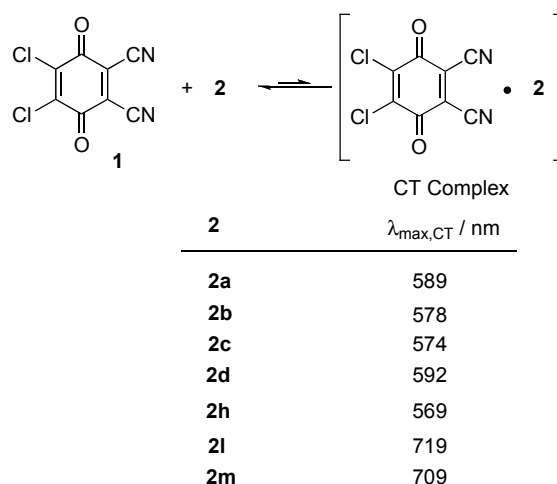
Because of its lower nucleophilicity, dichloromethane cannot act as a silyl-carrier, and the conversions **11**  $\rightarrow$  **3a-C** and **12**  $\rightarrow$  **3a-O** can only occur in the presence of other nucleophiles, e.g., methanol, or when bimolecular reactions of two molecules of **11** or **12** lead to the formation of **3a-C** and **3a-O**. In the absence of methanol or in highly dilute solutions in dichloromethane, silyl-transfers will be slow, and the formation of **11** that is thermodynamically less stable than **12** will be reversible. As a consequence, in highly dilute dichloromethane solutions (where also the concentrations of **11** and **12** will be small), the ratio  $[\mathbf{3a-O}]/[\mathbf{3a-C}]$  will be large because of the reversible formation of **11**. Already small amounts of methanol are sufficient to accelerate the silyl transfer, which results in an increase of the observed rate constant (factor of 2 in a  $0.05 \text{ mol L}^{-1}$  solution, Figure 4) as well as the yield of **3a-C**.

The observations with the *t*BuMe<sub>2</sub>Si substituted enol ether **2a'** are in line with these interpretations. As the transfer of the sterically more shielded *t*BuMe<sub>2</sub>Si group is slower than that of the Me<sub>3</sub>Si group, in dilute dichloromethane solution, C-attack at DDQ becomes completely reversible, and **4a-O** is the only product (entry 11, Scheme 10). In pure acetonitrile, C-attack (which is irreversible with **2a**, see above) becomes partially reversible in the reaction with **2a'**, and addition of the more nucleophilic methanol now leads to a decrease of the ratio  $[\mathbf{4a-O}]/[\mathbf{4a-C}]$  (entries 13–17, Scheme 10).

**Charge Transfer (CT) Complexes.** The formation of CT complexes between electron-deficient and electron-rich  $\pi$ -systems is well known.<sup>11</sup> As the association constants between the nucleophiles **2** and DDQ (**1**) are small, at room temperature the corresponding CT complexes could only be observed in few cases as short-lived intermediates when high

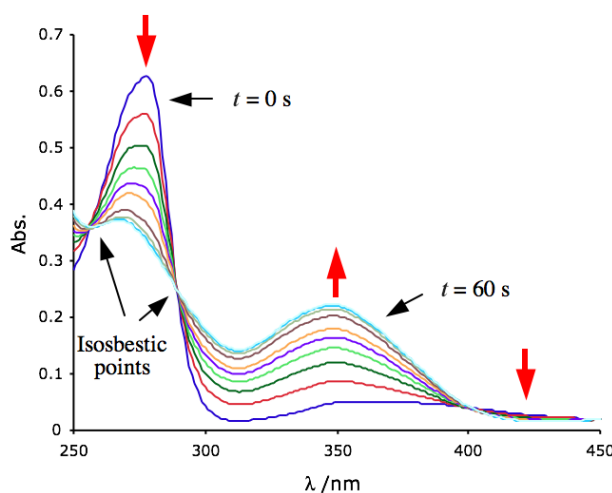
concentrations of the reactants were employed. Since lowering of the temperature increases the association constants and retards the reactions of **1** with **2**, we have been able to observe several CT complexes, however, when mixing the nucleophiles **2** with DDQ in CH<sub>2</sub>Cl<sub>2</sub> at –80 °C (Scheme 13). The new absorption bands observed under these conditions can be assigned to charge transfer complexes, because neither DDQ nor the nucleophiles **2** examined absorb beyond 450 nm.

**Scheme 13.** Characteristic Absorption Bands of the CT Complexes of Nucleophiles **2** with DDQ in CH<sub>2</sub>Cl<sub>2</sub> at –80 °C

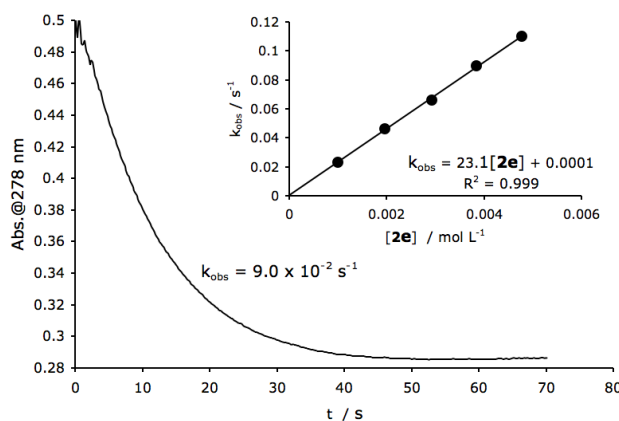


Though the CT complexes are likely to correspond to the encounter complexes preceding the formation of the reaction products from **1** and **2**, the kinetic data do not allow us to differentiate whether the CT complexes are intermediates on the way to the products or correspond to dead ends of a non-productive side channel (Curtin-Hammett principle<sup>12</sup>).

**Kinetic Studies.** All kinetic investigations of the reactions of DDQ with the nucleophiles **2** were performed in acetonitrile or dichloromethane solution at 20 °C. The reactions were monitored by UV-Vis spectroscopy at or close to the absorption maxima of DDQ (278 nm, Figure 5). For some nucleophiles (**2d**, **2l**, **2m**), the formation of the products (at 350 nm) was monitored because of the intensive absorbance of nucleophiles at lower wavelength (< 300 nm). Pseudo first-order rate constants  $k_{\text{obs}}$  were obtained by least-squares fitting of the absorbances to the monoexponential function  $A_t = A_0 e^{-k_{\text{obs}}t} + C$  or  $A_t = A_0 (1 - e^{-k_{\text{obs}}t}) + C$ . Second-order rate constants  $k_2$  were derived from the linear correlation of  $k_{\text{obs}}$  (s<sup>-1</sup>) against the concentrations of the nucleophiles (Figure 6).

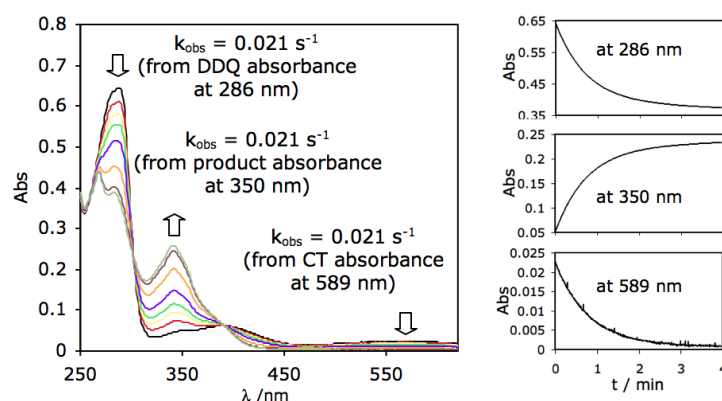


**Figure 5.** Time-dependent UV-Vis absorbance during the reaction of DDQ ( $1.0 \times 10^{-4} \text{ mol L}^{-1}$ ) with **2e** ( $3.9 \times 10^{-3} \text{ mol L}^{-1}$ ) in  $\text{CH}_3\text{CN}$  at  $20^\circ\text{C}$ .



**Figure 6.** UV-Vis spectroscopic monitoring of the reaction of DDQ ( $1.0 \times 10^{-4} \text{ mol L}^{-1}$ ) with **2e** ( $3.9 \times 10^{-3} \text{ mol L}^{-1}$ ) at 278 nm in  $\text{CH}_3\text{CN}$  at  $20^\circ\text{C}$ . Insert: Determination of the second-order rate constant  $k_2 = 23 \text{ L mol}^{-1} \text{ s}^{-1}$  from the dependence of the first-order rate constant  $k_{\text{obs}}$  on the concentration of **2e**.

In line with the fast reversible formation of the CT complexes, identical rate constants for the reaction of DDQ with **2a** were derived by following the decay of the absorption band of the CT complex (589 nm) and the absorption band of DDQ (286 nm) as well as the increase of the absorption of the product (350 nm) in  $\text{CH}_2\text{Cl}_2$  at  $-60^\circ\text{C}$  (Figure 7).



**Figure 7.** UV-Vis spectrum of a mixture of DDQ ( $1.0 \times 10^{-4} \text{ mol L}^{-1}$ ) and **2a** ( $4.0 \times 10^{-3} \text{ mol L}^{-1}$ ) in  $\text{CH}_2\text{Cl}_2$  at  $-60^\circ\text{C}$  and the time dependent UV-Vis absorbance.

The observation of second-order kinetics for the reactions of DDQ with nucleophiles **2** in  $\text{CH}_2\text{Cl}_2$  is surprising in view of the discussion of Schemes 10 and 12. Possibly, the perfect linearity of the  $k_{\text{obs}}$  vs  $[\mathbf{2}]$  correlations (Tables S18–S24) indicates that also **2a–f, k** may also act as silyl carriers under the conditions of the kinetic experiments.

Table 2 shows that the ratios of the second-order rate constants for the reactions of DDQ with nucleophiles **2** in  $\text{CH}_2\text{Cl}_2$  and  $\text{CH}_3\text{CN}$  solutions,  $k_2^{\text{CH}_2\text{Cl}_2}/k_2^{\text{MeCN}}$ , vary from 0.44 to 3.1 indicating that the kinetics are only slightly affected by solvent polarity.

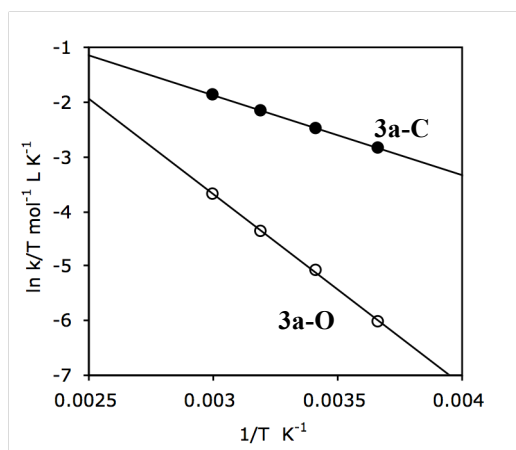
**Table 2.** Second-Order Rate Constants  $k$  for the Reaction of DDQ with Nucleophiles (**2a–n**) at  $20^\circ\text{C}$

Nucleophile	$k_2^{\text{CH}_2\text{Cl}_2} / \text{L mol}^{-1} \text{s}^{-1}$	$k_2^{\text{MeCN}} / \text{L mol}^{-1} \text{s}^{-1}$	$k_2^{\text{CH}_2\text{Cl}_2}/k_2^{\text{MeCN}}$	$k_{\text{O}} / \text{L mol}^{-1} \text{s}^{-1}$ (in $\text{CH}_3\text{CN}$ )	$k_{\text{C}} / \text{L mol}^{-1} \text{s}^{-1}$ (in $\text{CH}_3\text{CN}$ )
<b>2a</b>	$1.9 \times 10^1$	$2.5 \times 10^1$	0.76	1.9	$2.3 \times 10^1$
<b>2b</b>	$3.4 \times 10^2$	$5.5 \times 10^2$	0.62	-	$5.5 \times 10^2$
<b>2c</b>	$9.6 \times 10^2$	$7.1 \times 10^2$	1.4	-	$7.1 \times 10^2$
<b>2d</b>	$2.0 \times 10^2$	$4.5 \times 10^2$	0.44	-	$4.5 \times 10^2$
<b>2e</b>	$4.5 \times 10^1$	$2.3 \times 10^1$	2.0	-	$2.3 \times 10^1$
<b>2f</b>	$1.1 \times 10^4$	$3.5 \times 10^3$	3.1	-	$3.5 \times 10^3$
<b>2g</b>		$8.5 \times 10^5$	-	-	$8.5 \times 10^5$
<b>2h</b>		$1.8 \times 10^{-1}$	-	$1.8 \times 10^{-1}$	-
<b>2i</b>		$1.1 \times 10^7$	-	$6.6 \times 10^5$	$1.0 \times 10^7$
<b>2j</b>		$7.0 \times 10^4$	-	$7.0 \times 10^4$	-
<b>2k</b>	$3.9 \times 10^{-1}$	$3.9 \times 10^{-1}$	1.0	-	$3.9 \times 10^{-1}$
<b>2l</b>		6.8	-	6.8	-
<b>2m</b>		$2.3 \times 10^1$	-	$2.3 \times 10^1$	-
<b>2n</b>		$8.6 \times 10^3$	-	-	$8.6 \times 10^3$

**Temperature effect.** For the reaction of DDQ with **2a**, Table 3 shows how temperature affects the kinetics and the product selectivity. As temperature increasing, the rate constants slowly increase as well as the ratio of *O*-attack/*C*-attack.

**Table 3.** Temperature effect on the reaction of DDQ with **2a** in CH<sub>3</sub>CN

Entry	T / °C	$k_2 / \text{mol}^{-1} \text{L}^{-1} \text{s}^{-1}$	Relative yield / %		Activation energy	
			<b>3a-O</b>	<b>3a-C</b>	<b>3a-O</b>	<b>3a-C</b>
1	0	16.6	4	96 (1:4)	$\Delta H^\ddagger / \text{kJ mol}^{-1}$	
2	20	25.9	7	93 (1:3)	29.2	12.2
3	40	40.0	10	90 (1:2)	$\Delta S^\ddagger / \text{e.u.}$	
4	60	59.0	14	86 (1:1.5)	-140.5	-176.7



**Figure 8.** Eyring plot for the temperature-dependent rates of *C*-attack and *O*-attack in the reaction of DDQ with **2a**.

Figure 8 shows an Eyring plot of the kinetic data in the Table 3. The rate constant of each product was derived from the overall rate constant and the yield of corresponding product. The activation parameters  $\Delta H^\ddagger$  and  $\Delta S^\ddagger$  can be calculated from the slope and the intercept, respectively, according to Eyring equation (Eq. 2).

$$\ln \frac{k}{T} = -\frac{\Delta H^\ddagger}{R} \cdot \frac{1}{T} + \ln \frac{k_B}{h} + \frac{\Delta S^\ddagger}{R} \quad (2)$$

***Ab initio* Calculation of Adiabatic Ionization Potentials.** In order to elucidate the feasibility of single electron transfer (SET) processes, we have determined the ionization potentials of the  $\pi$ -nucleophiles **2(a-q)** by quantum chemical calculations using the Gaussian 09 program package.<sup>13</sup> Adiabatic ionization potentials were calculated at the G3(MP2) level of theory, which is a high-level composite *ab initio* molecular orbital theory method as the sum of the



QCISD(T) calculations with a double zeta basis set, and basis set corrections carried out at the MP2 level of theory to approximate QCISD(T) calculations with a large triple zeta basis. G3(MP2) has been shown to reproduce a large test set of gas-phase experimental data within chemical accuracy.<sup>14</sup> The adiabatic ionization potentials listed in Table 4 have been calculated as the difference of the enthalpies of the radical cations and those of the neutral molecules in the gas phase.

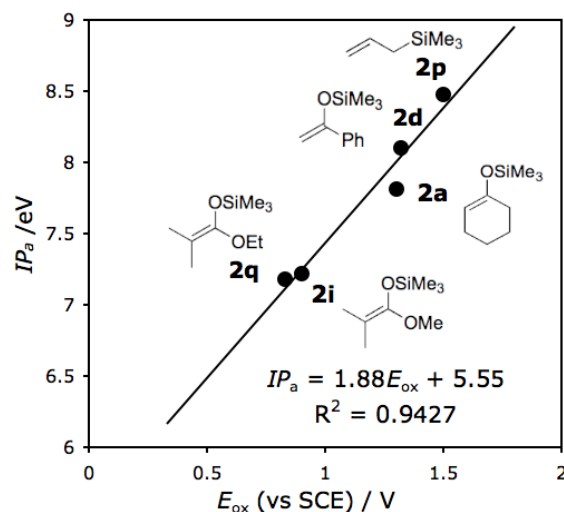
**Table 4.** Calculated Adiabatic Ionization Potentials [G3(MP2)] of Nucleophiles **2** and the Corresponding Electrochemical Oxidation Potentials.

Nucleophile	$IP_a$ / eV	$E_{ox}$ (vs. SCE) / V
<b>2a</b>	7.77	1.30 <sup>a</sup>
<b>2b</b>	7.83	1.21 <sup>b</sup>
<b>2c</b>	7.71	1.15 <sup>b</sup>
<b>2d</b>	8.10	1.32 <sup>a</sup>
<b>2e</b>	8.24	1.43 <sup>b</sup>
<b>2f</b>	7.89	1.24 <sup>b</sup>
<b>2g</b>	7.65	1.12 <sup>b</sup>
<b>2h</b>	7.77	1.18 <sup>b</sup>
<b>2i</b>	7.22	0.90 <sup>a</sup>
<b>2j</b>	7.05	0.80 <sup>b</sup>
<b>2k</b>	8.26	1.44 <sup>b</sup>
<b>2l</b>	7.71	1.15 <sup>b</sup>
<b>2m</b>	7.70	1.14 <sup>b</sup>
<b>2n</b>	7.87	1.23 <sup>b</sup>
<b>2p<sup>c</sup></b>	8.48	1.50 <sup>a</sup>
<b>2q<sup>c</sup></b>	7.18	0.83 <sup>a</sup>

<sup>a</sup> In CH<sub>3</sub>CN from ref. 15. <sup>b</sup> Calculated by substitution of calculated ionization potentials into equation (3). <sup>c</sup> See Figure 8 for the structures of these compounds.

Figure 9 shows that the calculated ionization potentials correlate with the experimental oxidation potentials<sup>15</sup> of **2a**, **2d**, **2i**, **2p** and **2q** as expressed by equation (3), which is similar to the correlation previously reported for aromatic compounds ( $IP_a = 1.5E_{ox} + 5.8$ ).<sup>16</sup> Using correlation (3) we have calculated experimentally not available oxidation potentials from their adiabatic ionization potentials (Table 4).

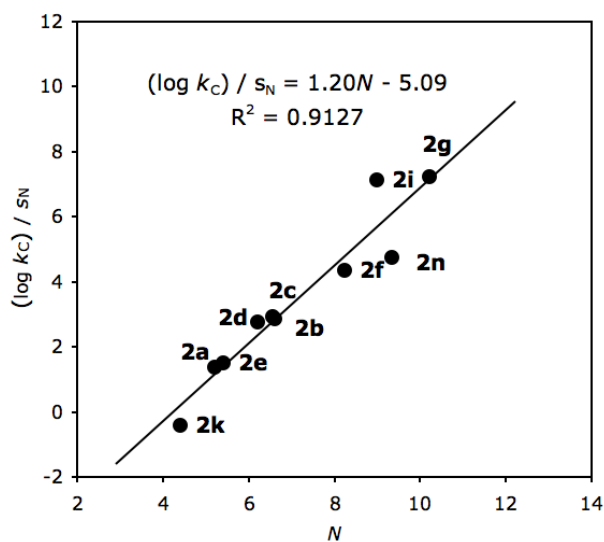
$$IP_a = 1.88E_{ox} + 5.55 \quad (3)$$



**Figure 9.** Correlation between calculated adiabatic ionization potentials and experimental oxidation potentials (vs. SCE in  $\text{CH}_3\text{CN}$ ).

## 2.3 Discussion

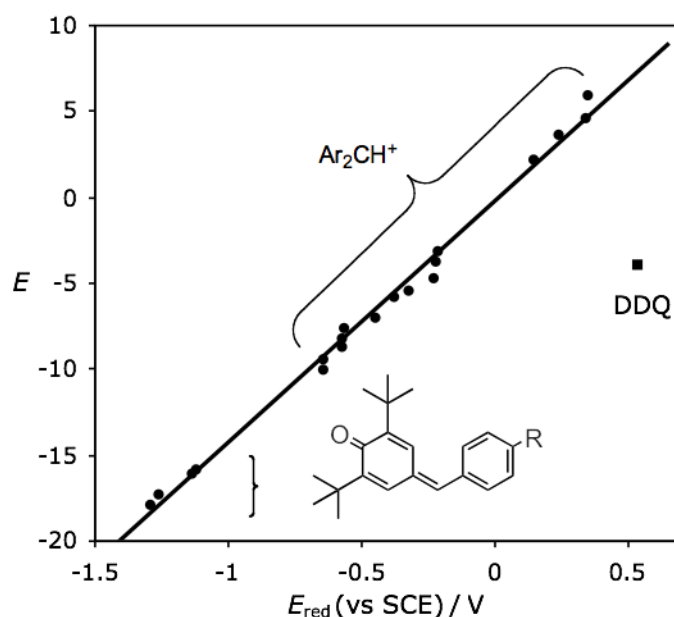
**Correlation Analysis.** In order to examine the validity of equation (1) for the reactions of DDQ (C-attack) with  $\pi$ -nucleophiles, a plot of  $(\log k_c)/s_N$  against the nucleophilicity parameters  $N$  of nucleophiles is presented in Figure 10. A fair linear correlation ( $R^2 = 0.91$ ) was obtained.



**Figure 10.** Plot of  $(\log k_c)/s_N$  vs  $N$  for the reactions of DDQ (C-attack) with  $\pi$ -nucleophiles in  $\text{CH}_3\text{CN}$  at 20 °C

According to equation (1), the electrophilicity parameter of DDQ (reactivity at C-2) was determined as  $E = -3.66$  by least-squares minimization of  $\Delta^2 = \sum (\log k_C - s_N(N + E))^2$  using the second-order rate constants  $k_C$  given in Table 2 and the  $N$  and  $s_N$  parameters of the nucleophiles **2a-n** from Table 1.

In previous work we have shown that the electrophilicity parameters of benzhydrylium ions and structurally related quinone methides correlate linearly with their reduction potentials (Figure 11).<sup>17</sup> When the data for DDQ are added to this correlation, one can see that DDQ reacts much more slowly with  $\pi$ -nucleophiles than expected from its reduction potential. The position of DDQ in Figure 11 implies that the transition states of the reactions of DDQ with  $\pi$ -CC-systems profit much less from the formation of the new CC-bond (product stabilizing factor) than the corresponding reactions of benzhydrylium ions and quinone methides. Yu and coworkers have demonstrated recently that a relationship between electrophilicities  $E$  and LUMO energies holds only within species that share similar substitution patterns.<sup>18</sup> Thus, arylidene Meldrum's acids and arylidene Barbituric acids were found to be 5 orders of magnitude more electrophilic than quinone methides of comparable LUMO energies, indicating that the product stabilizing factor must be more important in the transition states of the former species. The conclusion drawn from Figure 11 that product stabilizing factors are less important in the reactions of DDQ with  $\pi$ -nucleophiles implies that SET processes can be expected to be more likely in reactions of DDQ with nucleophiles than in the corresponding reactions of benzhydrylium ions having similar electrophilicity  $E$ .



**Figure 11.** Correlation between the electrophilicity parameters  $E$  and the reduction potentials  $E_{\text{red}}$  of reference electrophiles<sup>17</sup> and DDQ.

The kinetics of one-electron oxidations of silylated enol ethers and ketene acetals as well as of allylsilanes with one electron oxidants have previously been studied by Fukuzumi and coworkers.<sup>15</sup> The oxidation potentials of these  $\pi$ -systems as well as the intrinsic barriers for the electron transfer oxidation of these compounds by one-electron oxidants were derived from experimental rate constants using the Rehm-Weller Gibbs relationship (5), which derives the Gibbs energy of activation for the electron transfer ( $\Delta G_{\text{et}}^\ddagger$ ) from the Gibbs energy of electron transfer ( $\Delta G_{\text{et}}^0$  given by eq. (6)) and the intrinsic barrier ( $\Delta G_{0,\text{et}}^\ddagger$ ). The latter quantity represents the Gibbs activation free energy for a process where the driving force of electron transfer is zero, i.e.  $\Delta G_{\text{et}}^\ddagger = \Delta G_{0,\text{et}}^\ddagger$  for  $\Delta G_{\text{et}}^0 = 0$ . Due to the significant rearrangements of structure accompanying electron transfer, large intrinsic barriers  $\Delta G_{0,\text{et}}^\ddagger$  (15–20 kJ mol<sup>-1</sup>) were observed for the one-electron oxidation of a large variety of silylated  $\pi$ -nucleophiles, including several compounds shown in Figure 9.

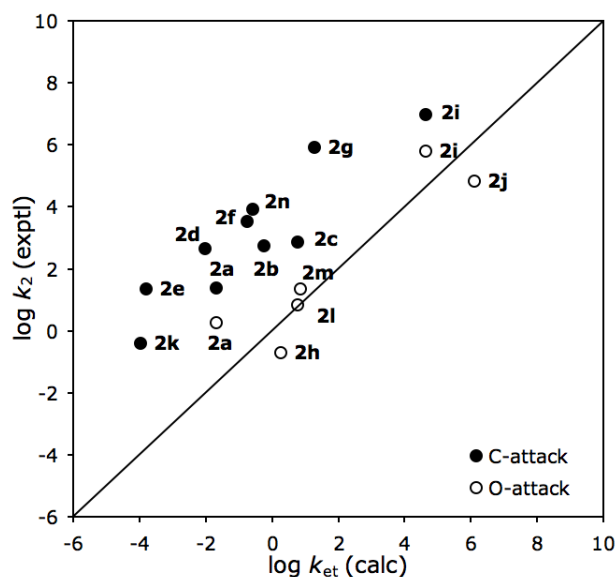
By applying the same methodology, we have now used the oxidation potentials in Table 4 to calculate the rate constants for the outer-sphere electron transfer of the reactions of DDQ with the  $\pi$ -nucleophiles **2a-n** according to equations (4)–(6), assuming an intrinsic barrier of  $\Delta G_{0,\text{et}}^\ddagger = 18 \text{ kJ mol}^{-1}$ , a typical value for such systems according to ref 15.

$$k_{\text{et}} = (k_{\text{b}}T/h) \exp(-\Delta G_{\text{et}}^\ddagger/RT) \quad (4)$$

$$\Delta G_{\text{et}}^\ddagger = \Delta G_{\text{et}}^0/2 + [(\Delta G_{\text{et}}^0/2)^2 + (\Delta G_{0,\text{et}}^\ddagger)^2]^{1/2} \quad (5)$$

$$\Delta G_{\text{et}}^0 = F(E_{\text{ox}} - E_{\text{red}}) \quad (6)$$

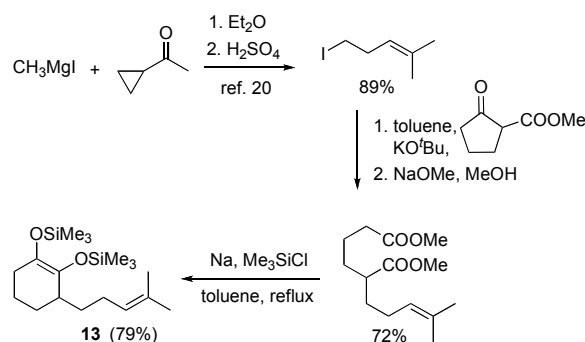
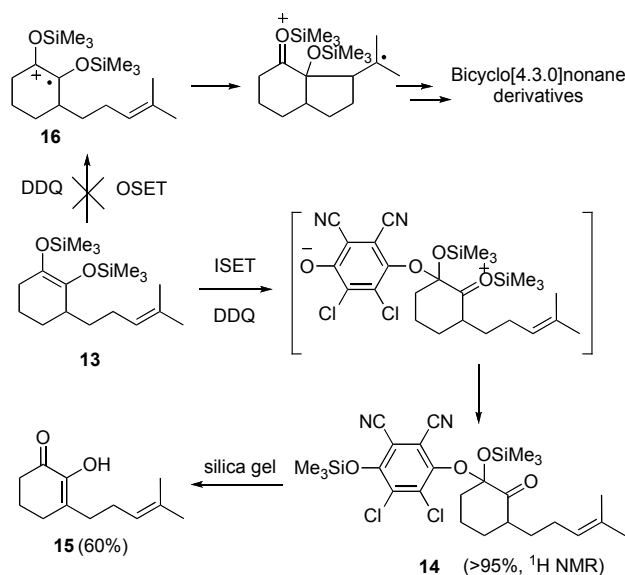
A plot of experimental rate constants  $\log k_{\text{C}}$  (●) and  $\log k_{\text{O}}$  (○) for the reactions of DDQ with various  $\pi$ -nucleophiles versus the calculated rates for SET ( $\log k_{\text{et}}$ , from eqs 4-6) is presented in Figure 12. The open circles for systems which react via O-attack are close to the diagonal, indicating that these reactions proceed with rates as expected for SET processes, while C-attack at DDQ (filled circles) is 2 to 5 orders of magnitude faster than calculated for SET processes. We, therefore, conclude that C-attack at DDQ usually occurs by a polar mechanism, which may be reversible if there is no fast subsequent reaction.



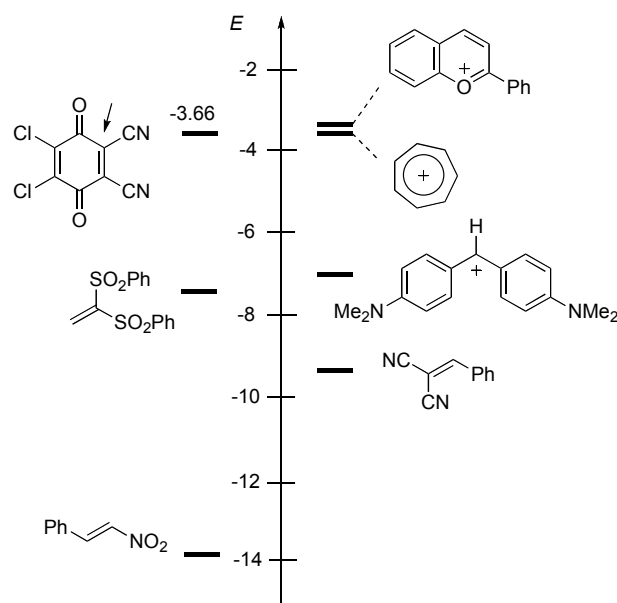
**Figure 12.** Correlation of experimental rate constants ( $\log k_2$ , in  $\text{CH}_3\text{CN}$ ) with calculated rate constants for SET ( $\log k_{\text{et}}$ ).

It should be noted that all experimental rate constants for the reactions of benzhydrylium ions with  $\pi$ -nucleophiles have been reported to be at least 8 orders of magnitude larger than the calculated rate constants for one-electron transfer processes.<sup>17</sup> Therefore, the reactions of DDQ with  $\pi$ -nucleophiles are generally closer to the borderline between polar reactions and electron transfer than the corresponding reactions with benzhydrylium ions.

**Outer Sphere Electron Transfer (OSET) vs. Inner Sphere Electron Transfer (ISET): Radical Clock Experiments.** According to Figure 12, the observed rate constant for the reaction of **2j** with DDQ corresponds to that expected for a SET process. In order to examine the occurrence of an OSET mechanism, a radical clock<sup>19</sup> substrate **13** was designed based on the structure of **2j** (Scheme 14). When **13** was combined with DDQ, only **14**, the product of O-attack, was observed in the  $^1\text{H}$  NMR spectrum of the crude material (>95%), and **15** was isolated in 60% yield after column chromatography, while no cyclization product was observed (Scheme 15). Though cyclization of the radical cation **16** may be slower than analogous cyclizations of radicals, the quantitative formation of **14** allows us to exclude the operation of a OSET mechanism because Mattay's report on the formation of carbocycles via photoinduced electron transfer oxidative cyclization of silyl enol ethers carrying side chains with olefinic double bonds indicates cyclizations of the intermediate radical cations to be faster than competing intermolecular processes.<sup>21</sup> Therefore, O-attack is suggested to proceed via an ISET mechanism.

**Scheme 14.** Synthesis of the Radical Clock Substrate **13****Scheme 15.** Exclusion of OSET by a Radical Clock Experiment ( $\text{CH}_3\text{CN}$ ,  $20^\circ\text{C}$ )**2.4 Conclusion**

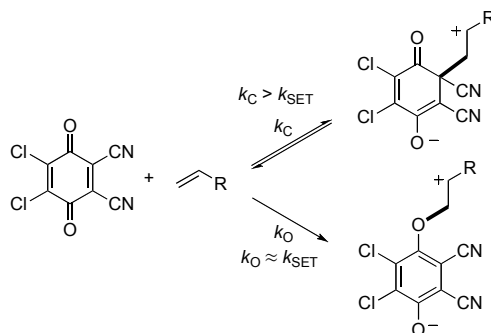
$\pi$ -Nucleophiles attack DDQ either at C-2 to give 4-hydroxycyclohexadienones or at oxygen to give O-substituted hydroquinones. In several cases initial C-attack and subsequent rearrangement to the thermodynamically more stable products of O-attack has been observed. Kinetics for the reactions of  $\pi$ -systems with DDQ have been determined photometrically, and it was found that the rate constants  $k_C$  for the attack of the  $\pi$ -nucleophiles **2** at C-2 of DDQ can be described by the linear free energy relationship (1), which allowed us to derive the electrophilicity parameter  $E = -3.66$  for the C-2 position of DDQ. It thus possesses an electrophilic reactivity comparable to the flavylum and tropylium ion, considerably more reactive than the bis(dimethylamino)-substituted benzhydrylium ion or other highly reactive Michael acceptors (Figure 13).<sup>8, 9a</sup>



**Figure 13.** Comparison of the electrophilic reactivity of DDQ with that of other electrophiles.<sup>8</sup>

The experimental rate constants for the attack of  $\pi$ -systems at C-2 of DDQ are larger than those calculated for SET processes from the electrochemical oxidation potentials of the  $\pi$ -systems and the reduction potential of DDQ, indicating that C-attack at DDQ usually occurs via polar processes. However, DDQ reacts about 12 orders of magnitude more slowly than benzhydrylium ions of comparable reduction potential showing that the transition states of the reactions of DDQ with  $\pi_{CC}$ -systems profit much less from the formation of the new CC-bond (product stabilizing factor) than the corresponding reactions of benzhydrylium ions, which can be explained by the high stabilization of the DDQ radical anion. O-Attack is probably restricted to reactions with sterically shielded nucleophiles or to cases, where the faster C-attack is highly reversible because the resulting intermediate cannot undergo fast subsequent reactions. The observed rate constants for O-attack are smaller than calculated by eq. 1 and thus are similar to those for SET processes (Scheme 16).

**Scheme 16.** C- versus O-Attack in Reactions of DDQ with  $\pi$ -Nucleophiles



Since radical-clock experiment did not provide evidence for the intermediacy of radical cations of the silylated enol ethers, these reactions are interpreted as inner sphere electron transfer processes.

## 2.5 Experimental Section

**Materials.** DDQ was purchased from ABCR and recrystallized from chloroform or dichloromethane before use. Silyl enol ethers **2(a-e, a', h)** were prepared as reported in literature.<sup>22</sup> Silyl ketene acetals **2(f, g, i)** were prepared according to ref. 23. The synthesis of disiloxy hexane **2j** was achieved by Rühlmann-type acyloin condensation.<sup>24</sup> Enamino esters **2l** and **2m** were prepared from amines and methyl propiolate. Diazomethanes **2n** and **2o** were prepared according to ref. 25 and ref. 26, respectively.

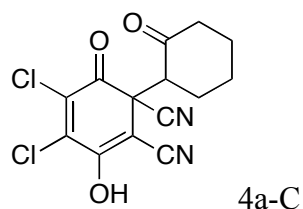
**Kinetics.** All the rates of reactions were determined photometrically in dry acetonitrile or in freshly distilled dry CH<sub>2</sub>Cl<sub>2</sub>. Fast reactions were determined by using the stopped-flow technique. Slow reactions were measured by conventional photodiode array UV-Vis spectrometers. The temperature was kept constant at  $20 \pm 0.1$  °C by using a circulating bath thermostat. In all runs, excess of nucleophiles (at least 8-fold) over DDQ was used to achieve pseudo first-order kinetics.

### 1) Experimental details and characterization data for products

**General information:** <sup>1</sup>H NMR and <sup>13</sup>C NMR spectra were recorded on Bruker 400 MHz (101 MHz), 300 MHz (75.5 MHz) or Varian 200 MHz spectrometers. The chemical shifts are reported in parts per million ( $\delta$ ) relative to internal TMS signal (0.00 ppm) or the internal solvent signals of CDCl<sub>3</sub> ( $\delta_H = 7.26$ ,  $\delta_C = 77.0$ ), d<sub>6</sub>-DMSO ( $\delta_H = 2.50$ ,  $\delta_C = 39.5$ ), CD<sub>3</sub>CN ( $\delta_H = 1.94$ ,  $\delta_C = 118.3$ , 1.3), d<sub>6</sub>-acetone ( $\delta_H = 2.05$ ,  $\delta_C = 206.3$ , 29.8). The peak patterns are indicated as follows: br, broad signal; s, singlet; d, doublet; t, triplet; m, multiplet; q, quartet. The coupling constants, *J*, are reported in Hertz (Hz). Mass spectra were determined with

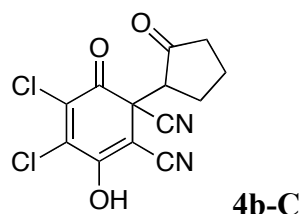


Finnigan MAT 95 for EI-MS (70 eV) and HR-MS, Thermo Finnigan LTQ FT for ESI-MS. IR spectra were recorded with a Perkin Elmer Spectrum BX infrared spectrometer from Perkin Elmer with ATR probe (diamond).



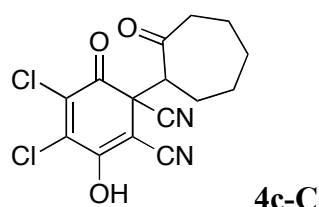
**4,5-Dichloro-3-hydroxy-6-oxo-1-(2-oxocyclohexyl)cyclohexa-2,4-diene-1,2-dicarbonitrile (4a-C, major isomer).** To a solution of DDQ (114 mg, 0.500 mmol) in CH<sub>3</sub>CN, **2a** (170 mg, 1.00 mmol) was added under nitrogen at -20 °C. After stirring for 1 min at -20 °C, the solvent was evaporated in the vacuum to afford the crude product. The residue was purified by flash column chromatography (silica gel, eluent: acetic acid/ethyl acetate/pentane = 1/10/20) to give **4a-C** (yellow solid, 135 mg, 83% yield), the major diastereoisomer was crystallized from CH<sub>2</sub>Cl<sub>2</sub>/pentane (95 mg, 0.29 mmol). M.p.: 183-185 °C (decomp., CH<sub>2</sub>Cl<sub>2</sub>). IR (neat):  $\nu_{\text{max}}$  3255, 2949, 2868, 2211, 1698, 1612, 1554, 1450, 1353, 1306, 1220, 1145, 1129, 1102, 1038, 956, 907, 837, 802, 772, 748 cm<sup>-1</sup>; <sup>1</sup>H NMR (d<sub>6</sub>-DMSO, 400 MHz)  $\delta$  13.72 (s, 1 H), 3.58 (dd,  $J$  = 13.0, 5.4 Hz, 1 H), 2.60 (td,  $J$  = 13.6, 6.3 Hz, 1 H), 2.50-2.45 (m, 1 H), 2.26-2.15 (m, 2 H), 2.08-2.00 (m, 1 H), 1.96-1.77 (m, 2 H), 1.53-1.43 (m, 1 H); <sup>13</sup>C NMR (d<sub>6</sub>-DMSO, 101 MHz)  $\delta$  207.7, 181.0, 158.1, 145.2, 135.4, 116.0, 115.2, 82.9, 62.1, 48.9, 41.2, 31.1, 27.3, 24.3; MS (EI)  $m/z$  (%): 324 (M<sup>+</sup>), 301, 299, 255, 230, 228, 202, 200, 194, 166, 110, 98, 96, 70, 68 (100), 55; HRMS (EI) calcd for C<sub>14</sub>H<sub>10</sub><sup>35</sup>Cl<sub>2</sub>N<sub>2</sub>O<sub>3</sub>: 324.0063; found: 324.0053.

The <sup>1</sup>H and <sup>13</sup>C NMR spectra agree with ref. 27.



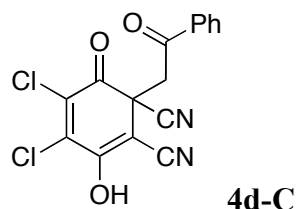
**4,5-Dichloro-3-hydroxy-6-oxo-1-(2-oxocyclopentyl)cyclohexa-2,4-diene-1,2-dicarbonitrile (4b-C).** A solution of DDQ (114 mg, 0.500 mmol) and **2b** (156 mg, 1.00 mmol) in CH<sub>3</sub>CN was stirred at -20 °C for 1 min. The solvent was removed under reduced pressure. The crude material was purified by flash column chromatography (silica gel, eluent: acetic acid/ethyl acetate/pentane = 1/10/20) to give a mixture of diastereomers of **4b-C**

(yellow solid, 136 mg, dr  $\approx$  1 : 2, 87%). IR (neat):  $\nu_{\max}$  3232, 2978, 2889, 2214, 1742, 1698, 1606, 1549, 1451, 1422, 1402, 1355, 1274, 1215, 1153, 1096, 1016, 890, 829, 767, 700, 635, 607  $\text{cm}^{-1}$ ;  $^1\text{H}$  NMR ( $d_6$ -DMSO, 400 MHz)  $\delta$  10.60 (s,  $>1$  H), 3.47 (dd,  $J = 11.4, 9.2$  Hz, 1 H), 3.14 (dd,  $J = 10.6, 8.1$  Hz, 2 H), 2.32-1.78 (m, 18 H); HRMS (EI) calcd for  $\text{C}_{13}\text{H}_9^{35}\text{Cl}_2\text{N}_2\text{O}_3[\text{M}^+ + \text{H}]$ : 310.9990; found: 310.9991.



**4,5-Dichloro-3-hydroxy-6-oxo-1-(2-oxocycloheptyl)cyclohexa-2,4-diene-1,2-**

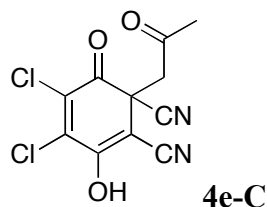
**dicarbonitrile (4c-C).** A solution of DDQ (114 mg, 0.500 mmol) and **2c** (184 mg, 1.00 mmol) in  $\text{CH}_3\text{CN}$  was stirred at  $-20$   $^\circ\text{C}$  for 1 min. The solvent was removed under reduced pressure. The crude material was purified by flash column chromatography (silica gel, eluent: acetic acid/ethyl acetate/pentane = 1/10/20) to afford **4c-C** (yellow solid, 140 mg, 83%), then crystallized from  $\text{CH}_2\text{Cl}_2$ /pentane. M.p.: 168-170  $^\circ\text{C}$  (decomp.,  $\text{CH}_2\text{Cl}_2$ /pentane). IR (neat):  $\nu_{\max}$  3234, 2937, 2210, 1698, 1611, 1554, 1454, 1354, 1217, 1131, 1008, 935, 898, 858, 808, 750, 645  $\text{cm}^{-1}$ ;  $^1\text{H}$  NMR ( $d_6$ -DMSO, 400 MHz)  $\delta$  13.91 (s, 1 H), 3.69 (dd,  $J = 10.8, 2.6$  Hz, 1 H), 2.57-2.50 (m, 1 H), 2.40-2.28 (m, 2 H), 1.95-1.76 (m, 3 H), 1.70-1.58 (m, 2 H), 1.56-1.47 (m, 1 H), 1.19-1.10 (m, 1 H);  $^{13}\text{C}$  NMR ( $d_6$ -DMSO, 101 MHz)  $\delta$  209.8, 180.4, 158.8, 145.1, 135.3, 116.3, 115.9, 81.1, 63.2, 50.2, 42.0, 28.3, 27.6, 27.5, 22.5; MS (EI)  $m/z$  (%): 338 ( $\text{M}^+$ ), 315, 313, 256, 230, 228, 202, 200, 194, 112, 84, 83, 55 (100); HRMS (EI) calcd for  $\text{C}_{15}\text{H}_{12}^{35}\text{Cl}_2\text{N}_2\text{O}_3$ : 338.0219; found: 338.0223.



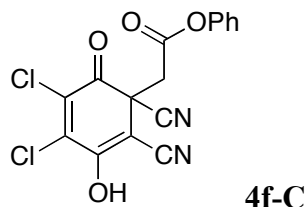
**4,5-Dichloro-3-hydroxy-6-oxo-1-(2-oxo-2-phenylethyl)cyclohexa-2,4-diene-1,2-**

**dicarbonitrile (4d-C).** A solution of DDQ (114 mg, 0.500 mmol) and **2d** (192 mg, 1.00 mmol) in  $\text{CH}_3\text{CN}$  was stirred at  $20$   $^\circ\text{C}$  for 1 min. The solvent was removed under reduced pressure. The crude material was purified by flash column chromatography (silica gel, eluent: acetic acid/ethyl acetate/pentane = 1/10/20) to afford **4d-C** (yellow solid, 168 mg, 97%). M.p.: 166-170  $^\circ\text{C}$  (decomp.,  $\text{Et}_2\text{O}$ ). IR (neat):  $\nu_{\max}$  2978, 2930, 2877, 2212, 1703, 1678, 1597, 1450,

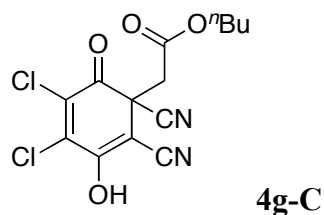
1352, 1216, 1144, 1095, 979, 901, 870, 819, 777, 760, 750, 686, 612  $\text{cm}^{-1}$ ;  $^1\text{H}$  NMR ( $\text{d}_6$ -DMSO, 400 MHz)  $\delta$  12.42 (s, 1 H), 8.04-8.02 (m, 2 H), 7.73-7.69 (m, 1 H), 7.58-7.53 (m, 2 H), 4.49-4.39 (m, 2 H);  $^{13}\text{C}$  NMR ( $\text{d}_6$ -DMSO, 101 MHz)  $\delta$  194.4, 181.0, 158.7, 147.5, 134.7, 134.6, 134.2, 129.0, 128.7, 116.0, 115.9, 81.6, 49.1, 45.2; MS (EI)  $m/z$  (%): 105 (100); HRMS (EI) calcd for  $\text{C}_{16}\text{H}_8^{35}\text{Cl}_2\text{N}_2\text{O}_3$ : 345.9906; found: 345.9907.



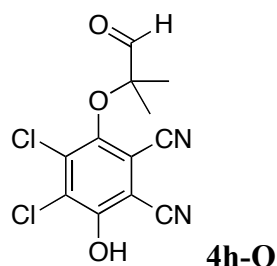
**4,5-Dichloro-3-hydroxy-6-oxo-1-(2-oxopropyl)cyclohexa-2,4-diene-1,2-dicarbonitrile (4e-C).** A solution of DDQ (114 mg, 0.500 mmol) and **2e** (130 mg, 1.00 mmol) in  $\text{CH}_3\text{CN}$  was stirred at 20  $^\circ\text{C}$  for 1 min. The solvent was removed under reduced pressure. The crude material was purified by flash column chromatography (silica gel, eluent: acetic acid/ethyl acetate/pentane = 1/10/20) to afford **4e-C** (yellow solid, 138 mg, 97%). M.p.: 172-175  $^\circ\text{C}$  (decomp.,  $\text{Et}_2\text{O}$ ). IR (neat):  $\nu_{\text{max}}$  3245, 2979, 2214, 1702, 1613, 1550, 1403, 1356, 1226, 1178, 1141, 1027, 894, 822, 786, 751, 633  $\text{cm}^{-1}$ ;  $^1\text{H}$  NMR ( $\text{d}_6$ -DMSO, 400 MHz)  $\delta$  13.85 (s, 1 H), 3.92 (d,  $J$  = 18.3 Hz, 1 H), 3.72 (d,  $J$  = 18.3 Hz, 1 H), 2.14 (s, 3 H);  $^{13}\text{C}$  NMR ( $\text{d}_6$ -DMSO, 101 MHz)  $\delta$  203.4, 180.9, 158.4, 147.0, 134.7, 115.8, 81.6, 81.5, 52.9, 45.0, 28.9; HRMS (EI) calcd for  $\text{C}_{11}\text{H}_6^{35}\text{Cl}^{37}\text{Cl}\text{N}_2\text{O}_3$ : 285.9720; found: 285.9725.



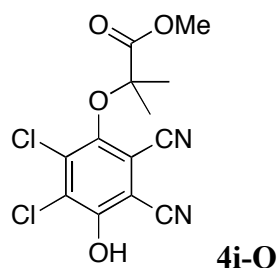
**Phenyl 2-(4,5-dichloro-1,2-dicyano-3-hydroxy-6-oxocyclohexa-2,4-dienyl)acetate (4f-C).** A solution of DDQ (114 mg, 0.500 mmol) and **2f** (208 mg, 1.00 mmol) in  $\text{CH}_3\text{CN}$  was stirred at 20  $^\circ\text{C}$  for 1 min. The solvent was removed under reduced pressure. The crude material was purified by flash column chromatography (silica gel, eluent: acetic acid/ethyl acetate/pentane = 1/10/20) to afford **4f-C** (yellow solid, 151 mg, 83%). M.p.: 132-135  $^\circ\text{C}$  (decomp.,  $\text{Et}_2\text{O}$ ). IR (neat):  $\nu_{\text{max}}$  2979, 2938, 2213, 1752, 1703, 1592, 1548, 1492, 1458, 1408, 1356, 1230, 1191, 1140, 1025, 994, 942, 902, 821, 762, 714, 688  $\text{cm}^{-1}$ ;  $^1\text{H}$  NMR ( $\text{d}_6$ -DMSO, 400 MHz)  $\delta$  12.73 (s, 1 H), 7.42 (t,  $J$  = 7.6 Hz, 2 H), 7.27 (t,  $J$  = 7.6 Hz, 1 H), 7.05 (d,  $J$  = 7.6 Hz, 2 H), 3.83 (d,  $J$  = 15.9 Hz, 1 H), 3.47 (d,  $J$  = 15.9 Hz, 1 H);  $^{13}\text{C}$  NMR ( $\text{d}_6$ -DMSO, 101 MHz)  $\delta$  181.2, 166.2, 159.5, 149.8, 133.8, 129.7, 126.4, 121.3, 117.1, 116.0, 77.9, 46.6, 43.9, 20.5; HRMS (EI) calcd for  $\text{C}_{16}\text{H}_8^{35}\text{Cl}_2\text{N}_2\text{O}_4$ : 361.9856; found: 361.9876.



**Butyl 2-(4,5-dichloro-1,2-dicyano-3-hydroxy-6-oxocyclohexa-2,4-dienyl)acetate (4g-C).** A solution of DDQ (114 mg, 0.500 mmol) and **2g** (188 mg, 1.00 mmol) in CH<sub>3</sub>CN was stirred at 20 °C for 1 min. The solvent was removed under reduced pressure. The crude material was purified by flash column chromatography (silica gel, eluent: acetic acid/ethyl acetate/pentane = 1/10/20) to afford **4g-C** (yellow solid, 135 mg, 79%). M.p.: 127-131 °C (decomp., Et<sub>2</sub>O). IR (neat):  $\nu_{\max}$  3241, 2962, 2936, 2874, 2215, 1726, 1706, 1613, 1549, 1465, 1410, 1351, 1206, 1142, 1028, 995, 945, 905, 870, 799, 753 cm<sup>-1</sup>; <sup>1</sup>H NMR (d<sub>6</sub>-DMSO, 400 MHz)  $\delta$  9.71 (s, 1 H), 4.04-3.93 (m, 2 H), 3.58 (d,  $J$  = 16.0 Hz, 1 H), 3.16 (d,  $J$  = 16.0 Hz, 1 H), 1.46 (pent,  $J$  = 7.2 Hz, 2 H), 1.26 (hex,  $J$  = 7.2 Hz, 2 H), 0.85 (t,  $J$  = 7.2 Hz, 3 H); <sup>13</sup>C NMR (d<sub>6</sub>-DMSO, 101 MHz)  $\delta$  181.3, 167.2, 159.7, 150.4, 133.7, 117.5, 116.2, 76.6, 65.1, 46.0, 43.9, 29.9, 18.4, 13.5; MS (EI)  $m/z$  (%): 245, 243, 215, 181, 153, 87, 56 (100); HRMS (EI) calcd for C<sub>14</sub>H<sub>12</sub><sup>35</sup>Cl<sub>2</sub>N<sub>2</sub>O<sub>4</sub>: 342.0169; found: 342.0192.

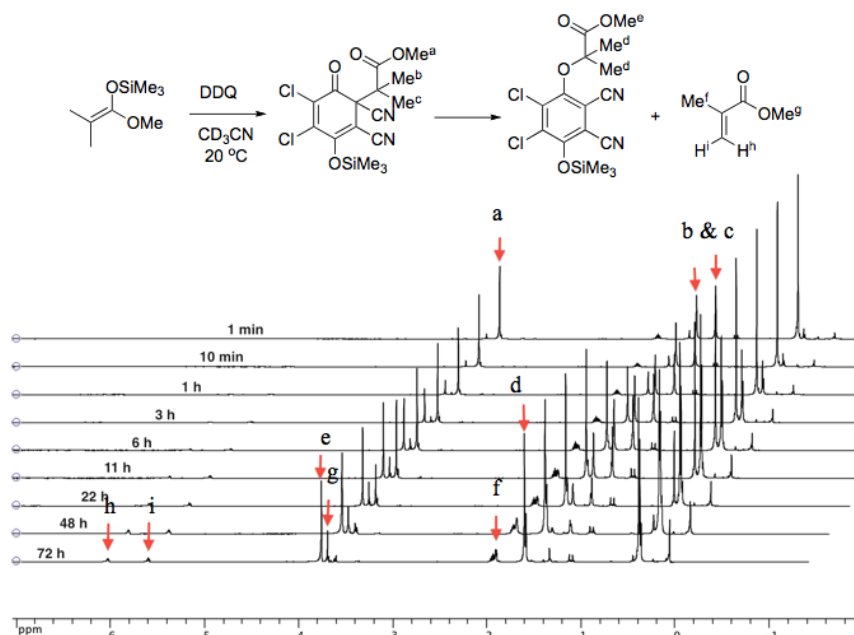


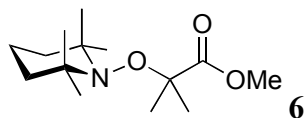
**4,5-Dichloro-3-hydroxy-6-(2-methyl-1-oxopropan-2-yloxy)phthalonitrile (4h-O).** A solution of DDQ (114 mg, 0.50 mmol) and **2h** (72 mg, 0.500 mmol) in CD<sub>3</sub>CN was stirred at 20 °C for 1 h. The reaction mixture was analyzed by <sup>1</sup>H NMR during the course of the reaction. The solvent was removed under reduced pressure. The crude material was purified by flash column chromatography (silica gel, eluent: triethylamine/methanol/ethyl acetate = 1/5/10). The remaining triethylamine was removed by a short column (silica gel, eluent: acetic acid/ethyl acetate = 1/20) to afford **4h-O** (white solid, 67 mg, 45%). M.p.: 150-153 °C (decomp., Et<sub>2</sub>O). IR (neat):  $\nu_{\max}$  3267, 2983, 2938, 2836, 2362, 2335, 2234, 1733, 1558, 1440, 1418, 1390, 1370, 1344, 1265, 1203, 1130, 1088, 995, 915, 834, 783 cm<sup>-1</sup>; <sup>1</sup>H NMR (CD<sub>3</sub>CN, 400 MHz)  $\delta$  9.96 (s, 1 H), 5.87 (br s, 1 H), 1.43 (s, 6 H); <sup>13</sup>C NMR (CD<sub>3</sub>CN, 101 MHz)  $\delta$  201.2, 155.4, 149.0, 136.9, 129.6, 114.8, 113.8, 112.6, 103.2, 91.0, 22.5; MS (EI)  $m/z$  (%): 298 (M<sup>+</sup>), 285, 230, 228, 202, 200, 87, 72, 43 (100); HRMS (EI) calcd for C<sub>12</sub>H<sub>9</sub><sup>35</sup>Cl<sub>2</sub>N<sub>2</sub>O<sub>3</sub>[M<sup>+</sup> + H]: 298.9985; found: 298.9978.



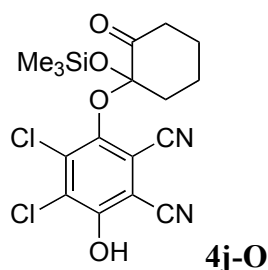
**Methyl 2-(2,3-dichloro-5,6-dicyano-4-hydroxyphenoxy)-2-methylpropanoate (4i-O).** A solution of DDQ (114 mg, 0.500 mmol) and **2i** (87 mg, 0.50 mmol) in CD<sub>3</sub>CN was stirred at 20 °C for 72 h. The reaction mixture was analyzed by <sup>1</sup>H NMR during the course of the reaction. The solvent was removed under reduced pressure. The crude material was purified by flash column chromatography (silica gel, eluent: triethylamine/methanol/ethyl acetate = 1/5/10). The remaining triethylamine was removed by a short column (silica gel, eluent: acetic acid/ethyl acetate = 1/20) to afford **4i-O** (white solid, 104 mg, 63%). M.p.: 153-154 °C (Et<sub>2</sub>O). IR (neat):  $\nu_{\max}$  3263, 2980, 2961, 2830, 2233, 1737, 1625, 1556, 1436, 1418, 1389, 1353, 1298, 1260, 1198, 1168, 1128, 1088, 1015, 993, 904, 791 cm<sup>-1</sup>; <sup>1</sup>H NMR (d<sub>6</sub>-DMSO, 101 MHz)  $\delta$  4.47 (br s, 1 H), 3.70 (s, 3 H), 1.47 (s, 6 H); <sup>13</sup>C NMR (d<sub>6</sub>-DMSO, 101 MHz)  $\delta$  171.9, 164.5, 137.4, 133.5, 131.9, 117.9, 115.3, 108.7, 95.8, 83.5, 52.2, 24.4; MS (EI)  $m/z$  (%): 328 (M<sup>+</sup>), 230, 228, 202, 200, 101, 69, 73, 70, 59, 43, 41 (100); HRMS (EI) calcd for C<sub>13</sub>H<sub>9</sub><sup>35</sup>Cl<sub>2</sub>N<sub>2</sub>O<sub>4</sub>[M<sup>+</sup>-H]: 326.9934; found: 326.9950.

#### Time-resolved <sup>1</sup>H NMR spectra of the reaction of **2i** with DDQ

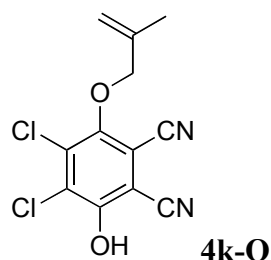




**Methyl 2-methyl-2-((2,2,6,6-tetramethylpiperidin-1-yl)oxy)propanoate (6)** A solution of DDQ (114 mg, 0.500 mmol) and **2i** (87 mg, 0.50 mmol) in CH<sub>3</sub>CN was stirred for 1 min at 20 °C under nitrogen. Then (2,2,6,6-tetramethylpiperidin-1-yl)oxyl (TEMPO, 78 mg, 0.50 mmol) was added to the reaction mixture which was stirred for 72 h at 20 °C. The solvent was removed under reduced pressure. The crude material was purified by flash column chromatography (silica gel, eluent: ethyl acetate/pentane = 1/10) to give **6** (colorless oil, 63 mg, 49%). IR (neat):  $\nu_{\text{max}}$  2975, 2932, 2872, 1736, 1471, 1448, 1376, 1360, 1282, 1259, 1206, 1190, 1160, 1132, 1012, 988, 950, 924, 878, 853, 812, 768, 720 cm<sup>-1</sup>; <sup>1</sup>H NMR (CDCl<sub>3</sub>, 300 MHz)  $\delta$  3.69 (s, 3 H), 1.45 (s, 6H) overlapping with m from 1.62 to 1.23 (12 H), 1.12 (s, 6 H), 0.97 (s, 6 H); <sup>13</sup>C NMR (CDCl<sub>3</sub>, 75.5 MHz)  $\delta$  176.6, 81.2, 59.7, 51.8, 40.7, 33.5, 24.6, 20.5, 17.2; MS (EI)  $m/z$  (%): 156.1 (100), 142.1, 140.1, 123.1, 83.0, 81.0, 69.1, 55.3; HRMS (ESI) calcd for C<sub>14</sub>H<sub>28</sub>NO<sub>3</sub>[M<sup>+</sup>+H]: 258.2064; found: 258.2067.

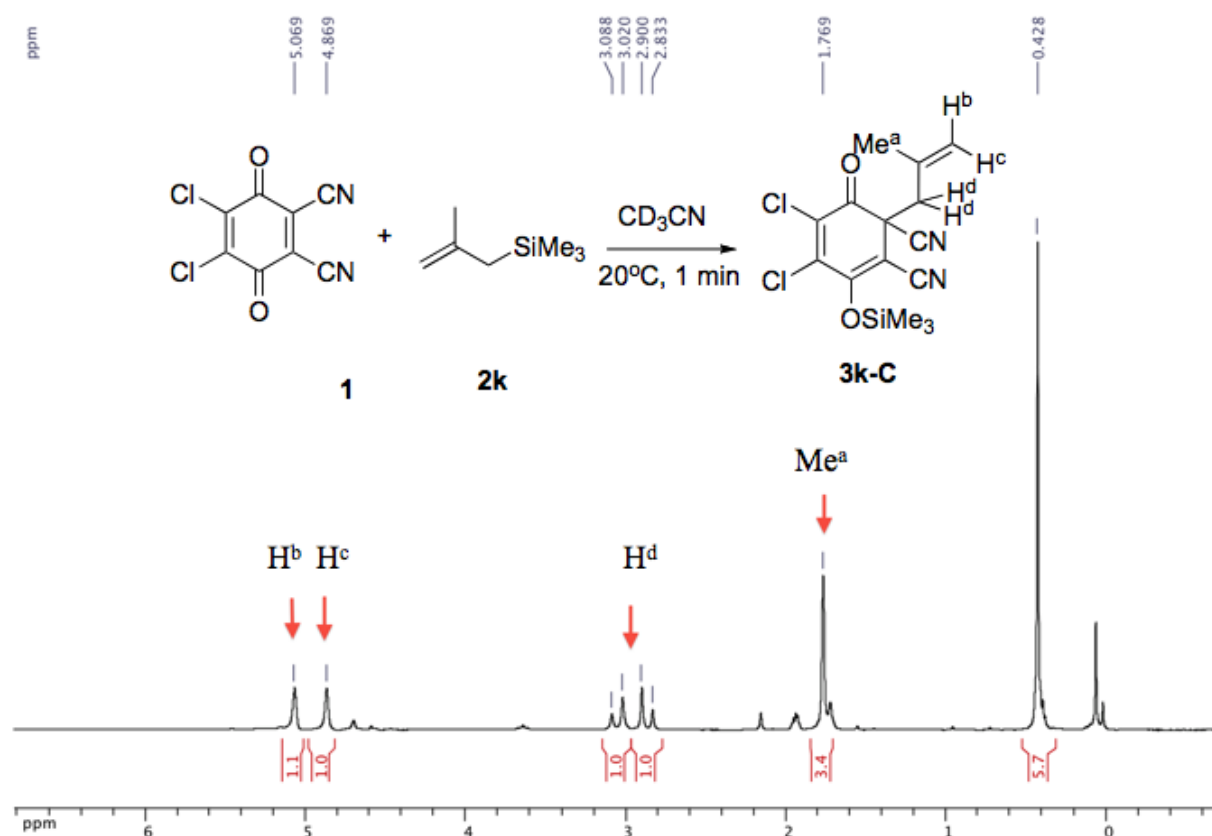


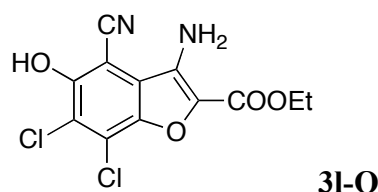
**4,5-Dichloro-3-hydroxy-6-(2-oxo-1-(trimethylsilyloxy)cyclohexyloxy)phthalonitrile (4j-O).** A solution of DDQ (114 mg, 0.500 mmol) and **2j** (259 mg, 1.00 mmol) in CH<sub>3</sub>CN was stirred at 20 °C for 1 min. A few drops of methanol or water was added and the solvent was removed under reduced pressure. The crude material was analyzed by <sup>1</sup>H NMR spectroscopy and then purified by crystallization from CH<sub>2</sub>Cl<sub>2</sub>/pentane to give **4j-O** (white solid, 88 mg, 43%). M.p.: <150 °C (decomp.). <sup>1</sup>H NMR (d<sub>6</sub>-DMSO, 400 MHz)  $\delta$  11.95 (s, 1 H), 2.68-2.65 (m, 4 H), 1.97-1.94 (m, 4 H), 0.35 (s, 9 H); <sup>13</sup>C NMR (d<sub>6</sub>-DMSO, 101 MHz)  $\delta$  197.2, 150.8 (br), 132.0 (br), 129.3 (br), 113.6, 101.7 (br), 42.3, 22.7, 0.6. MS (EI)  $m/z$  (%): 372.0, 359, 357.0, 284.9, 227.9, 199.9, 169.0 (100), 73.0; HRMS (EI) calcd for C<sub>16</sub>H<sub>15</sub><sup>35</sup>Cl<sub>2</sub>N<sub>2</sub>O<sub>4</sub>Si [M<sup>+</sup>-CH<sub>3</sub>]: 397.0173; found: 397.0158.



**4,5-Dichloro-3-hydroxy-6-(2-methylallyloxy)phthalonitrile (4k-O).** A solution of DDQ (114 mg, 0.50 mmol) and **2k** (64 mg, 0.50 mmol) in CD<sub>3</sub>CN was stirred at 20 °C for 24 h. The reaction mixture was analyzed by <sup>1</sup>H NMR during the course of the reaction. A few drops of methanol or water was added and then the solvent was removed under reduced pressure. The crude material was purified by crystallization from CH<sub>2</sub>Cl<sub>2</sub>/pentane to give **4k-O** (light yellow solid, 115 mg, 81%). M.p.: 156.5-157.0 °C (CH<sub>2</sub>Cl<sub>2</sub>). IR (neat):  $\nu_{\text{max}}$  3328, 3083, 2977, 2873, 2246, 2235, 1655, 1561, 1442, 1426, 1368, 1335, 1261, 1193, 1119, 1082, 1004, 943, 906, 892, 779, 746, 688 cm<sup>-1</sup>; <sup>1</sup>H NMR (d<sub>6</sub>-DMSO, 400 MHz)  $\delta$  9.20 (br s, 1 H), 5.14-5.13 (m, 1 H), 5.05-5.04 (m, 1 H), 4.53 (s, 2 H), 1.87 (s, 3 H); <sup>13</sup>C NMR (d<sub>6</sub>-DMSO, 101 MHz)  $\delta$  154.4, 150.6, 139.8, 133.9, 129.1, 115.1, 113.3, 113.0, 108.4, 102.0, 78.8, 19.4; MS (EI)  $m/z$  (%): 282 (M<sup>+</sup>), 55 (100); HRMS (EI) calcd for C<sub>12</sub>H<sub>8</sub><sup>35</sup>Cl<sub>2</sub>N<sub>2</sub>O<sub>2</sub>: 281.9957; found: 281.9956.

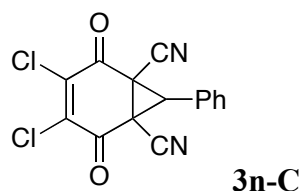
**<sup>1</sup>H NMR spectrum of the reaction of 2k with DDQ after 1 min**





**Ethyl 3-amino-6,7-dichloro-4-cyano-5-hydroxybenzofuran-2-carboxylate (3l-O).** A solution of DDQ (114 mg, 0.500 mmol) and **2l** (185 mg, 1.00 mmol) or **2m** (143 mg, 1.00 mmol) in CH<sub>3</sub>CN was stirred at 20 °C for 10 min. A few drops of water were added. The mixture was stirred for another 30 min. The solvent was removed under reduced pressure. The crude material was purified by crystallization from AcOH/CH<sub>3</sub>CN to give **3l-O** as light yellow solid (76 mg, 48% from **2l**; 83 mg, 53% from **2m**). M.p.: 274-277 °C (decomp., AcOH/CH<sub>3</sub>CN), literature report<sup>2</sup>: 227 °C (AcOH). IR (neat):  $\nu_{\max}$  3369, 2228, 1678, 1629, 1554, 1399, 1336, 1275, 1185, 1126, 903, 760, 626 cm<sup>-1</sup>; <sup>1</sup>H NMR (d<sub>6</sub>-DMSO, 300 MHz)  $\delta$  5.62 (s, 2 H), 4.35 (q,  $J$  = 7.1 Hz, 2 H), 3.48 (br s, 1 H), 1.33 (t,  $J$  = 7.1 Hz, 3 H); <sup>13</sup>C NMR (d<sub>6</sub>-DMSO, 75.5 MHz)  $\delta$  159.8, 154.2, 143.3, 137.3, 127.1, 123.4, 122.1, 119.7, 114.1, 90.4, 60.4, 14.3; MS (EI)  $m/z$  (%): 316 ( $M^+$  + 2), 314 ( $M^+$ ), 268, 242, 58, 43 (100); HRMS (EI) calcd for C<sub>12</sub>H<sub>7</sub><sup>35</sup>Cl<sub>2</sub>N<sub>2</sub>O<sub>4</sub>[ $M^+$  - H]: 312.9777; found: 312.9795.

IR, <sup>1</sup>H and <sup>13</sup>C NMR spectra agree with ref. 28, while m.p. does not agree with the value reported from ref. S2.



**3,4-Dichloro-2,5-dioxo-7-phenylbicyclo[4.1.0]hept-3-ene-1,6-dicarbonitrile (3n-C, major isomer).** A solution of DDQ (114 mg, 0.500 mmol) and **2n** (118 mg, 1.00 mmol) in CH<sub>3</sub>CN was stirred at 20 °C for 1 min. The solvent was removed under reduced pressure. The crude material was analyzed by <sup>1</sup>H NMR spectroscopy and then purified by flash column chromatography (silica gel, eluent: ethyl acetate/pentane = 1/20) to give the major isomer (white solid, 68 mg, 43% yield). M.p.: 220-222 °C (decomp., CH<sub>2</sub>Cl<sub>2</sub>), literature report<sup>29</sup>: 215-216 °C (methanol). IR (neat):  $\nu_{\max}$  2921, 2258, 1702, 1570, 1498, 1488, 1450, 1364, 1279, 1229, 1162, 956, 888, 830, 791, 783, 752, 724, 702, 677 cm<sup>-1</sup>; <sup>1</sup>H NMR (d<sub>6</sub>-acetone, 400 MHz)  $\delta$  7.46-7.42 (m, 3 H), 7.26-7.22 (m, 2 H), 5.20 (s, 1 H); <sup>13</sup>C NMR (d<sub>6</sub>-acetone, 101 MHz)  $\delta$  176.1, 143.4, 130.9, 130.7, 129.7, 128.5, 113.6, 47.0, 37.3; MS (EI)  $m/z$  (%): 318 ( $M^+$  + 2),



316 ( $M^+$ ), 263, 261, 253, 239, 237 (100), 225, 202, 189, 166, 139, 89, 87, 63, 51; HRMS (EI) calcd for  $C_{15}H_6^{35}Cl_2N_2O_2$ : 315.9801; found: 315.9797.

$^1H$  NMR spectrum agrees with ref. S3.

## 2) Kinetic studies of the reaction of DDQ with **2a-n** in $CH_3CN$

The rate constants of all investigated reactions were determined photometrically. The temperature of the solutions during all kinetic studies was kept constant ( $20.0 \pm 0.1$  °C) by using a circulating bath thermostat. For the evaluation of fast kinetics ( $\tau_{1/2} < 10$  s) a stopped-flow spectrophotometer (Hi-Tech SF-61DX2) was used. The rates of slow reactions ( $\tau_{1/2} > 10$  s) were determined by using a conventional UV/Vis diode array spectrophotometer (J&M TIDAS) connected to a Hellma 661.502-QX quartz Suprasil immersion probe (5 mm light path) via fiber optic cables. Rate constants  $k_{obs}$  ( $s^{-1}$ ) were obtained by least-squares fitting of the absorbances to the monoexponential function  $A_t = A_0 e^{-k_{obs}t} + C$  (for decreasing absorbance) or  $A_t = A_0 (1 - e^{-k_{obs}t}) + C$  (for increasing absorbance).

Table 1. Kinetics of the reaction of DDQ with **2a** in  $CH_3CN$  (0 °C, Conventional UV/Vis, at 278 nm)

[DDQ] / mol L <sup>-1</sup>	[ <b>2a</b> ] / mol L <sup>-1</sup>	$k_{obs}$ / s <sup>-1</sup>
$1.0 \times 10^{-4}$	$1.2 \times 10^{-3}$	$2.4 \times 10^{-2}$
$1.0 \times 10^{-4}$	$1.6 \times 10^{-3}$	$3.2 \times 10^{-2}$
$1.0 \times 10^{-4}$	$2.0 \times 10^{-3}$	$3.8 \times 10^{-2}$
$1.0 \times 10^{-4}$	$2.3 \times 10^{-3}$	$4.3 \times 10^{-2}$
$k_2 = 1.7 \times 10^1$ L mol <sup>-1</sup> s <sup>-1</sup>		

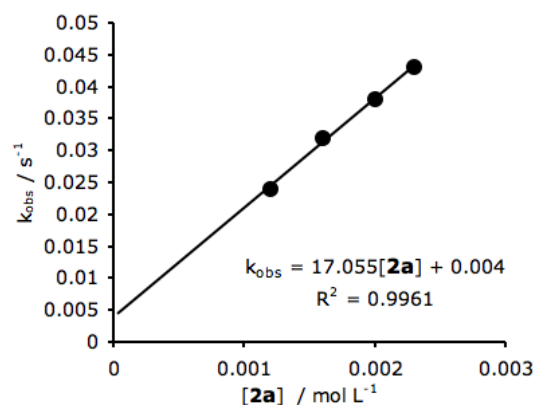
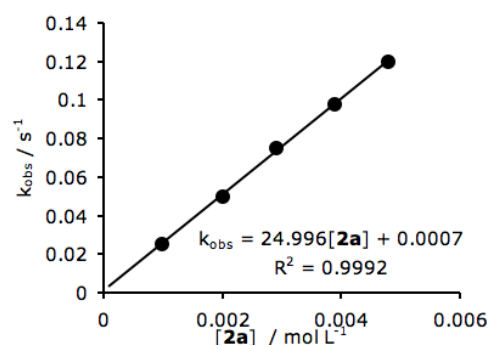


Table S2. Kinetics of the reaction of DDQ with **2a** in CH<sub>3</sub>CN (20 °C, Conventional UV/Vis, at 278 nm)

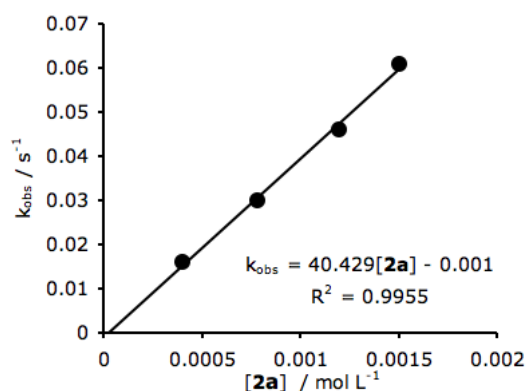
[DDQ] / mol L <sup>-1</sup>	additive	[ <b>2a</b> ] / mol L <sup>-1</sup>	$k_{\text{obs}}$ / s <sup>-1</sup>
$1.0 \times 10^{-4}$	-	$9.9 \times 10^{-4}$	$2.5 \times 10^{-2}$
$1.0 \times 10^{-4}$	NBu <sub>4</sub> OTs ( $5.0 \times 10^{-3}$ M)	$9.9 \times 10^{-4}$	$1.8 \times 10^{-2}$
$1.0 \times 10^{-4}$	-	$2.0 \times 10^{-3}$	$5.0 \times 10^{-2}$
$1.0 \times 10^{-4}$	-	$2.9 \times 10^{-3}$	$7.5 \times 10^{-2}$
$1.0 \times 10^{-4}$	-	$3.9 \times 10^{-3}$	$9.8 \times 10^{-2}$
$1.0 \times 10^{-4}$	-	$4.8 \times 10^{-3}$	$1.2 \times 10^{-1}$

$k_2 = 2.5 \times 10^1 \text{ L mol}^{-1} \text{ s}^{-1}$

Table 3. Kinetics of the reaction of DDQ with **2a** in CH<sub>3</sub>CN (40 °C, Conventional UV/Vis, at 278 nm)

[DDQ] / mol L <sup>-1</sup>	[ <b>2a</b> ] / mol L <sup>-1</sup>	$k_{\text{obs}}$ / s <sup>-1</sup>
$1.0 \times 10^{-4}$	$4.0 \times 10^{-4}$	$1.6 \times 10^{-2}$
$1.0 \times 10^{-4}$	$7.8 \times 10^{-4}$	$3.0 \times 10^{-2}$
$1.0 \times 10^{-4}$	$1.2 \times 10^{-3}$	$4.6 \times 10^{-2}$
$1.0 \times 10^{-4}$	$1.5 \times 10^{-3}$	$6.1 \times 10^{-2}$

$k_2 = 4.0 \times 10^1 \text{ mol}^{-1} \text{ L s}^{-1}$

Table 4. Kinetics of the reaction of DDQ with **2a** in CH<sub>3</sub>CN (60 °C, Conventional UV/Vis, at 278 nm)

[DDQ] / mol L <sup>-1</sup>	[ <b>2a</b> ] / mol L <sup>-1</sup>	$k_{\text{obs}}$ / s <sup>-1</sup>
$1.0 \times 10^{-4}$	$3.8 \times 10^{-3}$	$2.1 \times 10^{-2}$
$1.0 \times 10^{-4}$	$7.5 \times 10^{-3}$	$4.3 \times 10^{-2}$
$1.0 \times 10^{-4}$	$1.1 \times 10^{-3}$	$6.5 \times 10^{-2}$
$1.0 \times 10^{-4}$	$1.5 \times 10^{-3}$	$8.6 \times 10^{-2}$

$k_2 = 5.9 \times 10^1 \text{ mol}^{-1} \text{ L s}^{-1}$

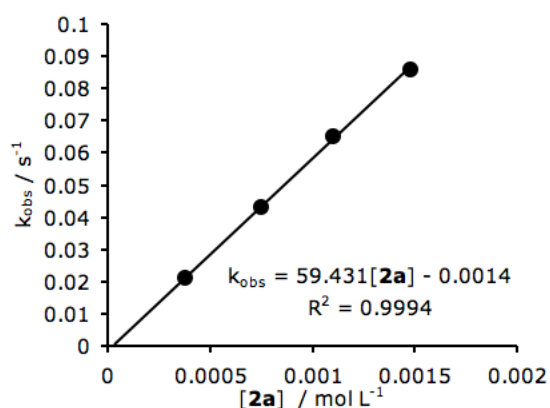
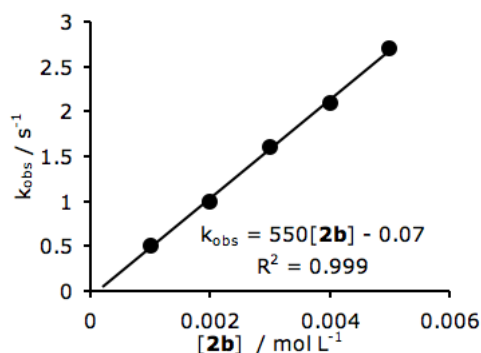


Table S5. Kinetics of the reaction of DDQ with **2b** in CH<sub>3</sub>CN (20 °C, Stopped-flow, at 278 nm)

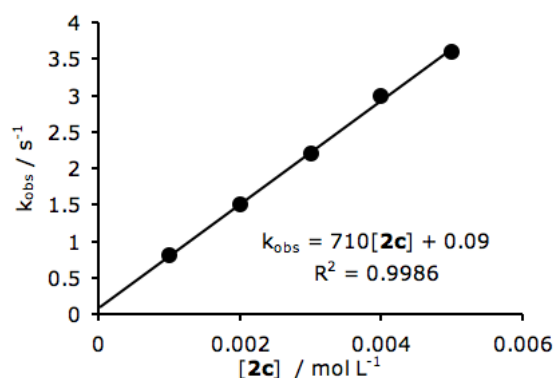
[DDQ] / mol L <sup>-1</sup>	[ <b>2b</b> ] / mol L <sup>-1</sup>	<i>k</i> <sub>obs</sub> / s <sup>-1</sup>
1.0 × 10 <sup>-4</sup>	1.0 × 10 <sup>-3</sup>	0.50
1.0 × 10 <sup>-4</sup>	2.0 × 10 <sup>-3</sup>	1.0
1.0 × 10 <sup>-4</sup>	3.0 × 10 <sup>-3</sup>	1.6
1.0 × 10 <sup>-4</sup>	4.0 × 10 <sup>-3</sup>	2.1
1.0 × 10 <sup>-4</sup>	5.0 × 10 <sup>-3</sup>	2.7

$$k_2 = 5.5 \times 10^2 \text{ L mol}^{-1} \text{ s}^{-1}$$

Table S6. Kinetics of the reaction of DDQ with **2c** in CH<sub>3</sub>CN (20 °C, Stopped-flow, at 278 nm)

[DDQ] / mol L <sup>-1</sup>	[ <b>2c</b> ] / mol L <sup>-1</sup>	<i>k</i> <sub>obs</sub> / s <sup>-1</sup>
1.0 × 10 <sup>-4</sup>	1.0 × 10 <sup>-3</sup>	0.80
1.0 × 10 <sup>-4</sup>	2.0 × 10 <sup>-3</sup>	1.5
1.0 × 10 <sup>-4</sup>	3.0 × 10 <sup>-3</sup>	2.2
1.0 × 10 <sup>-4</sup>	4.0 × 10 <sup>-3</sup>	3.0
1.0 × 10 <sup>-4</sup>	5.0 × 10 <sup>-3</sup>	3.6

$$k_2 = 7.1 \times 10^2 \text{ L mol}^{-1} \text{ s}^{-1}$$

Table S7. Kinetics of the reaction of DDQ with **2d** in CH<sub>3</sub>CN (20 °C, Stopped-flow, at 350 nm)

[DDQ] / mol L <sup>-1</sup>	[ <b>2d</b> ] / mol L <sup>-1</sup>	<i>k</i> <sub>obs</sub> / s <sup>-1</sup>
1.0 × 10 <sup>-4</sup>	5.0 × 10 <sup>-2</sup>	2.4 × 10 <sup>1</sup>
1.0 × 10 <sup>-4</sup>	6.0 × 10 <sup>-2</sup>	2.7 × 10 <sup>1</sup>
1.0 × 10 <sup>-4</sup>	8.0 × 10 <sup>-2</sup>	3.6 × 10 <sup>1</sup>
1.0 × 10 <sup>-4</sup>	1.0 × 10 <sup>-1</sup>	4.6 × 10 <sup>1</sup>

$$k_2 = 4.5 \times 10^2 \text{ mol}^{-1} \text{ L s}^{-1}$$

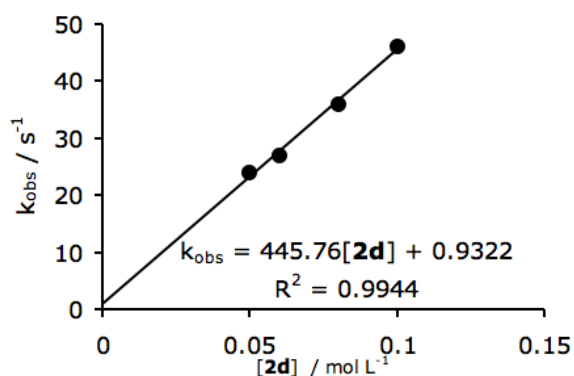
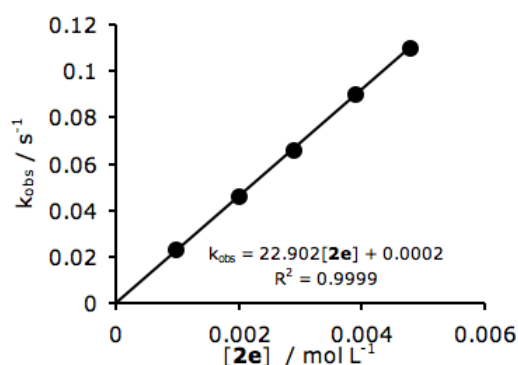


Table S8. Kinetics of the reaction of DDQ with **2e** in CH<sub>3</sub>CN (20 °C, Conventional UV/Vis, at 278 nm)

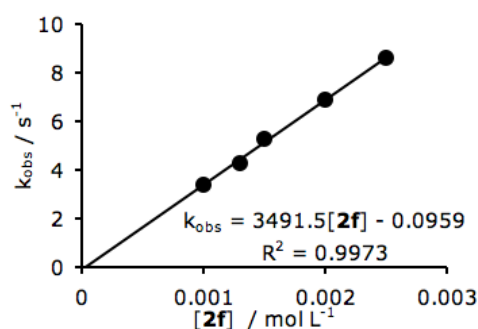
[DDQ] / mol L <sup>-1</sup>	[ <b>2e</b> ] / mol L <sup>-1</sup>	<i>k</i> <sub>obs</sub> / s <sup>-1</sup>
1.0 × 10 <sup>-4</sup>	9.9 × 10 <sup>-4</sup>	2.3 × 10 <sup>-2</sup>
1.0 × 10 <sup>-4</sup>	2.0 × 10 <sup>-3</sup>	4.6 × 10 <sup>-2</sup>
1.0 × 10 <sup>-4</sup>	2.9 × 10 <sup>-3</sup>	6.6 × 10 <sup>-2</sup>
1.0 × 10 <sup>-4</sup>	3.9 × 10 <sup>-3</sup>	9.0 × 10 <sup>-2</sup>
1.0 × 10 <sup>-4</sup>	4.8 × 10 <sup>-3</sup>	1.1 × 10 <sup>-1</sup>

$$k_2 = 2.3 \times 10^1 \text{ L mol}^{-1} \text{ s}^{-1}$$

Table S9. Kinetics of the reaction of DDQ with **2f** in CH<sub>3</sub>CN (20 °C, Stopped-flow, at 278 nm)

[DDQ] / mol L <sup>-1</sup>	[ <b>2f</b> ] / mol L <sup>-1</sup>	<i>k</i> <sub>obs</sub> / s <sup>-1</sup>
1.0 × 10 <sup>-4</sup>	1.0 × 10 <sup>-3</sup>	3.4
1.0 × 10 <sup>-4</sup>	1.3 × 10 <sup>-3</sup>	4.3
1.0 × 10 <sup>-4</sup>	1.5 × 10 <sup>-3</sup>	5.3
1.0 × 10 <sup>-4</sup>	2.0 × 10 <sup>-3</sup>	6.9
1.0 × 10 <sup>-4</sup>	2.5 × 10 <sup>-3</sup>	8.6

$$k_2 = 3.5 \times 10^3 \text{ L mol}^{-1} \text{ s}^{-1}$$

Table S10. Kinetics of the reaction of DDQ with **2g** in CH<sub>3</sub>CN (20 °C, Stopped-flow, at 278 nm)

[DDQ] / mol L <sup>-1</sup>	[ <b>2g</b> ] / mol L <sup>-1</sup>	<i>k</i> <sub>obs</sub> / s <sup>-1</sup>
2.0 × 10 <sup>-5</sup>	2.0 × 10 <sup>-4</sup>	1.7 × 10 <sup>2</sup>
2.0 × 10 <sup>-5</sup>	4.0 × 10 <sup>-4</sup>	3.4 × 10 <sup>2</sup>
2.0 × 10 <sup>-5</sup>	6.0 × 10 <sup>-4</sup>	5.2 × 10 <sup>2</sup>
2.0 × 10 <sup>-5</sup>	8.0 × 10 <sup>-4</sup>	7.1 × 10 <sup>2</sup>
2.0 × 10 <sup>-5</sup>	1.0 × 10 <sup>-3</sup>	8.3 × 10 <sup>2</sup>

$$k_2 = 8.5 \times 10^5 \text{ L mol}^{-1} \text{ s}^{-1}$$

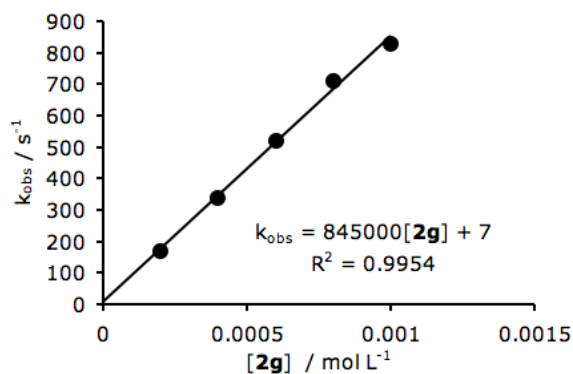
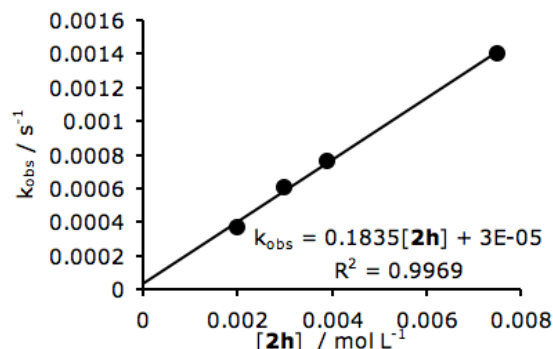


Table S11. Kinetics of the reaction of DDQ with **2h** in CH<sub>3</sub>CN (20 °C, Conventional UV/Vis, at 278 nm)

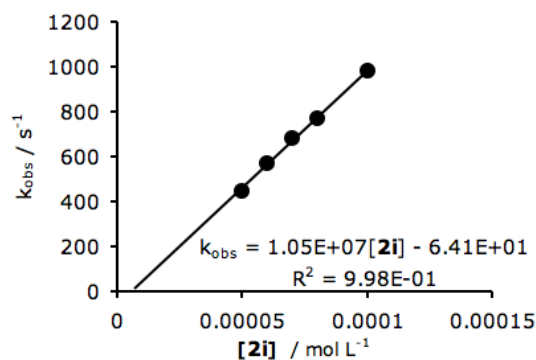
[DDQ] / mol L <sup>-1</sup>	[ <b>2h</b> ] / mol L <sup>-1</sup>	<i>k</i> <sub>obs</sub> / s <sup>-1</sup>
1.0 × 10 <sup>-4</sup>	2.0 × 10 <sup>-3</sup>	3.7 × 10 <sup>-4</sup>
1.0 × 10 <sup>-4</sup>	3.0 × 10 <sup>-3</sup>	6.1 × 10 <sup>-4</sup>
1.0 × 10 <sup>-4</sup>	3.9 × 10 <sup>-3</sup>	7.6 × 10 <sup>-4</sup>
1.0 × 10 <sup>-4</sup>	7.5 × 10 <sup>-3</sup>	1.4 × 10 <sup>-3</sup>

$$k_2 = 1.8 \times 10^{-1} \text{ L mol}^{-1} \text{ s}^{-1}$$


 Table S12. Kinetics of the reaction of DDQ with **2i** in CH<sub>3</sub>CN (20 °C, Stopped-flow, at 278 nm)

[DDQ] / mol L <sup>-1</sup>	[ <b>2i</b> ] / mol L <sup>-1</sup>	<i>k</i> <sub>obs</sub> / s <sup>-1</sup>
1.0 × 10 <sup>-5</sup>	5.0 × 10 <sup>-5</sup>	4.5 × 10 <sup>2</sup>
1.0 × 10 <sup>-5</sup>	6.0 × 10 <sup>-5</sup>	5.7 × 10 <sup>2</sup>
1.0 × 10 <sup>-5</sup>	7.0 × 10 <sup>-5</sup>	6.8 × 10 <sup>2</sup>
1.0 × 10 <sup>-5</sup>	8.0 × 10 <sup>-5</sup>	7.7 × 10 <sup>2</sup>
1.0 × 10 <sup>-5</sup>	1.0 × 10 <sup>-4</sup>	9.8 × 10 <sup>2</sup>

$$k_2 = 1.1 \times 10^7 \text{ L mol}^{-1} \text{ s}^{-1}$$


 Table S13. Kinetics of the reaction of DDQ with **2j** in CH<sub>3</sub>CN (20 °C, Stopped-flow, at 278 nm)

[DDQ] / mol L <sup>-1</sup>	[ <b>2j</b> ] / mol L <sup>-1</sup>	<i>k</i> <sub>obs</sub> / s <sup>-1</sup>
1.0 × 10 <sup>-4</sup>	1.0 × 10 <sup>-3</sup>	6.7 × 10 <sup>1</sup>
1.0 × 10 <sup>-4</sup>	2.0 × 10 <sup>-3</sup>	1.4 × 10 <sup>2</sup>
1.0 × 10 <sup>-4</sup>	2.5 × 10 <sup>-3</sup>	1.7 × 10 <sup>2</sup>
1.0 × 10 <sup>-4</sup>	3.0 × 10 <sup>-3</sup>	2.0 × 10 <sup>2</sup>
1.0 × 10 <sup>-4</sup>	4.0 × 10 <sup>-3</sup>	2.8 × 10 <sup>2</sup>

$$k_2 = 7.0 \times 10^4 \text{ L mol}^{-1} \text{ s}^{-1}$$

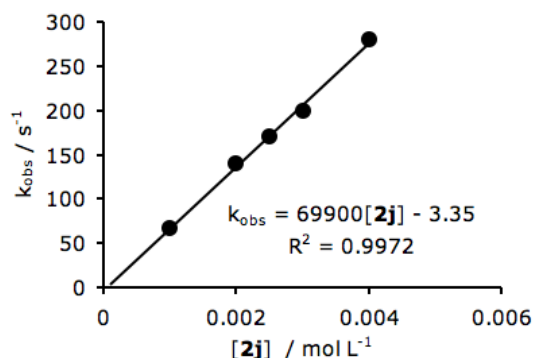
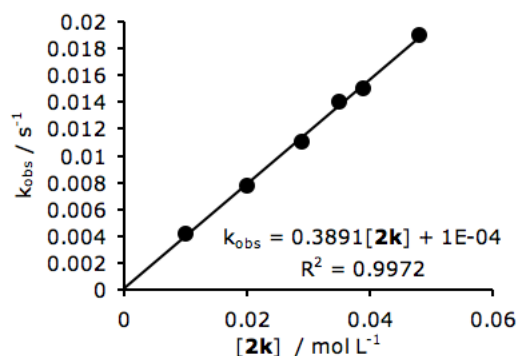


Table S14. Kinetics of the reaction of DDQ with **2k** in CH<sub>3</sub>CN (20 °C, Conventional UV/Vis, at 278 nm)

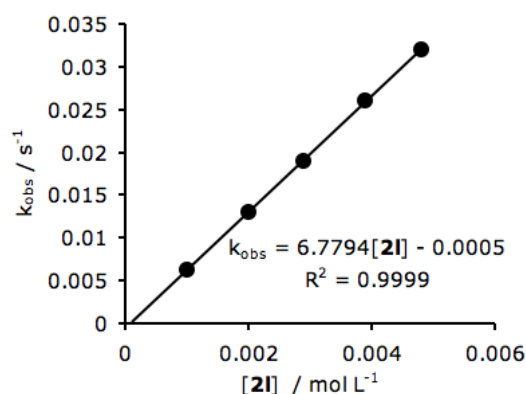
[DDQ] / mol L <sup>-1</sup>	additive	[ <b>2k</b> ] / mol L <sup>-1</sup>	<i>k</i> <sub>obs</sub> / s <sup>-1</sup>
1.0 × 10 <sup>-4</sup>	NBu <sub>4</sub> OTs (5.0 × 10 <sup>-3</sup> M)	1.0 × 10 <sup>-2</sup>	4.2 × 10 <sup>-3</sup>
1.0 × 10 <sup>-4</sup>		1.0 × 10 <sup>-2</sup>	3.2 × 10 <sup>-3</sup>
1.0 × 10 <sup>-4</sup>		2.0 × 10 <sup>-2</sup>	7.8 × 10 <sup>-3</sup>
1.0 × 10 <sup>-4</sup>		2.9 × 10 <sup>-2</sup>	1.1 × 10 <sup>-2</sup>
1.0 × 10 <sup>-4</sup>		3.5 × 10 <sup>-2</sup>	1.4 × 10 <sup>-2</sup>
1.0 × 10 <sup>-4</sup>		3.9 × 10 <sup>-2</sup>	1.5 × 10 <sup>-2</sup>
1.0 × 10 <sup>-4</sup>		4.8 × 10 <sup>-2</sup>	1.9 × 10 <sup>-2</sup>



$$k_2 = 3.9 \times 10^{-1} \text{ L mol}^{-1} \text{ s}^{-1}$$

Table S14. Kinetics of the reaction of DDQ with **2l** in CH<sub>3</sub>CN (20 °C, Conventional UV/Vis, at 350 nm)

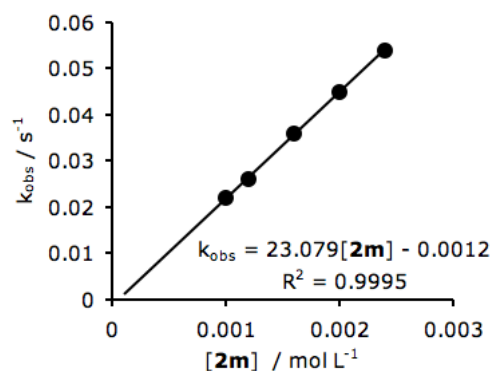
[DDQ] / mol L <sup>-1</sup>	[ <b>2l</b> ] / mol L <sup>-1</sup>	<i>k</i> <sub>obs</sub> / s <sup>-1</sup>
1.0 × 10 <sup>-4</sup>	1.0 × 10 <sup>-3</sup>	6.3 × 10 <sup>-3</sup>
1.0 × 10 <sup>-4</sup>	2.0 × 10 <sup>-3</sup>	1.3 × 10 <sup>-2</sup>
1.0 × 10 <sup>-4</sup>	2.9 × 10 <sup>-3</sup>	1.9 × 10 <sup>-2</sup>
1.0 × 10 <sup>-4</sup>	3.9 × 10 <sup>-3</sup>	2.6 × 10 <sup>-2</sup>
1.0 × 10 <sup>-4</sup>	4.8 × 10 <sup>-3</sup>	3.2 × 10 <sup>-2</sup>



$$k_2 = 6.8 \text{ L mol}^{-1} \text{ s}^{-1}$$

Table S16. Kinetics of the reaction of DDQ with **2m** in CH<sub>3</sub>CN (20 °C, Conventional UV/Vis, at 350 nm)

[DDQ] / mol L <sup>-1</sup>	[ <b>2m</b> ] / mol L <sup>-1</sup>	<i>k</i> <sub>obs</sub> / s <sup>-1</sup>
1.0 × 10 <sup>-4</sup>	1.0 × 10 <sup>-3</sup>	2.2 × 10 <sup>-2</sup>
1.0 × 10 <sup>-4</sup>	1.2 × 10 <sup>-3</sup>	2.6 × 10 <sup>-2</sup>
1.0 × 10 <sup>-4</sup>	1.6 × 10 <sup>-3</sup>	3.6 × 10 <sup>-2</sup>
1.0 × 10 <sup>-4</sup>	2.0 × 10 <sup>-3</sup>	4.5 × 10 <sup>-2</sup>
1.0 × 10 <sup>-4</sup>	2.4 × 10 <sup>-3</sup>	5.4 × 10 <sup>-2</sup>

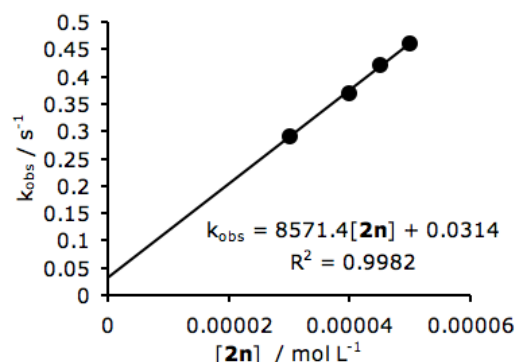


$$k_2 = 2.3 \times 10^1 \text{ mol}^{-1} \text{ L s}^{-1}$$

Table S17. Kinetics of the reaction of DDQ with **2n** in CH<sub>3</sub>CN (20 °C, Stopped-flow, at 278 nm)

[DDQ] / mol L <sup>-1</sup>	[ <b>2n</b> ] / mol L <sup>-1</sup>	<i>k</i> <sub>obs</sub> / s <sup>-1</sup>
5.0 × 10 <sup>-6</sup>	3.0 × 10 <sup>-5</sup>	0.29
5.0 × 10 <sup>-6</sup>	4.0 × 10 <sup>-5</sup>	0.37
5.0 × 10 <sup>-6</sup>	4.5 × 10 <sup>-5</sup>	0.42
5.0 × 10 <sup>-6</sup>	5.0 × 10 <sup>-5</sup>	0.46

$$k_2 = 8.6 \times 10^3 \text{ L mol}^{-1} \text{ s}^{-1}$$

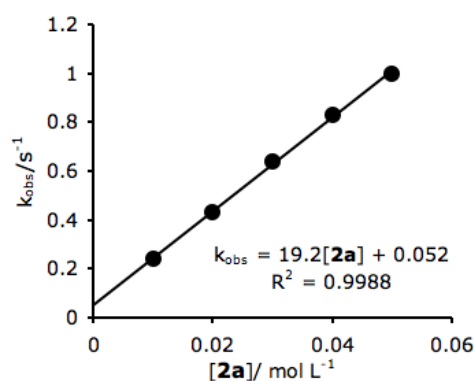


### 3) Kinetics of the Reaction of DDQ with **2** (a-f, k) in CH<sub>2</sub>Cl<sub>2</sub>

Table S18. Kinetics of the reaction of DDQ with **2a** in CH<sub>2</sub>Cl<sub>2</sub> (20 °C, Stopped-flow, at 420 nm)

[DDQ] / mol L <sup>-1</sup>	[ <b>2a</b> ] / mol L <sup>-1</sup>	<i>k</i> <sub>obs</sub> / s <sup>-1</sup>
1.0 × 10 <sup>-3</sup>	1.0 × 10 <sup>-2</sup>	0.24
1.0 × 10 <sup>-3</sup>	2.0 × 10 <sup>-2</sup>	0.43
1.0 × 10 <sup>-3</sup>	3.0 × 10 <sup>-2</sup>	0.64
1.0 × 10 <sup>-3</sup>	4.0 × 10 <sup>-2</sup>	0.83
1.0 × 10 <sup>-3</sup>	5.0 × 10 <sup>-2</sup>	1.0

$$k_2 = 1.9 \times 10^1 \text{ L mol}^{-1} \text{ s}^{-1}$$

Table S19. Kinetics of the reaction of DDQ with **2b** in CH<sub>2</sub>Cl<sub>2</sub> (20 °C, Stopped-flow, at 420 nm)

[DDQ] / mol L <sup>-1</sup>	[ <b>2b</b> ] / mol L <sup>-1</sup>	<i>k</i> <sub>obs</sub> / s <sup>-1</sup>
1.0 × 10 <sup>-3</sup>	1.0 × 10 <sup>-2</sup>	5.0
1.0 × 10 <sup>-3</sup>	1.5 × 10 <sup>-2</sup>	6.5
1.0 × 10 <sup>-3</sup>	2.0 × 10 <sup>-2</sup>	8.0
1.0 × 10 <sup>-3</sup>	2.5 × 10 <sup>-2</sup>	9.7
1.0 × 10 <sup>-3</sup>	3.0 × 10 <sup>-2</sup>	12

$$k_2 = 3.4 \times 10^2 \text{ L mol}^{-1} \text{ s}^{-1}$$

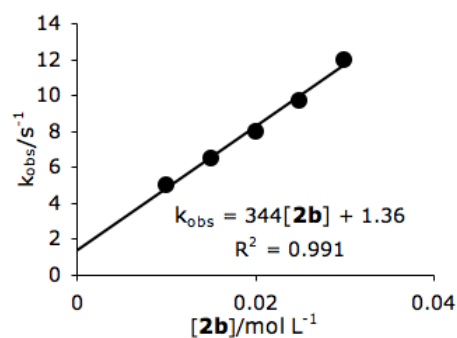
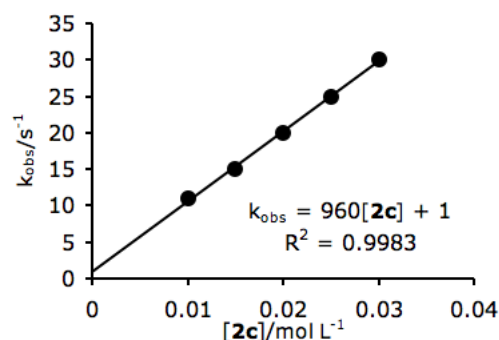


Table S20. Kinetics of the reaction of DDQ with **2c** in CH<sub>2</sub>Cl<sub>2</sub> (20 °C, Stopped-flow, at 420 nm)

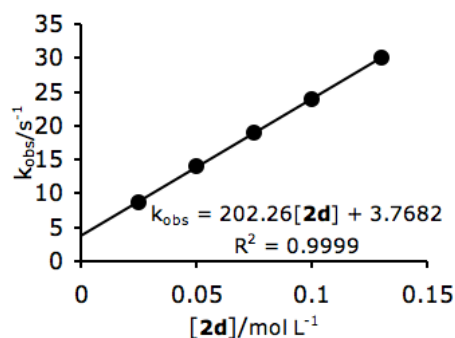
[DDQ] / mol L <sup>-1</sup>	[ <b>2c</b> ] / mol L <sup>-1</sup>	<i>k</i> <sub>obs</sub> / s <sup>-1</sup>
1.0 × 10 <sup>-3</sup>	1.0 × 10 <sup>-2</sup>	11
1.0 × 10 <sup>-3</sup>	1.5 × 10 <sup>-2</sup>	15
1.0 × 10 <sup>-3</sup>	2.0 × 10 <sup>-2</sup>	20
1.0 × 10 <sup>-3</sup>	2.5 × 10 <sup>-2</sup>	25
1.0 × 10 <sup>-3</sup>	3.0 × 10 <sup>-2</sup>	30

$$k_2 = 9.6 \times 10^2 \text{ L mol}^{-1} \text{ s}^{-1}$$

Table S21. Kinetics of the reaction of DDQ with **2d** in CH<sub>2</sub>Cl<sub>2</sub> (20 °C, Stopped-flow, at 420 nm)

[DDQ] / mol L <sup>-1</sup>	[ <b>2d</b> ] / mol L <sup>-1</sup>	<i>k</i> <sub>obs</sub> / s <sup>-1</sup>
1.0 × 10 <sup>-3</sup>	2.5 × 10 <sup>-2</sup>	8.7
1.0 × 10 <sup>-3</sup>	5.0 × 10 <sup>-2</sup>	14
1.0 × 10 <sup>-3</sup>	7.5 × 10 <sup>-2</sup>	19
1.0 × 10 <sup>-3</sup>	1.0 × 10 <sup>-1</sup>	24
1.0 × 10 <sup>-3</sup>	1.3 × 10 <sup>-1</sup>	30

$$k_2 = 2.0 \times 10^2 \text{ L mol}^{-1} \text{ s}^{-1}$$

Table S22. Kinetics of the reaction of DDQ with **2e** in CH<sub>2</sub>Cl<sub>2</sub> (20 °C, Stopped-flow, at 420 nm)

[DDQ] / mol L <sup>-1</sup>	[ <b>2e</b> ] / mol L <sup>-1</sup>	<i>k</i> <sub>obs</sub> / s <sup>-1</sup>
5.0 × 10 <sup>-4</sup>	4.0 × 10 <sup>-3</sup>	0.21
5.0 × 10 <sup>-4</sup>	6.0 × 10 <sup>-3</sup>	0.30
5.0 × 10 <sup>-4</sup>	8.0 × 10 <sup>-3</sup>	0.39
5.0 × 10 <sup>-4</sup>	1.0 × 10 <sup>-2</sup>	0.47
5.0 × 10 <sup>-4</sup>	1.2 × 10 <sup>-2</sup>	0.57

$$k_2 = 4.5 \times 10^1 \text{ L mol}^{-1} \text{ s}^{-1}$$

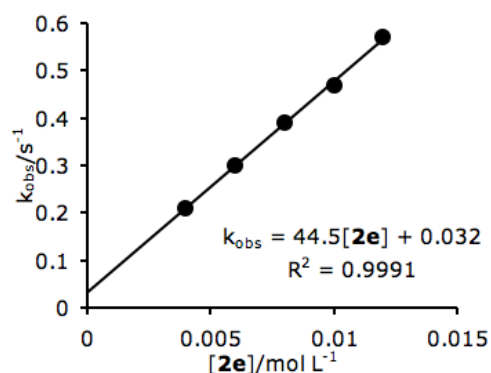
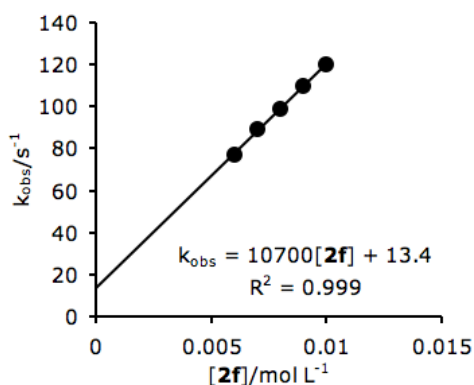




Table S23. Kinetics of the reaction of DDQ with **2f** in CH<sub>2</sub>Cl<sub>2</sub> (20 °C, Stopped-flow, at 420 nm)

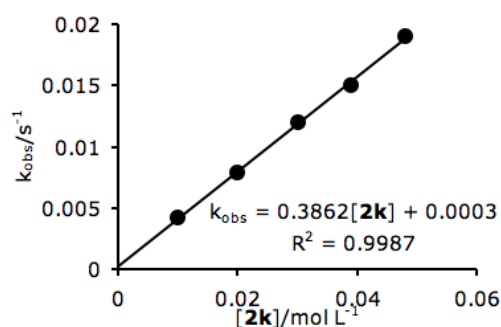
[DDQ] / mol L <sup>-1</sup>	[ <b>2f</b> ] / mol L <sup>-1</sup>	<i>k</i> <sub>obs</sub> / s <sup>-1</sup>
1.0 × 10 <sup>-3</sup>	6.0 × 10 <sup>-3</sup>	7.7 × 10 <sup>1</sup>
1.0 × 10 <sup>-3</sup>	7.0 × 10 <sup>-3</sup>	8.9 × 10 <sup>1</sup>
1.0 × 10 <sup>-3</sup>	8.0 × 10 <sup>-3</sup>	9.9 × 10 <sup>1</sup>
1.0 × 10 <sup>-3</sup>	9.0 × 10 <sup>-3</sup>	1.1 × 10 <sup>2</sup>
1.0 × 10 <sup>-3</sup>	1.0 × 10 <sup>-2</sup>	1.2 × 10 <sup>2</sup>

$$k_2 = 1.1 \times 10^4 \text{ L mol}^{-1} \text{ s}^{-1}$$

Table S24. Kinetics of the reaction of DDQ with **2k** in CH<sub>2</sub>Cl<sub>2</sub> (20 °C, Conventional UV/Vis, at 420 nm)

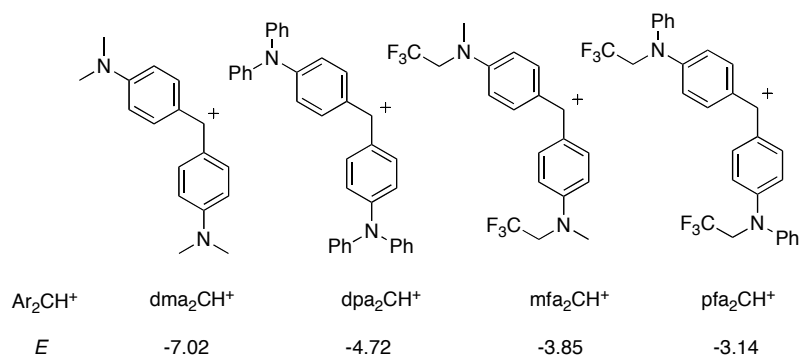
[DDQ] / mol L <sup>-1</sup>	[ <b>2k</b> ] / mol L <sup>-1</sup>	<i>k</i> <sub>obs</sub> / s <sup>-1</sup>
1.0 × 10 <sup>-3</sup>	1.0 × 10 <sup>-2</sup>	4.2 × 10 <sup>-3</sup>
1.0 × 10 <sup>-3</sup>	2.0 × 10 <sup>-2</sup>	7.9 × 10 <sup>-3</sup>
1.0 × 10 <sup>-3</sup>	3.0 × 10 <sup>-2</sup>	1.2 × 10 <sup>-2</sup>
1.0 × 10 <sup>-3</sup>	3.9 × 10 <sup>-2</sup>	1.5 × 10 <sup>-2</sup>
1.0 × 10 <sup>-3</sup>	4.8 × 10 <sup>-2</sup>	1.9 × 10 <sup>-2</sup>

$$k_2 = 3.9 \times 10^{-1} \text{ L mol}^{-1} \text{ s}^{-1}$$



#### 4) Determination of the Nucleophilicity Parameters of **2j**

In order to determine the nucleophilicity parameters  $N$  and  $s_N$  for the nucleophile **2j** the rates of the reactions with the benzhydrylium ions  $\text{Ar}_2\text{CH}^+$  have been determined photometrically in CH<sub>2</sub>Cl<sub>2</sub> solution. The nucleophilicity parameters of **2j** in CH<sub>2</sub>Cl<sub>2</sub> were determined according to the correlation  $\log k_2 = s_N (N + E)$  by plots of the second-order rate constants ( $\log k_2$ ) for the reactions of **2j** with the employed benzhydrylium ions  $\text{Ar}_2\text{CH}^+$  versus the corresponding electrophilicity parameters  $E$ .



**Figure S1.** Benzhydrylium ions  $\text{Ar}_2\text{CH}^+$  and their electrophilicity parameters  $E^{[31]}$  used for the determination of the nucleophilicity parameters ( $N$  and  $s_N$ ) for **2j** in  $\text{CH}_2\text{Cl}_2$ .

Table S25. Kinetics of the reaction of **2j** with  $\text{pfa}_2\text{CH}^+$  in  $\text{CH}_2\text{Cl}_2$  (20 °C, Conventional UV/Vis, at 601 nm)

$[\text{pfa}_2\text{CH}^+]$ / mol L <sup>-1</sup>	$[\text{2j}]$ / mol L <sup>-1</sup>	$k_{\text{obs}}$ / s <sup>-1</sup>
$1.0 \times 10^{-5}$	$1.0 \times 10^{-4}$	$4.9 \times 10^{-3}$
$1.0 \times 10^{-5}$	$2.0 \times 10^{-4}$	$9.9 \times 10^{-3}$
$1.0 \times 10^{-5}$	$2.9 \times 10^{-4}$	$1.5 \times 10^{-2}$
$1.0 \times 10^{-5}$	$3.9 \times 10^{-4}$	$2.1 \times 10^{-2}$
$1.0 \times 10^{-5}$	$4.8 \times 10^{-4}$	$2.5 \times 10^{-2}$

$$k_2 = 5.4 \times 10^1 \text{ L mol}^{-1} \text{ s}^{-1}$$

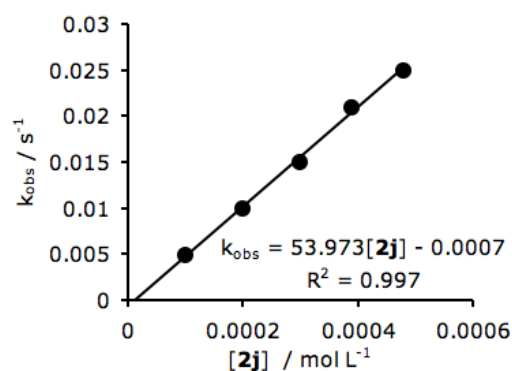


Table S26. Kinetics of the reaction of **2j** with  $\text{mfa}_2\text{CH}^+$  in  $\text{CH}_2\text{Cl}_2$  (20 °C, Conventional UV/Vis, at 593 nm)

$[\text{mfa}_2\text{CH}^+]$ / mol L <sup>-1</sup>	$[\text{2j}]$ / mol L <sup>-1</sup>	$k_{\text{obs}}$ / s <sup>-1</sup>
$1.0 \times 10^{-5}$	$1.0 \times 10^{-4}$	$6.3 \times 10^{-4}$
$1.0 \times 10^{-5}$	$2.0 \times 10^{-4}$	$1.1 \times 10^{-3}$
$1.0 \times 10^{-5}$	$3.0 \times 10^{-4}$	$1.8 \times 10^{-3}$
$1.0 \times 10^{-5}$	$3.9 \times 10^{-4}$	$2.2 \times 10^{-3}$

$$k_2 = 5.6 \text{ L mol}^{-1} \text{ s}^{-1}$$

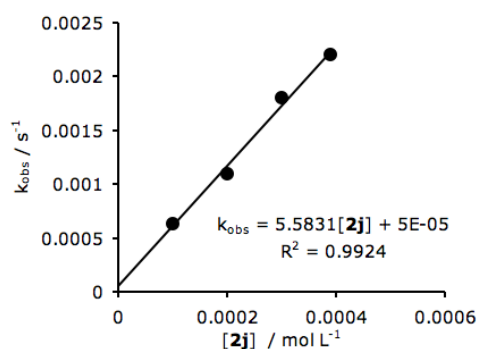
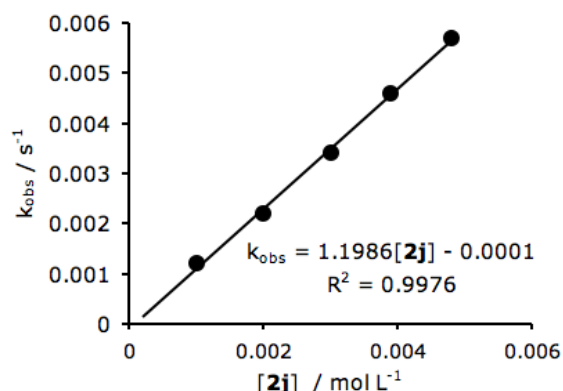
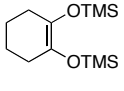


Table S27. Kinetics of the reaction of **2j** with  $\text{dpa}_2\text{CH}^+$  in  $\text{CH}_2\text{Cl}_2$  (20 °C, Conventional UV/Vis, at 672 nm)

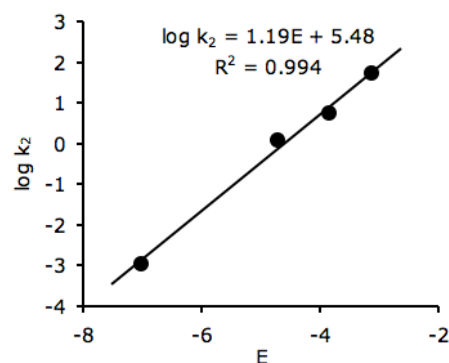
$[\text{dpa}_2\text{CH}^+]$ / $\text{mol L}^{-1}$	$[\mathbf{2j}]$ / $\text{mol L}^{-1}$	$k_{\text{obs}}$ / $\text{s}^{-1}$
$1.0 \times 10^{-5}$	$1.0 \times 10^{-3}$	$1.2 \times 10^{-3}$
$1.0 \times 10^{-5}$	$2.0 \times 10^{-3}$	$2.2 \times 10^{-3}$
$1.0 \times 10^{-5}$	$3.0 \times 10^{-3}$	$3.4 \times 10^{-3}$
$1.0 \times 10^{-5}$	$3.9 \times 10^{-3}$	$4.6 \times 10^{-3}$
$1.0 \times 10^{-5}$	$4.8 \times 10^{-3}$	$5.7 \times 10^{-3}$

$$k_2 = 1.2 \text{ L mol}^{-1} \text{ s}^{-1}$$

Table S28. Determination of the nucleophilicity parameters ( $N$  and  $s_N$ ) of **2j**.

<b>2j</b>	Electrophile	$E$	$k_2$ / $\text{L mol}^{-1} \text{ s}^{-1}$	$\log k_2$
	$\text{dma}_2\text{CH}^+$	-7.02	$1.2 \times 10^{-3}$ <sup>a</sup>	-2.94
	$\text{dpa}_2\text{CH}^+$	-4.72	1.2	0.08
	$\text{mfa}_2\text{CH}^+$	-3.85	5.6	0.75
	$\text{pfa}_2\text{CH}^+$	-3.14	$5.4 \times 10^1$	1.73

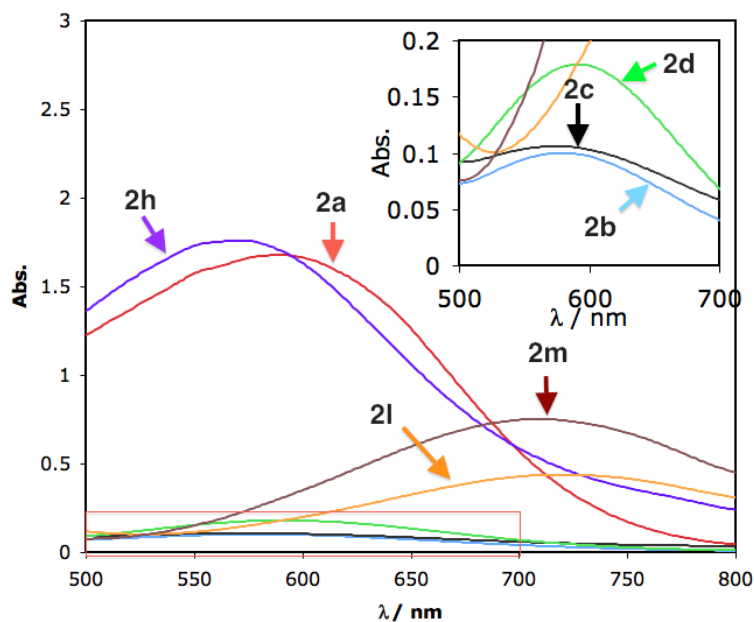
$$N = 4.61, s_N = 1.19$$



<sup>a</sup>From ref. 32

### 5) Vis Spectra of the Charge Transfer Complexes of DDQ with **2(a-d, h, l, m)**

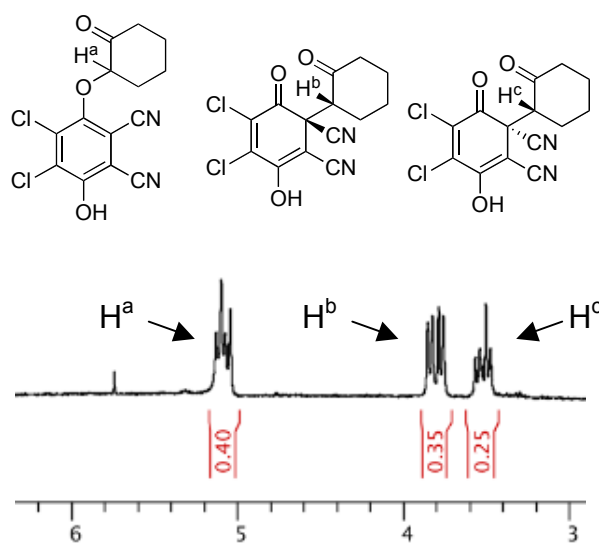
The UV-vis spectra of the charge transfer (CT) complexes of DDQ ( $0.01 \text{ mol L}^{-1}$ ) with **2(a-d, h, l, m)** ( $0.01 \text{ mol L}^{-1}$ ) were recorded by using a conventional UV/Vis diode array spectrophotometer (J&M TIDAS) connected to a Hellma 661.502-QX quartz Suprasil immersion probe (5 mm light path) via fiber optic cables in  $\text{CH}_2\text{Cl}_2$  at -80 °C. The spectra were taken immediately just after mixing the reactants. The low absorbance of the CT complexes of DDQ with **2b-d** was attributed to their fast reactions and the limit of mixing speed of conventional stirring.

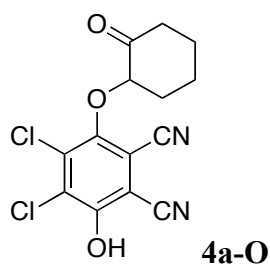


**Figure S1.** Characteristic Absorption Bands of the CT Complexes of Nucleophiles **2(a-d, h, l, m)** with DDQ in  $\text{CH}_2\text{Cl}_2$  at  $-80\text{ }^\circ\text{C}$

#### 6) Solvent Effects on the Reaction of DDQ with **2a**

**General procedure for the solvent effects on the reaction of DDQ with **2a** (entry 1, Scheme 9).** A solution of DDQ (22.7 mg, 0.100 mmol) and **2a** (170 mg, 1.00 mmol) in  $\text{CH}_2\text{Cl}_2$  (10 mL) was stirred at  $20\text{ }^\circ\text{C}$  for 1 min. One drop of water was added, and then the solvent was removed under reduced pressure. The crude product was analyzed by  $^1\text{H}$  NMR spectroscopy with mesitylene as an internal standard. The ratios of **4a-O** and two diastereoisomers of **4a-C** were obtained by integrating their characteristic proton signals (at  $\delta = 5.07$ , 3.81 and 3.58 ppm, respectively).





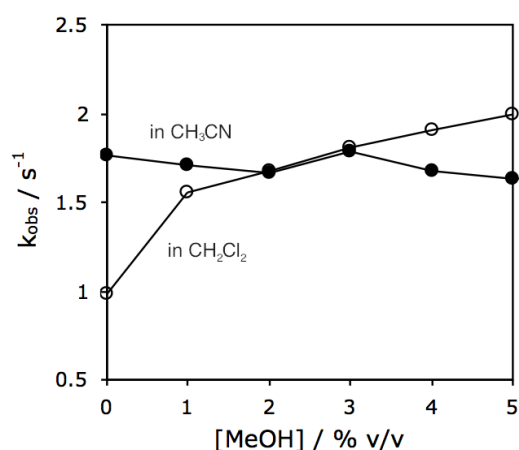
**4,5-Dichloro-3-hydroxy-6-(2-oxocyclohexyloxy)phthalonitrile (4a-O).** A solution of DDQ (114 mg, 0.500 mmol) and **2a** (170 mg, 1.00 mmol) in  $\text{CH}_2\text{Cl}_2$  (50 mL) was stirred at 20 °C for 1 min. The solvent was removed under reduced pressure. The crude material was purified by flash column chromatography (silica gel, eluent: acetic acid/ethyl acetate/pentane = 1/10/20) to give **4a-O** (107 mg, 66%).  $^1\text{H}$  NMR ( $\text{d}_6$ -DMSO, 400 MHz)  $\delta$  9.96 (s, 1 H), 5.07 (dd,  $J$  = 11.2, 6.8 Hz, 1 H), 2.50-2.44 (m, 1 H), 2.40-2.32 (m, 2 H), 1.98-1.90 (m, 1 H), 1.90-1.80 (m, 2 H), 1.80-1.55 (m, 2 H);  $^{13}\text{C}$  NMR ( $\text{d}_6$ -DMSO, 101 MHz)  $\delta$  204.9, 154.4, 149.3, 133.4, 129.1, 113.6, 113.3, 108.4, 101.9, 85.8, 40.3, 33.9, 26.5, 22.8; MS (EI)  $m/z$  (%): 326 ( $\text{M}^+ + 2$ ), 324 ( $\text{M}^+$ ), 281, 270, 268, 255, 230, 228, 202, 200, 194, 166, 110, 98, 70, 55 (100); HRMS (EI) calcd for  $\text{C}_{14}\text{H}_{10}^{35}\text{Cl}_2\text{N}_2\text{O}_3$ : 324.0063; found: 324.0064.

The  $^1\text{H}$  and  $^{13}\text{C}$  NMR spectra agree with ref. S1.

#### Methanol effects on kinetics of the reaction of DDQ with **2a**.

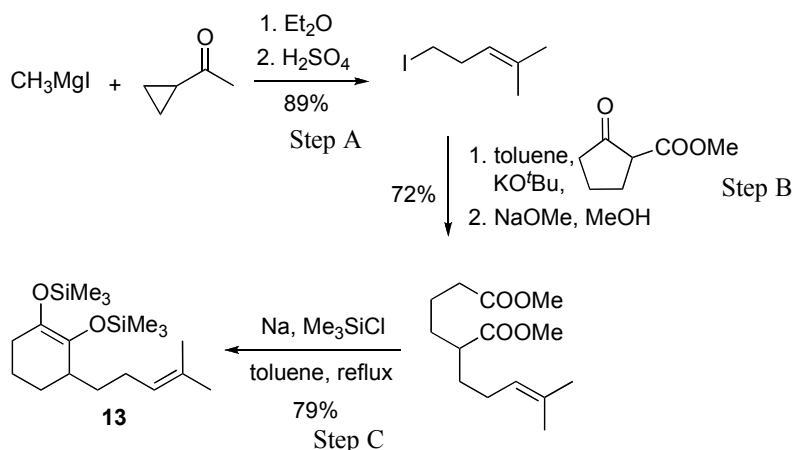
**Table S29.** Effect of methanol on the rate of the reaction of DDQ ( $5.00 \times 10^{-3} \text{ mol L}^{-1}$ ) with **2a** ( $5.00 \times 10^{-2} \text{ mol L}^{-1}$ ) in  $\text{CH}_2\text{Cl}_2$  and in  $\text{CH}_3\text{CN}$  (monitoring the CT complex at 570 nm)

[MeOH] / %v/v	$k_{\text{obs}} / \text{s}^{-1}$ (in $\text{CH}_2\text{Cl}_2$ )	$k_{\text{obs}} / \text{s}^{-1}$ (in $\text{CH}_3\text{CN}$ )
0	0.98	1.76
1.0	1.55	1.71
2.0	1.68	1.66
3.0	1.81	1.79
4.0	1.91	1.68
5.0	2.00	1.63



## 7) Radical Clock Experiments.

## Procedure for synthesis of 13

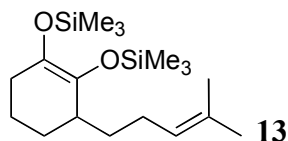


**Step A**<sup>[30]</sup>: A solution of cyclopropyl methyl ketone (8.4 g, 0.10 mol) in diethyl ether (50 mL) was slowly added via addition funnel to a solution of MeMgI (50 mL of a 2 M solution in diethyl ether, 100 mmol) at 0 °C under nitrogen. Then the solution was allowed to stir at room temperature for 1 hour. The reaction mixture was poured into a cooled 25% aqueous  $\text{H}_2\text{SO}_4$  solution (100 mL) and allowed to stir for 1 h at room temperature. The aqueous layer was separated and extracted with diethyl ether (2 x 50 mL). The combined organic layers were then washed with brine, dried with  $\text{Na}_2\text{SO}_4$ , and concentrated under reduced pressure. The resulting residue was purified by distillation (70 °C, 10 mbar) to give 5-iodo-2-methylpent-2-ene (18.7 g, 89% yield).

**Step B**:  $\text{KO}^t\text{Bu}$  (6.2 g, 55 mmol) was slowly added to a mixture of methyl 2-oxocyclopentanecarboxylate (7.1 g, 50 mmol) and 5-iodo-2-methylpent-2-ene (10.5 g, 50 mmol) in toluene (100 mL). Then the mixture was stirred for 6 h at 80 °C. After removing the solvent under vacuum the residue was dissolved in methanol (100 mL) and NaOMe (2.7 g, 50 mmol) was added to the resulting solution. Then the solution was allowed to stir under reflux for 4 h. The solvent was removed under reduced pressure.  $\text{H}_2\text{O}$  100 mL was added and extract with diethyl ether (2 x 50 mL). The combined organic layers were then washed with brine, dried with  $\text{Na}_2\text{SO}_4$ , and concentrated under reduced pressure. The resulting residue was purified by distillation (130 °C, 1 mbar) to give dimethyl 2-(4-methylpent-3-enyl)hexanedioate (9.2 g, 72% yield).

**Step C**: Sodium (1.8 g, 80 mmol) was stirred vigorously in refluxing toluene (100 mL) until sodium sand was obtained. After being cooled to room temperature, chlorotrimethylsilane (8.7 g, 80 mmol) and dimethyl 2-(4-methylpent-3-enyl)hexanedioate (5.1 g, 20 mmol) were added to the mixture. After being refluxed for 1.5 h, the mixture was filtrated immediately

and the solvent was evaporated under reduced pressure. The residue was purified by Kugelrohr distillation to afford **13** (5.4 g, 79% yield).



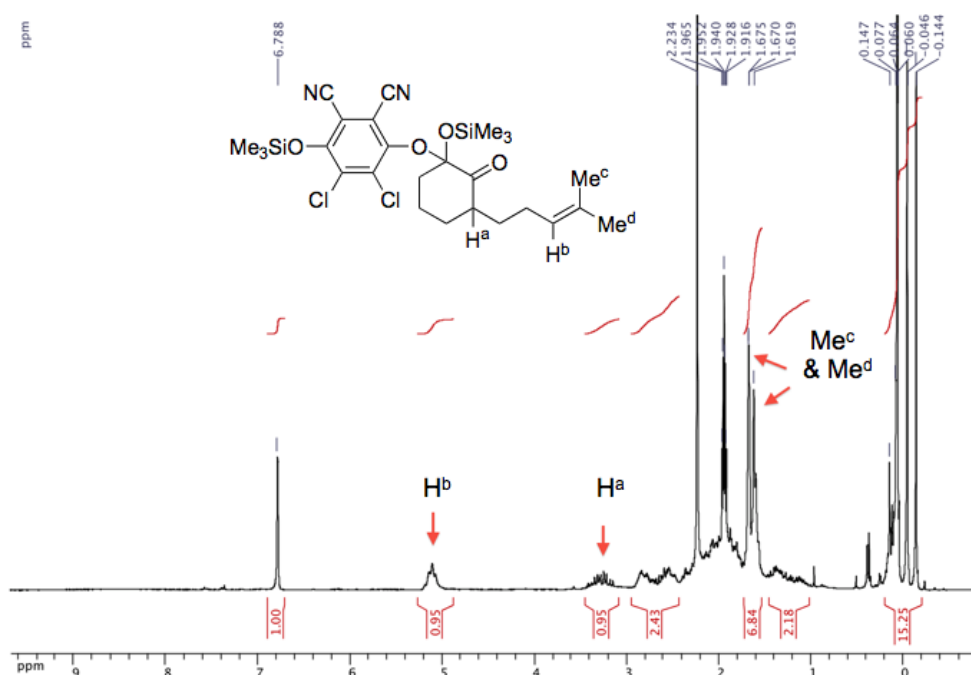
**(3-(4-Methylpent-3-enyl)cyclohex-1-ene-1,2-diyl)bis(oxy)bis(trimethylsilane) (13).**

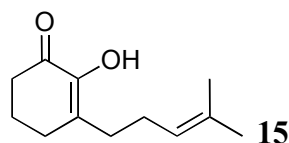
Colorless oil. IR (neat):  $\nu_{\text{max}}$  2956, 2928, 2858, 1715, 1694, 1682, 1447, 1355, 1345, 1249, 1212, 1123, 950, 903, 840, 750  $\text{cm}^{-1}$ ;  $^1\text{H}$  NMR ( $\text{CDCl}_3$ , 300 MHz)  $\delta$  5.13-5.07 (m, 1 H), 2.46-2.22 (m, 1 H), 2.10-1.84 (m, 6 H), 1.75-1.62 (m, 6 H), 1.58 (s, 3 H), 1.52-1.42 (m, 1 H), 1.40-1.30 (m, 1 H), 1.29-1.14 (m, 1 H), 0.13 (s, 18 H);  $^{13}\text{C}$  NMR ( $\text{CDCl}_3$ , 75.5 MHz)  $\delta$  135.8, 133.1, 131.5, 125.1, 38.8, 32.8, 30.2, 28.3, 25.9, 25.7, 21.0, 17.8, 1.2, 1.0; MS (EI)  $m/z$  (%): 340 ( $\text{M}^+$ ), 258, 257, 169, 82, 73 (100); HRMS (EI) calcd for  $\text{C}_{18}\text{H}_{36}\text{O}_2\text{Si}_2$ : 340.2248; found: 340.2250.

**Procedure for radical clock experiment.**

A solution of DDQ (114 mg, 0.500 mmol) and **13** (170 mg, 0.500 mmol) in  $\text{CH}_3\text{CN}$  was stirred at 20  $^\circ\text{C}$  for 1 min. The solvent was removed under reduced pressure. The crude material was analyzed by  $^1\text{H}$  NMR spectroscopy with mesitylene as an internal standard and then purified by flash column chromatography (silica gel, eluent: ethyl acetate/pentane = 1/20) to give **15** (58 mg, 60% yield).

**$^1\text{H}$  NMR of the crude material of the reaction of **13** with DDQ.**





**2-Hydroxy-3-(4-methylpent-3-enyl)cyclohex-2-enone (15).** Colorless oil. IR (neat):  $\nu_{\max}$  3419, 2924, 2862, 1671, 1645, 1436, 1383, 1325, 1278, 1196, 1166, 1128, 877, 800  $\text{cm}^{-1}$ ;  $^1\text{H}$  NMR ( $\text{CDCl}_3$ , 300 MHz)  $\delta$  6.02 (s, 1 H), 5.13-5.09 (m, 1 H), 2.46 (t,  $J = 6.9$  Hz, 2 H), 2.39-2.28 (m, 4 H), 2.16 (q,  $J = 7.5$  Hz, 2 H), 1.93 (quintet,  $J = 6.3$  Hz, 2 H), 1.67 (s, 3 H), 1.59 (s, 3 H);  $^{13}\text{C}$  NMR ( $\text{CDCl}_3$ , 75.5 MHz)  $\delta$  194.8, 143.9, 134.7, 132.6, 123.7, 36.1, 31.3, 28.9, 25.9, 25.8, 22.7, 17.9; MS (EI)  $m/z$  (%): 194 ( $\text{M}^+$ ), 126, 112, 79, 69 (100), 53, 41; HRMS (EI) calcd for  $\text{C}_{12}\text{H}_{18}\text{O}_2$ : 194.1301; found: 194.1302.

## 8) Quantum Chemical Calculations of Adiabatic Ionization Potentials

All calculations were carried out with Gaussian 09 at G3MP2 level of theory. Conformer search was carried out with Avogadro 1.1.0 software by using molecular mechanics with force field MMFF94. Three most stable conformers of each compound were subjected to Gaussian 09 for structure optimization and energy calculations. In some cases, same structures were obtained after structure optimizations from different conformers. The adiabatic ionization potentials were calculated as the difference of the enthalpies of the radical cations and those of the neutral molecules (with lowest energies among the conformers) in gas phase. Only the most stable conformer for each compound was listed as follow.

2a

O	0.59667	-0.39176	-0.92547
Si	1.90847	0.00424	0.06849
C	3.35286	-0.90152	-0.69678
H	3.17415	-1.97983	-0.71299
H	3.51598	-0.57417	-1.72719
H	4.27558	-0.71994	-0.13703
C	1.56039	-0.58984	1.81321
H	2.38405	-0.32994	2.48590
H	0.65159	-0.12678	2.20915
H	1.42970	-1.67513	1.84758
C	2.23096	1.85228	0.08394
H	3.15710	2.07217	0.62559
H	2.33735	2.24407	-0.93171
H	1.42200	2.39971	0.57477
C	-0.70923	-0.13866	-0.53757
C	-1.22235	1.10180	-0.50220
C	-2.63666	1.37706	-0.07444
H	-0.60137	1.93613	-0.81996
H	-3.24847	1.64081	-0.94931
H	-2.65967	2.25611	0.58206



## Chapter 2: Manifestation of Polar Reaction Pathways of DDQ

C	-1.48797	-1.37985	-0.21815
H	-1.25681	-2.12947	-0.98428
H	-1.13109	-1.79590	0.73449
C	-2.98771	-1.10010	-0.15389
H	-3.37766	-0.97738	-1.17194
H	-3.51200	-1.95469	0.28812
C	-3.25300	0.17558	0.63832
H	-2.80756	0.07781	1.63664
H	-4.32842	0.33059	0.78034

-----			
Temperature=	298.150000	Pressure=	1.000000
E(ZPE)=	0.241068	E(Thermal)=	0.255972
E(QCISD(T))=	-716.729721	E(Empiric)=	-0.296928
DE(MP2)=	-0.613483		
G3MP2 (0 K)=	-717.399064	G3MP2 Energy=	-717.384160
G3MP2 Enthalpy=	-717.383216	G3MP2 Free Energy=	-717.442181
-----			

### 2a<sup>+</sup>

O	-0.46868	0.80039	0.05113
Si	-2.08231	-0.03859	-0.01247
C	-2.24931	-0.88649	1.63441
H	-1.58708	-1.74733	1.75340
H	-2.06985	-0.19355	2.46080
H	-3.27569	-1.25460	1.73870
C	-2.04056	-1.16759	-1.49070
H	-3.06583	-1.48105	-1.71574
H	-1.66278	-0.65820	-2.38186
H	-1.45520	-2.07528	-1.32983
C	-3.18963	1.42989	-0.22348
H	-4.23597	1.11082	-0.26190
H	-3.08809	2.13091	0.60875
H	-2.97397	1.96582	-1.15133
C	0.75565	0.39764	0.02918
C	1.74358	1.41562	0.08811
C	3.19262	1.12940	0.06057
H	1.38274	2.43726	0.18401
H	3.57401	1.32770	1.07786
H	3.69347	1.87388	-0.57149
C	1.13560	-1.04243	-0.07796
H	0.43605	-1.64517	0.51038
H	0.99364	-1.33572	-1.12890
C	2.58785	-1.28720	0.34097
H	2.68062	-1.18343	1.42823
H	2.85684	-2.31854	0.09761
C	3.51817	-0.30356	-0.35889
H	3.41334	-0.40342	-1.44530
H	4.56181	-0.52463	-0.12104

-----			
Temperature=	298.150000	Pressure=	1.000000
E(ZPE)=	0.240388	E(Thermal)=	0.255550
E(QCISD(T))=	-716.468744	E(Empiric)=	-0.292120
DE(MP2)=	-0.593313		
G3MP2(0 K)=	-717.113789	G3MP2 Energy=	-717.098627
G3MP2 Enthalpy=	-717.097683	G3MP2 Free Energy=	-717.156678
-----			

### 2b

O	0.21900	0.85419	-0.00919
Si	1.68148	-0.01035	0.00899
C	2.97870	1.33365	0.00231

H	2.88818	1.96043	-0.88872
H	2.87663	1.97991	0.87807
H	3.98710	0.90850	0.01372
C	1.82259	-1.07560	-1.52741
H	2.79290	-1.58182	-1.55487
H	1.04460	-1.84114	-1.57431
H	1.74057	-0.46282	-2.42960
C	1.80747	-1.04091	1.57024
H	2.78029	-1.54045	1.62203
H	1.70982	-0.40850	2.45721
H	1.03346	-1.80999	1.62497
C	-1.03957	0.32861	-0.02611
C	-2.17993	1.30132	-0.14881
C	-1.45769	-0.95049	0.00490
C	-3.38785	0.43117	0.22569
H	-2.24158	1.67788	-1.17871
H	-2.04540	2.16904	0.50482
C	-2.95759	-1.01294	-0.10700
H	-0.82630	-1.83138	0.04162
H	-3.56281	0.51002	1.30307
H	-4.30844	0.72985	-0.28373
H	-3.41143	-1.74264	0.57292
H	-3.26706	-1.29444	-1.12365

```

-----
Temperature=      298.150000 Pressure=      1.000000
E(ZPE)=          0.213072 E(Thermal)=      0.226987
E(QCISD(T))=     -677.539158 E(Empirc)=     -0.269091
DE(MP2)=         -0.561820
G3MP2 (0 K)=     -678.156998 G3MP2 Energy=   -678.143082
G3MP2 Enthalpy=  -678.142138 G3MP2 Free Energy= -678.198219
-----

```

**2b\*\***

O	0.17315	0.79282	-0.06916
Si	1.78847	-0.05577	0.02087
C	2.92490	1.40309	0.00715
H	2.80755	1.99312	-0.90529
H	2.74631	2.05777	0.86385
H	3.96681	1.07107	0.05539
C	1.86158	-1.10629	-1.51197
H	2.87068	-1.51988	-1.61231
H	1.17010	-1.95235	-1.49612
H	1.66590	-0.51596	-2.41132
C	1.74910	-0.98980	1.62850
H	2.74756	-1.39166	1.83101
H	1.49105	-0.33500	2.46534
H	1.05865	-1.83678	1.62639
C	-1.03197	0.37154	-0.07945
C	-2.19417	1.30546	-0.17401
C	-1.49245	-0.97860	-0.03413
C	-3.38857	0.44239	0.26049
H	-2.28158	1.62098	-1.22433
H	-2.02873	2.21036	0.41721
C	-2.97003	-1.00333	-0.08330
H	-0.85143	-1.85249	-0.00491
H	-3.54039	0.53422	1.33875
H	-4.31652	0.73447	-0.23234
H	-3.39875	-1.76621	0.57525
H	-3.28139	-1.28025	-1.10516

```

-----
Temperature=      298.150000 Pressure=      1.000000
E(ZPE)=          0.212055 E(Thermal)=      0.226250

```

E(QCISD(T))=	-677.275831	E(Empiric)=	-0.264283
DE(MP2)=	-0.541418		
G3MP2 (0 K)=	-677.869478	G3MP2 Energy=	-677.855283
G3MP2 Enthalpy=	-677.854339	G3MP2 Free Energy=	-677.911348

2c

O	0.90382	-0.47564	-0.92166
Si	2.16926	-0.01034	0.10048
C	3.63993	-0.98653	-0.51411
H	3.45120	-2.06129	-0.44873
H	3.85610	-0.74814	-1.55909
H	4.53628	-0.76409	0.07306
C	1.73041	-0.45682	1.86914
H	2.53061	-0.16280	2.55605
H	0.81758	0.05603	2.18714
H	1.57074	-1.53289	1.98214
C	2.51359	1.83028	-0.01502
H	3.40662	2.08705	0.56467
H	2.68830	2.13655	-1.05044
H	1.68181	2.42164	0.37666
C	-0.41792	-0.17740	-0.60411
C	-0.88789	1.07186	-0.77033
C	-2.25527	1.57207	-0.38478
H	-0.19830	1.79795	-1.19581
H	-2.95422	1.52689	-1.23293
H	-2.15473	2.63796	-0.14795
C	-1.18727	-1.39927	-0.17924
H	-0.73478	-2.23386	-0.72688
H	-1.01800	-1.61186	0.88636
C	-2.68158	-1.33553	-0.49020
H	-2.79905	-0.94228	-1.50633
H	-3.09021	-2.35287	-0.50733
C	-3.49573	-0.49335	0.48983
H	-4.49270	-0.32606	0.06304
H	-3.64932	-1.05724	1.41861
C	-2.85552	0.85355	0.82642
H	-3.60746	1.49305	1.30405
H	-2.05723	0.71305	1.56478

Temperature=	298.150000	Pressure=	1.000000
E(ZPE)=	0.268791	E(Thermal)=	0.284817
E(QCISD(T))=	-755.903577	E(Empiric)=	-0.324765
DE(MP2)=	-0.665862		
G3MP2 (0 K)=	-756.625413	G3MP2 Energy=	-756.609386
G3MP2 Enthalpy=	-756.608442	G3MP2 Free Energy=	-756.669246

2c<sup>+</sup>

O	0.77456	0.78441	-0.21032
Si	2.36365	-0.05445	0.06553
C	2.58294	-1.20240	-1.38211
H	1.94018	-2.08509	-1.34827
H	2.41382	-0.68610	-2.33101
H	3.61846	-1.55966	-1.39055
C	2.23726	-0.87640	1.72974
H	3.23961	-1.18761	2.04321
H	1.86521	-0.18712	2.49310
H	1.60850	-1.76931	1.72843
C	3.49703	1.40943	0.03678

H	4.53297	1.08735	0.18249
H	3.44620	1.93628	-0.91941
H	3.25712	2.11927	0.83244
C	-0.46661	0.42917	-0.16229
C	-1.38260	1.49345	-0.39631
C	-2.85356	1.46483	-0.22713
H	-0.91261	2.42391	-0.70925
H	-3.31258	1.35261	-1.22504
H	-3.15207	2.46879	0.09872
C	-0.86603	-0.99090	0.08546
H	-0.04278	-1.62545	-0.25333
H	-0.94934	-1.14670	1.17108
C	-2.16840	-1.38675	-0.62279
H	-2.17642	-0.94303	-1.62499
H	-2.15558	-2.46936	-0.78055
C	-3.43176	-1.00303	0.14630
H	-4.29005	-1.09322	-0.52825
H	-3.60014	-1.72015	0.95716
C	-3.38820	0.40489	0.73738
H	-4.39585	0.69615	1.04806
H	-2.78273	0.42181	1.65103

```

-----
Temperature=          298.150000 Pressure=          1.000000
E(ZPE)=              0.268094 E(Thermal)=          0.284532
E(QCISD(T))=        -755.644489 E(Empiric)=        -0.319957
DE(MP2)=             -0.645919
G3MP2(0 K)=         -756.342271 G3MP2 Energy=      -756.325833
G3MP2 Enthalpy=     -756.324889 G3MP2 Free Energy=   -756.386853
-----

```

2d

C	0.00535	1.12827	-0.68255
C	-0.15632	2.45979	-0.74994
H	-1.11458	2.88640	-1.02172
H	0.67785	3.12985	-0.58325
O	-1.02726	0.27023	-1.01598
Si	-2.04999	-0.35317	0.18856
C	-3.01228	-1.69534	-0.68462
H	-3.55132	-1.29188	-1.54598
H	-2.34474	-2.48260	-1.04529
H	-3.74497	-2.15609	-0.01490
C	-3.18117	1.00814	0.80454
H	-3.86180	0.63270	1.57544
H	-2.60584	1.83032	1.23956
H	-3.78684	1.41603	-0.00963
C	-1.03729	-1.03868	1.60824
H	-1.69544	-1.46237	2.37439
H	-0.35680	-1.82514	1.27131
H	-0.43134	-0.26127	2.08207
C	1.27717	0.45966	-0.33831
C	2.17400	1.03046	0.57498
C	1.59529	-0.77090	-0.92970
C	3.37659	0.39324	0.87308
H	1.91492	1.96448	1.06807
C	2.79792	-1.40563	-0.62752
H	0.89773	-1.21268	-1.63567
C	3.69276	-0.82662	0.27366
H	4.06152	0.84205	1.58842
H	3.03894	-2.35591	-1.09799
H	4.62861	-1.32577	0.51195

## Chapter 2: Manifestation of Polar Reaction Pathways of DDQ

Temperature=	298.150000	Pressure=	1.000000
E(ZPE)=	0.228841	E(Thermal)=	0.244698
E(QCISD(T))=	-791.539325	E(Empiric)=	-0.324765
DE(MP2)=	-0.663699		
G3MP2 (0 K)=	-792.298948	G3MP2 Energy=	-792.283091
G3MP2 Enthalpy=	-792.282146	G3MP2 Free Energy=	-792.343330

2d<sup>+</sup>

C	-0.23445	-0.70653	-0.00007
C	0.14227	-2.09375	0.00003
H	1.18482	-2.37646	-0.00018
H	-0.58806	-2.88870	0.00028
O	0.69262	0.19977	-0.00020
Si	2.48751	0.22737	0.00003
C	2.78452	2.05701	-0.00061
H	2.35622	2.53158	-0.88728
H	2.35586	2.53226	0.88552
H	3.85865	2.26731	-0.00047
C	3.03067	-0.61117	-1.57118
H	4.10003	-0.42739	-1.71971
H	2.88940	-1.69447	-1.56624
H	2.50953	-0.20114	-2.44072
C	3.03007	-0.61007	1.57202
H	4.09955	-0.42688	1.72046
H	2.50914	-0.19891	2.44115
H	2.88805	-1.69327	1.56805
C	-1.60027	-0.25205	-0.00004
C	-2.66947	-1.14267	-0.00005
C	-1.85947	1.11847	-0.00001
C	-3.94551	-0.68785	-0.00003
H	-2.50938	-2.21590	-0.00010
C	-3.12946	1.57733	0.00002
H	-1.02737	1.81588	-0.00001
C	-4.16249	0.66701	0.00001
H	-4.78374	-1.37589	-0.00005
H	-3.34108	2.64123	0.00005
H	-5.18617	1.03493	0.00003

Temperature=	298.150000	Pressure=	1.000000
E(ZPE)=	0.226172	E(Thermal)=	0.242768
E(QCISD(T))=	-791.264690	E(Empiric)=	-0.319957
DE(MP2)=	-0.643306		
G3MP2 (0 K)=	-792.001781	G3MP2 Energy=	-791.985185
G3MP2 Enthalpy=	-791.984241	G3MP2 Free Energy=	-792.047430

2e

C	2.91107	0.95886	-0.00006
H	3.87101	0.43928	-0.00002
H	2.85249	1.60328	-0.88183
H	2.85244	1.60332	0.88167
C	1.77139	-0.01046	-0.00007
C	1.91598	-1.34375	-0.00002
H	1.08045	-2.03132	-0.00004
H	2.90927	-1.77356	0.00002
O	0.57188	0.65859	-0.00013
Si	-1.00890	0.04350	0.00002
C	-2.06412	1.58548	-0.00006
H	-1.86297	2.19723	0.88329
H	-1.86308	2.19706	-0.88356
H	-3.12937	1.33442	0.00003
C	-1.32839	-0.96413	1.54934
H	-2.37977	-1.26609	1.59512

H	-0.71899	-1.86949	1.59648
H	-1.11322	-0.37240	2.44365
C	-1.32859	-0.96441	-1.54908
H	-2.38001	-1.26630	-1.59472
H	-1.11346	-0.37287	-2.44352
H	-0.71928	-1.86983	-1.59610

Temperature=	298.150000	Pressure=	1.000000
E(ZPE)=	0.177675	E(Thermal)=	0.190603
E(QCISD(T))=	-600.353626	E(Empirc)=	-0.222696
DE(MP2)=	-0.480367		
G3MP2 (0 K)=	-600.879014	G3MP2 Energy=	-600.866087
G3MP2 Enthalpy=	-600.865143	G3MP2 Free Energy=	-600.918389

2e<sup>+</sup>

C	-2.94284	0.96623	-0.00015
H	-3.56167	0.76509	-0.88132
H	-3.56288	0.76435	0.87997
H	-2.62308	2.00692	0.00041
C	-1.76449	0.06090	0.00010
C	-1.94495	-1.35940	-0.00004
H	-1.10551	-2.04068	-0.00028
H	-2.94581	-1.77224	-0.00001
O	-0.60777	0.59758	0.00014
Si	1.13801	0.01125	0.00004
C	2.00874	1.64177	-0.00184
H	1.75841	2.22959	-0.88850
H	1.75860	2.23153	0.88360
H	3.09269	1.48856	-0.00179
C	1.31049	-0.96064	-1.57475
H	2.37260	-1.16894	-1.74293
H	0.79585	-1.92429	-1.55906
H	0.95663	-0.39169	-2.43893
C	1.31098	-0.95759	1.57663
H	2.37293	-1.16744	1.74392
H	0.95914	-0.38620	2.44000
H	0.79456	-1.92033	1.56357

Temperature=	298.150000	Pressure=	1.000000
E(ZPE)=	0.175882	E(Thermal)=	0.188662
E(QCISD(T))=	-600.075324	E(Empirc)=	-0.217888
DE(MP2)=	-0.458418		
G3MP2 (0 K)=	-600.575748	G3MP2 Energy=	-600.562967
G3MP2 Enthalpy=	-600.562023	G3MP2 Free Energy=	-600.615171

2f

O	-1.64501	1.14009	-0.00005
Si	-2.58162	-0.29215	0.00002
C	-4.32113	0.39153	-0.00011
H	-4.49933	1.01047	0.88319
H	-4.49927	1.01031	-0.88353
H	-5.06032	-0.41556	-0.00006
C	-2.26464	-1.28952	1.55219
H	-2.98347	-2.11155	1.63342
H	-1.25855	-1.71359	1.55374
H	-2.37273	-0.66481	2.44367
C	-2.26451	-1.28977	-1.55197
H	-2.98336	-2.11178	-1.63316
H	-2.37247	-0.66517	-2.44355

H	-1.25842	-1.71386	-1.55334
C	-0.30130	1.21678	-0.00007
C	0.37792	2.36923	-0.00025
H	-0.17836	3.29535	-0.00039
H	1.45659	2.39410	-0.00025
O	0.25101	-0.05374	0.00011
C	1.64224	-0.12939	0.00006
C	2.31646	-0.19739	-1.21559
C	2.31656	-0.19711	1.21567
C	3.70344	-0.34083	-1.20903
H	1.75154	-0.14319	-2.14190
C	3.70355	-0.34055	1.20903
H	1.75172	-0.14269	2.14201
C	4.39779	-0.41078	-0.00002
H	4.24206	-0.39907	-2.15123
H	4.24224	-0.39857	2.15120
H	5.47844	-0.52414	-0.00006

```

-----
Temperature=          298.150000 Pressure=          1.000000
E(ZPE)=              0.232826 E(Thermal)=          0.249806
E(QCISD(T))=        -866.571700 E(Empirc)=         -0.352602
DE(MP2)=             -0.745548
G3MP2(0 K)=         -867.437024 G3MP2 Energy=        -867.420044
G3MP2 Enthalpy=     -867.419100 G3MP2 Free Energy=    -867.483734
-----

```

2r<sup>+</sup>

O	-1.35459	-0.00075	-0.57140
Si	-3.07474	-0.00002	0.01028
C	-3.25876	1.57184	0.98708
H	-2.71971	1.56665	1.93768
H	-2.93304	2.44107	0.40917
H	-4.31791	1.72102	1.22237
C	-3.25849	-1.56944	0.99102
H	-4.31750	-1.71780	1.22750
H	-2.93338	-2.44013	0.41499
H	-2.71868	-1.56203	1.94118
C	-3.96533	-0.00204	-1.60995
H	-5.04776	-0.00195	-1.44745
H	-3.71791	0.88256	-2.20203
H	-3.71774	-0.88801	-2.19991
C	-0.19510	-0.00015	-0.04634
C	0.04171	0.00232	1.37531
H	-0.79869	0.00459	2.05305
H	1.04672	0.00187	1.77001
O	0.78099	-0.00209	-0.91378
C	2.14036	-0.00098	-0.46015
C	2.76725	1.22492	-0.29539
C	2.76833	-1.22599	-0.29295
C	4.11086	1.21222	0.08303
H	2.23282	2.15279	-0.47831
C	4.11192	-1.21135	0.08544
H	2.23467	-2.15467	-0.47397
C	4.77819	0.00092	0.27569
H	4.63551	2.15325	0.21877
H	4.63739	-2.15164	0.22307
H	5.82481	0.00167	0.56464

```

-----
Temperature=          298.150000 Pressure=          1.000000
E(ZPE)=              0.231419 E(Thermal)=          0.249036
E(QCISD(T))=        -866.306808 E(Empirc)=         -0.347794
DE(MP2)=             -0.724572
G3MP2(0 K)=         -867.147754 G3MP2 Energy=        -867.130138
-----

```

G3MP2 Enthalpy= -867.129193 G3MP2 Free Energy= -867.195633

2g

C	0.27337	2.88596	0.00004
H	-0.72790	3.28690	0.00002
H	1.10954	3.56969	0.00011
C	0.52473	1.56920	-0.00005
C	-1.77531	0.93943	-0.00003
H	-1.98344	1.54800	-0.88917
H	-1.98333	1.54791	0.88921
C	-2.59542	-0.33226	-0.00005
H	-2.32619	-0.92574	0.88110
H	-2.32629	-0.92565	-0.88128
C	-4.09485	-0.04971	0.00005
H	-4.35145	0.55467	0.87842
H	-4.35155	0.55475	-0.87824
C	-4.92443	-1.32890	0.00003
H	-4.70543	-1.93478	0.88396
H	-5.99523	-1.10845	0.00010
H	-4.70553	-1.93470	-0.88397
O	1.78084	1.07170	-0.00007
Si	2.21027	-0.58160	0.00001
C	4.07781	-0.49167	0.00005
H	4.51996	-1.49285	0.00009
H	4.44470	0.03776	-0.88323
H	4.44467	0.03780	0.88332
C	1.59616	-1.43280	-1.55096
H	2.01472	-2.44179	-1.62684
H	0.50734	-1.51174	-1.55528
H	1.90018	-0.87878	-2.44382
C	1.59608	-1.43264	1.55104
H	2.01467	-2.44161	1.62707
H	1.90002	-0.87850	2.44386
H	0.50726	-1.51162	1.55529
O	-0.39576	0.55724	-0.00013

Temperature= 298.150000 Pressure= 1.000000  
 E(ZPE)= 0.264563 E(Thermal)= 0.282599  
 E(QCISD(T))= -792.936368 E(Empiric)= -0.334044  
 DE(MP2)= -0.717348  
 G3MP2(0 K)= -793.723196 G3MP2 Energy= -793.705160  
 G3MP2 Enthalpy= -793.704216 G3MP2 Free Energy= -793.770649

2g\*\*

C	-0.27572	2.88960	0.00000
H	0.71484	3.31843	0.00000
H	-1.14379	3.53338	-0.00000
C	-0.50113	1.46860	-0.00000
C	1.88117	0.95418	0.00000
H	2.06361	1.54916	0.89798
H	2.06361	1.54916	-0.89798
C	2.66618	-0.33291	-0.00000
H	2.39450	-0.91954	-0.88391
H	2.39449	-0.91954	0.88391
C	4.17014	-0.05357	0.00000
H	4.43142	0.54574	-0.87980
H	4.43142	0.54574	0.87981
C	4.98236	-1.34408	0.00000
H	4.76135	-1.94616	-0.88524
H	6.05262	-1.12767	0.00000



H	4.76135	-1.94616	0.88524
O	-1.71095	1.05980	-0.00000
Si	-2.32367	-0.66658	0.00000
C	-4.14736	-0.34572	-0.00002
H	-4.69606	-1.29282	-0.00002
H	-4.45662	0.21476	0.88579
H	-4.45660	0.21475	-0.88586
C	-1.67031	-1.41442	1.57053
H	-2.11082	-2.40731	1.70876
H	-0.58506	-1.53405	1.55226
H	-1.94260	-0.81620	2.44435
C	-1.67027	-1.41444	-1.57050
H	-2.11078	-2.40733	-1.70873
H	-1.94255	-0.81623	-2.44434
H	-0.58502	-1.53407	-1.55221
O	0.44618	0.57577	-0.00000

```

-----
Temperature=          298.150000 Pressure=          1.000000
E(ZPE)=              0.263426 E(Thermal)=          0.281971
E(QCISD(T))=        -792.681546 E(Empirc)=         -0.329236
DE(MP2)=             -0.694960
G3MP2(0 K)=         -793.442316 G3MP2 Energy=       -793.423771
G3MP2 Enthalpy=     -793.422827 G3MP2 Free Energy=   -793.490464
-----

```

**2h**

C	-1.08123	0.63769	-0.54370
C	-2.21295	0.02858	-0.15920
O	0.05937	-0.04060	-0.92541
Si	1.44642	0.01227	0.04312
C	2.74737	-0.88904	-0.94892
H	2.42987	-1.91180	-1.16919
H	2.93328	-0.38426	-1.90058
H	3.69474	-0.94147	-0.40366
C	1.10191	-0.84981	1.67173
H	1.96890	-0.79975	2.33812
H	0.25631	-0.38536	2.18754
H	0.85789	-1.90431	1.51503
C	1.93916	1.79669	0.35048
H	2.87955	1.84715	0.90863
H	2.08121	2.33599	-0.59051
H	1.18335	2.33070	0.93365
H	-1.01829	1.72311	-0.63408
C	-2.33432	-1.46163	-0.06047
H	-2.55438	-1.76827	0.96887
H	-3.15984	-1.82156	-0.68510
H	-1.41549	-1.95215	-0.38404
C	-3.42725	0.84307	0.17622
H	-4.26339	0.59014	-0.48587
H	-3.76077	0.64592	1.20158
H	-3.23402	1.91562	0.08248

```

-----
Temperature=          298.150000 Pressure=          1.000000
E(ZPE)=              0.204547 E(Thermal)=          0.219184
E(QCISD(T))=        -639.536316 E(Empirc)=         -0.250533
DE(MP2)=             -0.530656
G3MP2 (0 K)=         -640.112959 G3MP2 Energy=       -640.098322
G3MP2 Enthalpy=     -640.097377 G3MP2 Free Energy=   -640.156122
-----

```

**2h<sup>+</sup>**

C	-1.10227	0.46866	-0.00255
C	-2.43560	-0.00361	-0.01129
O	-0.11491	-0.35543	-0.00975
Si	1.67111	0.02661	0.00093
C	2.23655	-0.78000	-1.56891
H	2.00603	-1.84832	-1.57485
H	1.77992	-0.32347	-2.45094
H	3.32179	-0.67630	-1.66984
C	2.22374	-0.80110	1.56437
H	3.30839	-0.70051	1.67442
H	1.76150	-0.35518	2.44890
H	1.99140	-1.86899	1.55483
C	1.80210	1.88195	0.01386
H	2.86433	2.15021	0.01848
H	1.36684	2.34821	-0.87450
H	1.36217	2.33644	0.90600
H	-0.89920	1.54202	0.00982
C	-2.72620	-1.45499	-0.00470
H	-3.04117	-1.74570	1.00728
H	-3.56588	-1.67746	-0.66901
H	-1.85914	-2.05452	-0.27898
C	-3.54761	0.97494	0.00278
H	-4.13790	0.86963	-0.91632
H	-4.22994	0.75084	0.83106
H	-3.20975	2.00891	0.08733

```

-----
Temperature=          298.150000 Pressure=          1.000000
E(ZPE)=              0.204016 E(Thermal)=          0.219139
E(QCISD(T))=        -639.276279 E(Empiric)=         -0.245725
DE(MP2)=             -0.509977
G3MP2 (0 K)=        -639.827965 G3MP2 Energy=        -639.812842
G3MP2 Enthalpy=     -639.811898 G3MP2 Free Energy=    -639.871865
-----

```

2i

O	-0.18771	-0.13716	-0.81694
Si	-1.63354	-0.22163	0.08487
C	-2.45691	1.45909	0.17910
H	-3.42570	1.38471	0.68405
H	-1.83956	2.16674	0.73809
H	-2.63454	1.87235	-0.81810
C	-1.22981	-0.86064	1.79659
H	-2.14047	-0.98056	2.39219
H	-0.72764	-1.83120	1.74897
H	-0.56948	-0.16769	2.32490
C	0.98034	0.20041	-0.18169
C	2.03520	-0.62443	-0.07891
O	0.97903	1.46263	0.37264
C	-2.70002	-1.41493	-0.88199
H	-3.68690	-1.52668	-0.42231
H	-2.84666	-1.06418	-1.90735
H	-2.23596	-2.40375	-0.93020
C	3.31451	-0.18316	0.56626
H	3.54722	-0.81502	1.43175
H	4.15382	-0.28088	-0.13266
H	3.25646	0.85198	0.90340
C	1.97565	-2.03240	-0.58922
H	2.12742	-2.74788	0.22839
H	1.01885	-2.24488	-1.06740
H	2.77363	-2.21126	-1.31948
C	0.92045	2.49246	-0.62652
H	0.01937	2.39864	-1.23632
H	0.90676	3.43825	-0.08507

## Chapter 2: Manifestation of Polar Reaction Pathways of DDQ

H            1.80591            2.44199            -1.26848

```

-----
Temperature=      298.150000 Pressure=      1.000000
E(ZPE)=           0.236281 E(Thermal)=      0.253503
E(QCISD(T))=     -753.753750 E(Empirc)=     -0.306207
DE(MP2)=          -0.662993
G3MP2 (0 K)=     -754.486668 G3MP2 Energy=   -754.469447
G3MP2 Enthalpy=  -754.468502 G3MP2 Free Energy= -754.531633
-----

```

2i\*\*

O	-0.12817	0.45390	-0.44903
Si	-1.72871	-0.15786	0.09401
C	-2.66294	1.42619	0.34291
H	-3.69971	1.20821	0.61914
H	-2.23425	2.03423	1.14400
H	-2.68757	2.02478	-0.57151
C	-1.41755	-1.08495	1.67663
H	-2.38189	-1.31820	2.14069
H	-0.89514	-2.03187	1.52785
H	-0.85555	-0.48464	2.39812
C	1.12486	0.35361	-0.17886
C	1.86382	-0.86606	-0.04212
O	1.83552	1.44756	-0.07078
C	-2.38274	-1.16711	-1.32042
H	-3.44581	-1.36880	-1.15043
H	-2.30469	-0.62219	-2.26519
H	-1.88640	-2.13281	-1.43759
C	3.27957	-0.80471	0.40668
H	3.60069	-1.77858	0.78028
H	3.92609	-0.54207	-0.44213
H	3.43732	-0.04677	1.17573
C	1.27855	-2.16754	-0.44607
H	1.16874	-2.82341	0.42650
H	0.31730	-2.07023	-0.94654
H	1.97402	-2.67483	-1.12478
C	1.15786	2.73305	-0.21910
H	0.39990	2.83424	0.55596
H	1.95014	3.46492	-0.09550
H	0.71135	2.79152	-1.21019

```

-----
Temperature=      298.150000 Pressure=      1.000000
E(ZPE)=           0.235861 E(Thermal)=      0.253659
E(QCISD(T))=     -753.511559 E(Empirc)=     -0.301399
DE(MP2)=          -0.644846
G3MP2 (0 K)=     -754.221943 G3MP2 Energy=   -754.204145
G3MP2 Enthalpy=  -754.203201 G3MP2 Free Energy= -754.268842
-----

```

2j

O	-1.00599	-0.22245	0.79688
Si	-2.18096	-1.04293	-0.11683
C	-2.61532	-2.53054	0.93094
H	-1.75259	-3.18507	1.07873
H	-2.97432	-2.22067	1.91614
H	-3.40465	-3.12197	0.45622
C	-1.52489	-1.53846	-1.79802
H	-2.32028	-2.00301	-2.39096
H	-1.15419	-0.66838	-2.34574
H	-0.69859	-2.24625	-1.71408

C	-3.69577	0.04271	-0.35537
H	-4.47706	-0.51805	-0.87975
H	-4.11148	0.37787	0.59898
H	-3.46964	0.92686	-0.95868
C	-0.51624	0.99467	0.33984
C	0.58638	1.04601	-0.43308
C	1.21558	2.33031	-0.88527
H	1.00819	2.48412	-1.95358
H	2.30532	2.22664	-0.80259
C	-1.19026	2.21949	0.88334
H	-2.27580	2.07901	0.84685
H	-0.93363	2.32839	1.94707
C	-0.78588	3.47044	0.10783
H	-1.26183	3.45352	-0.88084
H	-1.15005	4.36609	0.62380
C	0.72793	3.52108	-0.06333
H	1.19948	3.49317	0.92716
H	1.03761	4.45883	-0.53837
O	1.19636	-0.10188	-0.89865
Si	2.18794	-1.03934	0.11198
C	1.53574	-2.79382	0.15333
H	2.21411	-3.44266	0.71754
H	0.55627	-2.83066	0.63505
H	1.44120	-3.21063	-0.85345
C	3.89814	-1.03053	-0.65829
H	3.86383	-1.39709	-1.68827
H	4.31806	-0.02061	-0.67840
H	4.58836	-1.66989	-0.09842
C	2.22148	-0.30450	1.83382
H	2.89582	-0.88046	2.47652
H	2.57089	0.73211	1.82920
H	1.22287	-0.32596	2.27754

```

-----
Temperature=          298.150000 Pressure=          1.000000
E(ZPE)=              0.341967 E(Thermal)=          0.366040
E(QCISD(T))=        -1199.574716 E(Empirc)=         -0.436113
DE(MP2)=             -0.936508
G3MP2 (0 K)=         -1200.605369 G3MP2 Energy=      -1200.581296
G3MP2 Enthalpy=      -1200.580352 G3MP2 Free Energy=  -1200.660398
-----

```

2j<sup>+</sup>

O	-1.28396	-0.39863	0.02384
Si	-2.97370	-0.95278	0.01112
C	-2.73733	-2.76413	0.33317
H	-2.10982	-3.22411	-0.43437
H	-2.26829	-2.93717	1.30513
H	-3.70066	-3.28327	0.33164
C	-3.63599	-0.59019	-1.69240
H	-4.61130	-1.07446	-1.80886
H	-3.78186	0.47551	-1.88520
H	-2.97833	-0.99317	-2.46729
C	-3.87988	-0.08121	1.38725
H	-4.83105	-0.59495	1.56308
H	-3.31927	-0.11647	2.32578
H	-4.11394	0.96116	1.16034
C	-0.71367	0.76989	-0.00163
C	0.71367	0.76989	0.00163
C	1.49812	2.04297	-0.00171
H	1.90903	2.18074	-1.01242
H	2.35803	1.92850	0.66769
C	-1.49812	2.04297	0.00171
H	-2.35802	1.92850	-0.66769

## Chapter 2: Manifestation of Polar Reaction Pathways of DDQ

H	-1.90903	2.18074	1.01242
C	-0.65502	3.25621	-0.38778
H	-0.45024	3.23645	-1.46453
H	-1.22557	4.16806	-0.19012
C	0.65502	3.25621	0.38778
H	0.45024	3.23645	1.46453
H	1.22558	4.16806	0.19011
O	1.28396	-0.39863	-0.02384
Si	2.97370	-0.95278	-0.01112
C	2.73733	-2.76413	-0.33316
H	3.70066	-3.28327	-0.33164
H	2.10982	-3.22411	0.43437
H	2.26829	-2.93718	-1.30513
C	3.87988	-0.08121	-1.38725
H	3.31927	-0.11647	-2.32578
H	4.11393	0.96115	-1.16034
H	4.83105	-0.59495	-1.56308
C	3.63598	-0.59019	1.69240
H	4.61130	-1.07446	1.80886
H	3.78185	0.47551	1.88520
H	2.97833	-0.99317	2.46729

```

-----
Temperature=          298.150000 Pressure=          1.000000
E(ZPE)=              0.342137 E(Thermal)=          0.366555
E(QCISD(T))=        -1199.341596 E(Empirc)=         -0.431305
DE(MP2)=             -0.915753
G3MP2 (0 K)=        -1200.346518 G3MP2 Energy=       -1200.322099
G3MP2 Enthalpy=     -1200.321155 G3MP2 Free Energy=   -1200.402455
-----

```

2k

C	2.48351	-1.17566	0.02188
H	3.36089	-1.01222	0.65296
H	1.80313	-1.85447	0.54510
H	2.80744	-1.68885	-0.89085
C	1.80393	0.12059	-0.32355
C	2.31683	1.30282	0.05315
H	1.84387	2.24180	-0.21957
H	3.23229	1.36697	0.63321
Si	-1.01895	-0.01527	0.01198
C	-2.51817	-0.43302	-1.05235
H	-2.64074	0.28804	-1.86639
H	-2.42287	-1.42672	-1.50073
H	-3.43872	-0.42320	-0.46045
C	-1.24281	1.68633	0.78445
H	-2.11563	1.70566	1.44449
H	-0.36735	1.96533	1.37722
H	-1.38811	2.45538	0.01935
C	-0.84722	-1.29678	1.38208
H	-1.75361	-1.32163	1.99574
H	-0.69255	-2.30391	0.98323
H	-0.00839	-1.06143	2.04339
C	0.52066	0.01221	-1.10132
H	0.53230	-0.88570	-1.73253
H	0.41293	0.86987	-1.77796

```

-----
Temperature=          298.150000 Pressure=          1.000000
E(ZPE)=              0.200044 E(Thermal)=          0.213127
E(QCISD(T))=        -564.454761 E(Empirc)=         -0.222696
DE(MP2)=             -0.448929
G3MP2 (0 K)=        -564.926342 G3MP2 Energy=       -564.913259
G3MP2 Enthalpy=     -564.912315 G3MP2 Free Energy=   -564.964960
-----

```

2k<sup>+</sup>

C	-2.39778	-1.15733	-0.03793
H	-2.66143	-1.13262	-1.09848
H	-1.80412	-2.04736	0.17103
H	-3.33582	-1.23742	0.52577
C	-1.70389	0.09579	0.38621
C	-2.20927	1.33790	-0.05055
H	-1.74291	2.27058	0.24599
H	-3.09384	1.39371	-0.67494
Si	1.05557	-0.02120	-0.10627
C	2.43384	-0.19851	1.13431
H	2.47934	0.64531	1.82745
H	2.35240	-1.12123	1.71433
H	3.38693	-0.23226	0.59423
C	1.07031	1.60061	-1.02145
H	1.99863	1.66106	-1.60050
H	0.24285	1.69838	-1.72851
H	1.06057	2.46005	-0.34524
C	0.82068	-1.51362	-1.19283
H	1.72586	-1.64006	-1.79793
H	0.69144	-2.43354	-0.61629
H	-0.01801	-1.41209	-1.88559
C	-0.57125	0.05532	1.21935
H	-0.40193	-0.86694	1.77709
H	-0.31386	0.97027	1.75679

```

-----
Temperature=          298.150000 Pressure=          1.000000
E(ZPE)=              0.198278 E(Thermal)=          0.211915
E(QCISD(T))=        -564.171822 E(Empirc)=         -0.217888
DE(MP2)=             -0.431618
G3MP2 (0 K)=        -564.623050 G3MP2 Energy=       -564.609414
G3MP2 Enthalpy=     -564.608469 G3MP2 Free Energy=   -564.662842
-----

```

2l

C	-0.25958	0.48278	-0.18695
C	0.77569	-0.38842	-0.13684
H	0.67128	-1.45089	0.04135
C	2.12365	0.14172	-0.31586
O	3.04386	-0.85839	-0.19838
C	4.41970	-0.44080	-0.33765
H	4.94673	-1.35074	-0.63050
H	4.48914	0.29486	-1.14128
C	4.94955	0.11715	0.96657
H	4.82550	-0.61307	1.76928
H	6.01396	0.35233	0.87197
H	4.41395	1.03081	1.22701
O	2.42431	1.31021	-0.53500
H	-0.02268	1.53544	-0.33674
C	-2.03795	-1.13796	0.21581
C	-2.48490	1.25700	0.36539
C	-3.48577	-1.31363	-0.20795
H	-1.93364	-1.32100	1.29691
H	-1.41385	-1.86022	-0.31804
C	-3.90238	0.97122	-0.09025
H	-2.46384	1.30229	1.46530
H	-2.14006	2.21920	-0.02701
H	-3.87437	-2.27410	0.13962
H	-3.55307	-1.27748	-1.30565
H	-4.60187	1.69337	0.33825

## Chapter 2: Manifestation of Polar Reaction Pathways of DDQ

H	-3.95938	1.02257	-1.18791
N	-1.59809	0.20622	-0.12633
O	-4.31809	-0.31198	0.36439

Temperature=	298.150000	Pressure=	1.000000
E(ZPE)=	0.231765	E(Thermal)=	0.245228
E(QCISD(T))=	-630.576493	E(Empiric)=	-0.343323
DE(MP2)=	-0.733576		
G3MP2 (0 K)=	-631.421627	G3MP2 Energy=	-631.408165
G3MP2 Enthalpy=	-631.407220	G3MP2 Free Energy=	-631.462919

### 2I<sup>+</sup>

C	-0.33260	0.47782	0.19759
C	0.73216	-0.44077	0.11739
H	0.64229	-1.50596	0.28784
C	2.07533	0.14325	-0.21523
O	2.97311	-0.82164	-0.27211
C	4.35198	-0.39680	-0.58480
H	4.80019	-1.30247	-0.98979
H	4.29439	0.37171	-1.35611
C	5.04317	0.08857	0.66665
H	5.02993	-0.68277	1.43862
H	6.08511	0.32118	0.43206
H	4.56960	0.99523	1.04573
O	2.22958	1.33487	-0.39759
H	-0.06893	1.52159	0.03021
C	-2.14061	-1.12690	0.66455
C	-2.58765	1.27900	0.49158
C	-3.25425	-1.33882	-0.36298
H	-2.56119	-1.14970	1.67444
H	-1.36699	-1.88927	0.57837
C	-3.67630	0.94615	-0.52707
H	-3.01676	1.29416	1.49812
H	-2.10752	2.23811	0.28301
H	-3.75343	-2.29007	-0.16859
H	-2.83045	-1.35685	-1.37762
H	-4.48611	1.67425	-0.45182
H	-3.26292	0.97355	-1.54559
N	-1.57237	0.21236	0.45592
O	-4.23119	-0.32426	-0.23735

Temperature=	298.150000	Pressure=	1.000000
E(ZPE)=	0.230653	E(Thermal)=	0.244325
E(QCISD(T))=	-630.317217	E(Empiric)=	-0.338515
DE(MP2)=	-0.713381		
G3MP2 (0 K)=	-631.138461	G3MP2 Energy=	-631.124788
G3MP2 Enthalpy=	-631.123844	G3MP2 Free Energy=	-631.180791

### 2m

C	1.41046	-0.37942	0.06573
C	0.33455	0.42949	-0.09983
H	0.39214	1.50808	-0.16890
C	-0.97799	-0.19325	-0.20890
O	-1.94014	0.75770	-0.39694
C	-3.28597	0.24811	-0.51188
H	-3.82407	1.03173	-1.04873
H	-3.27293	-0.66236	-1.11419

## Chapter 2: Manifestation of Polar Reaction Pathways of DDQ

C	-3.88673	-0.00587	0.85491
H	-3.84631	0.90193	1.46095
H	-4.93256	-0.31263	0.75739
H	-3.33755	-0.80001	1.36206
O	-1.22403	-1.39415	-0.15733
H	1.23399	-1.45345	0.08765
N	2.70501	-0.00391	0.26071
C	3.75957	-0.95619	-0.03902
H	4.07732	-0.90776	-1.08956
H	4.62591	-0.75492	0.59664
H	3.40176	-1.96555	0.17089
C	3.05087	1.39778	0.14287
H	2.38622	1.99102	0.77459
H	4.07651	1.53921	0.48881
H	2.96932	1.75979	-0.89173

```

-----
Temperature=          298.150000 Pressure=          1.000000
E(ZPE)=              0.190304 E(Thermal)=          0.202539
E(QCISD(T))=        -478.357848 E(Empirc)=         -0.269091
DE(MP2)=             -0.568729
G3MP2 (0 K)=        -479.005364 G3MP2 Energy=        -478.993129
G3MP2 Enthalpy=     -478.992185 G3MP2 Free Energy=    -479.044267
-----

```

### 2m<sup>++</sup>

C	1.42594	-0.33848	-0.04349
C	0.31316	0.52586	-0.10761
H	0.36600	1.60618	-0.06710
C	-1.02488	-0.14385	-0.24622
O	-1.96929	0.77295	-0.32373
C	-3.34882	0.26327	-0.45900
H	-3.87352	1.09996	-0.91693
H	-3.32200	-0.58447	-1.14415
C	-3.90282	-0.10367	0.89660
H	-3.85902	0.74980	1.57538
H	-4.94894	-0.40070	0.78627
H	-3.35486	-0.94321	1.32663
O	-1.13482	-1.35350	-0.28099
H	1.19688	-1.40160	-0.09975
N	2.66944	-0.00330	0.07236
C	3.71673	-1.03248	0.11919
H	4.41013	-0.86719	-0.70805
H	4.25490	-0.94524	1.06533
H	3.26859	-2.02136	0.03618
C	3.16863	1.37199	0.16119
H	2.35438	2.09018	0.15915
H	3.74114	1.47137	1.08543
H	3.82549	1.55799	-0.69113

```

-----
Temperature=          298.150000 Pressure=          1.000000
E(ZPE)=              0.189074 E(Thermal)=          0.201618
E(QCISD(T))=        -478.098774 E(Empirc)=         -0.264283
DE(MP2)=             -0.548424
G3MP2 (0 K)=        -478.722407 G3MP2 Energy=        -478.709864
G3MP2 Enthalpy=     -478.708920 G3MP2 Free Energy=    -478.762776
-----

```

### 2n

C	1.48078	-0.91959	-0.00002
---	---------	----------	----------



H	1.74048	-1.97016	-0.00003
N	2.50393	-0.08921	-0.00002
N	3.37509	0.66358	-0.00003
C	0.12763	-0.39896	-0.00000
C	-0.94745	-1.30400	0.00002
C	-0.15230	0.97820	-0.00001
C	-2.26035	-0.84384	0.00003
H	-0.74734	-2.37376	0.00002
C	-1.46883	1.42985	0.00001
H	0.66195	1.70102	-0.00002
C	-2.53103	0.52524	0.00003
H	-3.07754	-1.56121	0.00005
H	-1.66426	2.49952	0.00001
H	-3.55715	0.88263	0.00004

```

-----
Temperature=          298.150000 Pressure=          1.000000
E(ZPE)=              0.109718 E(Thermal)=          0.117223
E(QCISD(T))=        -378.705558 E(Empirc)=         -0.204138
DE(MP2)=             -0.391596
G3MP2 (0 K)=        -379.191574 G3MP2 Energy=       -379.184069
G3MP2 Enthalpy=     -379.183125 G3MP2 Free Energy=    -379.224032
-----

```

**2n<sup>+</sup>**

C	1.41008	-0.90138	-0.00001
H	1.67337	-1.95131	-0.00001
N	2.48123	-0.07133	-0.00003
N	3.35524	0.59200	-0.00004
C	0.12635	-0.37659	0.00000
C	-0.95084	-1.30393	0.00002
C	-0.15332	1.01499	-0.00000
C	-2.22703	-0.85974	0.00003
H	-0.73400	-2.36788	0.00002
C	-1.43229	1.43907	0.00001
H	0.65770	1.73675	-0.00002
C	-2.47849	0.50985	0.00003
H	-3.05478	-1.56065	0.00004
H	-1.65994	2.49970	0.00001
H	-3.50429	0.86498	0.00003

```

-----
Temperature=          298.150000 Pressure=          1.000000
E(ZPE)=              0.107181 E(Thermal)=          0.114954
E(QCISD(T))=        -378.435999 E(Empirc)=         -0.199330
DE(MP2)=             -0.374228
G3MP2 (0 K)=        -378.902377 G3MP2 Energy=       -378.894604
G3MP2 Enthalpy=     -378.893660 G3MP2 Free Energy=    -378.935345
-----

```

**2p**

C	0.78128	-0.24740	-1.08467
H	0.94752	0.65809	-1.68234
H	0.57253	-1.06266	-1.78934
C	1.99644	-0.55807	-0.26957
H	2.06525	-1.57141	0.12644
C	2.96308	0.31642	0.04040
H	3.80417	0.03753	0.66610
H	2.94615	1.33721	-0.33188
Si	-0.74324	0.02401	0.01525
C	-0.49698	1.59636	1.01886
H	-1.32832	1.75965	1.71148
H	0.42484	1.54401	1.60494

H	-0.42904	2.47426	0.36882
C	-0.94787	-1.44966	1.17080
H	-1.85001	-1.34658	1.78184
H	-1.03296	-2.38707	0.61217
H	-0.09664	-1.54190	1.85147
C	-2.26984	0.19015	-1.07776
H	-3.16772	0.37042	-0.47848
H	-2.16771	1.02385	-1.77921
H	-2.43943	-0.71821	-1.66392

```

-----
Temperature=          298.150000 Pressure=          1.000000
E(ZPE)=              0.173042 E(Thermal)=          0.184809
E(QCISD(T))=        -525.268071 E(Empirc)=         -0.194859
DE(MP2)=             -0.396516
G3MP2 (0 K)=        -525.686404 G3MP2 Energy=        -525.674638
G3MP2 Enthalpy=     -525.673694 G3MP2 Free Energy=    -525.723358
-----

```

## 2p\*\*

C	0.81432	-0.57032	-1.12960
H	0.85542	0.23895	-1.86076
H	0.37245	-1.50037	-1.48896
C	1.87760	-0.68122	-0.22200
H	1.97930	-1.60366	0.34783
C	2.79752	0.34040	0.01238
H	3.62094	0.20656	0.70368
H	2.72684	1.28735	-0.51230
Si	-0.78052	0.07313	0.10543
C	-0.33475	1.78882	0.67162
H	-1.20434	2.22327	1.17766
H	0.49239	1.79899	1.38599
H	-0.08909	2.45054	-0.16382
C	-0.92099	-1.19406	1.46032
H	-1.84792	-1.01337	2.01611
H	-0.97720	-2.21370	1.06850
H	-0.09774	-1.13910	2.17731
C	-2.15451	0.01674	-1.14917
H	-3.07675	0.36098	-0.66632
H	-1.96687	0.67312	-2.00269
H	-2.33539	-0.99547	-1.51961

```

-----
Temperature=          298.150000 Pressure=          1.000000
E(ZPE)=              0.171756 E(Thermal)=          0.183982
E(QCISD(T))=        -524.978143 E(Empirc)=         -0.190051
DE(MP2)=             -0.378707
G3MP2 (0 K)=        -525.375145 G3MP2 Energy=        -525.362919
G3MP2 Enthalpy=     -525.361975 G3MP2 Free Energy=    -525.413044
-----

```

## 2q

C	1.64097	-1.44011	-0.07376
C	0.83772	-0.36966	-0.18830
C	1.20976	-2.79318	-0.55268
C	2.99934	-1.33507	0.55169
O	-0.38511	-0.40467	-0.80929
O	1.17428	0.86110	0.33334
H	3.21305	-0.31553	0.87369
H	3.77632	-1.65325	-0.15376
H	3.07369	-1.99503	1.42431
H	0.22125	-2.75852	-1.01190
H	1.18747	-3.50931	0.27802
H	1.91969	-3.18523	-1.29055

C	1.41751	1.84741	-0.69129
Si	-1.78927	-0.03276	0.08416
C	1.79344	3.13264	0.00713
H	0.51966	1.97020	-1.30488
H	2.22900	1.48745	-1.33612
H	0.97695	3.47072	0.64886
H	2.00623	3.91495	-0.72674
H	2.68042	2.98234	0.62601
C	-3.15130	-0.94600	-0.81446
C	-2.12254	1.81138	0.06279
C	-1.56214	-0.64865	1.83642
H	-3.20588	-0.63322	-1.86094
H	-4.12663	-0.75403	-0.35660
H	-2.97647	-2.02515	-0.79694
H	-1.34529	-1.72064	1.85395
H	-2.46566	-0.47732	2.43032
H	-0.73250	-0.13113	2.32540
H	-2.17884	2.19344	-0.96076
H	-1.33681	2.35812	0.58983
H	-3.07572	2.03577	0.55300

Temperature=	298.150000	Pressure=	1.000000
E(ZPE)=	0.263312	E(Thermal)=	0.281885
E(QCISD(T))=	-792.941925	E(Empiric)=	-0.334044
DE(MP2)=	-0.714229		
G3MP2 (0 K)=	-793.726886	G3MP2 Energy=	-793.708313
G3MP2 Enthalpy=	-793.707369	G3MP2 Free Energy=	-793.774068

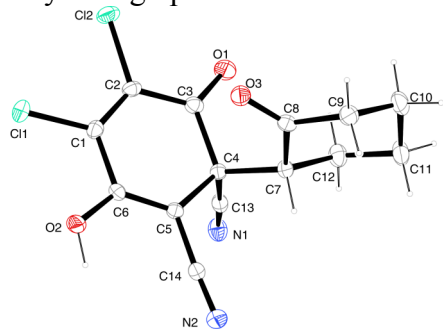
2q<sup>+</sup>

C	1.40260	-1.55027	0.08266
C	1.02232	-0.17136	-0.00670
C	0.55036	-2.53600	0.79131
C	2.72784	-1.96900	-0.44443
O	-0.13241	0.30515	0.31188
O	1.97029	0.64123	-0.39011
H	2.98757	-1.44922	-1.36817
H	2.74558	-3.04718	-0.61283
H	3.51050	-1.73192	0.28946
H	-0.29814	-2.08271	1.30006
H	1.15964	-3.06439	1.53399
H	0.18893	-3.30037	0.09235
C	1.70214	2.09156	-0.47067
Si	-1.86149	0.06901	-0.09755
C	1.87412	2.72065	0.89063
H	0.70260	2.22811	-0.88218
H	2.44978	2.42851	-1.18671
H	1.12233	2.35643	1.59224
H	1.76029	3.80382	0.79616
H	2.87039	2.51567	1.28559
C	-2.67850	-0.43976	1.49012
C	-1.90670	-1.18879	-1.46814
C	-2.35685	1.77120	-0.65002
H	-2.43799	-1.45998	1.79702
H	-3.76540	-0.38655	1.36647
H	-2.41219	0.23727	2.30644
H	-2.15649	2.51697	0.12405
H	-3.43117	1.79850	-0.85969
H	-1.84050	2.07316	-1.56535
H	-1.64574	-2.19618	-1.13799
H	-1.25110	-0.91207	-2.29913
H	-2.92503	-1.23441	-1.86888

Temperature=	298.150000	Pressure=	1.000000
E(ZPE)=	0.262995	E(Thermal)=	0.282051
E(QCISD(T))=	-792.701024	E(Empiric)=	-0.329236
DE(MP2)=	-0.696249		
G3MP2(0 K)=	-793.463514	G3MP2 Energy=	-793.444458
G3MP2 Enthalpy=	-793.443514	G3MP2 Free Energy=	-793.512359

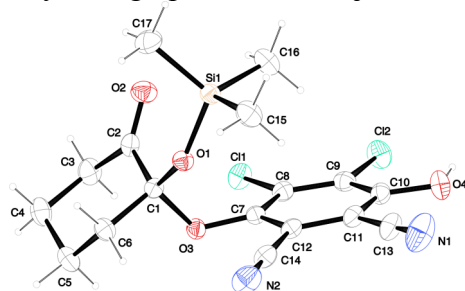
## 9) X-ray crystallography data for 3a-C and 3j-O

### Crystallographic data for 3a-C



net formula	C <sub>14</sub> H <sub>10</sub> Cl <sub>2</sub> N <sub>2</sub> O <sub>3</sub>
<i>M<sub>r</sub></i> /g mol <sup>-1</sup>	325.146
crystal size/mm	0.15 × 0.03 × 0.03
<i>T</i> /K	200(2)
radiation	MoKα
diffractometer	'KappaCCD'
crystal system	monoclinic
space group	<i>P</i> 2 <sub>1</sub> / <i>c</i>
<i>a</i> /Å	14.0747(5)
<i>b</i> /Å	6.6201(2)
<i>c</i> /Å	15.0699(6)
α/°	90
β/°	93.3281(18)
γ/°	90
<i>V</i> /Å <sup>3</sup>	1401.78(9)
<i>Z</i>	4
calc. density/g cm <sup>-3</sup>	1.54069(10)
μ/mm <sup>-1</sup>	0.474
absorption correction	none
refls. measured	11160
<i>R</i> <sub>int</sub>	0.0504
mean σ( <i>I</i> )/ <i>I</i>	0.0444
θ range	3.15–27.49
observed refls.	2370
<i>x</i> , <i>y</i> (weighting scheme)	0.0492, 0.6356
hydrogen refinement	mixed
refls in refinement	3218

parameters	194
restraints	0
$R(F_{\text{obs}})$	0.0435
$R_w(F^2)$	0.1100
$S$	1.047
shift/error <sub>max</sub>	0.001
max electron density/e $\text{\AA}^{-3}$	0.312
min electron density/e $\text{\AA}^{-3}$	-0.454

Crystallographic data for **3j-O**

net formula	$\text{C}_{17}\text{H}_{18}\text{Cl}_2\text{N}_2\text{O}_4\text{Si}$
$M_r/\text{g mol}^{-1}$	413.327
crystal size/mm	$0.49 \times 0.38 \times 0.07$
$T/\text{K}$	173(2)
radiation	MoK $\alpha$
diffractometer	'Oxford XCalibur'
crystal system	orthorhombic
space group	$Pbca$
$a/\text{\AA}$	10.2550(6)
$b/\text{\AA}$	15.1590(11)
$c/\text{\AA}$	24.5615(14)
$\alpha/^\circ$	90
$\beta/^\circ$	90
$\gamma/^\circ$	90
$V/\text{\AA}^3$	3818.2(4)
$Z$	8
calc. density/ $\text{g cm}^{-3}$	1.43807(15)
$\mu/\text{mm}^{-1}$	0.428
absorption correction	'multi-scan'
transmission factor range	0.86251–1.00000
refls. measured	12912
$R_{\text{int}}$	0.0334
mean $\sigma(I)/I$	0.0369
$\theta$ range	4.27–28.76
observed refls.	3495
$x, y$ (weighting scheme)	0.0344, 2.1970
hydrogen refinement	mixed

refls in refinement	4430
parameters	242
restraints	0
$R(F_{\text{obs}})$	0.0365
$R_w(F^2)$	0.0935
$S$	1.048
shift/error <sub>max</sub>	0.001
max electron density/e Å <sup>-3</sup>	0.342
min electron density/e Å <sup>-3</sup>	-0.272

## 2.6 References:

- (1) Thiele, J.; Günther, F. *Liebigs Ann. Chem.* **1906**, 349, 45–66.
- (2) Andrieux, C. P.; Merz, A.; Saveant, J.-M.; Tomahogh, R. *J. Am. Chem. Soc.* **1984**, 106, 1957–1962.
- (3) (a) Walker, D.; Hiebert, J. D. *Chem. Rev.* **1967**, 67, 153–195. (b) Becker, H.-D. In *The Chemistry of the Quinoid Compounds, Part I*; Patai, S., Ed.; Wiley: Chichester, UK, 1974; pp 335–423. (c) Becker, H.-D. Turner, A. B. In *The Chemistry of the Quinoid Compounds Vol. 2*; Patai, S., Rappoport, Z., Eds.; Wiley: Chichester, UK, 1988; pp 1351–1384. (d) Buckle, D. R. In *Encyclopedia of Reagents for Organic Synthesis Vol. 3*; Paquette, L. A., Ed.; Wiley: Chichester, UK, 1995; p 1699.
- (4) (a) Zhang, Y.; Li, C.-J. *Angew. Chem., Int. Ed.* **2006**, 45, 1949–1952. (b) Zhang, Y.; Li, C.-J. *J. Am. Chem. Soc.* **2006**, 128, 4242–4243. (c) Tu, W.; Floreancig, P. E. *Angew. Chem., Int. Ed.* **2009**, 48, 4567–4571. (d) Liu, L.; Floreancig, P. E. *Angew. Chem., Int. Ed.* **2010**, 49, 3069–3072. (e) Guo, C.; Song, J.; Luo, S.-W.; Gong, L.-Z. *Angew. Chem., Int. Ed.* **2010**, 49, 5558–5562. (f) Liu, L.; Floreancig, P. E. *Angew. Chem., Int. Ed.* **2010**, 49, 5894–5897. (g) Hayashi, Y.; Itoh, T.; Ishikawa, H. *Angew. Chem., Int. Ed.* **2011**, 50, 3920–3924. (h) Tsang, A. S.-K.; Jensen, P.; Hook, J. M.; Hashmi, A. S. K.; Todd, M. H. *Pure Appl. Chem.* **2011**, 83, 655–665. (i) Alagiri, K.; Devadig, P.; Prabhu, K. R. *Chem. Eur. J.* **2012**, 18, 5160–5164. (j) Rohlmann, R.; Garcia Mancheño, O. *Synlett.* **2013**, 24, 6–10.
- (5) Bhattacharya, A.; DiMichele, L. M.; Dolling, U.-H.; Douglas, A. W.; Grabowski, E. J. J. *J. Am. Chem. Soc.* **1988**, 110, 3318–3319.
- (6) (a) Bhattacharya, A.; DiMichele, L. M.; Dolling, U.-H.; Grabowski, E. J. J.; Grenda, V. J. *J. Org. Chem.* **1989**, 54, 6118–6120. (b) For an earlier report on the formation of enones by oxidation of silyl enol ethers with DDQ, see: Ryu, I.; Murai, S.; Hatayama, Y.; Sonoda, N. *Tetrahedron Lett.* **1978**, 19, 3455–3458.

- (7) (a) Mayr, H.; Patz, M. *Angew. Chem., Int. Ed. Engl.* **1994**, *33*, 938–957. (b) Mayr, H.; Ofial, A. R. *Pure Appl. Chem.* **2005**, *77*, 1807–1821. (c) Mayr, H.; Ofial, A. R. *J. Phys. Org. Chem.* **2008**, *21*, 584–595. (d) Mayr, H.; Kempf, B.; Ofial, A. R. *Acc. Chem. Res.* **2003**, *36*, 66–77.
- (8) For a comprehensive database of nucleophilicity parameters  $N$  and  $s_N$  as well as electrophilicity parameters  $E$ , see <http://www.cup.lmu.de/oc/mayr/DBintro.html>.
- (9) (a) Mayr, H.; Bug, T.; Gotta, M. F.; Hering, N.; Irrgang, B.; Janker, B.; Kempf, B.; Loos, R.; Ofial, A. R.; Remennikov, G.; Schimmel, H. *J. Am. Chem. Soc.* **2001**, *123*, 9500–9512. (b) Lucius, R.; Loos, R.; Mayr, H. *Angew. Chem., Int. Ed.* **2002**, *41*, 91–95. (c) Richter, D.; Hampel, N.; Singer, T.; Ofial, A. R.; Mayr, H. *Eur. J. Org. Chem.* **2009**, 3203–3211. (d) Ammer, J.; Nolte, C.; Mayr, H. *J. Am. Chem. Soc.* **2012**, *134*, 13902–13911.
- (10) Kucklaender, U.; Bollig, R.; Frank, W.; Gratz, A.; Jose, J. *Bioorg. Med. Chem.* **2011**, *19*, 2666–2674.
- (11) (a) Mulliken, R. S.; Person, W. B. *Molecular Complexes, a Lecture and Reprint Volume*; Wiley-Interscience: New York, 1969. (b) Mataga, N.; Kubota, T. *Molecular Interactions and Electronic Spectra*; Marcel Dekker: New York, 1970.
- (12) (a) Seeman, J. I. *Chem. Rev.* **1983**, *83*, 83–134. (b) Curtin, D. Y. *Rec. Chem. Prog.* **1954**, *15*, 111. (c) Hammett, L. P. *Physical Organic Chemistry*; McGraw-Hill: New York, 1970.
- (13) Frisch, M. J.; Trucks, G. W.; Schlegel, H.; Scuseria, G. E.; Robb, M. A.; Cheeseman, J. R.; Scalmani, G.; Barone, V.; Mennucci, B.; Petersson, G. A.; Nakatsuji, H.; Caricato, M.; Li, X.; Hratchian, H. P.; Izmaylov, A. F.; Bloino, J.; Zheng, G.; Sonnenberg, J. L.; Hada, M.; Ehara, M.; Toyota, K.; Fukuda, R.; Hasegawa, J.; Ishida, M.; Nakajima, T.; Honda, Y.; Kitao, O.; Nakai, H.; Vreven, T.; Montgomery, J. A.; Peralta, J. E.; Ogliaro, F.; Bearpark, M.; Heyd, J. J.; Brothers, E.; Kudin, K. N.; Staroverov, V. N.; Kobayashi, R.; Normand, J.; Raghavachari, K.; Rendell, A.; Burant, J. C.; Iyengar, S. S.; Tomasi, J.; Cossi, M.; Rega, N.; Millam, J. M.; Klene, M.; Knox, J. E.; Cross, J. B.; Bakken, V.; Adamo, C.; Jaramillo, J.; Gomperts, R.; Stratmann, R. E.; Yazyev, O.; Austin, A. J.; Cammi, R.; Pomelli, C.; Ochterski, J. W.; Martin, R. L.; Morokuma, K.; Zakrzewski, V. G.; Voth, G. A.; Salvador, P.; Dannenberg, J. J.; Dapprich, S.; Daniels, A. D.; Farkas; Foresman, J. B.; Ortiz, J. V.; Cioslowski, J.; Fox, D. J. *Gaussian 09*, Revision A.02; Gaussian, Inc.: Wallingford CT, 2009.
- (14) Henry, D. J.; Sullivan, M. B.; Radom, L. *J. Chem. Phys.* **2003**, *118*, 4849–4860.

- (15) Fukuzumi, S.; Fujita, M.; Otera, J.; Fujita, Y. *J. Am. Chem. Soc.* **1992**, *114*, 10271–10278.
- (16) Pysh, E. S.; Yang, N. C. *J. Am. Chem. Soc.* **1963**, *85*, 2124–2130.
- (17) Ofial, A. R.; Ohkubo, K.; Fukuzumi, S.; Lucius, R.; Mayr, H. *J. Am. Chem. Soc.* **2003**, *125*, 10906–10912.
- (18) Zhou, L.-G.; Liao, W.; Yu, Z.-X. *Asian J. Org. Chem.* **2012**, *1*, 336–345.
- (19) (a) Newcomb, M.; Curran, D. P. *Acc. Chem. Res.* **1988**, *21*, 206–214. (b) Tolbert, L. M.; Sun, X.-J.; Ashby, E. C. *J. Am. Chem. Soc.* **1995**, *117*, 2681–2685. (c) Zard, S. Z. *Radical Reactions in Organic Synthesis*; Oxford University Press, New York, **2003**.
- (20) Liu, Z.; Peng, L.; Zhang, T.; Li, Y. L. *Synth. Commun.* **2001**, *31*, 2549–2555.
- (21) (a) Bunte, J. O.; Rinne, S.; Schäfer, C.; Neumann, B.; Stammeler, H.-G.; Mattay, J. *Tetrahedron Lett.* **2003**, *44*, 45–48. (b) MacMillan's observation of the intramolecular attack of an enamine radical cation at a 1,2-dialkylated ethylene with formation of a five-membered ring, which has a much lower driving-force confirms this conclusion: Beeson, T. D.; Mastracchio, A.; Hong, J.-B.; Ashton, K.; MacMillan, D. W. C. *Science* **2007**, *316*, 582–585.
- (22) (a) Cazeau, P.; Duboudin, F.; Moulines, F.; Babot, O.; Dunogues, J. *Tetrahedron* **1987**, *43*, 2075–2088. (b) Cazeau, P.; Duboudin, F.; Moulines, F.; Babot, O.; Dunogues, J. *Tetrahedron* **1987**, *43*, 2089–2100.
- (23) Oisaki, K.; Suto, Y.; Kanai, M.; Shibasaki, M. *J. Am. Chem. Soc.* **2003**, *125*, 5644–5645.
- (24) Rühlmann, K. *Synthesis* **1971**, 236–253.
- (25) Wulfman, D. S.; Yousefian, S.; White, J. M. *Synth. Commun.* **1988**, *18*, 2349–2352.
- (26) Searle, N. E. *Org. Synth.* **1956**, *36*, 25–27.
- (27) Bhattacharya, A.; DiMichele, L. M.; Dolling, U.-H.; Grabowski, E. J. J.; Grenda, V. J. *J. Org. Chem.* **1989**, *54*, 6118–6120.
- (28) Kucklaender, U.; Bollig, R.; Frank, W.; Gratz, A.; Jose, J. *Bioorg. Med. Chem.* **2011**, *19*, 2666–2674.
- (29) Oshima, T.; Nagai, T. *Bull. Chem. Soc. Jpn.* **1986**, *59*, 3865–3869.
- (30) Liu, Z. S.; Peng, L. Z.; Zhang, T.; Li, Y. L. *Synth. Commun.* **2001**, *31*, 2549–2555.
- (31) For details on the electrophilicity parameters see Mayr, H.; Bug, T.; Gotta, M. F.; Hering, N.; Irrgang, B.; Janker, B.; Kempf, B.; Loos, R.; Ofial, A. R.; Remennikov, G.; Schimmel, H. *J. Am. Chem. Soc.* **2001**, *123*, 9500–9512.
- (32) Burfeindt, J.; Patz, M.; Müller, M.; Mayr, H. *J. Am. Chem. Soc.* **1998**, *120*, 3629–3634.



## Chapter 3: Quantification of the Ambident Electrophilicities of Halogen-Substituted Quinones

### 3.1 Introduction

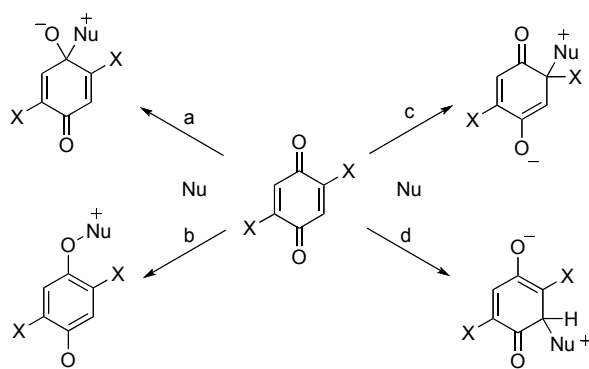
Since Wöhler carried out the first 1,4-addition of HCl to *p*-benzoquinone in 1844,<sup>1</sup> the chemistry of quinones has continuously been attracting the attention of chemists.<sup>2</sup> The realization of the oxidizing properties of quinones in the early 20th century<sup>3</sup> also paved the way to understanding the important role of quinones in biological processes.<sup>4</sup> In spite of this long history, quantitative mechanistic studies concerning the reactivities and selectivities of quinones in organic synthesis are still missing, especially in the border area between electron transfer and polar reaction pathways.

We have previously reported that the reactions of DDQ with *p*-nucleophiles usually proceed by polar pathways,<sup>5</sup> the rates of which can be described by eq. (1), which had been developed to predict rates and selectivities of polar reactions.<sup>6</sup>

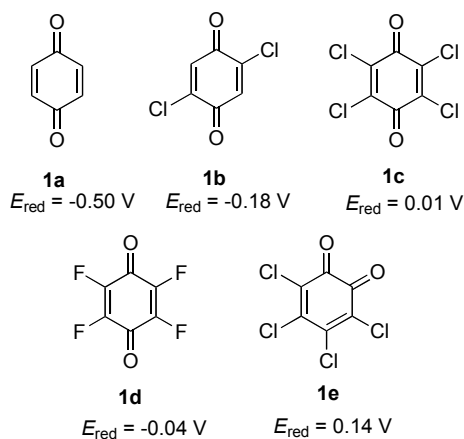
$$\log k(20\text{ }^{\circ}\text{C}) = s_{\text{N}}(E + N) \quad (1)$$

In equation (1) the second-order rate constant ( $\log k$ ) is calculated by two solvent-dependent nucleophile-specific parameters ( $s_{\text{N}}$ ,  $N$ ) and one electrophile-specific parameter ( $E$ ). A comprehensive nucleophilicity scale covering more than 30 orders of magnitude<sup>7</sup> has been created by using a series of benzhydrylium ions and structurally related quinone methides as reference electrophiles.<sup>8</sup>

Nucleophilic attack at quinones may either occur at the carbonyl group (paths *a*, *b*, Scheme 1) or at conjugate positions (paths *c*, *d*). Depending on the substitution pattern of the quinone, one or more types of conjugate attack are conceivable.

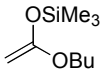
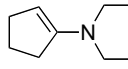
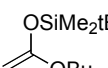
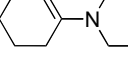
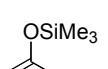
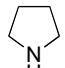
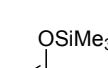
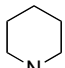
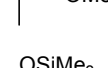
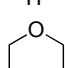
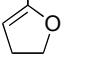
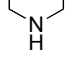
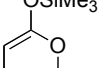
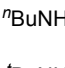
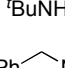

**Scheme 1.** Ambident Reactivities of 2,5-Disubstituted Quinones

We have now used the linear free energy relationship (1) to elucidate the mechanisms of the reactions of different halogen-substituted quinones (Figure 1) with  $\pi$ -systems and amines (Table 1) and to quantify their ambident electrophilicities and selectivities.



**Figure 1.** Quinones **1a-e** studied in this work and their reduction potentials  $E_{\text{red}}$  (vs SCE)<sup>9</sup> in acetonitrile.

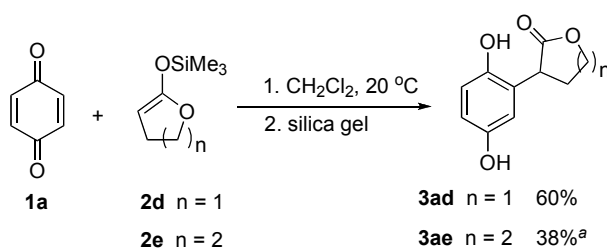
**Table 1.** Nucleophiles **2a-o** and their Reactivity Parameters  $N$  and  $s_N$  in  $\text{CH}_2\text{Cl}_2$  (**2a-h**) or  $\text{CH}_3\text{CN}$  (**2i-o**) and Their Oxidation Potentials in  $\text{CH}_3\text{CN}$  (vs SCE)

Nucleophile	$N$ ( $s_N$ )	$E_{\text{ox}}$	Nucleophile	$N$ ( $s_N$ )	$E_{\text{ox}}$
 <b>2a</b>	10.21 (0.82)	1.12 <sup>a</sup>	 <b>2g</b>	13.41 (0.82)	0.60 <sup>c</sup>
 <b>2a'</b>	10.32 (0.79)		 <b>2h</b>	11.40 (0.83)	0.60 <sup>c</sup>
 <b>2b</b>	8.23 (0.81)	1.24 <sup>a</sup>	 <b>2i</b>	18.64 (0.60)	0.86 <sup>d</sup>
 <b>2c</b>	9.00 (0.98)	0.90 <sup>b</sup>	 <b>2j</b>	17.35 (0.68)	1.04 <sup>d</sup>
 <b>2d</b>	12.56 (0.70)		 <b>2k</b>	15.65 (0.74)	1.13 <sup>d</sup>
 <b>2e</b>	10.61 (0.86)		 <b>2l</b>	15.27 (0.63)	1.51 <sup>e</sup>
 <b>2f</b>	6.22 (0.96)	1.32 <sup>b</sup>	 <b>2m</b>	12.35 (0.72)	1.53 <sup>e</sup>
			 <b>2n</b>	14.29 (0.67)	
			 <b>2o</b>	15.51 (0.62)	

<sup>a</sup>calculated values from ref 5. <sup>b</sup>from ref 10. <sup>c</sup>peak potentials from ref 11. <sup>d</sup>from ref 12. <sup>e</sup>from ref 13.

## 3.2 Results

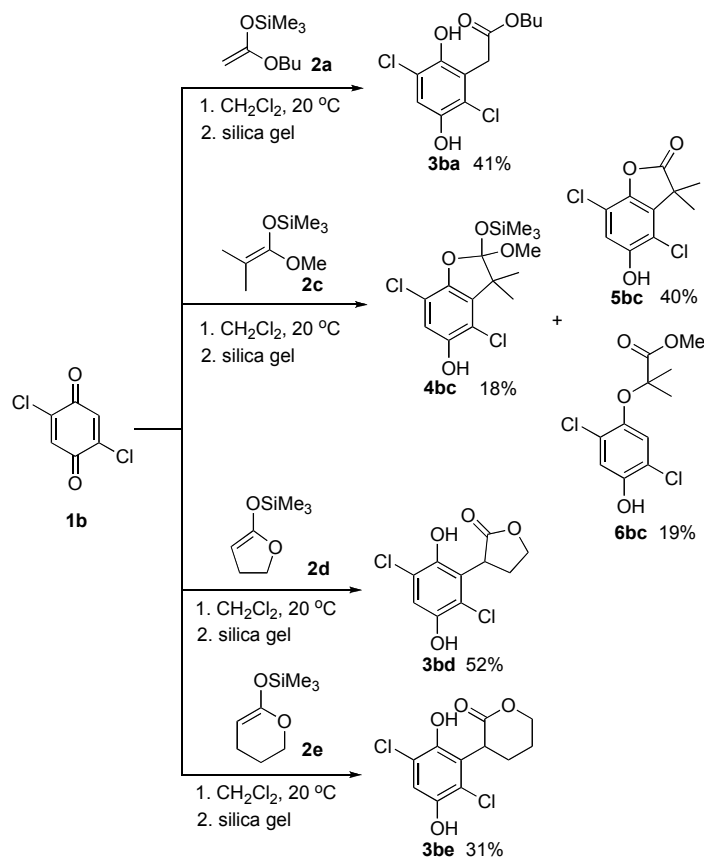
**Product Studies: Reactions with p-Nucleophiles.** 1,4-Benzoquinone **1a** reacted with the silyl ketene acetals **2d** and **2e** to give products of C-H attack selectively. Chromatography of the crude mixture on silica gel led to hydrolysis with formation of the substituted hydroquinones **3ad** and **3ae** (Scheme 1), which were fully characterized. Due to the low electrophilicity of **1a**, the reactions with less reactive silyl ketene acetals are rather slow and were not studied in this work.

**Scheme 1.** Reactions of Benzoquinone (**1a**) with Silyl Ketene Acetals

<sup>a</sup>yield includes traces of impurities which could not be removed by chromatography.

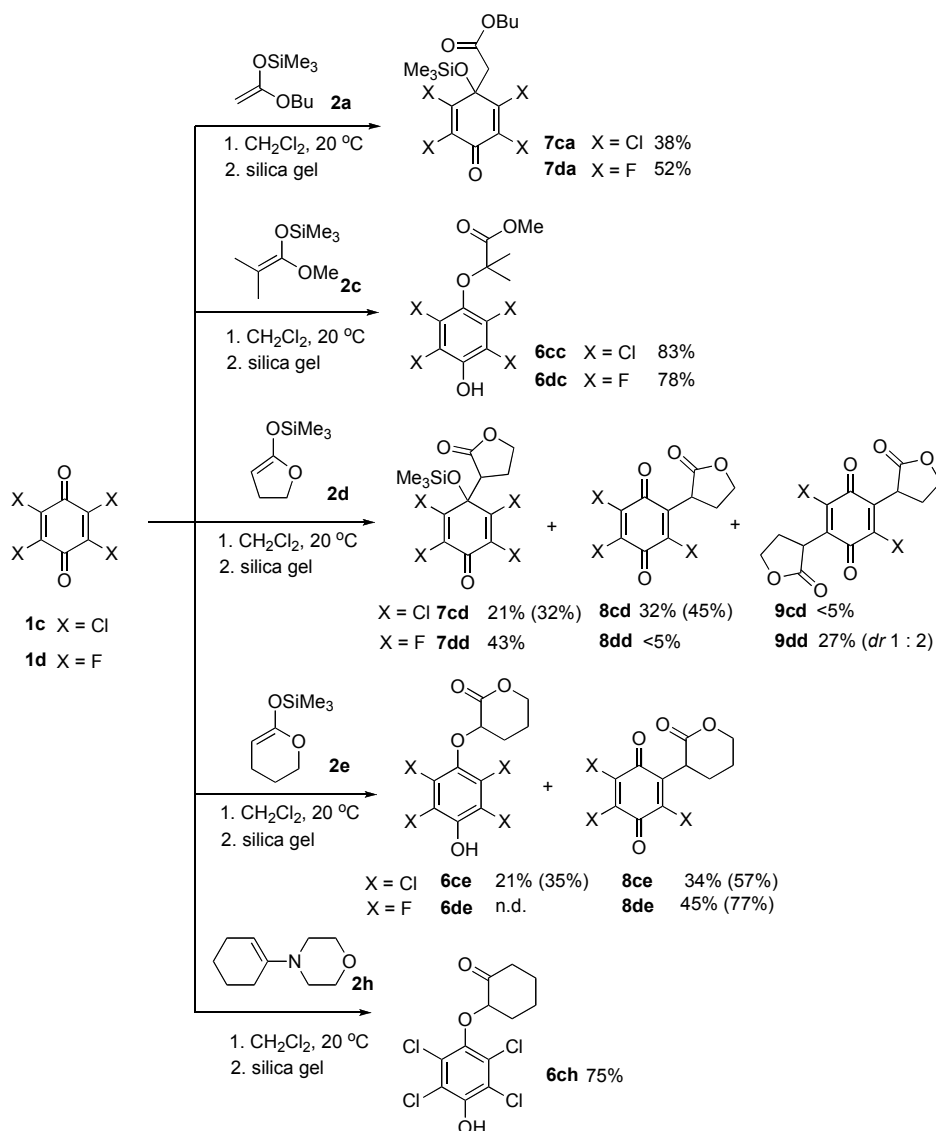
2,5-Dichlorobenzoquinone (**1b**) reacted analogously with the silyl ketene acetals **2(a,d,e)** and gave **3ba**, **3bd**, and **3be**, respectively (Scheme 2). In the reaction of **1b** with **2c**, the [3+2] cyclization products **4bc** (18%) and **5bc** (40%) were formed along with 19% of **6bc**, a product of O attack.

**Scheme 2.** Reactions of 2,5-Dichlorobenzoquinone (**1b**) with Silyl Ketene Acetals



In line with Fukuzumi's and Otera's report,<sup>9</sup> the tetrachloro- and tetrafluoro-substituted para-quinones **1c** and **1d** were found to give 1,2-addition products (**7**) with the terminal silyl ketene acetal **2a**, and products of O attack (**6**) with **2c** (Scheme 3).

**Scheme 3.** Isolated and (in parentheses) NMR Yields for the Reactions of Chloranil (**1c**) and Fluoranil (**1d**) with Silyl Ketene Acetals and an Enamine

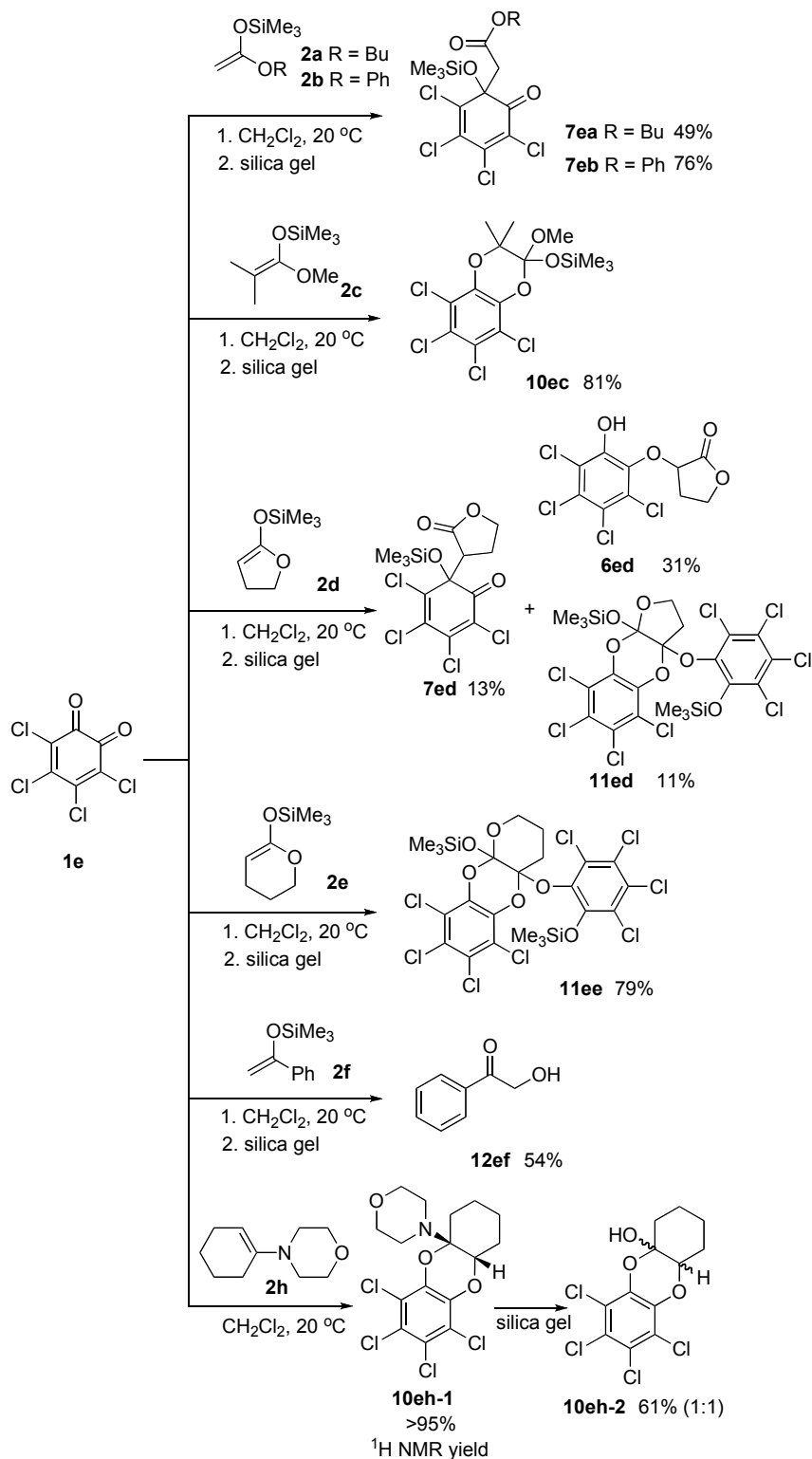


Mixtures of products were formed with cyclic silyl ketene acetals. When **2d** was combined with *p*-chloranil **1c**, both products from C-1 addition (**7cd**), C-2 mono-substitution (**8cd**), and traces of a disubstitution product (**9cd**) were formed. The C-1 addition product **7dd** was the major product of the reaction of **2d** with tetrafluoro-benzoquinone **1d**. While only a trace of the mono-substitution product (**8dd**) was observed, the disubstitution product **9dd** was isolated in 27% yield as a 1 : 2 mixture of diastereomers.

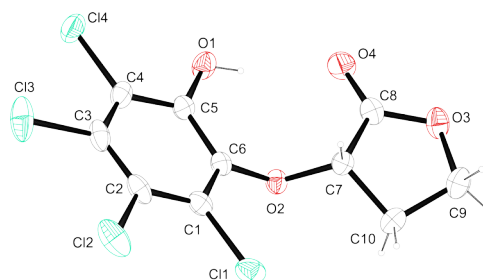
Concomitant C- and O-attack was observed in the reaction of the six-membered ring silyl ketene acetal **2e** with *p*-chloranil **1c**, to give the quinone **8ce** and the hydroquinone **6ce**. In the reaction of **2e** with tetrafluoro-*p*-benzoquinone (**1d**), only the substitution product **8de** was obtained.

While **1c** reacted with enamine **2h** in the same way as with **2c** to give **6ch** by O-attack, the corresponding reaction of **1d** with **2h** gave a complex mixture of products, which was not analyzed.

**Scheme 4.** Reaction of ortho-Chloranil (**1e**) with Silyl Ketene Acetals and an Enamine

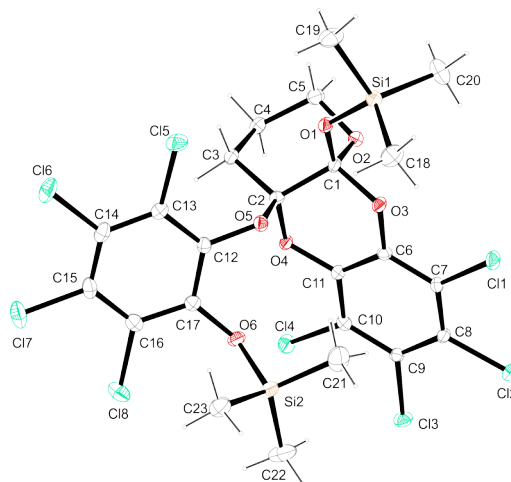


o-Chloranil (**1e**) reacted with the terminal silyl ketene acetals **2a** and **2b** to give the C-1 addition products **7ea** and **7eb**, respectively, while its reaction with **2c** yielded the [4+2] cycloaddition product **10ec** exclusively.



**Figure 2.** Crystal structure of **6ed** (thermal ellipsoids are drawn at the 50% probability level).

The reaction of **1e** with **2d** gave a mixture, from which the C-1 addition product **7ed**, the product of O-attack **6ed** (X-ray structure in Figure 2), and the tricyclic compound **11ed** were isolated in 13%, and 31%, and 11% yield, respectively. Only a single diastereomer of **11ed** was observed and fully characterized by  $^1\text{H}$  NMR,  $^{13}\text{C}$  NMR, and high-resolution mass spectroscopy. The analogous tricyclic compound **11ee**, which was the only product obtained in the reaction of **1e** with **2e**, was characterized by X-ray crystallography (Figure 3).

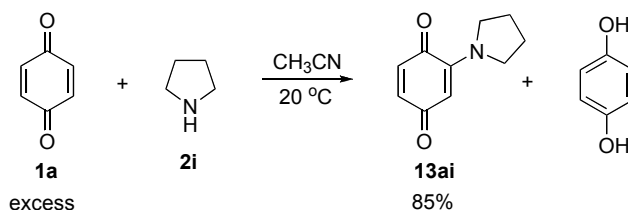


**Figure 3.** Crystal structure of **11ee** (thermal ellipsoids are drawn at the 50% probability level).

The reaction of **1e** with silyl enol ether **2f** proceeded with attack at the carbonyl oxygen and gave hydroxyacetophenone (**12ef**) after chromatography on silica gel. NMR-spectroscopic investigation of the reaction of **1e** with enamine **2h** showed the exclusive formation of the [4+2] cycloaddition product **10eh-1**; its chromatography on silica gel led to hydrolysis, and **10eh-2** was isolated in 61% yield as a 1:1 mixture of diastereomers.

**Reactions with Amines.** In agreement with earlier reports,<sup>2b,14</sup> pyrrolidine was found to react with 1,4-benzoquinone with formation of the mono-substituted benzoquinone **13ai** in 85% yield, when 4 equivalents of quinone was used (Scheme 6).

**Scheme 6.** Reaction of Pyrrolidine with p-Benzoquinone (**1a**)



Products arising from C-2 and C-3 attack were formed by the reaction of 2,5-dichloroquinone (**1b**) with pyrrolidine.<sup>2b,15</sup> Scheme 7 shows that the ratio **13bi**/**8bi** depends strongly on the concentration of the reactants. The ratio **13bi**/**8bi** decreases from 58/26 to 3/82 when reducing the concentration of quinone **1b** from 0.25 mol L<sup>-1</sup> to 0.001 mol L<sup>-1</sup> in CH<sub>3</sub>CN while keeping the ratio [**1b**]/[**2i**] = 5 constant.

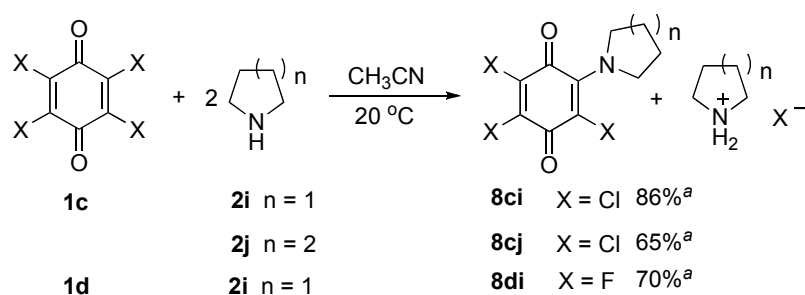
**Scheme 7.** Reactions of Pyrrolidine with 2,5-Dichloroquinone (**1b**) in Acetonitrile

[ <b>1b</b> ] / mol L <sup>-1</sup>	[ <b>2i</b> ] / mol L <sup>-1</sup>	<sup>1</sup> H NMR yield / %	
		<b>13bi</b>	<b>8bi</b>
0.25	0.05	58	26 <sup>a</sup>
0.05	0.01	41	50 <sup>a</sup>
0.005	0.001	13	76 <sup>a</sup>
0.001	0.0002	3	82 <sup>a</sup>

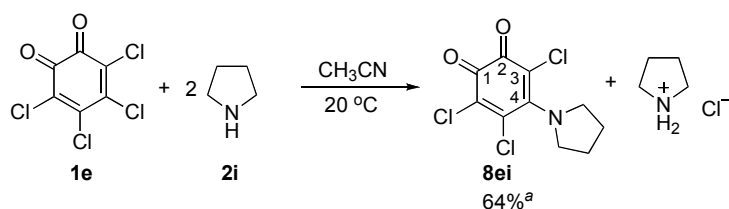
<sup>a</sup>Yield based on **2i**, considering that two amine molecules are needed per quinone

As chloranil **1c** has previously been reported to react with more than one molecule of amine, the reactions of **1c-e** with **2i** and **2j** have been performed with 4 equivalents of quinones (Schemes 8 and 9).



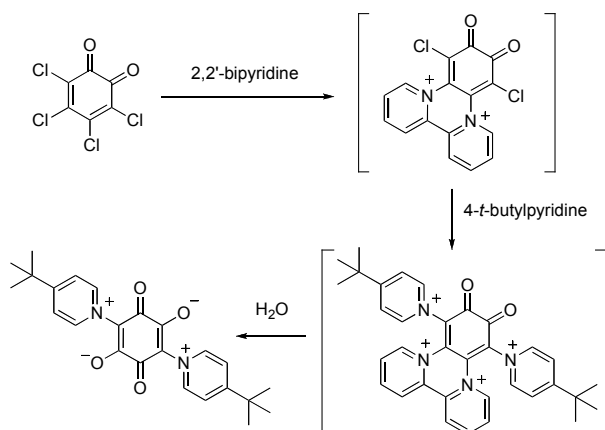
**Scheme 8.** Reactions of Quinones **1c** and **1d** with Amines **2i,j**

<sup>a</sup>Isolated yield based on **2i** or **2j**, considering that two amine molecules are needed per quinone

**Scheme 9.** Reaction of ortho-Quinone **1e** with Pyrrolidine

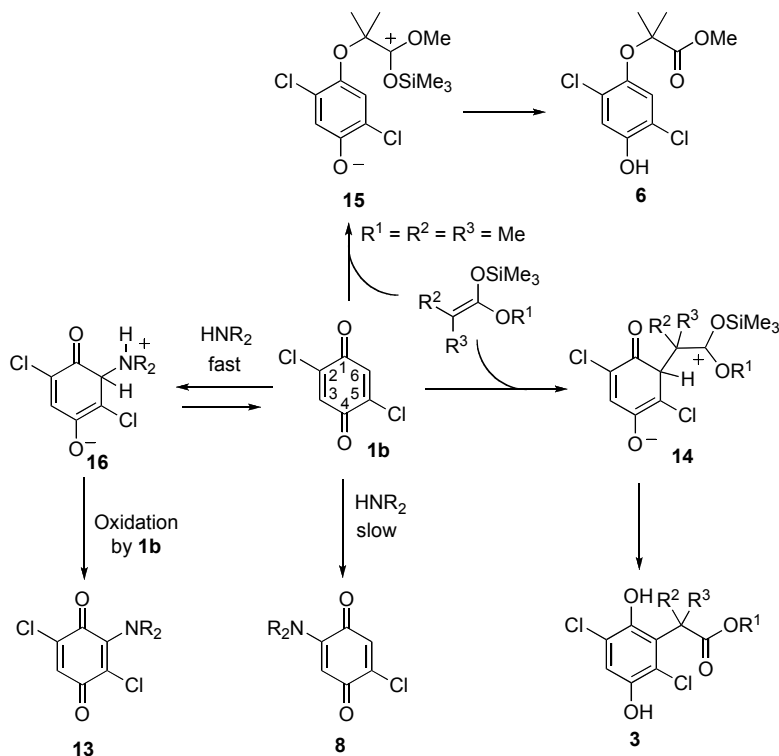
<sup>a</sup>Isolated yield based on **2i**, considering that two amine molecules are needed per quinone

The  $^{13}\text{C}$  NMR spectrum of pyrrolidine-substituted ortho-quinone **8ei** shows a similar pattern as that of **8ci**, i.e., only one carbon signal (C-3) is significantly shifted to high field because of the mesomeric electron donation of the lone pair of the nitrogen atom, in line with structure **8ei**, where the pyrrolidino group is located at C-4 position. The corresponding C-3 substitution by pyrrolidine would result in an NMR spectrum in which two carbon signals (conjugate C-4 and C-6 positions) are shifted to higher field. This assignment is in line with Koch's report<sup>16</sup> that the reaction of o-chloranil with 2,2'-bipyridine proceeds via C-4,5 substitution (Scheme 10).

**Scheme 10.** Reactions of o-Chloranil with Pyridine Derivatives Reported in Ref. 16

**Reaction Mechanism.** From the fact that *p*-benzoquinone **1a** as well as 2,5-dichloro-benzoquinone **1b** do not give products of C-1 attack with any of the investigated nucleophiles, we can conclude that conjugate attack at a C-H center of these quinones is generally preferred over attack at the carbonyl carbon C-1. For that reason, the nucleophilic attack at the carbonyl carbon of **1b** is not considered in Scheme 11.

**Scheme 11.** Reaction Pathways of 2,5-Dichloro-benzoquinone (**1b**)

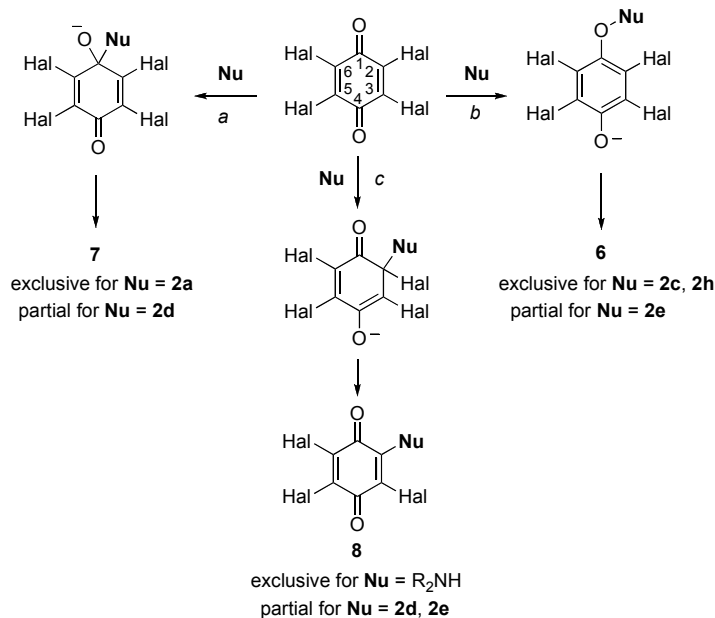


As summarized in Scheme 11, ketene acetals attack exclusively at O or C-6 (C-H) of **1b** with formation of the zwitterions **15** or **14**, respectively, which undergo subsequent desilylation to give the isolated products **6** and **3**; nucleophilic attack at CCl is not observed. Analogously, amines also attack faster at CH than at CCl to give the zwitterion **16**. However, the intermediate **16** may undergo retroaddition and the subsequent slower attack at C-2 leads to nucleophilic substitution of the chloride with formation of **8**. Only in the presence of high concentrations of quinones, oxidation of **16** can take place to give the amino-substituted quinones **13**. This situation – fast reversible nucleophilic attack at a CH position followed by slow irreversible attack at a CCl position reminds of the mechanisms of nucleophilic aromatic substitution of Cl<sup>-</sup> in acceptor substituted chlorobenzenes, where the initial nucleophilic attack also occurs at a CH group.<sup>17</sup>

If a highly electrophilic CH position is not available, as in the tetrahalo-substituted quinones **1c-e**, attack of *p*-nucleophiles at the carbonyl carbon, which was not observed in the reactions

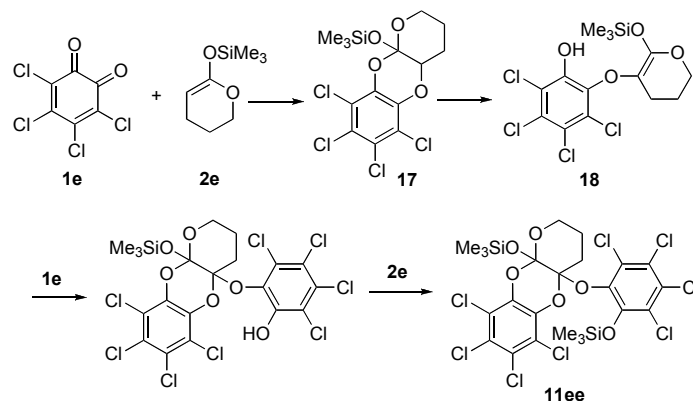
with **1a** and **1b**, becomes competitive. As shown in Scheme 12, nucleophiles may either attack at a halogen-substituted position (Scheme 12, path *c*) or at the carbonyl group, where C or O attack may occur (paths *a* and *b*).

**Scheme 12.** Reaction Pathways of Tetrahalogen-Substituted Quinones

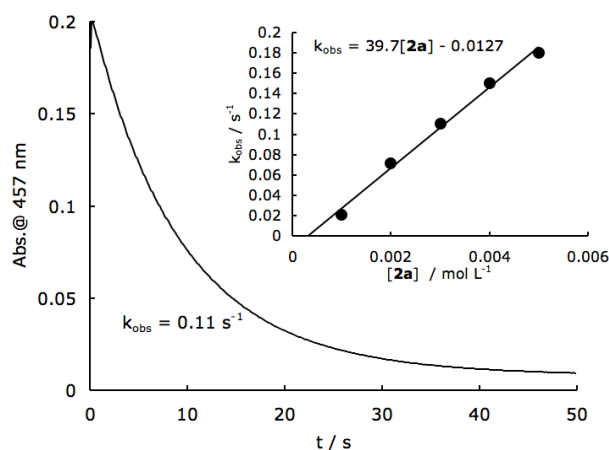


Pathway *a* (C-1 attack) is only followed by the terminal ketene acetal **2a**, and it is the only pathway followed by this nucleophile. Pathway *b* (O attack) is partially followed by the cyclic ketene acetal **2e**, and it is the only pathway followed by the enamine **2h** and the sterically demanding ketene acetal **2c**. Pathway *c* (C-2 attack), which leads to substitution via initial conjugate addition, is the exclusive process for all amines and is partially followed by the ketene acetals **2d** and **2e**, which concomitantly react via pathways *a* or *b*.

The presence of an *s*-cis configured hetero-diene system in the ortho-quinone **1e** provides additional reaction pathways. While amines selectively substitute 4-Cl of chloranil (**1c**) according to reaction pathway *c* in Scheme 12, and the terminal ketene acetal **2a** attacks the carbonyl carbon C-1 according to pathway *a* in Scheme 12, all other investigated *p*-nucleophiles **2c-e,h** behave as dienophiles in Diels-Alder reactions with inverse electron demand. The formation of the tricyclic compounds can be rationalized by the mechanism shown in Scheme 13. Initial [4+2] cycloaddition gives intermediate **17**, which undergoes ring-opening and proton transfer to form the silyl ketene acetal **18**. Its Diels-Alder reaction with **1e** and subsequent silylation of the hydroxyl group gives the isolated product **11ee**. Alternatively, silylation of the hydroxyl group may occur at an earlier stage of the reaction cascade.

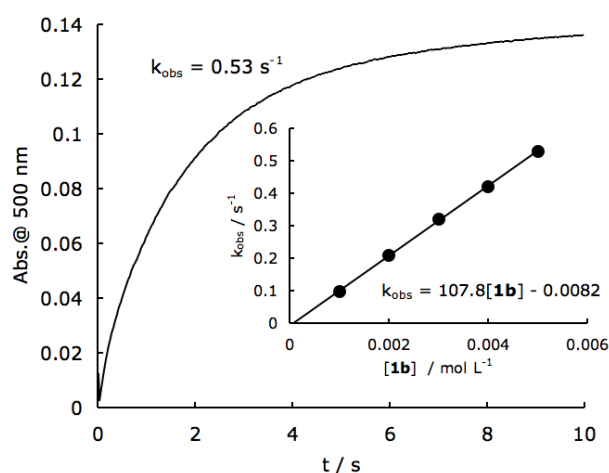
**Scheme 13.** Possible Mechanism for the Reaction of **1e** with **2e**

**Kinetic Studies: Reactions with p-Nucleophiles.** Kinetic investigations of the reactions of the quinones **1a-e** with the p-nucleophiles **2a-h** were performed in dichloromethane solution at 20 °C. Most of these reactions were monitored by UV-vis spectroscopy at or close to the absorption maxima of the quinones (2,5-dichloro-p-benzoquinone (**1b**): 275 nm, *p*-chloranil (**1c**): 290 nm, tetrafluoro-benzoquinone (**1d**): 256 nm, *o*-chloranil (**1e**): 457 nm). Only the reaction of **1a** with **2d** as well as the reaction of **1d** with **2b** were monitored by UV-vis spectroscopy at or close to the absorption maxima of the products (at ~350 nm), and the reaction of **1a** with **2e** was followed by  $^1\text{H}$  NMR spectroscopy. In all runs, an excess of the nucleophiles (at least 10-fold) over the quinones was used to achieve pseudo-first-order kinetics. The pseudo-first-order rate constants  $k_{\text{obs}}$  were obtained by least-squares fitting of the monoexponential function  $A_t = A_0 e^{-k_{\text{obs}}t} + C$  (for decrease) or  $A_t = A_0 (1 - e^{-k_{\text{obs}}t}) + C$  (for increase) to the absorbances. The second-order rate constants  $k_2$  (summarized in Table 2) were derived from the linear correlations of  $k_{\text{obs}}$  ( $\text{s}^{-1}$ ) against the concentrations of the nucleophiles as illustrated in Figure 4.



**Figure 4.** UV-Vis spectroscopic monitoring of the reaction of o-chloranil (**1e**,  $1.0 \times 10^{-4}$  mol  $\text{L}^{-1}$ ) with **2a** ( $3.0 \times 10^{-3}$  mol  $\text{L}^{-1}$ ) at 457 nm in  $\text{CH}_3\text{CN}$  at 20 °C. Insert: Determination of the second-order rate constant  $k_2 = 40 \text{ L mol}^{-1} \text{ s}^{-1}$  from the dependence of the first-order rate constants  $k_{\text{obs}}$  on the concentrations of **2a**.

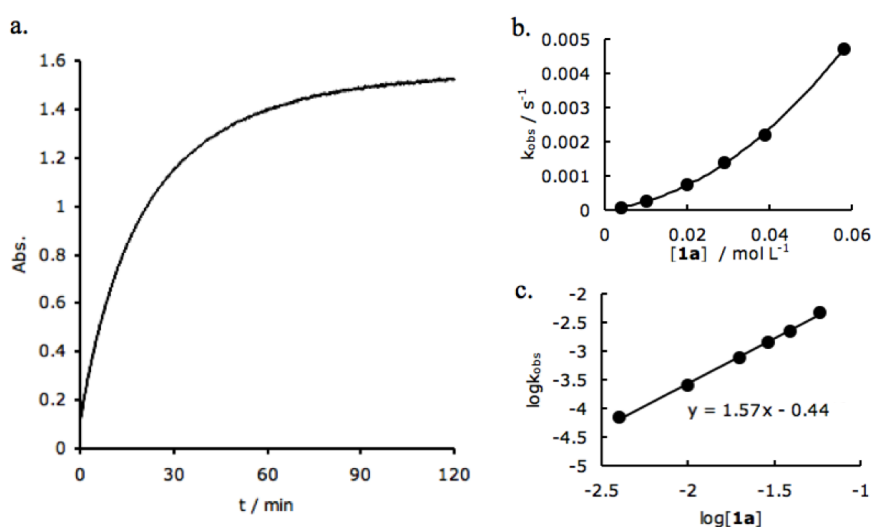
**Reactions with amines.** Kinetic investigations of the reactions of the quinones with the amines **2i-o** were performed in  $\text{CH}_3\text{CN}$  solution at 20 °C. The formation of the colored amino-substituted benzoquinones was monitored by UV-vis spectroscopy. In all runs, an excess of the quinones (at least 10-fold) over the amines was used to achieve pseudo-first-order kinetics and to avoid multiple substitutions. The pseudo-first-order rate constants  $k_{\text{obs}}$  were obtained by least-squares fitting of the monoexponential function  $A_t = A_0 (1 - e^{-k_{\text{obs}}t}) + C$  to the increasing absorbances.



**Figure 5.** UV-Vis spectroscopic monitoring of the reaction of 2,5-dichloro-benzoquinone (**1b**,  $5.0 \times 10^{-3}$  mol  $\text{L}^{-1}$ ) with **2i** ( $1.0 \times 10^{-4}$  mol  $\text{L}^{-1}$ ) at 500 nm in  $\text{CH}_3\text{CN}$  at 20 °C. Insert: Determination of the second-order rate constant  $k_2 = 54 \text{ L mol}^{-1} \text{ s}^{-1}$  from the dependence of the first-order rate constants  $k_{\text{obs}}$  on the concentrations of **1b**.

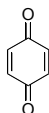
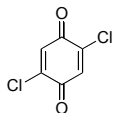
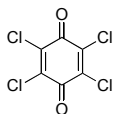
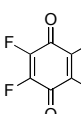
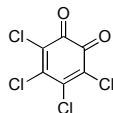
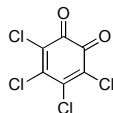
Like the reactions with *p*-nucleophiles, the reactions of the quinones **1b-e** with the amines **2i-o** also followed second-order kinetics. The second-order rate constants  $k_2$  (summarized in Table 2) were derived from the linear correlations of  $k_{\text{obs}}$  ( $\text{s}^{-1}$ ) against the concentrations of the nucleophiles (Figure 5). As two amine molecules are consumed by each substitution process, the slopes of the plots of  $k_{\text{obs}}$  vs. [quinone] have been multiplied by a factor of 0.5 to give the second-order rate constants  $k_2$  which are listed in Table 2.

Only the reaction of *p*-benzoquinone **1a** with pyrrolidine **2i** did not follow a second-order rate law. As shown in Figure 6, a reaction order of 2.6 (1 for **2i** and 1.6 for **1a**) was observed, indicating that a second molecule of quinone is needed for the oxidation of the reversibly generated initial adduct.



**Figure 6.** a) UV-Vis spectroscopic monitoring of the reaction of **2i** ( $1.0 \times 10^{-3} \text{ mol L}^{-1}$ ) with **1a** ( $2.0 \times 10^{-2} \text{ mol L}^{-1}$ ) at 500 nm in  $\text{CH}_3\text{CN}$  at 20 °C. b) Correlation of the observed pseudo-first-order rate constant  $k_{\text{obs}}$  with the concentration of **1a**. c) Correlation of  $\log k_{\text{obs}}$  vs.  $\log [\mathbf{1a}]$ .

**Table 2.** Rate Constants for The Reactions of The Quinones **1a-e** with The Nucleophiles **2a-o** (20 °C, L mol<sup>-1</sup> s<sup>-1</sup>)

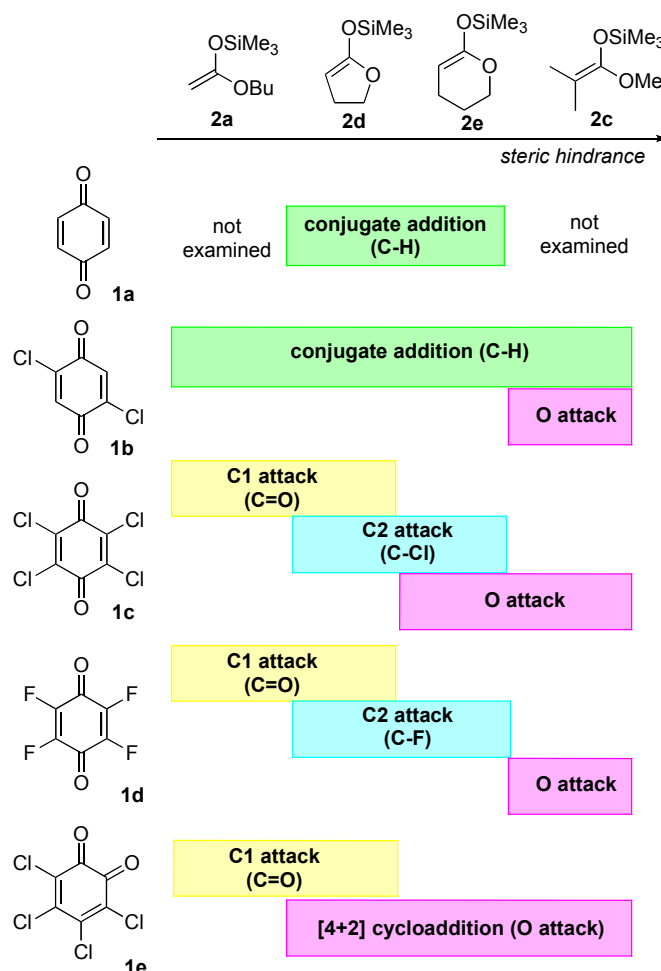
Quinone	attacked position	<i>E</i> parameter	Nucleophile	<i>k</i> <sub>2</sub> <sup>exp</sup>	<i>k</i> <sub>2</sub> <sup>calcd, a</sup>	log( <i>k</i> <sub>2</sub> <sup>exp</sup> / <i>k</i> <sub>2</sub> <sup>calcd</sup> )	<i>k</i> <sub>et</sub> <sup>max, b</sup>	log( <i>k</i> <sub>2</sub> <sup>exp</sup> / <i>k</i> <sub>et</sub> <sup>max</sup> )		
	C(-H)	-16.19	2d	2.2 x 10 <sup>-3</sup>	2.9 x 10 <sup>-3</sup>	-0.12				
			2e	2.0 x 10 <sup>-5</sup>	1.6 x 10 <sup>-5</sup>	0.10				
	O		2c	2.8 x 10 <sup>-4 c</sup>			8.5 x 10 <sup>-5</sup>	0.52		
	C(-H)	-12.28	2a	3.3 x 10 <sup>-2</sup>	2.0 x 10 <sup>-2</sup>	0.22	1.4 x 10 <sup>-8</sup>	6.37		
			2a'	1.0 x 10 <sup>-2</sup>	3.0 x 10 <sup>-2</sup>	-0.47				
			2c	8.3 x 10 <sup>-4 c</sup>	6.1 x 10 <sup>-4</sup>	0.13	8.5 x 10 <sup>-5</sup>	0.99		
			2d	3.1	1.6	0.30				
			2e	2.5 x 10 <sup>-2</sup>	3.7 x 10 <sup>-2</sup>	-0.17				
	C(-Cl)	-16.11	2i	5.4 x 10 <sup>1</sup>	3.3 x 10 <sup>1</sup>	0.21	4.2 x 10 <sup>-4</sup>	5.11		
			2j	8.0	7.0	0.06	3.3 x 10 <sup>-7</sup>	7.38		
			2k	2.6 x 10 <sup>-1</sup>	4.6 x 10 <sup>-1</sup>	-0.24	9.4 x 10 <sup>-9</sup>	7.44		
			2l	2.7 x 10 <sup>-1</sup>	3.0 x 10 <sup>-1</sup>	-0.04	2.7 x 10 <sup>-15</sup>	13.99		
			2o	4.7 x 10 <sup>-1</sup>	4.2 x 10 <sup>-1</sup>	0.04				
	O		2c	2.1 x 10 <sup>-2</sup>			1.6 x 10 <sup>-1</sup>	-0.88		
			2e	1.3 x 10 <sup>-2 c</sup>						
			2g	6.9 x 10 <sup>3</sup>			2.3 x 10 <sup>4</sup>	-0.52		
			2h	9.4 x 10 <sup>1</sup>			2.3 x 10 <sup>4</sup>	-2.38		
	C(=O)	-12.13	2a	1.0 x 10 <sup>-1</sup>	2.7 x 10 <sup>-2</sup>	0.57	2.6 x 10 <sup>-5</sup>	3.59		
			2a'	3.4 x 10 <sup>-2</sup>	3.9 x 10 <sup>-2</sup>	-0.05				
	C(-Cl)	-13.84	2d	4.8 x 10 <sup>-1 c</sup>	2.0	-0.62				
			2d	7.2 x 10 <sup>-1 c</sup>	1.3 x 10 <sup>-1</sup>	0.75				
			2e	2.1 x 10 <sup>-2 c</sup>	1.7 x 10 <sup>-3</sup>	1.10				
			2i	5.6 x 10 <sup>2</sup>	7.6 x 10 <sup>2</sup>	-0.13	7.7 x 10 <sup>-1</sup>	2.86		
2j			8.8 x 10 <sup>1</sup>	2.4 x 10 <sup>2</sup>	-0.44	6.2 x 10 <sup>-4</sup>	5.15			
2k			1.9	2.2 x 10 <sup>1</sup>	-1.06	1.7 x 10 <sup>-5</sup>	5.04			
	C(-Cl)	-13.84	2l	4.7	8.0	-0.23	5.1 x 10 <sup>-12</sup>	11.97		
			2n	6.8 x 10 <sup>-1</sup>	2.0	-0.47				
			2o	1.8 x 10 <sup>1</sup>	1.1 x 10 <sup>1</sup>	0.22				
			O		2c	3.1 x 10 <sup>-1</sup>			2.2 x 10 <sup>-2</sup>	1.15
					2g	6.1 x 10 <sup>4</sup>			3.1 x 10 <sup>3</sup>	1.29
					2h	9.2 x 10 <sup>2</sup>			3.1 x 10 <sup>3</sup>	-0.53
	C(=O)	-9.37			2a	2.0 x 10 <sup>1</sup>	4.9	0.61	3.6 x 10 <sup>-6</sup>	6.75
			2a'	1.2 x 10 <sup>1</sup>	5.5	0.34				
			2b	3.3 x 10 <sup>-2</sup>	1.2 x 10 <sup>-1</sup>	-0.56	3.1 x 10 <sup>-8</sup>	6.09		
			2d	5.9 x 10 <sup>1 c</sup>	1.7 x 10 <sup>2</sup>	-0.46				
	C(-F)	-11.12	2d	3.8 x 10 <sup>1 c</sup>	1.0 x 10 <sup>1</sup>	0.57				
			2e	1.8	3.6 x 10 <sup>-1</sup>	0.69				
			2i	3.5 x 10 <sup>4</sup>	3.3 x 10 <sup>4</sup>	0.04	1.1 x 10 <sup>-1</sup>	5.52		
			2j	1.6 x 10 <sup>4</sup>	1.7 x 10 <sup>4</sup>	-0.03	8.5 x 10 <sup>-5</sup>	8.27		
			2k	3.0 x 10 <sup>2</sup>	2.3 x 10 <sup>3</sup>	-0.88	2.4 x 10 <sup>-6</sup>	8.09		
			2l	5.0 x 10 <sup>2</sup>	4.1 x 10 <sup>2</sup>	0.08	7.0 x 10 <sup>-13</sup>	14.85		
			2m	2.5	7.7	-0.49	3.2 x 10 <sup>-13</sup>	12.90		
			2n	6.9 x 10 <sup>1</sup>	1.3 x 10 <sup>2</sup>	-0.29				
	2o	9.2 x 10 <sup>2</sup>	5.3 x 10 <sup>2</sup>	0.24						
		O		2c	4.6 x 10 <sup>2</sup>			2.7 x 10 <sup>1</sup>	1.23	
2d				1.2 x 10 <sup>3 c</sup>						
2e				1.0 x 10 <sup>2</sup>						
2g				1.4 x 10 <sup>6</sup>			3.9 x 10 <sup>6</sup>	-0.45		
2h				>10 <sup>6</sup>						
2f				3.2 x 10 <sup>-3</sup>			1.6 x 10 <sup>-6</sup>	3.29		
C(=O)		-8.77	2a	4.0 x 10 <sup>1</sup>	1.5 x 10 <sup>1</sup>	0.42	4.5 x 10 <sup>-3</sup>	3.95		
			2b	1.6 x 10 <sup>-1</sup>	3.7 x 10 <sup>-1</sup>	-0.36	3.9 x 10 <sup>-5</sup>	3.62		
			2d	3.8 x 10 <sup>2 c</sup>	4.5 x 10 <sup>2</sup>	-0.07				
			C(-Cl)	-12.02	2i	2.5 x 10 <sup>4</sup>	9.4 x 10 <sup>3</sup>	0.43	1.3 x 10 <sup>2</sup>	2.28
2j	5.5 x 10 <sup>3</sup>	4.2 x 10 <sup>3</sup>			0.12	1.1 x 10 <sup>-1</sup>	4.71			
2k	1.3 x 10 <sup>2</sup>	4.9 x 10 <sup>2</sup>			-0.57	3.0 x 10 <sup>-3</sup>	4.64			
2l	2.0 x 10 <sup>2</sup>	1.1 x 10 <sup>2</sup>			0.25	8.8 x 10 <sup>-10</sup>	11.36			
		2n	2.7 x 10 <sup>1</sup>	3.3 x 10 <sup>1</sup>	-0.09					

a) *k*<sub>2</sub><sup>calcd</sup> are rate constants calculated by eq. 1 from the *E* parameters in this table and *N*/*s<sub>N</sub>* from Table 1.b) *k*<sub>et</sub><sup>max</sup> are the maximal rate constants calculated by eq. 4 for single electron transfer.

c) calculated from overall rate constant based on the ratio of products

### 3.3 Discussion

**Linear Free Energy Relationships.** The changes of selectivity due to increasing steric hindrance of the silyl ketene acetals are shown in Figure 7. In the reactions with **1a** and **1b** conjugate addition at the C-H positions is always favored; only the sterically demanding ketene acetal **2c** also attacks at the carbonyl oxygen. Both tetrahalogen-substituted quinones **1c,d** react with the terminal ketene acetal **2a** exclusively at the carbonyl carbon, but increasing steric shielding of the nucleophiles (**2d**, **2e**) leads to C-2 attack (substitution) and further increase of steric demand results in attack at O which is the least shielded position and gives the thermodynamically most stable product. Like the para-quinones **1c,d**, the ortho-quinone **1e** also reacts exclusively at C-1 with the terminal ketene acetal **2a**, but increasing steric shielding now leads to Diels-Alder reactions.

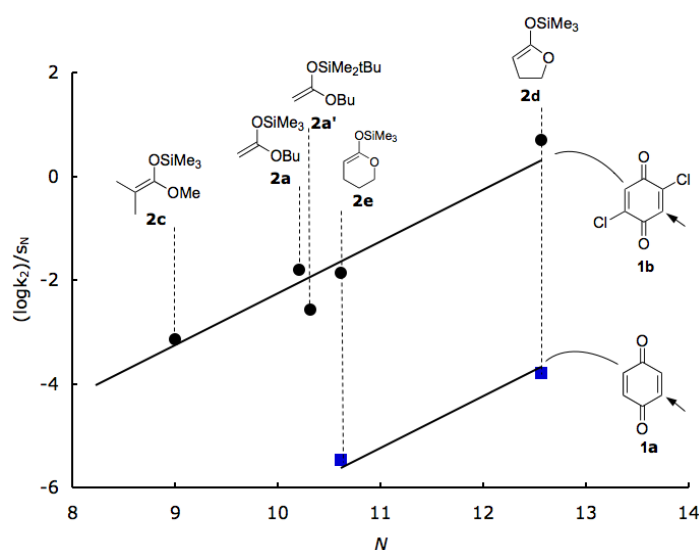


**Figure 7.** Steric effect on the product selectivities of quinones with silyl ketene acetals.

The linear plots of  $(\log k)/s_N$  vs. the benzhydrylium-derived nucleophilicity parameters  $N$  of the ketene acetals **2** in Figure 8 show that the conjugate attack of the ketene acetals at a C-H



position of **1a** and **1b** follows eq. (1). Please note that also the two-point correlation for the parent quinone **1a** has significance because a slope of 1.0, as required by eq. (1), was enforced for the least-squares minimizations. The similar reactivities of the trimethylsilyl (**2a**) and *tert*-butyldimethylsilyl (**2a'**) ketene acetals indicate that the silyl transfer must occur after the rate-determining step. Comparison of the reactivities of **1a** and **1b** shows that the dichloro-substitution in **1b** increases the electrophilicities of the C-H positions by approximately three orders of magnitude. It should be noted, however, that the high electrophilicities of these positions can only become effective when the initially formed zwitterions undergo fast subsequent reactions, e.g. silyl transfer in the reactions with silylated ketene acetals or oxidation by a second molecule of quinone in the reactions with amines.

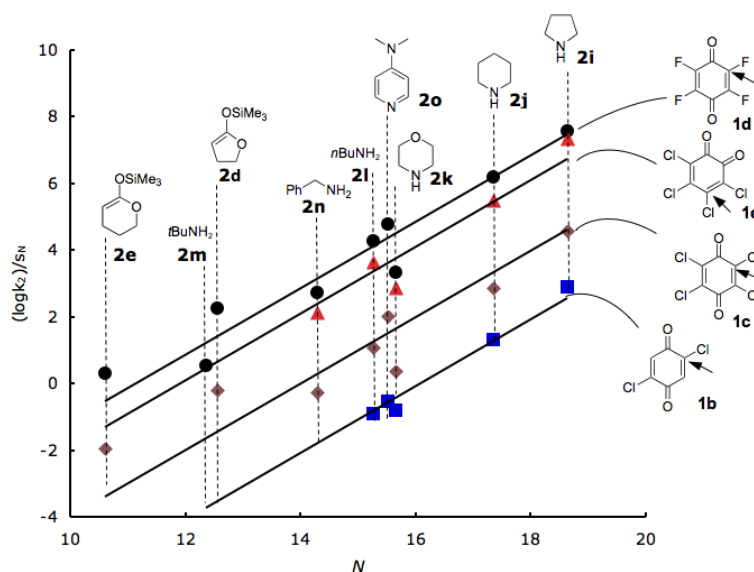


**Figure 8.** Plot of  $(\log k_2)/s_N$  vs  $N$  for the addition (at C(-H)) reactions of **1a,b** with p-nucleophiles in  $\text{CH}_2\text{Cl}_2$  at 20 °C (the slope is enforced to 1).

When studying the kinetics of the reactions of **1b** with amines, the concentrations of the quinone **1b** were rather small, with the consequence that the measured rate constants referred to the attack at C-Cl and formation of **8**. From the fact that second-order kinetics were observed from low to high degree of conversion, we conclude that the concentration of the rapidly formed zwitterion **16** (Scheme 11) remains so small under the conditions of the kinetic experiments that its intermediacy is not relevant for the kinetics.

The linear correlations for the attack at the C-Cl or C-F positions of **1b-e** show (Figure 9) that also for these reactions, eq. (1) and the benzhydrylium-derived nucleophile-specific reactivity parameters  $N$  and  $s_N$  are applicable; as mentioned above, a slope of 1.0 is enforced in this type of plots. Since the partial rate constants<sup>18</sup> for the attack of the ketene acetals **2d** and **2e** at the C-Hal positions of **1c** and **1d** are on the same correlation line (deviation less than a factor of

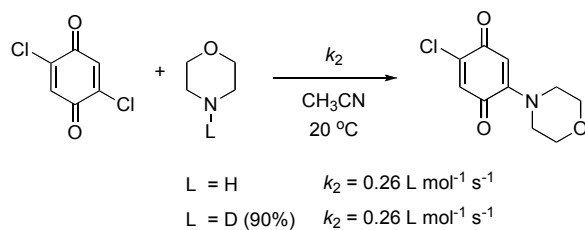
20, see Table 2) as the rate constants for the reactions with amines, it is demonstrated that the electrophilic reactivities ( $E$ ) of the halogen-substituted positions of the quinones are again almost independent of the nature of the nucleophilic reaction partner.



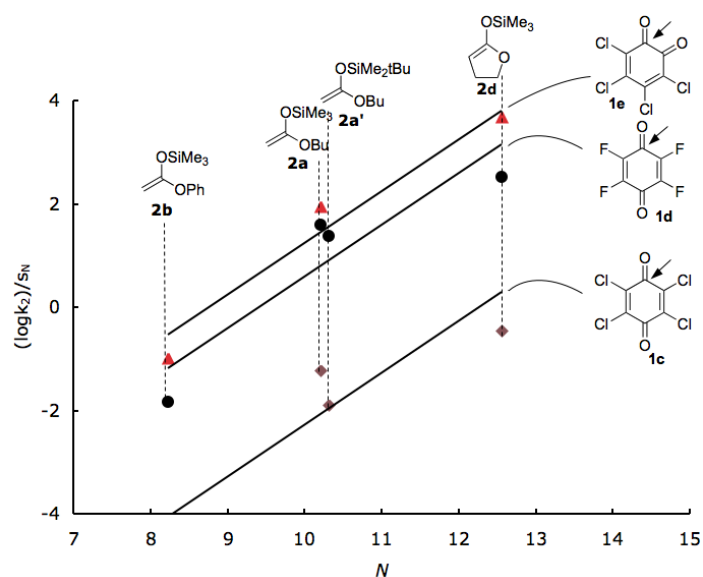
**Figure 9.** Plot of  $(\log k_2)/s_N$  vs  $N$  for the substitution or addition reactions of **1b-e** with amines **2i-o** in  $\text{CH}_3\text{CN}$  and silyl ketene acetals **2d** and **2e** (at C-Hal) in  $\text{CH}_2\text{Cl}_2$  at 20 °C (the slope is enforced to 1).

The absence of a kinetic isotope effect ( $k_H/k_D = 1.0$ , Scheme 14) in the reaction of 2,5-dichloro-benzoquinone (**1b**) with  $N$ -deuterated-morpholine (90% D) indicates that proton transfer is not involved in the rate-determining-step.

**Scheme 14.** Kinetic Isotope Effect for the Reaction of **1b** with Morpholine



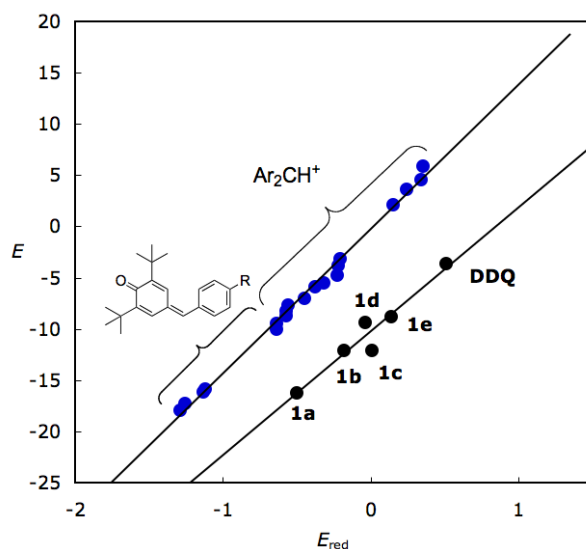
Analogous correlations in Figure 10 show that the carbonyl carbons of tetrachloro-o-quinone (**1e**) and fluoranil (**1d**) have similar electrophilicities, 2-3 orders of magnitude greater than that of the carbonyl carbon of chloranil (**1c**).



**Figure 10.** Plot of  $(\log k_2)/s_N$  vs  $N$  for the attack of p-nucleophiles at the carbonyl carbon of **1c-e** in  $\text{CH}_2\text{Cl}_2$  at 20 °C (the slope is enforced to 1).

According to equation (1), the electrophilicity parameters of the C-1, C-2, and C-3 positions of the quinones listed in Table 2 were determined by least-squares minimization of  $\Delta^2 = \sum (\log k_2 - s_N(N + E))^2$  using the second-order rate constants  $k_2$  given in Table 2 and the  $N$  and  $s_N$  parameters of the nucleophiles **2a-o** from Table 1, which have been derived from reactions with benzhydrylium ions.<sup>6-8</sup>

**SET vs Polar Reaction.** In previous work we have shown that DDQ reacts much more slowly with p-nucleophiles than expected from the correlation between electrophilicity and redox potential of benzhydrylium ions and quinone methides,<sup>19</sup> i.e., DDQ is far below the correlation line for benzhydrylium ions and quinone methides (Figure 11). After adding data for the quinones studied in this work to the plot, one can see that the electrophilic reactivities of the most reactive positions of quinones also correlate linearly with their redox potentials. The correlation line for quinones is ~10 orders of magnitude below the line for benzhydrylium ions and quinone methides.



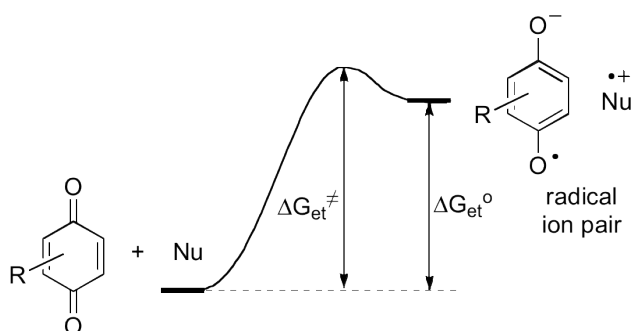
**Figure 11.** Correlation between the electrophilicity parameters  $E$  and the reduction potentials  $E_{\text{red}}$  of benzhydrylium ions and quinone methides (reference electrophiles)<sup>19</sup> and quinones.

As the rate constant for electron transfer can be calculated by the Eyring equation (eq. 2), and  $\Delta G_{\text{et}}^\ddagger$  must be greater than  $\Delta G_{\text{et}}^\circ$  (eq. 3) according to Figure 12, the maximal accessible rate constants for electron transfer from nucleophiles to quinones are given by eq. (4), where  $c$  is the Coulomb term, i.e., the energy needed to separate the radical ion pair to infinite distance in  $\text{CH}_2\text{Cl}_2$  solution; a value of  $c = 9.6$  kJ/mol as suggested by Fukuzumi and Otera was used for the Coulomb term in the following analyses.<sup>9</sup>

$$k_{\text{et}} = (k_{\text{b}}T/h) \exp(-\Delta G_{\text{et}}^\ddagger/RT) \quad (2)$$

$$\Delta G_{\text{et}}^\ddagger > \Delta G_{\text{et}}^\circ = F(E_{\text{ox}} - E_{\text{red}}) - c \quad (3)$$

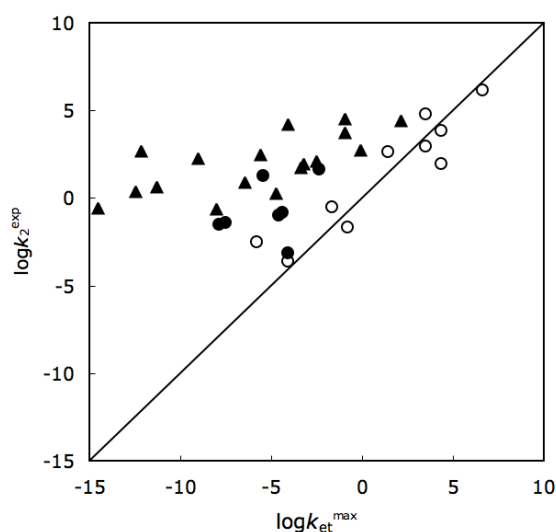
$$k_{\text{et}}^{\text{max}} = (k_{\text{b}}T/h) \exp\{-F(E_{\text{ox}} - E_{\text{red}}) + c\}/RT\} \quad (4)$$



**Figure 12.** Energy profile for electron transfer process.

The comparison of the experimental rate constants with the maximal rate constants for electron transfer (i.e., for  $\Delta G_{\text{et}}^\ddagger = \Delta G_{\text{et}}^\circ$ ), which is given in the last column of Table 2, is illustrated in Figure 13. Since the drawn diagonal characterizes reactions of quinones with nucleophiles which proceed with the same rate as the fastest conceivable SET processes, one

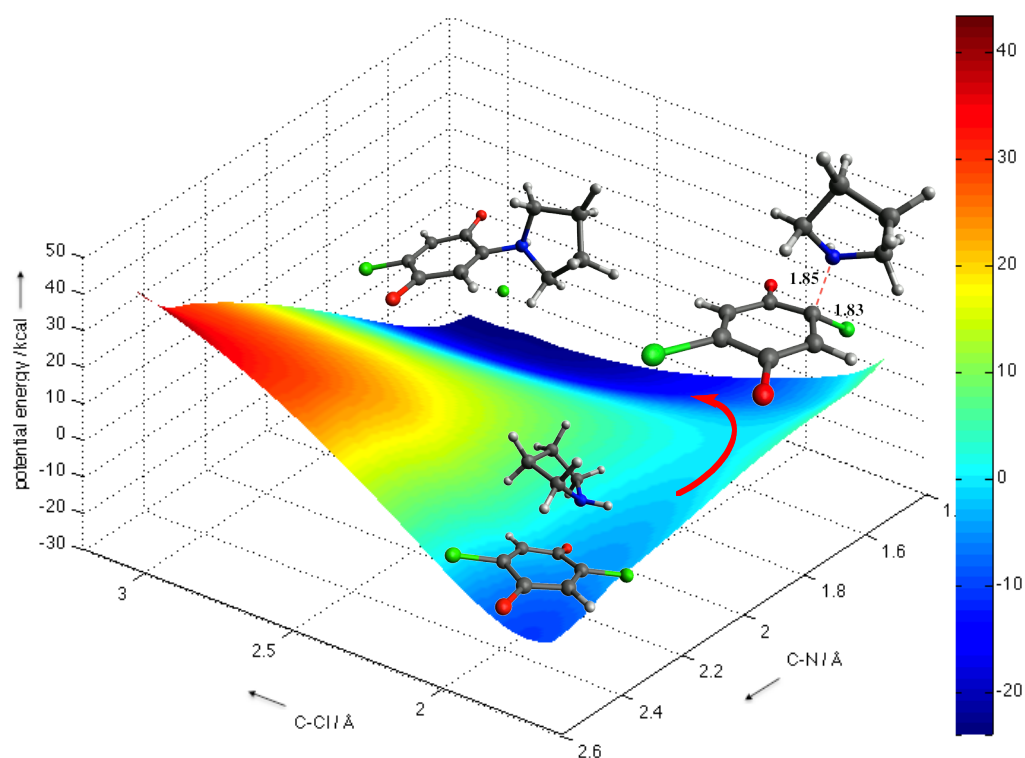
can derive that the operation of SET processes can certainly be excluded for the reactions of quinones with amines ( $\blacktriangle$ ). As all amines react several orders of magnitude faster than the SET can proceed, they must react via polar processes. Most of the reactions of p-nucleophiles with a carbon center of the quinones are also 4-7 orders of magnitude faster than the fastest conceivable SET processes ( $\bullet$ , exception **1b** + **2c** which gives both C- and O-attack products), and only the reactions, which involve O attack at the quinones ( $\circ$ ), proceed with rate constants which are compatible with SET processes.



**Figure 13.** Correlation of measured rate constants ( $\log k_{\text{exp}}$ ) with calculated maximal rate constants of SET ( $\log k_{\text{et,max}}$ ) for the reactions of quinones with amines ( $\blacktriangle$ ) and p-nucleophiles via C attack ( $\bullet$ ) and p-nucleophiles via O attack ( $\circ$ ).

**Computational Studies: Stepwise or Concerted Substitution?** The question whether conjugate addition or elimination of chloride is rate-determining in the reaction of 2,5-dichloro-benzoquinone (**1b**) with pyrrolidine (**2i**) was studied by quantum chemical calculations using Gaussian 09<sup>20</sup> at B97D/6-31+G(d,p)//B97D/6-31+G(d,p)//PCM/UFF level of theory in CH<sub>3</sub>CN. The potential energy surface for the substitution process was calculated by a relaxed PES scan (with geometry optimization at each point) on the bond length of C-N and C-Cl.

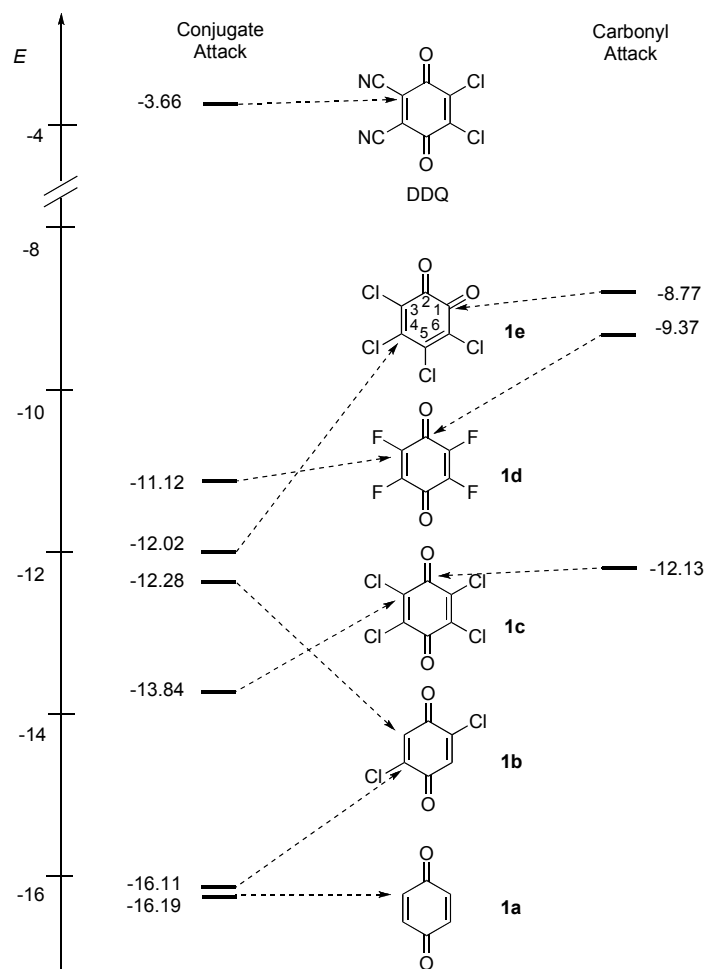
Interestingly, the potential energy surface for the substitution reaction of **1b** with **2i** shows that there is no intermediate between the reactants and products (Figure 14). The substitution proceeds via an asymmetric concerted process, in which breaking of the C-Cl bond starts before the formation of C-N bond is complete.



**Figure 14.** Potential energy surface of the reaction of **1b** with **2i**

### 3.4 Conclusion

The electrophilicity scale in Figure 15 summarizes the behavior of the quinones **1(a-e)** toward nucleophiles. The most electrophilic position in the parent compound **1a** is the CH-group. Attack at this position can only lead to products, however, when the initially formed intermediate can be stabilized, e.g., by silyl migration, as in the reactions with silyl ketene acetals or by subsequent hydride abstraction, as in the reactions with amines.



**Figure 15.** The ambident electrophilicities of halo-substituted quinones.

Introduction of two chlorine atoms, as in **1b**, increases the electrophilicities of the CH-positions by 3-4 units, while the electrophilicities of the chlorine substituted positions remain the same as in the parent **1a**. As a consequence, attack at a CH-position of **1b** occurs, when the corresponding intermediate can undergo subsequent reactions as described for **1a**. Otherwise, the CH attack is reversible, and the final product is formed by the slower attack at the CCl position.

The additional chlorine substituents in **1c** increase the electrophilicities of the CCl positions in **1c** relative to those of **1b** by more than two units of  $E$ . The four halogen substituents in chloranil **1c** and fluoranil **1d** activate the carbonyl groups so strongly that the carbonyl carbons adopt similar electrophilicities as the halogen-substituted positions, and it depends on the nature of the nucleophile and the rate of the subsequent reactions which products will eventually be formed. It is interesting to note that the CCl positions in chloranil **1c** are still less reactive than the CH positions in the dichloroquinone **1b**.

The higher electrophilicity of both positions of fluoranil **1d** compared to those of chloranil **1c** is in analogy to the relative reactivities of nitrated fluoro- and chlorobenzenes in nucleophilic aromatic substitutions.<sup>17</sup>

Both, C-4 and C-1 of ortho-chloranil **1e** are more electrophilic than the corresponding positions in para-chloranil **1c**, and the regioselectivity of nucleophilic attack at **1e** is again controlled by the feasibility of subsequent reactions.

Comparison with the previously reported electrophilicity of DDQ reveals the enormous activating effect of the cyano groups – ten units in *E* compared with chloranil **1c**.

As equation (1) is only applicable to electrophile-nucleophile combinations, when at least one of the reaction centers is carbon, Figure 15 does not include electrophilicity parameters for O-attack.

Because of the weakness of N-O bonds, O-attack is not observed in reactions with amines, but is encountered in reactions of chloranil (**1c**) and fluoranil (**1d**) with the sterically shielded ketene acetal **2c** and the enamines **2g,h**. For these reactions SET processes appear feasible, because the observed rate constants are comparable to those calculated from the redox potentials of the reactants. The significantly lower electrophilicity of the CCl position compared with the carbonyl carbon of the ortho-quinone **1e** reflects that p<sub>CC</sub>-nucleophiles do not usually attack at the halogenated position. However, ketene acetals attack the carbonyl carbon with comparable rates as they undergo Diels-Alder reactions with inverse electron demand across the cis-1,2-diketone fragment of **1e**. As decreasing nucleophilicity of the p<sub>CC</sub>-system retards the C-attack more than the hetero-Diels-Alder reaction, one can explain why ordinary alkenes give benzo-1,4-dioxines with ortho-chloranil (**1e**).<sup>21</sup>



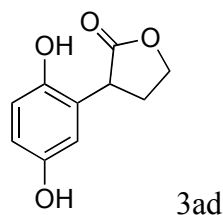
### 3.5 Experimental Section

**Materials.** Commercially available **1a** was purified by sublimation before use. **1b** was prepared by chlorination and subsequent oxidation of 1,4-dimethoxybenzene as reported in the literature.<sup>22</sup> Commercially available **1c** was recrystallized from chloroform. Silyl ketene acetals **2(a, a', b, d, e)** were prepared by silylation of the deprotonated esters according to ref. 23. Silyl enol ether **2f** was prepared from acetophenone as reported in the literature.<sup>24</sup> Enamines **2g** and **2h** were synthesized by condensation of the cycloalkanones with morpholine according to a literature procedure.<sup>25</sup> *N*-deuterated-morpholine was synthesized by deuterium exchange of morpholine with D<sub>4</sub>-methanol followed by evaporation of the remaining methanol (3 ×) before it was dried with sodium. All other chemicals were purchased from commercial sources without further purification.

#### 1) Experimental details and characterization data for products

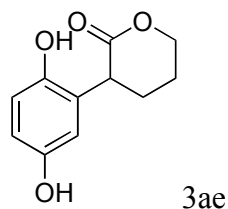
**General information:** <sup>1</sup>H NMR and <sup>13</sup>C NMR spectra were recorded on Bruker 400 MHz (101 MHz), 300 MHz (75.5 MHz) or Varian 600 MHz (151 MHz) spectrometers. The chemical shifts are reported in parts per million (δ) relative to internal TMS signal (0.00 ppm) or the internal solvent signals of CDCl<sub>3</sub> (δ<sub>H</sub> = 7.26, δ<sub>C</sub> = 77.0), d<sub>6</sub>-DMSO (δ<sub>H</sub> = 2.50, δ<sub>C</sub> = 39.5), CD<sub>3</sub>CN (δ<sub>H</sub> = 1.94, δ<sub>C</sub> = 118.3, 1.3), d<sub>4</sub>-methanol (δ<sub>H</sub> = 3.31, δ<sub>C</sub> = 49.0). The peak patterns are indicated as follows: br, broad signal; s, singlet; d, doublet; t, triplet; m, multiplet; q, quartet. The coupling constants, *J*, are reported in Hertz (Hz). Mass spectra were determined with Finnigan MAT 95 for EI-MS (70 eV) and HR-MS, Thermo Finnigan LTQ FT for ESI-MS. IR spectra were recorded with a Perkin Elmer Spectrum BX infrared spectrometer from Perkin Elmer with ATR probe (diamond).

**Reaction of quinone **1a** with ketene acetal **2d**.** A mixture of **2d** (317 mg, 2.00 mmol) and **1a** (54 mg, 0.50 mmol) in CH<sub>2</sub>Cl<sub>2</sub> (2.0 mL) was stirred for 24 h under nitrogen at 20 °C. Then the solvent was evaporated and the residue was purified by column chromatography (silica gel, eluent: MeOH/dichloromethane = 1/50, very low flow rate is needed for complete hydrolysis of the silylated **3ad**) to give **3ad** (colorless sticky oil, 58 mg, 60% yield).



**3-(2,5-Dihydroxyphenyl)dihydrofuran-2(3H)-one (3ad).** IR (neat):  $\nu_{\max}$  3323, 2971, 2914, 1738, 1508, 1451, 1378, 1253, 1174, 1021, 952, 868, 813, 793, 733, 702  $\text{cm}^{-1}$ ;  $^1\text{H}$  NMR (400 MHz,  $\text{d}_6$ -DMSO)  $\delta$  8.92 (s, 1H), 8.68 (s, 1H), 6.63-6.60 (m, 1H), 6.53-6.49 (m, 2H), 4.37 (apparent td,  $J$  = 8.8, 2.4 Hz, 1H), 4.24 (apparent ddd,  $J$  = 8.8, 10.0, 7.2 Hz, 1H), 3.84 (apparent dd,  $J$  = 10.4, 9.6 Hz, 1H), 2.50-2.42 (m, 1H), 2.35-2.25 (m, 1H);  $^{13}\text{C}$  NMR (101 MHz,  $\text{d}_6$ -DMSO)  $\delta$  177.7 (s), 149.7 (s), 147.4 (s), 125.1 (s), 116.8 (d), 115.9 (d), 114.6 (d), 66.4 (t), 41.6 (d), 29.6 (t); MS (DEI)  $m/z$ : 194, 176, 147, 136, 107, 77, 43; HRMS (DEI) calcd for  $[\text{C}_{10}\text{H}_{10}\text{O}_4]^+$ : 194.0574; found: 194.0562.

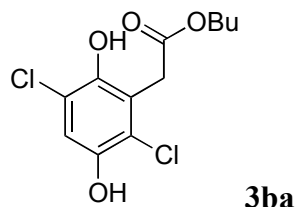
**Reaction of quinone 1a with ketene acetal 2e.** A mixture of **2e** (345 mg, 2.00 mmol) and **1a** (54 mg, 0.50 mmol) in  $\text{CH}_2\text{Cl}_2$  (2.0 mL) was stirred for 24 h under nitrogen at 20 °C. Then the solvent was evaporated and the residue was purified by column chromatography (silica gel, eluent: diethyl ether/dichloromethane = 1/5, very low flow rate is needed for complete hydrolysis of the silylated **3ae**) to give crude **3ae** (light yellow sticky oil, 40 mg, 38% yield).



**3-(2,5-Dihydroxyphenyl)tetrahydro-2H-pyran-2-one (3ae).** IR (neat):  $\nu_{\max}$  3343, 2951, 2883, 1707, 1507, 1451, 1203, 1084, 1053, 815  $\text{cm}^{-1}$ ;  $^1\text{H}$  NMR (600 MHz,  $\text{d}_4$ -methanol) 6.65-6.61 (m, 2H), 6.52 (dd,  $J$  = 8.6, 2.9 Hz, 1H), 3.97 (apparent t,  $J$  = 7.7 Hz, 1H), 3.54 (apparent t,  $J$  = 6.6 Hz, 2H), 2.05-1.98 (m, 1H), 1.81-1.76 (m, 1H), 1.54-1.44 (m, 2H);  $^{13}\text{C}$  NMR (151 MHz,  $\text{d}_4$ -methanol)  $\delta$  176.9 (s), 151.2 (s), 149.0 (s), 127.9 (s), 117.0 (d), 115.8 (d), 115.4 (d), 62.7 (t), 45.2 (d), 31.5 (t), 29.9 (t); MS (DEI)  $m/z$ : 208, 190, 162, 147; HRMS (DEI) calcd for  $[\text{C}_{11}\text{H}_{12}\text{O}_4]^+$ : 208.0730; found: 208.0740.

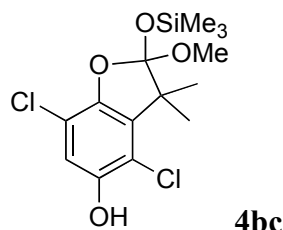
**Reaction of quinone 1b with ketene acetal 2a.** To a solution of **2a** (377 mg, 2.00 mmol) in  $\text{CH}_2\text{Cl}_2$  (2.0 mL), a solution of **1b** (89 mg, 0.50 mmol) in 5 mL  $\text{CH}_2\text{Cl}_2$  was slowly added over 2 h under nitrogen at 20 °C. After stirring for 12 h at 20 °C, the solvent was evaporated

and the residue was purified by flash column chromatography (silica gel, eluent: MeOH/dichloromethane = 1/50, very low flow rate is needed for complete hydrolysis of the silylated **3ba**, or the crude mixture was treated with methanol for 1 h before column) to give **3ba** (white solid, 60 mg, 41% yield).



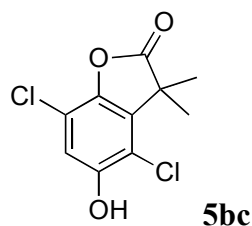
**Butyl 2-(2,5-dichloro-3,6-dihydroxyphenyl)acetate (3ba).** M.p.: 127-129 °C (CH<sub>2</sub>Cl<sub>2</sub>); IR (neat):  $\nu_{\max}$  3429, 3316, 2960, 2928, 2861, 1709, 1586, 1483, 1448, 1408, 1388, 1341, 1323, 1276, 1252, 1189, 1138, 1055, 1009, 964, 946, 846, 809, 758, 736 cm<sup>-1</sup>; <sup>1</sup>H NMR (400 MHz, d<sub>6</sub>-DMSO)  $\delta$  9.87 (s, 1H), 9.07 (s, 1H), 6.90 (s, 1H), 4.04 (t, *J* = 6.4 Hz, 2H), 3.78 (s, 2H), 1.57-1.50 (m, 2H), 1.35-1.25 (m, 2H), 0.87 (t, *J* = 7.2 Hz, 3H); <sup>13</sup>C NMR (101 MHz, d<sub>6</sub>-DMSO)  $\delta$  169.7 (s), 146.6 (s), 144.1 (s), 124.1 (s), 120.3 (s), 119.7 (s), 114.8 (d), 64.0 (t), 33.5 (t), 30.1 (t), 18.5 (t), 13.5 (q); MS (DEI) *m/z*: 294, 292, 220, 218, 192, 190, 99, 57, 41, 29; HRMS (DEI) calcd for [C<sub>12</sub>H<sub>14</sub><sup>35</sup>Cl<sub>2</sub>O<sub>4</sub>]<sup>+</sup>: 292.0264; found: 292.0248.

**Reaction of quinone 1b with ketene acetal 2c.** To a solution of **2c** (350 mg, 2.00 mmol) in CH<sub>2</sub>Cl<sub>2</sub> (2.0 mL), a solution of **1b** (89 mg, 0.50 mmol) in 5 mL CH<sub>2</sub>Cl<sub>2</sub> was slowly added over 2 h under nitrogen at 20 °C. After stirring for 12 h at 20 °C, the solvent was evaporated and the residue was purified by flash column chromatography (silica gel, eluent: MeOH/dichloromethane = 1/50, very low flow rate is needed for complete hydrolysis of the silylated **5bc** and **6bc**) to give **4bc** (white solid, 32 mg, 18% yield) and **5bc** (white solid, 48 mg, 39% yield) and **6bc** (colorless sticky oil, 27 mg, 19% yield).

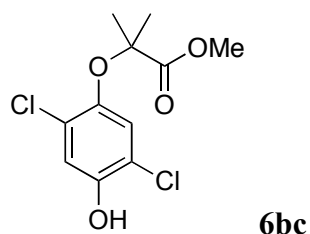


**4,7-Dichloro-2-methoxy-3,3-dimethyl-2-(trimethylsilyloxy)-2,3-dihydrobenzofuran-5-ol (4bc).** M.p.: 213-215 °C (CH<sub>2</sub>Cl<sub>2</sub>); IR (neat):  $\nu_{\max}$  3445, 2955, 1453, 1416, 1254, 1187, 1150, 1116, 1074, 1010, 916, 871, 840 cm<sup>-1</sup>; <sup>1</sup>H NMR (400 MHz, CDCl<sub>3</sub>)  $\delta$  6.85 (s, 1H), 3.43 (s, 3H), 1.44 (s, 3H), 1.34 (s, 3H), 0.21 (s, 9H); <sup>13</sup>C NMR (101 MHz, CDCl<sub>3</sub>)  $\delta$  146.3 (s), 145.2

(s), 133.8 (s), 124.7 (s), 115.0 (s), 114.8 (s), 114.5 (d), 51.7 (s), 50.0 (q), 22.8 (q), 21.1 (q), 1.5 (q).

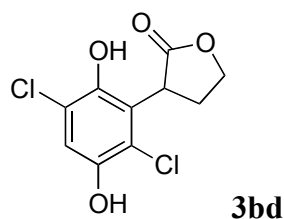


**4,7-Dichloro-5-hydroxy-3,3-dimethylbenzofuran-2(3H)-one (5bc).** M.p.: 222-224 °C (CH<sub>2</sub>Cl<sub>2</sub>); IR (neat):  $\nu_{\text{max}}$  3357, 2919, 2852, 1795, 1448, 1357, 1300, 1291, 1167, 1118, 1068, 990, 912, 843, 732, 681 cm<sup>-1</sup>; <sup>1</sup>H NMR (400 MHz, d<sub>6</sub>-DMSO)  $\delta$  10.57 (s, 1H), 6.97 (s, 1H), 1.56 (s, 6H); <sup>13</sup>C NMR (101 MHz, d<sub>6</sub>-DMSO)  $\delta$  178.4 (s), 150.7 (s), 140.8 (s), 131.6 (s), 115.6 (s), 115.1 (s), 113.1 (d), 45.7 (s), 22.0 (q); MS (DEI)  $m/z$ : 248, 246, 220, 218, 205, 203; HRMS (DEI) calcd for [C<sub>10</sub>H<sub>8</sub><sup>35</sup>Cl<sub>2</sub>O<sub>3</sub>]<sup>+</sup>: 245.9845; found: 245.9855.



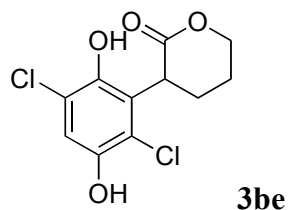
**Methyl 2-(2,5-dichloro-4-hydroxyphenoxy)-2-methylpropanoate (6bc).** IR (neat):  $\nu_{\text{max}}$  3417, 2991, 2953, 1731, 1477, 1385, 1285, 1193, 1169, 1131, 1074, 982, 881, 869, 824, 764 cm<sup>-1</sup>; <sup>1</sup>H NMR (400 MHz, d<sub>6</sub>-DMSO)  $\delta$  7.05 (s, 1H), 7.02 (s, 1H), 3.75 (s, 3H), 1.51 (s, 6H); <sup>13</sup>C NMR (101 MHz, d<sub>6</sub>-DMSO)  $\delta$  174.7 (s), 149.7 (s), 145.6 (s), 127.3 (s), 124.0 (s), 119.5 (d), 118.3 (d), 82.9 (s), 53.1 (q), 25.2 (q); MS (DEI)  $m/z$ : 280, 278, 221, 219, 180, 178; HRMS (DEI) calcd for [C<sub>11</sub>H<sub>12</sub><sup>35</sup>Cl<sub>2</sub>O<sub>4</sub>]<sup>+</sup>: 278.0113; found: 278.0110.

**Reaction of quinone 1b with ketene acetal 2d.** To a solution of **2d** (317 mg, 2.00 mmol) in CH<sub>2</sub>Cl<sub>2</sub> (2.0 mL), a solution of **1b** (89 mg, 0.50 mmol) in 5 mL CH<sub>2</sub>Cl<sub>2</sub> was slowly added over 2 h under nitrogen at 20 °C. After stirring for 2 h at 20 °C, the solvent was evaporated and the residue was purified by flash column chromatography (silica gel, eluent: MeOH/dichloromethane = 1/50, very low flow rate is needed for complete hydrolysis of the silylated **3bd**) to give **3bd** (white solid, 68 mg, 52% yield).



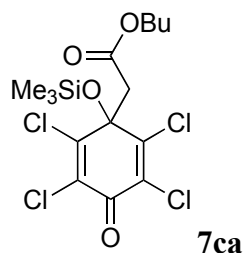
**3-(2,5-Dichloro-3,6-dihydroxyphenyl)dihydrofuran-2(3H)-one (3bd).** M.p.: 220-222 °C (CH<sub>2</sub>Cl<sub>2</sub>); IR (neat):  $\nu_{\text{max}}$  3400, 3281, 2914, 1747, 1463, 1441, 1379, 1348, 1301, 1219, 1174, 1125, 1026, 953, 858, 844 cm<sup>-1</sup>; <sup>1</sup>H NMR (600 MHz, d<sub>6</sub>-DMSO)  $\delta$  9.97 (s, 1H), 9.45 (s, 1H), 6.93 (s, 1H), 4.50-4.28 (m, 3H), 2.50-2.30 (m, 2H); <sup>13</sup>C NMR (151 MHz, d<sub>6</sub>-DMSO)  $\delta$  176.6 (s), 146.7 (s), 143.6 (s), 127.4 (s), 120.2 (s), 120.0 (s), 115.0 (d), 66.6 (t), 40.5 (d), 27.7 (t); MS (DEI)  $m/z$ : 264, 262, 246, 244, 218, 217, 216, 215, 206, 204, 192, 190, 148, 147; HRMS (DEI) calcd for [C<sub>10</sub>H<sub>8</sub><sup>35</sup>Cl<sub>2</sub>O<sub>4</sub>]<sup>+</sup>: 261.9794; found: 261.9781.

**Reaction of quinone 1b with ketene acetal 2d.** To a solution of **2e** (345 mg, 2.00 mmol) in CH<sub>2</sub>Cl<sub>2</sub> (2.0 mL), a solution of **1b** (89 mg, 0.50 mmol) in 5 mL CH<sub>2</sub>Cl<sub>2</sub> was slowly added over 2 h under nitrogen at 20 °C. After stirring for 12 h at 20 °C, the solvent was evaporated and the residue was purified by flash column chromatography (silica gel, eluent: MeOH/dichloromethane = 1/50, very low flow rate is needed for complete hydrolysis of the silylated **3be**) to give **3be** (white solid, 43 mg, 31% yield).



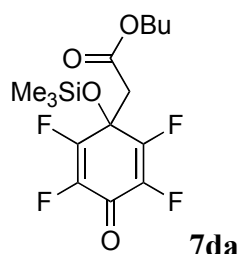
**3-(2,5-Dichloro-3,6-dihydroxyphenyl)tetrahydro-2H-pyran-2-one (3be).** M.p.: 229-231 °C (CH<sub>2</sub>Cl<sub>2</sub>); IR (neat):  $\nu_{\text{max}}$  3477, 3332, 2908, 2852, 1682, 1580, 1488, 1472, 1454, 1441, 1409, 1278, 1260, 1237, 1181, 1133, 1090, 954, 909, 835 cm<sup>-1</sup>; <sup>1</sup>H NMR (400 MHz, d<sub>6</sub>-DMSO)  $\delta$  9.92 (s, 1H), 9.36 (s, 1H), 6.89 (s, 1H), 4.46-4.41 (m, 1H), 4.37-4.31 (m, 1H), 4.19 (apparent br s, 1H), 2.00-1.87 (m, 4H); <sup>13</sup>C NMR (101 MHz, d<sub>6</sub>-DMSO)  $\delta$  170.1 (s), 146.8 (s), 143.0 (s), 130.9 (s), 120.1 (s), 119.1 (s), 114.4 (d), 69.7 (t), 41.9 (d), 26.1 (t), 22.6 (t); MS (EI)  $m/z$ : 278, 276, 260, 258, 232, 230, 217, 215, 204, 84, 66; HRMS (EI) calcd for [C<sub>11</sub>H<sub>9</sub><sup>35</sup>Cl<sub>2</sub>O<sub>4</sub>]<sup>+</sup>: 274.9872; found: 274.9884.

**Reaction of quinone 1c with ketene acetal 2a.** To a solution of **1c** (123 mg, 0.50 mmol) in CH<sub>2</sub>Cl<sub>2</sub> (5.0 mL), **2a** (188 mg, 1.00 mmol) was added under nitrogen at 20 °C. After stirring for 12 h at 20 °C, the solvent was evaporated and the residue was purified by flash column chromatography (silica gel, eluent: acetic acid/ethyl acetate/pentane = 1/10/100) to give **7ca** (colorless oil, 82 mg, 38% yield).

**Butyl 2-(2,3,5,6-tetrachloro-4-oxo-1-(trimethylsilyloxy)cyclohexa-2,5-dienyl)acetate (7ca).**

IR (neat):  $\nu_{\text{max}}$  2959, 2934, 2874, 1736, 1689, 1458, 1413, 1339, 1253, 1198, 1132, 1098, 874, 841, 755, 725  $\text{cm}^{-1}$ ;  $^1\text{H}$  NMR (300 MHz,  $\text{CDCl}_3$ )  $\delta$  3.97 (t,  $J$  = 8.8 Hz, 2H), 3.29 (s, 2H), 1.52-1.42 (m, 2H), 1.34-1.22 (m, 2H), 0.12 (s, 9H);  $^{13}\text{C}$  NMR (75 MHz,  $\text{CDCl}_3$ )  $\delta$  169.9 (s), 167.1 (s), 151.7 (s), 131.8 (s), 77.2 (s), 65.2 (t), 45.8 (t), 30.5 (t), 19.1 (t), 13.7 (q), 1.3 (q); MS (EI)  $m/z$ : 367, 365, 363, 361, 323, 321, 319, 317, 117, 75, 73, 57, 41; HRMS (EI) calcd for  $[\text{C}_{15}\text{H}_{20}^{35}\text{Cl}_4\text{O}_4\text{Si}]^+$ : 431.9879; found: 431.9890.

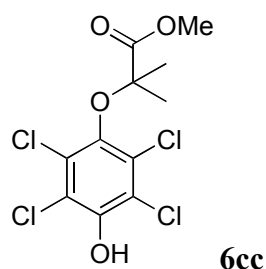
**Reaction of quinone 1d with ketene acetal 2a.** To a solution of **1d** (90 mg, 0.50 mmol) in  $\text{CH}_2\text{Cl}_2$  (5.0 mL), **2a** (188 mg, 1.00 mmol) was added under nitrogen at 20 °C. After stirring for 12 h at 20 °C, the solvent was evaporated and the residue was purified by flash column chromatography (silica gel, eluent: acetic acid/ethyl acetate/pentane = 1/10/100) to give **7da** (colorless oil, 96 mg, 52% yield).

**Butyl 2-(2,3,5,6-tetrafluoro-4-oxo-1-(trimethylsilyloxy)cyclohexa-2,5-dienyl)acetate (7da).**

IR (neat):  $\nu_{\text{max}}$  2963, 2876, 1739, 1702, 1687, 1297, 1257, 1185, 1088, 1014, 865, 847, 760  $\text{cm}^{-1}$ ;  $^1\text{H}$  NMR (300 MHz,  $\text{CDCl}_3$ )  $\delta$  4.04 (t,  $J$  = 8.8 Hz, 2H), 3.19 (s, 2H), 1.58-1.49 (m, 2H), 1.38-1.25 (m, 2H), 0.16 (s, 9H);  $^{13}\text{C}$  NMR (75 MHz,  $\text{CDCl}_3$ )  $\delta$  172.1 (s\*), 166.8 (s), 153.3 (d\*,  $^1J_{\text{F-C}}$  = 293 Hz), 138.1 (d\*,  $^1J_{\text{F-C}}$  = 263 Hz), 70.8 (t,  $^2J_{\text{F-C}}$  = 24 Hz), 65.5 (t), 40.8 (t), 30.5 (t), 19.1 (t), 13.7 (q), 1.1 (q), \*splitting due to remote F-C couplings are not given; MS (DEI)  $m/z$ : 312, 297, 253, 240, 181, 77, 75, 73, 57; HRMS (DEI) calcd for  $[\text{C}_{15}\text{H}_{20}\text{F}_4\text{O}_4\text{Si}]^+$ : 368.1061; found: 368.1043.

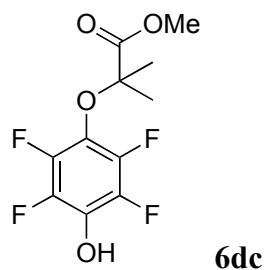
**Reaction of quinone 1c with ketene acetal 2c.** To a solution of **1c** (123 mg, 0.50 mmol) in  $\text{CH}_2\text{Cl}_2$  (5.0 mL), **2c** (176 mg, 1.00 mmol) was added under nitrogen at 20 °C. After stirring

for 12 h at 20 °C, the solvent was evaporated and the residue was purified by column chromatography (silica gel, eluent: ethyl acetate/pentane = 1/2) to give **6cc** (white solid, 144 mg, 83% yield).



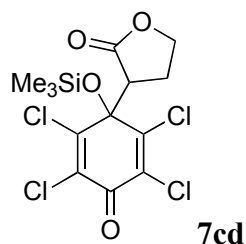
**Methyl 2-methyl-2-(2,3,5,6-tetrachloro-4-hydroxyphenoxy)propanoate (6cc).** M.p.: 125-127 °C (CH<sub>2</sub>Cl<sub>2</sub>); IR (neat):  $\nu_{\text{max}}$  3083, 2985, 2925, 2848, 1705, 1446, 1435, 1382, 1374, 1328, 1301, 1209, 1199, 1170, 1129, 1036, 977, 957, 921, 912, 846, 766, 713, 677 cm<sup>-1</sup>; <sup>1</sup>H NMR (400 MHz, d<sub>6</sub>-DMSO)  $\delta$  10.90 (br s, 1H), 3.73 (s, 3H), 1.47 (s, 6H); <sup>13</sup>C NMR (101 MHz, d<sub>6</sub>-DMSO)  $\delta$  172.2 (s), 148.0 (s), 142.1 (s), 128.1 (s), 120.4 (s), 83.3 (s), 52.3 (q), 24.4 (q); MS (DEI)  $m/z$ : 291, 289, 287, 250, 248, 246, 211, 209, 147, 101, 87, 41; HRMS (DEI) calcd for [C<sub>11</sub>H<sub>10</sub><sup>35</sup>Cl<sub>3</sub><sup>37</sup>ClO<sub>4</sub>]<sup>+</sup>: 347.9304; found: 347.9313.

**Reaction of quinone 1d with ketene acetal 2c.** To a solution of **1d** (90 mg, 0.50 mmol) in CH<sub>2</sub>Cl<sub>2</sub> (5.0 mL), **2c** (176 mg, 1.00 mmol) was added under nitrogen at 20 °C. After stirring for 12 h at 20 °C, the solvent was evaporated and the residue was purified by column chromatography (silica gel, eluent: ethyl acetate/pentane = 1/2) to give **6dc** (white solid, 110 mg, 78% yield).

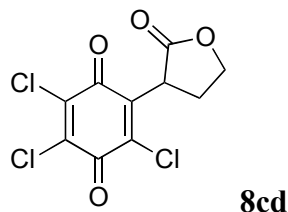


**Methyl 2-methyl-2-(2,3,5,6-tetrafluoro-4-hydroxyphenoxy)propanoate (6dc).** M.p.: 95-97 °C (CH<sub>2</sub>Cl<sub>2</sub>); IR (neat):  $\nu_{\text{max}}$  3273, 2998, 2961, 2922, 2851, 1715, 1520, 1504, 1467, 1437, 1388, 1372, 1310, 1299, 1233, 1202, 1173, 1133, 1030, 1003, 969, 806, 770, 692 cm<sup>-1</sup>; <sup>1</sup>H NMR (400 MHz, d<sub>6</sub>-DMSO)  $\delta$  11.24 (s, 1H), 3.71 (s, 3H), 1.47 (s, 6H); <sup>13</sup>C NMR (101 MHz, d<sub>6</sub>-DMSO)  $\delta$  171.3 (s), 144.27 (d\*, <sup>1</sup>J<sub>F-C</sub> = 243 Hz), 138.2 (d\*, <sup>1</sup>J<sub>F-C</sub> = 241 Hz), 133.0 (t, <sup>2</sup>J<sub>F-C</sub> = 15 Hz), 123.2 (t, <sup>2</sup>J<sub>F-C</sub> = 15 Hz), 83.4 (s), 52.4 (q), 23.7 (q\*), \*splitting due to remote F-C couplings are not given; MS (DEI)  $m/z$ : 282, 223, 182, 101, 73, 69, 41; HRMS (DEI) calcd for [C<sub>11</sub>H<sub>10</sub>F<sub>4</sub>O<sub>4</sub>]<sup>+</sup>: 282.0510; found: 282.0499.

**Reaction of quinone 1c with ketene acetal 2d.** To a solution of **1c** (123 mg, 0.50 mmol) in CH<sub>2</sub>Cl<sub>2</sub> (5.0 mL), **2d** (158 mg, 1.00 mmol) was added under nitrogen at 20 °C. After stirring for 1 h at 20 °C, the solvent was evaporated and the residue was purified by flash column chromatography (silica gel, eluent: acetic acid/ethyl acetate/pentane = 1/10/100) to give **7cd** (colorless oil, 42 mg, 21% yield) and **8cd** (yellow solid, 47 mg, 32% yield)



**3-(2,3,5,6-Tetrachloro-4-oxo-1-(trimethylsilyloxy)cyclohexa-2,5-dienyl)dihydrofuran-2(3H)-one (7cd).** <sup>1</sup>H NMR (300 MHz, CDCl<sub>3</sub>) δ 4.32 (apparent td, J = 8.8, 4.6 Hz, 1H), 4.22 (apparent dt, J = 9.1, 7.8 Hz, 1H), 3.55 (apparent dd, J = 10.4, 8.8 Hz, 1H), 2.67 (apparent dtd, J = 13.8, 8.8, 7.8 Hz, 1H), 2.47 (apparent dddd, J = 13.8, 10.5, 7.9, 4.7 Hz, 1H), 0.18 (s, 9H); <sup>13</sup>C NMR (75 MHz, CDCl<sub>3</sub>) δ 172.8 (s), 169.4 (s), 151.5 (s), 149.8 (s), 132.8 (s), 132.6 (s), 79.0 (s), 66.0 (t), 48.5 (d), 24.7 (t), 1.3 (q); MS (DEI) *m/z*: 391, 389, 387, 321, 319, 317, 158, 143, 73; HRMS (DEI) calcd for [C<sub>13</sub>H<sub>14</sub><sup>35</sup>Cl<sub>3</sub><sup>37</sup>ClO<sub>4</sub>Si]<sup>+</sup>: 403.9387; found: 403.9401.

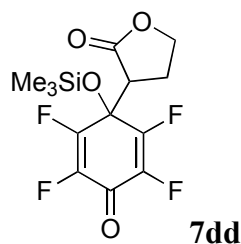


**2,3,5-Trichloro-6-(2-oxotetrahydrofuran-3-yl)cyclohexa-2,5-diene-1,4-dione (8cd).** IR (neat):  $\nu_{\text{max}}$  1761, 1687, 1668, 1577, 1376, 1316, 1300, 1249, 1220, 1170, 1043, 1023, 993, 951, 894, 803, 725, 719, 668 cm<sup>-1</sup>; <sup>1</sup>H NMR (400 MHz, CDCl<sub>3</sub>) δ 4.70-4.57 (m, 1H), 4.48-4.36 (m, 1H), 4.39-4.18 (br, m, 1H), 2.67-2.37 (m, 2H); <sup>13</sup>C NMR (101 MHz, CDCl<sub>3</sub>) δ 174.7 (s), 174.2 (br, s), 170.5 (s), 143.5 (br, s), 141.4 (s), 141.2 (s), 140.7 (s), 67.4 (t), 41.4 (br, d), 27.8 (t); MS (DEI) *m/z*: 298, 296, 252, 250, 217, 215, 189, 187, 159, 87; HRMS (ESI) calcd for [C<sub>10</sub>H<sub>5</sub><sup>35</sup>Cl<sub>3</sub>O<sub>4</sub>]<sup>+</sup>: 293.9248; found: 293.9257.

**Reaction of quinone 1d with ketene acetal 2d.** To a solution of **1d** (90 mg, 0.50 mmol) in CH<sub>2</sub>Cl<sub>2</sub> (5.0 mL), **2d** (158 mg, 1.00 mmol) was added under nitrogen at 20 °C. After stirring for 24 h at 20 °C, the solvent was evaporated and the residue was purified by flash column

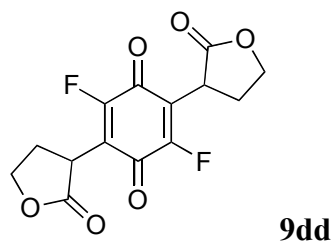


chromatography (silica gel, eluent: acetic acid/ethyl acetate/pentane = 1/10/100) to give **7dd** (colorless oil, 73 mg, 43% yield) and **9dd** (yellow solid, 42 mg, 27% yield).



**3-(2,3,5,6-Tetrafluoro-4-oxo-1-(trimethylsilyloxy)cyclohexa-2,5-dienyl)dihydrofuran-**

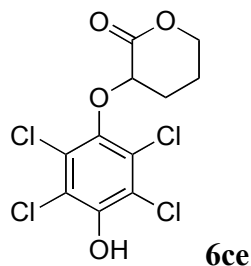
**2(3H)-one (7dd).** IR (neat):  $\nu_{\max}$  2962, 2921, 1767, 1702, 1681, 1379, 1298, 1255, 1218, 1165, 1112, 1083, 1036, 967, 889, 843, 756, 728, 686  $\text{cm}^{-1}$ ;  $^1\text{H}$  NMR (400 MHz,  $\text{CDCl}_3$ )  $\delta$  4.46-4.34 (m, 1H), 4.34-4.19 (m, 1H), 3.53 (apparent t,  $J = 9.7$  Hz, 1H), 2.75-2.48 (m, 2H), 0.19 (s, 9H);  $^{13}\text{C}$  NMR (101 MHz,  $\text{CDCl}_3$ )  $\delta$  172.3 (s), 171.6 (s\*), 153.2 (d\*,  $^1J_{\text{F-C}} = 283$  Hz), 138.6 (d\*,  $^1J_{\text{F-C}} = 290$  Hz), 72.0 (t\*,  $^2J_{\text{F-C}} = 22$  Hz), 66.4 (t), 46.1 (d), 24.6 (t), 0.9 (q), \*splitting due to remote F-C couplings are not given; MS (DEI)  $m/z$ : 338, 323, 253, 158, 143, 115, 73; HRMS (DEI) calcd for  $[\text{C}_{13}\text{H}_{14}\text{F}_4\text{O}_4\text{Si}]^+$ : 338.0592; found: 338.0597.



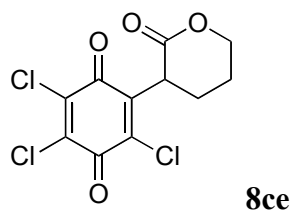
**2,5-Difluoro-3,6-bis(2-oxotetrahydrofuran-3-yl)cyclohexa-2,5-diene-1,4-dione (9dd).** IR (neat):  $\nu_{\max}$  2961, 2922, 2852, 1764, 1695, 1682, 1660, 1646, 1374, 1304, 1257, 1157, 1095, 1012, 797  $\text{cm}^{-1}$ ;  $^1\text{H}$  NMR (600 MHz,  $\text{CDCl}_3$ )  $\delta$  4.63-4.59 (m, 1H), 4.41-4.36 (m, 1H), 4.05 (“apparent”, t,  $J = 10.3$  Hz, 0.3H), 3.99 (“apparent”, t,  $J = 10.3$  Hz, 0.7H), 2.61-2.52 (m, 1H), 2.48-2.39 (m, 1H);  $^{13}\text{C}$  NMR (151 MHz,  $\text{CDCl}_3$ )  $\delta$  183.1 (s\*), 174.6\*\* (s), 174.3 (s), 170.3\*\* (s), 156.8\*\* (d\*), 156.6 (d\*), 125.0\*\* (s), 124.9 (s), 67.5\*\* (d), 67.4 (d), 35.7\*\* (t), 35.5 (t), 28.7\*\* (t), 28.4 (t), \*splitting due to remote F-C couplings are not given, \*\*major diastereomer; MS (DEI)  $m/z$ : 312, 268, 209, 181, 133; HRMS (ESI) calcd for  $[\text{C}_{14}\text{H}_{10}\text{F}_2\text{O}_6]^+$ : 312.0440; found: 312.0449.

**Reaction of quinone 1c with ketene acetal 2e.** To a solution of **1c** (123 mg, 0.50 mmol) in  $\text{CH}_2\text{Cl}_2$  (5.0 mL), **2e** (172 mg, 1.00 mmol) was added under nitrogen at 20 °C. After stirring for 1 h at 20 °C, the solvent was evaporated and the residue was purified by flash column

chromatography (silica gel, eluent: ethyl acetate/pentane = 1/10) to give **6ce** (white solid, 36 mg, 21% yield) and **8ce** (brown sticky oil, 53 mg, 34% yield)

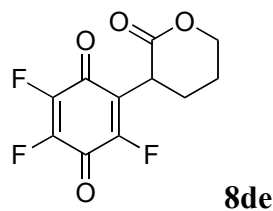


**3-(2,3,5,6-Tetrachloro-4-hydroxyphenoxy)tetrahydro-2H-pyran-2-one (6ce).** M.p.: 206-208 °C (CH<sub>2</sub>Cl<sub>2</sub>); IR (neat):  $\nu_{\text{max}}$  3286, 2968, 1712, 1436, 1419, 1389, 1332, 1312, 1260, 1168, 1110, 1052, 1037, 991, 957, 932, 897, 801, 712 cm<sup>-1</sup>; <sup>1</sup>H NMR (400 MHz, d<sub>6</sub>-DMSO)  $\delta$  10.90 (s, 1H), 4.91 (apparent dd, *J* = 7.2, 6.4 Hz, 1H), 4.43-4.31 (m, 2H), 2.33-2.24 (m, 1H), 2.17-2.08 (m, 1H), 2.06-1.97 (m, 1H), 1.93-1.83 (m, 1H); <sup>13</sup>C NMR (101 MHz, d<sub>6</sub>-DMSO)  $\delta$  167.6 (s), 147.9 (s), 143.5 (s), 126.4 (s), 120.6 (s), 76.3 (d), 68.6 (t), 25.5 (t), 19.5 (t); MS (EI) *m/z*: 350, 348, 346, 344, 252, 251, 250, 248, 246, 231, 229, 194, 100, 87, 55; HRMS (EI) calcd for [C<sub>11</sub>H<sub>8</sub><sup>35</sup>Cl<sub>3</sub><sup>37</sup>ClO<sub>4</sub>]<sup>+</sup>: 345.9147; found: 345.9125.



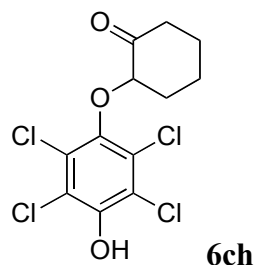
**2,3,5-Trichloro-6-(2-oxotetrahydro-2H-pyran-3-yl)cyclohexa-2,5-diene-1,4-dione (8ce).** IR (neat):  $\nu_{\text{max}}$  2961, 2907, 1720, 1686, 1666, 1575, 1476, 1456, 1401, 1348, 1236, 1160, 1080, 1036, 953, 924, 877, 803, 792, 779, 719, 712 cm<sup>-1</sup>; <sup>1</sup>H NMR (300 MHz, CDCl<sub>3</sub>)  $\delta$  4.53 (apparent t, *J* = 7.2 Hz, 2H), 4.09 (apparent t, *J* = 8.8 Hz, 1H), 2.17-1.80 (m, 4H); <sup>13</sup>C NMR (75 MHz, CDCl<sub>3</sub>)  $\delta$  174.9 (s), 170.8 (s), 168.5 (s), 143.9 (s), 141.8 (s), 141.3 (s), 140.7 (s), 70.5 (t), 42.5 (br, d), 25.7 (t), 22.9 (t); MS (EI) *m/z*: 310, 294, 292, 275, 273, 251, 249, 231, 229, 201, 194, 165, 87; HRMS (EI) calcd for [C<sub>11</sub>H<sub>7</sub><sup>35</sup>Cl<sub>3</sub>O<sub>4</sub>]<sup>+</sup>: 307.9404; found: 307.9394.

**Reaction of quinone 1d with ketene acetal 2e.** To a solution of **1d** (90 mg, 0.50 mmol) in CH<sub>2</sub>Cl<sub>2</sub> (5.0 mL), **2e** (172 mg, 1.00 mmol) was added under nitrogen at 20 °C. After stirring for 12 h at 20 °C, the solvent was evaporated and the residue was purified by column chromatography (silica gel, eluent: ethyl acetate/pentane = 1/10) to give **8de** (brown sticky oil, 59 mg, 45% yield).

**2,3,5-Trifluoro-6-(2-oxotetrahydro-2H-pyran-3-yl)cyclohexa-2,5-diene-1,4-dione (8de).**

IR (neat):  $\nu_{\max}$  2964, 1698, 1678, 1651, 1306, 1244, 1167, 1081, 1068, 1009, 957, 924, 739  $\text{cm}^{-1}$ ;  $^1\text{H}$  NMR (300 MHz,  $\text{CDCl}_3$ )  $\delta$  4.64-4.40 (m, 2H), 3.95-3.87 (m, 1H), 2.16-1.93 (m, 4H);  $^{13}\text{C}$  NMR (75 MHz,  $\text{CDCl}_3$ )  $\delta$  177.4 (s\*), 171.5 (s\*), 168.4 (s\*), 155.3 (d\*,  $^1J_{\text{F-C}} = 285$  Hz), 144.3 (d\*,  $^1J_{\text{F-C}} = 285$  Hz), 143.5 (d\*,  $^1J_{\text{F-C}} = 284$  Hz), 124.8 (d,  $^2J_{\text{F-C}} = 9$  Hz), 70.4 (t), 36.6 (d\*), 26.1 (t\*), 22.8 (t), \*splitting due to remote F-C couplings are not given; MS (EI)  $m/z$ : 262, 260, 258, 244, 216, 214, 201, 196, 167, 148, 132, 101, 43; HRMS (EI) calcd for  $[\text{C}_{11}\text{H}_7\text{F}_3\text{O}_4]^+$ : 260.0291; found: 260.0289.

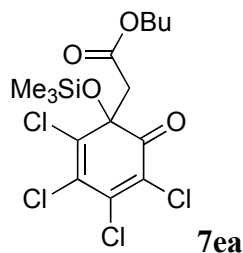
**Reaction of quinone 1c with enamine 2h.** To a solution of **1c** (123 mg, 0.50 mmol) in  $\text{CH}_2\text{Cl}_2$  (5.0 mL), **2h** (168 mg, 1.00 mmol) was added under nitrogen at 20 °C. After stirring for 1 h at 20 °C, the solvent was evaporated and the residue was purified by column chromatography (silica gel, eluent: ethyl acetate/pentane = 1/5) to give **6ch** (white solid, 129 mg, 75% yield).



**2-(2,3,5,6-Tetrachloro-4-hydroxyphenoxy)cyclohexanone (6ch).** M.p.: 185-187 °C (ethyl acetate/pentane); IR (neat):  $\nu_{\max}$  3188, 2946, 2866, 1708, 1441, 1385, 1328, 1260, 1175, 1167, 1056, 1024, 921, 896, 709  $\text{cm}^{-1}$ ;  $^1\text{H}$  NMR (400 MHz,  $d_6$ -DMSO)  $\delta$  10.84 (s, 1H), 4.83 (apparent ddd,  $J = 11.0, 5.8, 1.0$  Hz, 1H), 2.52-2.36 (m, 3H), 2.21-2.16 (m, 1H), 1.97-1.54 (m, 4H);  $^{13}\text{C}$  NMR (101 MHz,  $d_6$ -DMSO)  $\delta$  205.0 (s), 147.7 (s), 143.9 (s), 126.3 (s), 120.6 (s), 85.2 (d), 40.3 (t), 33.9 (t), 26.6 (t), 22.5 (t); MS (EI)  $m/z$ : 348, 346, 344, 342, 252, 250, 248, 246, 97, 69; HRMS (EI) calcd for  $[\text{C}_{12}\text{H}_{10}^{35}\text{Cl}_4\text{O}_3]^+$ : 341.9379; found: 341.9387.

**Reaction of quinone 1e with ketene acetal 2a.** To a solution of **1e** (123 mg, 0.50 mmol) in  $\text{CH}_2\text{Cl}_2$  (5.0 mL), **2a** (188 mg, 1.00 mmol) was added under nitrogen at 20 °C. After stirring for 1 h at 20 °C, the solvent was evaporated and the residue was purified by flash column

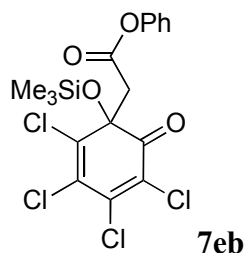
chromatography (silica gel, eluent: acetic acid/ethyl acetate/pentane = 1/10/100) to give **7ea** (yellow oil, 106 mg, 49% yield).



**Butyl 2-(2,3,4,5-tetrachloro-6-oxo-1-(trimethylsilyloxy)cyclohexa-2,4-dienyl)acetate (**7ea**).**

IR (neat):  $\nu_{\max}$  2959, 2934, 2875, 1727, 1697, 1590, 1533, 1466, 1407, 1340, 1253, 1195, 1093, 866, 842, 743  $\text{cm}^{-1}$ ;  $^1\text{H}$  NMR (300 MHz,  $\text{CDCl}_3$ )  $\delta$  3.97 (td,  $J$  = 6.7, 1.5 Hz, 2H), 3.40 (d,  $J$  = 16.4 Hz, 1H), 3.20 (d,  $J$  = 16.3 Hz, 1H), 1.55-1.45 (m, 2H), 1.35-1.22 (m, 2H), 0.89 (t,  $J$  = 7.3 Hz, 3H), 0.07 (s, 9H);  $^{13}\text{C}$  NMR (75 MHz,  $\text{CDCl}_3$ )  $\delta$  188.6 (s), 168.7 (s), 144.6 (s), 140.5 (s), 130.4 (s), 126.9 (s), 77.2 (s), 65.3 (t), 46.9 (t), 30.5 (t), 19.1 (t), 13.8 (q), 1.4 (q); MS (EI)  $m/z$ : 434, 432, 399, 397, 328, 326, 304, 253, 251, 159, 117, 115, 93, 75, 73, 57; HRMS (EI) calcd for  $[\text{C}_{15}\text{H}_{20}^{35}\text{Cl}_4\text{O}_4\text{Si}]^+$ : 431.9879; found: 431.9896.

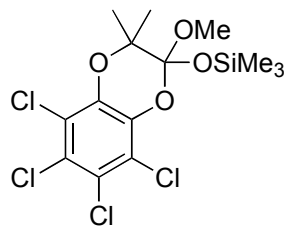
**Reaction of quinone 1e with ketene acetal 2b.** To a solution of **1e** (123 mg, 0.50 mmol) in  $\text{CH}_2\text{Cl}_2$  (5.0 mL), **2b** (208 mg, 1.00 mmol) was added under nitrogen at 20 °C. After stirring for 12 h at 20 °C, the solvent was evaporated and the residue was purified by flash column chromatography (silica gel, eluent: acetic acid/ethyl acetate/pentane = 1/5/100) to give **7eb** (yellow oil, 157 mg, 76% yield).



**Phenyl 2-(2,3,4,5-tetrachloro-6-oxo-1-(trimethylsilyloxy)cyclohexa-2,4-dienyl)acetate (**7eb**).**

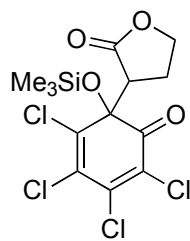
IR (neat):  $\nu_{\max}$  2958, 1748, 1694, 1589, 1532, 1491, 1342, 1252, 1186, 1085, 954, 864, 841, 754, 739, 685  $\text{cm}^{-1}$ ;  $^1\text{H}$  NMR (300 MHz,  $\text{CDCl}_3$ )  $\delta$  7.38-7.33 (m, 2H), 7.25-7.20 (m, 1H), 7.00-6.97 (m, 2H), 3.69 (d,  $J$  = 16.7 Hz, 1H), 3.48 (d,  $J$  = 16.7 Hz, 1H), 0.12 (s, 9H);  $^{13}\text{C}$  NMR (75 MHz,  $\text{CDCl}_3$ )  $\delta$  188.6 (s), 167.6 (s), 150.0 (s), 145.0 (s), 140.1 (s), 130.4 (d), 129.7 (s), 127.3 (s), 126.5 (d), 121.4 (d), 77.1 (s), 46.7 (t), 1.4 (q); MS (EI)  $m/z$ : 246, 244, 242, 216, 151, 94, 75, 75, 43; HRMS (EI) calcd for  $[\text{C}_{17}\text{H}_{16}^{35}\text{Cl}_4\text{O}_4\text{Si}]^+$ : 451.9566; found: 451.9544.

**Reaction of quinone 1e with ketene acetal 2c.** To a solution of **1e** (123 mg, 0.50 mmol) in CH<sub>2</sub>Cl<sub>2</sub> (5.0 mL), **2c** (176 mg, 1.00 mmol) was added under nitrogen at 20 °C. After stirring for 1 h at 20 °C, the solvent was evaporated and the residue was purified by flash column chromatography (silica gel, eluent: ethyl acetate/pentane = 1/10) to give **10ec** (white solid, 170 mg, 81% yield).

**10ec**

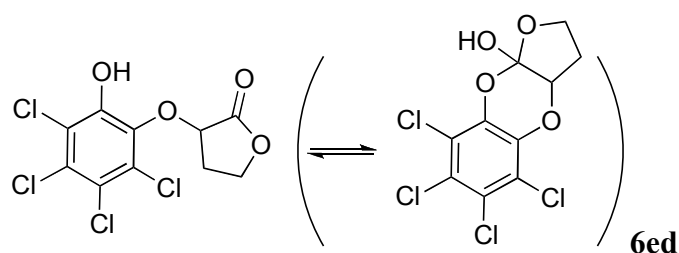
**Trimethyl(5,6,7,8-tetrachloro-2-methoxy-3,3-dimethyl-2,3-dihydrobenzo[b][1,4]dioxin-2-yl)oxy)silane (10ec).** M.p.: 129-131 °C (ethyl acetate/pentane); IR (neat):  $\nu_{\text{max}}$  2987, 2948, 1427, 1398, 1383, 1367, 1315, 1252, 1211, 1184, 1148, 1120, 1021, 989, 957, 903, 846, 834, 821, 763, 727, 703 cm<sup>-1</sup>; <sup>1</sup>H NMR (400 MHz, CDCl<sub>3</sub>)  $\delta$  3.30 (s, 3H), 1.52 (s, 3H), 1.29 (s, 3H), 0.33 (s, 9H); <sup>13</sup>C NMR (101 MHz, CDCl<sub>3</sub>)  $\delta$  139.3 (s), 137.6 (s), 125.7 (s), 124.0 (s), 120.8 (s), 120.1 (s), 110.8 (s), 79.9 (s), 49.1 (q), 22.2 (q), 22.1 (q), 1.9 (q); MS (EI)  $m/z$ : 422, 420, 418, 322, 320, 318, 304, 302, 174, 73, 70; HRMS (EI) calcd for [C<sub>14</sub>H<sub>18</sub><sup>35</sup>Cl<sub>4</sub>O<sub>4</sub>Si]<sup>+</sup>: 417.9723; found: 417.9735.

**Reaction of quinone 1e with ketene acetal 2d.** To a solution of **2d** (158 mg, 1.00 mmol) in CH<sub>2</sub>Cl<sub>2</sub> (2.0 mL), a solution of **1e** (123 mg, 0.50 mmol) in 5.0 mL CH<sub>2</sub>Cl<sub>2</sub> was added under nitrogen at 20 °C. After stirring for 1 h at 20 °C, the solvent was evaporated and the residue was purified by flash column chromatography (silica gel, eluent: acetic acid/ethyl acetate/pentane = 1/10/100) to give **7ed** (colorless oil, 26 mg, 13% yield) and **6ed** (white solid, 51 mg, 31% yield) and **11ed** (white solid, 20 mg, 11% yield).

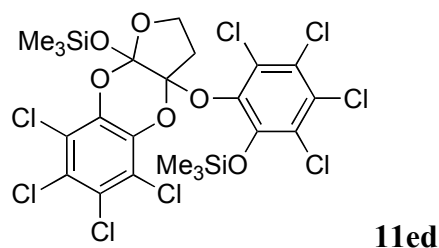
**7ed**

**3-(2,3,4,5-Tetrachloro-6-oxo-1-(trimethylsilyloxy)cyclohexa-2,4-dienyl)dihydrofuran-2(3H)-one (7ed).** <sup>1</sup>H NMR (300 MHz, CDCl<sub>3</sub>)  $\delta$  4.38-4.23 (m, 2H), 3.25 (apparent dd, J = 10.2, 6.2 Hz, 1H), 2.65-2.50 (m, 1H), 2.37-2.23 (m, 1H), 0.15 (s, 9H); <sup>13</sup>C NMR (75 MHz,

CDCl<sub>3</sub>)  $\delta$  191.1 (s), 173.4 (s), 145.5 (s), 141.3 (s), 129.7 (s), 126.6 (s), 83.4 (s), 67.9 (t), 51.7 (d), 24.2 (t), 1.3 (q).

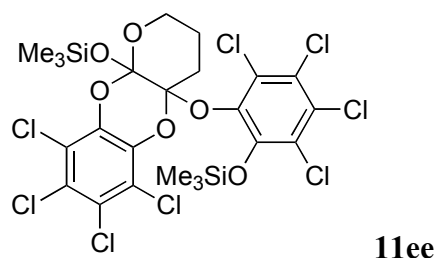


**3-(2,3,4,5-Tetrachloro-6-hydroxyphenoxy)dihydrofuran-2(3H)-one (6ed).** M.p.: 202-204 °C (CH<sub>2</sub>Cl<sub>2</sub>); IR (neat):  $\nu_{\text{max}}$  3412, 1784, 1431, 1391, 1385, 1307, 1286, 1262, 1227, 1208, 1185, 1098, 1054, 1023, 966, 955, 908, 821, 808, 756, 725 cm<sup>-1</sup>; <sup>1</sup>H NMR (400 MHz, d<sub>6</sub>-DMSO)  $\delta$  10.92 (br s, 0.5H), 6.49 (br s, 1H), 5.21 (apparent t, J = 8.0 Hz, 1.5H), 4.50-4.44 (m, 2H), 4.28 (apparent td, J = 8.6, 6.8 Hz, 1H), 2.64 (apparent dddd, J = 12.8, 8.1, 6.7, 3.6 Hz, 1H), 2.48-2.41 (m, 2H); <sup>13</sup>C NMR (101 MHz, d<sub>6</sub>-DMSO)  $\delta$  173.6, 152.9, 147.7, 142.0, 139.2, 128.2, 127.3, 127.0, 126.1, 121.4, 121.2, 120.6, 104.4, 75.9, 65.6, 64.5, 32.5, 28.8; MS (EI) *m/z*: 334, 332, 330, 328, 288, 287, 286, 285, 284, 283, 274, 272, 270, 250, 248, 246, 183, 181, 167, 165, 147, 86; HRMS (EI) calcd for [C<sub>10</sub>H<sub>6</sub><sup>35</sup>Cl<sub>3</sub><sup>37</sup>ClO<sub>4</sub>]<sup>+</sup>: 331.8991; found: 331.8999.



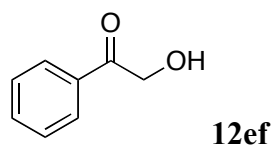
**Trimethyl(5,6,7,8-tetrachloro-3a-(2,3,4,5-tetrachloro-6-(trimethylsilyloxy)phenoxy)-2,3,3a,9a-tetrahydrobenzo[b]furo[2,3-e][1,4]dioxin-9a-yl)silane (11ed).** M.p.: 141 °C (decomp, CH<sub>2</sub>Cl<sub>2</sub>); IR (neat):  $\nu_{\text{max}}$  2957, 2910, 2852, 1431, 1417, 1395, 1379, 1323, 1291, 1254, 1199, 1176, 1141, 1099, 1066, 1043, 1002, 988, 840, 757 cm<sup>-1</sup>; <sup>1</sup>H NMR (300 MHz, CDCl<sub>3</sub>)  $\delta$  4.04 (apparent ddd, J = 9.3, 8.2, 1.6 Hz, 1H), 3.87 (apparent ddd, J = 9.5, 8.2, 7.1 Hz, 1H), 3.05 (apparent dt, J = 12.8, 9.5 Hz, 1H), 2.37 (apparent ddd, J = 12.8, 7.1, 1.6 Hz, 1H), 0.38 (s, 9H), 0.18 (s, 9H); <sup>13</sup>C NMR (75 MHz, CDCl<sub>3</sub>)  $\delta$  147.0 (s), 141.8 (s), 137.7 (s), 137.1 (s), 130.0 (s), 129.1 (s), 126.2 (s), 125.8 (s), 125.7 (s), 120.7 (s), 120.4 (s), 111.6 (s), 103.8 (s), 77.2 (s), 62.6 (t), 32.5 (t), 1.1 (q), 0.3 (q); MS (EI) *m/z*: 478, 476, 474, 405, 403, 401, 330, 304, 287, 285, 283, 250, 248, 246, 147, 103, 73; HRMS (EI) calcd for [C<sub>22</sub>H<sub>22</sub><sup>35</sup>Cl<sub>8</sub>O<sub>6</sub>Si<sub>2</sub>]<sup>+</sup>: 717.8458; found: 717.8489.

**Reaction of quinone 1e with ketene acetal 2e.** To a solution of **2e** (172 mg, 1.00 mmol) in CH<sub>2</sub>Cl<sub>2</sub> (2.0 mL), a solution of **1e** (123 mg, 0.50 mmol) in 5.0 mL CH<sub>2</sub>Cl<sub>2</sub> was added under nitrogen at 20 °C. After stirring for 1 h at 20 °C, the solvent was evaporated and the residue was purified by flash column chromatography (silica gel, eluent: acetic acid/ethyl acetate/pentane = 1/10/100) to give **11ee** (white solid, 145 mg, 79% yield).



**Trimethyl(6,7,8,9-tetrachloro-4a-(2,3,4,5-tetrachloro-6-(trimethylsilyloxy)phenoxy)-3,4,4a,10a-tetrahydro-2H-benzo[b]pyrano[2,3-e][1,4]dioxin-10a-yloxy)silane (11ee).** M.p.: 172 °C (decomp, CH<sub>2</sub>Cl<sub>2</sub>) IR (neat):  $\nu_{\text{max}}$  2966, 2944, 2892, 1432, 1417, 1375, 1251, 1212, 1140, 1111, 1073, 1038, 1013, 978, 906, 847, 832, 811, 757 cm<sup>-1</sup>; <sup>1</sup>H NMR (600 MHz, CDCl<sub>3</sub>)  $\delta$  3.97-3.91 (m, 2H), 3.78 (apparent dd, J = 11.4, 5.1 Hz, 1H), 2.57 (apparent td, J = 13.4, 4.6 Hz, 1H), 1.99 (apparent d, J = 13.3 Hz, 1H), 1.87 (apparent dddd, J = 18.0, 13.4, 9.1, 4.6 Hz, 1H), 1.56 (apparent d, J = 13.4 Hz, 1H), 0.41 (s, 9H), 0.01 (s, 9H); <sup>13</sup>C NMR (151 MHz, CDCl<sub>3</sub>)  $\delta$  147.9 (s), 140.9 (s), 138.6 (s), 138.3 (s), 130.0 (s), 129.5 (s), 126.6 (s), 126.1 (s), 125.8 (s), 125.2 (s), 121.1 (s), 120.6 (s), 106.9 (s), 101.5 (s), 64.4 (t), 29.0 (t), 23.1 (t), 1.4 (q), 0.1 (q); MS (EI) *m/z*: 418, 346, 344, 342, 274, 272, 270, 280, 278, 276, 172.

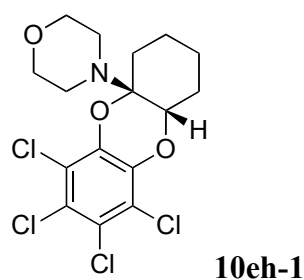
**Reaction of quinone 1e with silyl enol ether 2f.** To a solution of **1e** (123 mg, 0.50 mmol) in CH<sub>2</sub>Cl<sub>2</sub> (5.0 mL), **2f** (192 mg, 1.00 mmol) was added under nitrogen at 20 °C. After stirring for 24 h at 20 °C, the solvent was evaporated and the residue was purified by flash column chromatography (silica gel, eluent: diethyl ether/CH<sub>2</sub>Cl<sub>2</sub> = 1/10) to give **12ef** (pale yellow solid, 37 mg, 54% yield).



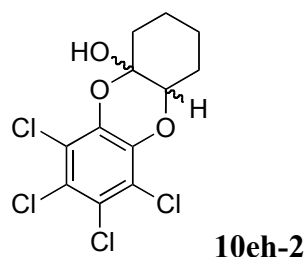
**2-Hydroxy-1-phenylethanone (12ef).** M.p.: 85-87 °C (CH<sub>2</sub>Cl<sub>2</sub>); <sup>1</sup>H NMR (300 MHz, CDCl<sub>3</sub>)  $\delta$  7.94-7.90 (m, 2H), 7.66-7.60 (m, 1H), 7.53-7.48 (m, 2H), 4.88 (s, 2H), 3.50 (br, s, 1H); <sup>13</sup>C NMR (75 MHz, CDCl<sub>3</sub>)  $\delta$  198.5 (s), 134.4 (d), 133.5 (s), 129.1 (d), 127.8 (d), 65.6 (t).

The <sup>1</sup>H and <sup>13</sup>C NMR spectra agree with ref. 26.

**Reaction of quinone 1e with enamine 2h.** To a solution of **1e** (123 mg, 0.50 mmol) in CH<sub>2</sub>Cl<sub>2</sub> (5.0 mL), **2h** (84 mg, 0.50 mmol) was added under nitrogen at 20 °C. After stirring for 10 min at 20 °C, the solvent was evaporated under vacuum to give crude **10eh-1** and purification by column chromatography (silica gel, eluent: ethyl acetate/pentane = 1/10) lead to hydrolysis to give **10eh-2** (white solid, 105 mg, 61% yield).



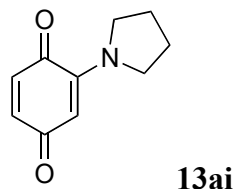
**(±)4-((4aR,10aS)-6,7,8,9-tetrachloro-1,2,3,4,4a,10a-hexahydrodibenzo[b,e][1,4]dioxin-4a-yl)morpholine (10eh-1).** <sup>1</sup>H NMR (400 MHz, CDCl<sub>3</sub>) δ 4.39 (dd, J = 7.5, 3.6 Hz, 1H), 3.67-3.56 (m, 4H), 2.88-2.69 (m, 4H), 2.03-1.90 (m, 2H), 1.87-1.66 (m, 3H), 1.66-1.53 (m, 2H), 1.51-1.38 (m, 1H); <sup>13</sup>C NMR (101 MHz, CDCl<sub>3</sub>) δ 139.1 (s), 138.9 (s), 124.2 (s), 123.9 (s), 120.6 (s), 120.0 (s), 90.5 (s), 72.5 (d), 67.3 (t), 44.8 (t), 27.9 (t), 27.0 (t), 21.7(t), 21.2(t).



**6,7,8,9-Tetrachloro-1,2,3,4,4a,10a-hexahydrodibenzo[b,e][1,4]dioxin-4a-ol (10eh-2).** IR (neat):  $\nu_{\max}$  3182, 2944, 2685, 1420, 1397, 1347, 1262, 1132, 1102, 1038, 1019, 996, 969, 950, 934, 886, 860, 852, 808, 800, 786 cm<sup>-1</sup>; <sup>1</sup>H NMR (600 MHz, CDCl<sub>3</sub>) δ 5.19 (s, 1H), 4.67 (s, 1H), 4.21 (dd, J = 9.8, 4.4 Hz, 1H), 3.81 (dd, J = 11.8, 4.7 Hz, 1H), 2.29 (apparent d, J = 10.0 Hz, 1H), 2.16 (apparent d, J = 12.2 Hz, 2H), 1.98-1.94 (m, 1H), 1.88 (d, J = 14.7 Hz, 1H), 1.87-1.76 (m, 1H), 1.76-1.69 (m, 3H), 1.69-1.53 (m, 2H), 1.44-1.35 (m, 2H); <sup>13</sup>C NMR (151 MHz, CDCl<sub>3</sub>) δ 140.4 (s), 138.9 (s), 138.4 (s), 138.1 (s), 124.8 (s), 124.6 (s), 124.4 (s), 120.9 (s), 120.6 (s), 120.5 (s), 120.3 (s), 95.6 (s), 95.5 (s), 78.1 (d), 76.5 (d), 35.4 (t), 35.0 (t), 28.2 (t), 27.9 (t), 23.7 (t), 22.3 (t), 22.2 (t); MS (EI) *m/z*: 348, 346, 344, 342, 250, 248, 246, 98, 97, 69; HRMS (EI) calcd for [C<sub>12</sub>H<sub>10</sub><sup>35</sup>Cl<sub>4</sub>O<sub>3</sub>]<sup>+</sup>: 341.9379; found: 341.9390.



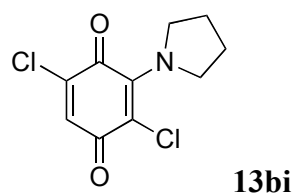
**Reaction of quinone 1a with amine 2i.** To a solution of **1a** (108 mg, 1.00 mmol) in CH<sub>3</sub>CN (5.0 mL), a solution of **2i** (18 mg, 0.25 mmol) in 1.0 mL CH<sub>3</sub>CN was added under nitrogen at 20 °C. After stirring for 30 min at 20 °C, the solvent was evaporated and the residue was purified by flash column chromatography (silica gel, eluent: ethyl acetate/pentane = 1/10) to give **13ai** (dark red solid, 38 mg, 85% yield).



**2-(Pyrrolidin-1-yl)cyclohexa-2,5-diene-1,4-dione (13ai).** M.p.: 117-119 °C (CH<sub>2</sub>Cl<sub>2</sub>); IR (neat):  $\nu_{\max}$  3043, 2979, 2969, 2940, 2869, 1676, 1632, 1582, 1555, 1410, 1389, 1355, 1340, 1302, 1294, 1136, 1094, 1042, 962, 848, 816, 761 cm<sup>-1</sup>; <sup>1</sup>H NMR (400 MHz, d<sub>6</sub>-DMSO)  $\delta$  6.61-6.50 (m, 2H), 5.37-5.35 (m, 1H), 3.67 (br, s, 2H), 3.24 (br, s, 2H), 1.91-1.83 (m, 4H); <sup>13</sup>C NMR (101 MHz, d<sub>6</sub>-DMSO)  $\delta$  184.8 (s), 183.6 (s), 147.3 (s), 138.3 (d), 133.4 (d), 101.0 (d), 50.3 (t), 25.8 (br, t), 23.7 (br, t); MS (EI)  $m/z$ : 177, 149, 121, 93, 67, 53, 41; HRMS (EI) calcd for [C<sub>10</sub>H<sub>11</sub>NO<sub>2</sub>]<sup>+</sup>: 177.0784; found: 177.0791.

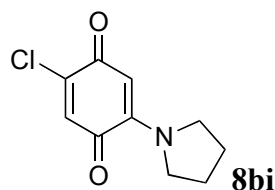
The IR, <sup>1</sup>H NMR spectra agree with ref. 27.

**Reaction of quinone 1b with amine 2i.** To a solution of **1b** (446 mg, 2.50 mmol) in CH<sub>3</sub>CN (50 mL), a solution of **2i** (18 mg, 0.50 mmol) in 1.0 mL CH<sub>3</sub>CN was added dropwise under nitrogen at 20 °C. After stirring for 30 min at 20 °C, the solvent was evaporated and the residue was purified by flash column chromatography (silica gel, eluent: diethyl ether/CH<sub>2</sub>Cl<sub>2</sub> = 1/10) to give **13bi** (dark violet solid, 42 mg, 34% yield) and **8bi** (dark red solid, 21 mg, 40% yield).



**2,5-Dichloro-3-(pyrrolidin-1-yl)cyclohexa-2,5-diene-1,4-dione (13bi).** M.p.: 101-103 °C (CH<sub>2</sub>Cl<sub>2</sub>); IR (neat):  $\nu_{\max}$  3045, 2921, 1689, 1631, 1598, 1512, 1453, 1441, 1363, 1284, 1172, 1147, 1018, 911, 880, 858, 845, 767, 691 cm<sup>-1</sup>; <sup>1</sup>H NMR (400 MHz, d<sub>6</sub>-DMSO)  $\delta$  7.13 (s, 1H), 3.84-3.80 (m, 4H), 1.85-1.81 (m, 4H); <sup>13</sup>C NMR (101 MHz, d<sub>6</sub>-DMSO)  $\delta$  176.7 (s), 175.9 (s), 147.7 (s), 138.5 (s), 133.0 (s), 106.7 (d), 53.8 (t), 25.2 (t); MS (EI)  $m/z$ : 247, 245, 217, 154, 118, 87, 53, 43, 41; HRMS (ESI) calcd for [C<sub>10</sub>H<sub>10</sub><sup>35</sup>Cl<sub>2</sub>NO<sub>2</sub>]<sup>+</sup>: 246.0083; found: 246.0086.

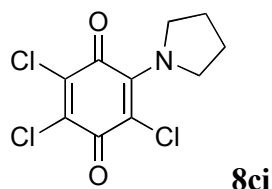
The IR,  $^1\text{H}$  and  $^{13}\text{C}$  NMR spectra agree with ref. 28.



**2-Chloro-5-(pyrrolidin-1-yl)cyclohexa-2,5-diene-1,4-dione (8bi).** M.p.: 138-140 °C ( $\text{CH}_2\text{Cl}_2$ ); IR (neat):  $\nu_{\text{max}}$  3032, 2914, 2868, 1659, 1614, 1597, 1556, 1453, 1410, 1361, 1319, 1254, 1237, 1205, 1040, 1006, 919, 883, 828, 815  $\text{cm}^{-1}$ ;  $^1\text{H}$  NMR (400 MHz,  $\text{d}_6\text{-DMSO}$ )  $\delta$  6.99 (s, 1H), 5.50 (s, 1H), 3.73 (br, s, 2H), 3.27 (br, s, 2H), 1.91-1.86 (m, 4H);  $^{13}\text{C}$  NMR (101 MHz,  $\text{d}_6\text{-DMSO}$ )  $\delta$  182.3 (s), 174.6 (s), 147.8 (s), 145.6 (s), 130.5 (d), 99.5 (d), 50.9 (br, t), 50.5 (br, t), 26.0 (br, t), 23.3 (br, t); MS (EI)  $m/z$ : 213, 211, 176, 148, 120, 43; HRMS (EI) calcd for  $[\text{C}_{10}\text{H}_{10}^{35}\text{ClNO}_2]^+$ : 211.0395; found: 211.0390.

The IR,  $^1\text{H}$  and  $^{13}\text{C}$  NMR spectra agree with ref. 29.

**Reaction of quinone 1c with amine 2i.** To a solution of **1c** (246 mg, 1.00 mmol) in  $\text{CH}_3\text{CN}$  (5.0 mL), a solution of **2i** (36 mg, 0.50 mmol) in 1.0 mL  $\text{CH}_3\text{CN}$  was added dropwise under nitrogen at 20 °C. After stirring for 30 min at 20 °C, the solvent was evaporated and the residue was purified by flash column chromatography (silica gel, eluent: acetic acid/ethyl acetate/pentane = 1/10/50) to give **8ci** (dark violet solid, 60 mg, 86% yield).

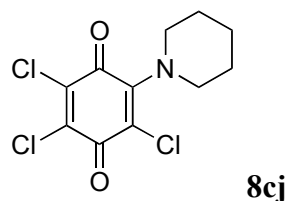


**2,3,5-Trichloro-6-(pyrrolidin-1-yl)cyclohexa-2,5-diene-1,4-dione (8ci).** IR (neat):  $\nu_{\text{max}}$  1692, 1618, 1524, 1476, 1456, 1376, 1276, 1078, 930, 861, 810, 723  $\text{cm}^{-1}$ ;  $^1\text{H}$  NMR (300 MHz,  $\text{CDCl}_3$ )  $\delta$  3.95-3.90 (m, 4H), 1.96-1.91 (m, 4H);  $^{13}\text{C}$  NMR (75 MHz,  $\text{CDCl}_3$ )  $\delta$  175.9 (s), 170.3 (s), 146.6 (s), 142.3 (s), 135.9 (s), 108.2 (s), 54.7 (t), 25.8 (t); MS (EI)  $m/z$ : 283, 281, 279, 240, 238, 216, 188, 152, 87; HRMS (EI) calcd for  $[\text{C}_{10}\text{H}_8^{35}\text{Cl}_3\text{NO}_2]^+$ : 278.9615; found: 278.9617.

The IR,  $^1\text{H}$  and  $^{13}\text{C}$  NMR spectra agree with ref. 29.

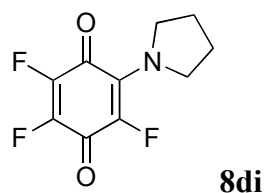
**Reaction of quinone 1c with amine 2j.** To a solution of **1c** (246 mg, 1.00 mmol) in  $\text{CH}_3\text{CN}$  (5.0 mL), a solution of **2j** (43 mg, 0.50 mmol) in 1.0 mL  $\text{CH}_3\text{CN}$  was added dropwise under

nitrogen at 20 °C. After stirring for 30 min at 20 °C, the solvent was evaporated and the residue was purified by flash column chromatography (silica gel, eluent: acetic acid/ethyl acetate/pentane = 1/10/50) to give **8cj** (dark violet solid, 48 mg, 65% yield).



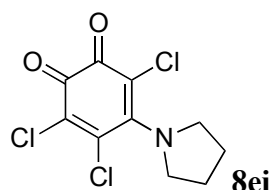
**2,3,5-Trichloro-6-(piperidin-1-yl)cyclohexa-2,5-diene-1,4-dione (8cj).** M.p.: 92-94 °C (AcOH); IR (neat):  $\nu_{\max}$  2948, 2939, 2894, 2853, 1688, 1633, 1547, 1443, 1434, 1355, 1342, 1280, 1261, 1249, 1218, 1191, 1152, 1127, 1075, 1062, 1018, 1007, 934, 903, 887, 855, 798, 719  $\text{cm}^{-1}$ ;  $^1\text{H}$  NMR (400 MHz,  $\text{d}_6$ -DMSO)  $\delta$  3.47-3.42 (m, 4H), 1.67-1.61 (m, 6H);  $^{13}\text{C}$  NMR (101 MHz,  $\text{d}_6$ -DMSO)  $\delta$  173.7 (s), 170.7 (s), 149.5 (s), 138.9 (s), 137.7 (s), 115.0 (s), 52.4 (t), 26.5 (t), 23.3 (t); MS (EI)  $m/z$ : 297, 295, 293, 240, 238, 166, 87, 43, 41; HRMS (EI) calcd for  $[\text{C}_{11}\text{H}_{10}^{35}\text{Cl}_3\text{NO}_2]^+$ : 292.9772; found: 292.9768.

**Reaction of quinone 1d with amine 2i.** To a solution of **1d** (180 mg, 1.00 mmol) in  $\text{CH}_3\text{CN}$  (5.0 mL), a solution of **2i** (36 mg, 0.50 mmol) in 1.0 mL  $\text{CH}_3\text{CN}$  was added dropwise under nitrogen at 20 °C. After stirring for 30 min at 20 °C, the solvent was evaporated and the residue was purified by flash column chromatography (silica gel, eluent: acetic acid/ethyl acetate/pentane = 1/10/50) to give **8di** (dark violet solid, 40 mg, 70% yield).



**2,3,5-Trifluoro-6-(pyrrolidin-1-yl)cyclohexa-2,5-diene-1,4-dione (8di).** IR (neat):  $\nu_{\max}$  2988, 2958, 2921, 2884, 1716, 1694, 1626, 1566, 1454, 1447, 1386, 1319, 1250, 1171, 1140, 1113, 1099, 1049, 1026, 999, 969, 857, 812, 730  $\text{cm}^{-1}$ ;  $^1\text{H}$  NMR (400 MHz,  $\text{d}_6$ -DMSO)  $\delta$  3.80-3.70 (m, 4H), 1.90-1.80 (m, 4H);  $^{13}\text{C}$  NMR (101 MHz,  $\text{d}_6$ -DMSO)  $\delta$  176.1 (s\*), 167.2 (s\*), 141.5 (d\*,  $^1J_{\text{F-C}} = 279$  Hz), 140.6 (d\*,  $^1J_{\text{F-C}} = 273$  Hz), 138.1 (d\*,  $^1J_{\text{F-C}} = 238$  Hz), 133.5 (s\*), 52.5 (t\*), 24.9 (t\*), \*splitting due to remote F-C couplings are not given; MS (EI)  $m/z$ : 231, 203, 190, 119, 106, 69, 43; HRMS (EI) calcd for  $[\text{C}_{10}\text{H}_8\text{F}_3\text{NO}_2]^+$ : 231.0502; found: 231.0494.

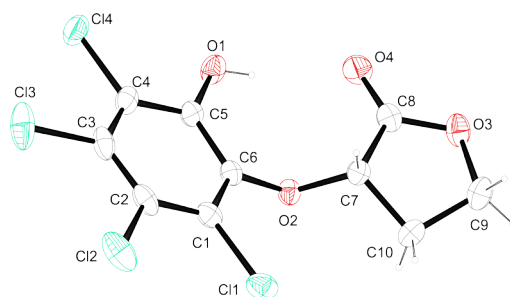
**Reaction of quinone 1e with amine 2i.** To a solution of **1e** (246 mg, 1.00 mmol) in CH<sub>3</sub>CN (5.0 mL), a solution of **2i** (36 mg, 0.50 mmol) in 1.0 mL CH<sub>3</sub>CN was added dropwise under nitrogen at 20 °C. After stirring for 30 min at 20 °C, the solvent was evaporated and the residue was purified by flash column chromatography (silica gel, eluent: acetic acid/ethyl acetate/pentane = 1/10/50) to give **8ei** (dark violet solid, 46 mg, 64% yield).



**3,4,6-Trichloro-5-(pyrrolidin-1-yl)cyclohexa-3,5-diene-1,2-dione (8ei).** IR (neat):  $\nu_{\text{max}}$  2955, 2921, 1693, 1612, 1555, 1479, 1446, 1360, 1344, 1297, 1206, 1163, 1063, 937, 900, 780, 761, 674 cm<sup>-1</sup>; <sup>1</sup>H NMR (400 MHz, CD<sub>3</sub>CN)  $\delta$  3.95-3.90 (m, 4H), 1.99-1.95 (m, 4H); <sup>13</sup>C NMR (101 MHz, CD<sub>3</sub>CN)  $\delta$  173.6 (s), 171.1 (s), 153.0 (s), 143.4 (s), 133.9 (s), 109.6 (s), 56.3 (t), 26.0 (t); MS (EI)  $m/z$ : 286, 285, 284, 283, 282, 281, 280, 248, 246, 212, 69, 55, 44, 43; HRMS (ESI) calcd for [C<sub>10</sub>H<sub>9</sub><sup>35</sup>Cl<sub>3</sub>NO<sub>2</sub>]<sup>+</sup>: 279.9693; found: 279.9697.

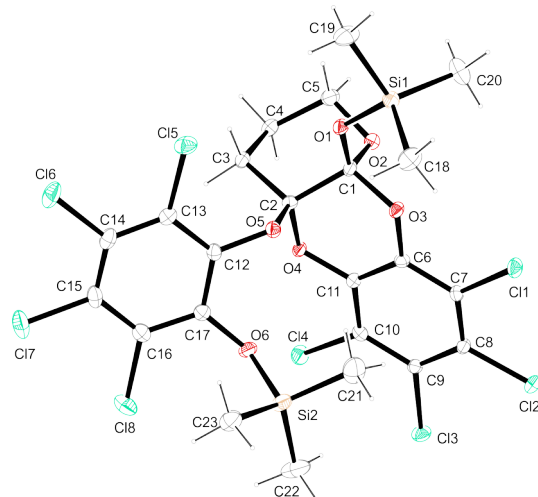
## 2) X-ray crystallography data for 6ed and 11ee

Crystallographic data for **6ed**



	<b>6ed</b>
net formula	C <sub>10</sub> H <sub>6</sub> Cl <sub>4</sub> O <sub>4</sub>
$M_r/\text{g mol}^{-1}$	331.963
crystal size/mm	0.235 × 0.145 × 0.072
$T/\text{K}$	173(2)
radiation	'Mo K $\alpha$
diffractometer	'Bruker D8Quest'
crystal system	monoclinic
space group	$P2_1/c$
$a/\text{\AA}$	12.0384(7)
$b/\text{\AA}$	6.1634(4)

$c/\text{\AA}$	16.5271(9)
$\alpha/^\circ$	90
$\beta/^\circ$	101.491(2)
$\gamma/^\circ$	90
$V/\text{\AA}^3$	1201.69(12)
$Z$	4
calc. density/ $\text{g cm}^{-3}$	1.83490(18)
$\mu/\text{mm}^{-1}$	0.986
absorption correction	multi-scan
transmission factor range	0.8863–0.9585
refls. measured	11649
$R_{\text{int}}$	0.0530
mean $\sigma(I)/I$	0.0458
$\theta$ range	2.52–26.41
observed refls.	1872
$x, y$ (weighting scheme)	0.0307, 1.7135
hydrogen refinement	mixed
refls in refinement	2387
parameters	167
restraints	0
$R(F_{\text{obs}})$	0.0524
$R_w(F^2)$	0.1020
$S$	1.136
shift/error $_{\text{max}}$	0.001
max electron density/ $\text{e \AA}^{-3}$	0.404
min electron density/ $\text{e \AA}^{-3}$	−0.365

Crystallographic data for **11ee**

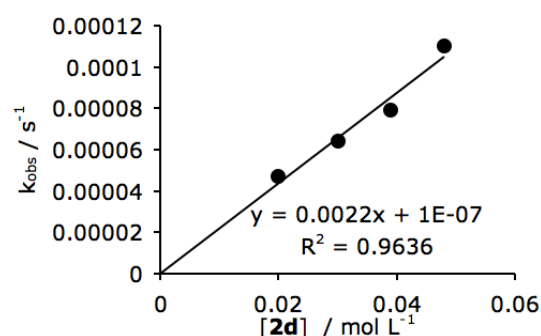
	<b>11ee</b>
net formula	C <sub>23</sub> H <sub>24</sub> Cl <sub>8</sub> O <sub>6</sub> Si <sub>2</sub>
$M_r/\text{g mol}^{-1}$	736.226
crystal size/mm	0.40 × 0.25 × 0.15
$T/\text{K}$	173(2)
radiation	MoK $\alpha$
diffractometer	'Oxford XCalibur'
crystal system	triclinic
space group	$P1bar$
$a/\text{\AA}$	8.8302(5)
$b/\text{\AA}$	11.9810(7)
$c/\text{\AA}$	15.2909(8)
$\alpha/^\circ$	79.908(5)
$\beta/^\circ$	81.840(5)
$\gamma/^\circ$	83.374(5)
$V/\text{\AA}^3$	1569.72(16)
$Z$	2
calc. density/ $\text{g cm}^{-3}$	1.55767(16)
$\mu/\text{mm}^{-1}$	0.831
absorption correction	'multi-scan'
transmission factor range	0.99060–1.00000
refls. measured	9306
$R_{\text{int}}$	0.0232
mean $\sigma(I)/I$	0.0485
$\theta$ range	4.28–26.37
observed refls.	5074
$x, y$ (weighting scheme)	0.0321, 0.3493
hydrogen refinement	constr
refls in refinement	6317
parameters	358
restraints	0
$R(F_{\text{obs}})$	0.0360
$R_w(F^2)$	0.0875
$S$	1.040
shift/error <sub>max</sub>	0.001
max electron density/ $\text{e \AA}^{-3}$	0.336
min electron density/ $\text{e \AA}^{-3}$	–0.336

3) Kinetics of the Reactions of Quinones with **2** in CH<sub>2</sub>Cl<sub>2</sub> or CH<sub>3</sub>CN

The rate constants of the reactions of **1a** with **2e** were determined by time-resolved <sup>1</sup>H NMR spectroscopy. The integrations of the proton signal of **1a** (6.75-6.80 ppm) were extracted to give a monoexponential decay vs. reaction time. The rate constants of all other investigated reactions were determined photometrically. The temperature of the solutions during all kinetic studies was kept constant (20.0 ± 0.1 °C) by using a circulating bath thermostat. For the evaluation of fast kinetics ( $\tau_{1/2} < 10$  s) a stopped-flow spectrophotometer (Hi-Tech SF-61DX2) was used. The rates of slow reactions ( $\tau_{1/2} > 10$  s) were determined by using a conventional UV/Vis diode array spectrophotometer (J&M TIDAS) connected to a Hellma 661.502-QX quartz Suprasil immersion probe (5 mm light path) via fiber optic cables. Rate constants  $k_{\text{obs}}$  (s<sup>-1</sup>) were obtained by least-squares fitting of the absorbances to the monoexponential function  $A_t = A_0 e^{-k_{\text{obs}}t} + C$  (for decreasing absorbance) or  $A_t = A_0 (1 - e^{-k_{\text{obs}}t}) + C$  (for increasing absorbance).

Table S1. Kinetics of the reaction of **1a** with **2d** in CH<sub>2</sub>Cl<sub>2</sub> (20 °C, Conventional UV/Vis, 290 nm)

[ <b>1a</b> ] / mol L <sup>-1</sup>	[ <b>2d</b> ] / mol L <sup>-1</sup>	$k_{\text{obs}}$ / s <sup>-1</sup>
1.0 × 10 <sup>-4</sup>	2.0 × 10 <sup>-2</sup>	4.7 × 10 <sup>-5</sup>
1.0 × 10 <sup>-4</sup>	3.0 × 10 <sup>-2</sup>	6.4 × 10 <sup>-5</sup>
1.0 × 10 <sup>-4</sup>	3.9 × 10 <sup>-2</sup>	7.9 × 10 <sup>-5</sup>
1.0 × 10 <sup>-4</sup>	4.8 × 10 <sup>-2</sup>	1.1 × 10 <sup>-4</sup>
$k_2 = 2.2 \times 10^{-3} \text{ L mol}^{-1} \text{ s}^{-1}$		

Table S2. Kinetics of the reaction of **1a** with **2e** in CD<sub>2</sub>Cl<sub>2</sub> (20 °C, <sup>1</sup>H NMR, 6.75-6.80 ppm)

[ <b>1a</b> ] / mol L <sup>-1</sup>	[ <b>2e</b> ] / mol L <sup>-1</sup>	$k_{\text{obs}}$ / s <sup>-1</sup>
5.0 × 10 <sup>-2</sup>	0.50	2.0 × 10 <sup>-5</sup>
5.0 × 10 <sup>-2</sup>	1.0	3.3 × 10 <sup>-5</sup>
5.0 × 10 <sup>-2</sup>	1.5	4.1 × 10 <sup>-5</sup>
5.0 × 10 <sup>-2</sup>	2.0	5.0 × 10 <sup>-5</sup>
$k_2 = 2.0 \times 10^{-5} \text{ L mol}^{-1} \text{ s}^{-1}$		

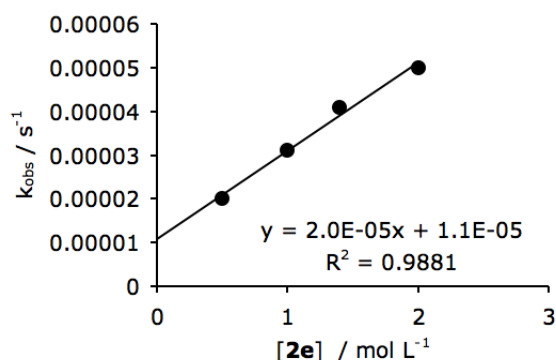
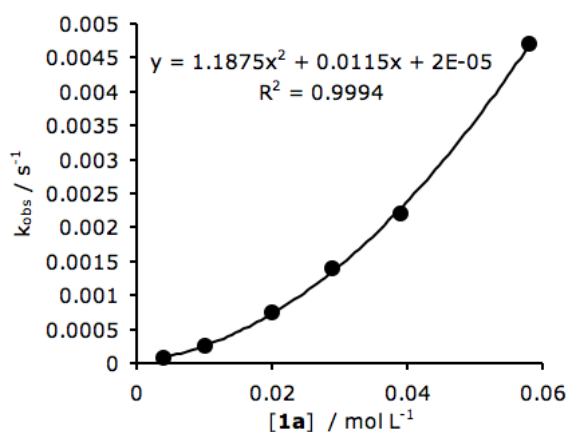


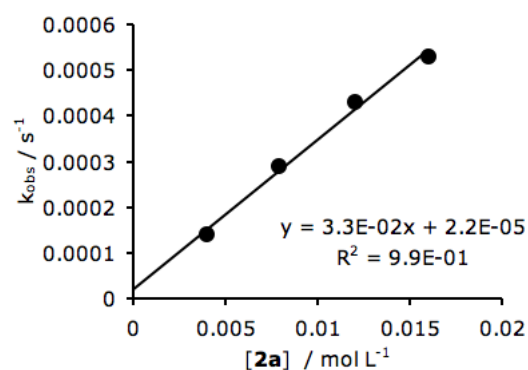
Table S3. Kinetics of the reaction of **1a** with **2i** in CH<sub>3</sub>CN (20 °C, Conventional UV/Vis, 510 nm)

[ <b>2i</b> ] / mol L <sup>-1</sup>	[ <b>1a</b> ] / mol L <sup>-1</sup>	<i>k</i> <sub>obs</sub> / s <sup>-1</sup>
4.0 × 10 <sup>-4</sup>	4.0 × 10 <sup>-3</sup>	7.0 × 10 <sup>-5</sup>
1.0 × 10 <sup>-3</sup>	1.0 × 10 <sup>-2</sup>	2.5 × 10 <sup>-4</sup>
1.0 × 10 <sup>-3</sup>	2.0 × 10 <sup>-2</sup>	7.5 × 10 <sup>-4</sup>
1.0 × 10 <sup>-3</sup>	2.9 × 10 <sup>-2</sup>	1.4 × 10 <sup>-3</sup>
1.0 × 10 <sup>-3</sup>	3.9 × 10 <sup>-2</sup>	2.2 × 10 <sup>-3</sup>
1.0 × 10 <sup>-3</sup>	5.8 × 10 <sup>-2</sup>	4.7 × 10 <sup>-3</sup>

Table S4. Kinetics of the reaction of **1b** with **2a** in CH<sub>2</sub>Cl<sub>2</sub> (20 °C, Conventional UV/Vis, 275 nm)

[ <b>1b</b> ] / mol L <sup>-1</sup>	[ <b>2a</b> ] / mol L <sup>-1</sup>	<i>k</i> <sub>obs</sub> / s <sup>-1</sup>
1.0 × 10 <sup>-4</sup>	4.0 × 10 <sup>-3</sup>	1.4 × 10 <sup>-4</sup>
1.0 × 10 <sup>-4</sup>	7.9 × 10 <sup>-3</sup>	2.9 × 10 <sup>-4</sup>
1.0 × 10 <sup>-4</sup>	1.2 × 10 <sup>-2</sup>	4.3 × 10 <sup>-4</sup>
1.0 × 10 <sup>-4</sup>	1.6 × 10 <sup>-2</sup>	5.3 × 10 <sup>-4</sup>

$$k_2 = 3.3 \times 10^{-2} \text{ L mol}^{-1} \text{ s}^{-1}$$

Table S5. Kinetics of the reaction of **1b** with **2a'** in CH<sub>2</sub>Cl<sub>2</sub> (20 °C, Conventional UV/Vis, 275 nm)

[ <b>1b</b> ] / mol L <sup>-1</sup>	[ <b>2a'</b> ] / mol L <sup>-1</sup>	<i>k</i> <sub>obs</sub> / s <sup>-1</sup>
5.0 × 10 <sup>-5</sup>	1.0 × 10 <sup>-2</sup>	8.6 × 10 <sup>-5</sup>
5.0 × 10 <sup>-5</sup>	2.0 × 10 <sup>-2</sup>	1.7 × 10 <sup>-4</sup>
5.0 × 10 <sup>-5</sup>	3.0 × 10 <sup>-2</sup>	2.9 × 10 <sup>-4</sup>
5.0 × 10 <sup>-5</sup>	4.0 × 10 <sup>-2</sup>	3.8 × 10 <sup>-4</sup>

$$k_2 = 1.0 \times 10^{-2} \text{ L mol}^{-1} \text{ s}^{-1}$$

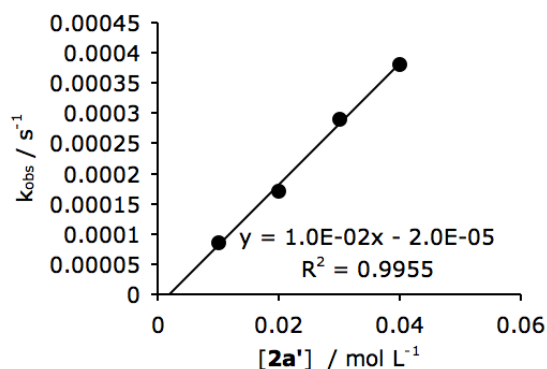
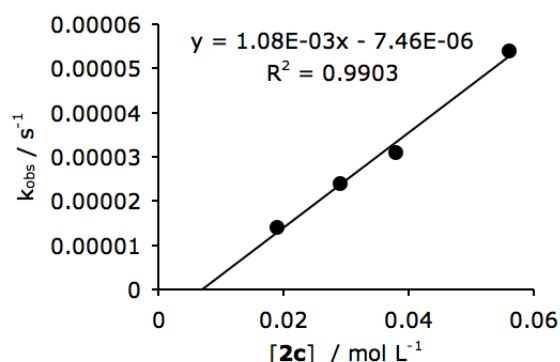


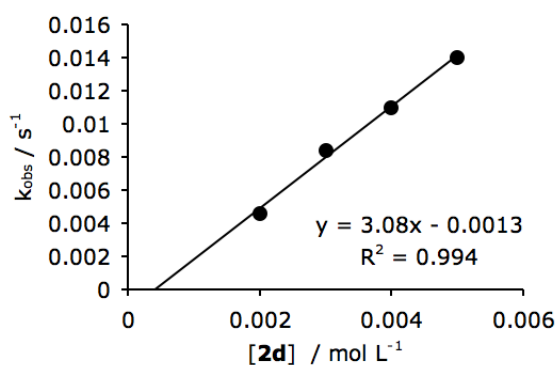


Table S6. Kinetics of the reaction of **1b** with **2c** in CH<sub>2</sub>Cl<sub>2</sub> (20 °C, Conventional UV/Vis, 275 nm)

[ <b>1b</b> ] / mol L <sup>-1</sup>	[ <b>2c</b> ] / mol L <sup>-1</sup>	<i>k</i> <sub>obs</sub> / s <sup>-1</sup>
1.0 × 10 <sup>-4</sup>	1.9 × 10 <sup>-2</sup>	1.4 × 10 <sup>-5</sup>
1.0 × 10 <sup>-4</sup>	2.9 × 10 <sup>-2</sup>	2.4 × 10 <sup>-5</sup>
1.0 × 10 <sup>-4</sup>	3.8 × 10 <sup>-2</sup>	3.1 × 10 <sup>-5</sup>
1.0 × 10 <sup>-4</sup>	5.6 × 10 <sup>-2</sup>	5.4 × 10 <sup>-5</sup>
<i>k</i> <sub>2</sub> = 1.1 × 10 <sup>-3</sup> L mol <sup>-1</sup> s <sup>-1</sup>		

Table S7. Kinetics of the reaction of **1b** with **2d** in CH<sub>2</sub>Cl<sub>2</sub> (20 °C, Conventional UV/Vis, 275 nm)

[ <b>1b</b> ] / mol L <sup>-1</sup>	[ <b>2d</b> ] / mol L <sup>-1</sup>	<i>k</i> <sub>obs</sub> / s <sup>-1</sup>
5.0 × 10 <sup>-5</sup>	2.0 × 10 <sup>-3</sup>	4.6 × 10 <sup>-3</sup>
5.0 × 10 <sup>-5</sup>	3.0 × 10 <sup>-3</sup>	8.4 × 10 <sup>-3</sup>
5.0 × 10 <sup>-5</sup>	4.0 × 10 <sup>-3</sup>	1.1 × 10 <sup>-2</sup>
5.0 × 10 <sup>-5</sup>	5.0 × 10 <sup>-3</sup>	1.4 × 10 <sup>-2</sup>
<i>k</i> <sub>2</sub> = 3.1 L mol <sup>-1</sup> s <sup>-1</sup>		

Table S8. Kinetics of the reaction of **1b** with **2e** in CH<sub>2</sub>Cl<sub>2</sub> (20 °C, Conventional UV/Vis, 275 nm)

[ <b>1b</b> ] / mol L <sup>-1</sup>	[ <b>2e</b> ] / mol L <sup>-1</sup>	<i>k</i> <sub>obs</sub> / s <sup>-1</sup>
1.0 × 10 <sup>-4</sup>	5.0 × 10 <sup>-3</sup>	1.3 × 10 <sup>-4</sup>
1.0 × 10 <sup>-4</sup>	9.9 × 10 <sup>-3</sup>	2.0 × 10 <sup>-4</sup>
1.0 × 10 <sup>-4</sup>	1.5 × 10 <sup>-2</sup>	3.5 × 10 <sup>-4</sup>
1.0 × 10 <sup>-4</sup>	1.9 × 10 <sup>-2</sup>	4.7 × 10 <sup>-4</sup>
<i>k</i> <sub>2</sub> = 2.5 × 10 <sup>-2</sup> L mol <sup>-1</sup> s <sup>-1</sup>		

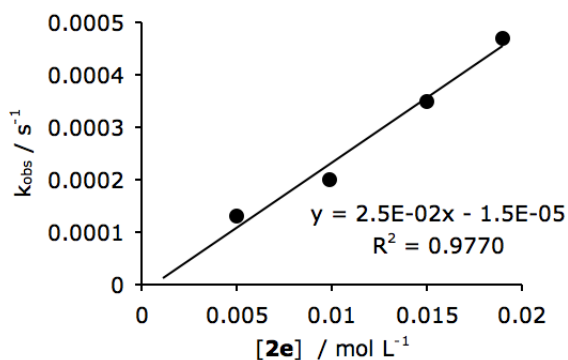
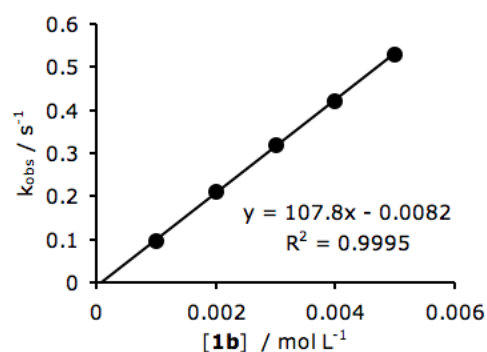
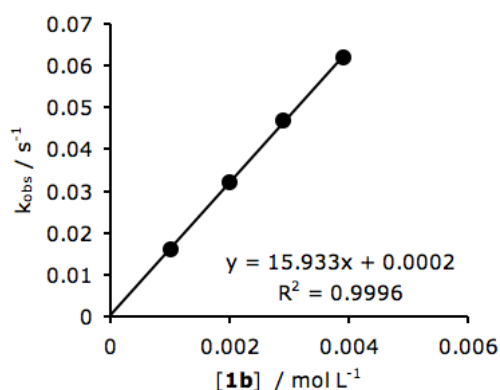


Table S9. Kinetics of the reaction of **1b** with **2i** in CH<sub>3</sub>CN (20 °C, Conventional UV/Vis, 525 nm)

[ <b>2i</b> ] / mol L <sup>-1</sup>	[ <b>1b</b> ] / mol L <sup>-1</sup>	<i>k</i> <sub>obs</sub> / s <sup>-1</sup>
1.0 × 10 <sup>-4</sup>	1.0 × 10 <sup>-3</sup>	0.096
1.0 × 10 <sup>-4</sup>	2.0 × 10 <sup>-3</sup>	0.21
1.0 × 10 <sup>-4</sup>	3.0 × 10 <sup>-3</sup>	0.32
1.0 × 10 <sup>-4</sup>	4.0 × 10 <sup>-3</sup>	0.42
1.0 × 10 <sup>-4</sup>	5.0 × 10 <sup>-3</sup>	0.53
<i>k</i> <sub>2</sub> = 5.4 × 10 <sup>1</sup> L mol <sup>-1</sup> s <sup>-1</sup>		
As two molecules of amine are consumed per quinone, the slope of the depicted graph is divided by 2		

Table S10. Kinetics of the reaction of **1b** with **2j** in CH<sub>3</sub>CN (20 °C, Conventional UV/Vis, 510 nm)

[ <b>2j</b> ] / mol L <sup>-1</sup>	[ <b>1b</b> ] / mol L <sup>-1</sup>	<i>k</i> <sub>obs</sub> / s <sup>-1</sup>
1.0 × 10 <sup>-4</sup>	1.0 × 10 <sup>-3</sup>	1.6 × 10 <sup>-2</sup>
1.0 × 10 <sup>-4</sup>	2.0 × 10 <sup>-3</sup>	3.2 × 10 <sup>-2</sup>
1.0 × 10 <sup>-4</sup>	2.9 × 10 <sup>-3</sup>	4.7 × 10 <sup>-2</sup>
1.0 × 10 <sup>-4</sup>	3.9 × 10 <sup>-3</sup>	6.2 × 10 <sup>-2</sup>
<i>k</i> <sub>2</sub> = 8.0 L mol <sup>-1</sup> s <sup>-1</sup>		
As two molecules of amine are consumed per quinone, the slope of the depicted graph is divided by 2		

Table S11. Kinetics of the reaction of **1b** with **2k** in CH<sub>3</sub>CN (20 °C, Conventional UV/Vis, 500 nm)

[ <b>2k</b> ] / mol L <sup>-1</sup>	[ <b>1b</b> ] / mol L <sup>-1</sup>	<i>k</i> <sub>obs</sub> / s <sup>-1</sup>
1.0 × 10 <sup>-4</sup>	1.0 × 10 <sup>-3</sup>	5.6 × 10 <sup>-4</sup>
1.0 × 10 <sup>-4</sup>	2.0 × 10 <sup>-3</sup>	1.1 × 10 <sup>-3</sup>
1.0 × 10 <sup>-4</sup>	2.9 × 10 <sup>-3</sup>	1.5 × 10 <sup>-3</sup>
1.0 × 10 <sup>-4</sup>	3.9 × 10 <sup>-3</sup>	2.1 × 10 <sup>-3</sup>
<i>k</i> <sub>2</sub> = 0.26 L mol <sup>-1</sup> s <sup>-1</sup>		
As two molecules of amine are consumed per quinone, the slope of the depicted graph is divided by 2		

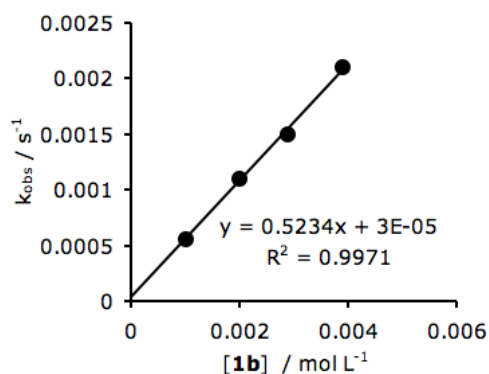
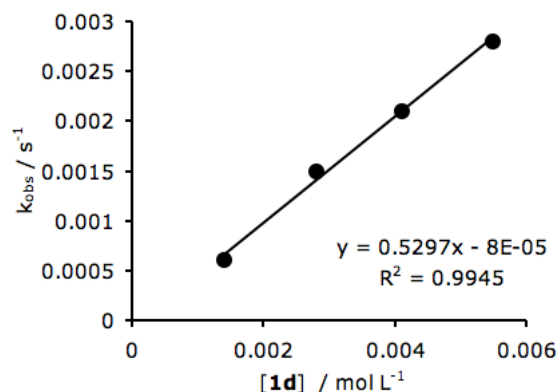
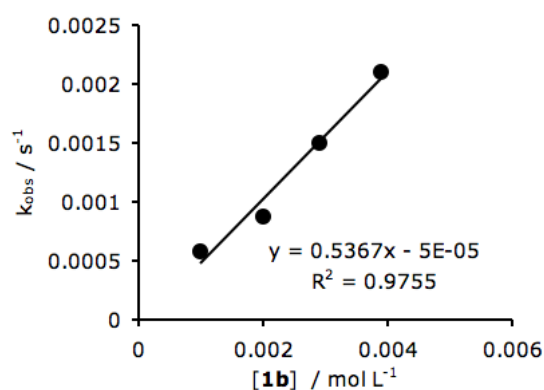


Table S12. Kinetics of the reaction of **1b** with **2k-D** in CH<sub>3</sub>CN (20 °C, Conventional UV/Vis, 500 nm)

[ <b>2k-D</b> ] / mol L <sup>-1</sup>	[ <b>1b</b> ] / mol L <sup>-1</sup>	<i>k</i> <sub>obs</sub> / s <sup>-1</sup>
1.0 × 10 <sup>-4</sup>	1.4 × 10 <sup>-3</sup>	6.0 × 10 <sup>-4</sup>
1.0 × 10 <sup>-4</sup>	2.8 × 10 <sup>-3</sup>	1.5 × 10 <sup>-3</sup>
1.0 × 10 <sup>-4</sup>	4.1 × 10 <sup>-3</sup>	2.1 × 10 <sup>-3</sup>
1.0 × 10 <sup>-4</sup>	5.5 × 10 <sup>-3</sup>	2.8 × 10 <sup>-3</sup>
<i>k</i> <sub>2</sub> = 0.26 L mol <sup>-1</sup> s <sup>-1</sup>		
As two molecules of amine are consumed per quinone, the slope of the depicted graph is divided by 2		

Table S13. Kinetics of the reaction of **1b** with **2l** in CH<sub>3</sub>CN (20 °C, Conventional UV/Vis, 500 nm)

[ <b>2l</b> ] / mol L <sup>-1</sup>	[ <b>1b</b> ] / mol L <sup>-1</sup>	<i>k</i> <sub>obs</sub> / s <sup>-1</sup>
1.0 × 10 <sup>-4</sup>	9.9 × 10 <sup>-4</sup>	5.8 × 10 <sup>-4</sup>
1.0 × 10 <sup>-4</sup>	2.0 × 10 <sup>-3</sup>	8.8 × 10 <sup>-4</sup>
1.0 × 10 <sup>-4</sup>	2.9 × 10 <sup>-3</sup>	1.5 × 10 <sup>-3</sup>
1.0 × 10 <sup>-4</sup>	3.9 × 10 <sup>-3</sup>	2.1 × 10 <sup>-3</sup>
<i>k</i> <sub>2</sub> = 0.27 L mol <sup>-1</sup> s <sup>-1</sup>		
As two molecules of amine are consumed per quinone, the slope of the depicted graph is divided by 2		

Table S14. Kinetics of the reaction of **1b** with **2o** in CH<sub>3</sub>CN (20 °C, Conventional UV/Vis, nm)

[ <b>2o</b> ] / mol L <sup>-1</sup>	[ <b>1b</b> ] / mol L <sup>-1</sup>	<i>k</i> <sub>obs</sub> / s <sup>-1</sup>
1.0 × 10 <sup>-4</sup>	9.9 × 10 <sup>-4</sup>	1.0 × 10 <sup>-3</sup>
1.0 × 10 <sup>-4</sup>	2.0 × 10 <sup>-3</sup>	2.0 × 10 <sup>-3</sup>
1.0 × 10 <sup>-4</sup>	2.9 × 10 <sup>-3</sup>	3.0 × 10 <sup>-3</sup>
1.0 × 10 <sup>-4</sup>	3.8 × 10 <sup>-3</sup>	3.6 × 10 <sup>-3</sup>
<i>k</i> <sub>2</sub> = 0.47 L mol <sup>-1</sup> s <sup>-1</sup>		
As two molecules of amine are consumed per quinone, the slope of the depicted graph is divided by 2		

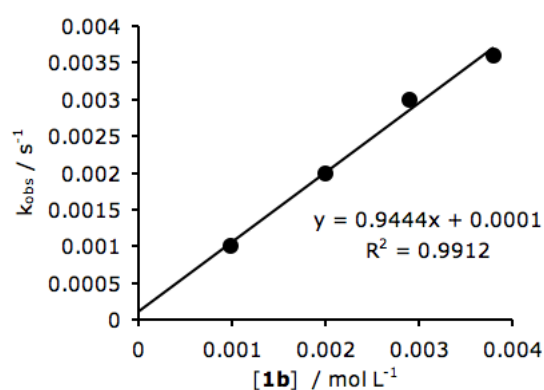
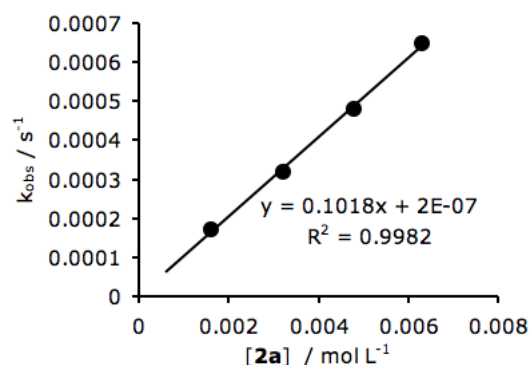
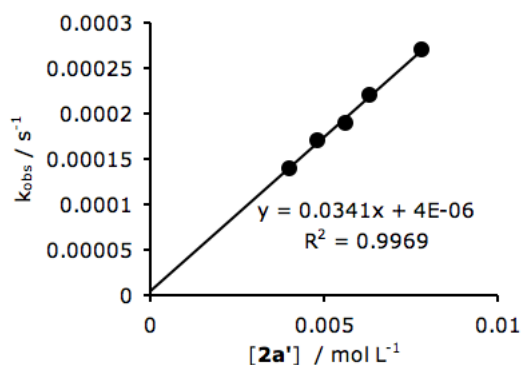


Table S15. Kinetics of the reaction of **1c** with **2a** in CH<sub>2</sub>Cl<sub>2</sub> (20 °C, Conventional UV/Vis, 290 nm)

[ <b>1c</b> ] / mol L <sup>-1</sup>	[ <b>2a</b> ] / mol L <sup>-1</sup>	<i>k</i> <sub>obs</sub> / s <sup>-1</sup>
1.0 × 10 <sup>-4</sup>	1.6 × 10 <sup>-3</sup>	1.7 × 10 <sup>-4</sup>
1.0 × 10 <sup>-4</sup>	3.2 × 10 <sup>-3</sup>	3.2 × 10 <sup>-4</sup>
1.0 × 10 <sup>-4</sup>	4.8 × 10 <sup>-3</sup>	4.8 × 10 <sup>-4</sup>
1.0 × 10 <sup>-4</sup>	6.3 × 10 <sup>-3</sup>	6.5 × 10 <sup>-4</sup>
<i>k</i> <sub>2</sub> = 0.10 L mol <sup>-1</sup> s <sup>-1</sup>		

Table S16. Kinetics of the reaction of **1c** with **2a'** in CH<sub>2</sub>Cl<sub>2</sub> (20 °C, Conventional UV/Vis, 293 nm)

[ <b>1c</b> ] / mol L <sup>-1</sup>	[ <b>2a'</b> ] / mol L <sup>-1</sup>	<i>k</i> <sub>obs</sub> / s <sup>-1</sup>
1.0 × 10 <sup>-4</sup>	4.0 × 10 <sup>-3</sup>	1.4 × 10 <sup>-4</sup>
1.0 × 10 <sup>-4</sup>	4.8 × 10 <sup>-3</sup>	1.7 × 10 <sup>-4</sup>
1.0 × 10 <sup>-4</sup>	5.6 × 10 <sup>-3</sup>	1.9 × 10 <sup>-4</sup>
1.0 × 10 <sup>-4</sup>	6.3 × 10 <sup>-3</sup>	2.2 × 10 <sup>-4</sup>
1.0 × 10 <sup>-4</sup>	7.8 × 10 <sup>-3</sup>	2.7 × 10 <sup>-4</sup>
<i>k</i> <sub>2</sub> = 3.4 × 10 <sup>-2</sup> L mol <sup>-1</sup> s <sup>-1</sup>		

Table S17. Kinetics of the reaction of **1c** with **2c** in CH<sub>2</sub>Cl<sub>2</sub> (20 °C, Stopped-flow, 290 nm)

[ <b>1c</b> ] / mol L <sup>-1</sup>	[ <b>2c</b> ] / mol L <sup>-1</sup>	<i>k</i> <sub>obs</sub> / s <sup>-1</sup>
1.0 × 10 <sup>-4</sup>	1.0 × 10 <sup>-2</sup>	2.2 × 10 <sup>-4</sup>
1.0 × 10 <sup>-4</sup>	1.9 × 10 <sup>-2</sup>	4.1 × 10 <sup>-4</sup>
1.0 × 10 <sup>-4</sup>	2.9 × 10 <sup>-2</sup>	6.3 × 10 <sup>-4</sup>
1.0 × 10 <sup>-4</sup>	3.8 × 10 <sup>-2</sup>	8.0 × 10 <sup>-4</sup>
<i>k</i> <sub>2</sub> = 2.1 × 10 <sup>-2</sup> L mol <sup>-1</sup> s <sup>-1</sup>		

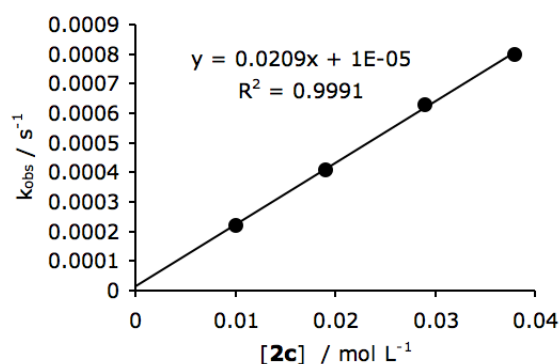
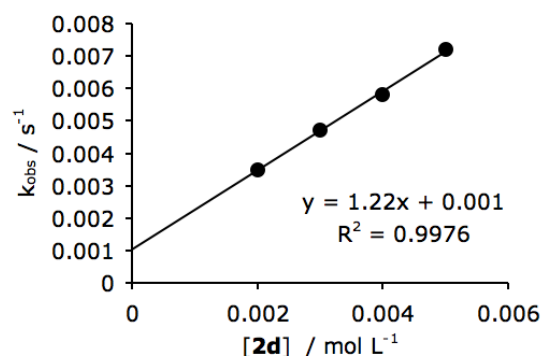


Table S18. Kinetics of the reaction of **1c** with **2d** in CH<sub>2</sub>Cl<sub>2</sub> (20 °C, Stopped-flow, 293 nm)

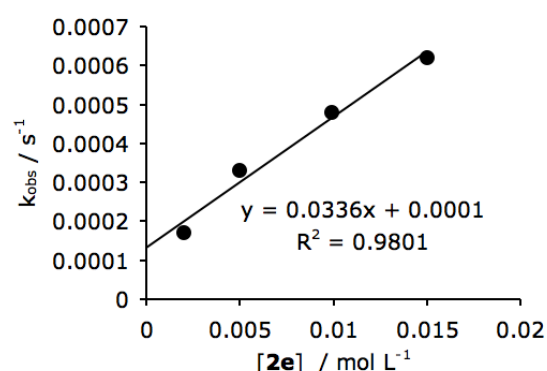
[ <b>1c</b> ] / mol L <sup>-1</sup>	[ <b>2d</b> ] / mol L <sup>-1</sup>	<i>k</i> <sub>obs</sub> / s <sup>-1</sup>
1.0 × 10 <sup>-4</sup>	2.0 × 10 <sup>-3</sup>	3.5 × 10 <sup>-3</sup>
1.0 × 10 <sup>-4</sup>	3.0 × 10 <sup>-3</sup>	4.7 × 10 <sup>-3</sup>
1.0 × 10 <sup>-4</sup>	4.0 × 10 <sup>-3</sup>	5.8 × 10 <sup>-3</sup>
1.0 × 10 <sup>-4</sup>	5.0 × 10 <sup>-3</sup>	7.2 × 10 <sup>-3</sup>

$k_2 = 1.2 \text{ L mol}^{-1} \text{ s}^{-1}$

Table S19. Kinetics of the reaction of **1c** with **2e** in CH<sub>2</sub>Cl<sub>2</sub> (20 °C, Conventional UV/Vis, 293 nm)

[ <b>1c</b> ] / mol L <sup>-1</sup>	[ <b>2e</b> ] / mol L <sup>-1</sup>	<i>k</i> <sub>obs</sub> / s <sup>-1</sup>
1.0 × 10 <sup>-4</sup>	2.0 × 10 <sup>-3</sup>	1.7 × 10 <sup>-4</sup>
1.0 × 10 <sup>-4</sup>	5.0 × 10 <sup>-3</sup>	3.3 × 10 <sup>-4</sup>
1.0 × 10 <sup>-4</sup>	9.9 × 10 <sup>-3</sup>	4.8 × 10 <sup>-4</sup>
1.0 × 10 <sup>-4</sup>	1.5 × 10 <sup>-2</sup>	6.2 × 10 <sup>-4</sup>

$k_2 = 3.4 \times 10^{-2} \text{ L mol}^{-1} \text{ s}^{-1}$

Table S20. Kinetics of the reaction of **1c** with **2g** in CH<sub>2</sub>Cl<sub>2</sub> (20 °C, Stopped-flow, 293 nm)

[ <b>1c</b> ] / mol L <sup>-1</sup>	[ <b>2g</b> ] / mol L <sup>-1</sup>	<i>k</i> <sub>obs</sub> / s <sup>-1</sup>
1.0 × 10 <sup>-4</sup>	1.0 × 10 <sup>-3</sup>	7.1
1.0 × 10 <sup>-4</sup>	2.0 × 10 <sup>-3</sup>	15
1.0 × 10 <sup>-4</sup>	3.0 × 10 <sup>-3</sup>	22
1.0 × 10 <sup>-4</sup>	4.0 × 10 <sup>-3</sup>	28
1.0 × 10 <sup>-4</sup>	5.0 × 10 <sup>-3</sup>	35

$k_2 = 6.9 \times 10^3 \text{ L mol}^{-1} \text{ s}^{-1}$

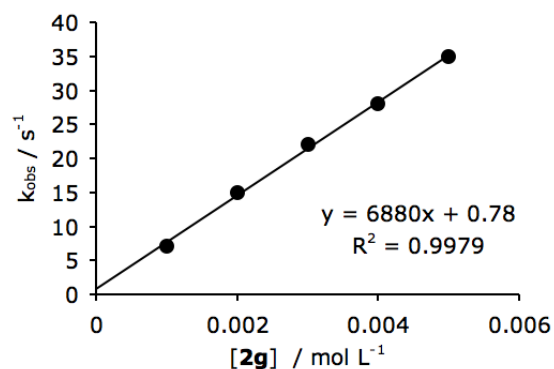
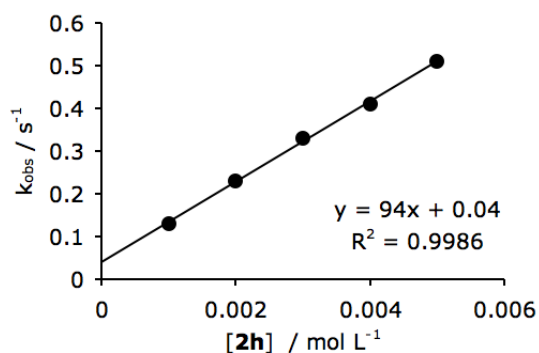


Table S21. Kinetics of the reaction of **1c** with **2h** in CH<sub>2</sub>Cl<sub>2</sub> (20 °C, Stopped-flow, 293 nm)

[ <b>1c</b> ] / mol L <sup>-1</sup>	[ <b>2h</b> ] / mol L <sup>-1</sup>	<i>k</i> <sub>obs</sub> / s <sup>-1</sup>
1.0 × 10 <sup>-4</sup>	1.0 × 10 <sup>-3</sup>	0.13
1.0 × 10 <sup>-4</sup>	2.0 × 10 <sup>-3</sup>	0.23
1.0 × 10 <sup>-4</sup>	3.0 × 10 <sup>-3</sup>	0.33
1.0 × 10 <sup>-4</sup>	4.0 × 10 <sup>-3</sup>	0.41
1.0 × 10 <sup>-4</sup>	5.0 × 10 <sup>-2</sup>	0.51

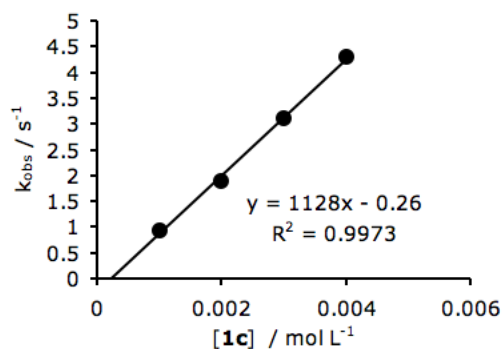
$k_2 = 94 \text{ L mol}^{-1} \text{ s}^{-1}$

Table S22. Kinetics of the reaction of **1c** with **2i** in CH<sub>3</sub>CN (20 °C, Stopped-flow, 525 nm)

[ <b>2i</b> ] / mol L <sup>-1</sup>	[ <b>1c</b> ] / mol L <sup>-1</sup>	<i>k</i> <sub>obs</sub> / s <sup>-1</sup>
1.0 × 10 <sup>-4</sup>	1.0 × 10 <sup>-3</sup>	0.94
1.0 × 10 <sup>-4</sup>	2.0 × 10 <sup>-3</sup>	1.9
1.0 × 10 <sup>-4</sup>	3.0 × 10 <sup>-3</sup>	3.1
1.0 × 10 <sup>-4</sup>	4.0 × 10 <sup>-3</sup>	4.3

$k_2 = 5.6 \times 10^2 \text{ L mol}^{-1} \text{ s}^{-1}$

As two molecules of amine are consumed per quinone, the slope of the depicted graph is divided by 2

Table S23. Kinetics of the reaction of **1c** with **2j** in CH<sub>3</sub>CN (20 °C, Stopped-flow, 525 nm)

[ <b>2j</b> ] / mol L <sup>-1</sup>	[ <b>1c</b> ] / mol L <sup>-1</sup>	<i>k</i> <sub>obs</sub> / s <sup>-1</sup>
1.0 × 10 <sup>-4</sup>	1.0 × 10 <sup>-3</sup>	0.17
1.0 × 10 <sup>-4</sup>	2.0 × 10 <sup>-3</sup>	0.35
1.0 × 10 <sup>-4</sup>	3.0 × 10 <sup>-3</sup>	0.53
1.0 × 10 <sup>-4</sup>	4.0 × 10 <sup>-3</sup>	0.71
1.0 × 10 <sup>-4</sup>	5.0 × 10 <sup>-3</sup>	0.87

$k_2 = 8.8 \times 10^1 \text{ L mol}^{-1} \text{ s}^{-1}$

As two molecules of amine are consumed per quinone, the slope of the depicted graph is divided by 2

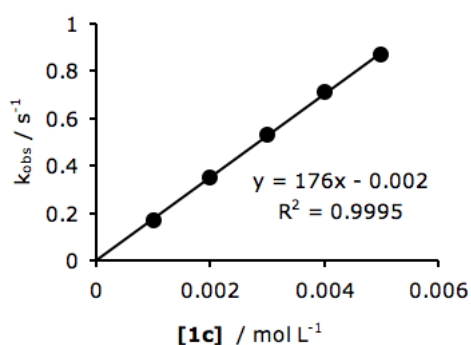
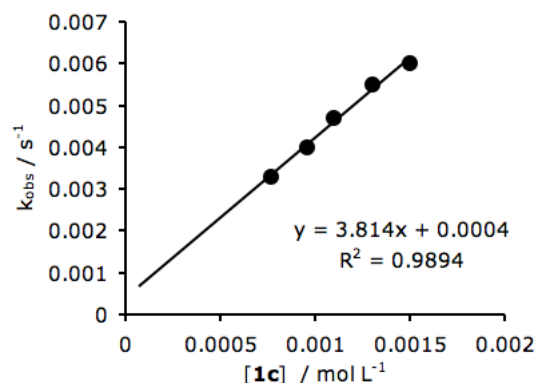


Table S24. Kinetics of the reaction of **1c** with **2k** in CH<sub>3</sub>CN (20 °C, Conventional UV/Vis, 550 nm)

[ <b>2k</b> ] / mol L <sup>-1</sup>	[ <b>1c</b> ] / mol L <sup>-1</sup>	<i>k</i> <sub>obs</sub> / s <sup>-1</sup>
1.0 × 10 <sup>-4</sup>	7.7 × 10 <sup>-4</sup>	3.3 × 10 <sup>-3</sup>
1.0 × 10 <sup>-4</sup>	9.6 × 10 <sup>-4</sup>	4.0 × 10 <sup>-3</sup>
1.0 × 10 <sup>-4</sup>	1.1 × 10 <sup>-3</sup>	4.7 × 10 <sup>-3</sup>
1.0 × 10 <sup>-4</sup>	1.3 × 10 <sup>-3</sup>	5.5 × 10 <sup>-3</sup>
1.0 × 10 <sup>-4</sup>	1.5 × 10 <sup>-3</sup>	6.0 × 10 <sup>-3</sup>

$$k_2 = 1.9 \text{ L mol}^{-1} \text{ s}^{-1}$$

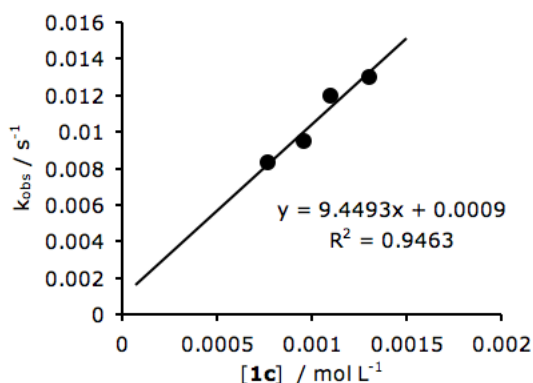
As two molecules of amine are consumed per quinone, the slope of the depicted graph is divided by 2

Table S25. Kinetics of the reaction of **1c** with **2l** in CH<sub>3</sub>CN (20 °C, Conventional UV/Vis, 535 nm)

[ <b>2l</b> ] / mol L <sup>-1</sup>	[ <b>1c</b> ] / mol L <sup>-1</sup>	<i>k</i> <sub>obs</sub> / s <sup>-1</sup>
1.0 × 10 <sup>-4</sup>	7.7 × 10 <sup>-4</sup>	8.3 × 10 <sup>-3</sup>
1.0 × 10 <sup>-4</sup>	9.6 × 10 <sup>-4</sup>	9.5 × 10 <sup>-3</sup>
1.0 × 10 <sup>-4</sup>	1.1 × 10 <sup>-3</sup>	1.2 × 10 <sup>-2</sup>
1.0 × 10 <sup>-4</sup>	1.3 × 10 <sup>-3</sup>	1.3 × 10 <sup>-2</sup>

$$k_2 = 4.7 \text{ L mol}^{-1} \text{ s}^{-1}$$

As two molecules of amine are consumed per quinone, the slope of the depicted graph is divided by 2

Table S26. Kinetics of the reaction of **1c** with **2n** in CH<sub>3</sub>CN (20 °C, Conventional UV/Vis, 535 nm)

[ <b>2n</b> ] / mol L <sup>-1</sup>	[ <b>1c</b> ] / mol L <sup>-1</sup>	<i>k</i> <sub>obs</sub> / s <sup>-1</sup>
7.7 × 10 <sup>-5</sup>	7.7 × 10 <sup>-4</sup>	9.1 × 10 <sup>-4</sup>
7.7 × 10 <sup>-5</sup>	1.1 × 10 <sup>-3</sup>	1.2 × 10 <sup>-3</sup>
7.7 × 10 <sup>-5</sup>	1.5 × 10 <sup>-3</sup>	1.8 × 10 <sup>-3</sup>
7.7 × 10 <sup>-5</sup>	1.8 × 10 <sup>-3</sup>	2.3 × 10 <sup>-3</sup>

$$k_2 = 0.68 \text{ L mol}^{-1} \text{ s}^{-1}$$

As two molecules of amine are consumed per quinone, the slope of the depicted graph is divided by 2

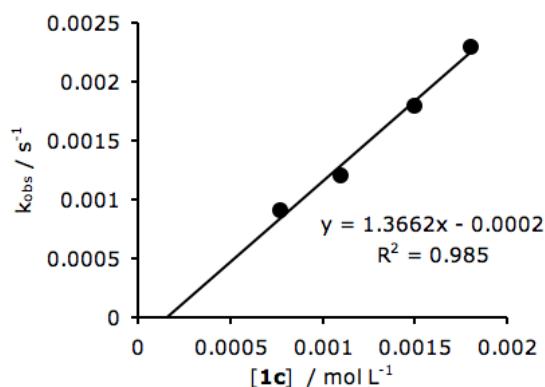
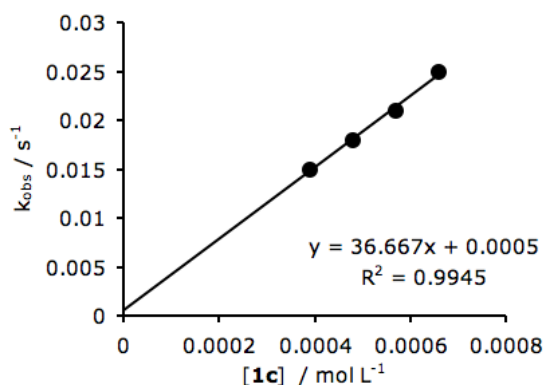


Table S27. Kinetics of the reaction of **1c** with **2o** in CH<sub>3</sub>CN (20 °C, Conventional UV/Vis, 535 nm)

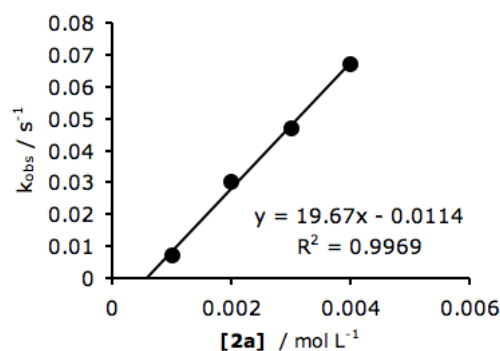
[ <b>2o</b> ] / mol L <sup>-1</sup>	[ <b>1c</b> ] / mol L <sup>-1</sup>	<i>k</i> <sub>obs</sub> / s <sup>-1</sup>
1.0 × 10 <sup>-4</sup>	3.9 × 10 <sup>-4</sup>	1.5 × 10 <sup>-2</sup>
1.0 × 10 <sup>-4</sup>	4.8 × 10 <sup>-4</sup>	1.8 × 10 <sup>-2</sup>
1.0 × 10 <sup>-4</sup>	5.7 × 10 <sup>-4</sup>	2.1 × 10 <sup>-2</sup>
1.0 × 10 <sup>-4</sup>	6.6 × 10 <sup>-4</sup>	2.5 × 10 <sup>-2</sup>

$k_2 = 1.8 \times 10^1 \text{ L mol}^{-1} \text{ s}^{-1}$   
As two molecules of amine are consumed per quinone, the slope of the depicted graph is divided by 2

Table S28. Kinetics of the reaction of **1d** with **2a** in CH<sub>2</sub>Cl<sub>2</sub> (20 °C, Stopped-flow, 256 nm)

[ <b>1d</b> ] / mol L <sup>-1</sup>	[ <b>2a</b> ] / mol L <sup>-1</sup>	<i>k</i> <sub>obs</sub> / s <sup>-1</sup>
1.0 × 10 <sup>-4</sup>	1.0 × 10 <sup>-3</sup>	0.0071
1.0 × 10 <sup>-4</sup>	2.0 × 10 <sup>-3</sup>	0.03
1.0 × 10 <sup>-4</sup>	3.0 × 10 <sup>-3</sup>	0.047
1.0 × 10 <sup>-4</sup>	4.0 × 10 <sup>-3</sup>	0.067

$k_2 = 2.0 \times 10^1 \text{ L mol}^{-1} \text{ s}^{-1}$

Table S29. Kinetics of the reaction of **1d** with **2a'** in CH<sub>2</sub>Cl<sub>2</sub> (20 °C, Conventional UV/Vis, 256 nm)

[ <b>1d</b> ] / mol L <sup>-1</sup>	[ <b>2a'</b> ] / mol L <sup>-1</sup>	<i>k</i> <sub>obs</sub> / s <sup>-1</sup>
1.0 × 10 <sup>-4</sup>	4.0 × 10 <sup>-3</sup>	4.6 × 10 <sup>-2</sup>
1.0 × 10 <sup>-4</sup>	4.8 × 10 <sup>-3</sup>	5.7 × 10 <sup>-2</sup>
1.0 × 10 <sup>-4</sup>	5.5 × 10 <sup>-3</sup>	6.5 × 10 <sup>-2</sup>
1.0 × 10 <sup>-4</sup>	6.3 × 10 <sup>-3</sup>	7.4 × 10 <sup>-2</sup>

$k_2 = 1.2 \times 10^1 \text{ L mol}^{-1} \text{ s}^{-1}$

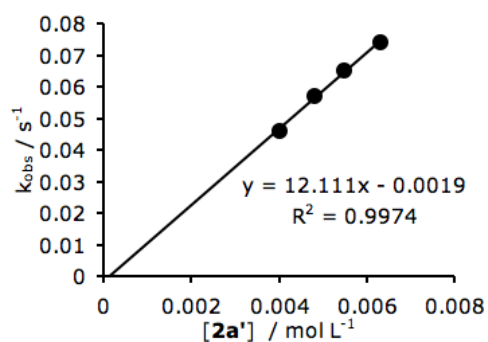
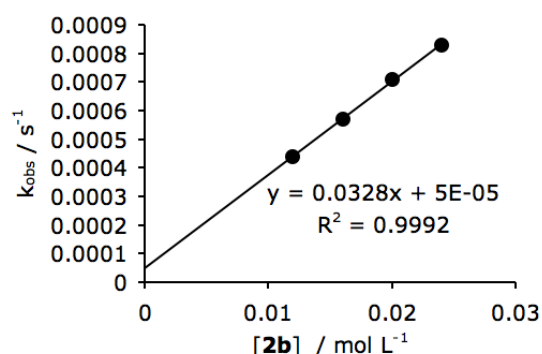




Table S30. Kinetics of the reaction of **1d** with **2b** in CH<sub>2</sub>Cl<sub>2</sub> (20 °C, Conventional UV/Vis, 340 nm)

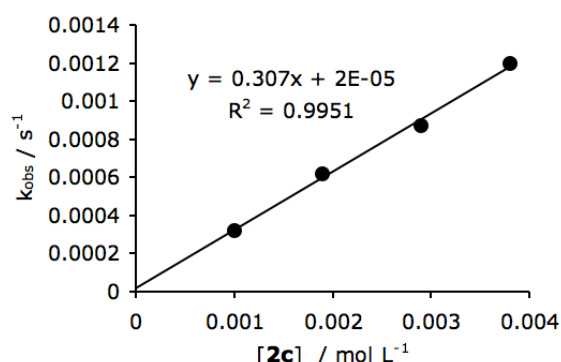
[ <b>1d</b> ] / mol L <sup>-1</sup>	[ <b>2b</b> ] / mol L <sup>-1</sup>	<i>k</i> <sub>obs</sub> / s <sup>-1</sup>
4.0 × 10 <sup>-5</sup>	1.4 × 10 <sup>-2</sup>	4.4 × 10 <sup>-4</sup>
4.0 × 10 <sup>-5</sup>	1.6 × 10 <sup>-2</sup>	5.7 × 10 <sup>-4</sup>
2.0 × 10 <sup>-4</sup>	2.0 × 10 <sup>-2</sup>	7.1 × 10 <sup>-4</sup>
2.0 × 10 <sup>-4</sup>	3.4 × 10 <sup>-2</sup>	8.3 × 10 <sup>-4</sup>

$$k_2 = 3.3 \times 10^{-2} \text{ L mol}^{-1} \text{ s}^{-1}$$

Table S31. Kinetics of the reaction of **1d** with **2c** in CH<sub>2</sub>Cl<sub>2</sub> (20 °C, Conventional UV/Vis, 256 nm)

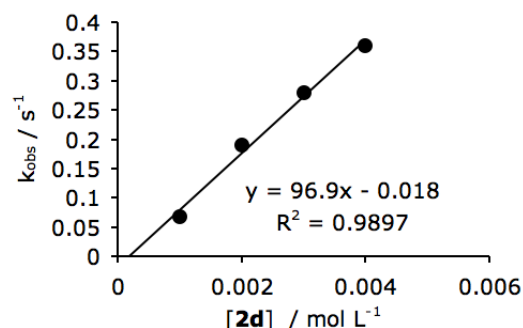
[ <b>1d</b> ] / mol L <sup>-1</sup>	[ <b>2c</b> ] / mol L <sup>-1</sup>	<i>k</i> <sub>obs</sub> / s <sup>-1</sup>
1.0 × 10 <sup>-4</sup>	1.0 × 10 <sup>-3</sup>	3.2 × 10 <sup>-4</sup>
1.0 × 10 <sup>-4</sup>	1.9 × 10 <sup>-3</sup>	6.2 × 10 <sup>-4</sup>
1.0 × 10 <sup>-4</sup>	2.9 × 10 <sup>-3</sup>	8.7 × 10 <sup>-4</sup>
1.0 × 10 <sup>-4</sup>	3.8 × 10 <sup>-3</sup>	1.2 × 10 <sup>-3</sup>

$$k_2 = 0.31 \text{ L mol}^{-1} \text{ s}^{-1}$$

Table S32. Kinetics of the reaction of **1d** with **2d** in CH<sub>2</sub>Cl<sub>2</sub> (20 °C, Stopped-flow, 256 nm)

[ <b>1d</b> ] / mol L <sup>-1</sup>	[ <b>2d</b> ] / mol L <sup>-1</sup>	<i>k</i> <sub>obs</sub> / s <sup>-1</sup>
1.0 × 10 <sup>-4</sup>	1.0 × 10 <sup>-3</sup>	6.7 × 10 <sup>-2</sup>
1.0 × 10 <sup>-4</sup>	2.0 × 10 <sup>-3</sup>	0.19
1.0 × 10 <sup>-4</sup>	3.0 × 10 <sup>-3</sup>	0.28
1.0 × 10 <sup>-4</sup>	4.0 × 10 <sup>-3</sup>	0.36

$$k_2 = 97 \text{ L mol}^{-1} \text{ s}^{-1}$$

Table S33. Kinetics of the reaction of **1d** with **2e** in CH<sub>2</sub>Cl<sub>2</sub> (20 °C, Stopped-flow, 265 nm)

[ <b>1d</b> ] / mol L <sup>-1</sup>	[ <b>2e</b> ] / mol L <sup>-1</sup>	<i>k</i> <sub>obs</sub> / s <sup>-1</sup>
1.0 × 10 <sup>-4</sup>	5.0 × 10 <sup>-3</sup>	1.5 × 10 <sup>-2</sup>
1.0 × 10 <sup>-4</sup>	1.0 × 10 <sup>-2</sup>	2.4 × 10 <sup>-2</sup>
1.0 × 10 <sup>-4</sup>	1.5 × 10 <sup>-2</sup>	3.3 × 10 <sup>-2</sup>
1.0 × 10 <sup>-4</sup>	2.0 × 10 <sup>-2</sup>	4.2 × 10 <sup>-2</sup>
1.0 × 10 <sup>-4</sup>	2.5 × 10 <sup>-2</sup>	5.0 × 10 <sup>-2</sup>

$$k_2 = 1.8 \text{ L mol}^{-1} \text{ s}^{-1}$$

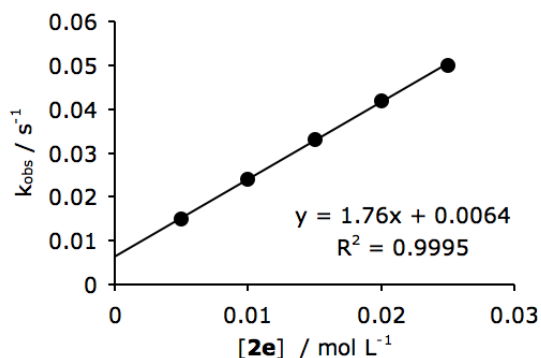
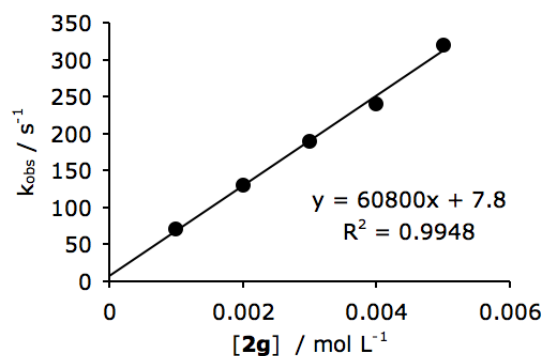


Table S34. Kinetics of the reaction of **1d** with **2g** in CH<sub>2</sub>Cl<sub>2</sub> (20 °C, Stopped-flow, 265 nm)

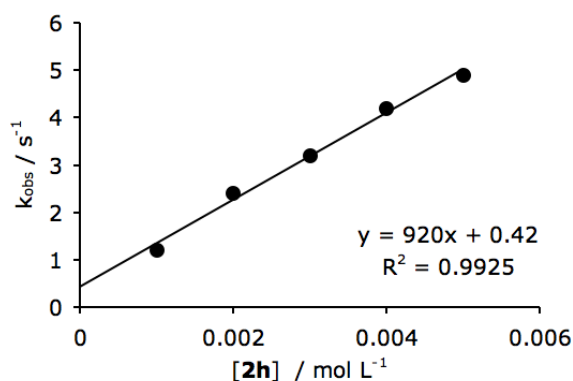
[ <b>1d</b> ] / mol L <sup>-1</sup>	[ <b>2g</b> ] / mol L <sup>-1</sup>	<i>k</i> <sub>obs</sub> / s <sup>-1</sup>
1.0 × 10 <sup>-4</sup>	1.0 × 10 <sup>-3</sup>	71
1.0 × 10 <sup>-4</sup>	2.0 × 10 <sup>-3</sup>	1.3 × 10 <sup>2</sup>
1.0 × 10 <sup>-4</sup>	3.0 × 10 <sup>-3</sup>	1.9 × 10 <sup>2</sup>
1.0 × 10 <sup>-4</sup>	4.0 × 10 <sup>-3</sup>	2.4 × 10 <sup>2</sup>
1.0 × 10 <sup>-4</sup>	5.0 × 10 <sup>-3</sup>	3.2 × 10 <sup>2</sup>

$$k_2 = 6.1 \times 10^4 \text{ L mol}^{-1} \text{ s}^{-1}$$

Table S35. Kinetics of the reaction of **1d** with **2h** in CH<sub>2</sub>Cl<sub>2</sub> (20 °C, Stopped-flow, 265 nm)

[ <b>1d</b> ] / mol L <sup>-1</sup>	[ <b>2h</b> ] / mol L <sup>-1</sup>	<i>k</i> <sub>obs</sub> / s <sup>-1</sup>
1.0 × 10 <sup>-4</sup>	1.0 × 10 <sup>-3</sup>	1.2
1.0 × 10 <sup>-4</sup>	2.0 × 10 <sup>-3</sup>	2.4
1.0 × 10 <sup>-4</sup>	3.0 × 10 <sup>-3</sup>	3.2
1.0 × 10 <sup>-4</sup>	4.0 × 10 <sup>-3</sup>	4.2
1.0 × 10 <sup>-4</sup>	5.0 × 10 <sup>-3</sup>	4.9

$$k_2 = 9.2 \times 10^2 \text{ L mol}^{-1} \text{ s}^{-1}$$

Table S36. Kinetics of the reaction of **1d** with **2i** in CH<sub>3</sub>CN (20 °C, Stopped-flow, 525 nm)

[ <b>2i</b> ] / mol L <sup>-1</sup>	[ <b>1d</b> ] / mol L <sup>-1</sup>	<i>k</i> <sub>obs</sub> / s <sup>-1</sup>
1.0 × 10 <sup>-4</sup>	1.0 × 10 <sup>-3</sup>	95
1.0 × 10 <sup>-4</sup>	2.0 × 10 <sup>-3</sup>	1.9 × 10 <sup>2</sup>
1.0 × 10 <sup>-4</sup>	3.0 × 10 <sup>-3</sup>	2.5 × 10 <sup>2</sup>
1.0 × 10 <sup>-4</sup>	4.0 × 10 <sup>-3</sup>	3.1 × 10 <sup>2</sup>

$$k_2 = 3.5 \times 10^4 \text{ L mol}^{-1} \text{ s}^{-1}$$

As two molecules of amine are consumed per quinone, the slope of the depicted graph is divided by 2

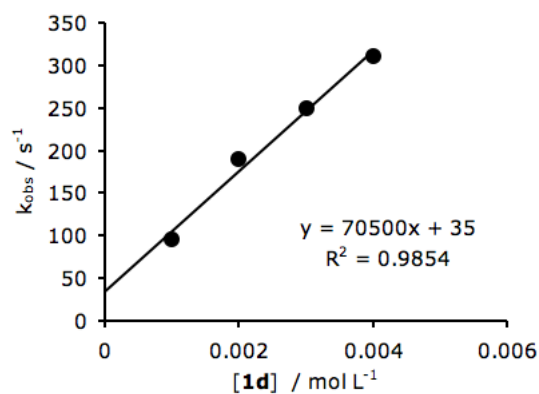
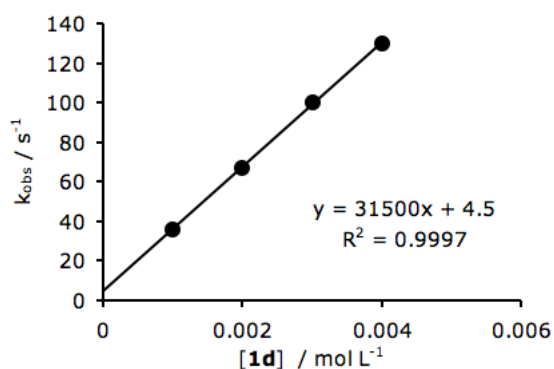


Table S37. Kinetics of the reaction of **1d** with **2j** in CH<sub>3</sub>CN (20 °C, Stopped-flow, 525 nm)

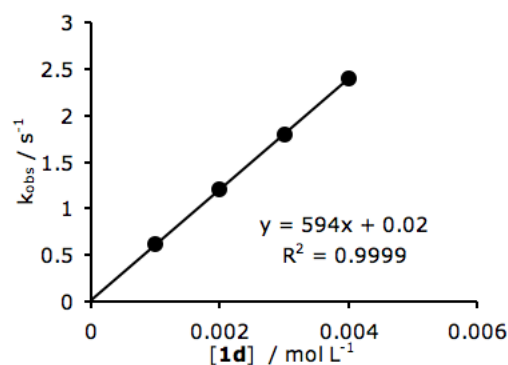
[ <b>2j</b> ] / mol L <sup>-1</sup>	[ <b>1d</b> ] / mol L <sup>-1</sup>	<i>k</i> <sub>obs</sub> / s <sup>-1</sup>
1.0 × 10 <sup>-4</sup>	1.0 × 10 <sup>-3</sup>	36
1.0 × 10 <sup>-4</sup>	2.0 × 10 <sup>-3</sup>	67
1.0 × 10 <sup>-4</sup>	3.0 × 10 <sup>-3</sup>	1.0 × 10 <sup>2</sup>
1.0 × 10 <sup>-4</sup>	4.0 × 10 <sup>-3</sup>	1.3 × 10 <sup>2</sup>

$k_2 = 1.6 \times 10^4 \text{ L mol}^{-1} \text{ s}^{-1}$   
As two molecules of amine are consumed per quinone, the slope of the depicted graph is divided by 2

Table S38. Kinetics of the reaction of **1d** with **2k** in CH<sub>3</sub>CN (20 °C, Stopped-flow, 525 nm)

[ <b>2k</b> ] / mol L <sup>-1</sup>	[ <b>1d</b> ] / mol L <sup>-1</sup>	<i>k</i> <sub>obs</sub> / s <sup>-1</sup>
1.0 × 10 <sup>-4</sup>	1.0 × 10 <sup>-3</sup>	0.62
1.0 × 10 <sup>-4</sup>	2.0 × 10 <sup>-3</sup>	1.2
1.0 × 10 <sup>-4</sup>	3.0 × 10 <sup>-3</sup>	1.8
1.0 × 10 <sup>-4</sup>	4.0 × 10 <sup>-3</sup>	2.4

$k_2 = 3.0 \times 10^2 \text{ L mol}^{-1} \text{ s}^{-1}$   
As two molecules of amine are consumed per quinone, the slope of the depicted graph is divided by 2

Table S39. Kinetics of the reaction of **1d** with **2l** in CH<sub>3</sub>CN (20 °C, Stopped-flow, 525 nm)

[ <b>2l</b> ] / mol L <sup>-1</sup>	[ <b>1d</b> ] / mol L <sup>-1</sup>	<i>k</i> <sub>obs</sub> / s <sup>-1</sup>
1.0 × 10 <sup>-4</sup>	1.0 × 10 <sup>-3</sup>	1.2
1.0 × 10 <sup>-4</sup>	2.0 × 10 <sup>-3</sup>	2.2
1.0 × 10 <sup>-4</sup>	3.0 × 10 <sup>-3</sup>	3.2
1.0 × 10 <sup>-4</sup>	4.0 × 10 <sup>-3</sup>	4.3

$k_2 = 5.0 \times 10^2 \text{ L mol}^{-1} \text{ s}^{-1}$   
As two molecules of amine are consumed per quinone, the slope of the depicted graph is divided by 2

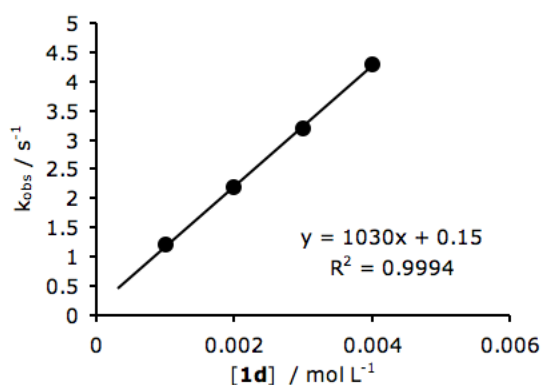
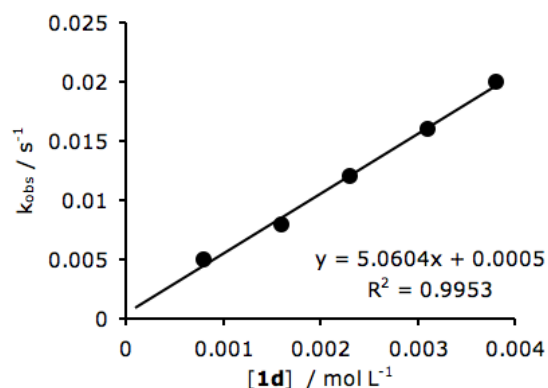


Table S40. Kinetics of the reaction of **1d** with **2m** in CH<sub>3</sub>CN (20 °C, Conventional UV/Vis, 515 nm)

[ <b>2m</b> ] / mol L <sup>-1</sup>	[ <b>1d</b> ] / mol L <sup>-1</sup>	<i>k</i> <sub>obs</sub> / s <sup>-1</sup>
1.0 × 10 <sup>-4</sup>	8.0 × 10 <sup>-4</sup>	5.0 × 10 <sup>-3</sup>
1.0 × 10 <sup>-4</sup>	1.6 × 10 <sup>-3</sup>	8.0 × 10 <sup>-3</sup>
1.0 × 10 <sup>-4</sup>	2.3 × 10 <sup>-3</sup>	1.2 × 10 <sup>-2</sup>
1.0 × 10 <sup>-4</sup>	3.1 × 10 <sup>-3</sup>	1.6 × 10 <sup>-2</sup>
1.0 × 10 <sup>-4</sup>	3.8 × 10 <sup>-3</sup>	2.0 × 10 <sup>-2</sup>

$$k_2 = 2.5 \text{ L mol}^{-1} \text{ s}^{-1}$$

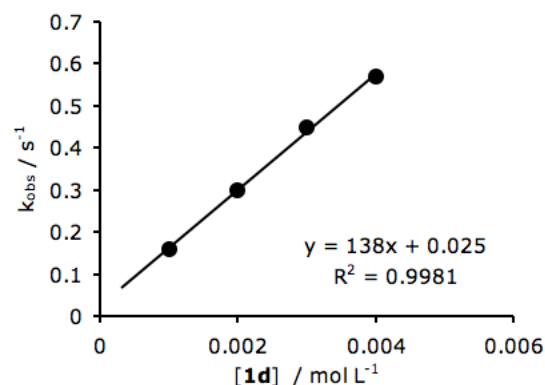
As two molecules of amine are consumed per quinone, the slope of the depicted graph is divided by 2

Table S41. Kinetics of the reaction of **1d** with **2n** in CH<sub>3</sub>CN (20 °C, Stopped-flow, 525 nm)

[ <b>2n</b> ] / mol L <sup>-1</sup>	[ <b>1d</b> ] / mol L <sup>-1</sup>	<i>k</i> <sub>obs</sub> / s <sup>-1</sup>
1.0 × 10 <sup>-4</sup>	1.0 × 10 <sup>-3</sup>	0.16
1.0 × 10 <sup>-4</sup>	2.0 × 10 <sup>-3</sup>	0.30
1.0 × 10 <sup>-4</sup>	3.0 × 10 <sup>-3</sup>	0.45
1.0 × 10 <sup>-4</sup>	4.0 × 10 <sup>-3</sup>	0.57

$$k_2 = 6.9 \times 10^1 \text{ L mol}^{-1} \text{ s}^{-1}$$

As two molecules of amine are consumed per quinone, the slope of the depicted graph is divided by 2

Table S42. Kinetics of the reaction of **1d** with **2o** in CH<sub>3</sub>CN (20 °C, Stopped-flow, 525 nm)

[ <b>2o</b> ] / mol L <sup>-1</sup>	[ <b>1d</b> ] / mol L <sup>-1</sup>	<i>k</i> <sub>obs</sub> / s <sup>-1</sup>
1.0 × 10 <sup>-4</sup>	5.0 × 10 <sup>-4</sup>	0.97
1.0 × 10 <sup>-4</sup>	1.0 × 10 <sup>-3</sup>	1.8
1.0 × 10 <sup>-4</sup>	1.5 × 10 <sup>-3</sup>	2.7
1.0 × 10 <sup>-4</sup>	2.0 × 10 <sup>-3</sup>	3.5
1.0 × 10 <sup>-4</sup>	3.0 × 10 <sup>-3</sup>	5.6

$$k_2 = 9.2 \times 10^2 \text{ L mol}^{-1} \text{ s}^{-1}$$

As two molecules of amine are consumed per quinone, the slope of the depicted graph is divided by 2

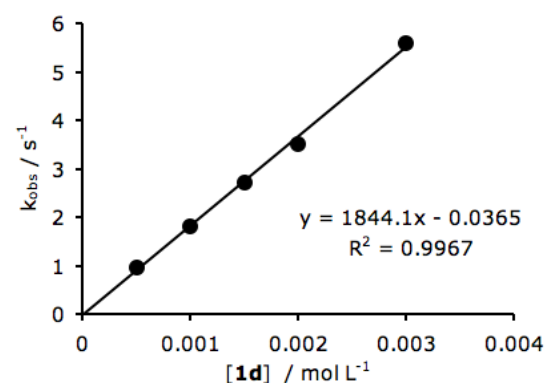
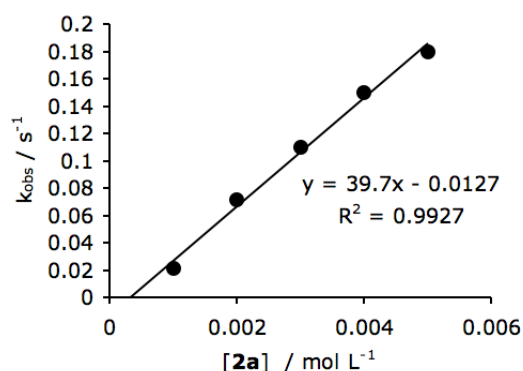


Table S43. Kinetics of the reaction of **1e** with **2a** in CH<sub>2</sub>Cl<sub>2</sub> (20 °C, Stopped-flow, 457 nm)

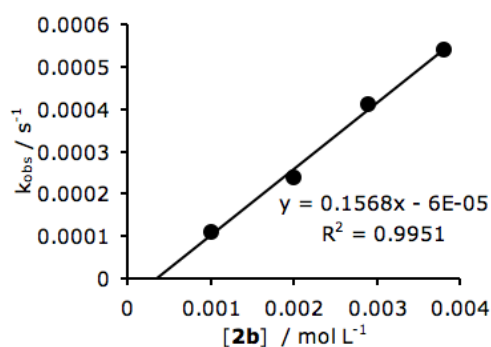
[ <b>1e</b> ] / mol L <sup>-1</sup>	[ <b>2a</b> ] / mol L <sup>-1</sup>	<i>k</i> <sub>obs</sub> / s <sup>-1</sup>
1.0 × 10 <sup>-4</sup>	1.0 × 10 <sup>-3</sup>	2.1 × 10 <sup>2</sup>
1.0 × 10 <sup>-4</sup>	2.0 × 10 <sup>-3</sup>	7.1 × 10 <sup>2</sup>
1.0 × 10 <sup>-4</sup>	3.0 × 10 <sup>-3</sup>	0.11
1.0 × 10 <sup>-4</sup>	4.0 × 10 <sup>-3</sup>	0.15
1.0 × 10 <sup>-4</sup>	5.0 × 10 <sup>-3</sup>	0.18

$k_2 = 40 \text{ L mol}^{-1} \text{ s}^{-1}$

Table S44. Kinetics of the reaction of **1e** with **2b** in CH<sub>2</sub>Cl<sub>2</sub> (20 °C, Conventional UV/Vis, 360 nm)

[ <b>1e</b> ] / mol L <sup>-1</sup>	[ <b>2b</b> ] / mol L <sup>-1</sup>	<i>k</i> <sub>obs</sub> / s <sup>-1</sup>
1.0 × 10 <sup>-4</sup>	1.0 × 10 <sup>-3</sup>	1.1 × 10 <sup>-4</sup>
1.0 × 10 <sup>-4</sup>	2.0 × 10 <sup>-3</sup>	2.4 × 10 <sup>-4</sup>
1.0 × 10 <sup>-4</sup>	2.9 × 10 <sup>-3</sup>	4.1 × 10 <sup>-4</sup>
1.0 × 10 <sup>-4</sup>	3.8 × 10 <sup>-3</sup>	5.4 × 10 <sup>-4</sup>

$k_2 = 0.16 \text{ L mol}^{-1} \text{ s}^{-1}$

Table S45. Kinetics of the reaction of **1e** with **2c** in CH<sub>2</sub>Cl<sub>2</sub> (20 °C, Stopped-flow, 457 nm)

[ <b>1e</b> ] / mol L <sup>-1</sup>	[ <b>2c</b> ] / mol L <sup>-1</sup>	<i>k</i> <sub>obs</sub> / s <sup>-1</sup>
1.0 × 10 <sup>-4</sup>	1.0 × 10 <sup>-3</sup>	0.45
1.0 × 10 <sup>-4</sup>	2.0 × 10 <sup>-3</sup>	0.91
1.0 × 10 <sup>-4</sup>	3.0 × 10 <sup>-3</sup>	1.4
1.0 × 10 <sup>-4</sup>	4.0 × 10 <sup>-3</sup>	1.8
1.0 × 10 <sup>-4</sup>	5.0 × 10 <sup>-3</sup>	2.3

$k_2 = 4.6 \times 10^2 \text{ L mol}^{-1} \text{ s}^{-1}$

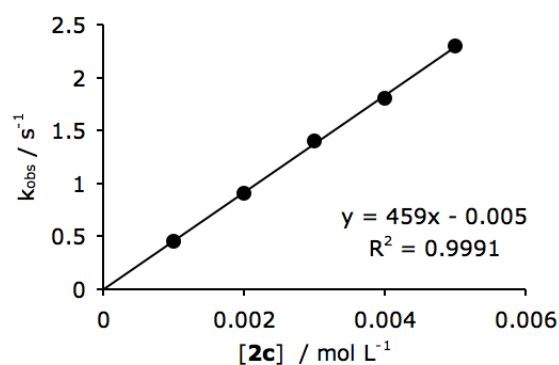
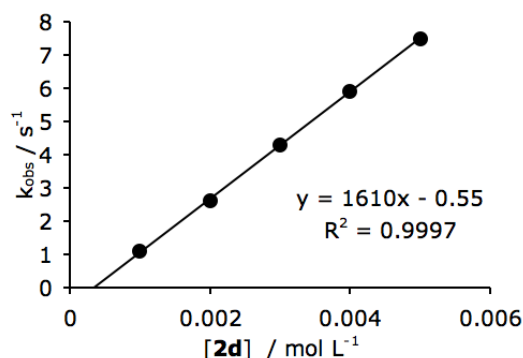


Table S46. Kinetics of the reaction of **1e** with **2d** in CH<sub>2</sub>Cl<sub>2</sub> (20 °C, Stopped-flow, 457 nm)

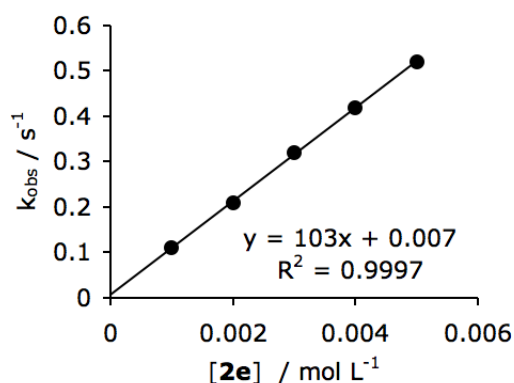
[ <b>1e</b> ] / mol L <sup>-1</sup>	[ <b>2d</b> ] / mol L <sup>-1</sup>	<i>k</i> <sub>obs</sub> / s <sup>-1</sup>
1.0 × 10 <sup>-4</sup>	1.0 × 10 <sup>-3</sup>	1.1
1.0 × 10 <sup>-4</sup>	2.0 × 10 <sup>-3</sup>	2.6
1.0 × 10 <sup>-4</sup>	3.0 × 10 <sup>-3</sup>	4.3
1.0 × 10 <sup>-4</sup>	4.0 × 10 <sup>-3</sup>	5.9
1.0 × 10 <sup>-4</sup>	5.0 × 10 <sup>-3</sup>	7.5

$$k_2 = 1.6 \times 10^3 \text{ L mol}^{-1} \text{ s}^{-1}$$

Table S47. Kinetics of the reaction of **1e** with **2e** in CH<sub>2</sub>Cl<sub>2</sub> (20 °C, Stopped-flow, 457 nm)

[ <b>1e</b> ] / mol L <sup>-1</sup>	[ <b>2e</b> ] / mol L <sup>-1</sup>	<i>k</i> <sub>obs</sub> / s <sup>-1</sup>
1.0 × 10 <sup>-4</sup>	1.0 × 10 <sup>-3</sup>	0.11
1.0 × 10 <sup>-4</sup>	2.0 × 10 <sup>-3</sup>	0.21
1.0 × 10 <sup>-4</sup>	3.0 × 10 <sup>-3</sup>	0.32
1.0 × 10 <sup>-4</sup>	4.0 × 10 <sup>-3</sup>	0.42
1.0 × 10 <sup>-4</sup>	5.0 × 10 <sup>-3</sup>	0.52

$$k_2 = 1.0 \times 10^2 \text{ L mol}^{-1} \text{ s}^{-1}$$

Table S48. Kinetics of the reaction of **1e** with **2f** in CH<sub>2</sub>Cl<sub>2</sub> (20 °C, Conventional UV/Vis, 457 nm)

[ <b>1e</b> ] / mol L <sup>-1</sup>	[ <b>2f</b> ] / mol L <sup>-1</sup>	<i>k</i> <sub>obs</sub> / s <sup>-1</sup>
2.0 × 10 <sup>-4</sup>	7.7 × 10 <sup>-3</sup>	3.4 × 10 <sup>-5</sup>
2.0 × 10 <sup>-4</sup>	1.5 × 10 <sup>-2</sup>	5.3 × 10 <sup>-5</sup>
2.0 × 10 <sup>-4</sup>	2.3 × 10 <sup>-2</sup>	7.6 × 10 <sup>-5</sup>
2.0 × 10 <sup>-4</sup>	3.1 × 10 <sup>-2</sup>	1.1 × 10 <sup>-4</sup>

$$k_2 = 3.2 \times 10^{-3} \text{ L mol}^{-1} \text{ s}^{-1}$$

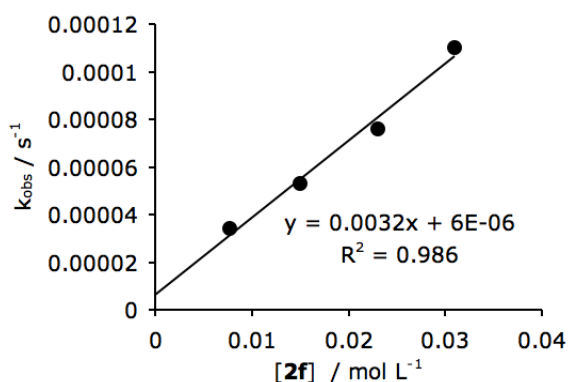
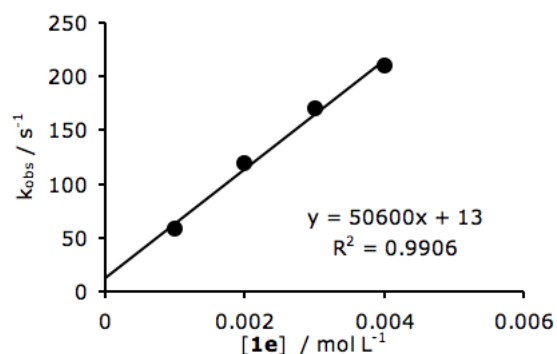
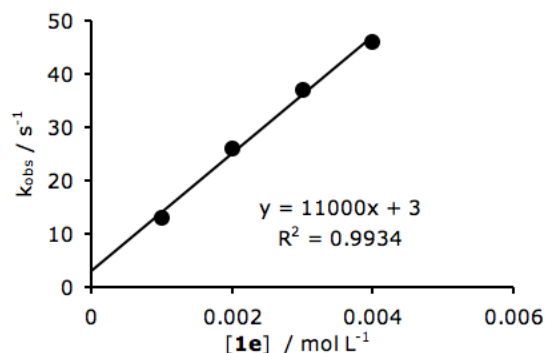


Table S49. Kinetics of the reaction of **1e** with **2i** in CH<sub>3</sub>CN (20 °C, Stopped-flow, 570 nm)

[ <b>2i</b> ] / mol L <sup>-1</sup>	[ <b>1e</b> ] / mol L <sup>-1</sup>	<i>k</i> <sub>obs</sub> / s <sup>-1</sup>
1.0 × 10 <sup>-4</sup>	1.0 × 10 <sup>-3</sup>	58
1.0 × 10 <sup>-4</sup>	2.0 × 10 <sup>-3</sup>	1.2 × 10 <sup>2</sup>
1.0 × 10 <sup>-4</sup>	3.0 × 10 <sup>-3</sup>	1.7 × 10 <sup>2</sup>
1.0 × 10 <sup>-4</sup>	4.0 × 10 <sup>-3</sup>	2.1 × 10 <sup>2</sup>
<i>k</i> <sub>2</sub> = 2.5 × 10 <sup>4</sup> L mol <sup>-1</sup> s <sup>-1</sup>		
As two molecules of amine are consumed per quinone, the slope of the depicted graph is divided by 2		

Table S50. Kinetics of the reaction of **1e** with **2j** in CH<sub>3</sub>CN (20 °C, Stopped-flow, 570 nm)

[ <b>2j</b> ] / mol L <sup>-1</sup>	[ <b>1e</b> ] / mol L <sup>-1</sup>	<i>k</i> <sub>obs</sub> / s <sup>-1</sup>
1.0 × 10 <sup>-4</sup>	1.0 × 10 <sup>-3</sup>	13
1.0 × 10 <sup>-4</sup>	2.0 × 10 <sup>-3</sup>	26
1.0 × 10 <sup>-4</sup>	3.0 × 10 <sup>-3</sup>	37
1.0 × 10 <sup>-4</sup>	4.0 × 10 <sup>-3</sup>	46
<i>k</i> <sub>2</sub> = 5.5 × 10 <sup>3</sup> L mol <sup>-1</sup> s <sup>-1</sup>		
As two molecules of amine are consumed per quinone, the slope of the depicted graph is divided by 2		

Table S51. Kinetics of the reaction of **1e** with **2k** in CH<sub>3</sub>CN (20 °C, Stopped-flow, 570 nm)

[ <b>2k</b> ] / mol L <sup>-1</sup>	[ <b>1e</b> ] / mol L <sup>-1</sup>	<i>k</i> <sub>obs</sub> / s <sup>-1</sup>
1.0 × 10 <sup>-4</sup>	1.0 × 10 <sup>-3</sup>	0.32
1.0 × 10 <sup>-4</sup>	2.0 × 10 <sup>-3</sup>	0.61
1.0 × 10 <sup>-4</sup>	3.0 × 10 <sup>-3</sup>	0.86
1.0 × 10 <sup>-4</sup>	4.0 × 10 <sup>-3</sup>	1.1
<i>k</i> <sub>2</sub> = 1.3 × 10 <sup>2</sup> L mol <sup>-1</sup> s <sup>-1</sup>		
As two molecules of amine are consumed per quinone, the slope of the depicted graph is divided by 2		

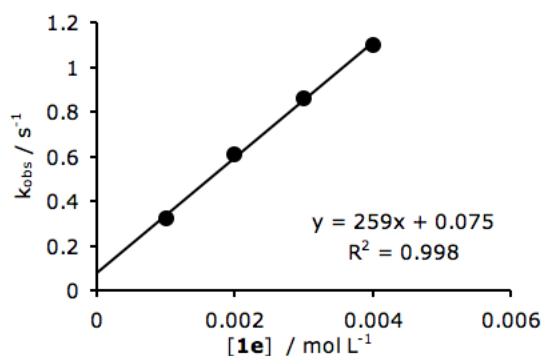
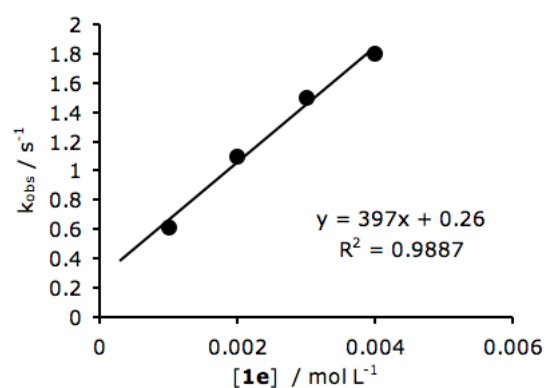


Table S52. Kinetics of the reaction of **1e** with **2l** in CH<sub>3</sub>CN (20 °C, Stopped-flow, 570 nm)

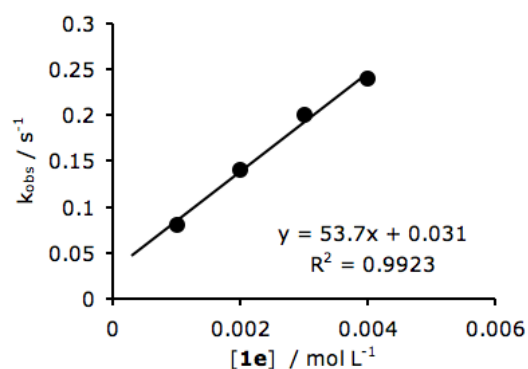
[ <b>2l</b> ] / mol L <sup>-1</sup>	[ <b>1e</b> ] / mol L <sup>-1</sup>	<i>k</i> <sub>obs</sub> / s <sup>-1</sup>
1.0 × 10 <sup>-4</sup>	1.0 × 10 <sup>-3</sup>	0.61
1.0 × 10 <sup>-4</sup>	2.0 × 10 <sup>-3</sup>	1.1
1.0 × 10 <sup>-4</sup>	3.0 × 10 <sup>-3</sup>	1.5
1.0 × 10 <sup>-4</sup>	4.0 × 10 <sup>-3</sup>	1.8

$k_2 = 2.0 \times 10^2 \text{ L mol}^{-1} \text{ s}^{-1}$   
As two molecules of amine are consumed per quinone, the slope of the depicted graph is divided by 2

Table S53. Kinetics of the reaction of **1e** with **2n** in CH<sub>3</sub>CN (20 °C, Stopped-flow, 570 nm)

[ <b>2n</b> ] / mol L <sup>-1</sup>	[ <b>1e</b> ] / mol L <sup>-1</sup>	<i>k</i> <sub>obs</sub> / s <sup>-1</sup>
1.0 × 10 <sup>-4</sup>	1.0 × 10 <sup>-3</sup>	0.081
1.0 × 10 <sup>-4</sup>	2.0 × 10 <sup>-3</sup>	0.14
1.0 × 10 <sup>-4</sup>	3.0 × 10 <sup>-3</sup>	0.20
1.0 × 10 <sup>-4</sup>	4.0 × 10 <sup>-3</sup>	0.24

$k_2 = 2.7 \times 10^1 \text{ L mol}^{-1} \text{ s}^{-1}$   
As two molecules of amine are consumed per quinone, the slope of the depicted graph is divided by 2

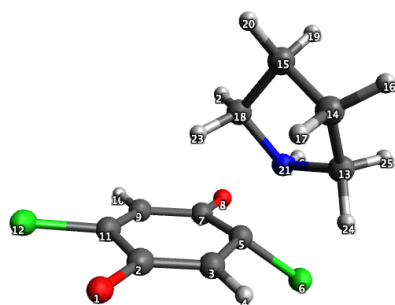




#### 4) Computational Study: Potential Energy Surface for the Reaction of **1b** with Pyrrolidine

The potential energy surface for the substitution reaction of 2,5-dichloro-benzoquinone (**1b**) with pyrrolidine (**2i**) was studied by quantum chemical method using Gaussian 09 program at B97D/6-31+G(d,p)//B97D/6-31+G(d,p)//IEFPCM level of theory using CH<sub>3</sub>CN as the solvent. A relaxed PES scan (with geometry optimization at each point) on the bond length of C-N and C-Cl was carried out. The geometry of transition state was verified by vibrational frequency analysis and the intrinsic reaction coordinate (IRC) method.

Transition structure:



O	2.06674	-0.99640	2.07623
C	1.46941	-0.33180	1.19124
C	0.16759	0.21838	1.32851
H	-0.34015	0.06693	2.27946
C	-0.49078	0.92249	0.29175
Cl	-1.53265	2.32119	0.85507
C	0.29783	1.29433	-0.98788
O	-0.22305	1.96880	-1.88187
C	1.64784	0.74556	-1.11609
H	2.18238	0.97184	-2.03746
C	2.18434	-0.02075	-0.12863
Cl	3.77744	-0.68857	-0.33301
C	-2.81934	-0.62427	0.49980
C	-2.73146	-2.16122	0.43384
C	-2.20750	-2.43476	-0.99029
H	-3.70588	-2.62480	0.63295
H	-2.00884	-2.52811	1.17687
C	-1.17422	-1.31551	-1.16497
H	-3.01412	-2.33143	-1.73102
H	-1.75025	-3.42679	-1.09888
N	-1.79353	-0.11957	-0.49818
H	-0.91675	-1.06465	-2.19911
H	-0.26097	-1.55065	-0.59707
H	-2.58119	-0.21969	1.49010
H	-3.79892	-0.24645	0.18613
H	-2.22379	0.50230	-1.18831

SCF Energy= -1512.886953 Hartree

Table S54. Relative potential energies (relative to transition state energy, in kcal mol<sup>-1</sup>) for the partial optimized structures at fixed bond length (Å) of C-N and C-Cl.

C-N \ C-Cl	1.467	1.567	1.667	1.767	1.867	1.967	2.067	2.167	2.267	2.367	2.467	2.567
1.6702	8.7	6.0	5.5	5.1	4.1	2.6	0.9	-0.9	-2.5	-3.9	-7.6	-9.0
1.7702	1.4	-0.4	0.1	0.6	0.3	-0.6	-1.9	-3.2	-4.4	-5.5	-9.2	-10.5
1.8702	-3.0	-4.1	-2.5	-0.6	0.2	-0.1	-0.8	-1.7	-2.5	-3.3	-7.0	-8.1
1.9702	-6.4	-6.9	-4.4	-1.2	1.2	2.2	2.2	1.8	1.3	0.8	-2.7	-3.7
2.0702	-9.7	-9.5	-6.3	-2.1	1.7	4.4	5.7	6.1	6.1	5.9	2.5	1.6
2.1702	-12.6	-11.9	-8.2	-3.3	1.6	5.6	8.5	10.2	10.9	11.1	7.9	7.2
2.2702	-15.3	-14.1	-9.9	-4.5	1.1	6.1	10.1	13.1	15.2	16.1	13.4	12.7
2.3702	-17.6	-16.1	-11.5	-5.7	0.4	6.1	11.0	14.9	18.0	20.5	18.5	17.9
2.4702	-19.6	-17.8	-12.9	-6.7	-0.3	5.9	11.4	16.1	20.0	23.0	23.3	22.8
2.5702	-21.1	-19.1	-14.1	-7.6	-0.9	5.7	11.6	16.9	21.3	25.0	28.0	27.3
2.6702	-22.3	-20.1	-14.9	-8.3	-1.4	5.4	11.7	17.3	22.3	26.4	29.9	31.4
2.7702	-23.1	-20.8	-15.5	-8.8	-1.7	5.1	11.9	17.6	22.8	27.4	31.2	35.0
2.8702	-23.0	-21.3	-15.9	-9.1	-2.0	5.0	11.5	17.6	23.1	28.0	32.1	38.2
2.9702	-23.8	-21.5	-16.1	-9.3	-2.1	4.9	11.5	17.6	23.2	28.3	32.7	41.0
3.0702	-23.9	-21.5	-16.1	-9.3	-2.3	4.7	11.4	17.5	23.3	28.5	33.1	43.4

### 3.6 References:

- (1) Wöhler, F. *Justus Liebigs Ann. Chem.* **1844**, *51*, 145-163.
- (2) (a) Thiele, J. *Chem. Ber.* **1898**, *31*, 1247. (b) Suida, H.; Suida, W. *Justus Liebigs Ann. Chem.* **1918**, *416*, 113-163. (c) *The Chemistry of the Quinoid Compounds, Part I*; Patai, S., Ed.; Wiley: Chichester, UK, 1974. (d) *The Chemistry of the Quinoid Compounds Vol. 2*; Patai, S., Rappoport, Z., Eds.; Wiley: Chichester, UK, 1988. (e) Moody, C. J.; Nawrat, C. C. *Angew. Chem., Int. Ed.* **2014**, *53*, 2-24.
- (3) (a) Conant, J. B.; Fieser, L. F. *J. Am. Chem. Soc.* **1923**, *45*, 2194–2218. (b) Conant, J. B.; Fieser, L. F. *J. Am. Chem. Soc.* **1923**, *46*, 1858–1881.
- (4) (a) *Biochemistry of Quinones*; Morton, R. A., Ed.; Academic Press Inc., New York-London, 1965. (b) Nohl, H.; Jordan, W.; Youngman, R. J. *Adv. Free Radical Biol.* **1986**, *2*, 211-279. (c) *Enzyme-Catalyzed Electron and Radical Transfer*; Holzenburg, A., Scrutton, N. S., Eds.; Kluwer, New York, 2000.
- (5) Guo, X.; Mayr, H. *J. Am. Chem. Soc.* **2013**, *135*, 12377-12387.

- (6) (a) Mayr, H.; Patz, M. *Angew. Chem., Int. Ed. Engl.* **1994**, *33*, 938–957. (b) Mayr, H.; Kempf, B.; Ofial, A. R. *Acc. Chem. Res.* **2003**, *36*, 66–77. (c) Mayr, H.; Ofial, A. R. *Pure Appl. Chem.* **2005**, *77*, 1807–1821. (d) Mayr, H.; Ofial, A. R. *J. Phys. Org. Chem.* **2008**, *21*, 584–595.
- (7) For a comprehensive database of nucleophilicity parameters  $N$  and  $s_N$  as well as electrophilicity parameters  $E$ , see [www.cup.lmu.de/oc/mayr/DBintro.html](http://www.cup.lmu.de/oc/mayr/DBintro.html).
- (8) (a) Mayr, H.; Bug, T.; Gotta, M. F.; Hering, N.; Irrgang, B.; Janker, B.; Kempf, B.; Loos, R.; Ofial, A. R.; Remennikov, G.; Schimmel, H. *J. Am. Chem. Soc.* **2001**, *123*, 9500–9512. (b) Lucius, R.; Loos, R.; Mayr, H. *Angew. Chem., Int. Ed.* **2002**, *41*, 91–95. (c) Richter, D.; Hampel, N.; Singer, T.; Ofial, A. R.; Mayr, H. *Eur. J. Org. Chem.* **2009**, 3203–3211. (d) Ammer, J.; Nolte, C.; Mayr, H. *J. Am. Chem. Soc.* **2012**, *134*, 13902–13911.
- (9) Fukuzumi, S.; Fujita, M.; Matsubayashi, G.; Otera, J. *Chem. Lett.* **1993**, 1451–1454.
- (10) Fukuzumi, S.; Fujita, M.; Otera, J.; Fujita, Y. *J. Am. Chem. Soc.* **1992**, *114*, 10271–10278.
- (11) Renaud, P.; Schubert, S. *Angew. Chem., Int. Ed. Engl.* **1990**, *29*, 433–434.
- (12) Liu, W.-Z.; Bordwell, F. G. *J. Org. Chem.* **1996**, *61*, 4778–4783.
- (13) Bourdelande, J. L.; Gallardo, I.; Guirado, G. *J. Am. Chem. Soc.* **2007**, *129*, 2817–2821.
- (14) (a) Ott, R.; Pinter, E. *Monatsh. Chem.* **1997**, *128*, 901–909. (b) Tandon, V. K.; Maurya, H. K. *Tetrahedron Lett.* **2009**, *50*, 5896–5902.
- (15) Chapyshev, S. V.; Ibata, T. *Mendeleev Commun.* **1994**, *4*, 150–152.
- (16) Koch, A. S.; Harbison, W. G.; Hubbard, J. M.; Kort, M.; Roe, B. A. *J. Org. Chem.* **1996**, *61*, 5959–5963.
- (17) (a) Terrier, F. *Modern Nucleophilic Aromatic Substitution*, Wiley-VCH, Weinheim (Germany), 2013; (b) Makosza, M.; Winiarski, J. *Acc. Chem. Res.* **1987**, *20*, 282–289; (c) Makosza, M.; Kwast, A. *J. Phys. Org. Chem.* **1998**, *11*, 341–349.
- (18) Throughout this article we define “partial rate constants” as the sum of the reactivities of all equivalent positions.
- (19) Ofial, A. R.; Ohkubo, K.; Fukuzumi, S.; Lucius, R.; Mayr, H. *J. Am. Chem. Soc.* **2003**, *125*, 10906–10912.
- (20) Frisch, M. J.; Trucks, G. W.; Schlegel, H.; Scuseria, G. E.; Robb, M. A.; Cheeseman, J. R.; Scalmani, G.; Barone, V.; Mennucci, B.; Petersson, G. A.; Nakatsuji, H.; Caricato, M.; Li, X.; Hratchian, H. P.; Izmaylov, A. F.; Bloino, J.; Zheng, G.; Sonnenberg, J. L.; Hada, M.; Ehara, M.; Toyota, K.; Fukuda, R.; Hasegawa, J.; Ishida, M.; Nakajima, T.; Honda,

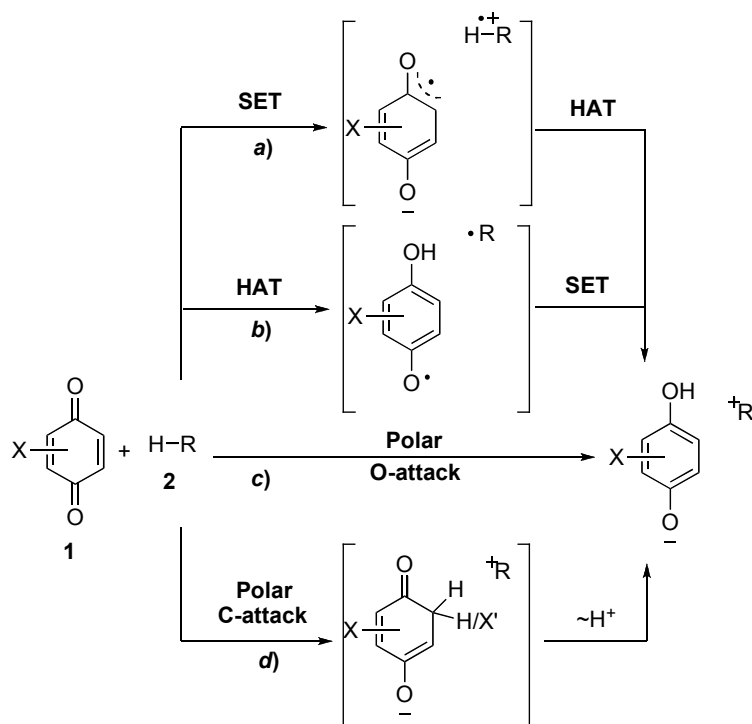
- Y.; Kitao, O.; Nakai, H.; Vreven, T.; Montgomery, J. A.; Peralta, J. E.; Ogliaro, F.; Bearpark, M.; Heyd, J. J.; Brothers, E.; Kudin, K. N.; Staroverov, V. N.; Kobayashi, R.; Normand, J.; Raghavachari, K.; Rendell, A.; Burant, J. C.; Iyengar, S. S.; Tomasi, J.; Cossi, M.; Rega, N.; Millam, J. M.; Klene, M.; Knox, J. E.; Cross, J. B.; Bakken, V.; Adamo, C.; Jaramillo, J.; Gomperts, R.; Stratmann, R. E.; Yazyev, O.; Austin, A. J.; Cammi, R.; Pomelli, C.; Ochterski, J. W.; Martin, R. L.; Morokuma, K.; Zakrzewski, V. G.; Voth, G. A.; Salvador, P.; Dannenberg, J. J.; Dapprich, S.; Daniels, A. D.; Farkas; Foresman, J. B.; Ortiz, J. V.; Cioslowski, J.; Fox, D. J. *Gaussian 09*, Revision A.02; Gaussian, Inc.: Wallingford CT, 2009.
- (21) Horner, L.; Merz, H. *Liebigs Ann. Chem.* **1950**, 570, 89-120.
- (22) López-Alvarado, P.; Avendaño, C.; Menéndez, J. C. *Synth. Commun.* **2002**, 32, 3233-3239.
- (23) Oisaki, K.; Suto, Y.; Kanai, M.; Shibasaki, M. *J. Am. Chem. Soc.* **2003**, 125, 5644–5645.
- (24) (a) Cazeau, P.; Duboudin, F.; Moulines, F.; Babot, O.; Dunogues, J. *Tetrahedron* **1987**, 43, 2075–2088. (b) Cazeau, P.; Duboudin, F.; Moulines, F.; Babot, O.; Dunogues, J. *Tetrahedron* **1987**, 43, 2089–2100.
- (25) Hünig, S.; Lücke, E.; Brenninger, W. *Org. Synth.* **1961**, 41, 65.
- (26) Baranac-Stojanovic, M.; Markovic, R.; Stojanovic, M. *Tetrahedron* **2011**, 67, 8000-8008.
- (27) Ott, R.; Pinter, E., *Monatsh. Chem.* **1997**, 128, 901-909.
- (28) Chapyshev, S. V. and Ibata, T. *Mendeleev Commun.* **1994**, 4, 150-152.
- (29) Chapyshev, S. V. and Ibata, T. *Mendeleev Commun.* **1994**, 3, 109-110.

## Chapter 4: Mechanisms of Hydride Abstractions by Quinones

### 4.1 Introduction

Quinones belong to the most important oxidizing reagents in organic chemistry.<sup>1</sup> As shown in a series of studies by Linstead, Jackman, and coworkers,<sup>2</sup> the oxidations of hydrocarbons by quinones often occur via rate-determining hydride transfer, leading to delocalized carbocations, which rapidly lose a proton or are trapped by a nucleophile in a subsequent step. Hydrogen atom transfer (HAT) processes have an essential significance for biosystems and have been well studied.<sup>3</sup> However, mechanistic details of the hydride abstraction by quinones are still discussed controversially.<sup>4</sup> As depicted in Scheme 1, the process may occur through stepwise or one-step pathways, e.g. *a*) initial single electron transfer (SET), followed by hydrogen atom transfer, *b*) initial hydrogen atom transfer, followed by an electron transfer, *c*) one-step hydride transfer via O-attack or *d*) one-step hydride transfer via C-attack.

**Scheme 1.** Possible Hydride Transfer Mechanisms of Quinones



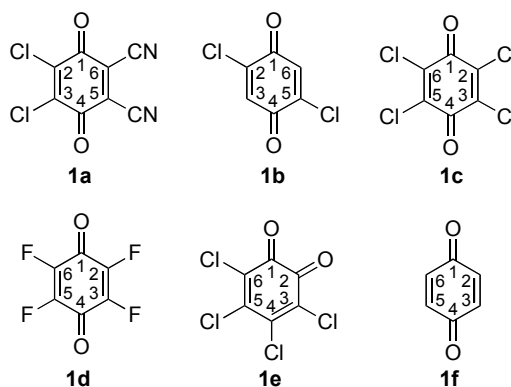
Among quinones, 2,3-dichloro-5,6-dicyano-*p*-benzoquinone (DDQ, **1a**) is the most frequently used hydride acceptor in oxidations of hydrocarbons<sup>5</sup> and dehydrogenative cross coupling reactions.<sup>6</sup>

We have previously reported that the reactions of DDQ with *p*-nucleophiles<sup>7</sup> proceed by polar pathways, the rates of which can be described by eq. (1),<sup>8</sup> which had been developed to predict rates and selectivities for polar reactions.

$$\log k(20\text{ }^{\circ}\text{C}) = s_N(E + N) \quad (1)$$

In eq. (1) the second-order rate constant ( $\log k$ ) is described by two solvent-dependent, nucleophile-specific parameters ( $s_N$ ,  $N$ ) and one electrophile-specific parameter ( $E$ ). Using a series of benzhydrylium ions and structurally related quinone methides as reference electrophiles, comprehensive nucleophilicity scales<sup>9</sup> have been established for different types of nucleophiles including a variety of hydride donors,<sup>10</sup> which serve as the basis of the present study.

**Scheme 2.** Quinones Investigated in This Work

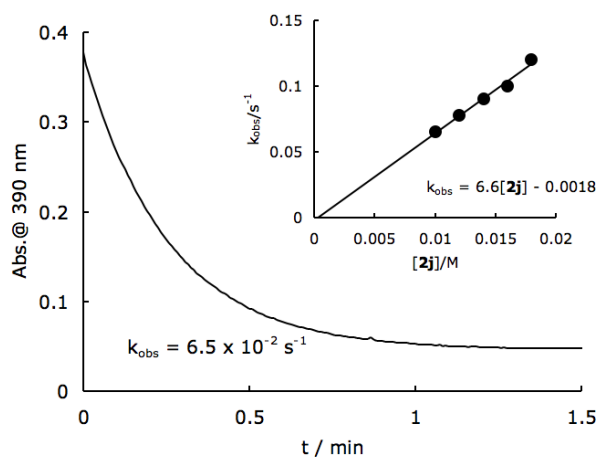


Structurally different hydride donors **2a-t** were selected in this work, e.g. allylic and benzylic C-H hydride donors, tin hydrides, and boron hydrides (Table 1), to elucidate hydride transfer mechanisms of quinones (Scheme 2) by using eq. (1).

## 4.2 Results and Discussion

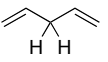
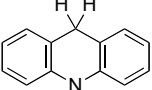
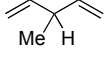
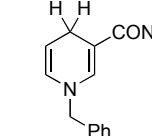
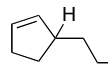
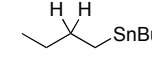
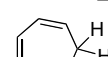
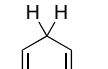
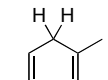
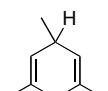
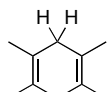
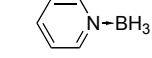
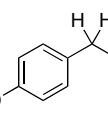
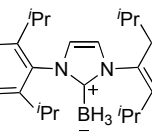
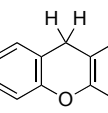
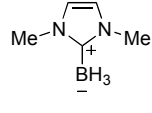
**Kinetic Studies.** Most kinetic investigations of the reactions of DDQ with the hydride donors **2** were performed in  $\text{CH}_2\text{Cl}_2$  solution at  $20\text{ }^{\circ}\text{C}$ , and for some reactions of DDQ, solvent effects were investigated.  $\text{CH}_3\text{CN}$  or  $\text{CD}_3\text{CN}$  were employed as solvents for the kinetic investigations of the reactions of  $\text{Bu}_3\text{SnH}$  (**2n**) with **1b-f**. Most reactions were monitored by UV-vis spectroscopy at or close to the absorption maxima of the quinones (DDQ (**1a**):  $286\text{ nm}$  or  $390\text{ nm}$ , 2,5-dichloro-*p*-benzoquinone (**1b**):  $275\text{ nm}$ , *p*-chloranil (**1c**):  $290\text{ nm}$ , tetrafluoro-*p*-benzoquinone (**1d**):  $256\text{ nm}$ , *o*-chloranil (**1e**):  $457\text{ nm}$ ). When acetone was used as a solvent, the formation of the hydroquinones was monitored at  $350\text{ nm}$  because the absorption of the solvent covered that of the quinone. In all runs, at least 10 equivalents of hydride donors were used to achieve pseudo-first-order kinetics; the rate constants were obtained by least-squares

fitting of the monoexponential function  $A_t = A_0 e^{-k_{\text{obs}}t} + C$  (for decrease) or  $A_t = A_0 (1 - e^{-k_{\text{obs}}t}) + C$  (for increase) to the observed absorbances.  $^1\text{H}$  NMR spectroscopy was employed to study the slow reaction of tributylstannane (**2n**) with *p*-benzoquinone, which was used in excess over **2n**. The second order rate constants shown in Table 1 were derived from the slopes of the correlations between the first order rate constants  $k_{\text{obs}}$  and the concentrations of the hydride donors, which were linear with negligible intercepts.



**Figure 2.** UV-Vis spectroscopic monitoring of the reaction of DDQ ( $1.0 \times 10^{-3} \text{ mol L}^{-1}$ ) with **2j** ( $1.0 \times 10^{-2} \text{ mol L}^{-1}$ ) at 390 nm in  $\text{CH}_2\text{Cl}_2$  at  $20^\circ\text{C}$ . Insert: Determination of the second-order rate constant  $k_2 = 6.6 \text{ L mol}^{-1} \text{ s}^{-1}$  from the dependence of the first-order rate constant  $k_{\text{obs}}$  on the concentration of **2j**.

**Table 1.** Experimental Rate Constants of the Reactions of DDQ (**1a**) with **2** in CH<sub>2</sub>Cl<sub>2</sub> at 20 °C and Calculated Rate Constants for C-Attack from eq 1 by Using the Electrophilicity Parameter of *E* (**1a**) = -3.66 (from ref. 7).

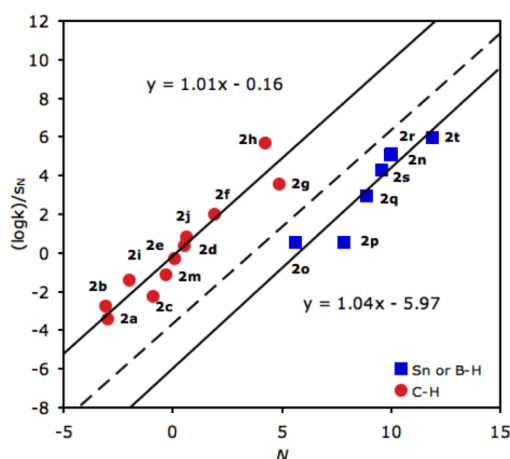
H-donor	<i>N</i> ( <i>s<sub>N</sub></i> ) <sup>a</sup>	<i>k</i> <sub>2</sub> / M <sup>-1</sup> s <sup>-1</sup>	<i>k</i> <sub>cal</sub> / M <sup>-1</sup> s <sup>-1</sup>	log( <i>k</i> <sub>2</sub> / <i>k</i> <sub>cal</sub> )	H-donor	<i>N</i> ( <i>s<sub>N</sub></i> ) <sup>a</sup>	<i>k</i> <sub>2</sub> / M <sup>-1</sup> s <sup>-1</sup>	<i>k</i> <sub>cal</sub> / M <sup>-1</sup> s <sup>-1</sup>	log( <i>k</i> <sub>2</sub> / <i>k</i> <sub>cal</sub> )
<b>2a</b> 	-2.99(0.97)	5.2 x 10 <sup>-4</sup>	3.5 x 10 <sup>-7</sup>	3.2	<b>2k</b> 	5.54(0.90)	>10 <sup>7</sup>	49	>5
<b>2b</b> 	-3.08(0.97)	2.2 x 10 <sup>-3</sup>	2.9 x 10 <sup>-7</sup>	3.9	<b>2l</b> 	8.67(0.82)	>10 <sup>7</sup>	1.3 x 10 <sup>4</sup>	>3
<b>2c</b> 	-0.88(0.94)	7.5 x 10 <sup>-3</sup>	5.4 x 10 <sup>-5</sup>	2.1	<b>2m</b> 	-0.30(1.07)	6.2 x 10 <sup>-2</sup>	5.8 x 10 <sup>-5</sup>	3.0
<b>2d</b> 	0.52(0.97)	2.2	9.0 x 10 <sup>-4</sup>	3.4	<b>2n</b> Bu <sub>3</sub> SnH	9.96(0.55)	6.2 x 10 <sup>2</sup>	2.9 x 10 <sup>3</sup>	-0.7
<b>2e</b> 	0.09(0.98)	0.49	3.2 x 10 <sup>-4</sup>	3.2	<b>2o</b> Ph <sub>3</sub> SnH	5.64(0.59)	2.1	15	-0.9
<b>2f</b> 	1.93(1.01)	1.1 x 10 <sup>2</sup>	1.8 x 10 <sup>-2</sup>	3.8	<b>2p</b> Me <sub>3</sub> N→BH <sub>3</sub>	7.97(0.75)	3.1	1.7 x 10 <sup>3</sup>	-2.7
<b>2g</b> 	4.86(0.86)	1.2 x 10 <sup>3</sup>	11	2.0	<b>2q</b> Et <sub>3</sub> N→BH <sub>3</sub>	8.90(0.75)	1.7 x 10 <sup>2</sup>	8.5 x 10 <sup>3</sup>	-1.7
<b>2h</b> 	4.24(0.84)	5.9 x 10 <sup>4</sup>	3.1	4.3	<b>2r</b> 	10.01(0.75)	5.1 x 10 <sup>3</sup>	5.8 x 10 <sup>4</sup>	-1.1
<b>2i</b> 	-2.11(0.98)	3.8 x 10 <sup>-2</sup>	2.2 x 10 <sup>-6</sup>	4.2	<b>2s</b> 	9.55(0.81)	2.9 x 10 <sup>3</sup>	5.9 x 10 <sup>4</sup>	-1.3
<b>2j</b> 	0.64(0.97)	6.6	1.2 x 10 <sup>-3</sup>	3.7	<b>2t</b> 	11.88(0.71)	1.7 x 10 <sup>4</sup>	6.9 x 10 <sup>5</sup>	-1.6

a) From ref. 10. The *N* and *s<sub>N</sub>* parameters of **2f-i** have been determined in this work using our standard procedure (SI pages S20-24). As only two reference electrophiles were employed, the splitting up of log *k*<sub>2</sub> into *N* and *s<sub>N</sub>* has not been independently justified.

**Correlation Analysis.** In previous work we have determined the electrophilicity parameter of DDQ (*E* = -3.66 at C-5) from the rates of its reactions with p-nucleophiles.<sup>7</sup> When this electrophilicity parameter and the previously reported *N* and *s<sub>N</sub>* parameters for the hydride donors **2** were substituted in eq. (1) one obtains the calculated rate constants *k*<sub>cal</sub> for hydride transfer to C-5 of DDQ, which are listed in Table 1. The last column of Table 1 shows that all C-H hydride donors investigated (**2a-m**) react 2-5 orders of magnitude faster than calculated, while the tin hydrides **2n**, **2o** and the borane complexes **2p-t** react somewhat slower than



calculated. This situation is illustrated in Figure 3 by the plot of  $(\log k)/s_N$  against the nucleophilicity parameters  $N$  of hydride donors. One can see a fair linear correlation line ( $r^2 = 0.91$ ) for the C-H hydride donors which is 3-4 units higher than the calculated correlation line and a second correlation for B-H or Sn-H hydride donors which is slightly below the calculated correlation line. Two different mechanisms are thus indicated. As tributylstannane (**2n**) reacted 300 times faster with DDQ than triphenylstannane (**2o**), we excluded rate-determining hydrogen atom transfer for these reactions, because Ingold reported that homolytic SnH cleavage is faster in  $\text{Ph}_3\text{SnH}$  than in  $\text{Bu}_3\text{SnH}$ .<sup>11</sup>

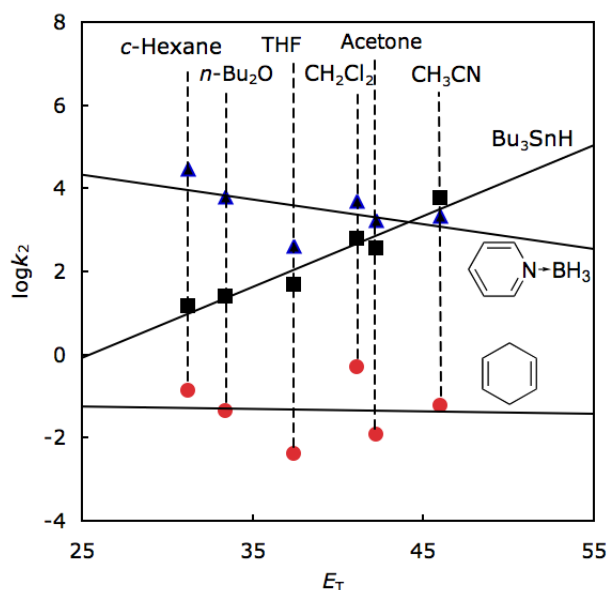


**Figure 3.** Correlation of  $(\log k)/s_N$  vs  $N$  for the reactions of DDQ (**1a**) with hydride donors **2**, the broken line represents the calculated line according to eq. 1 using the electrophilicity parameter  $E = -3.66$ , which was derived from reactions of DDQ with C-nucleophiles.

**Solvent and Kinetic Isotope Effects.** Table 2 and Figure 4 show that the rates of hydride abstraction from cyclohexa-1,4-diene (**2e**) do not correlate with Reichardt's solvent polarity parameter  $E_T$ . In contrast, the rate constants for the reactions of DDQ with  $\text{Bu}_3\text{SnH}$  (**2n**) increase linearly with  $E_T$ , while the hydride abstractions from pyridine-borane become slightly slower with increasing  $E_T$ .

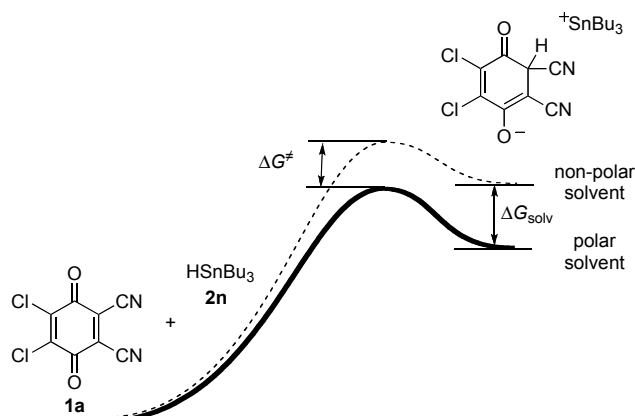
**Table 2.** Solvent and Kinetic Isotope Effect for Reactions of DDQ with **2e**, **2n** and **2r** (20 °C)

solvent	$E_T$	DDQ + cyclohexa-1,4-diene/D <sub>8</sub> ( <b>2e</b> )		
		$k_H / M^{-1} s^{-1}$	$k_D / M^{-1} s^{-1}$	$k_H/k_D$
c-Hexane	31.2	$1.4 \times 10^{-1}$		
<i>n</i> -Bu <sub>2</sub> O	32.0	$4.6 \times 10^{-2}$	$5.1 \times 10^{-3}$	9.0
THF	37.4	$4.2 \times 10^{-3}$	$7.3 \times 10^{-4}$	5.8
CH <sub>2</sub> Cl <sub>2</sub>	41.1	$4.9 \times 10^{-1}$	$6.8 \times 10^{-2}$	7.2
Acetone	42.2	$1.2 \times 10^{-2}$		
CH <sub>3</sub> CN	46.0	$6.2 \times 10^{-2}$	$9.7 \times 10^{-3}$	6.4
DDQ + Bu <sub>3</sub> SnH/D ( <b>2n</b> )				
c-Hexane	31.2	$1.5 \times 10^1$	$1.6 \times 10^1$	0.94
<i>n</i> -Bu <sub>2</sub> O	32.0	$2.5 \times 10^1$	$1.4 \times 10^1$	1.8
THF	37.4	$4.8 \times 10^1$	$3.7 \times 10^1$	1.3
CH <sub>2</sub> Cl <sub>2</sub>	41.1	$6.2 \times 10^2$	$3.7 \times 10^2$	1.7
Acetone	42.2	$3.6 \times 10^2$	$2.7 \times 10^2$	1.3
CH <sub>3</sub> CN	46.0	$6.0 \times 10^3$	$2.7 \times 10^3$	2.2
DDQ + Pyridine-BH <sub>3</sub> /D <sub>3</sub> ( <b>2r</b> )				
c-Hexane	31.2	$3.0 \times 10^4$	$1.3 \times 10^4$	2.3
<i>n</i> -Bu <sub>2</sub> O	32.0	$6.4 \times 10^3$	$4.2 \times 10^3$	1.5
THF	37.4	$5.4 \times 10^2$	$2.2 \times 10^2$	2.5
CH <sub>2</sub> Cl <sub>2</sub>	41.1	$5.1 \times 10^3$	$2.8 \times 10^3$	1.8
Acetone	42.2	$1.7 \times 10^3$	$7.9 \times 10^2$	2.2
CH <sub>3</sub> CN	46.0	$2.2 \times 10^3$	$1.0 \times 10^3$	2.2

**Figure 4.** Solvent effects for the reactions of DDQ with **2e**, **2n** and **2r**.

The large solvent effect for the reaction of DDQ with tributylstannane (**2n**) indicates charge separation in the transition state, as shown in Figure 5, where C attack of **2n** on DDQ forms an ion pair, which can be stabilized by polar solvent. From Hammond's principle, we can expect a large solvent effect based on a late transition state. The slight decrease of the reaction rates with increasing solvent polarity in the corresponding reaction with borane pyridine

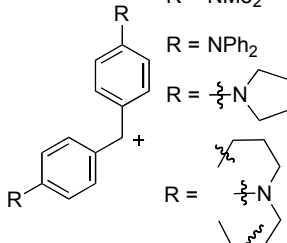
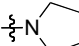
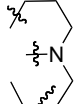
complex can be attributed to the dipolar character of the borane amine complex, which can be stabilized by polar solvent as well.

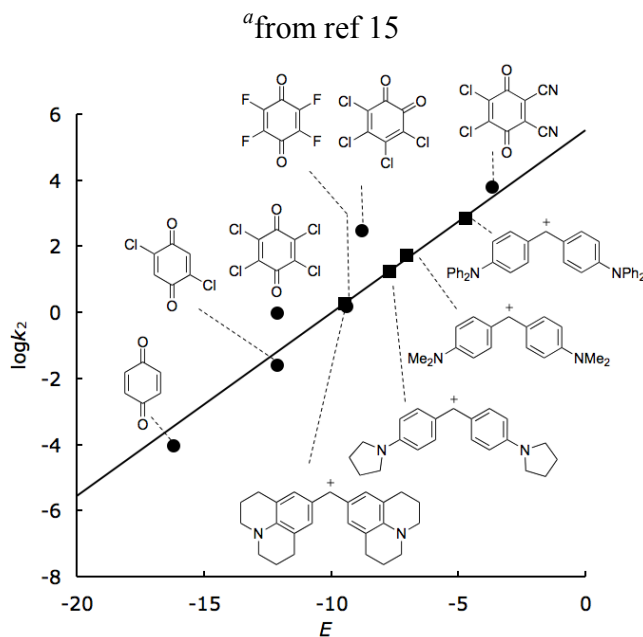


**Figure 5.** Solvent effect on the reaction profile for the proposed C attack pathway in the reaction of DDQ with tributylstannane (**2n**).

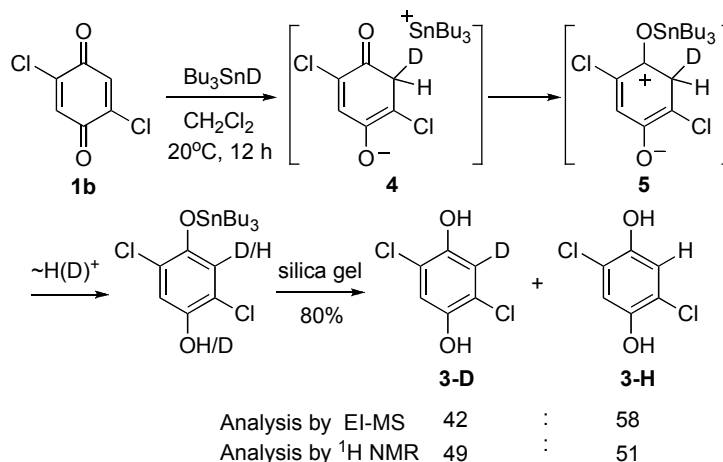
In line with an earlier report on dehydrogenations of hydroaromatic compounds with quinones,<sup>4f</sup> large primary isotope effects of  $k_{\text{H}}/k_{\text{D}} = 5.8\text{--}9.0$  were observed for the reactions of DDQ with cyclohexa-1,4-diene (Table 2). Only small, solvent-dependent kinetic isotope effects were observed for the corresponding reactions with tributylstannane (0.94–2.2), which are similar to those for the reaction of tributylstannane with tetracyanoethylene.<sup>12</sup> The borane pyridine complex also gave small kinetic isotope effects ( $k_{\text{H}}/k_{\text{D}} = 1.5\text{--}2.5$ ), though slightly larger than those previously reported for borohydride reductions of heteroaromatic cations (e.g. tri-*p*-methylphenylpyrylium ion,  $k_{\text{H}}/k_{\text{D}} = 1.25$ )<sup>13</sup> or ketones (e.g. benzophenone,  $k_{\text{H}}/k_{\text{D}} = 0.72\text{--}1.1$ ).<sup>14</sup>

**Reactions of Tributylstannane with Different Oxidants.** Table 3 and the corresponding plot in Figure 6 show that the rate constants ( $\log k_2$ ) for the reactions of  $\text{Bu}_3\text{SnH}$  with quinones and benzhydrylium ions follow a common correlation with the electrophilicity parameters of quinones and benzhydrylium ions, which were derived from reactions with *p*-nucleophiles. As the reactions of stannanes with benzhydrylium ions have previously been shown to proceed by a polar mechanism, the correlation in Figure 6 supports a polar reaction mechanism via C attack for the reactions of Sn-H hydride donors with quinones.

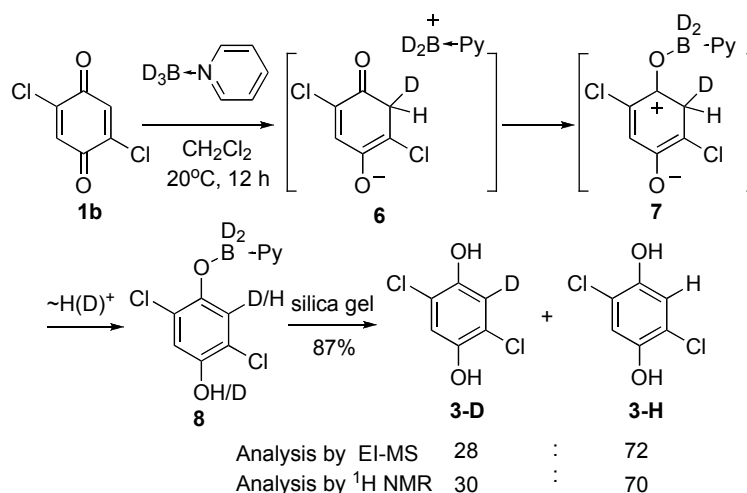
electrophile	<i>E</i>	<i>k</i> <sub>2</sub> / M <sup>-1</sup> s <sup>-1</sup>	<i>k</i> <sub>calc</sub> / M <sup>-1</sup> s <sup>-1</sup>	log( <i>k</i> <sub>2</sub> / <i>k</i> <sub>calc</sub> )	
	R = NMe <sub>2</sub>	-4.72	7.2 x 10 <sup>2</sup> <sup>a</sup>	7.6 x 10 <sup>2</sup>	-0.03
	R = NPh <sub>2</sub>	-7.02	5.4 x 10 <sup>1</sup> <sup>a</sup>	4.1 x 10 <sup>1</sup>	0.12
	R = 	-7.69	1.7 x 10 <sup>1</sup> <sup>a</sup>	1.8 x 10 <sup>1</sup>	-0.02
	R = 	-9.45	1.8 <sup>a</sup>	1.9	-0.03
DDQ ( <b>1a</b> )	-3.66	6.0 x 10 <sup>3</sup>	2.9 x 10 <sup>3</sup>	0.31	
2,5-Dichloro- <i>p</i> -benzoquinone ( <b>1b</b> )	-12.12	2.5 x 10 <sup>-2</sup>	6.5 x 10 <sup>-2</sup>	-0.41	
<i>p</i> -Chloranil ( <b>1c</b> )	-12.13	9.3 x 10 <sup>-1</sup>	6.4 x 10 <sup>-2</sup>	1.16	
<i>o</i> -Chloranil ( <b>1d</b> )	-8.79	3.0 x 10 <sup>2</sup>	4.4	1.83	
Tetrafluoro- <i>p</i> -benzoquinone ( <b>1e</b> )	-9.37	1.5	2.1	-0.15	
<i>p</i> -benzoquinone ( <b>1f</b> )	-16.19	9.4 x 10 <sup>-5</sup>	3.7 x 10 <sup>-4</sup>	-0.60	



Deuterium labeling experiments with 2,5-dichlorobenzoquinone provide a further tool to differentiate between C- and O-attack of different hydride donors. When 2,5-dichlorobenzoquinone (**1b**) was treated with Bu<sub>3</sub>SnD in CH<sub>2</sub>Cl<sub>2</sub> at 20 °C, a ~1:1 mixture of the deuterated and non-deuterated hydroquinones **3-D** and **3-H** was isolated in 80% yield (Scheme 2). The formation of **3-D**, i.e., a product with deuterium at C-3, requires a C attack pathway, e.g. via intermediates **4** and **5**.

**Scheme 2.** Reaction of 2,5-Dichloro-p-benzoquinone (**1b**) with Bu<sub>3</sub>SnD

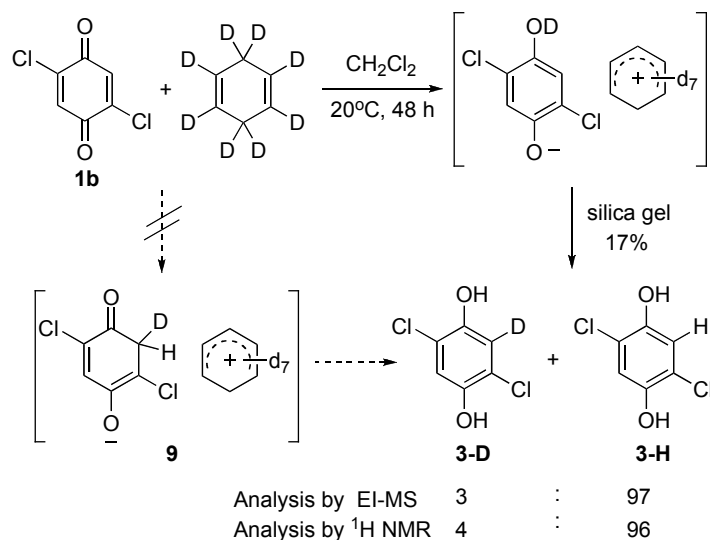
Similarly, when 2,5-dichlorobenzoquinone reacted with the deuterated borane pyridine complex **D<sub>3</sub>-2r**, a 3:7 mixture of **3-D** and **3-H** was isolated in 87% yield (Scheme 3), which also supports a C attack pathway via intermediates **6** and **7**. The smaller ratio **3-D/3-H** may be due to the proton exchange of pyridine-BD<sub>3</sub> with the phenolic proton of **8**, as an early study showed that amine borane complexes undergo a rapid proton-deuterium exchange with heavy water under acidic conditions.<sup>16</sup>

**Scheme 3.** Reaction of 2,5-Dichloro-benzoquinone (**1b**) with Pyridine Borane Deuteride Complex (**D<sub>3</sub>-2r**)

In contrast, only a trace amount of deuterium was found in the hydroquinone which was obtained in 17% yield from the reaction of 2,5-dichloro-p-benzoquinone (**1b**) with D<sub>8</sub>-cyclohexadiene in CH<sub>2</sub>Cl<sub>2</sub> at 20 °C after 48 h (Scheme 4).<sup>17</sup> While the E-parameters for C-attack at quinones cannot be applied to derive the rate of O-attack, the formation of a small yield of **3** from **1b** and D<sub>8</sub>-cyclohexadiene is surprising in view of the fact that a rate constant

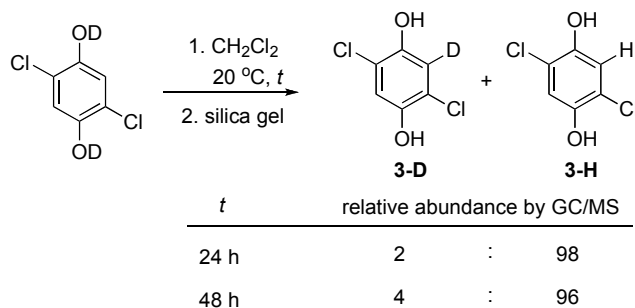
of  $10^{-12} \text{ M}^{-1}\text{s}^{-1}$  can be calculated for the attack of cyclohexa-1,4-diene **2e** at the CH position of **1b**, which is far too small to explain the observed traces of **3-D**.

**Scheme 4.** Reaction of 2,5-Dichloro-p-benzoquinone (**1b**) with D<sub>8</sub>-cyclohexadiene (**D<sub>8</sub>-2e**)



In order to examine the origin of **3-D**, *O*-deuterated 2,5-dichloro-hydroquinone was prepared by deuterium exchange with heavy water and dissolved in CH<sub>2</sub>Cl<sub>2</sub>, the solvent used for the hydride transfer reaction. Scheme 5 shows that the exchange of deuterium at C-3 position occurs slowly at 20 °C. The small amount (4%) of **3-D** observed after 48 h, therefore, suggests that the trace amount (3%) of **3-D** found in the reaction of **1b** with C<sub>6</sub>D<sub>8</sub> comes from deuterium exchange at the product stage and not from the intermediacy of **9**.

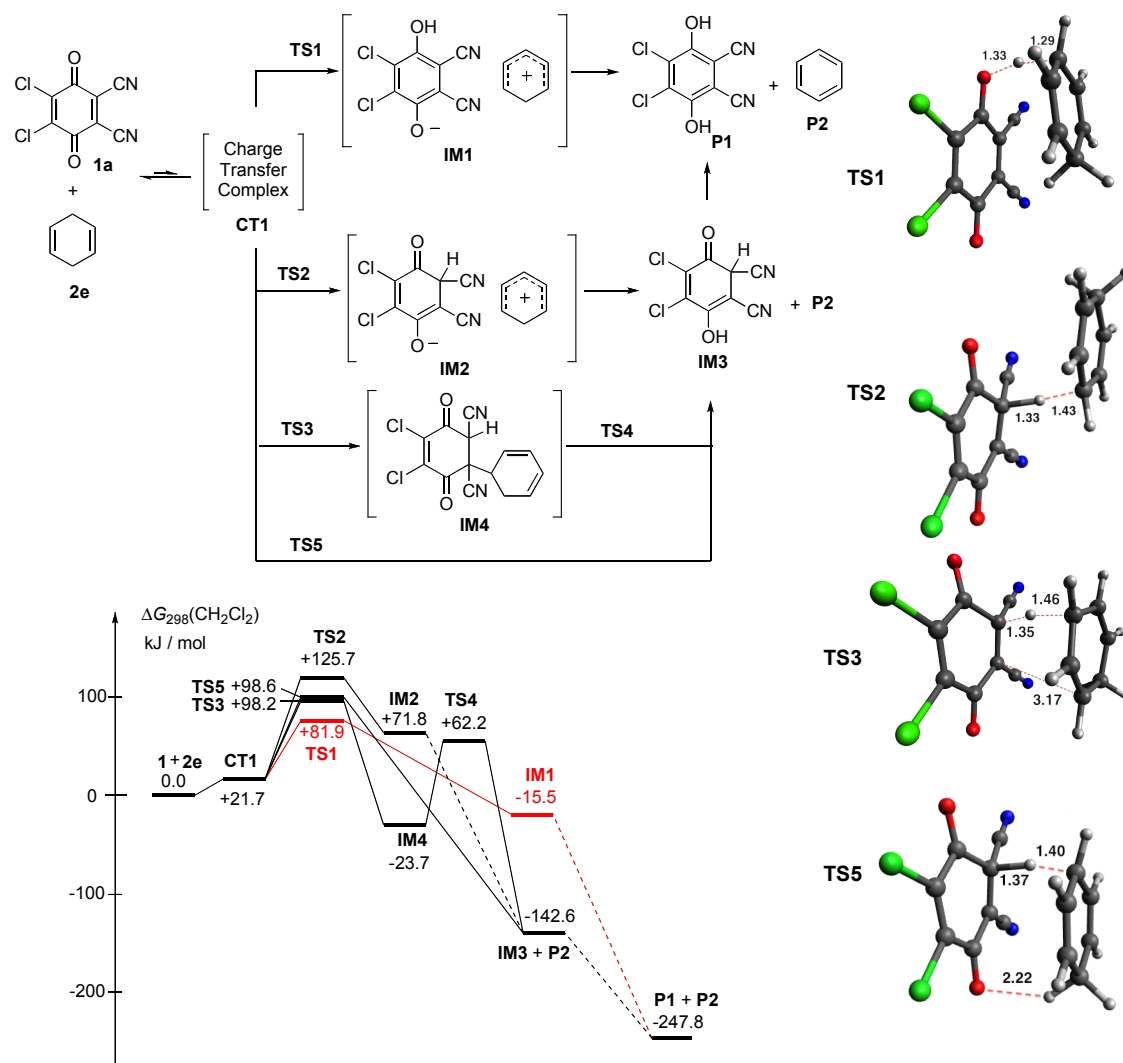
**Scheme 5.** Examination of Deuterium Exchange in Product Stage



**Computational studies.** DFT studies on the reactions of DDQ with cyclohexa-1,4-diene (**2e**), Me<sub>3</sub>SnH (**2n'**), and trimethylamine borane complex (**2p**) were performed using Gaussian 09.<sup>18</sup> The B97D functional was used in combination with the 6-31+G(d,p) basis set (LANL2DZ ECP for Sn atoms) for structure optimization and frequency calculations together with the PCM/UFF model for CH<sub>2</sub>Cl<sub>2</sub>. Geometries of the transition states were verified by vibrational frequency calculations. The nature of the most favorable transition states was further verified by IRC calculations (50 steps in each direction) and subsequent structure optimizations to the next local minimum energy structure. Thermal corrections were calculated from unscaled

frequencies at 298.15 K and 1 atm. Refined electronic energies were obtained from single-point calculations on the B97D geometries using Truhlar's meta hybrid exchange–correlation functional M06-2X with the triple- $\zeta$  quality def2-TZVPP basis sets, again using the PCM/UFF model for CH<sub>2</sub>Cl<sub>2</sub>. All free energies in solution have been corrected to correspond to a standard state of 1 mol/L.<sup>19</sup> The stabilities of the restricted wave functions (RB97D and RM06-2X) have been checked for all transition states. An ultrafine grid was used throughout this study for numerical integration of the density.

The energy profile as well as the optimized transition structures for the different modes of reaction of DDQ (**1a**) with cyclohexadiene (**2e**) are shown in Figure 7. The formation of CT complex (**CT1**) between DDQ (**1a**) and **2e** is endergonic by 22 kJ/mol. From **CT1**, hydride transfer to O of DDQ via **TS1** requires an activation free energy of 60 kJ/mol, resulting in an overall barrier of 82 kJ/mol. Surprisingly, the generation of the ion pair intermediate **IM1** from DDQ (**1a**) and cyclohexa-1,4-diene (**2e**) is exergonic by 16 kJ/mol. Further stabilization by proton transfer and separation of the product complex gives the final products **P1** and **P2**.

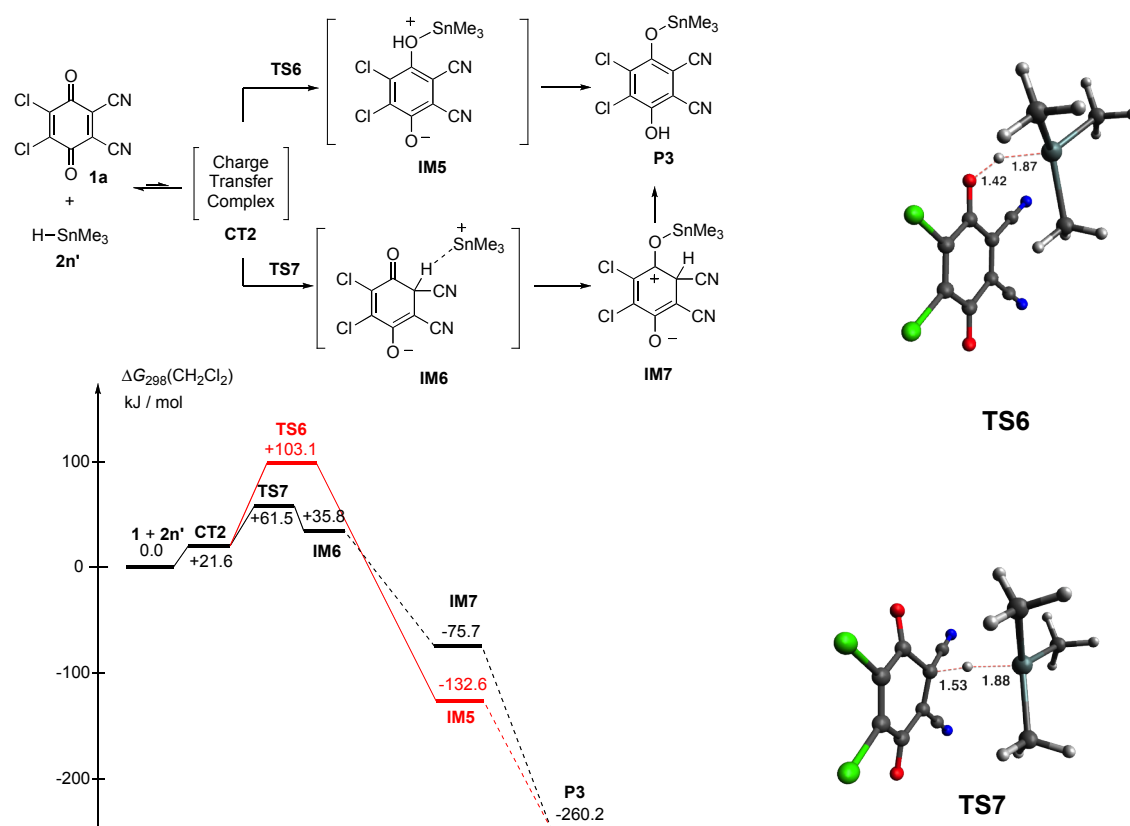


**Figure 7.** Free energy profile for the reaction of DDQ (**1a**) with cyclohexadiene (**2e**) [RM06-2X/def2-TZVPP//B97D/6-31+G(d,p)//PCM/UFF] in  $\text{CH}_2\text{Cl}_2$  together with selected transition structures.

The barrier for hydride transfer from **2e** to C-5 of DDQ via **TS2** is 44  $\text{kJ/mol}$  higher than that for O-attack and the free energy of the generated ion pair intermediate **IM2** is 87  $\text{kJ/mol}$  higher than that of **IM1**. Also the transition state of the ene-reaction **TS3** is favored by 28  $\text{kJ/mol}$  over **TS2**, and the formation of the ene adduct **IM4** is exergonic by 24  $\text{kJ/mol}$ . Further elimination of benzene from **IM4** requires an activation free energy of 86  $\text{kJ/mol}$  (for structure of **TS4** see SI, page S49). Interestingly, concerted transfer of two hydrogen atoms via **TS5** faces a comparable reaction barrier (99  $\text{kJ/mol}$ ) as the stepwise process through **TS3** and **IM4**. The restricted wave functions were examined to be stable for the structures in Fig. 7, which indicates that these stationary points are not of biradical type. The charge

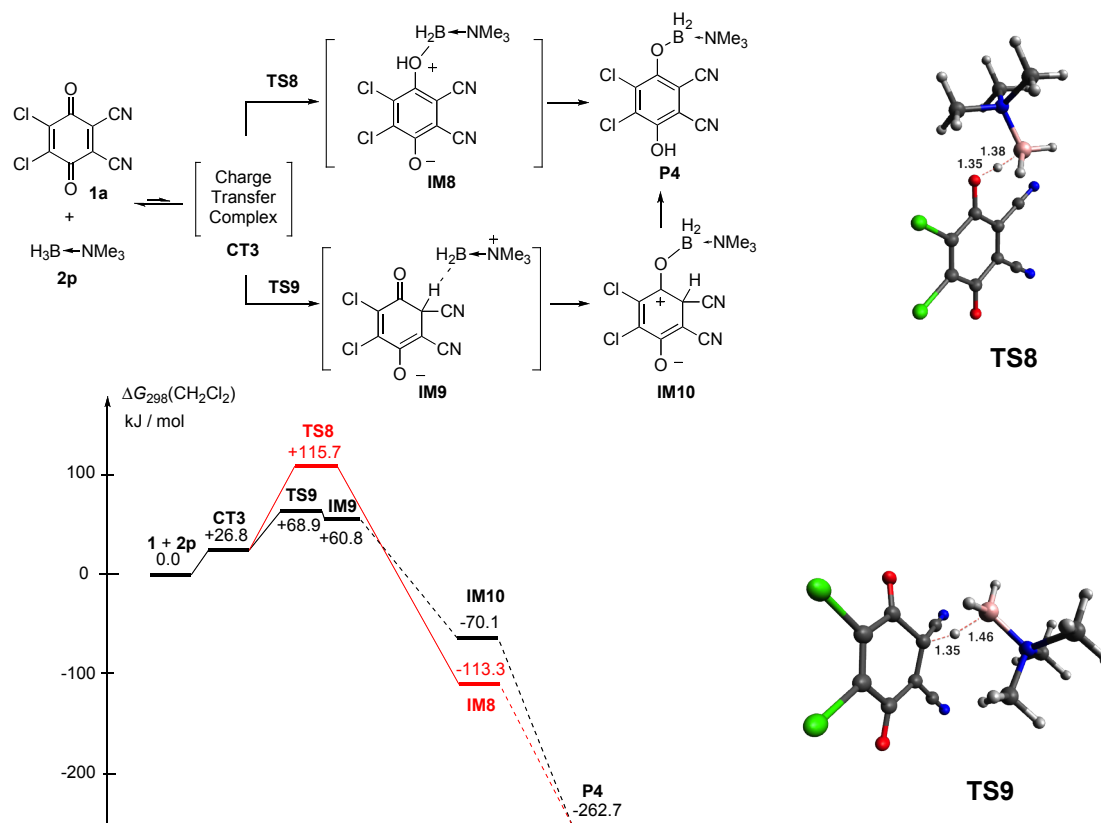


distributions in these structures further confirm the nature of these polar pathways (see SI, pages S33-34).



**Figure 8.** Free energy profile for the reaction of DDQ (**1a**) with trimethylstannane (**2n'**) [RM06-2X/def2-TZVPP//B97D/6-31+G(d,p)/PCM/UFF] in  $\text{CH}_2\text{Cl}_2$  together with selected transition structures.

Figure 8 shows the free energy profiles of the two different reaction pathways for the reaction of DDQ (**1a**) with trimethylstannane (**2n'**), a model for the experimentally studied tributylstannane **2n**. The O-attack pathway, i.e., hydride transfer via **TS6** requires an overall activation free energy of 103 kJ/mol to form the zwitterionic intermediate **IM5**. The formation of **IM5** from DDQ (**1a**) and **2n'** is exergonic by 133 kJ/mol and a subsequent proton shift leads to the more stable final product **P3**. The competing hydride transfer to C-5 of DDQ (**1a**) via **TS7** is favored by 42 kJ/mol over the O-attack pathway. While the generation of the ion pair intermediate **IM6** from **1a** and **2n'** is endergonic by 36 kJ/mol, stabilization comes from the following migration of the  $\text{SnMe}_3$  group to the adjacent oxygen atom and the subsequent proton transfer, which gives the final product **P3**. Though there seems to be a small barrier of ~10 kJ/mol, the transition state for the migration of the  $\text{SnMe}_3$  group could not be located due to the exceedingly flat potential energy surface.



**Figure 9.** Free energy profile for the reaction of DDQ (**1a**) with trimethylamine borane (**2p**) [RM06-2X/def2-TZVPP//B97D/6-31+G(d,p)//PCM/UFF] in  $\text{CH}_2\text{Cl}_2$  together with selected transition structures.

As illustrated in Figure 9, the O- and C-attack pathways of the reaction of DDQ (**1a**) with trimethylamine borane complex **2p** show a similar pattern as the reactions with trimethylstannane. C-attack is favored over O-attack by 47  $\text{kJ/mol}$ . The formation of **IM9** is a highly endergonic process by 61  $\text{kJ/mol}$ , i.e. **IM9** is only 8  $\text{kJ/mol}$  more stable than the transition state **TS9**. As in the reaction with the stannane, the major stabilization comes through migration of boron to the oxygen.

The activation Gibbs free energies for C- and O-attack pathways of the reaction of DDQ with various hydride donors **2**, which were analogously calculated on the same level of theory (Table S64) were converted into second-order rate constants by the Eyring equation. The numbers given in Table 4 include statistical corrections, considering the number of equivalent positions in the quinones and the hydride donors. As shown in Table 4, O-attack is favored for all computationally examined C-H hydride donors,<sup>20</sup> while C-attack is favored for all computationally examined B-H and Sn-H hydride donors, in agreement with the interpretation of our experimental observations. Efforts to rationalize the different behavior of these two

groups of hydride donors by analysis of transition state charge distribution or distortion/interaction energy analysis<sup>21</sup> (see SI pages S32-34) have, unfortunately, not been successful. Obviously, there is not ONE dominant component which accounts for the barrier variations, and the different selectivity of C-H and Sn-H/B-H donors is not due to a simple change.

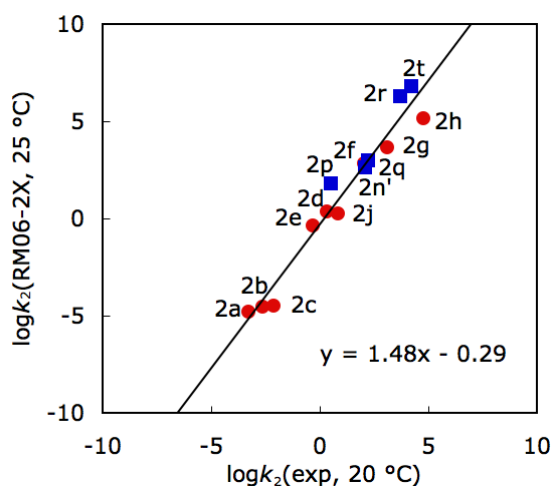
**Table 4.** Rate Constants Derived from Activation Gibbs Free Energies (RM06-2X/def2-TZVPP//B97D/6-31+G(d,p)//PCM/UFF) for O-Attack and C-Attack Pathways of Reactions of DDQ with **2** in CH<sub>2</sub>Cl<sub>2</sub> at 25 °C and Experimental Values in CH<sub>2</sub>Cl<sub>2</sub> at 20 °C

Nucleophile	log ( $k_2/\text{M}^{-1}\text{s}^{-1}$ )		log ( $k_2/\text{M}^{-1}\text{s}^{-1}$ ) exp., 20 °C
	RM06-2X, 25 °C		
	O-attack <sup>a</sup>	C-attack <sup>a</sup>	
<b>2a</b>	-4.79 (8)	-7.50 (8)	-3.28
<b>2b</b>	-4.54 (4)	-6.49 (4)	-2.66
<b>2c</b>	-4.47 (4)	-4.60 (4)	-2.12
<b>2d</b>	0.38 (8)	-2.00 (8)	0.34
<b>2e</b>	-0.35 (16)	-3.21 (16)	-0.31
<b>2f</b>	2.86 (16)	-0.23 (16)	2.04
<b>2g</b>	3.67 (4)	2.43 (4)	3.08
<b>2h</b>	5.15 (16)	2.08 (16)	4.77
<b>2j</b>	0.28 (8)	-3.02 (8)	0.82
Bu <sub>3</sub> SnH ( <b>2n</b> )	-	-	2.79
Me <sub>3</sub> SnH ( <b>2n'</b> )	-4.67 (4)	2.62 (4)	2.10 <sup>b</sup>
<b>2p</b>	-6.40 (12)	1.80 (12)	0.49
<b>2q</b>	-5.98 (12)	3.01 (12)	2.23
<b>2r</b>	-1.98 (12)	6.27 (12)	3.71
<b>2t</b>	-0.25 (12)	6.83 (12)	4.23

a) Statistical factor in parentheses

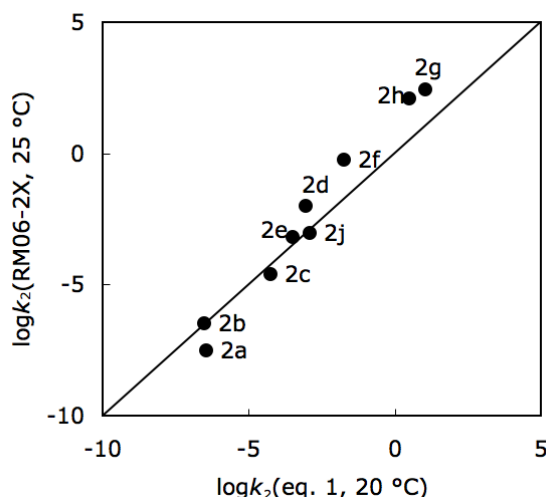
b) Calculated from the rate constant  $k_2 = 125 \text{ M}^{-1}\text{s}^{-1}$  in CH<sub>3</sub>CN at 25 °C reported in ref. (12)

As shown in Figure 10, the rate constants derived from quantum chemically calculated activation free energies for O-attack of C-H hydride donors and for C-attack of tin and boron hydrides correlate well with the experimental values, which demonstrates the consistency of the computational method employed in this work.



**Figure 10.** Correlation of quantum chemically calculated rate constants ( $\log k_2$  (RM06-2X, 25 °C), from Table 4) for the reactions of DDQ with C-H hydride donors (O-attack, red circles) and Sn-H and B-H hydride donors (C-attack, blue squares) with the experimental values from Table 1.

The deviation of the experimental rate constants for the reactions of DDQ (**1a**) with C-H hydride donors from those calculated from the reactivity parameters  $E$ ,  $N$ , and  $s_N$  by eq. 1 was explained by the fact that the experimental data refer to transfer of  $H^-$  to the quinone oxygen, while the  $E$  parameters of quinones refer to the quinone carbons, with the consequence that eq. 1 calculates transfer of  $H^-$  to the quinone carbon atoms. For that reason we have compared the quantum chemically calculated rate constants for the non-observed transfer of hydride from C-H to C-5 of DDQ (**1a**) with the corresponding rate constants obtained from the linear free energy relationship (eq. 1). Figure 11 shows a remarkably good agreement of the absolute rate constants obtained by two completely different approaches. The applicability of eq. 1 also for hydride transfer reactions from C-H hydride donors to quinones has thus been demonstrated.



**Figure 11.** Rate constants for the non-observed reactions of C-H hydride donors with C-5 of DDQ (**1a**): Comparison of quantum chemically calculated rate constants ( $\log k_2$  (RM06-2X, 25 °C, from Table 4) with the  $\log k_2$  (20 °C) derived from eq. 1, by using the electrophilicity parameter of **E** (**1a**) = -3.66 and the  $N$  and  $s_N$  parameters from Table 1.

### 4.3 Conclusion.

Correlation equation (1), which has previously been demonstrated to hold for a large variety of reactions of carbocations and Michael acceptors with  $\pi$ -,  $n$ -, and  $\sigma$ -nucleophiles, has now been demonstrated also to hold for the reactions of quinones with Sn-H and B-H hydride donors, but not for the corresponding reactions with C-H hydride donors. The contrasting behavior of the different hydride donors turned out to be due to the fact that Sn-H and B-H groups transfer hydrogen to the conjugate carbons of the investigated quinones, while C-H hydride donors transfer hydrogen to the carbonyl oxygens. This conclusion is supported by deuterium labelling experiments, and quantum chemical intrinsic reaction coordinate calculations.

The electrophilicity parameters  $E$  of quinones, which have been derived from their reactivities towards  $\pi_{CC}$ -nucleophiles (preceding paper), can be combined with the benzhydrylium-derived  $N$  and  $s_N$  parameters of Sn-H and B-H hydride donors to calculate the rate constants for the reactions of quinones with these hydride donors. The analogy of the involved mechanisms is thus demonstrated. The polar nature of these processes is further supported by the higher reactivity of  $\text{Bu}_3\text{SnH}$  compared to  $\text{Ph}_3\text{SnH}$ , which would not be the case if the Sn-H bond would be cleaved homolytically.

As the  $E$  parameters of electrophiles are based on their reactivities toward C-centered reference nucleophiles, and the  $N$  and  $s_N$  parameters of nucleophiles are based on their reactivities toward C-centered reference electrophiles (typically benzhydrylium ions and quinone methides), the applicability of eq. (1) is limited to electrophile-nucleophile combinations, in which at least one of the reaction centers is carbon. Since this condition is not fulfilled for the hydride shift from C-H groups to the carbonyl oxygen of quinones (formation of an O-H bond), the failure of eq. (1) to reproduce the rate constants for this reaction series can be rationalized. Figure 11 shows, however, that eq. 1 accurately predicts the quantum chemically derived rate constants for the non-observed transfer of hydride from C-H groups to C-5 of DDQ (**1a**).

## 4.4 Experimental Section.

**Materials.** **2f-h** were synthesized by Birch reduction according to literature procedure.<sup>22</sup> **2i** was prepared through reduction of 4,4'-dimethoxybenzophenone with triethylsilane in presence of HBF<sub>4</sub>. **2k** and **2l** were synthesized by reduction of the corresponding acridinium and pyridinium salts with NaS<sub>2</sub>O<sub>4</sub> according to ref 23 and ref 24. **2s** and **2t** were prepared by deprotonation of their carbene precursors and treated with THF-borane complex according to literature procedures.<sup>25</sup> D<sub>8</sub>-1,4-cyclohexadiene was prepared by birch reduction of D<sub>6</sub>-benzene in liquid deuterated ammonia according to ref 26. Bu<sub>3</sub>SnD was synthesized from the reaction of tributyltin chloride with LiAlD<sub>4</sub>. The pyridine-BD<sub>3</sub> complex was obtained in pyridine solution by treatment of NaBD<sub>4</sub> with pyridine deuterium chloride which was prepared from the deuterium exchange of pyridine hydrogen chloride with heavy water. **1b** was prepared by chlorination and subsequent oxidation of 1,4-dimethoxybenzene as reported in the literature.<sup>27</sup> All other compounds were purchased from commercial sources and (if necessary) purified by crystallization, or sublimation (for benzoquinone), or distillation prior to use.

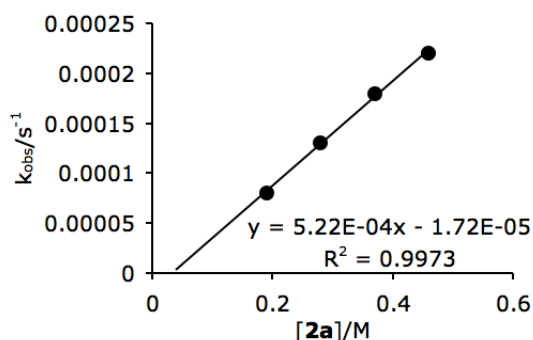
### 4.4.1 Kinetics of the Reactions of DDQ with **2**

CH<sub>2</sub>Cl<sub>2</sub> was freshly distilled over CaH<sub>2</sub> before use. Commercially available *c*-Hexane, *n*-Bu<sub>2</sub>O and THF were further purified by distillation over DDQ to remove the impurities which may react with DDQ. Acetone and CH<sub>3</sub>CN were purchased from Acros and used without further purification. The rate constants of all investigated reactions were determined photometrically. The temperature of the solutions during all kinetic studies was kept constant (20.0 ± 0.1 °C) by using a circulating bath thermostat. For the evaluation of fast kinetics ( $\tau_{1/2} < 10$  s) a stopped-flow spectrophotometer (Hi-Tech SF-61DX2) was used. The rates of slow reactions ( $\tau_{1/2} > 10$  s) were determined by using a conventional UV/Vis diode array spectrophotometer (J&M TIDAS) connected to a Hellma 661.502-QX quartz Suprasil immersion probe (5 mm light path) via fiber optic cables. Rate constants  $k_{\text{obs}}$  (s<sup>-1</sup>) were obtained by least-squares fitting of the absorbances to the monoexponential function  $A_t = A_0 e^{-k_{\text{obs}}t} + C$  (for decreasing absorbance) or  $A_t = A_0 (1 - e^{-k_{\text{obs}}t}) + C$  (for increasing absorbance).

Table S1. Kinetics of the reaction of DDQ (**1a**) with penta-1,4-diene (**2a**) in CH<sub>2</sub>Cl<sub>2</sub> (20 °C, Conventional UV/Vis, at 340 nm)

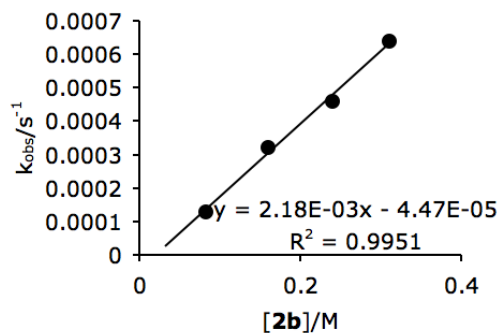
[DDQ] / mol L <sup>-1</sup>	[ <b>2a</b> ] / mol L <sup>-1</sup>	k <sub>obs</sub> / s <sup>-1</sup>
2.0 × 10 <sup>-4</sup>	0.19	8.0 × 10 <sup>-5</sup>
2.0 × 10 <sup>-4</sup>	0.28	1.3 × 10 <sup>-4</sup>
2.0 × 10 <sup>-4</sup>	0.37	1.8 × 10 <sup>-4</sup>
2.0 × 10 <sup>-4</sup>	0.46	2.2 × 10 <sup>-4</sup>

$$k_2 = 5.2 \times 10^{-4} \text{ L mol}^{-1} \text{ s}^{-1}$$

Table S2. Kinetics of the reaction of DDQ (**1a**) with 3-methylpenta-1,4-diene (**2b**) in CH<sub>2</sub>Cl<sub>2</sub> (20 °C, Conventional UV/Vis, at 340 nm)

[DDQ] / mol L <sup>-1</sup>	[ <b>2b</b> ] / mol L <sup>-1</sup>	k <sub>obs</sub> / s <sup>-1</sup>
2.0 × 10 <sup>-4</sup>	0.082	1.3 × 10 <sup>-4</sup>
2.0 × 10 <sup>-4</sup>	0.16	3.2 × 10 <sup>-4</sup>
2.0 × 10 <sup>-4</sup>	0.24	4.6 × 10 <sup>-4</sup>
2.0 × 10 <sup>-4</sup>	0.31	6.4 × 10 <sup>-4</sup>

$$k_2 = 2.2 \times 10^{-3} \text{ L mol}^{-1} \text{ s}^{-1}$$

Table S3. Kinetics of the reaction of DDQ (**1a**) with 3-propylcyclopent-1-ene (**2c**) in CH<sub>2</sub>Cl<sub>2</sub> (20 °C, Stopped-flow, at 390 nm)

[DDQ] / mol L <sup>-1</sup>	[ <b>2c</b> ] / mol L <sup>-1</sup>	k <sub>obs</sub> / s <sup>-1</sup>
1.0 × 10 <sup>-3</sup>	0.5	3.7 × 10 <sup>-3</sup>
1.0 × 10 <sup>-3</sup>	1.0	7.3 × 10 <sup>-3</sup>
1.0 × 10 <sup>-3</sup>	1.5	1.1 × 10 <sup>-2</sup>
1.0 × 10 <sup>-3</sup>	2.0	1.5 × 10 <sup>-2</sup>

$$k_2 = 7.5 \times 10^{-3} \text{ L mol}^{-1} \text{ s}^{-1}$$

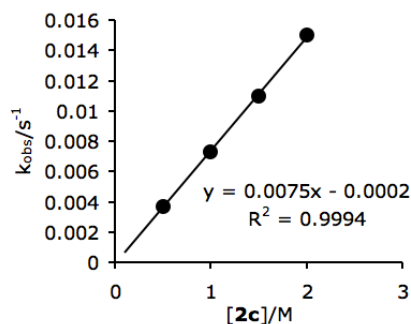
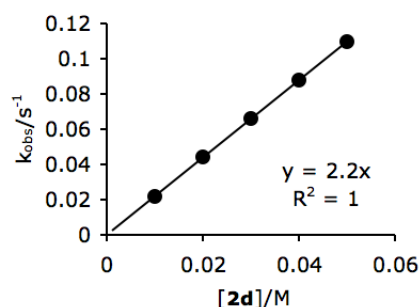




Table S4. Kinetics of the reaction of DDQ (**1a**) with cyclohepta-1,3,5-triene (**2d**) in CH<sub>2</sub>Cl<sub>2</sub> (20 °C, Stopped-flow, at 350 nm)

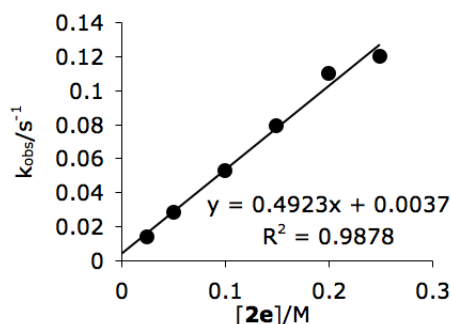
[DDQ] / mol L <sup>-1</sup>	[ <b>2d</b> ] / mol L <sup>-1</sup>	k <sub>obs</sub> / s <sup>-1</sup>
1.0 × 10 <sup>-4</sup>	1.0 × 10 <sup>-2</sup>	2.2 × 10 <sup>-2</sup>
1.0 × 10 <sup>-4</sup>	2.0 × 10 <sup>-2</sup>	4.4 × 10 <sup>-2</sup>
1.0 × 10 <sup>-4</sup>	3.0 × 10 <sup>-2</sup>	6.6 × 10 <sup>-2</sup>
1.0 × 10 <sup>-4</sup>	4.0 × 10 <sup>-2</sup>	8.8 × 10 <sup>-2</sup>
1.0 × 10 <sup>-4</sup>	5.0 × 10 <sup>-2</sup>	1.1 × 10 <sup>-1</sup>

$$k_2 = 2.2 \text{ L mol}^{-1} \text{ s}^{-1}$$

Table S5. Kinetics of the reaction of DDQ (**1a**) with cyclohexa-1,4-diene (**2e**) in CH<sub>2</sub>Cl<sub>2</sub> (20 °C, Stopped-flow, at 390 nm)

[DDQ] / mol L <sup>-1</sup>	[ <b>2e</b> ] / mol L <sup>-1</sup>	k <sub>obs</sub> / s <sup>-1</sup>
1.0 × 10 <sup>-3</sup>	2.5 × 10 <sup>-2</sup>	1.4 × 10 <sup>-2</sup>
1.0 × 10 <sup>-3</sup>	5.0 × 10 <sup>-2</sup>	2.8 × 10 <sup>-2</sup>
1.0 × 10 <sup>-3</sup>	1.0 × 10 <sup>-1</sup>	5.3 × 10 <sup>-2</sup>
1.0 × 10 <sup>-3</sup>	1.5 × 10 <sup>-1</sup>	7.9 × 10 <sup>-2</sup>
1.0 × 10 <sup>-3</sup>	2.0 × 10 <sup>-1</sup>	1.1 × 10 <sup>-1</sup>
1.0 × 10 <sup>-3</sup>	2.5 × 10 <sup>-1</sup>	1.2 × 10 <sup>-1</sup>

$$k_2 = 0.49 \text{ L mol}^{-1} \text{ s}^{-1}$$

Table S6. Kinetics of the reaction of DDQ (**1a**) with cyclohexa-1,4-diene (**2e**) in CH<sub>3</sub>CN (20 °C, Conventional UV/Vis, at 286 nm)

[DDQ] / mol L <sup>-1</sup>	[ <b>2e</b> ] / mol L <sup>-1</sup>	k <sub>obs</sub> / s <sup>-1</sup>
1.0 × 10 <sup>-4</sup>	3.9 × 10 <sup>-3</sup>	2.8 × 10 <sup>-4</sup>
1.0 × 10 <sup>-4</sup>	5.7 × 10 <sup>-3</sup>	3.8 × 10 <sup>-4</sup>
1.0 × 10 <sup>-4</sup>	7.5 × 10 <sup>-3</sup>	4.9 × 10 <sup>-4</sup>
1.0 × 10 <sup>-4</sup>	9.2 × 10 <sup>-3</sup>	6.1 × 10 <sup>-4</sup>

$$k_2 = 6.2 \times 10^{-2} \text{ L mol}^{-1} \text{ s}^{-1}$$

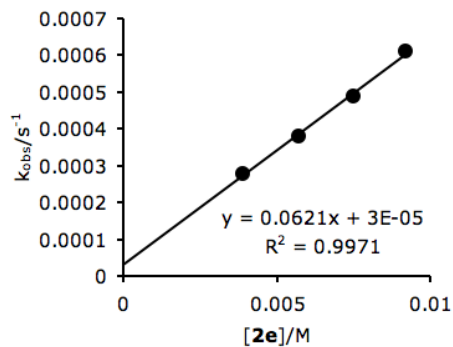
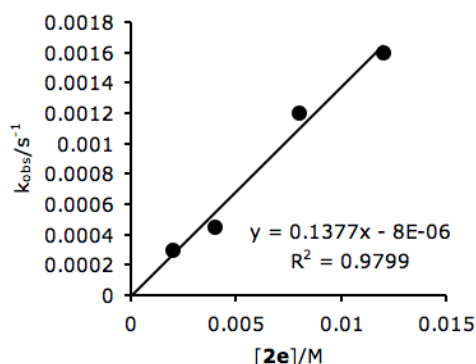


Table S7. Kinetics of the reaction of DDQ (**1a**) with cyclohexa-1,4-diene (**2e**) in *c*-Hexane (20 °C, Conventional UV/Vis, at 286 nm)

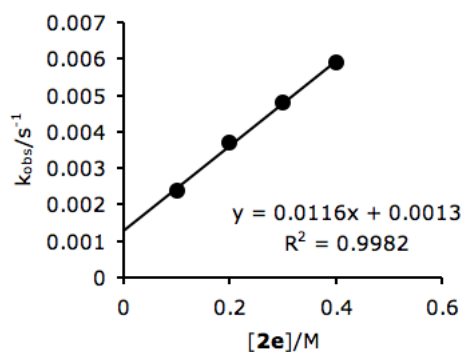
[DDQ] / mol L <sup>-1</sup>	[ <b>2e</b> ] / mol L <sup>-1</sup>	k <sub>obs</sub> / s <sup>-1</sup>
1.0 × 10 <sup>-4</sup>	2.0 × 10 <sup>-3</sup>	3.0 × 10 <sup>-4</sup>
1.0 × 10 <sup>-4</sup>	4.0 × 10 <sup>-3</sup>	4.5 × 10 <sup>-4</sup>
1.0 × 10 <sup>-4</sup>	8.0 × 10 <sup>-3</sup>	1.2 × 10 <sup>-3</sup>
1.0 × 10 <sup>-4</sup>	1.2 × 10 <sup>-2</sup>	1.6 × 10 <sup>-3</sup>

$$k_2 = 0.14 \text{ L mol}^{-1} \text{ s}^{-1}$$

Table S8. Kinetics of the reaction of DDQ (**1a**) with cyclohexa-1,4-diene (**2e**) in acetone (20 °C, Stopped-flow, at 350 nm)

[DDQ] / mol L <sup>-1</sup>	[ <b>2e</b> ] / mol L <sup>-1</sup>	k <sub>obs</sub> / s <sup>-1</sup>
1.0 × 10 <sup>-4</sup>	1.0 × 10 <sup>-1</sup>	2.4 × 10 <sup>-3</sup>
1.0 × 10 <sup>-4</sup>	2.0 × 10 <sup>-1</sup>	3.7 × 10 <sup>-3</sup>
1.0 × 10 <sup>-4</sup>	3.0 × 10 <sup>-1</sup>	4.8 × 10 <sup>-3</sup>
1.0 × 10 <sup>-4</sup>	4.0 × 10 <sup>-1</sup>	5.9 × 10 <sup>-3</sup>

$$k_2 = 1.2 \times 10^{-2} \text{ L mol}^{-1} \text{ s}^{-1}$$

Table S9. Kinetics of the reaction of DDQ (**1a**) with cyclohexa-1,4-diene (**2e**) in THF (20 °C, Conventional UV/Vis, at 286 nm)

[DDQ] / mol L <sup>-1</sup>	[ <b>2e</b> ] / mol L <sup>-1</sup>	k <sub>obs</sub> / s <sup>-1</sup>
1.0 × 10 <sup>-4</sup>	1.0 × 10 <sup>-2</sup>	4.5 × 10 <sup>-5</sup>
1.0 × 10 <sup>-4</sup>	2.0 × 10 <sup>-2</sup>	1.0 × 10 <sup>-4</sup>
1.0 × 10 <sup>-4</sup>	3.9 × 10 <sup>-2</sup>	1.7 × 10 <sup>-4</sup>

$$k_2 = 4.2 \times 10^{-3} \text{ L mol}^{-1} \text{ s}^{-1}$$

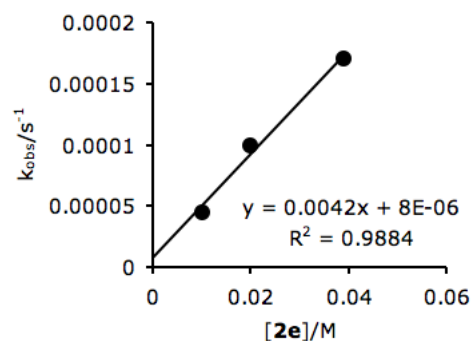
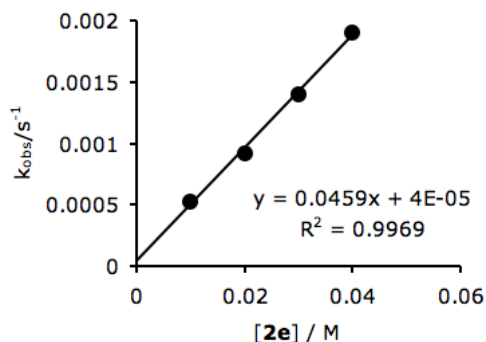


Table S10. Kinetics of the reaction of DDQ (**1a**) with cyclohexa-1,4-diene (**2e**) in *n*-Bu<sub>2</sub>O (20 °C, Conventional UV/Vis, at 390 nm)

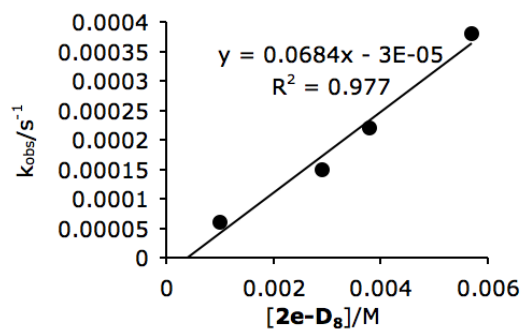
[DDQ] / mol L <sup>-1</sup>	[ <b>2e</b> ] / mol L <sup>-1</sup>	k <sub>obs</sub> / s <sup>-1</sup>
1.0 × 10 <sup>-3</sup>	1.0 × 10 <sup>-2</sup>	5.3 × 10 <sup>-4</sup>
1.0 × 10 <sup>-3</sup>	2.0 × 10 <sup>-2</sup>	9.2 × 10 <sup>-4</sup>
1.0 × 10 <sup>-3</sup>	3.0 × 10 <sup>-2</sup>	1.4 × 10 <sup>-3</sup>
1.0 × 10 <sup>-3</sup>	4.0 × 10 <sup>-2</sup>	1.9 × 10 <sup>-3</sup>

$$k_2 = 4.6 \times 10^{-2} \text{ L mol}^{-1} \text{ s}^{-1}$$

Table S11. Kinetics of the reaction of DDQ (**1a**) with **2e-D<sub>8</sub>** in CH<sub>2</sub>Cl<sub>2</sub> (20 °C, Conventional UV/Vis, at 286 nm)

[DDQ] / mol L <sup>-1</sup>	[ <b>2e-D<sub>8</sub></b> ] / mol L <sup>-1</sup>	k <sub>obs</sub> / s <sup>-1</sup>
1.0 × 10 <sup>-4</sup>	1.0 × 10 <sup>-3</sup>	6.0 × 10 <sup>-5</sup>
1.0 × 10 <sup>-4</sup>	2.9 × 10 <sup>-3</sup>	1.5 × 10 <sup>-4</sup>
1.0 × 10 <sup>-4</sup>	3.8 × 10 <sup>-3</sup>	2.2 × 10 <sup>-4</sup>
1.0 × 10 <sup>-4</sup>	5.7 × 10 <sup>-3</sup>	3.8 × 10 <sup>-4</sup>

$$k_2 = 6.8 \times 10^{-2} \text{ L mol}^{-1} \text{ s}^{-1}$$

Table S12. Kinetics of the reaction of DDQ (**1a**) with **2e-D<sub>8</sub>** in CH<sub>3</sub>CN (20 °C, Conventional UV/Vis, at 390 nm)

[DDQ] / mol L <sup>-1</sup>	[ <b>2e-D<sub>8</sub></b> ] / mol L <sup>-1</sup>	k <sub>obs</sub> / s <sup>-1</sup>
1.0 × 10 <sup>-3</sup>	1.0 × 10 <sup>-2</sup>	1.6 × 10 <sup>-4</sup>
1.0 × 10 <sup>-3</sup>	2.0 × 10 <sup>-2</sup>	2.7 × 10 <sup>-4</sup>
1.0 × 10 <sup>-3</sup>	3.0 × 10 <sup>-2</sup>	3.4 × 10 <sup>-4</sup>
1.0 × 10 <sup>-3</sup>	4.0 × 10 <sup>-2</sup>	4.6 × 10 <sup>-4</sup>

$$k_2 = 9.7 \times 10^{-3} \text{ L mol}^{-1} \text{ s}^{-1}$$

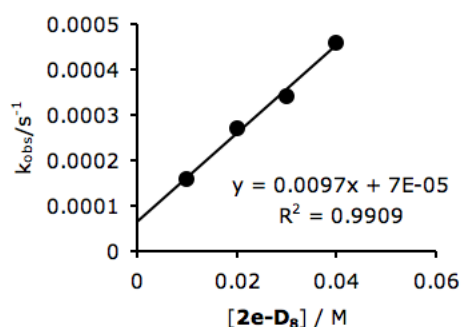
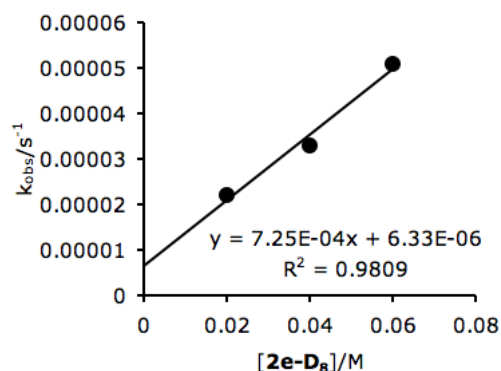


Table S13. Kinetics of the reaction of DDQ (**1a**) with **2e-D<sub>8</sub>** in THF (20 °C, Conventional UV/Vis, at 390 nm)

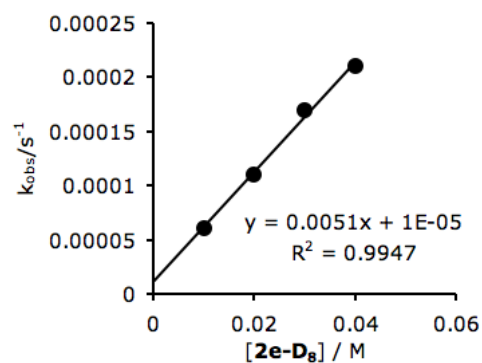
[DDQ] / mol L <sup>-1</sup>	[ <b>2e-D<sub>8</sub></b> ] / mol L <sup>-1</sup>	k <sub>obs</sub> / s <sup>-1</sup>
1.0 × 10 <sup>-3</sup>	2.0 × 10 <sup>-2</sup>	2.2 × 10 <sup>-5</sup>
1.0 × 10 <sup>-3</sup>	4.0 × 10 <sup>-2</sup>	3.3 × 10 <sup>-5</sup>
1.0 × 10 <sup>-3</sup>	6.0 × 10 <sup>-2</sup>	5.1 × 10 <sup>-5</sup>

$$k_2 = 7.3 \times 10^{-4} \text{ L mol}^{-1} \text{ s}^{-1}$$

Table S14. Kinetics of the reaction of DDQ (**1a**) with **2e-D<sub>8</sub>** in *n*-Bu<sub>2</sub>O (20 °C, Conventional UV/Vis, at 390 nm)

[DDQ] / mol L <sup>-1</sup>	[ <b>2e-D<sub>8</sub></b> ] / mol L <sup>-1</sup>	k <sub>obs</sub> / s <sup>-1</sup>
1.0 × 10 <sup>-3</sup>	1.0 × 10 <sup>-2</sup>	6.1 × 10 <sup>-5</sup>
1.0 × 10 <sup>-3</sup>	2.0 × 10 <sup>-2</sup>	1.1 × 10 <sup>-4</sup>
1.0 × 10 <sup>-3</sup>	3.0 × 10 <sup>-2</sup>	1.7 × 10 <sup>-4</sup>
1.0 × 10 <sup>-3</sup>	4.0 × 10 <sup>-2</sup>	2.1 × 10 <sup>-4</sup>

$$k_2 = 5.1 \times 10^{-3} \text{ L mol}^{-1} \text{ s}^{-1}$$

Table S15. Kinetics of the reaction of DDQ (**1a**) with 1,4-dimethylcyclohexa-1,4-diene (**2f**) in CH<sub>2</sub>Cl<sub>2</sub> (20 °C, Stopped-flow, at 286 nm)

[DDQ] / mol L <sup>-1</sup>	[ <b>2f</b> ] / mol L <sup>-1</sup>	k <sub>obs</sub> / s <sup>-1</sup>
1.0 × 10 <sup>-4</sup>	1.0 × 10 <sup>-3</sup>	0.10
1.0 × 10 <sup>-4</sup>	2.0 × 10 <sup>-3</sup>	0.21
1.0 × 10 <sup>-4</sup>	3.0 × 10 <sup>-3</sup>	0.31
1.0 × 10 <sup>-4</sup>	4.0 × 10 <sup>-3</sup>	0.42
1.0 × 10 <sup>-4</sup>	5.0 × 10 <sup>-3</sup>	0.53

$$k_2 = 1.1 \times 10^2 \text{ L mol}^{-1} \text{ s}^{-1}$$

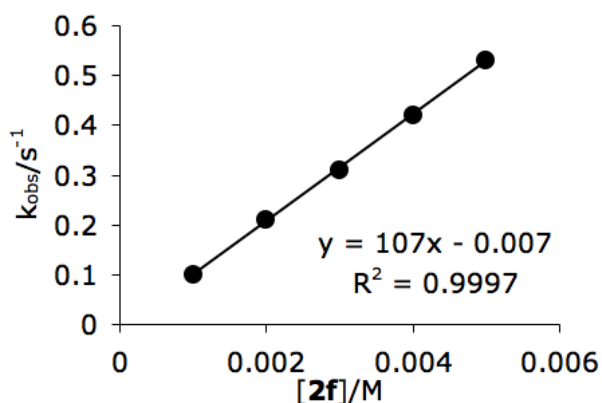
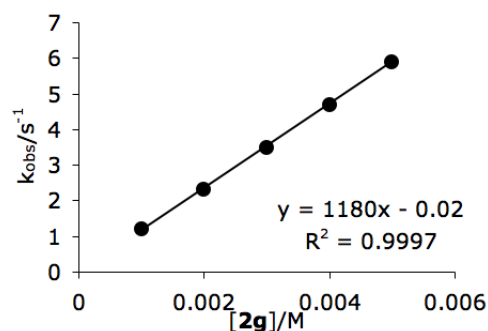


Table S16. Kinetics of the reaction of DDQ (**1a**) with 1,3,5-trimethylcyclohexa-1,4-diene (**2g**) in CH<sub>2</sub>Cl<sub>2</sub> (20 °C, Stopped-flow, at 286 nm)

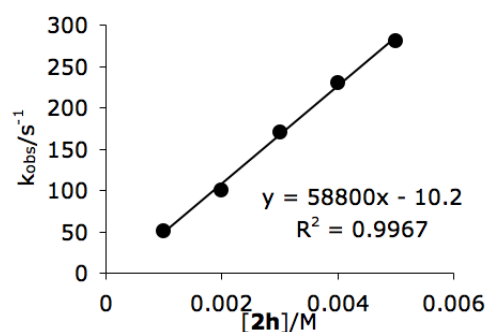
[DDQ] / mol L <sup>-1</sup>	[ <b>2g</b> ] / mol L <sup>-1</sup>	k <sub>obs</sub> / s <sup>-1</sup>
1.0 × 10 <sup>-4</sup>	1.0 × 10 <sup>-3</sup>	1.2
1.0 × 10 <sup>-4</sup>	2.0 × 10 <sup>-3</sup>	2.3
1.0 × 10 <sup>-4</sup>	3.0 × 10 <sup>-3</sup>	3.5
1.0 × 10 <sup>-4</sup>	4.0 × 10 <sup>-3</sup>	4.7
1.0 × 10 <sup>-4</sup>	5.0 × 10 <sup>-3</sup>	5.9

$$k_2 = 1.2 \times 10^3 \text{ mol}^{-1} \text{ L s}^{-1}$$

Table S17. Kinetics of the reaction of DDQ (**1a**) with 1,2,4,5-tetramethylcyclohexa-1,4-diene (**2h**) in CH<sub>2</sub>Cl<sub>2</sub> (20 °C, Stopped-flow, at 286 nm)

[DDQ] / mol L <sup>-1</sup>	[ <b>2h</b> ] / mol L <sup>-1</sup>	k <sub>obs</sub> / s <sup>-1</sup>
1.0 × 10 <sup>-4</sup>	1.0 × 10 <sup>-3</sup>	51
1.0 × 10 <sup>-4</sup>	2.0 × 10 <sup>-3</sup>	1.0 × 10 <sup>2</sup>
1.0 × 10 <sup>-4</sup>	3.0 × 10 <sup>-3</sup>	1.7 × 10 <sup>2</sup>
1.0 × 10 <sup>-4</sup>	4.0 × 10 <sup>-3</sup>	2.3 × 10 <sup>2</sup>
1.0 × 10 <sup>-4</sup>	5.0 × 10 <sup>-3</sup>	2.8 × 10 <sup>2</sup>

$$k_2 = 5.9 \times 10^4 \text{ L mol}^{-1} \text{ s}^{-1}$$

Table S18. Kinetics of the reaction of DDQ (**1a**) with bis(4-methoxyphenyl)methane (**2i**) in CH<sub>2</sub>Cl<sub>2</sub> (20 °C, Conventional UV/Vis, at 350 nm)

[DDQ] / mol L <sup>-1</sup>	[ <b>2i</b> ] / mol L <sup>-1</sup>	k <sub>obs</sub> / s <sup>-1</sup>
1.0 × 10 <sup>-4</sup>	1.0 × 10 <sup>-3</sup>	5.3 × 10 <sup>-5</sup>
1.0 × 10 <sup>-4</sup>	2.0 × 10 <sup>-3</sup>	9.0 × 10 <sup>-5</sup>
1.0 × 10 <sup>-4</sup>	2.9 × 10 <sup>-3</sup>	1.1 × 10 <sup>-4</sup>
1.0 × 10 <sup>-4</sup>	3.9 × 10 <sup>-3</sup>	1.6 × 10 <sup>-4</sup>
1.0 × 10 <sup>-4</sup>	4.8 × 10 <sup>-3</sup>	2.0 × 10 <sup>-4</sup>

$$k_2 = 3.8 \times 10^{-2} \text{ L mol}^{-1} \text{ s}^{-1}$$

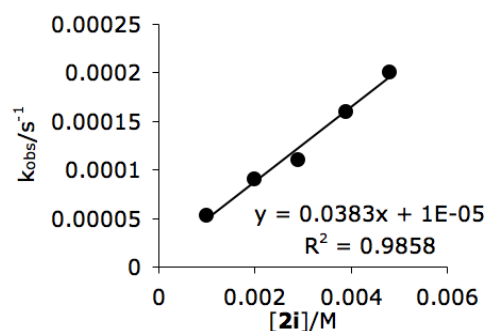
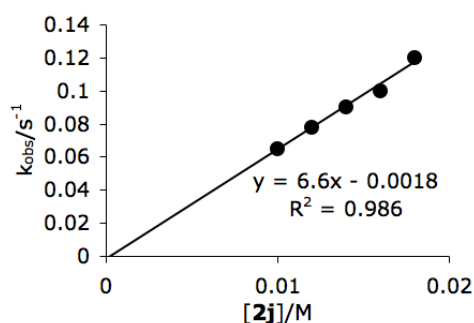


Table S19. Kinetics of the reaction of DDQ (**1a**) with 9H-xanthene (**2j**) in CH<sub>2</sub>Cl<sub>2</sub> (20 °C, Conventional UV/Vis, at 390 nm)

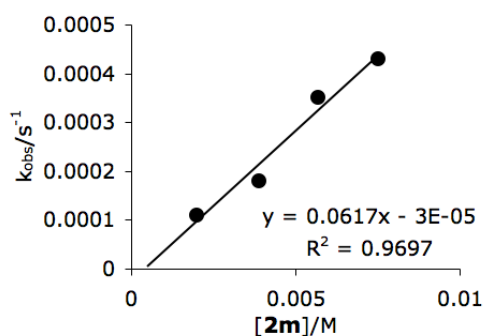
[DDQ] / mol L <sup>-1</sup>	[ <b>2j</b> ] / mol L <sup>-1</sup>	k <sub>obs</sub> / s <sup>-1</sup>
1.0 × 10 <sup>-3</sup>	1.0 × 10 <sup>-2</sup>	6.5 × 10 <sup>-2</sup>
1.0 × 10 <sup>-3</sup>	1.2 × 10 <sup>-2</sup>	7.8 × 10 <sup>-2</sup>
1.0 × 10 <sup>-3</sup>	1.4 × 10 <sup>-2</sup>	9.0 × 10 <sup>-2</sup>
1.0 × 10 <sup>-3</sup>	1.6 × 10 <sup>-2</sup>	1.0 × 10 <sup>-1</sup>
1.0 × 10 <sup>-3</sup>	1.8 × 10 <sup>-2</sup>	1.2 × 10 <sup>-1</sup>

$$k_2 = 6.6 \text{ L mol}^{-1} \text{ s}^{-1}$$

Table S20. Kinetics of the reaction of DDQ (**1a**) with tetrabutylstannane (**2m**) in CH<sub>2</sub>Cl<sub>2</sub> (20 °C, Conventional UV/Vis, at 286 nm)

[DDQ] / mol L <sup>-1</sup>	[ <b>2m</b> ] / mol L <sup>-1</sup>	k <sub>obs</sub> / s <sup>-1</sup>
1.0 × 10 <sup>-4</sup>	2.0 × 10 <sup>-3</sup>	1.1 × 10 <sup>-4</sup>
1.0 × 10 <sup>-4</sup>	3.9 × 10 <sup>-3</sup>	1.8 × 10 <sup>-4</sup>
1.0 × 10 <sup>-4</sup>	5.7 × 10 <sup>-3</sup>	3.5 × 10 <sup>-4</sup>
1.0 × 10 <sup>-4</sup>	7.5 × 10 <sup>-3</sup>	4.3 × 10 <sup>-4</sup>

$$k_2 = 6.2 \times 10^{-2} \text{ L mol}^{-1} \text{ s}^{-1}$$

Table S21. Kinetics of the reaction of DDQ (**1a**) with Bu<sub>3</sub>SnH (**2n**) in CH<sub>2</sub>Cl<sub>2</sub> (20 °C, Stopped-flow, at 286 nm)

[DDQ] / mol L <sup>-1</sup>	[ <b>2n</b> ] / mol L <sup>-1</sup>	k <sub>obs</sub> / s <sup>-1</sup>
1.0 × 10 <sup>-4</sup>	1.0 × 10 <sup>-3</sup>	0.55
1.0 × 10 <sup>-4</sup>	2.0 × 10 <sup>-3</sup>	1.1
1.0 × 10 <sup>-4</sup>	3.0 × 10 <sup>-3</sup>	1.7
1.0 × 10 <sup>-4</sup>	4.0 × 10 <sup>-3</sup>	2.4
1.0 × 10 <sup>-4</sup>	5.0 × 10 <sup>-3</sup>	3.0

$$k_2 = 6.2 \times 10^2 \text{ L mol}^{-1} \text{ s}^{-1}$$

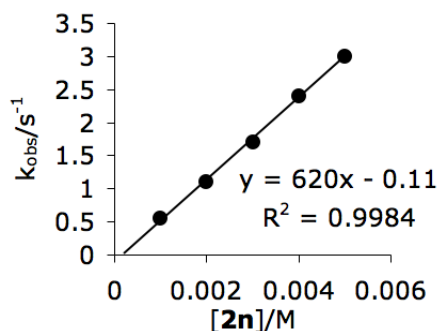
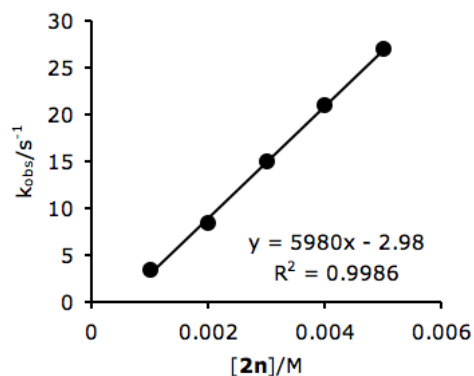


Table S22. Kinetics of the reaction of DDQ (**1a**) with Bu<sub>3</sub>SnH (**2n**) in CH<sub>3</sub>CN (20 °C, Stopped-flow, at 286 nm)

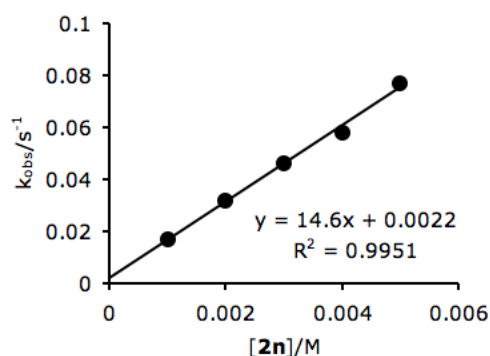
[DDQ] / mol L <sup>-1</sup>	[ <b>2n</b> ] / mol L <sup>-1</sup>	k <sub>obs</sub> / s <sup>-1</sup>
1.0 × 10 <sup>-4</sup>	1.0 × 10 <sup>-3</sup>	3.4
1.0 × 10 <sup>-4</sup>	2.0 × 10 <sup>-3</sup>	8.4
1.0 × 10 <sup>-4</sup>	3.0 × 10 <sup>-3</sup>	15
1.0 × 10 <sup>-4</sup>	4.0 × 10 <sup>-3</sup>	21
1.0 × 10 <sup>-4</sup>	5.0 × 10 <sup>-3</sup>	27

$$k_2 = 6.0 \times 10^3 \text{ L mol}^{-1} \text{ s}^{-1}$$

Table S23. Kinetics of the reaction of DDQ (**1a**) with Bu<sub>3</sub>SnH (**2n**) in c-Hexane (20 °C, Stopped-flow, at 286 nm)

[DDQ] / mol L <sup>-1</sup>	[ <b>2n</b> ] / mol L <sup>-1</sup>	k <sub>obs</sub> / s <sup>-1</sup>
1.0 × 10 <sup>-4</sup>	1.0 × 10 <sup>-3</sup>	1.7 × 10 <sup>-2</sup>
1.0 × 10 <sup>-4</sup>	2.0 × 10 <sup>-3</sup>	3.2 × 10 <sup>-2</sup>
1.0 × 10 <sup>-4</sup>	3.0 × 10 <sup>-3</sup>	4.6 × 10 <sup>-2</sup>
1.0 × 10 <sup>-4</sup>	4.0 × 10 <sup>-3</sup>	5.8 × 10 <sup>-2</sup>
1.0 × 10 <sup>-4</sup>	5.0 × 10 <sup>-3</sup>	7.7 × 10 <sup>-2</sup>

$$k_2 = 15 \text{ L mol}^{-1} \text{ s}^{-1}$$

Table S24. Kinetics of the reaction of DDQ (**1a**) with Bu<sub>3</sub>SnH (**2n**) in acetone (20 °C, Stopped-flow, at 350 nm)

[DDQ] / mol L <sup>-1</sup>	[ <b>2n</b> ] / mol L <sup>-1</sup>	k <sub>obs</sub> / s <sup>-1</sup>
1.0 × 10 <sup>-4</sup>	1.0 × 10 <sup>-3</sup>	0.26
1.0 × 10 <sup>-4</sup>	2.0 × 10 <sup>-3</sup>	0.57
1.0 × 10 <sup>-4</sup>	3.0 × 10 <sup>-3</sup>	0.96
1.0 × 10 <sup>-4</sup>	4.0 × 10 <sup>-3</sup>	1.3
1.0 × 10 <sup>-4</sup>	5.0 × 10 <sup>-3</sup>	1.7

$$k_2 = 3.6 \times 10^2 \text{ L mol}^{-1} \text{ s}^{-1}$$

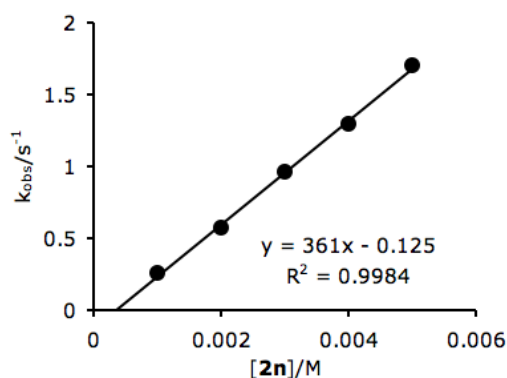
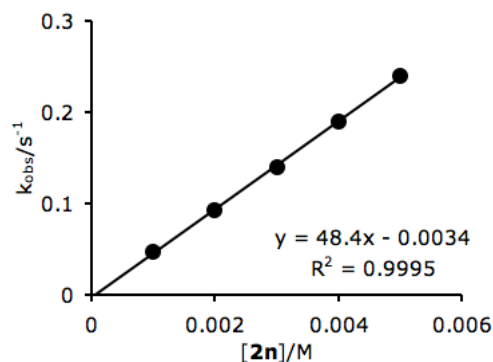


Table S25. Kinetics of the reaction of DDQ (**1a**) with Bu<sub>3</sub>SnH (**2n**) in THF (20 °C, Stopped-flow, at 286 nm)

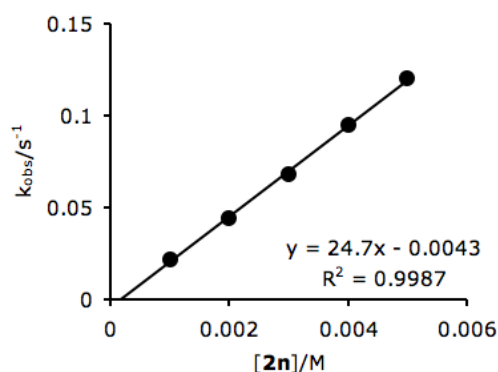
[DDQ] / mol L <sup>-1</sup>	[ <b>2n</b> ] / mol L <sup>-1</sup>	k <sub>obs</sub> / s <sup>-1</sup>
1.0 × 10 <sup>-4</sup>	1.0 × 10 <sup>-3</sup>	4.7 × 10 <sup>-2</sup>
1.0 × 10 <sup>-4</sup>	2.0 × 10 <sup>-3</sup>	9.2 × 10 <sup>-2</sup>
1.0 × 10 <sup>-4</sup>	3.0 × 10 <sup>-3</sup>	0.14
1.0 × 10 <sup>-4</sup>	4.0 × 10 <sup>-3</sup>	0.19
1.0 × 10 <sup>-4</sup>	5.0 × 10 <sup>-3</sup>	0.24

$$k_2 = 4.8 \times 10^1 \text{ L mol}^{-1} \text{ s}^{-1}$$

Table S26. Kinetics of the reaction of DDQ (**1a**) with Bu<sub>3</sub>SnH (**2n**) in *n*-Bu<sub>2</sub>O (20 °C, Stopped-flow, at 286 nm)

[DDQ] / mol L <sup>-1</sup>	[ <b>2n</b> ] / mol L <sup>-1</sup>	k <sub>obs</sub> / s <sup>-1</sup>
1.0 × 10 <sup>-4</sup>	1.0 × 10 <sup>-3</sup>	2.2 × 10 <sup>-2</sup>
1.0 × 10 <sup>-4</sup>	2.0 × 10 <sup>-3</sup>	4.4 × 10 <sup>-2</sup>
1.0 × 10 <sup>-4</sup>	3.0 × 10 <sup>-3</sup>	6.8 × 10 <sup>-2</sup>
1.0 × 10 <sup>-4</sup>	4.0 × 10 <sup>-3</sup>	9.5 × 10 <sup>-2</sup>
1.0 × 10 <sup>-4</sup>	5.0 × 10 <sup>-3</sup>	1.2 × 10 <sup>-1</sup>

$$k_2 = 2.5 \times 10^1 \text{ L mol}^{-1} \text{ s}^{-1}$$

Table S27. Kinetics of the reaction of DDQ (**1a**) with **2n-D** in CH<sub>2</sub>Cl<sub>2</sub> (20 °C, Stopped-flow, at 286 nm)

[DDQ] / mol L <sup>-1</sup>	[ <b>2n-D</b> ] / mol L <sup>-1</sup>	k <sub>obs</sub> / s <sup>-1</sup>
1.0 × 10 <sup>-4</sup>	1.0 × 10 <sup>-3</sup>	0.34
1.0 × 10 <sup>-4</sup>	2.0 × 10 <sup>-3</sup>	0.67
1.0 × 10 <sup>-4</sup>	3.0 × 10 <sup>-3</sup>	1.0
1.0 × 10 <sup>-4</sup>	4.0 × 10 <sup>-3</sup>	1.4
1.0 × 10 <sup>-4</sup>	5.0 × 10 <sup>-3</sup>	1.8

$$k_2 = 3.7 \times 10^2 \text{ L mol}^{-1} \text{ s}^{-1}$$

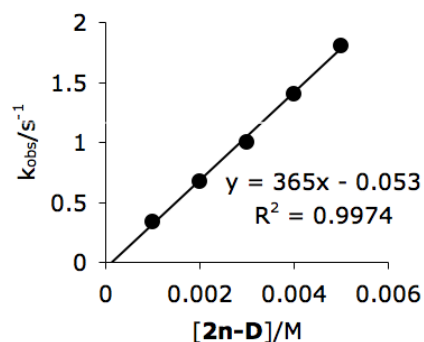
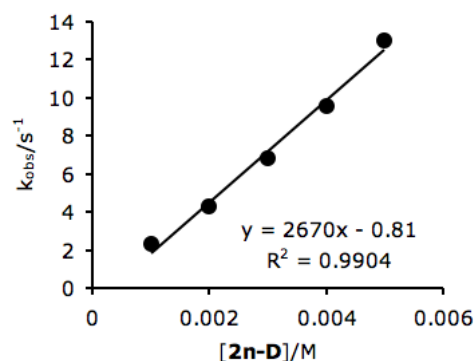




Table S28. Kinetics of the reaction of DDQ (**1a**) with **2n-D** in CH<sub>3</sub>CN (20 °C, Stopped-flow, at 286 nm)

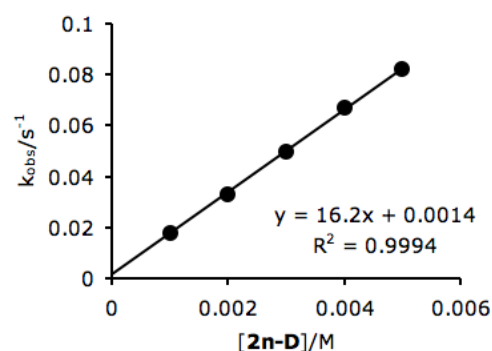
[DDQ] / mol L <sup>-1</sup>	[ <b>2n-D</b> ] / mol L <sup>-1</sup>	k <sub>obs</sub> / s <sup>-1</sup>
1.0 × 10 <sup>-4</sup>	1.0 × 10 <sup>-3</sup>	2.3
1.0 × 10 <sup>-4</sup>	2.0 × 10 <sup>-3</sup>	4.3
1.0 × 10 <sup>-4</sup>	3.0 × 10 <sup>-3</sup>	6.8
1.0 × 10 <sup>-4</sup>	4.0 × 10 <sup>-3</sup>	9.6
1.0 × 10 <sup>-4</sup>	5.0 × 10 <sup>-3</sup>	13

$$k_2 = 2.7 \times 10^3 \text{ L mol}^{-1} \text{ s}^{-1}$$

Table S29. Kinetics of the reaction of DDQ (**1a**) with **2n-D** in c-Hexane (20 °C, Stopped-flow, at 286 nm)

[DDQ] / mol L <sup>-1</sup>	[ <b>2n-D</b> ] / mol L <sup>-1</sup>	k <sub>obs</sub> / s <sup>-1</sup>
1.0 × 10 <sup>-4</sup>	1.0 × 10 <sup>-3</sup>	1.8 × 10 <sup>-2</sup>
1.0 × 10 <sup>-4</sup>	2.0 × 10 <sup>-2</sup>	3.3 × 10 <sup>-2</sup>
1.0 × 10 <sup>-4</sup>	3.0 × 10 <sup>-2</sup>	5.0 × 10 <sup>-2</sup>
1.0 × 10 <sup>-4</sup>	4.0 × 10 <sup>-2</sup>	6.7 × 10 <sup>-2</sup>
1.0 × 10 <sup>-4</sup>	5.0 × 10 <sup>-2</sup>	8.2 × 10 <sup>-2</sup>

$$k_2 = 1.6 \times 10^1 \text{ L mol}^{-1} \text{ s}^{-1}$$

Table S30. Kinetics of the reaction of DDQ (**1a**) with **2n-D** in acetone (20 °C, Stopped-flow, at 350 nm)

[DDQ] / mol L <sup>-1</sup>	[ <b>2n-D</b> ] / mol L <sup>-1</sup>	k <sub>obs</sub> / s <sup>-1</sup>
1.0 × 10 <sup>-4</sup>	1.0 × 10 <sup>-3</sup>	0.26
1.0 × 10 <sup>-4</sup>	2.0 × 10 <sup>-3</sup>	0.49
1.0 × 10 <sup>-4</sup>	3.0 × 10 <sup>-3</sup>	0.77
1.0 × 10 <sup>-4</sup>	4.0 × 10 <sup>-3</sup>	1.1
1.0 × 10 <sup>-4</sup>	5.0 × 10 <sup>-3</sup>	1.3

$$k_2 = 2.7 \times 10^2 \text{ L mol}^{-1} \text{ s}^{-1}$$

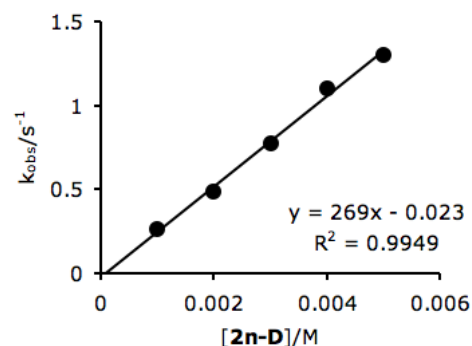
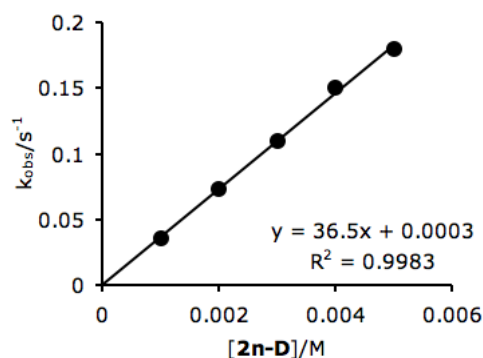


Table S31. Kinetics of the reaction of DDQ (**1a**) with **2n-D** in THF (20 °C, Stopped-flow, at 286 nm)

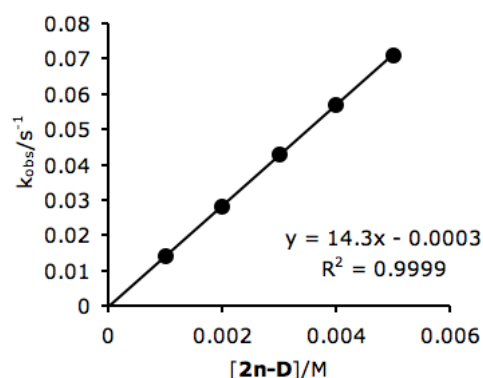
[DDQ] / mol L <sup>-1</sup>	[ <b>2n-D</b> ] / mol L <sup>-1</sup>	k <sub>obs</sub> / s <sup>-1</sup>
1.0 × 10 <sup>-4</sup>	1.0 × 10 <sup>-3</sup>	3.6 × 10 <sup>-2</sup>
1.0 × 10 <sup>-4</sup>	2.0 × 10 <sup>-3</sup>	7.3 × 10 <sup>-2</sup>
1.0 × 10 <sup>-4</sup>	3.0 × 10 <sup>-3</sup>	0.11
1.0 × 10 <sup>-4</sup>	4.0 × 10 <sup>-3</sup>	0.15
1.0 × 10 <sup>-4</sup>	5.0 × 10 <sup>-3</sup>	0.18

$$k_2 = 3.7 \times 10^1 \text{ L mol}^{-1} \text{ s}^{-1}$$

Table S32. Kinetics of the reaction of DDQ (**1a**) with **2n-D** in *n*-Bu<sub>2</sub>O (20 °C, Stopped-flow, at 286 nm)

[DDQ] / mol L <sup>-1</sup>	[ <b>2n-D</b> ] / mol L <sup>-1</sup>	k <sub>obs</sub> / s <sup>-1</sup>
1.0 × 10 <sup>-4</sup>	1.0 × 10 <sup>-3</sup>	1.4 × 10 <sup>-2</sup>
1.0 × 10 <sup>-4</sup>	2.0 × 10 <sup>-3</sup>	2.8 × 10 <sup>-2</sup>
1.0 × 10 <sup>-4</sup>	3.0 × 10 <sup>-3</sup>	4.3 × 10 <sup>-2</sup>
1.0 × 10 <sup>-4</sup>	4.0 × 10 <sup>-3</sup>	5.7 × 10 <sup>-2</sup>
1.0 × 10 <sup>-4</sup>	5.0 × 10 <sup>-3</sup>	7.1 × 10 <sup>-2</sup>

$$k_2 = 1.4 \times 10^1 \text{ L mol}^{-1} \text{ s}^{-1}$$

Table S33. Kinetics of the reaction of DDQ (**1a**) with Ph<sub>3</sub>SnH (**2o**) in CH<sub>2</sub>Cl<sub>2</sub> (20 °C, Stopped-flow, at 350 nm)

[DDQ] / mol L <sup>-1</sup>	[ <b>2o</b> ] / mol L <sup>-1</sup>	k <sub>obs</sub> / s <sup>-1</sup>
1.0 × 10 <sup>-4</sup>	1.0 × 10 <sup>-2</sup>	1.6 × 10 <sup>-2</sup>
1.0 × 10 <sup>-4</sup>	2.0 × 10 <sup>-2</sup>	3.4 × 10 <sup>-2</sup>
1.0 × 10 <sup>-4</sup>	3.0 × 10 <sup>-2</sup>	5.3 × 10 <sup>-2</sup>
1.0 × 10 <sup>-4</sup>	4.0 × 10 <sup>-2</sup>	7.7 × 10 <sup>-2</sup>
1.0 × 10 <sup>-4</sup>	5.0 × 10 <sup>-2</sup>	0.10

$$k_2 = 2.1 \text{ L mol}^{-1} \text{ s}^{-1}$$

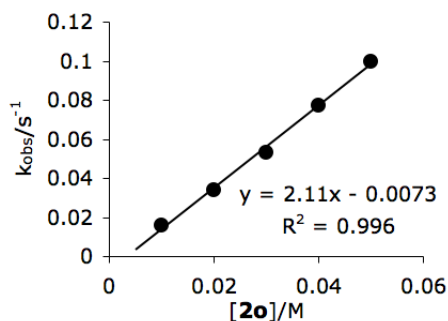
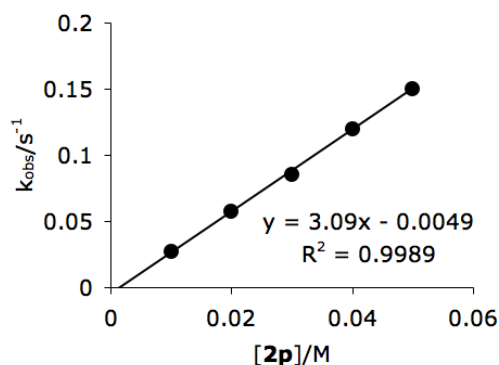


Table S34. Kinetics of the reaction of DDQ (**1a**) with Me<sub>3</sub>N-BH<sub>3</sub> (**2p**) in CH<sub>2</sub>Cl<sub>2</sub> (20 °C, Stopped-flow, at 286 nm)

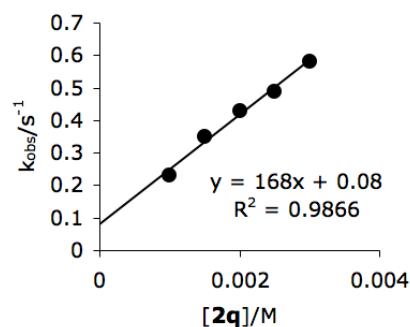
[DDQ] / mol L <sup>-1</sup>	[ <b>2p</b> ] / mol L <sup>-1</sup>	k <sub>obs</sub> / s <sup>-1</sup>
1.0 × 10 <sup>-4</sup>	1.0 × 10 <sup>-2</sup>	2.7 × 10 <sup>-2</sup>
1.0 × 10 <sup>-4</sup>	2.0 × 10 <sup>-2</sup>	5.7 × 10 <sup>-2</sup>
1.0 × 10 <sup>-4</sup>	3.0 × 10 <sup>-2</sup>	8.5 × 10 <sup>-2</sup>
1.0 × 10 <sup>-4</sup>	4.0 × 10 <sup>-2</sup>	0.12
1.0 × 10 <sup>-4</sup>	5.0 × 10 <sup>-2</sup>	0.15

$$k_2 = 3.1 \text{ L mol}^{-1} \text{ s}^{-1}$$

Table S35. Kinetics of the reaction of DDQ (**1a**) with Et<sub>3</sub>N-BH<sub>3</sub> (**2q**) in CH<sub>2</sub>Cl<sub>2</sub> (20 °C, Stopped-flow, at 286 nm)

[DDQ] / mol L <sup>-1</sup>	[ <b>2q</b> ] / mol L <sup>-1</sup>	k <sub>obs</sub> / s <sup>-1</sup>
1.0 × 10 <sup>-4</sup>	1.0 × 10 <sup>-3</sup>	0.23
1.0 × 10 <sup>-4</sup>	1.5 × 10 <sup>-3</sup>	0.35
1.0 × 10 <sup>-4</sup>	2.0 × 10 <sup>-3</sup>	0.43
1.0 × 10 <sup>-4</sup>	2.5 × 10 <sup>-3</sup>	0.49
1.0 × 10 <sup>-4</sup>	3.0 × 10 <sup>-3</sup>	0.58

$$k_2 = 1.7 \times 10^2 \text{ L mol}^{-1} \text{ s}^{-1}$$

Table S36. Kinetics of the reaction of DDQ (**1a**) with Py-BH<sub>3</sub> (**2r**) in CH<sub>2</sub>Cl<sub>2</sub> (20 °C, Stopped-flow, at 286 nm)

[DDQ] / mol L <sup>-1</sup>	[ <b>2r</b> ] / mol L <sup>-1</sup>	k <sub>obs</sub> / s <sup>-1</sup>
1.0 × 10 <sup>-4</sup>	1.0 × 10 <sup>-3</sup>	7.3
1.0 × 10 <sup>-4</sup>	2.0 × 10 <sup>-3</sup>	13
1.0 × 10 <sup>-4</sup>	3.0 × 10 <sup>-3</sup>	17
1.0 × 10 <sup>-4</sup>	4.0 × 10 <sup>-3</sup>	23
1.0 × 10 <sup>-4</sup>	5.0 × 10 <sup>-3</sup>	28

$$k_2 = 5.1 \times 10^3 \text{ mol}^{-1} \text{ L s}^{-1}$$

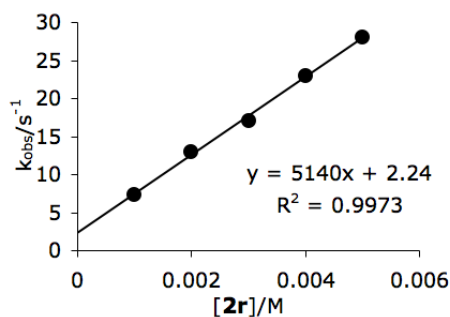
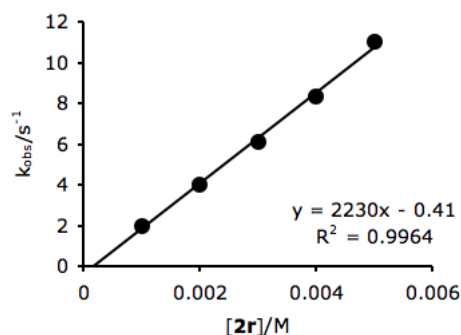


Table S37. Kinetics of the reaction of DDQ (**1a**) with Py-BH<sub>3</sub> (**2r**) in CH<sub>3</sub>CN (20 °C, Stopped-flow, at 286 nm)

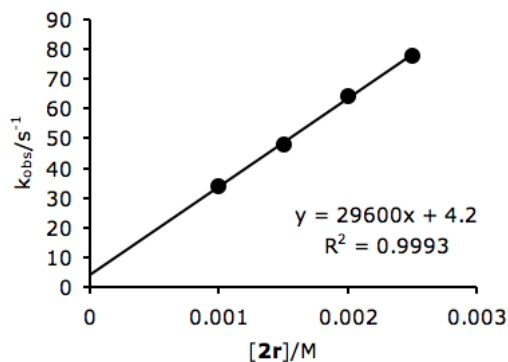
[DDQ] / mol L <sup>-1</sup>	[ <b>2r</b> ] / mol L <sup>-1</sup>	k <sub>obs</sub> / s <sup>-1</sup>
1.0 × 10 <sup>-4</sup>	1.0 × 10 <sup>-3</sup>	2.0
1.0 × 10 <sup>-4</sup>	2.0 × 10 <sup>-3</sup>	4.0
1.0 × 10 <sup>-4</sup>	3.0 × 10 <sup>-3</sup>	6.1
1.0 × 10 <sup>-4</sup>	4.0 × 10 <sup>-3</sup>	8.3
1.0 × 10 <sup>-4</sup>	5.0 × 10 <sup>-3</sup>	11

$$k_2 = 2.2 \times 10^3 \text{ L mol}^{-1} \text{ s}^{-1}$$

Table S38. Kinetics of the reaction of DDQ (**1a**) with Py-BH<sub>3</sub> (**2r**) in c-Hexane (20 °C, Stopped-flow, at 286 nm)

[DDQ] / mol L <sup>-1</sup>	[ <b>2r</b> ] / mol L <sup>-1</sup>	k <sub>obs</sub> / s <sup>-1</sup>
1.0 × 10 <sup>-4</sup>	1.0 × 10 <sup>-3</sup>	34
1.0 × 10 <sup>-4</sup>	1.5 × 10 <sup>-3</sup>	48
1.0 × 10 <sup>-4</sup>	2.0 × 10 <sup>-3</sup>	64
1.0 × 10 <sup>-4</sup>	2.5 × 10 <sup>-3</sup>	78

$$k_2 = 3.0 \times 10^4 \text{ L mol}^{-1} \text{ s}^{-1}$$

Table S39. Kinetics of the reaction of DDQ (**1a**) with Py-BH<sub>3</sub> (**2r**) in acetone (20 °C, Stopped-flow, at 350 nm)

[DDQ] / mol L <sup>-1</sup>	[ <b>2r</b> ] / mol L <sup>-1</sup>	k <sub>obs</sub> / s <sup>-1</sup>
1.0 × 10 <sup>-4</sup>	1.0 × 10 <sup>-3</sup>	0.90
1.0 × 10 <sup>-4</sup>	2.0 × 10 <sup>-3</sup>	2.0
1.0 × 10 <sup>-4</sup>	3.0 × 10 <sup>-3</sup>	3.6
1.0 × 10 <sup>-4</sup>	4.0 × 10 <sup>-3</sup>	5.4
1.0 × 10 <sup>-4</sup>	5.0 × 10 <sup>-3</sup>	7.6

$$k_2 = 1.7 \times 10^3 \text{ L mol}^{-1} \text{ s}^{-1}$$

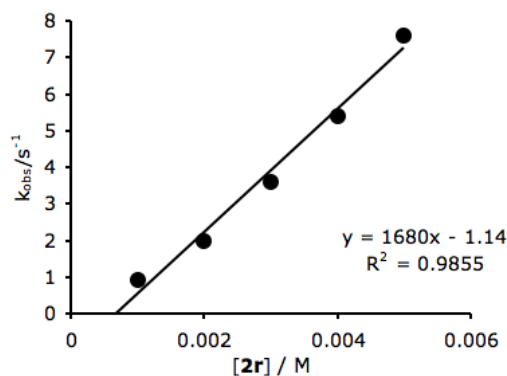
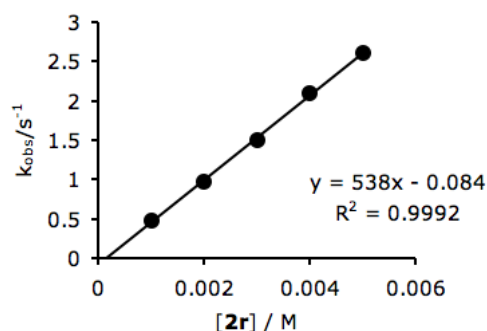


Table S40. Kinetics of the reaction of DDQ (**1a**) with Py-BH<sub>3</sub> (**2r**) in THF (20 °C, Stopped-flow, at 286 nm)

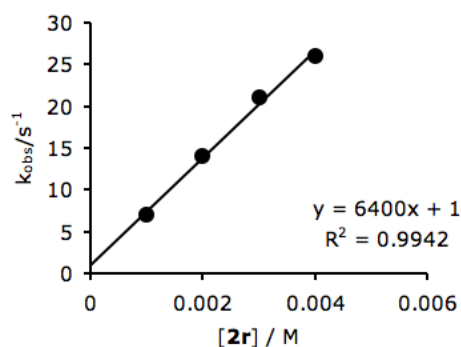
[DDQ] / mol L <sup>-1</sup>	[ <b>2r</b> ] / mol L <sup>-1</sup>	k <sub>obs</sub> / s <sup>-1</sup>
1.0 × 10 <sup>-4</sup>	1.0 × 10 <sup>-3</sup>	0.47
1.0 × 10 <sup>-4</sup>	2.0 × 10 <sup>-3</sup>	0.98
1.0 × 10 <sup>-4</sup>	3.0 × 10 <sup>-3</sup>	1.5
1.0 × 10 <sup>-4</sup>	4.0 × 10 <sup>-3</sup>	2.1
1.0 × 10 <sup>-4</sup>	5.0 × 10 <sup>-3</sup>	2.6

$$k_2 = 5.4 \times 10^2 \text{ L mol}^{-1} \text{ s}^{-1}$$

Table S41. Kinetics of the reaction of DDQ (**1a**) with Py-BH<sub>3</sub> (**2r**) in *n*-Bu<sub>2</sub>O (20 °C, Stopped-flow, at 286 nm)

[DDQ] / mol L <sup>-1</sup>	[ <b>2r</b> ] / mol L <sup>-1</sup>	k <sub>obs</sub> / s <sup>-1</sup>
1.0 × 10 <sup>-4</sup>	1.0 × 10 <sup>-3</sup>	7.0
1.0 × 10 <sup>-4</sup>	2.0 × 10 <sup>-3</sup>	14
1.0 × 10 <sup>-4</sup>	3.0 × 10 <sup>-3</sup>	21
1.0 × 10 <sup>-4</sup>	4.0 × 10 <sup>-3</sup>	26

$$k_2 = 6.4 \times 10^3 \text{ L mol}^{-1} \text{ s}^{-1}$$

Table S42. Kinetics of the reaction of DDQ (**1a**) with **2r-D<sub>3</sub>** in CH<sub>2</sub>Cl<sub>2</sub> (20 °C, Stopped-flow, at 286 nm)

[DDQ] / mol L <sup>-1</sup>	[ <b>2r-D<sub>3</sub></b> ] / mol L <sup>-1</sup>	k <sub>obs</sub> / s <sup>-1</sup>
1.0 × 10 <sup>-4</sup>	1.0 × 10 <sup>-3</sup>	2.8
1.0 × 10 <sup>-4</sup>	2.0 × 10 <sup>-3</sup>	5.8
1.0 × 10 <sup>-4</sup>	3.0 × 10 <sup>-3</sup>	8.7
1.0 × 10 <sup>-4</sup>	4.0 × 10 <sup>-3</sup>	11
1.0 × 10 <sup>-4</sup>	5.0 × 10 <sup>-3</sup>	14

$$k_2 = 2.8 \times 10^3 \text{ L mol}^{-1} \text{ s}^{-1}$$

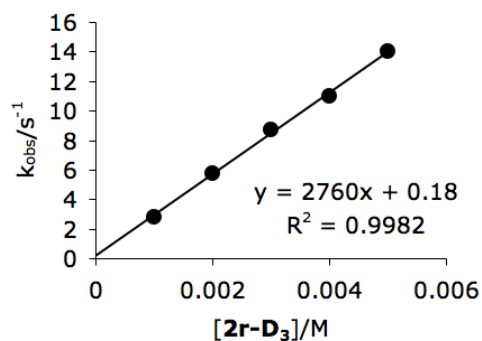
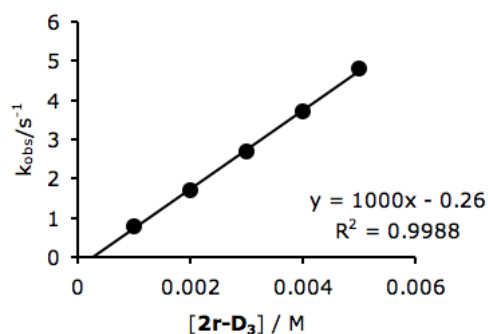


Table S43. Kinetics of the reaction of DDQ (**1a**) with **2r-D<sub>3</sub>** in CH<sub>3</sub>CN (20 °C, Stopped-flow, at 286 nm)

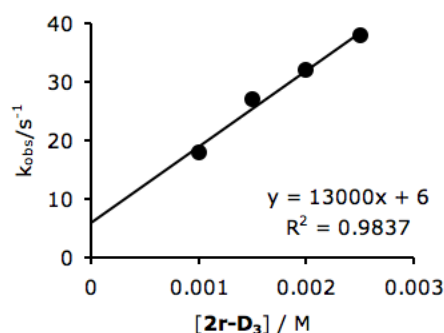
[DDQ] / mol L <sup>-1</sup>	[ <b>2r-D<sub>3</sub></b> ] / mol L <sup>-1</sup>	k <sub>obs</sub> / s <sup>-1</sup>
1.0 × 10 <sup>-4</sup>	1.0 × 10 <sup>-3</sup>	0.8
1.0 × 10 <sup>-4</sup>	2.0 × 10 <sup>-3</sup>	1.7
1.0 × 10 <sup>-4</sup>	3.0 × 10 <sup>-3</sup>	2.7
1.0 × 10 <sup>-4</sup>	4.0 × 10 <sup>-3</sup>	3.7
1.0 × 10 <sup>-4</sup>	5.0 × 10 <sup>-3</sup>	4.8

$$k_2 = 1.0 \times 10^3 \text{ L mol}^{-1} \text{ s}^{-1}$$

Table S44. Kinetics of the reaction of DDQ (**1a**) with **2r-D<sub>3</sub>** in c-Hexane (20 °C, Stopped-flow, at 286 nm)

[DDQ] / mol L <sup>-1</sup>	[ <b>2r-D<sub>3</sub></b> ] / mol L <sup>-1</sup>	k <sub>obs</sub> / s <sup>-1</sup>
1.0 × 10 <sup>-4</sup>	1.0 × 10 <sup>-3</sup>	18
1.0 × 10 <sup>-4</sup>	1.5 × 10 <sup>-3</sup>	27
1.0 × 10 <sup>-4</sup>	2.0 × 10 <sup>-3</sup>	32
1.0 × 10 <sup>-4</sup>	2.5 × 10 <sup>-3</sup>	38

$$k_2 = 1.3 \times 10^4 \text{ L mol}^{-1} \text{ s}^{-1}$$

Table S45. Kinetics of the reaction of DDQ (**1a**) with **2r-D<sub>3</sub>** in acetone (20 °C, Stopped-flow, at 350 nm)

[DDQ] / mol L <sup>-1</sup>	[ <b>2r-D<sub>3</sub></b> ] / mol L <sup>-1</sup>	k <sub>obs</sub> / s <sup>-1</sup>
1.0 × 10 <sup>-4</sup>	1.0 × 10 <sup>-3</sup>	0.55
1.0 × 10 <sup>-4</sup>	2.0 × 10 <sup>-3</sup>	1.2
1.0 × 10 <sup>-4</sup>	3.0 × 10 <sup>-3</sup>	2.0
1.0 × 10 <sup>-4</sup>	4.0 × 10 <sup>-3</sup>	2.8
1.0 × 10 <sup>-4</sup>	5.0 × 10 <sup>-3</sup>	3.7

$$k_2 = 7.9 \times 10^2 \text{ L mol}^{-1} \text{ s}^{-1}$$

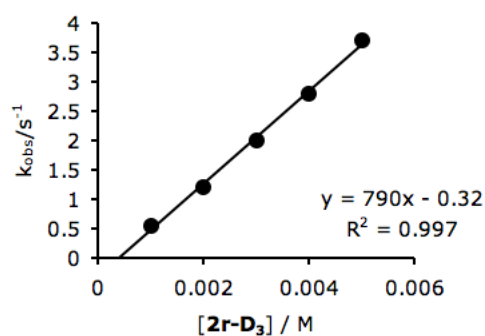
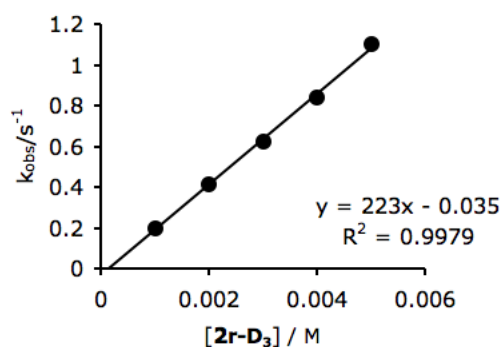


Table S46. Kinetics of the reaction of DDQ (**1a**) with **2r-D<sub>3</sub>** in THF (20 °C, Stopped-flow, at 286 nm)

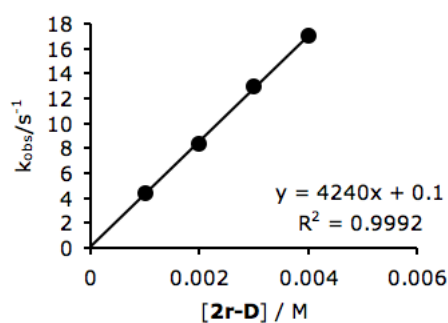
[DDQ] / mol L <sup>-1</sup>	[ <b>2r-D<sub>3</sub></b> ] / mol L <sup>-1</sup>	k <sub>obs</sub> / s <sup>-1</sup>
1.0 × 10 <sup>-4</sup>	1.0 × 10 <sup>-3</sup>	0.20
1.0 × 10 <sup>-4</sup>	2.0 × 10 <sup>-3</sup>	0.41
1.0 × 10 <sup>-4</sup>	3.0 × 10 <sup>-3</sup>	0.62
1.0 × 10 <sup>-4</sup>	4.0 × 10 <sup>-3</sup>	0.84
1.0 × 10 <sup>-4</sup>	5.0 × 10 <sup>-3</sup>	1.1

$$k_2 = 2.2 \times 10^2 \text{ L mol}^{-1} \text{ s}^{-1}$$

Table S47. Kinetics of the reaction of DDQ (**1a**) with **2r-D<sub>3</sub>** in *n*-Bu<sub>2</sub>O (20 °C, Stopped-flow, at 286 nm)

[DDQ] / mol L <sup>-1</sup>	[ <b>2r-D<sub>3</sub></b> ] / mol L <sup>-1</sup>	k <sub>obs</sub> / s <sup>-1</sup>
1.0 × 10 <sup>-4</sup>	1.0 × 10 <sup>-3</sup>	4.4
1.0 × 10 <sup>-4</sup>	2.0 × 10 <sup>-3</sup>	8.4
1.0 × 10 <sup>-4</sup>	3.0 × 10 <sup>-3</sup>	13
1.0 × 10 <sup>-4</sup>	4.0 × 10 <sup>-3</sup>	17

$$k_2 = 4.2 \times 10^3 \text{ L mol}^{-1} \text{ s}^{-1}$$

Table S48. Kinetics of the reaction of DDQ (**1a**) with 1,3-bis-(2,6-diisopropylphenyl)imidazolydene borane complex (**2s**) in CH<sub>2</sub>Cl<sub>2</sub> (20 °C, Stopped-flow, at 286 nm)

[DDQ] / mol L <sup>-1</sup>	[ <b>2s</b> ] / mol L <sup>-1</sup>	k <sub>obs</sub> / s <sup>-1</sup>
1.0 × 10 <sup>-4</sup>	1.0 × 10 <sup>-3</sup>	2.8
1.0 × 10 <sup>-4</sup>	1.5 × 10 <sup>-3</sup>	4.0
1.0 × 10 <sup>-4</sup>	2.0 × 10 <sup>-3</sup>	5.4
1.0 × 10 <sup>-4</sup>	2.5 × 10 <sup>-3</sup>	7.1

$$k_2 = 2.9 \times 10^3 \text{ mol}^{-1} \text{ L s}^{-1}$$

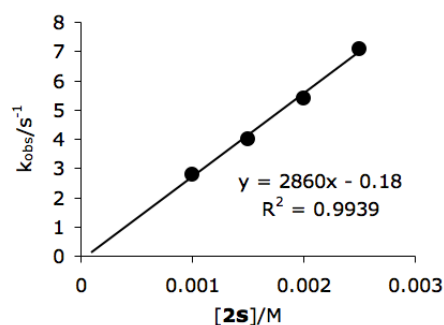
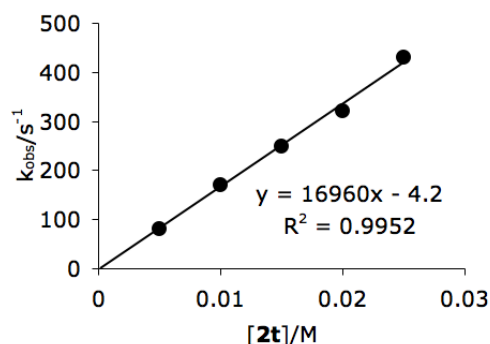


Table S49. Kinetics of the reaction of DDQ (**1a**) with 1,3-dimethylimidazolydene borane complex (**2t**) in CH<sub>2</sub>Cl<sub>2</sub> (20 °C, Stopped-flow, at 286 nm)

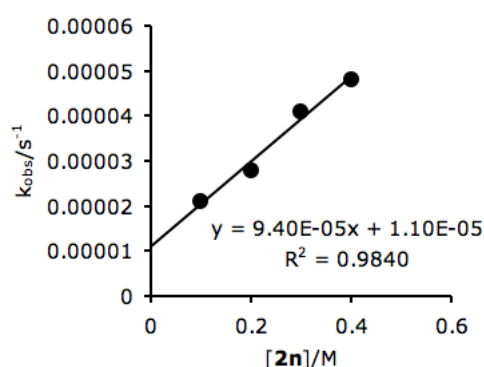
[DDQ] / mol L <sup>-1</sup>	[ <b>2t</b> ] / mol L <sup>-1</sup>	k <sub>obs</sub> / s <sup>-1</sup>
1.0 × 10 <sup>-4</sup>	5.0 × 10 <sup>-3</sup>	81
1.0 × 10 <sup>-4</sup>	1.0 × 10 <sup>-2</sup>	1.7 × 10 <sup>2</sup>
1.0 × 10 <sup>-4</sup>	1.5 × 10 <sup>-2</sup>	2.5 × 10 <sup>2</sup>
1.0 × 10 <sup>-4</sup>	2.0 × 10 <sup>-2</sup>	3.2 × 10 <sup>2</sup>
1.0 × 10 <sup>-4</sup>	2.5 × 10 <sup>-2</sup>	4.3 × 10 <sup>2</sup>

$$k_2 = 1.7 \times 10^4 \text{ mol}^{-1} \text{ L s}^{-1}$$

2). Kinetics of the Reactions of Bu<sub>3</sub>SnH (**2n**) with Other QuinonesTable S50. Kinetics of the reaction of Bu<sub>3</sub>SnH (**2n**) with benzoquinone (**1f**) in CD<sub>3</sub>CN (20 °C, <sup>1</sup>H NMR, 4.58-4.69 ppm)

[ <b>1f</b> ] / mol L <sup>-1</sup>	[ <b>2n</b> ] / mol L <sup>-1</sup>	k <sub>obs</sub> / s <sup>-1</sup>
1.5 × 10 <sup>-2</sup>	1.0 × 10 <sup>-1</sup>	2.1 × 10 <sup>-5</sup>
2.0 × 10 <sup>-2</sup>	2.0 × 10 <sup>-1</sup>	2.8 × 10 <sup>-5</sup>
2.0 × 10 <sup>-2</sup>	3.0 × 10 <sup>-1</sup>	4.1 × 10 <sup>-5</sup>
2.0 × 10 <sup>-2</sup>	4.0 × 10 <sup>-1</sup>	4.8 × 10 <sup>-5</sup>

$$k_2 = 9.4 \times 10^{-5} \text{ L mol}^{-1} \text{ s}^{-1}$$

Table S51. Kinetics of the reaction of Bu<sub>3</sub>SnH (**2n**) with 2,5-dichloro-benzoquinone (**1b**) in CD<sub>3</sub>CN (20 °C, Conventional UV/Vis, 270 nm)

[ <b>1b</b> ] / mol L <sup>-1</sup>	[ <b>2n</b> ] / mol L <sup>-1</sup>	k <sub>obs</sub> / s <sup>-1</sup>
1.0 × 10 <sup>-4</sup>	1.5 × 10 <sup>-2</sup>	4.5 × 10 <sup>-4</sup>
1.0 × 10 <sup>-4</sup>	2.9 × 10 <sup>-2</sup>	7.9 × 10 <sup>-4</sup>
1.0 × 10 <sup>-4</sup>	4.3 × 10 <sup>-2</sup>	1.1 × 10 <sup>-3</sup>
1.0 × 10 <sup>-4</sup>	5.7 × 10 <sup>-2</sup>	1.5 × 10 <sup>-3</sup>

$$k_2 = 2.5 \times 10^{-2} \text{ L mol}^{-1} \text{ s}^{-1}$$

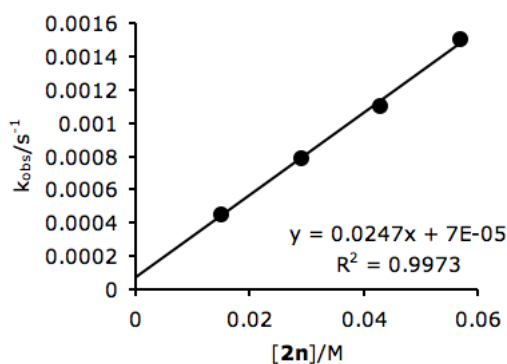
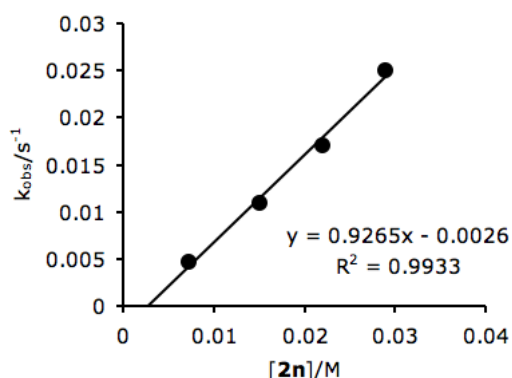




Table S52. Kinetics of the reaction of Bu<sub>3</sub>SnH (**2n**) with p-chloranil (**1c**) in CD<sub>3</sub>CN (20 °C, Conventional UV/Vis, 287 nm)

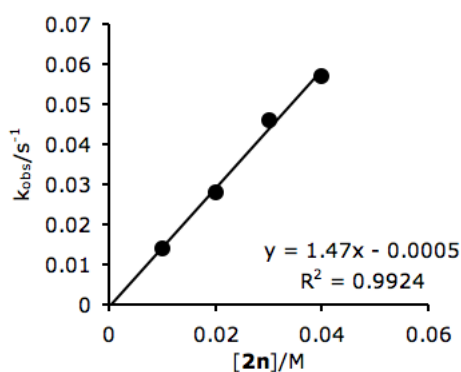
[ <b>1c</b> ] / mol L <sup>-1</sup>	[ <b>2n</b> ] / mol L <sup>-1</sup>	k <sub>obs</sub> / s <sup>-1</sup>
1.0 × 10 <sup>-4</sup>	7.3 × 10 <sup>-3</sup>	4.7 × 10 <sup>-3</sup>
1.0 × 10 <sup>-4</sup>	1.5 × 10 <sup>-2</sup>	1.1 × 10 <sup>-2</sup>
1.0 × 10 <sup>-4</sup>	2.2 × 10 <sup>-2</sup>	1.7 × 10 <sup>-2</sup>
1.0 × 10 <sup>-4</sup>	2.9 × 10 <sup>-2</sup>	2.5 × 10 <sup>-2</sup>

$$k_2 = 9.3 \times 10^{-1} \text{ L mol}^{-1} \text{ s}^{-1}$$

Table S53. Kinetics of the reaction of Bu<sub>3</sub>SnH (**2n**) with p-fluoranil (**1d**) in CD<sub>3</sub>CN (20 °C, Stopped-flow, 256 nm)

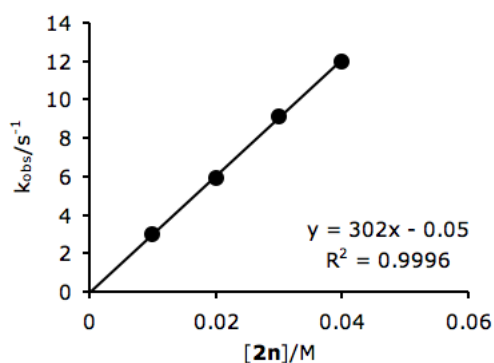
[ <b>1d</b> ] / mol L <sup>-1</sup>	[ <b>2n</b> ] / mol L <sup>-1</sup>	k <sub>obs</sub> / s <sup>-1</sup>
5.0 × 10 <sup>-5</sup>	1.0 × 10 <sup>-2</sup>	1.4 × 10 <sup>-2</sup>
5.0 × 10 <sup>-5</sup>	2.0 × 10 <sup>-2</sup>	2.8 × 10 <sup>-2</sup>
5.0 × 10 <sup>-5</sup>	3.0 × 10 <sup>-2</sup>	4.6 × 10 <sup>-2</sup>
5.0 × 10 <sup>-5</sup>	4.0 × 10 <sup>-2</sup>	5.7 × 10 <sup>-2</sup>

$$k_2 = 1.5 \text{ L mol}^{-1} \text{ s}^{-1}$$

Table S54. Kinetics of the reaction of Bu<sub>3</sub>SnH (**2n**) with o-chloranil (**1e**) in CD<sub>3</sub>CN (20 °C, Stopped-flow, 457 nm)

[ <b>1e</b> ] / mol L <sup>-1</sup>	[ <b>2n</b> ] / mol L <sup>-1</sup>	k <sub>obs</sub> / s <sup>-1</sup>
1.0 × 10 <sup>-4</sup>	1.0 × 10 <sup>-2</sup>	3.0
1.0 × 10 <sup>-4</sup>	2.0 × 10 <sup>-2</sup>	5.9
1.0 × 10 <sup>-4</sup>	3.0 × 10 <sup>-2</sup>	9.1
1.0 × 10 <sup>-4</sup>	4.0 × 10 <sup>-2</sup>	12

$$k_2 = 3.0 \times 10^2 \text{ L mol}^{-1} \text{ s}^{-1}$$



#### 4.4.3 Determination of the Nucleophilicity Parameters of **2f-i**

In order to determine the nucleophilicity parameters  $N$  and  $s_N$  for the nucleophiles **2f-i** the rates of the reactions with the benzhydrylium ions  $\text{Ar}_2\text{CH}^+$  have been determined photometrically in CH<sub>2</sub>Cl<sub>2</sub> solution. The nucleophilicity parameters of **2f-i** in CH<sub>2</sub>Cl<sub>2</sub> were

determined according to the correlation  $\log k_2 = s_N (N + E)$  by plots of the second-order rate constants ( $\log k_2$ ) for the reactions of **2f-i** with the employed benzhydrylium ions  $\text{Ar}_2\text{CH}^+$  versus the corresponding electrophilicity parameters  $E$ .

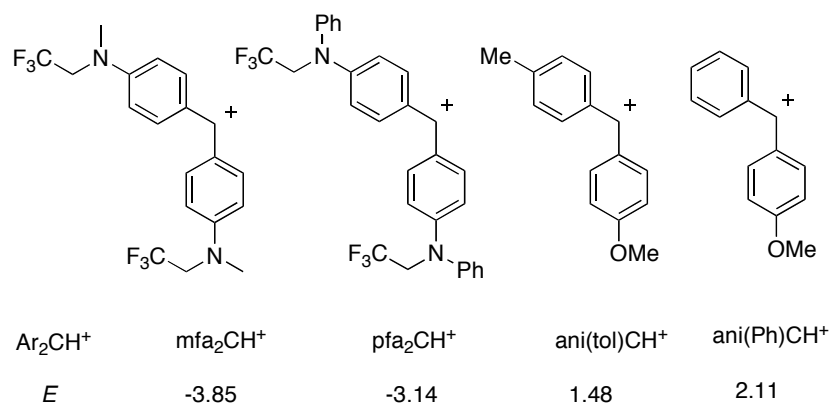


Figure S1. Benzhydrylium ions  $\text{Ar}_2\text{CH}^+$  and their electrophilicity parameters  $E^{[S5]}$  used for the determination of the nucleophilicity parameters ( $N$  and  $s_N$ ) for **2f-i** in  $\text{CH}_2\text{Cl}_2$ .

Table S55. Kinetics of the reaction of 1,4-dimethylcyclohexa-1,4-diene (**2f**) with  $\text{mfa}_2\text{CH}^+$  in  $\text{CH}_2\text{Cl}_2$  (20 °C, J&M, at 593 nm)

$[\text{mfa}_2\text{CH}^+]$ / $\text{mol L}^{-1}$	$[\text{2f}]$ / $\text{mol L}^{-1}$	$k_{\text{obs}}$ / $\text{s}^{-1}$
$1.0 \times 10^{-5}$	$3.9 \times 10^{-3}$	$4.5 \times 10^{-5}$
$1.0 \times 10^{-5}$	$4.8 \times 10^{-3}$	$5.6 \times 10^{-5}$
$1.0 \times 10^{-5}$	$5.7 \times 10^{-3}$	$6.9 \times 10^{-5}$
$1.0 \times 10^{-5}$	$7.4 \times 10^{-3}$	$8.9 \times 10^{-5}$

$$k_2 = 1.3 \times 10^{-2} \text{ L mol}^{-1} \text{ s}^{-1}$$

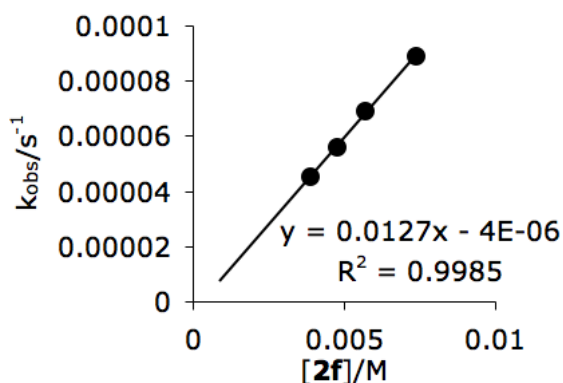


Table S56. Kinetics of the reaction of 1,4-dimethylcyclohexa-1,4-diene (**2f**) with  $\text{pfa}_2\text{CH}^+$  in  $\text{CH}_2\text{Cl}_2$  (20 °C, J&M, at 601 nm)

$[\text{pfa}_2\text{CH}^+]$ / $\text{mol L}^{-1}$	$[\text{2f}]$ / $\text{mol L}^{-1}$	$k_{\text{obs}}$ / $\text{s}^{-1}$
$1.0 \times 10^{-5}$	$1.0 \times 10^{-3}$	$6.1 \times 10^{-5}$
$1.0 \times 10^{-5}$	$2.0 \times 10^{-3}$	$1.2 \times 10^{-4}$
$1.0 \times 10^{-5}$	$3.9 \times 10^{-3}$	$2.5 \times 10^{-4}$
$1.0 \times 10^{-5}$	$4.8 \times 10^{-3}$	$2.9 \times 10^{-4}$

$$k_2 = 6.2 \times 10^{-2} \text{ L mol}^{-1} \text{ s}^{-1}$$

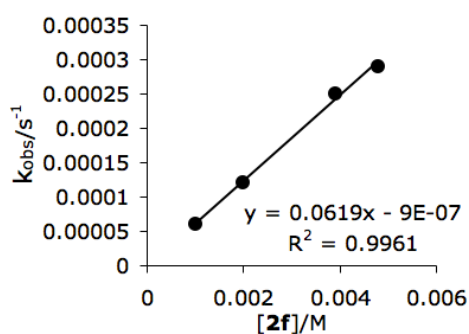
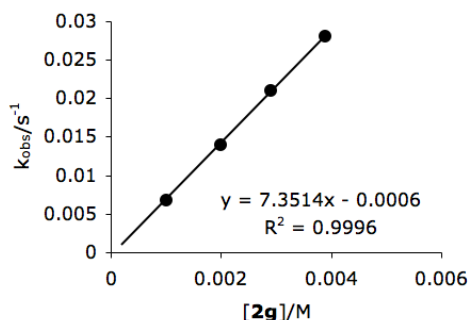


Table S57. Kinetics of the reaction of 1,3,5-trimethylcyclohexa-1,4-diene (**2g**) with mfa<sub>2</sub>CH<sup>+</sup> in CH<sub>2</sub>Cl<sub>2</sub> (20 °C, J&M, at 593 nm)

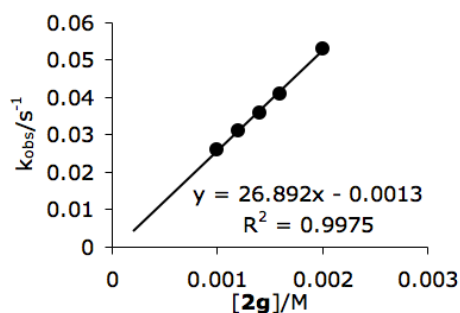
[mfa <sub>2</sub> CH <sup>+</sup> ] / mol L <sup>-1</sup>	[ <b>2g</b> ] / mol L <sup>-1</sup>	k <sub>obs</sub> / s <sup>-1</sup>
1.0 × 10 <sup>-5</sup>	1.0 × 10 <sup>-3</sup>	6.8 × 10 <sup>-3</sup>
1.0 × 10 <sup>-5</sup>	2.0 × 10 <sup>-3</sup>	1.4 × 10 <sup>-2</sup>
1.0 × 10 <sup>-5</sup>	2.9 × 10 <sup>-3</sup>	2.1 × 10 <sup>-2</sup>
1.0 × 10 <sup>-5</sup>	3.9 × 10 <sup>-3</sup>	2.8 × 10 <sup>-2</sup>

$$k_2 = 7.4 \text{ L mol}^{-1} \text{ s}^{-1}$$

Table S58. Kinetics of the reaction of 1,3,5-trimethylcyclohexa-1,4-diene (**2g**) with pfa<sub>2</sub>CH<sup>+</sup> in CH<sub>2</sub>Cl<sub>2</sub> (20 °C, Stopped-flow, at 601 nm)

[pfa <sub>2</sub> CH <sup>+</sup> ] / mol L <sup>-1</sup>	[ <b>2g</b> ] / mol L <sup>-1</sup>	k <sub>obs</sub> / s <sup>-1</sup>
1.0 × 10 <sup>-5</sup>	1.0 × 10 <sup>-3</sup>	2.6 × 10 <sup>-2</sup>
1.0 × 10 <sup>-5</sup>	1.2 × 10 <sup>-3</sup>	3.1 × 10 <sup>-2</sup>
1.0 × 10 <sup>-5</sup>	1.4 × 10 <sup>-3</sup>	3.6 × 10 <sup>-2</sup>
1.0 × 10 <sup>-5</sup>	1.6 × 10 <sup>-3</sup>	4.1 × 10 <sup>-2</sup>
1.0 × 10 <sup>-5</sup>	2.0 × 10 <sup>-3</sup>	5.3 × 10 <sup>-2</sup>

$$k_2 = 27 \text{ L mol}^{-1} \text{ s}^{-1}$$

Table S59. Kinetics of the reaction of 1,2,4,5-tetramethylcyclohexa-1,4-diene (**2h**) with mfa<sub>2</sub>CH<sup>+</sup> in CH<sub>2</sub>Cl<sub>2</sub> (20 °C, Stopped-flow, at 593 nm)

[mfa <sub>2</sub> CH <sup>+</sup> ] / mol L <sup>-1</sup>	[ <b>2h</b> ] / mol L <sup>-1</sup>	k <sub>obs</sub> / s <sup>-1</sup>
1.0 × 10 <sup>-5</sup>	1.0 × 10 <sup>-3</sup>	2.2 × 10 <sup>-3</sup>
1.0 × 10 <sup>-5</sup>	2.0 × 10 <sup>-3</sup>	4.4 × 10 <sup>-3</sup>
1.0 × 10 <sup>-5</sup>	2.9 × 10 <sup>-3</sup>	6.6 × 10 <sup>-3</sup>
1.0 × 10 <sup>-5</sup>	3.9 × 10 <sup>-3</sup>	8.8 × 10 <sup>-3</sup>

$$k_2 = 2.3 \text{ L mol}^{-1} \text{ s}^{-1}$$

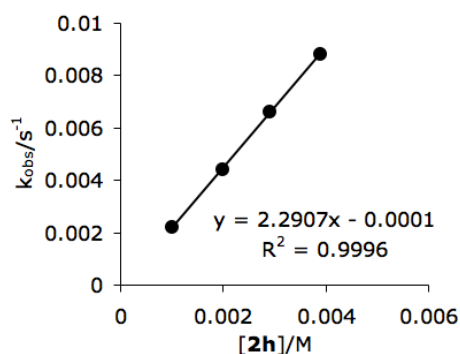
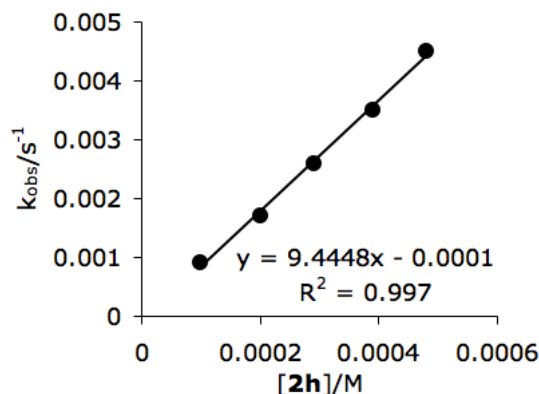


Table S60. Kinetics of the reaction of 1,2,4,5-tetramethylcyclohexa-1,4-diene (**2h**) with  $\text{pfa}_2\text{CH}^+$  in  $\text{CH}_2\text{Cl}_2$  (20 °C, J&M, at 601 nm)

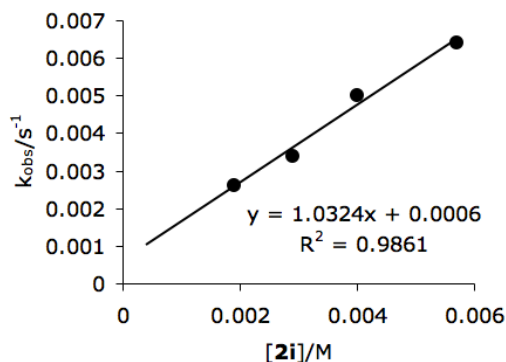
$[\text{pfa}_2\text{CH}^+]$ / mol L <sup>-1</sup>	<b>[2h]</b> / mol L <sup>-1</sup>	$k_{\text{obs}}$ / s <sup>-1</sup>
$1.0 \times 10^{-5}$	$1.0 \times 10^{-4}$	$9.1 \times 10^{-4}$
$1.0 \times 10^{-5}$	$2.0 \times 10^{-4}$	$1.7 \times 10^{-3}$
$1.0 \times 10^{-5}$	$2.9 \times 10^{-4}$	$2.6 \times 10^{-3}$
$1.0 \times 10^{-5}$	$3.9 \times 10^{-4}$	$3.5 \times 10^{-3}$
$1.0 \times 10^{-5}$	$4.8 \times 10^{-4}$	$4.5 \times 10^{-3}$

$$k_2 = 9.4 \text{ L mol}^{-1} \text{ s}^{-1}$$

Table S61. Kinetics of the reaction of bis(4-methoxyphenyl)methane (**2i**) with (ani,Ph)CH<sup>+</sup> in  $\text{CH}_2\text{Cl}_2$  (20 °C, J&M, at 513 nm)

$[(\text{ani,Ph})\text{CH}^+]$ / mol L <sup>-1</sup>	<b>[2i]</b> / mol L <sup>-1</sup>	$k_{\text{obs}}$ / s <sup>-1</sup>
$1.0 \times 10^{-5}$	$1.9 \times 10^{-3}$	$2.6 \times 10^{-3}$
$1.0 \times 10^{-5}$	$2.9 \times 10^{-3}$	$3.4 \times 10^{-3}$
$1.0 \times 10^{-5}$	$4.0 \times 10^{-3}$	$5.0 \times 10^{-3}$
$1.0 \times 10^{-5}$	$5.7 \times 10^{-3}$	$6.4 \times 10^{-3}$

$$k_2 = 1.0 \text{ L mol}^{-1} \text{ s}^{-1}$$

Table S62. Kinetics of the reaction of bis(4-methoxyphenyl)methane (**2i**) with (ani,tol)CH<sup>+</sup> in  $\text{CH}_2\text{Cl}_2$  (20 °C, J&M, at 513 nm)

$[(\text{ani,tol})\text{CH}^+]$ / mol L <sup>-1</sup>	<b>[2i]</b> / mol L <sup>-1</sup>	$k_{\text{obs}}$ / s <sup>-1</sup>
$1.0 \times 10^{-5}$	$4.0 \times 10^{-3}$	$1.2 \times 10^{-3}$
$1.0 \times 10^{-5}$	$8.1 \times 10^{-3}$	$2.0 \times 10^{-3}$
$1.0 \times 10^{-5}$	$1.6 \times 10^{-2}$	$3.8 \times 10^{-3}$
$1.0 \times 10^{-5}$	$2.0 \times 10^{-2}$	$5.1 \times 10^{-3}$

$$k_2 = 0.24 \text{ L mol}^{-1} \text{ s}^{-1}$$

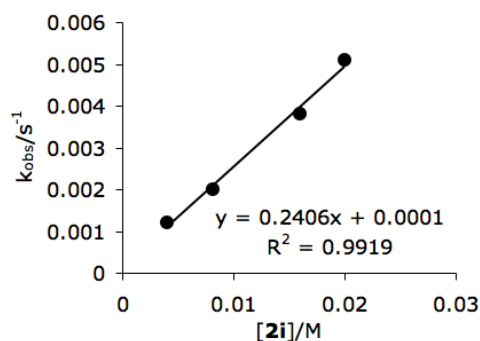


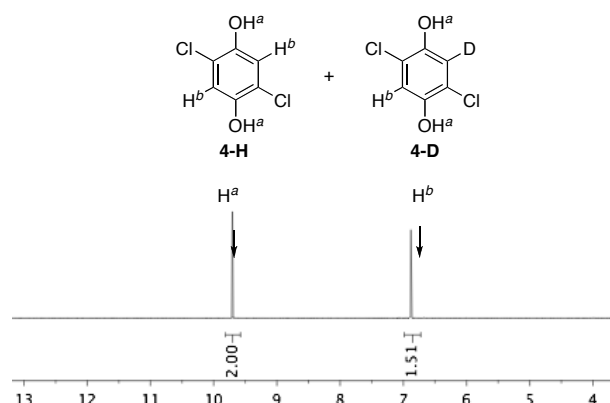
Table S63. Determination of the nucleophilicity parameters ( $N$  and  $s_N$ ) of **2f-i**.

<b>Nu</b>	Electrophile	$E$	$k_2/$ $\text{L mol}^{-1} \text{s}^{-1}$	$\log k_2$
<b>2f</b>	mfa <sub>2</sub> CH <sup>+</sup>	-3.85	$1.3 \times 10^{-2}$	-1.89
	pfa <sub>2</sub> CH <sup>+</sup>	-3.14	$6.2 \times 10^{-2}$	-1.21
	$N = 1.88, s_N = 0.96$			
<b>2g</b>	mfa <sub>2</sub> CH <sup>+</sup>	-3.85	7.4	0.87
	pfa <sub>2</sub> CH <sup>+</sup>	-3.14	27	1.43
	$N = 4.95, s_N = 0.79$			
<b>2h</b>	mfa <sub>2</sub> CH <sup>+</sup>	-3.85	2.3	0.36
	pfa <sub>2</sub> CH <sup>+</sup>	-3.14	9.4	0.97
	$N = 4.27, s_N = 0.86$			
<b>2i</b>	ani(tol)CH <sup>+</sup>	1.48	0.24	-0.62
	ani(Ph)CH <sup>+</sup>	2.11	1.0	0
	$N = -2.11, s_N = 0.98$			

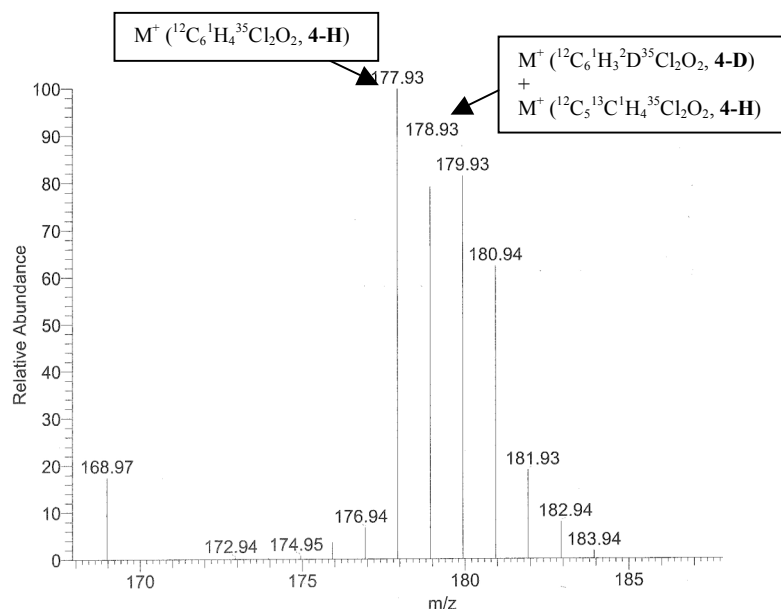
## 4.4.4 The Reaction of 2,5-Dichlorobenzoquinone (1b) with Deuterated Hydride Donors.

Procedure for the reaction of 2,5-dichlorobenzoquinone with Bu<sub>3</sub>SnD

A solution of 2,5-dichlorobenzoquinone (89 mg, 0.50 mmol) and Bu<sub>3</sub>SnD (293 mg, 1.00 mmol) in CH<sub>2</sub>Cl<sub>2</sub> was stirred at 20 °C for 6 h. The solvent was removed under reduced pressure. The crude material was purified by flash column chromatography (silica gel, eluent: MeOH/CH<sub>2</sub>Cl<sub>2</sub> = 1/10) to afford a mixture of **4-H** and **4-D** (white solid, 72 mg, 80%). The ratio [**4-H**/**4-D**] was analyzed by <sup>1</sup>H NMR and EI-MS spectroscopies.

<sup>1</sup>H NMR spectrum

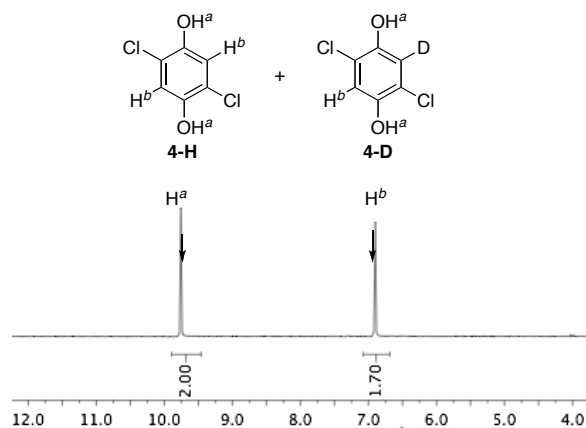
## EI-MS spectrum

Procedure for the reaction of 2,5-dichlorobenzoquinone with PyBD<sub>3</sub>

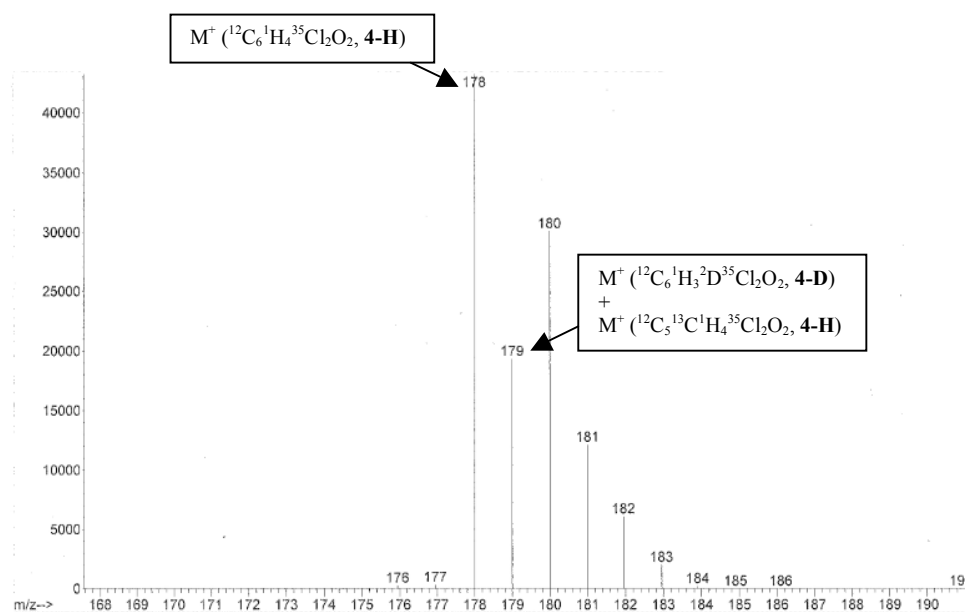
A solution of 2,5-dichlorobenzoquinone (89 mg, 0.50 mmol) and PyBD<sub>3</sub> (96 mg, 1.00 mmol) in CH<sub>2</sub>Cl<sub>2</sub> was stirred at 20 °C for 6 h. The solvent was removed under reduced pressure. The

crude material was purified by flash column chromatography (silica gel, eluent: ethyl MeOH/CH<sub>2</sub>Cl<sub>2</sub> = 1/10) to afford a mixture of **4-H** and **4-D** (white solid, 78 mg, 87%). The ratio [**4-H**/**4-D**] was analyzed by <sup>1</sup>H NMR and EI-MS spectroscopies.

### <sup>1</sup>H NMR spectrum

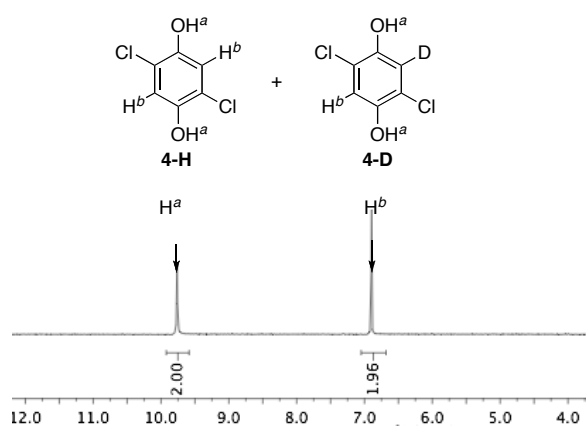
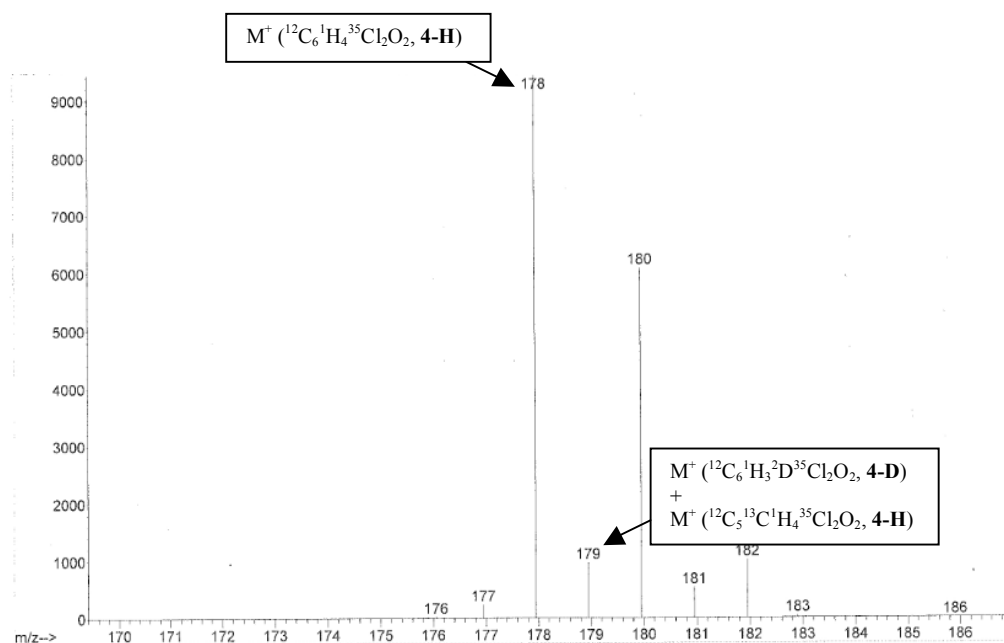


### EI-MS spectrum



**Procedure for the reaction of 2,5-dichlorobenzoquinone with cyclohexadiene-D<sub>8</sub>**

A solution of 2,5-dichlorobenzoquinone (89 mg, 0.50 mmol) and cyclohexadiene-D<sub>8</sub> (88 mg, 1.00 mmol) in CH<sub>2</sub>Cl<sub>2</sub> was stirred at 20 °C for 48 h. The solvent was removed under reduced pressure. The crude material was purified by flash column chromatography (silica gel, eluent: MeOH/CH<sub>2</sub>Cl<sub>2</sub> = 1/10) to afford a mixture of **4-H** and **4-D** (white solid, 15 mg, 17%). The ratio [**4-H**/**4-D**] was analyzed by <sup>1</sup>H NMR and EI-MS spectroscopies.

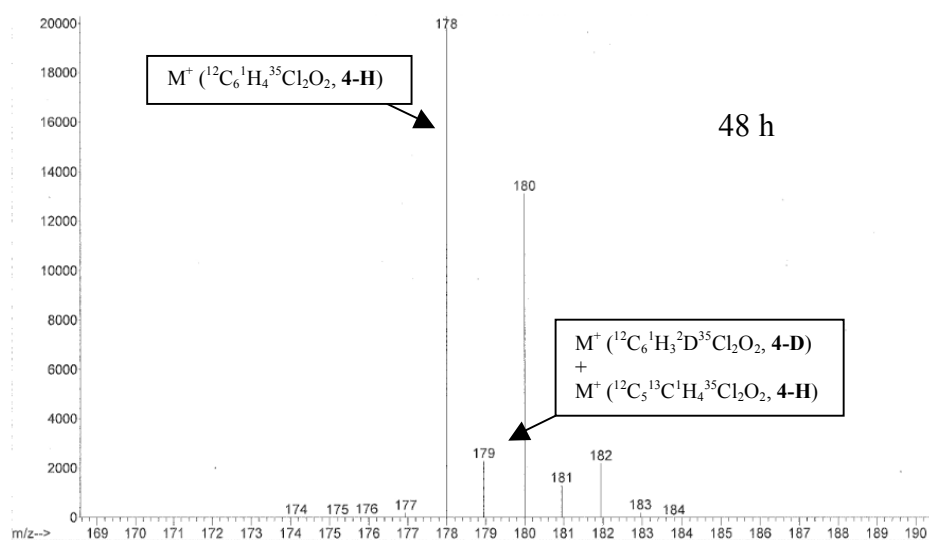
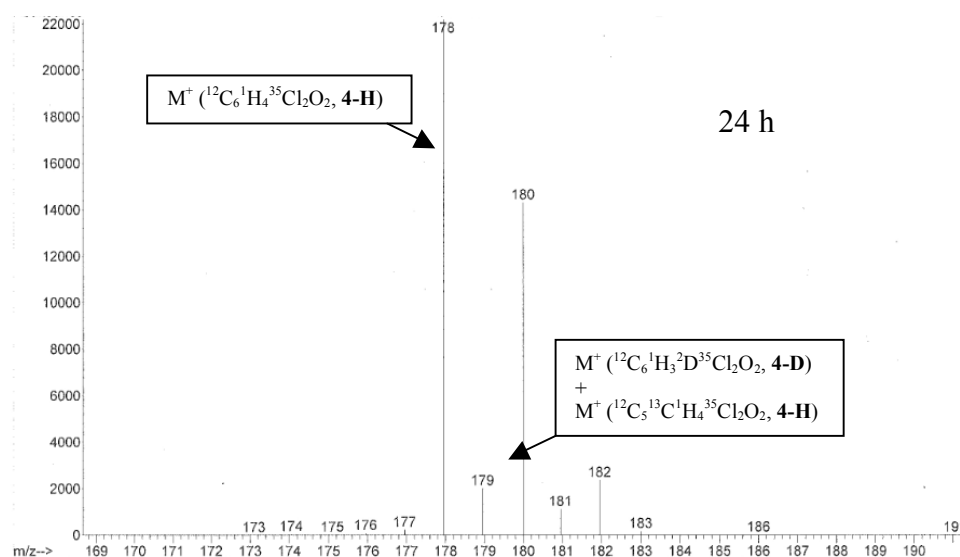
**<sup>1</sup>H NMR spectrum****EI-MS spectrum**



### Procedure for the examination for deuterium exchange of *O*-deuterated 2,5-dichlorobenzoquinone

*O*-deuterated 2,5-dichlorobenzoquinone was synthesized by deuterium exchange with heavy water and the remaining heavy water was removed under vacuum. *O*-deuterated 2,5-dichlorobenzoquinone (180 mg, 0.50 mmol) was dissolved in dichloromethane. The solution was stirring at 20 °C under nitrogen. After 24 h, a portion of the solution was taken out and passing through a short column on silica gel (MeOH/CH<sub>2</sub>Cl<sub>2</sub>) then the solvent was evaporated. The resulting mixture was analyzed by Mass spectroscopy. After another 24 h, the remaining solution was treated using the same method and analyzed by Mass spectroscopy

#### EI-MS spectra



#### 4.4.5 Quantum chemical calculations.

DFT studies on the reactions of DDQ with hydride donors **2** were performed using Gaussian 09.<sup>16</sup> The B97D functional was used in combination with the 6-31+G(d,p) basis set (LANL2DZ ECP for Sn atom) for structure optimization and frequency calculations together with the PCM/UFF model for CH<sub>2</sub>Cl<sub>2</sub>. Geometries of the transition states were verified by vibrational frequency calculations. The nature of the most favorable transition states was further verified by IRC calculations (50 steps in each direction) and subsequent structure optimizations to the next local minimum energy structure. Thermal corrections were calculated from unscaled frequencies at 298.15 K and 1 atm. Refined electronic energies were obtained from single-point calculations on the B97D geometries using Truhlar's meta hybrid exchange–correlation functional M06-2X with the triple- $\zeta$  quality def2-TZVPP basis sets, again using the PCM/UFF model for CH<sub>2</sub>Cl<sub>2</sub>. All free energies in solution have been corrected to correspond to a standard state of 1 mol/L. The stabilities of the restricted wave functions (RB97D and RM06-2X) have been checked for all transition states. An ultrafine grid was used throughout this study for numerical integration of the density. Transition state distortion/interaction analysis was carried out at the same level of theory as the single-point calculations. Conformer search was carried out with Avogadro 1.1.0 software by using molecular mechanics with force field MMFF94. The conformer search for transition structures was achieved by rotating the reactants along the reaction axes (approaching directions) and, in each case, 3-6 initial structures were submitted to transition structure optimization.

##### 4.4.5.1 Total energies and Gibbs free energies

**Table S64.** Energies for the optimized structures and transition states (the most favorable conformers are marked with yellow color)<sup>a</sup>

		RB97D/6-31+g(d,p)//PCM/UFF				RM06-2X/def2-TZVPP//PCM/UFF	
		E	ZPE	Hcorr	Gcorr	E	DG(°)/kJ mol <sup>-1</sup>
<b>1</b>		-1484.766118	0.05981	0.073476	0.018762	-1485.122467	
<b>2a</b>	cfr1	-195.173741	0.110202	0.117309	0.080756	-195.27242	
	cfr2	-195.173147	0.110082	0.117221	0.080488	-195.2720099	
<b>O-Attack-TS</b>	cfr1	-1679.932904	0.166893	0.187109	0.117752	-1680.363476	122.3
	cfr2	-1679.936348	0.166947	0.187203	0.117933	-1680.36747	112.3
	cfr3	-1679.936385	0.166911	0.187195	0.117651	-1680.367174	112.3
	cfr4	-1679.939193	0.166761	0.187082	0.11757	-1680.369712	105.5
<b>C-Attack-TS</b>	cfr1	-1679.923522	0.167941	0.188085	0.119519	-1680.356284	145.8

# Chapter 4: Mechanisms of Hydride Abstractions by Quinones

	cfr2	-1679.927948	0.167872	0.188017	0.119657	-1680.361245	133.1
	cfr3	-1679.929779	0.167464	0.187862	0.117853	-1680.362888	124.1
	cfr4	-1679.932340	0.167377	0.187685	0.118655	-1680.364888	121.0
<b>2b</b>	cfr1	-234.463280	0.137695	0.146067	0.106599	-234.5813468	
	cfr2	-234.463503	0.137458	0.145961	0.106095	-234.5810496	
<b>O-Attack-TS</b>	cfr1	-1719.226650	0.194182	0.215921	0.143733	-1719.676046	113.6
	cfr2	-1719.228843	0.194148	0.215984	0.143201	-1719.679131	104.2
	cfr3	-1719.228701	0.194267	0.216058	0.143464	-1719.678978	105.2
	cfr4	-1719.230562	0.194624	0.216326	0.143992	-1719.680602	102.4
<b>C-Attack-TS</b>	cfr1	-1719.219459	0.194902	0.216632	0.144589	-1719.671635	127.5
	cfr2	-1719.222502	0.195014	0.216727	0.14502	-1719.675218	119.2
	cfr3	-1719.223182	0.194952	0.216773	0.1445	-1719.675283	117.7
	cfr4	-1719.225252	0.195173	0.216867	0.144818	-1719.677169	113.5
<b>2c</b>	cfr1	-313.063878	0.195498	0.205352	0.161754	-313.2258501	
	cfr2	-313.063439	0.195457	0.205348	0.161592	-313.2252479	
	cfr3	-313.063472	0.19574	0.205485	0.162112	-313.2252958	
	cfr4	-313.062943	0.195761	0.205528	0.161929	-313.224474	
	cfr5	-313.062599	0.195681	0.205518	0.161681	-313.224165	
<b>O-Attack-TS</b>	cfr1	-1797.831672	0.251468	0.27497	0.198134	-1798.323079	104.5
	cfr2	-1797.832477	0.251601	0.275033	0.198267	-1798.323544	103.6
	cfr3	-1797.833042	0.251397	0.274893	0.197748	-1798.323631	102.0
<b>C-Attack-TS</b>	cfr1	-1797.829793	0.252508	0.2758	0.200376	-1798.326011	102.7
	cfr2	-1797.826774	0.252215	0.275707	0.199274	-1798.323063	107.5
<b>2d</b>		-271.329763	0.124339	0.131167	0.09515	-271.4840192	
<b>O-Attack-TS</b>		-1756.112002	0.182632	0.202716	0.134585	-1756.595164	76.0
<b>C-Attack-TS</b>		-1756.102697	0.182223	0.202795	0.132234	-1756.587636	89.6
<b>2e</b>		-233.259748	0.118152	0.124569	0.089419	-233.3941041	
<b>CT1</b>		-1718.047713	0.179395	0.199743	0.130555	-1718.527669	21.7
<b>O-Attack-TS (TS1)</b>	cfr1	-1718.031716	0.174512	0.194183	0.125888	-1718.492719	101.1
	cfr2	-1718.037176	0.17513	0.19441	0.128345	-1718.502472	81.9
	cfr3	-1718.023396	0.173558	0.193736	0.121085	-1718.478955	124.6
<b>IM1</b>		-1718.063448	0.179252	0.199773	0.129232	-1718.540516	-15.5
<b>P1</b>	cfr1	-1486.019698	0.083289	0.097554	0.042530	-1486.385654	
	cfr2	-1486.021198	0.083518	0.097604	0.043317	-1486.387632	
	cfr3	-1486.022499	0.083641	0.097622	0.043777	-1486.3894	
<b>P2</b>		-232.087702	0.097705	0.103176	0.070163	-232.227419	-247.8 (P1+P2)
<b>C-Attack-TS (TS2)</b>		-1718.018233	0.174547	0.194585	0.124432	-1718.481867	125.7
<b>IM2</b>		-1718.027054	0.178390	0.199313	0.124171	-1718.502180	71.8
<b>IM3</b>	cfr1	-1485.988857	0.082943	0.097003	0.041524	-1486.346905	
	cfr2	1485.989159	0.083282	0.097257	0.041517	-1486.34703	-142.6 (IM3+P2)
<b>C-Attack-TS (TS3)</b>		-1718.028250	0.175135	0.194761	0.127167	-1718.495116	98.2
<b>IM4</b>		-1718.057531	0.183085	0.20227	0.136152	-1718.550563	-23.7
<b>TS4</b>		-1718.039706	0.180495	0.199949	0.132229	-1718.513878	62.2
<b>C-Attack-TS</b>		-1718.027675	0.175005	0.194618	0.127353	-1718.495142	98.6

(TS5)							
2f		-311.848828	0.172061	0.181576	0.139436	-312.0206302	
O-Attack-TS	cfr1	-1796.634053	0.2289	0.25158	0.178171	-1797.135797	63.6
	cfr2	-1796.634428	0.229338	0.251822	0.179451	-1797.135828	66.9
C-Attack-TS	cfr1	-1796.625896	0.229322	0.251935	0.179315	-1797.12999	81.8
	cfr2	-1796.625299	0.229199	0.252009	0.178023	-1797.128952	81.2
2g		-351.139454	0.199234	0.210275	0.164579	-351.3296487	
O-Attack-TS		-1835.929165	0.256852	0.281009	0.205086	-1836.449672	55.5
C-Attack-TS		-1835.923408	0.256496	0.280811	0.204002	-1836.445901	62.6
2h		-390.431685	0.225917	0.239038	0.18813	-390.6396432	
O-Attack-TS		-1875.226388	0.283408	0.309301	0.229524	-1875.76246	50.5
C-Attack-TS		-1875.215109	0.28306	0.309408	0.227346	-1875.753634	68.0
2j		-576.238250	0.18694	0.198115	0.15065	-576.6113409	
O-Attack-TS	cfr1	-2061.019419	0.243884	0.268409	0.189957	-2061.719902	82.4
	cfr2	-2061.017238	0.243775	0.268318	0.189347	-2061.717224	87.9
	cfr3	-2061.022678	0.244091	0.268503	0.190809	-2061.722994	76.6
C-Attack-TS		-2061.010640	0.244151	0.268835	0.19023	-2061.715243	95.4
2n'		-123.658235	0.111696	0.121505	0.077524	-334.5387658	
CT2		-1608.419486	0.172485	0.197165	0.113321	-1819.667015	21.6
O-Attack-TS (TS6)		-1608.403904	0.170303	0.194051	0.114374	-1819.637008	103.1
IM5		-1608.469780	0.178993	0.202635	0.124053	-1819.736515	-132.6
P3	cfr1	-1608.512121	0.178759	0.202428	0.123544	-1819.784676	-260.2
	cfr2	-1608.510506	0.178974	0.202599	0.123921	-1819.782806	-254.3
C-Attack-TS (TS7)		-1608.412640	0.171078	0.194956	0.114264	-1819.652753	61.5
IM6		-1608.418232	0.175845	0.199628	0.120282	-1819.668542	35.8
IM7		-1608.458118	0.178051	0.201638	0.122712	-1819.713487	-75.7
2p		-201.034070	0.151429	0.159299	0.122401	-201.1165711	
CT3		-1685.810516	0.212024	0.233724	0.161165	-1686.245804	26.8
O-Attack-TS (TS8)	cfr1	-1685.789104	0.208612	0.230203	0.157749	-1686.204633	125.8
	cfr2	-1685.790876	0.208725	0.230381	0.157103	-1686.207682	116.1
	cfr3	-1685.790248	0.208564	0.230314	0.156389	-1686.207148	115.7
IM8		-1685.851078	0.21858	0.239683	0.169514	-1686.307572	-113.3
P4	cfr1	-1685.896354	0.218253	0.239289	0.168929	-1686.361559	-256.5
	cfr2	-1685.897855	0.218058	0.239146	0.168595	-1686.363597	-262.7
C-Attack-TS (TS9)		-1685.800183	0.210798	0.232267	0.160666	-1686.229238	68.9
IM9		-1685.801615	0.212767	0.234611	0.162124	-1686.233796	60.8
IM10		-1685.842842	0.217312	0.238348	0.166878	-1686.288474	-70.1

<b>2q</b>	cfr1	-318.893241	0.235569	0.246841	0.20225	-319.0307575	
	cfr2	-318.897413	0.235513	0.247094	0.201295	-319.0340045	
	cfr3	-318.901595	0.2355	0.247132	0.200948	-319.038377	
	cfr4	-318.900944	0.235475	0.247063	0.201125	-319.0377888	
	cfr5	-318.895345	0.235372	0.246877	0.201395	-319.0330159	
<b>O-Attack-TS</b>	cfr1	-1803.657073	0.292953	0.318266	0.237282	-1804.126972	127.0
	cfr2	-1803.661370	0.292865	0.318256	0.236722	-1804.131649	113.3
<b>C-Attack-TS</b>	cfr1	-1803.668551	0.294338	0.319669	0.239422	-1804.150189	71.7
	cfr2	-1803.673175	0.294737	0.319975	0.240071	-1804.15456	62.0
<hr/>							
<b>2r</b>		-274.773775	0.11846	0.12594	0.087839	-274.928951	
<b>O-Attack-TS</b>	cfr1	-1759.543913	0.17718	0.197727	0.127929	-1760.035228	90.5
	cfr2	-1759.542889	0.176337	0.197312	0.122862	-1760.024384	105.6
<b>C-Attack-TS</b>	cfr1	-1759.551594	0.178008	0.198619	0.128666	-1760.053935	43.4
	cfr2	-1759.545400	0.177686	0.198452	0.126972	-1760.045108	62.1
	cfr3	-1759.546186	0.177719	0.19847	0.126948	-1760.047138	56.7
<hr/>							
<b>2t</b>		-331.295022	0.155119	0.165432	0.120381	-331.4772843	
<b>O-Attack-TS</b>		-1816.076119	0.215151	0.237892	0.164424	-1816.591269	80.6
<b>C-Attack-TS</b>		-1816.081974	0.215817	0.238734	0.164676	-1816.606929	40.2

a) The stability check shows that the restricted wave function RB97D is always stable for all examined structures. However, the RM06-2X wave function shows a RHF→UHF instability for O-attack transition state **TS6** and **TS8** (resulting in stabilization of 2.4 and 10 kJ/mol, respectively, when using UM06-2X).

#### 4.4.5.2 Transition state distortion/interaction analysis

A transition state distortion/interaction analysis was carried out to rationalize the different barriers for O- and C-attack.

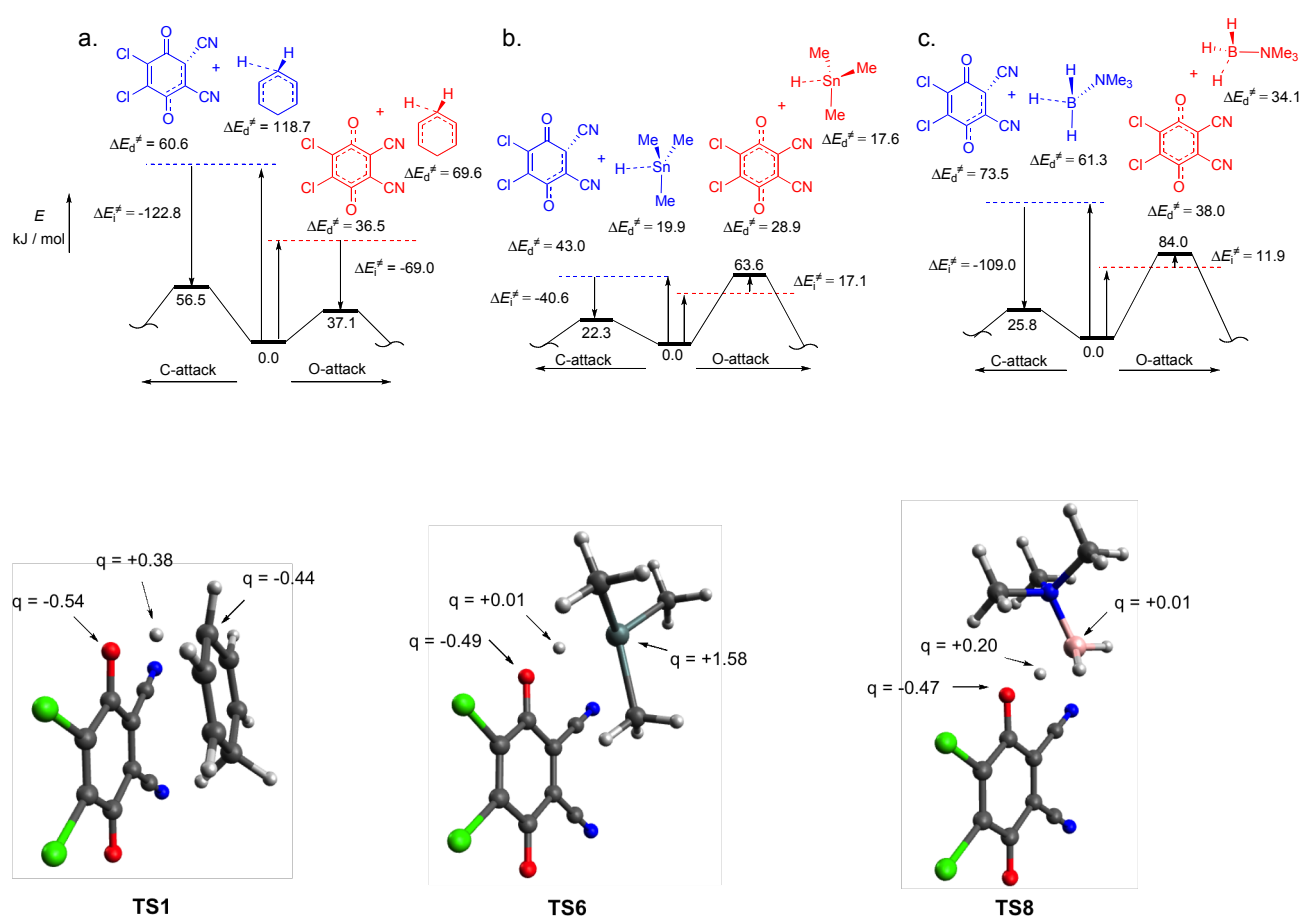
$$DE^\ddagger = DE_d^\ddagger + DE_i^\ddagger \quad (\text{S1})$$

In eq. (S1) the distortion energy term  $DE_d^\ddagger$  reflects the energy which is needed to distort the reactants into the transition structure while there is no interaction between the reactants. The interaction energy  $DE_i^\ddagger$  between these distorted fragments is calculated as the difference between the activation energy ( $DE^\ddagger$ ) and distortion energy ( $DE_d^\ddagger$ ).

**Table S65.** Transition state distortion and interaction energies in gas phase and  $\text{CH}_2\text{Cl}_2$  solution

		$E_d^\ddagger$ /kJ mol <sup>-1</sup> (distortion energy)		$E^\ddagger$ /kJ mol <sup>-1</sup> (activation energy)		$E_i^\ddagger$ /kJ mol <sup>-1</sup> (interaction energy)	
		gas	$\text{CH}_2\text{Cl}_2$	gas	$\text{CH}_2\text{Cl}_2$	gas	$\text{CH}_2\text{Cl}_2$
DDQ + <b>2e</b>	O-attack ( <b>TS1</b> )	106.5	105.7	41.2	37.0	-65.3	-68.7
	frag1 (DDQ)	37.0	36.3				
	frag2 ( <b>2e</b> )	69.5	69.4				
	C-attack ( <b>TS3</b> )	178.1	178.6	68.2	56.3	-109.9	-122.3

	frag1 (DDQ)	59.7	60.4				
	frag2 ( <b>2e</b> )	118.4	118.2				
DDQ + <b>2n'</b>	0-attack ( <b>TS6</b> )	50.3	46.5	66.4	63.6	16.1	17.1
	frag1 (DDQ)	29.6	28.9				
	frag2 ( <b>2n'</b> )	20.7	17.6				
	C-attack ( <b>TS7</b> )	66.9	62.9	40.8	22.3	-26.1	-40.6
	frag1 (DDQ)	42.6	43.0				
	frag2 ( <b>2n'</b> )	24.3	19.9				
DDQ + <b>2p</b>	0-attack ( <b>TS8</b> )	76.2	71.8	83.6	83.7	7.4	11.9
	frag1 (DDQ)	38.7	37.8				
	frag2 ( <b>2p</b> )	37.5	34.0				
	C-attack ( <b>TS9</b> )	139.7	134.3	46.4	25.7	-93.3	-108.6
	frag1 (DDQ)	72.8	73.2				
	frag2 ( <b>2p</b> )	66.9	61.1				



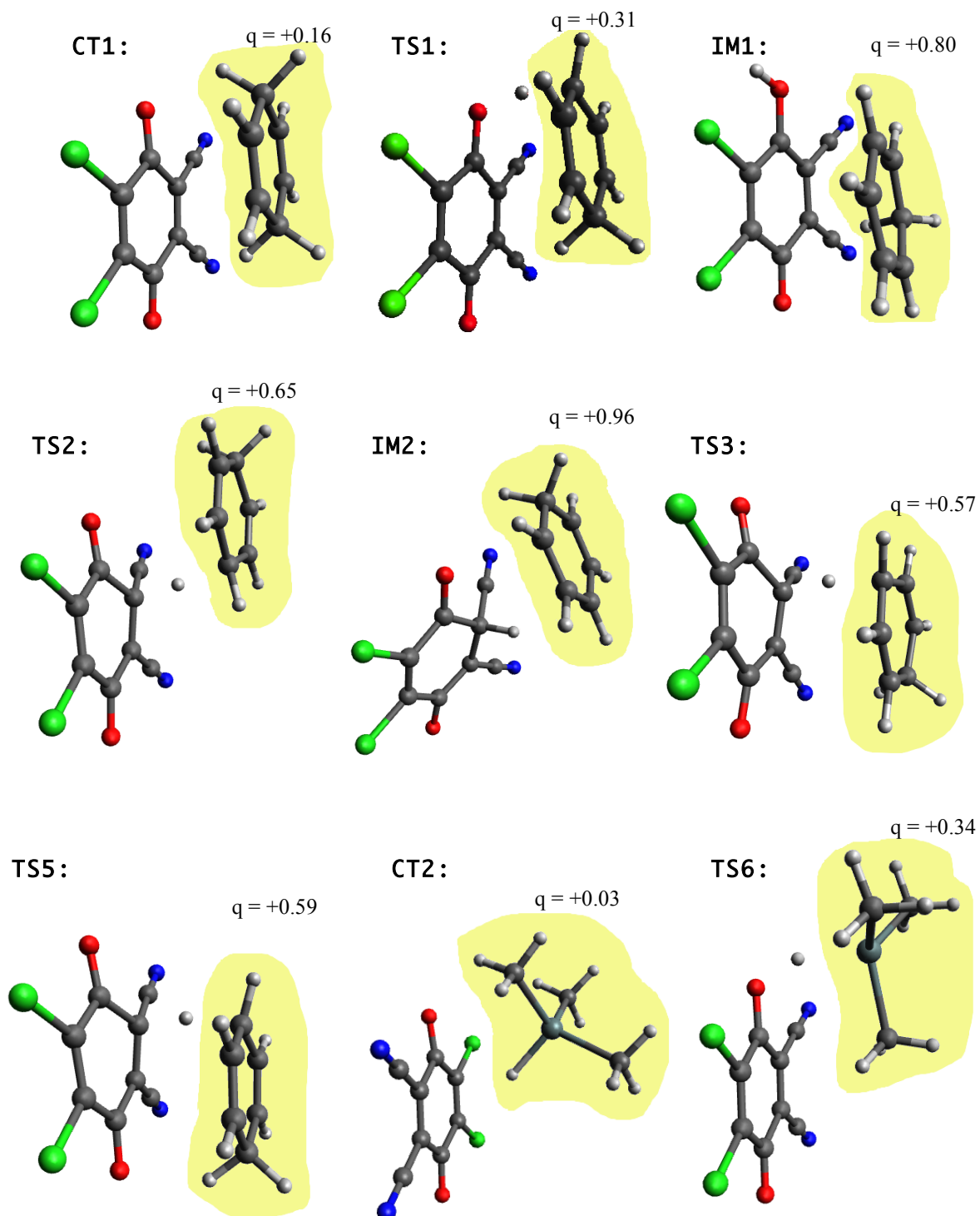
**Figure S2.** Transition state distortion/interaction analysis of the reactions of DDQ (**1a**) with a) cyclohexadiene (**2e**), b) Me<sub>3</sub>SnH (**2n'**), and c) trimethylamine borane (**2p**); and charge distribution in O-attack transition states for **TS1**, **TS6**, and **TS8** calculated from natural population analysis [RM06-2X/def2-TZVPP//PCM/UFF] in CH<sub>2</sub>Cl<sub>2</sub>.

The results of the transition state distortion/interaction analyses for the reactions of DDQ (**1a**) with cyclohexadiene (**2e**), trimethylstannane (**2n'**), and trimethylamine borane (**2p**) are shown

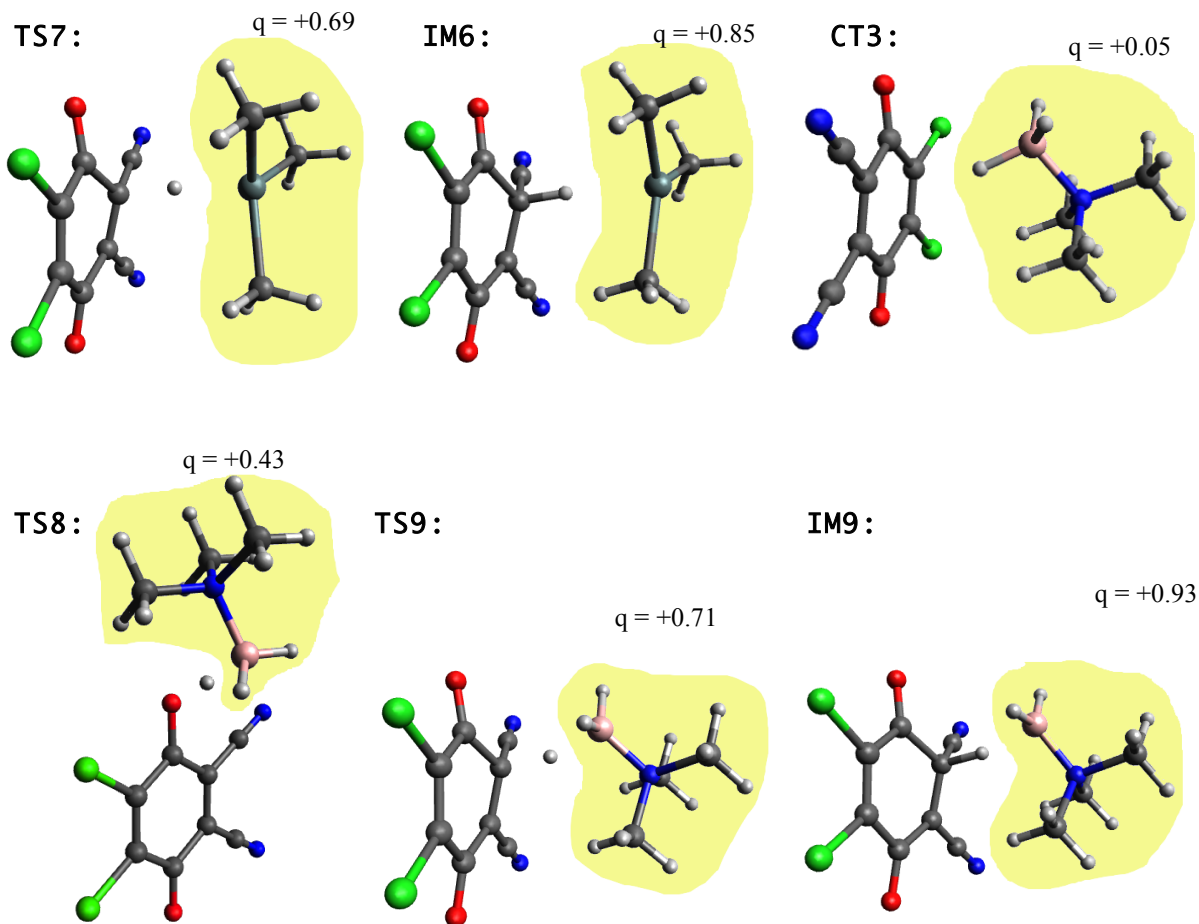
in Table S65 and illustrated in Fig. S2. In all three cases, the distortion energies  $DE_d^\ddagger$  for DDQ (**1a**) as well as for the hydride donor are higher in the case of C-attack than in the case of O-attack. While all transition states for C-attack show large interaction energies, large differences were observed for O-attack. While the interaction energy  $DE_i^\ddagger$  between DDQ (**1a**) and cyclohexadiene (**2e**) fragments of the O-attack transition state is stabilizing by 69 kJ/mol, the analogous interactions of the fragments of the O-attack are destabilizing by 17 kJ/mol for trimethylstannane **2n'** and by 12 kJ/mol for amine borane **2p**.

Different electrostatic interactions between the reaction centers and the migrating hydrogen, which can be derived from the charge distributions shown in the lower part of Figure 11, may be an important factor for the differences in  $DE_i^\ddagger$ . As expected from the higher electronegativity of C (**TS1**) compared to Sn (**TS6**) and B (**TS8**), the migrating hydrogen has a significantly higher positive charge in the transition state for the C-H hydride donor (**TS1**) than in that of Sn-H (**TS6**) and B-H (**TS8**) hydride donors (+0.38 compared with +0.01 and +0.20). As Figure S2 also shows large differences in distortion energies for the different transition states, detailed distortion/interaction analysis for reactions of other quinones with other hydride donors would be needed to arrive at a definite explanation for the origin of the different regioselectivities of C-H, Sn-H and B-H hydride donors.

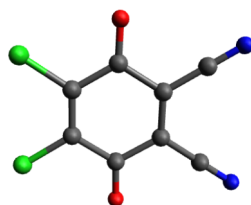
## 4.4.5.3 Mulliken charge distribution in some key structures





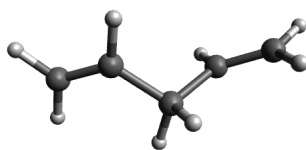


## 4.4.5.4 Geometries for the optimized structures and transition states (only the most favorable conformers are listed)



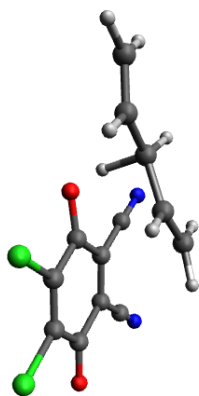
DDQ (1a)

C	1.41018	0.68519	-0.00011
C	0.11701	1.46908	0.00051
C	-1.16322	0.68597	-0.00026
C	-1.16331	-0.68593	-0.00040
C	0.11691	-1.46915	-0.00009
C	1.41006	-0.68531	0.00015
O	0.14303	2.69394	0.00169
Cl	-2.60640	1.62233	0.00011
Cl	-2.60649	-1.62222	-0.00043
O	0.14289	-2.69398	-0.00008
C	2.61848	-1.44904	0.00038
N	3.61026	-2.07493	0.00135
C	2.61857	1.44892	-0.00069
N	3.61027	2.07495	-0.00199

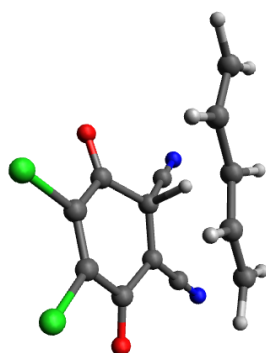


Penta-1,4-diene (2a)

C	0.00000	0.68521	-0.00000
C	1.17071	-0.16801	0.44794
C	-1.17071	-0.16801	-0.44794
H	0.32793	1.33535	-0.82947
H	-0.32793	1.33535	0.82947
C	2.37332	-0.19431	-0.15331
H	0.98448	-0.81275	1.31360
H	2.58376	0.43356	-1.02387
H	3.17807	-0.83788	0.20797
C	-2.37332	-0.19431	0.15331
H	-0.98448	-0.81275	-1.31360
H	-2.58376	0.43357	1.02387
H	-3.17807	-0.83788	-0.20797

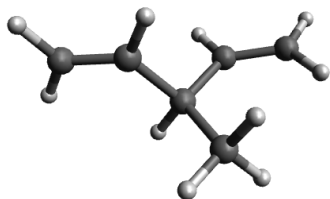
**O-Attack-TS (DDQ 1a + 2a)**

C	-3.12649	0.57664	0.66009
H	-2.36996	0.46813	-0.39002
C	0.68165	1.36252	-0.46110
C	2.00433	1.12500	-0.10450
C	-5.43246	0.30294	-0.22589
C	-0.24540	0.26108	-0.71853
Cl	-0.93047	-2.37118	-0.71378
Cl	2.11845	-2.95565	0.20012
C	2.92619	2.19678	0.09075
C	0.18668	2.69224	-0.65545
O	3.69090	-0.46136	0.44355
O	-1.39052	0.49544	-1.24765
N	3.68443	3.07849	0.25281
N	-0.22323	3.78257	-0.79268
C	1.52915	-1.35372	-0.08169
C	-4.31581	-0.22134	0.33573
C	2.51475	-0.25471	0.11253
C	0.22694	-1.10424	-0.46324
H	-4.26196	-1.29380	0.54213
C	-1.08254	0.83943	2.02725
C	-2.13834	0.08203	1.60677
H	-2.17303	-0.97891	1.86669
H	-3.26708	1.66645	0.64573
H	-0.30321	0.41783	2.66152
H	-1.02677	1.90335	1.79278
H	-5.50103	1.36805	-0.45822
H	-6.29601	-0.32277	-0.45277

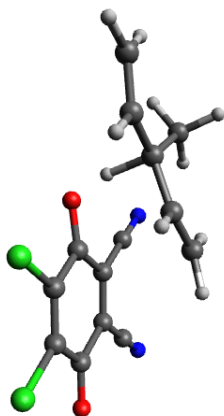
**C-Attack-TS (DDQ 1a + 2a)**

C	-1.57957	-0.92557	1.68097
H	-1.35026	-0.42603	0.37442
C	-1.10016	0.20839	-0.77584
C	-0.58642	1.51182	-0.42086
C	-2.37567	-3.23175	1.28018
C	-0.10527	-0.86551	-1.23692

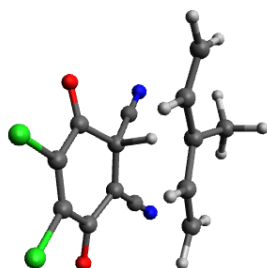
Cl	2.27942	-2.12831	-0.81289
Cl	3.28810	0.65873	0.49560
C	-1.42707	2.65746	-0.44273
C	-2.39020	0.14385	-1.43908
O	1.34465	2.82377	0.04981
O	-0.46687	-1.81273	-1.92086
N	-2.13355	3.59746	-0.46061
N	-3.44618	0.08029	-1.94051
C	1.69995	0.45996	-0.14217
C	-1.37764	-2.37009	1.59202
C	0.84189	1.71311	-0.14691
C	1.27084	-0.72716	-0.67872
H	-0.36634	-2.74289	1.77181
C	-0.80807	1.29396	2.37348
C	-0.60428	-0.05747	2.29039
H	0.37360	-0.47767	2.53674
H	-2.62200	-0.58007	1.68890
H	-0.03107	1.96223	2.74235
H	-1.78266	1.72838	2.14961
H	-3.38834	-2.87468	1.08085
H	-2.19502	-4.30514	1.22267

3-Methylpenta-1,4-diene (**2b**)

C	0.00000	0.31273	-0.23487
C	1.24251	-0.24687	0.43035
C	-1.24250	-0.24688	0.43036
C	2.18533	-0.97429	-0.19352
H	1.35192	-0.01628	1.49653
H	2.09844	-1.21798	-1.25610
H	3.06534	-1.34427	0.33657
C	-2.18533	-0.97429	-0.19352
H	-1.35190	-0.01631	1.49654
H	-2.09845	-1.21796	-1.25610
H	-3.06533	-1.34428	0.33657
C	-0.00001	1.86388	-0.15139
H	0.00000	0.01170	-1.29550
H	-0.89575	2.27394	-0.64172
H	0.89573	2.27395	-0.64172
H	-0.00001	2.19184	0.90043

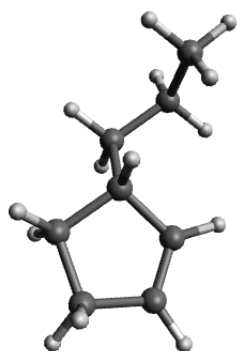
**O-Attack-TS (DDQ 1a + 2b)**

C	-3.00839	0.21562	0.55927
H	-2.22499	0.11107	-0.45205
C	0.71818	1.32866	-0.52443
C	2.04652	1.24914	-0.12308
C	-5.22015	-0.68019	-0.25816
C	-0.07379	0.12454	-0.77815
Cl	-0.46297	-2.56617	-0.71742
Cl	2.60687	-2.78564	0.28449
C	2.83613	2.42124	0.07541
C	0.08772	2.59035	-0.77226
O	3.87878	-0.12535	0.51955
O	-1.22836	0.21558	-1.32355
N	3.48521	3.38544	0.24143
N	-0.43118	3.62652	-0.95279
C	1.85066	-1.26713	-0.05307
C	-3.99541	-0.85627	0.29149
C	2.69960	-0.05962	0.14527
C	0.54077	-1.17339	-0.47497
H	-3.67336	-1.86969	0.54705
C	-0.99657	0.73589	1.97264
C	-1.96416	-0.11947	1.53518
H	-1.87868	-1.17446	1.80858
C	-3.47931	1.66790	0.44222
H	-0.19801	0.37928	2.62290
H	-1.01581	1.80073	1.74459
H	-5.59187	0.30372	-0.54594
H	-5.88111	-1.53255	-0.41739
H	-2.64120	2.37019	0.49793
H	-4.18500	1.89115	1.25705
H	-3.98854	1.83210	-0.51555

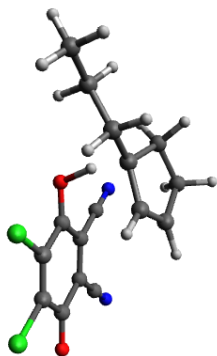
**C-Attack-TS (DDQ 1a + 2b)**

C	-1.74446	-0.75296	1.39549
H	-1.24946	-0.30628	0.16627
C	-0.81181	0.30679	-0.95841
C	-0.23881	1.56348	-0.54610
C	-2.53917	-3.08788	0.90883

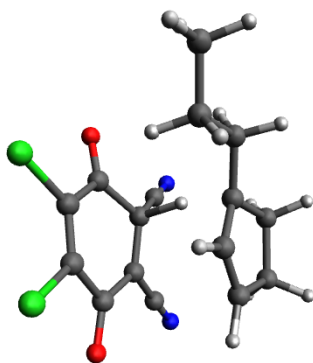
C	0.13348	-0.85244	-1.30172
Cl	2.35807	-2.29211	-0.64152
Cl	3.44890	0.42184	0.74990
C	-0.99286	2.76576	-0.61321
C	-2.02067	0.34032	-1.76031
O	1.72429	2.72484	0.13525
O	-0.23484	-1.77872	-2.01088
N	-1.62757	3.75455	-0.66563
N	-3.01064	0.35868	-2.38506
C	1.91966	0.34059	-0.03887
C	-1.58194	-2.21628	1.30295
C	1.16265	1.65494	-0.12157
C	1.45353	-0.81519	-0.61152
H	-0.59359	-2.60196	1.56688
C	-0.67756	1.31710	2.29677
C	-0.71232	-0.03765	2.13442
H	0.16006	-0.62087	2.43887
C	-3.14544	-0.16201	1.28659
H	0.17705	1.79036	2.77895
H	-1.50826	1.96300	2.01867
H	-3.54033	-2.76558	0.62185
H	-2.32846	-4.15673	0.87451
H	-3.69818	-0.60338	0.44959
H	-3.12024	0.92372	1.14365
H	-3.69084	-0.37663	2.21802

3-Propylcyclopent-1-ene (**2c**)

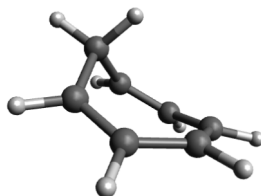
C	1.43649	1.23047	0.09843
C	0.33263	0.25543	0.47322
C	0.91120	-1.11023	-0.01477
C	2.45122	-0.90323	-0.12840
C	2.58161	0.60619	-0.23665
C	-1.04547	0.59923	-0.12584
C	-2.15072	-0.38489	0.29569
C	-3.52370	-0.01725	-0.29473
H	1.29563	2.31316	0.13645
H	0.22041	0.24368	1.57598
H	0.49992	-1.32305	-1.01543
H	0.63954	-1.94687	0.64376
H	2.88828	-1.43795	-0.98744
H	2.97688	-1.27072	0.77258
H	3.51361	1.10530	-0.51030
H	-0.96056	0.60625	-1.22748
H	-1.33329	1.62034	0.18067
H	-2.21068	-0.40433	1.39790
H	-1.87130	-1.40290	-0.02267
H	-3.83129	0.98950	0.03206
H	-4.30168	-0.73096	0.01851
H	-3.48511	-0.01576	-1.39625

**O-Attack-TS (DDQ 1a + 2c)**

C	-2.44358	0.47209	0.74782
H	-1.77485	0.30223	-0.36684
C	1.19744	1.13001	-0.73682
C	2.52125	0.94312	-0.33243
C	-0.69437	1.39238	1.97304
C	0.26875	0.01730	-0.83162
Cl	-0.41483	-2.59603	-0.50784
Cl	2.61196	-3.04887	0.52791
C	3.44284	2.03083	-0.29189
C	0.72696	2.41383	-1.15658
O	4.18680	-0.54532	0.49201
O	-0.91981	0.19484	-1.30600
N	4.19972	2.92840	-0.25476
N	0.33771	3.47169	-1.48261
C	2.03418	-1.49469	0.02908
C	-1.32523	0.21691	1.63916
C	3.01959	-0.38235	0.09844
C	0.73760	-1.29819	-0.40846
H	-0.98706	-0.77877	1.92185
C	-1.44961	2.58681	1.47389
C	-2.70142	1.98546	0.77842
C	-3.59534	-0.50657	0.58177
H	0.20975	1.46273	2.57827
H	-3.61323	2.17176	1.37022
H	-2.87500	2.40639	-0.22073
H	-1.71054	3.25104	2.31629
H	-0.83872	3.20587	0.79635
H	-4.23818	-0.40945	1.47732
H	-3.20350	-1.53501	0.57553
C	-4.44347	-0.25627	-0.67956
H	-4.83414	0.77349	-0.65661
C	-5.60828	-1.25409	-0.79114
H	-3.79571	-0.33382	-1.56750
H	-6.27614	-1.17337	0.08146
H	-5.23173	-2.28852	-0.83508
H	-6.20408	-1.06765	-1.69712

**C-Attack-TS (DDQ 1a + 2c)**

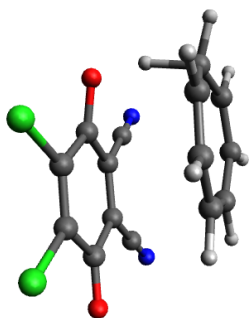
C	-1.04780	1.67366	-0.93543
H	-0.79338	0.86966	0.20095
C	-0.74860	-0.03747	1.18415
C	-1.16887	-1.28972	0.58904
C	-1.90541	-0.13444	-2.08908
C	0.74394	0.14582	1.50019
Cl	3.35377	-0.21546	0.77199
Cl	2.27114	-2.54074	-1.19763
C	-2.50403	-1.74170	0.71747
C	-1.62616	0.56689	2.17055
O	-0.52741	-3.21550	-0.65387
O	1.11797	0.94644	2.34745
N	-3.62503	-2.08550	0.82504
N	-2.35005	1.08174	2.93344
C	1.21898	-1.64939	-0.16398
C	-0.76417	0.60001	-1.85432
C	-0.22265	-2.13686	-0.12843
C	1.67655	-0.63731	0.64066
H	0.23309	0.33499	-2.19807
C	-3.12539	0.53501	-1.53480
C	-2.56870	1.80384	-0.83340
C	-0.15761	2.87406	-0.68874
H	-1.94066	-1.05047	-2.67824
H	-2.86733	2.72217	-1.36277
H	-2.91601	1.91200	0.20350
H	-3.81901	0.78305	-2.35670
H	-3.69419	-0.12796	-0.86300
H	-0.28346	3.21307	0.35258
H	-0.55755	3.69241	-1.31489
C	1.33106	2.66548	-1.00856
H	1.71000	1.79057	-0.46169
C	2.17123	3.89849	-0.63786
H	1.44401	2.44110	-2.08083
H	2.09318	4.11008	0.43995
H	1.82294	4.78770	-1.18667
H	3.23173	3.73782	-0.88097

**Cyclohepta-1,3,5-triene (2d)**

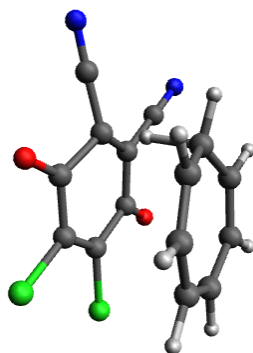
C	0.24922	-1.42743	0.69047
C	0.24922	-1.42743	-0.69047



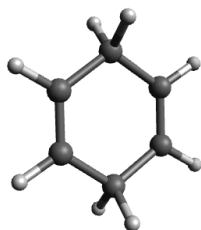
C	-0.25059	-0.36246	-1.53642
C	-0.25059	0.96536	-1.21874
C	-0.25059	-0.36246	1.53642
C	-0.25059	0.96536	1.21874
C	0.48095	1.48775	0.00000
H	0.50889	-2.36687	1.18623
H	0.50889	-2.36687	-1.18623
H	-0.68295	-0.66562	-2.49474
H	-0.77460	1.67565	-1.86324
H	-0.68295	-0.66562	2.49474
H	-0.77460	1.67565	1.86324
H	1.51510	1.09709	0.00000
H	0.52003	2.58455	0.00000

**O-Attack-TS (DDQ 1a + 2d)**

C	-0.89668	-2.89247	0.50094
H	-0.66422	-2.49925	-0.67350
C	-1.13423	0.43525	-1.07930
C	-0.89356	1.61740	-0.37086
C	0.85291	-1.61010	1.88500
C	-0.07679	-0.52872	-1.31150
Cl	2.54377	-1.27505	-1.34088
Cl	3.13465	1.45426	0.27718
C	-1.94728	2.53942	-0.09844
C	-2.44075	0.11995	-1.57432
O	0.67411	3.04241	0.72179
O	-0.35311	-1.70190	-1.76115
N	-2.82278	3.28475	0.14198
N	-3.51011	-0.11135	-1.99889
C	1.53759	1.01894	-0.23660
C	0.39051	-2.69410	1.16826
C	0.46023	1.98331	0.10786
C	1.28208	-0.15343	-0.92308
H	1.11206	-3.49569	1.00080
C	-2.20203	-0.92576	1.53404
C	-2.09023	-2.12730	0.86406
H	-3.02420	-2.54761	0.48658
H	-1.11303	-3.94853	0.28965
H	-3.21386	-0.52677	1.61941
C	-1.17923	-0.11386	2.12224
C	0.16734	-0.41240	2.26695
H	1.89393	-1.66616	2.20633
H	-1.51433	0.83239	2.54841
H	0.77331	0.33030	2.78698

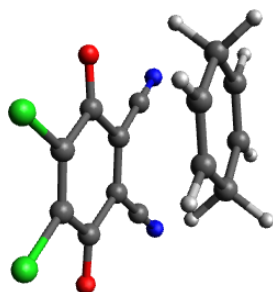
**C-Attack-TS (DDQ 1a + 2d)**

C	-1.09689	-1.90383	1.27111
H	-1.27729	-1.19006	0.13939
C	-1.49372	-0.20184	-0.83501
C	-1.59574	1.04272	-0.11326
C	1.27184	-2.82268	1.01872
C	-0.20259	-0.54552	-1.56580
Cl	2.49399	-0.27136	-1.87917
Cl	2.26139	2.33574	0.00393
C	-2.84499	1.46215	0.41315
C	-2.68875	-0.74011	-1.45105
O	-0.49168	2.95221	0.77347
O	-0.15051	-1.50243	-2.33434
N	-3.88537	1.79120	0.85527
N	-3.66267	-1.19219	-1.92036
C	0.88307	1.38527	-0.41336
C	-0.10485	-2.91206	0.94546
C	-0.43614	1.87980	0.14933
C	0.99021	0.26899	-1.20271
H	-0.51098	-3.83728	0.53388
C	0.33059	-0.20224	2.53064
C	-0.87191	-0.79731	2.19499
H	-1.77151	-0.35788	2.62636
H	-2.11773	-2.30075	1.31126
H	0.26274	0.67218	3.17975
C	1.65254	-0.58342	2.15263
C	2.06304	-1.73523	1.49532
H	1.82920	-3.68715	0.65575
H	2.44383	0.09581	2.47104
H	3.14001	-1.84884	1.36329

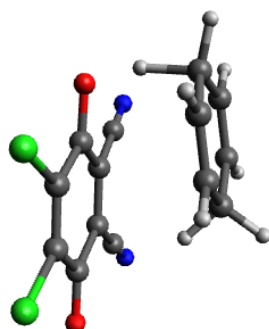
**Cyclohexa-1,4-diene (2e)**

C	-0.67331	1.26395	-0.00040
C	0.67334	1.26395	-0.00040
C	1.50969	-0.00003	0.00067
C	0.67331	-1.26395	-0.00040
H	2.18677	-0.00003	0.87663
H	2.18911	-0.00003	-0.87344
C	-0.67334	-1.26396	-0.00040
C	-1.50969	0.00003	0.00067
H	-2.18677	0.00003	0.87664
H	-2.18911	0.00003	-0.87344

H	-1.21422	2.21444	-0.00122
H	1.21427	2.21443	-0.00122
H	1.21422	-2.21444	-0.00122
H	-1.21428	-2.21443	-0.00122

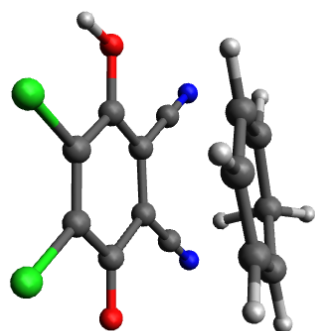
Charge transfer complex **CT1** (**1a** + **2e**)

C	-2.16004	-2.03485	0.85467
C	-1.06878	-3.02953	0.59630
C	0.24759	-2.66951	1.22270
C	0.42910	-1.55654	1.97008
C	-0.67601	-0.58166	2.26616
C	-1.98113	-0.92126	1.60861
O	-0.40340	-1.46185	-1.99929
C	-0.12054	-0.49214	-1.29377
C	-1.16866	0.51325	-0.91707
C	-0.83706	1.67367	-0.24588
C	0.57048	1.96930	0.17293
C	1.59381	0.92408	-0.13467
C	1.27410	-0.22413	-0.81613
C	-2.49139	0.28285	-1.41226
N	-3.57132	0.11908	-1.83943
C	-1.82072	2.65683	0.08114
N	-2.63515	3.45434	0.35965
Cl	3.19516	1.26401	0.41444
O	0.85443	3.03666	0.72075
Cl	2.45479	-1.40028	-1.26583
H	-0.93492	-3.14253	-0.50173
H	1.08579	-3.34457	1.04361
H	1.41182	-1.33946	2.39281
H	-0.36641	0.44462	1.96370
H	-0.81448	-0.47181	3.35911
H	-2.81528	-0.23492	1.76569
H	-3.13325	-2.22997	0.40165
H	-1.38985	-4.03928	0.91880

O-attack **TS1** (**1a** + **2e**)

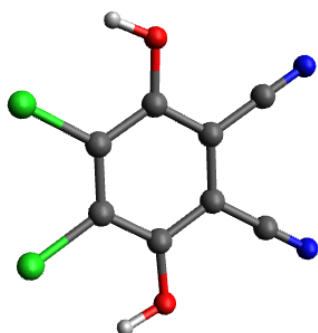
C	-1.63507	-2.74129	0.37551
H	-1.26447	-2.26953	-0.76585

C	-1.02007	0.74809	-0.85450
C	-0.46450	1.85428	-0.21051
C	0.08093	-1.77803	1.86166
C	-0.22403	-0.44029	-1.13364
Cl	2.13434	-1.80710	-1.21255
Cl	3.41766	0.70826	0.34959
C	-1.24576	3.01599	0.06673
C	-2.37183	0.77087	-1.33202
O	1.45282	2.88136	0.76087
O	-0.76340	-1.46202	-1.69367
N	-1.89474	3.96468	0.30706
N	-3.46968	0.82056	-1.74160
C	1.75145	0.67010	-0.11880
C	-0.34204	-2.79912	1.05899
C	0.96024	1.88657	0.20570
C	1.19313	-0.42037	-0.75808
H	0.31845	-3.63925	0.84691
H	1.07378	-1.81426	2.31148
C	-0.78510	-0.60657	2.19299
H	-0.27721	0.33973	1.88182
H	-0.85283	-0.47189	3.29037
C	-2.14931	-0.65681	1.58903
H	-2.84162	0.14855	1.83723
C	-2.55895	-1.68490	0.78375
H	-3.56512	-1.68444	0.36570
H	-2.07392	-3.69105	0.04592

**IM1****O-attack intermediate IM1 (1a + 2e)**

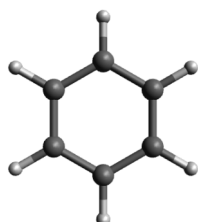
C	-2.42729	-0.20051	2.10706
H	-0.21641	3.32246	-0.20750
C	1.72534	0.79118	-0.30073
C	1.69202	-0.60600	-0.62888
C	-0.84119	-2.03237	2.03376
C	0.56517	1.57515	-0.41152
Cl	-2.04676	2.00358	-1.02718
Cl	-2.12149	-1.08203	-1.93617
C	2.87159	-1.39629	-0.51295
C	2.91573	1.38558	0.21642
O	0.47681	-2.45310	-1.55071
O	0.64003	2.88129	-0.05619
N	3.83908	-2.05549	-0.40011
N	3.89829	1.86217	0.64963
C	-0.67460	-0.36259	-1.30597
C	-2.14742	-1.58754	1.97792
C	0.50788	-1.24742	-1.21257
C	-0.63457	0.97271	-0.92598
H	-2.96795	-2.29222	1.85084
H	-0.60314	-3.09157	1.94218
C	0.27112	-1.07445	2.13986
H	0.79828	-1.10168	1.11905
H	1.10457	-1.42274	2.77316
C	-0.07909	0.34004	2.34834

H	0.72355	1.05445	2.52399
C	-1.40347	0.75142	2.30663
H	-1.65885	1.80272	2.43077
H	-3.46329	0.13648	2.06480



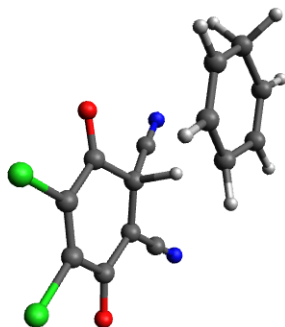
2,3-Dichloro-5,6-dicyanohydroquinone (P1)

O	-0.20072	-2.78029	-0.00027
C	-2.57937	-1.43691	-0.00012
C	-1.34707	-0.71318	-0.00017
C	-1.34710	0.71319	-0.00011
C	-2.57958	1.43660	0.00014
C	-0.12915	1.42970	-0.00040
O	-0.20100	2.78033	-0.00075
C	1.09076	0.70408	0.00004
Cl	2.57981	1.60946	-0.00001
C	1.09081	-0.70400	0.00002
Cl	2.57980	-1.60937	0.00042
C	-0.12906	-1.42974	-0.00010
H	0.69114	3.17302	-0.00043
N	-3.59314	2.02839	0.00124
N	-3.59309	-2.02845	-0.00038
H	0.69146	-3.17288	-0.00018



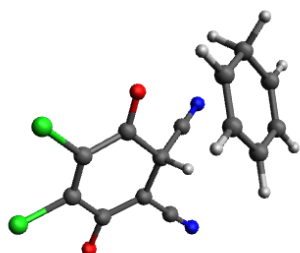
Benzene (P2)

H	2.42190	0.61396	-0.00000
C	1.36409	0.34582	-0.00000
C	0.38255	1.35422	0.00000
H	0.67916	2.40441	0.00000
C	-0.98152	1.00839	0.00000
H	-1.74267	1.79039	0.00000
C	-1.36409	-0.34582	-0.00000
H	-2.42190	-0.61396	-0.00001
C	-0.38255	-1.35422	0.00000
H	-0.67918	-2.40440	0.00001
C	0.98152	-1.00839	0.00000
H	1.74268	-1.79038	0.00000



C-attack TS2 (1a + 2e)

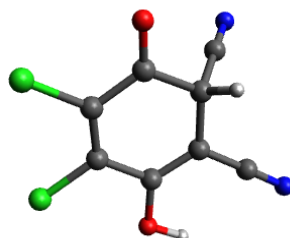
C	1.91339	-1.57346	-1.21488
C	1.82194	-0.14411	-1.47204
C	3.00666	0.68229	-1.29054
C	4.12349	0.16957	-0.69707
C	4.20598	-1.25992	-0.26625
C	3.02346	-2.10225	-0.62273
C	0.29108	0.77302	0.63471
C	-0.67832	1.76302	0.21778
C	-1.99331	1.37281	-0.25101
C	-2.33154	-0.10751	-0.15390
C	-1.50457	-1.03198	0.43626
C	-0.19674	-0.63422	1.01043
C	1.41230	1.22483	1.44096
N	2.34748	1.58465	2.04663
C	-0.31012	3.12789	0.12334
N	0.01055	4.25919	0.05192
O	0.52421	-1.38930	1.65464
Cl	-3.86546	-0.55211	-0.80524
O	-2.82907	2.17640	-0.69982
Cl	-1.92484	-2.70778	0.61576
H	0.97559	0.33910	-0.42081
H	2.96611	1.72733	-1.59605
H	4.99874	0.79922	-0.53509
H	4.36971	-1.30262	0.83110
H	5.13039	-1.72129	-0.66624
H	3.07688	-3.16981	-0.40755
H	1.06520	-2.20723	-1.47159
H	1.08303	0.18994	-2.21150



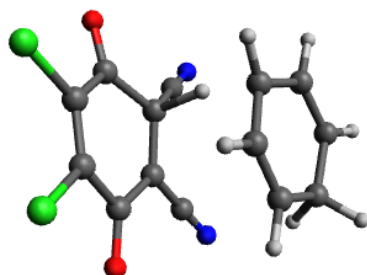
C-attack intermediate IM2 (1a + 2e)

C	-2.66148	-1.29801	1.65980
C	-2.88519	0.09293	1.83019
C	-3.64656	0.86055	0.90629
C	-4.16693	0.25122	-0.21522
C	-3.93916	-1.18868	-0.47514
C	-3.16750	-1.93458	0.54398
C	-0.20744	0.83743	-0.29115
C	0.96527	1.75621	-0.02534
C	2.28635	1.27080	0.19961

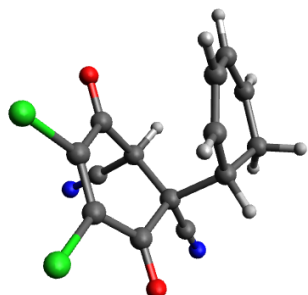
C	2.45890	-0.24111	0.08920
C	1.45893	-1.12160	-0.26351
C	0.10788	-0.65372	-0.59925
C	-1.12647	1.35538	-1.31933
N	-1.85359	1.77815	-2.13302
C	0.70141	3.13064	0.13220
N	0.44086	4.27670	0.25833
O	-0.78258	-1.38501	-1.03593
Cl	4.05326	-0.81079	0.43160
O	3.27833	1.98505	0.48011
Cl	1.71537	-2.84422	-0.40815
H	-0.81476	0.75045	0.64292
H	-3.79714	1.92362	1.08585
H	-4.74104	0.81984	-0.94555
H	-3.40562	-1.29003	-1.44655
H	-4.89780	-1.70196	-0.69407
H	-2.99830	-2.99813	0.38134
H	-2.08106	-1.84542	2.40062
H	-2.47582	0.58771	2.71213

4,5-Dichloro-3-hydroxy-6-oxocyclohexa-2,4-diene-1,2-dicarbonitrile (**IM3**)

H	1.75260	-1.38503	-1.37379
C	1.31506	-1.04618	-0.41968
C	1.51725	0.45737	-0.28321
C	-0.16698	-1.54109	-0.45199
Cl	-2.83533	-1.15166	-0.07051
Cl	-2.15614	1.94396	0.39157
C	2.83311	0.97288	-0.39634
C	2.01088	-1.76064	0.66849
O	0.55740	2.64061	0.06331
O	-0.39720	-2.71561	-0.70537
N	3.91770	1.42170	-0.48797
N	2.56780	-2.31016	1.53850
C	-0.92243	0.78908	0.04207
C	0.45648	1.30596	-0.06091
C	-1.22033	-0.54439	-0.14782
H	1.48396	2.93732	-0.00525

C-attack **TS3** (**1a** + **2e**)

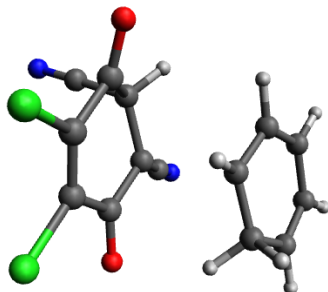
C	-1.32074	0.68704	-1.85590
H	-0.79743	0.97706	-0.58372
C	-0.40577	1.00847	0.71343
C	-0.48051	-0.35843	1.17690
C	-1.81090	-1.66129	-1.38570
C	0.97027	1.60335	0.41405
Cl	3.43647	1.27876	-0.71781
Cl	3.02791	-1.89240	-0.22067
C	-1.64042	-0.85687	1.80936
C	-1.36548	1.95388	1.24994
O	0.61050	-2.46759	1.33534
O	1.16031	2.81311	0.42479
N	-2.62323	-1.28499	2.29949
N	-2.17044	2.70674	1.64561
C	1.83722	-0.72868	0.23111
C	-0.94303	-0.71261	-1.86064
C	0.62465	-1.28989	0.95476
C	2.00737	0.61251	0.00135
H	0.06767	-0.98762	-2.16013
H	-1.49728	-2.70330	-1.31539
C	-3.22037	-1.33442	-1.02072
H	-3.39416	-1.59983	0.04948
H	-3.90937	-2.02446	-1.54583
C	-3.62059	0.08634	-1.25021
H	-4.66546	0.35080	-1.08545
C	-2.72741	1.03196	-1.65726
H	-3.03438	2.06732	-1.80032
H	-0.70036	1.38733	-2.42407

C-attack intermediate **IM4** (**1a** + **2e**)

C	1.24955	-2.30156	-1.21315
H	1.70869	-0.39011	1.37503
C	0.75428	0.12299	1.19506
C	0.86939	1.00312	-0.09723
C	1.59213	0.18035	-1.29776
C	-0.32802	-0.98572	1.08850
Cl	-2.83870	-1.78322	0.39953
Cl	-3.15116	1.02423	-1.14198
C	1.68088	2.19837	0.18063
C	0.42020	0.92209	2.38321
O	-0.62175	2.49576	-1.27529
O	-0.20447	-2.02084	1.72469
N	2.36348	3.12083	0.40807
N	0.13040	1.55027	3.32738
C	-1.67417	0.55086	-0.38338
C	0.82892	-1.08079	-1.64170
C	-0.51804	1.47044	-0.61296
C	-1.55687	-0.63413	0.31019
H	-0.08597	-0.98921	-2.22545
H	1.54639	0.88183	-2.14136
C	3.08706	-0.12967	-1.00339
H	3.57238	0.70929	-0.48623
H	3.58723	-0.20114	-1.98676

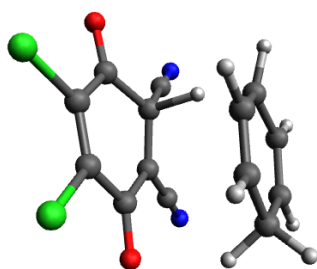


C	3.32601	-1.43070	-0.27320
H	4.24351	-1.53703	0.30713
C	2.45323	-2.46232	-0.39974
H	2.64065	-3.42153	0.08267
H	0.66003	-3.18638	-1.45732



Rearrangement TS4 (1a + 2e)

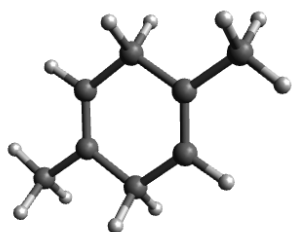
C	-3.74202	0.63498	-1.28229
H	-0.53802	2.29062	-0.39134
C	0.16727	1.65533	0.16249
C	-0.54625	0.42139	0.72484
C	-1.54721	-0.41480	-1.16654
C	1.32544	1.30503	-0.81695
Cl	3.57896	-0.13741	-1.36399
Cl	2.49260	-2.28208	0.78484
C	-1.69499	0.70461	1.52015
C	0.75066	2.46685	1.24967
O	-0.20496	-1.70078	1.72608
O	1.59060	2.05309	-1.74736
N	-2.65763	1.01175	2.12104
N	1.21877	3.09305	2.12162
C	1.60616	-0.85555	0.39694
C	-2.38346	0.67138	-1.55326
C	0.24080	-0.75193	1.05551
C	2.08988	0.06999	-0.49912
H	-1.94846	1.54602	-2.03545
H	-0.55753	-0.49430	-1.61572
C	-2.18368	-1.70338	-0.72883
H	-1.63953	-2.16778	0.11709
H	-2.02812	-2.43804	-1.54714
C	-3.64275	-1.63348	-0.41708
H	-4.10859	-2.52116	0.01128
C	-4.37450	-0.51216	-0.67955
H	-5.44039	-0.47471	-0.45798
H	-4.36101	1.48908	-1.55957



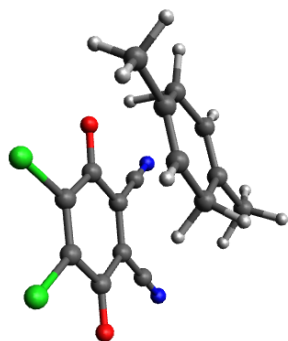
C-attack TS5 (1a + 2e)

C	1.35292	0.11800	2.11057
H	0.92929	0.89255	1.02237
C	0.66461	1.38477	-0.22577

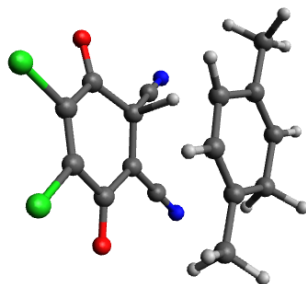
C	0.92328	0.26413	-1.09526
C	0.28947	-2.05343	1.66598
C	-0.78773	1.78011	0.06966
Cl	-3.38728	1.05393	0.47200
Cl	-2.58231	-1.78906	-0.83619
C	2.15605	0.13219	-1.79105
C	1.58176	2.50770	-0.27748
O	0.16767	-1.85920	-1.82690
O	-1.06092	2.90096	0.48566
N	3.15640	0.05473	-2.40568
N	2.34597	3.39479	-0.28961
C	-1.44635	-0.50241	-0.67053
C	0.23776	-0.81214	2.23575
C	-0.06833	-0.78387	-1.24487
C	-1.78829	0.69637	-0.09700
H	-0.65747	-0.48363	2.76321
H	-0.56051	-2.72999	1.75870
C	1.49015	-2.54593	0.93345
H	1.20198	-2.80764	-0.11357
H	1.81771	-3.52392	1.33858
C	2.63397	-1.59110	0.90781
H	3.54929	-1.91376	0.41104
C	2.58854	-0.37011	1.52509
H	3.45568	0.28958	1.50647
H	1.40951	0.94777	2.82315

1,4-Dimethylcyclohexa-1,4-diene (**2f**)

C	0.73940	-1.22066	-0.00001
C	1.45094	-0.07480	-0.00000
C	-0.77163	-1.28195	0.00002
C	-1.45094	0.07480	0.00000
C	-0.73940	1.22066	0.00001
C	0.77163	1.28195	0.00002
H	1.27155	-2.17721	-0.00003
C	2.96120	-0.05251	-0.00002
H	-1.12687	-1.86411	-0.87389
C	-2.96120	0.05251	-0.00001
H	-1.27155	2.17721	-0.00001
H	1.12685	1.86407	0.87396
H	1.12687	1.86411	-0.87389
H	-1.12684	-1.86407	0.87396
H	-3.34475	-0.48541	-0.88483
H	-3.38175	1.06914	-0.00001
H	-3.34477	-0.48541	0.88479
H	3.38175	-1.06914	-0.00007
H	3.34477	0.48536	0.88482
H	3.34475	0.48546	-0.88480

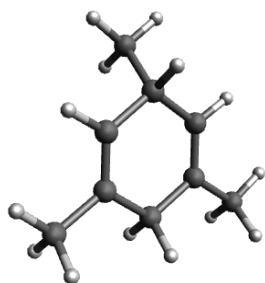
**O-Attack-TS (DDQ 1a + 2f)**

C	1.44219	-2.63351	0.01149
H	1.22621	-1.97718	-1.06403
C	-1.25869	-0.26454	-1.01729
C	-1.96743	0.70325	-0.30233
C	1.68227	-0.80570	1.62160
C	0.16979	-0.12766	-1.27329
Cl	2.50346	1.28380	-1.22479
Cl	0.93875	3.42774	0.60579
C	-3.38102	0.61113	-0.12345
C	-1.93221	-1.38479	-1.60520
O	-1.92675	2.75773	0.90443
O	0.79957	-1.03746	-1.92521
N	-4.54459	0.54350	0.02093
N	-2.50760	-2.28428	-2.09034
C	0.15720	2.01645	-0.02520
C	2.27785	-1.66419	0.73833
C	-1.29721	1.89950	0.26502
C	0.83906	1.07399	-0.77312
C	3.74683	-1.60896	0.41181
C	0.23779	-0.88075	1.99241
H	-0.26418	0.08755	1.75106
H	0.12423	-0.92743	3.09264
C	-0.53910	-1.99075	1.35379
C	-1.96606	-2.15884	1.77670
C	0.06912	-2.83364	0.45251
H	1.95530	-3.50975	-0.40602
H	2.28556	-0.04472	2.11956
H	-0.51037	-3.63301	-0.01002
H	-2.47886	-2.93439	1.19446
H	-2.50872	-1.20559	1.66728
H	-2.01768	-2.41912	2.84686
H	4.23291	-2.55871	0.68699
H	4.24400	-0.78763	0.94393
H	3.89447	-1.46887	-0.67027

**C-Attack-TS (DDQ 1a + 2f)**

C	1.11563	0.35133	2.02198
H	0.55951	1.07434	0.97664
C	0.22039	1.56987	-0.26658

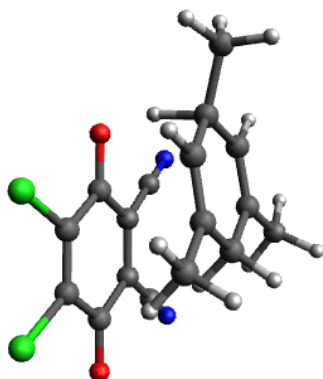
C	0.71428	0.55798	-1.16718
C	0.53863	-1.92312	1.35511
C	-1.28785	1.67555	-0.02646
Cl	-3.73734	0.48210	0.17208
Cl	-2.34440	-2.13011	-1.12302
C	1.96298	0.68397	-1.82736
C	0.91496	2.84211	-0.23482
O	0.39357	-1.62276	-2.03699
O	-1.78552	2.70832	0.41232
N	2.97473	0.78853	-2.42072
N	1.50728	3.85079	-0.17713
C	-1.47636	-0.66063	-0.86801
C	0.18731	-0.78228	2.02512
C	-0.05627	-0.65005	-1.40259
C	-2.06343	0.43522	-0.28613
C	-1.13252	-0.62120	2.73185
H	-0.15708	-2.76330	1.32690
C	1.86095	-2.11183	0.69365
H	1.69901	-2.35713	-0.38195
H	2.34830	-3.02850	1.07926
C	2.81039	-0.95860	0.80136
C	4.15805	-1.09725	0.16511
C	2.44808	0.17533	1.49409
H	3.15732	0.99835	1.58899
H	0.97032	1.11859	2.79130
H	-1.62230	0.32132	2.44407
H	-0.97433	-0.57417	3.82132
H	-1.81160	-1.45379	2.50936
H	4.85964	-0.33819	0.53505
H	4.05627	-0.95708	-0.92628
H	4.57475	-2.10231	0.32868



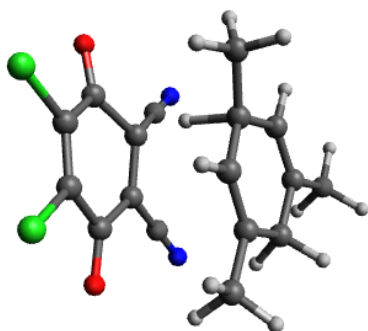
1,3,5-Trimethylcyclohexa-1,4-diene (2g)

C	-0.16786	0.74034	1.25831
C	-0.16786	-0.60792	1.27885
C	-0.14123	1.58066	0.00000
C	-0.16786	0.74034	-1.25831
C	-0.16786	-0.60792	-1.27885
C	-0.16363	-1.42257	0.00000
C	-0.17502	-1.40612	2.56139
H	-1.03510	2.23690	0.00000
C	-0.17502	-1.40612	-2.56139
H	0.71478	-2.09885	0.00000
H	-1.03303	-2.11051	0.00000
H	-0.17937	-0.75195	3.44574
H	0.70925	-2.06510	2.61666
H	-1.06023	-2.06461	2.60722
H	-0.17937	-0.75195	-3.44574
H	-1.06023	-2.06461	-2.60722
H	0.70925	-2.06510	-2.61666
C	1.08801	2.53256	0.00000
H	-0.16694	1.28810	-2.20650
H	-0.16694	1.28810	2.20650

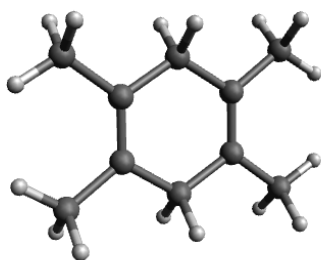
H	2.02019	1.94648	0.00000
H	1.07886	3.17680	0.89356
H	1.07886	3.17680	-0.89356

**O-Attack-TS (DDQ 1a + 2g)**

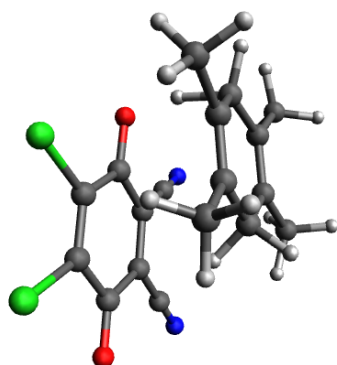
C	-2.57353	-1.39937	0.01336
H	-1.98726	-1.17921	-1.04420
C	-0.17582	1.29921	-1.01701
C	0.82957	1.94883	-0.30091
C	-0.66114	-1.51289	1.60896
C	-0.08160	-0.12331	-1.34053
Cl	1.25930	-2.49837	-1.40840
Cl	3.60983	-1.00458	0.22870
C	0.77003	3.35074	-0.03395
C	-1.29171	2.02602	-1.54582
O	2.94353	1.81982	0.78978
O	-1.01455	-0.69820	-1.99028
N	0.72975	4.50398	0.18376
N	-2.18022	2.64970	-1.98992
C	2.13661	-0.20255	-0.21511
C	-1.51553	-2.12354	0.73437
C	2.04739	1.23384	0.16345
C	1.12919	-0.84063	-0.91142
C	-0.83249	-0.06467	1.96681
H	0.10592	0.48665	1.72444
H	-0.89261	0.04649	3.06617
C	-1.98755	0.64239	1.32121
C	-2.21877	2.06839	1.72604
C	-2.80822	-0.01393	0.44200
C	-3.79704	-2.21046	-0.43989
C	0.45774	-2.24683	2.28874
H	-3.03134	2.53008	1.15150
H	-1.29924	2.65954	1.58732
H	-2.46104	2.12372	2.80031
H	0.52084	-3.29087	1.95653
H	0.32406	-2.22406	3.38290
H	1.41861	-1.74876	2.08110
H	-1.37343	-3.17753	0.49051
H	-3.63813	0.52285	-0.02015
H	-4.41083	-1.62523	-1.13794
H	-4.41209	-2.47062	0.43554
H	-3.48020	-3.13896	-0.93389

**C-Attack-TS (DDQ 1a + 2g)**

C	1.02830	-0.80571	-1.59256
H	0.49530	-1.06748	-0.40185
C	0.06101	-1.13640	0.96228
C	0.19874	0.21268	1.43322
C	1.32767	1.62264	-1.20694
C	-1.31052	-1.65734	0.57161
Cl	-3.70616	-1.18547	-0.65651
Cl	-3.15308	1.95125	-0.09256
C	1.36430	0.64810	2.10711
C	0.97920	-2.13448	1.46190
O	-0.76548	2.38330	1.55685
O	-1.55755	-2.85917	0.53450
N	2.33604	1.04311	2.64291
N	1.75242	-2.93288	1.83221
C	-2.04571	0.71972	0.39361
C	0.57084	0.57349	-1.67180
C	-0.83652	1.20662	1.17005
C	-2.27606	-0.60778	0.13603
C	0.81447	3.02829	-1.19512
C	2.73767	1.39520	-0.74138
H	2.85609	1.77654	0.29343
H	3.41115	2.04956	-1.32780
C	3.24336	-0.01995	-0.80299
C	2.43949	-1.02761	-1.24369
C	0.34108	-1.84693	-2.47101
C	4.65774	-0.24652	-0.35408
H	-0.13997	3.11827	-1.72941
H	1.55131	3.72054	-1.63072
H	0.65052	3.34547	-0.14921
H	4.95683	-1.29661	-0.46889
H	4.75558	0.03721	0.70802
H	5.35490	0.39396	-0.91858
H	-0.43494	0.76055	-2.05051
H	2.81208	-2.05220	-1.27777
H	0.73752	-1.76824	-3.49550
H	-0.74412	-1.68195	-2.50718
H	0.53950	-2.86258	-2.10387

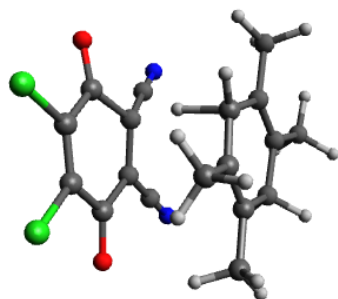
**1,2,4,5-Tetramethylcyclohexa-1,4-diene (2h)**

C	1.29553	0.67664	-0.00002
C	1.29553	-0.67664	-0.00002
C	0.00000	1.46547	-0.00015
C	-1.29553	0.67664	-0.00005
C	-1.29553	-0.67664	-0.00001
C	0.00000	-1.46547	-0.00009
C	2.52332	1.56163	0.00007
C	2.52332	-1.56163	0.00007
H	-0.00001	2.15183	0.87191
C	-2.52332	1.56163	0.00003
C	-2.52332	-1.56163	0.00011
H	-0.00001	-2.15162	-0.87232
H	0.00001	-2.15177	0.87203
H	-2.51471	2.22407	0.88374
H	-3.47015	1.00861	-0.00004
H	-2.51469	2.22425	-0.88355
H	3.47015	-1.00861	-0.00034
H	2.51452	-2.22448	-0.88333
H	2.51489	-2.22384	0.88396
H	0.00001	2.15155	-0.87245
H	3.47015	1.00861	0.00047
H	2.51447	2.22437	0.88356
H	2.51494	2.22395	-0.88374
H	-3.47015	-1.00861	0.00001
H	-2.51472	-2.22402	0.88386
H	-2.51469	-2.22430	-0.88343

**O-Attack-TS (DDQ 1a + 2h)**

C	-1.42520	-2.43354	-0.10037
H	-1.03038	-1.88417	-1.16650
C	-0.74479	1.12780	-1.00108
C	-0.21658	2.16331	-0.21990
C	0.24313	-1.57205	1.48526
C	0.05551	-0.03096	-1.36614
Cl	2.43100	-1.36045	-1.51892
Cl	3.67005	1.01508	0.27552
C	-1.00150	3.30530	0.12126
C	-2.06264	1.22380	-1.54835
O	1.65848	3.08065	0.93233
O	-0.45876	-0.98999	-2.04605
N	-1.64610	4.24497	0.40637
N	-3.13386	1.34826	-2.01152
C	1.99777	0.98734	-0.18889
C	-0.14522	-2.55892	0.60564
C	1.18850	2.15274	0.25066
C	1.46129	-0.03818	-0.94486
C	0.69707	-3.76449	0.27385
C	-0.69213	-0.46174	1.84653
H	-0.19397	0.51712	1.64530
H	-0.80204	-0.42251	2.94939
C	-2.04627	-0.45500	1.21834

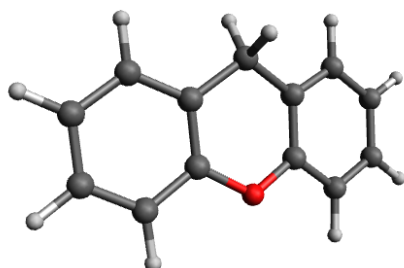
C	-3.00382	0.61147	1.67191
C	-2.41980	-1.45151	0.33407
H	-1.83461	-3.36923	-0.50489
C	1.57204	-1.57925	2.19584
C	-3.81139	-1.52896	-0.23802
H	-3.61559	0.98456	0.83876
H	-2.47227	1.45281	2.13600
H	-3.70021	0.19996	2.42328
H	0.67156	-3.96700	-0.80696
H	0.28335	-4.65143	0.78272
H	1.74109	-3.64864	0.58489
H	2.39968	-1.76006	1.49514
H	1.60527	-2.38250	2.95057
H	1.74899	-0.62483	2.70885
H	-3.89975	-2.35235	-0.95825
H	-4.09011	-0.59019	-0.73946
H	-4.54279	-1.69112	0.57031

**C-Attack-TS (DDQ 1a + 2h)**

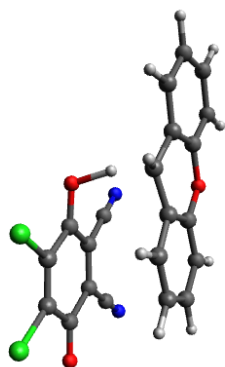
C	-1.20589	0.50402	-1.54764
H	-0.54706	0.92388	-0.43338
C	-0.00870	1.11391	0.86459
C	0.08035	-0.22065	1.40704
C	-1.42365	-1.83775	-0.90617
C	1.25040	1.80714	0.37943
Cl	3.71243	1.65022	-0.79797
Cl	3.69344	-1.47587	0.00464
C	-0.96334	-0.76612	2.18764
C	-1.00749	1.99682	1.42657
O	1.31985	-2.24580	1.52679
O	1.29369	3.02409	0.22029
N	-1.83936	-1.23053	2.82495
N	-1.84359	2.69018	1.86547
C	2.37674	-0.42357	0.38229
C	-0.70283	-0.85542	-1.56569
C	1.23636	-1.06573	1.14456
C	2.38410	0.90082	0.02785
C	-0.92628	-3.24758	-0.78269
C	-2.78424	-1.53734	-0.36141
H	-2.80577	-1.79218	0.72154
H	-3.48995	-2.27673	-0.78930
C	-3.33832	-0.15734	-0.55424
C	-2.58427	0.81861	-1.15481
C	-3.06848	2.23373	-1.40004
H	-0.74237	1.19871	-2.25936
C	0.59925	-1.14519	-2.27577
C	-4.74389	0.04751	-0.05981
H	-2.22120	2.90597	-1.59198
H	-3.62660	2.62764	-0.54157
H	-3.72956	2.26851	-2.28145
H	-0.07772	-3.28270	-0.07504
H	-0.55328	-3.62631	-1.74624



H	-1.71033	-3.91861	-0.40942
H	1.19270	-0.23171	-2.41060
H	0.38785	-1.55429	-3.27793
H	1.20635	-1.88742	-1.74282
H	-5.13621	1.04244	-0.29701
H	-4.77606	-0.09059	1.03461
H	-5.41725	-0.70979	-0.49314

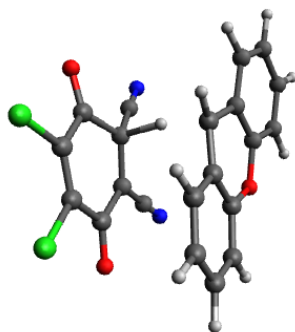
**9H-Xanthene (2j)**

C	-0.81628	-0.18427	3.59371
C	0.58826	-0.22842	3.68039
C	1.35948	-0.09029	2.51509
C	0.75852	0.09702	1.25616
C	-0.64811	0.12159	1.19545
C	-1.43937	-0.01450	2.34873
O	-1.33816	0.28421	0.00000
C	-0.64811	0.12159	-1.19545
C	0.75852	0.09702	-1.25616
C	1.58120	0.31076	0.00000
H	-1.42746	-0.28972	4.49083
H	1.07641	-0.36832	4.64532
H	2.44959	-0.11853	2.57373
H	-2.52513	0.00947	2.25490
C	-1.43937	-0.01450	-2.34873
C	1.35948	-0.09029	-2.51509
H	1.98487	1.34032	0.00000
H	2.45629	-0.35796	0.00000
C	-0.81628	-0.18427	-3.59371
C	0.58826	-0.22842	-3.68039
H	-2.52513	0.00947	-2.25490
H	2.44959	-0.11853	-2.57373
H	-1.42746	-0.28972	-4.49083
H	1.07641	-0.36832	-4.64532

**O-Attack-TS (DDQ 1a + 2j)**

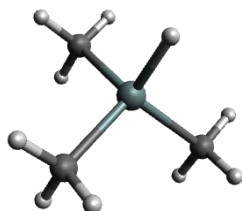
C	-1.78505	-1.30566	0.78564
H	-1.14757	-1.47638	-0.33495
C	0.73902	0.65213	-1.21984
C	1.84184	1.42834	-0.85127

C	-1.42966	1.12579	1.15502
C	0.74334	-0.78826	-1.05919
Cl	1.92644	-3.14623	-0.38628
Cl	4.53561	-1.39328	0.36147
C	1.82731	2.84674	-1.00063
C	-0.43013	1.24802	-1.79055
O	4.07400	1.50291	-0.02154
O	-0.31194	-1.48027	-1.33022
N	1.80884	4.01520	-1.11839
N	-1.38177	1.73831	-2.27120
C	3.07665	-0.66846	-0.22881
C	-0.98384	-0.22152	1.33733
C	3.08582	0.81628	-0.33122
C	1.96629	-1.41742	-0.56154
C	0.28776	-0.42571	1.93027
C	-0.63080	2.22108	1.51103
O	-2.65944	1.40237	0.63072
C	-3.53250	0.38936	0.29027
C	-4.80806	0.78253	-0.13986
C	-3.15523	-0.97540	0.38623
C	-4.11180	-1.95539	0.03011
H	-1.62890	-2.29886	1.22418
C	1.09136	0.65724	2.27946
H	0.62989	-1.44790	2.08833
C	0.63592	1.97953	2.05123
H	-0.99838	3.23156	1.34271
H	1.27508	2.82301	2.30935
H	2.07192	0.49062	2.72238
C	-5.38646	-1.57952	-0.39606
C	-5.73163	-0.20938	-0.48485
H	-5.05287	1.84187	-0.19822
H	-6.72613	0.08001	-0.82356
H	-6.11746	-2.34155	-0.66446
H	-3.83190	-3.00727	0.09483

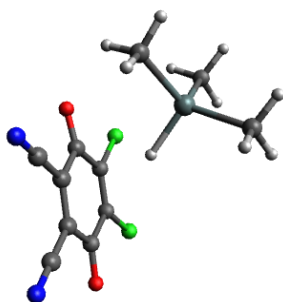
**C-Attack-TS (DDQ 1a + 2j)**

C	1.06887	-0.31135	-1.44121
H	0.45865	-0.89961	-0.31926
C	-0.07576	-1.21692	0.88658
C	-0.43135	0.04704	1.49472
C	1.13582	1.97445	-0.51425
C	-1.18214	-2.10543	0.31702
Cl	-3.58306	-2.33365	-0.96518
Cl	-4.14345	0.70702	-0.03968
C	0.48071	0.72270	2.34363
C	1.03144	-1.95223	1.46813
O	-2.02464	1.80102	1.64662
O	-0.99224	-3.29994	0.11103
N	1.24922	1.26643	3.05046
N	1.95097	-2.52382	1.91429
C	-2.67836	-0.11236	0.35568
C	0.46114	0.99233	-1.29881

C	-1.70599	0.68284	1.21245
C	-2.43968	-1.40058	-0.05024
C	-0.82536	1.31120	-1.81477
C	0.54565	3.21410	-0.22422
O	2.40020	1.76478	-0.03608
C	3.08952	0.61663	-0.36196
C	4.42442	0.54223	0.06030
C	2.47833	-0.43118	-1.10095
C	3.25458	-1.57528	-1.41186
H	0.67011	-0.98294	-2.20812
C	-1.40089	2.54898	-1.55553
H	-1.34403	0.56532	-2.41668
C	-0.72225	3.48936	-0.73908
H	1.08167	3.93076	0.39504
H	-1.19255	4.44556	-0.51341
H	-2.38478	2.78854	-1.95466
C	4.58618	-1.65443	-1.00802
C	5.16635	-0.59762	-0.26613
H	4.85513	1.36528	0.62814
H	6.20456	-0.66834	0.05727
H	5.17885	-2.53491	-1.25303
H	2.78783	-2.38904	-1.96736

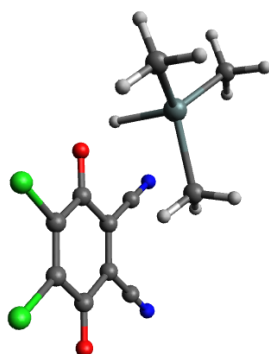
Trimethylstannane (**2n'**)

Sn	0.00009	-0.00004	-0.23693
C	-1.05397	-1.76086	0.46864
C	2.05202	-0.03191	0.46879
C	-0.99853	1.79300	0.46852
H	-1.06835	-1.78217	1.56999
H	-0.56258	-2.67976	0.11173
H	-2.09521	-1.76306	0.10945
H	-1.01282	1.81448	1.56987
H	-2.03904	1.82811	0.10880
H	-0.47838	2.69610	0.11206
H	0.00038	-0.00039	-1.96291
H	2.07748	-0.03149	1.57014
H	2.60245	0.85220	0.11015
H	2.57433	-0.93344	0.11149

Charge transfer complex **CT2** (**1a** + **2n'**)

O	0.10790	-0.02098	2.41450
C	0.84057	0.07031	1.43626
C	1.48040	-1.12241	0.78728
Cl	0.99903	-2.65123	1.40940

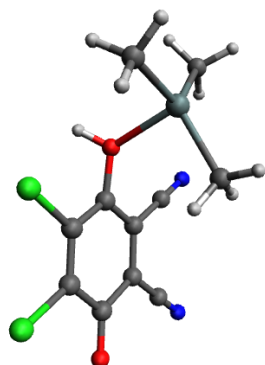
C	2.41036	-0.98019	-0.21103
Cl	3.19010	-2.32075	-0.95892
C	2.81161	0.37039	-0.72278
O	3.65663	0.52112	-1.59990
C	2.11716	1.56871	-0.12584
C	2.47743	2.84670	-0.65492
C	1.16712	1.42640	0.85300
C	0.47565	2.54472	1.41332
N	2.77226	3.89622	-1.08842
N	-0.09722	3.46296	1.86547
H	-0.68607	0.21538	-0.59335
Sn	-2.38541	-0.10452	-0.48041
C	-3.19223	1.19244	1.05379
C	-2.62910	-2.18772	0.06074
C	-3.25952	0.31446	-2.41799
H	-3.09641	1.36652	-2.69893
H	-4.34442	0.12581	-2.39288
H	-2.81322	-0.32692	-3.19376
H	-2.20196	-2.38216	1.05598
H	-2.12691	-2.84299	-0.66757
H	-3.69919	-2.44815	0.08369
H	-2.69623	1.00614	2.01836
H	-4.27122	1.00729	1.17535
H	-3.04734	2.25069	0.78807



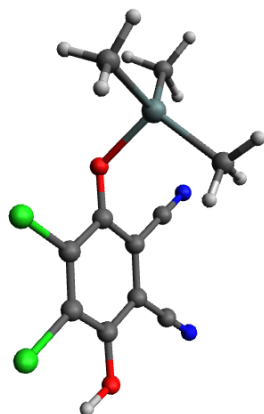
O-attack TS6 (1a + 2n')

O	-4.21253	0.05645	-1.11511
C	-3.16665	0.07092	-0.45331
C	-2.46142	-1.17174	-0.03246
Cl	-3.18052	-2.65818	-0.54069
C	-1.30039	-1.12700	0.71259
Cl	-0.43290	-2.55285	1.17617
C	-0.73028	0.14655	1.15824
O	0.32053	0.19683	1.88354
C	-1.35975	1.38133	0.69924
C	-0.72193	2.61284	1.05550
C	-2.53685	1.35758	-0.03713
C	-3.19151	2.55977	-0.44181
N	-0.18768	3.62100	1.32877
N	-3.72884	3.54885	-0.77618
H	1.56599	0.08726	1.20843
Sn	2.65593	0.02167	-0.30906
C	1.03501	0.26630	-1.73812
C	3.59581	-1.92438	-0.39818
C	4.03706	1.68439	-0.27181
H	3.48929	2.63240	-0.16864
H	4.60815	1.70220	-1.21420
H	4.74168	1.58339	0.56658
H	2.83326	-2.71620	-0.36848
H	4.28714	-2.05913	0.44656
H	4.16478	-2.00997	-1.33815
H	0.32398	-0.57022	-1.68831

H	1.47647	0.28793	-2.74844
H	0.49760	1.21180	-1.57795

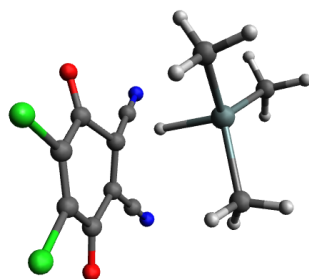
**IM5****O-attack intermediate IM5 (1a + 2n')**

O	4.37901	0.45553	0.66285
C	3.20568	0.33117	0.23254
C	2.58368	-0.98431	-0.02603
Cl	3.57041	-2.38118	0.29264
C	1.27478	-1.12046	-0.49565
Cl	0.53169	-2.68268	-0.78020
C	0.49895	0.03105	-0.77019
O	-0.85912	-0.08047	-1.15526
C	1.01035	1.31488	-0.54928
C	0.17001	2.44527	-0.80025
C	2.33707	1.47559	-0.05686
C	2.86273	2.77760	0.16747
N	-0.53557	3.36409	-0.99298
N	3.29871	3.85520	0.35482
H	-0.95811	-0.58388	-1.98517
Sn	-2.53134	-0.05962	0.35821
C	-1.24938	0.51129	1.97237
C	-3.14597	-2.10857	0.22279
C	-3.72320	1.42969	-0.61132
H	-3.09815	2.30616	-0.83258
H	-4.54783	1.73312	0.05156
H	-4.14671	1.02978	-1.54373
H	-2.44672	-2.75044	0.77558
H	-3.17611	-2.42526	-0.83039
H	-4.15446	-2.21665	0.65024
H	-0.36965	-0.14703	2.00548
H	-1.79700	0.41261	2.92186
H	-0.92320	1.55375	1.85785

**P3****O-Trimethylstannyl-2,3-dichloro-5,6-dicyanohydroquinone (P3)**

O	-0.87393	-0.20737	-0.97722
---	----------	----------	----------

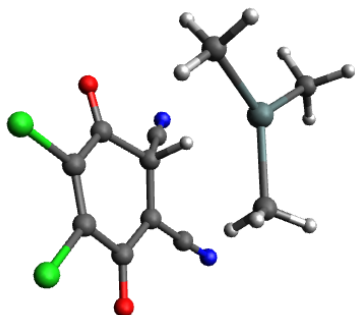
Sn	-2.53107	-0.07673	0.22705
C	0.04839	2.39214	-0.60619
C	0.92433	1.27973	-0.42678
C	2.29278	1.47965	-0.06881
C	2.81221	2.79861	0.10683
C	3.14605	0.37022	0.11594
O	4.43651	0.62082	0.44623
C	2.61432	-0.93758	-0.04897
Cl	3.69646	-2.28647	0.20353
C	1.26429	-1.13260	-0.39533
Cl	0.60067	-2.72785	-0.57096
C	0.38615	-0.02324	-0.60701
N	3.23010	3.88683	0.25143
N	-0.69097	3.29471	-0.74417
C	-3.79173	1.24982	-0.89473
C	-1.67623	0.68377	2.05097
C	-3.20521	-2.11715	0.31118
H	-1.43468	1.75178	1.95269
H	-0.75641	0.13074	2.29592
H	-2.38688	0.55887	2.88222
H	-3.31032	2.23391	-0.98517
H	-4.76412	1.36972	-0.39255
H	-3.96520	0.84037	-1.90140
H	-3.26985	-2.53135	-0.70634
H	-4.20174	-2.17083	0.77640
H	-2.50521	-2.72858	0.89903
H	4.93021	-0.21327	0.54766



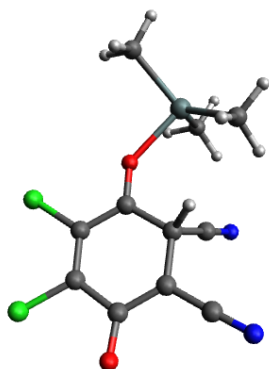
C-attack TS7 (1a + 2n')

Sn	2.05811	-0.62803	-0.52738
H	0.79120	0.40104	0.39953
C	-0.29479	1.26253	1.04304
C	0.56550	2.03114	1.91984
N	1.27153	2.65094	2.61857
C	-1.05085	1.94568	0.05944
C	-0.70692	3.26397	-0.34676
N	-0.41617	4.35451	-0.67825
C	-2.08479	1.24400	-0.70668
O	-2.71197	1.77729	-1.62934
C	-2.35613	-0.20036	-0.32097
Cl	-3.45255	-1.04516	-1.34540
C	-1.80446	-0.78141	0.79245
Cl	-2.17467	-2.38863	1.31505
C	-0.88427	-0.00886	1.67529
O	-0.56253	-0.36217	2.79989
C	1.92569	-2.59356	0.35379
C	3.89435	0.43993	-0.15178
C	1.22156	-0.41753	-2.50822
H	0.97516	-3.07433	0.08177
H	2.75958	-3.21150	-0.01508
H	1.99460	-2.52573	1.44935
H	3.82157	1.46895	-0.53170
H	4.72332	-0.07333	-0.66446

H	4.10547	0.46683	0.92697
H	1.93484	-0.81459	-3.24790
H	0.27775	-0.97633	-2.58495
H	1.03279	0.64273	-2.73183

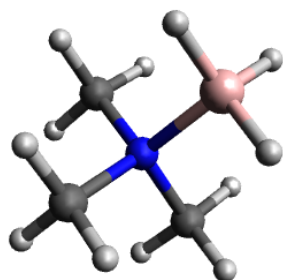
C-attack intermediate **IM6** (**1a** + **2n'**)

Sn	2.21232	-0.70902	-0.60315
H	0.71312	0.45613	0.58058
C	-0.17158	1.02136	1.09057
C	0.46957	1.74395	2.19647
N	0.98386	2.33184	3.06731
C	-0.86174	1.89128	0.10123
C	-0.31757	3.16123	-0.19193
N	0.16154	4.21461	-0.42555
C	-1.95852	1.41038	-0.68471
O	-2.53555	2.06487	-1.57864
C	-2.42786	-0.01378	-0.37948
Cl	-3.63389	-0.62692	-1.44826
C	-1.97731	-0.75906	0.68461
Cl	-2.59749	-2.33736	1.08077
C	-0.96695	-0.21800	1.61837
O	-0.67488	-0.73211	2.69029
C	1.68760	-2.67123	0.08795
C	3.95660	0.26260	0.18155
C	1.18039	0.13578	-2.27745
H	0.71737	-2.97159	-0.32961
H	2.46373	-3.38193	-0.23663
H	1.64041	-2.67933	1.18648
H	3.89147	1.34485	0.00460
H	4.84693	-0.13622	-0.33036
H	4.04273	0.06123	1.25843
H	1.89201	0.67356	-2.91997
H	0.67037	-0.65452	-2.84519
H	0.42944	0.85705	-1.91212

C-attack intermediate **IM7** (**1a** + **2n'**)

Sn	2.71754	-0.07600	-0.13632
----	---------	----------	----------

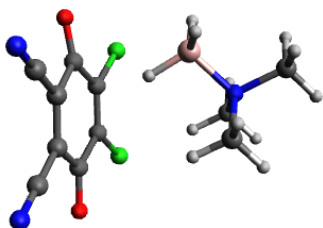
H	-0.15331	1.47702	-1.00862
C	-0.72010	1.15322	-0.11601
C	-0.07558	1.78284	1.05682
N	0.42515	2.29558	1.98265
C	-2.16144	1.61452	-0.23815
C	-2.37625	2.99198	-0.43896
N	-2.52535	4.15123	-0.61196
C	-3.27248	0.72808	-0.16247
O	-4.47981	1.05420	-0.23876
C	-2.89552	-0.73933	-0.00807
Cl	-4.22460	-1.81309	0.07607
C	-1.59210	-1.24101	0.04365
Cl	-1.23932	-2.94512	0.16991
C	-0.47427	-0.35380	-0.01449
O	0.71920	-0.80046	0.02557
C	3.45883	-1.76607	-1.22326
C	3.22094	0.05477	1.94174
C	2.51266	1.74554	-1.25985
H	2.91420	-1.87220	-2.17290
H	4.52942	-1.63410	-1.44206
H	3.32870	-2.68093	-0.62713
H	2.70708	0.90840	2.40340
H	4.30863	0.18249	2.04998
H	2.92102	-0.87277	2.45091
H	3.51717	2.08564	-1.55624
H	1.92957	1.57465	-2.17714
H	2.04562	2.53933	-0.66096



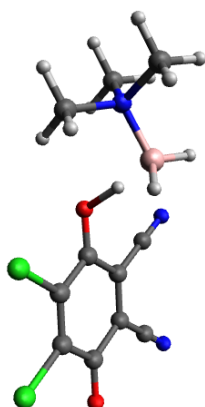
Trimethylamine borane complex (2p)

H	1.99948	0.99220	0.64696
B	1.66640	0.00299	0.00345
N	0.01270	0.00006	-0.00003
C	-0.49967	-0.07784	1.40505
C	-0.49286	-1.18031	-0.77068
C	-0.49776	1.25547	-0.63744
H	-1.59292	-1.18277	-0.77224
H	-0.11070	-2.09051	-0.29530
H	-0.11060	-1.11161	-1.79525
H	-1.59974	-0.08042	1.40226
H	-0.12218	0.78993	1.95731
H	-0.11778	-0.99859	1.86003
H	-1.59779	1.25363	-0.63899
H	-0.11546	1.30052	-1.66326
H	-0.11932	2.11002	-0.06552
H	2.00299	-1.04758	0.53880
H	2.00481	0.06588	-1.17351



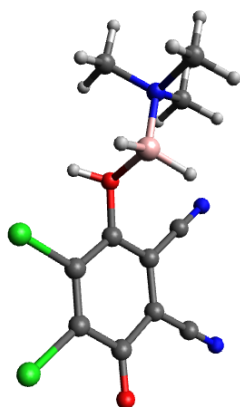
Charge transfer complex **CT3** (**1a** + **2p**)

C	-1.95198	-0.59319	-0.51786
C	-1.59974	-0.84928	0.78334
C	-0.85797	0.17692	1.61107
C	-0.32730	1.37718	0.87741
C	-0.65573	1.61518	-0.43204
C	-1.50730	0.66431	-1.21538
C	-1.97229	-2.05633	1.45128
N	-2.27080	-3.05104	1.99592
O	-0.75761	0.04325	2.82317
Cl	0.65250	2.44034	1.80694
Cl	-0.11274	3.01021	-1.29134
O	-1.82080	0.86794	-2.38558
C	-2.70774	-1.52405	-1.29619
N	-3.32640	-2.28866	-1.93531
B	1.97986	-1.46030	0.91075
N	2.85388	-1.32096	-0.46988
C	4.26106	-1.77407	-0.22106
C	2.87168	0.10664	-0.92460
C	2.24468	-2.16873	-1.54610
H	4.23385	-2.82006	0.10344
H	4.68826	-1.15070	0.57238
H	4.84983	-1.67468	-1.14440
H	1.83902	0.42176	-1.10544
H	3.46133	0.19597	-1.84792
H	3.30953	0.71860	-0.12881
H	1.21989	-1.82076	-1.71961
H	2.22823	-3.20749	-1.19851
H	2.83771	-2.08157	-2.46763
H	2.46249	-0.69295	1.72759
H	2.00328	-2.63727	1.23663
H	0.83755	-1.12108	0.59818

O-attack **TS8** (**1a** + **2p**)

C	2.41254	1.26498	0.06083
C	3.03665	-0.07401	0.22726
C	2.13296	-1.23805	0.03483
C	0.79931	-1.07876	-0.29002
C	0.22269	0.24575	-0.49727
C	1.06296	1.40416	-0.25580

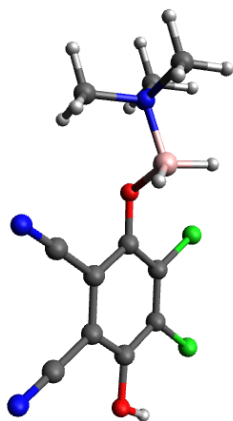
O	4.23915	-0.19484	0.50983
Cl	2.85640	-2.79991	0.23684
Cl	-0.27437	-2.42828	-0.49632
O	-1.00351	0.40617	-0.85696
C	0.45336	2.69475	-0.37902
N	-0.04516	3.75270	-0.47051
C	3.25650	2.40143	0.24128
N	3.95116	3.33647	0.39060
B	-2.88337	0.46113	1.12676
N	-4.21171	0.09413	0.31867
C	-4.09443	-1.27400	-0.29863
C	-4.46201	1.10947	-0.76505
C	-5.36548	0.10698	1.28885
H	-1.89919	0.45417	0.15726
H	-5.43980	1.10796	1.72782
H	-5.17176	-0.63626	2.07010
H	-6.28819	-0.14115	0.74627
H	-3.24099	-1.26847	-0.98432
H	-5.02221	-1.50763	-0.83715
H	-3.92280	-1.99944	0.50348
H	-3.61113	1.09464	-1.45414
H	-4.54849	2.09667	-0.29914
H	-5.38844	0.85041	-1.29410
H	-2.53286	-0.44100	1.85239
H	-2.88707	1.61380	1.49092



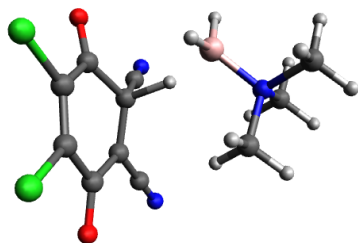
O-attack intermediate IM8 (1a + 2p)

B	-2.24738	-0.46212	0.77251
N	-1.23998	3.18187	-0.63614
C	-0.47663	2.30564	-0.47178
C	0.47044	1.25158	-0.27868
C	0.06347	-0.08136	-0.37640
C	0.97860	-1.14565	-0.20808
C	2.32164	-0.87277	0.06057
C	2.84063	0.50175	0.20992
C	1.83361	1.54819	0.01304
N	-3.75063	-0.17279	0.30049
C	-4.59307	-0.31453	1.54602
O	-1.32708	-0.34287	-0.59432
Cl	0.37191	-2.78289	-0.39654
Cl	3.47651	-2.16115	0.23746
O	4.04309	0.75004	0.47184
C	2.26180	2.90046	0.11457
N	2.62048	4.01829	0.19954
C	-4.22270	-1.17429	-0.72044
C	-3.92143	1.22063	-0.24904
H	-1.41474	-1.13134	-1.16936
H	-4.24393	0.41219	2.28762
H	-4.48314	-1.33398	1.93107
H	-5.63943	-0.11673	1.28251

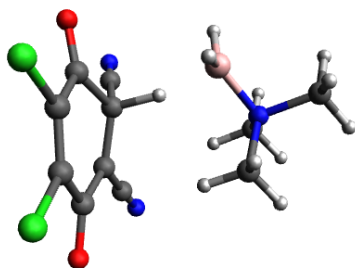
H	-3.65492	-1.03259	-1.64705
H	-5.28754	-1.00553	-0.92257
H	-4.06442	-2.18168	-0.32060
H	-3.30452	1.32265	-1.14592
H	-3.58815	1.93401	0.51001
H	-4.97958	1.37771	-0.49200
H	-2.15228	-1.59835	1.15085
H	-1.84882	0.42595	1.47175

O-attack product **P4** (**1a** + **2p**)

C	0.06860	-0.06335	-0.22960
C	-0.45070	1.25381	-0.15602
C	-1.84874	1.49147	0.01341
C	-2.74619	0.40477	0.10645
C	-2.23391	-0.91627	0.02162
C	-0.85412	-1.14777	-0.14028
C	0.45004	2.35614	-0.28620
N	1.16897	3.27531	-0.41339
C	-2.35807	2.82414	0.08539
N	-2.76936	3.92244	0.14460
O	-4.06043	0.69193	0.26642
Cl	-3.37741	-2.23421	0.12931
Cl	-0.22464	-2.76329	-0.25163
O	1.36880	-0.28456	-0.41937
B	2.27631	-0.23338	0.79775
N	3.78861	-0.14366	0.18896
C	3.96286	1.09122	-0.64892
C	4.09966	-1.35533	-0.64294
C	4.73867	-0.08778	1.34834
H	5.13076	-1.28465	-1.01560
H	3.39283	-1.39192	-1.47792
H	3.97914	-2.24371	-0.01317
H	4.99778	1.13675	-1.01430
H	3.73147	1.96324	-0.02908
H	3.26150	1.04131	-1.48698
H	-4.58424	-0.12870	0.31694
H	5.76828	-0.03616	0.96954
H	4.60037	-0.98987	1.95472
H	4.50695	0.80195	1.94419
H	2.22463	-1.26670	1.44605
H	2.09070	0.77899	1.45145

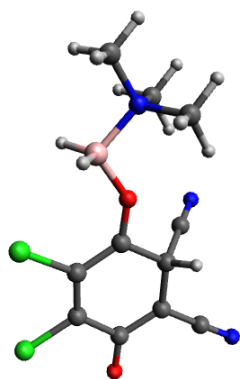
C-attack **TS9** (**1a** + **2p**)

O	-1.34316	2.08733	-1.91464
C	-1.06693	1.40220	-0.91653
C	-1.94291	0.20742	-0.55110
Cl	-3.16862	-0.18568	-1.69817
C	-1.80805	-0.48301	0.62518
Cl	-2.86257	-1.77381	1.10625
C	-0.75754	-0.11106	1.60726
O	-0.72070	-0.52010	2.75756
C	0.38301	0.77801	1.04524
C	1.25254	1.30960	2.08816
C	0.05866	1.67013	-0.04421
C	0.92265	2.74329	-0.38060
N	1.95877	1.74212	2.91444
N	1.65093	3.62795	-0.65341
H	1.12654	-0.26701	0.63907
B	1.73280	-1.58731	0.51287
N	2.64913	-1.46657	-0.77337
C	1.86986	-0.88875	-1.92844
C	3.07907	-2.87528	-1.12233
C	3.88248	-0.63590	-0.51916
H	3.73514	-2.82774	-2.00157
H	2.18657	-3.46984	-1.34265
H	3.62071	-3.29762	-0.26837
H	2.50504	-0.88705	-2.82261
H	1.57686	0.13600	-1.67734
H	0.98006	-1.50679	-2.08764
H	4.49475	-0.62536	-1.42915
H	4.43405	-1.08758	0.31139
H	3.58333	0.38296	-0.25754
H	0.74420	-2.23773	0.30995
H	2.34098	-1.62644	1.54686

C-attack intermediate **IM9** (**1a** + **2p**)

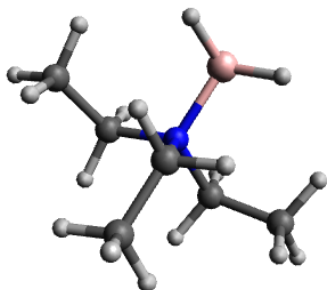
C	0.15467	1.44503	0.53023
C	-0.96746	1.63649	-0.34636
C	-1.96173	0.47757	-0.43609
C	-1.90568	-0.63572	0.36521
C	-0.84088	-0.78958	1.38181
C	0.38807	0.15846	1.20718
O	-1.16982	2.66954	-1.01398
Cl	-3.21830	0.68215	-1.59942
Cl	-3.09310	-1.90600	0.32522

O	-0.84190	-1.64467	2.25537
C	1.18663	0.23596	2.43300
N	1.83446	0.31543	3.40345
C	1.13893	2.45738	0.60278
N	1.98434	3.27767	0.66845
B	1.83672	-1.80096	-0.14874
N	2.69187	-1.01910	-1.20121
C	3.65942	-0.05750	-0.55034
C	1.81429	-0.27088	-2.17853
C	3.47429	-2.08698	-1.94448
H	1.04277	-0.59327	0.51038
H	4.08822	-1.58642	-2.70423
H	2.76694	-2.77422	-2.42122
H	4.11319	-2.61856	-1.23023
H	2.45395	0.20453	-2.93127
H	1.25538	0.49275	-1.62779
H	1.12902	-0.98474	-2.64607
H	4.28280	0.39340	-1.33137
H	4.27404	-0.61351	0.16421
H	3.08876	0.72213	-0.03661
H	0.87308	-2.34740	-0.59681
H	2.41765	-2.12273	0.84379

C-attack intermediate **IM10** (**1a** + **2p**)

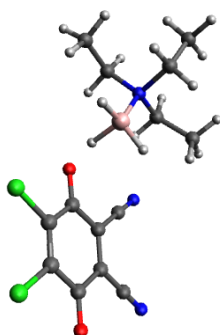
C	-2.05775	1.44834	-0.25792
C	-2.90034	0.32207	-0.04719
C	-2.15778	-1.00188	0.03924
C	-0.77007	-1.17960	-0.05595
C	0.07935	-0.04376	-0.19308
C	-0.54553	1.34934	-0.32092
O	-4.15029	0.34307	0.03261
Cl	-3.17194	-2.36512	0.24596
Cl	-0.05112	-2.76993	-0.01221
O	1.35512	-0.02434	-0.24251
C	0.08135	2.22411	0.69463
N	0.56039	2.92668	1.49856
C	-2.62976	2.72109	-0.44869
N	-3.08409	3.79860	-0.61520
B	2.55026	-0.98578	-0.09421
N	3.83144	0.01964	-0.09400
C	3.79378	0.95640	1.08345
C	3.90955	0.82018	-1.36516
C	5.05453	-0.84881	0.01257
H	-0.19938	1.70964	-1.30897
H	5.94564	-0.20834	0.03044
H	5.08444	-1.51914	-0.85337
H	4.98799	-1.43235	0.93742
H	4.81759	1.43664	-1.34654
H	3.02181	1.45736	-1.43172
H	3.93683	0.12319	-2.21003
H	4.69455	1.58376	1.07178

H	3.75765	0.35529	1.99853
H	2.89726	1.57941	1.00966
H	2.63849	-1.69174	-1.07178
H	2.52087	-1.53801	0.97969



Triethylamine borane complex (2q)

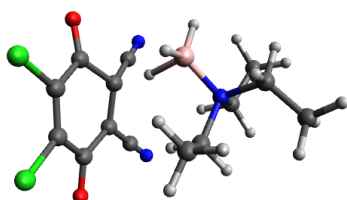
B	0.00013	-1.66985	1.08807
H	-1.00775	-1.58665	1.77456
N	0.00002	-0.36721	0.06111
H	0.00021	-2.66049	0.36304
H	1.00801	-1.58648	1.77455
C	-1.21307	-0.42792	-0.85577
C	1.21310	-0.42776	-0.85579
C	-0.00004	0.89896	0.88888
C	-2.56751	-0.23123	-0.17360
H	-1.16324	-1.41675	-1.32863
H	-1.07844	0.33392	-1.63797
C	2.56753	-0.23107	-0.17361
H	1.07842	0.33415	-1.63792
H	1.16332	-1.41655	-1.32875
H	-2.71782	-0.95696	0.63381
H	-3.35043	-0.37666	-0.93208
H	-2.67708	0.78400	0.23233
H	2.67702	0.78410	0.23249
H	3.35045	-0.37630	-0.93213
H	2.71791	-0.95693	0.63367
H	-0.88107	0.83482	1.53655
C	-0.00015	2.20422	0.08818
H	0.88102	0.83494	1.53651
H	-0.89244	2.29525	-0.54673
H	0.89216	2.29541	-0.54669
H	-0.00024	3.04578	0.79550



O-Attack-TS (DDQ 1a + 2q)

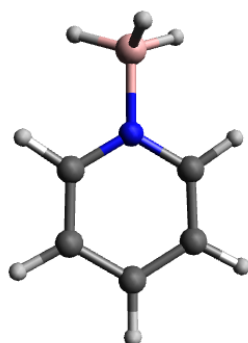
C	2.58610	1.52259	-0.11741
C	3.54388	0.48440	0.34640
C	3.07864	-0.92240	0.23446
C	1.83650	-1.24011	-0.28003

C	0.92609	-0.20407	-0.76477
C	1.32823	1.18351	-0.61087
O	4.65896	0.79115	0.79638
Cl	4.19017	-2.13277	0.78409
Cl	1.26947	-2.87576	-0.39766
O	-0.21014	-0.49162	-1.28997
C	0.39997	2.19083	-1.02826
N	-0.35739	3.02254	-1.36085
C	3.00979	2.88240	-0.02943
N	3.35683	4.00191	0.04443
H	-1.22015	-0.74777	-0.37733
H	-4.78290	-0.14394	-1.40112
H	-4.64092	-2.55084	-1.96551
H	-2.38920	1.38055	-0.81160
H	-5.21907	-2.35612	-0.29814
C	-4.35162	-2.22032	-0.95790
C	-3.93588	-0.75357	-1.06005
C	-3.19989	1.36207	-0.07530
H	-3.11696	-0.63063	-1.77964
H	-4.11323	1.72929	-0.56161
B	-2.06719	-0.82100	0.69590
H	-2.64062	3.24947	0.73941
N	-3.42645	-0.11881	0.23742
H	-1.97547	1.88341	1.66295
C	-2.85970	2.24424	1.12432
H	-3.53015	-2.85564	-0.60701
H	-2.20399	-2.00386	0.88532
H	-1.42389	-0.15496	1.47627
H	-3.70030	2.32436	1.82650
C	-4.42464	-0.30061	1.37609
H	-6.29774	-0.14502	0.24946
H	-4.49994	-1.37986	1.54615
C	-5.80299	0.31238	1.11649
H	-5.74725	1.39806	0.96237
H	-3.95764	0.14416	2.26219
H	-6.42680	0.12549	2.00166

**C-Attack-TS (DDQ 1a + 2q)**

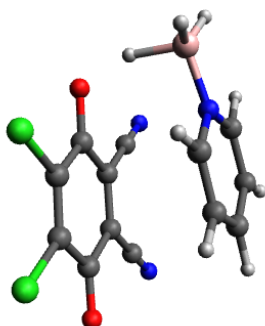
O	1.81923	0.43517	2.75407
C	1.60258	0.55055	1.53946
C	2.35466	-0.31925	0.54107
Cl	3.35558	-1.53932	1.23390
C	2.27379	-0.13047	-0.81403
Cl	3.18413	-1.05134	-1.96444
C	1.42703	0.95467	-1.38073
O	1.49684	1.34140	-2.53694
C	0.36688	1.52724	-0.41636
C	-0.33697	2.68749	-0.93600
C	0.63775	1.49187	0.98722
C	-0.14632	2.25224	1.89476
N	-0.91221	3.62251	-1.34091
N	-0.81147	2.87922	2.63623
H	-0.57315	0.51938	-0.80398
B	-1.42912	-0.38373	-1.42664
H	-0.67343	-1.23967	-1.79918
H	-1.97100	0.32876	-2.22736

H	-3.81082	-2.99445	1.01403
H	-4.94540	-3.19244	-0.33930
H	-3.72181	1.32876	-1.51560
C	-4.31489	-2.46735	0.19338
H	-4.57842	1.86168	-0.05104
H	-4.96910	-1.69303	0.61482
H	-2.37069	1.07326	0.64406
C	-4.16807	0.98711	-0.57476
C	-3.13805	0.34649	0.35295
C	-3.31790	-1.88972	-0.81350
H	-4.99972	0.30505	-0.79528
H	-2.68189	-2.67694	-1.23275
H	-3.62409	-0.00910	1.27007
N	-2.36951	-0.84466	-0.23060
H	-3.83658	-1.39895	-1.64472
C	-1.53836	-1.42170	0.92031
H	-0.06792	-2.56992	-0.22999
H	-1.43579	-3.54075	0.38559
C	-0.76453	-2.70045	0.60593
H	-2.22912	-1.59218	1.75541
H	-0.85805	-0.61482	1.21690
H	-0.18421	-2.95924	1.50245

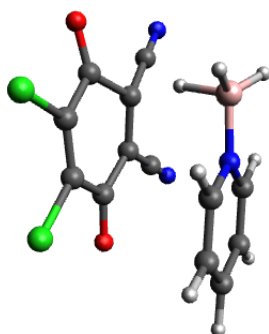
**2r****Pyridine borane complex (2r)**

H	2.84075	-0.02310	1.21013
B	2.52934	0.00025	0.02030
N	0.90595	0.00054	-0.02150
C	0.21735	-1.16939	-0.01558
C	0.21652	1.16998	-0.01565
C	-1.17876	-1.20771	0.00419
C	-1.17965	1.20718	0.00408
H	2.89708	-1.01171	-0.56366
H	2.89652	1.03349	-0.52506
C	-1.89496	-0.00051	0.01380
H	0.82585	2.07059	-0.02841
H	-1.68628	-2.17061	0.00730
H	0.82715	-2.06975	-0.02912
H	-2.98448	-0.00086	0.02534
H	-1.68801	2.16965	0.00750



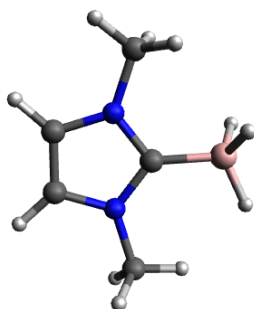
**O-Attack-TS (DDQ 1a + 2r)**

O	1.35639	2.87632	0.41209
C	1.00890	1.79561	-0.08318
C	1.90002	0.60668	-0.13348
Cl	3.47854	0.81892	0.54484
C	1.47908	-0.59466	-0.66361
Cl	2.48500	-2.00456	-0.68090
C	0.13899	-0.74707	-1.25322
O	-0.25677	-1.84592	-1.76286
C	-0.74772	0.41156	-1.23128
C	-2.04613	0.25613	-1.81527
C	-0.34791	1.62004	-0.67385
C	-1.21313	2.75557	-0.65667
N	-3.11202	0.13841	-2.29036
N	-1.93114	3.68392	-0.63116
H	-0.93871	-2.77850	-0.84687
B	-1.54107	-3.20170	0.29162
N	-1.55813	-1.87059	1.08371
C	-0.43577	-1.45277	1.74385
C	-2.64899	-1.04462	1.03409
C	-0.36784	-0.20352	2.35459
C	-2.64128	0.21049	1.63271
H	-0.73144	-3.98481	0.73339
H	-2.64534	-3.54173	-0.06133
C	-1.47913	0.65203	2.29058
H	-3.50576	-1.43501	0.49221
H	0.54844	0.09094	2.86166
H	0.38838	-2.16081	1.75941
H	-1.44542	1.63834	2.75099
H	-3.52737	0.83771	1.56475

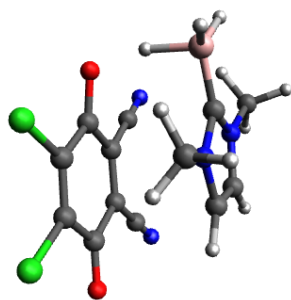
**C-Attack-TS (DDQ 1a + 2r)**

O	0.95723	-1.04463	-2.03888
C	0.24229	-0.31430	-1.34100
C	-1.08486	-0.81873	-0.80256
Cl	-1.44751	-2.46604	-1.16236
C	-1.95789	-0.01619	-0.11506
Cl	-3.50196	-0.55485	0.45048
C	-1.65031	1.42512	0.11687

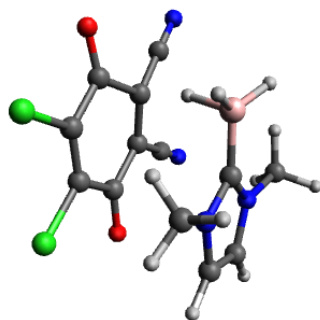
O	-2.47879	2.24158	0.49211
C	-0.18774	1.82412	-0.10658
C	0.08489	3.23881	0.02891
C	0.61455	1.05632	-0.98857
C	1.84516	1.56109	-1.49487
N	0.31726	4.38056	0.14247
N	2.85725	1.98604	-1.91584
H	0.09989	1.43571	1.35877
B	0.57272	0.81595	2.46937
N	1.32708	-0.35386	1.79604
C	0.77384	-1.60340	1.74073
C	2.50748	-0.11304	1.14975
C	1.39273	-2.64142	1.05339
C	3.16655	-1.11202	0.43798
H	-0.40492	0.46118	3.07642
H	1.31095	1.67540	2.88759
C	2.60194	-2.39477	0.37997
H	2.89389	0.89837	1.23767
H	0.92278	-3.62176	1.03512
H	-0.16701	-1.72277	2.27091
H	3.09386	-3.18958	-0.17826
H	4.09760	-0.87530	-0.07142

1,3-dimethylimidazolyli-dene borane complex (**2t**)

C	-0.77506	-1.52926	0.00510
C	0.59075	-1.60108	-0.00389
N	1.05577	-0.29302	-0.01367
C	0.02053	0.59907	-0.00517
N	-1.10376	-0.17745	0.00472
B	0.18969	2.20476	-0.00087
C	-2.48582	0.31302	0.00105
H	-1.53246	-2.30290	0.00727
H	-2.46180	1.40526	0.03714
H	-3.01470	-0.08163	0.87870
H	-2.99150	-0.02090	-0.91505
H	1.26339	-2.44945	-0.00743
C	2.46615	0.10283	0.00798
H	3.07738	-0.76553	-0.26184
H	2.73998	0.45928	1.01024
H	2.61612	0.91466	-0.71313
H	0.82722	2.51509	1.01380
H	-0.89847	2.77204	-0.02087
H	0.86294	2.51606	-0.99225

**O-Attack-TS (DDQ 1a + 2t)**

C	0.65427	0.02412	-2.19457
C	1.94471	0.35615	-1.82621
N	2.41924	-0.67207	-1.05722
C	1.47460	-1.67131	-0.93858
N	0.38886	-1.20518	-1.64666
C	-0.83415	-1.97744	-1.91501
H	-0.06151	0.55344	-2.81055
H	-0.96026	-2.72312	-1.12791
H	-0.73724	-2.47547	-2.88817
H	-1.68691	-1.29163	-1.92903
H	2.53875	1.23230	-2.05271
C	3.79189	-0.76125	-0.53262
H	4.20834	0.24954	-0.48927
H	4.39067	-1.39318	-1.20032
H	3.76334	-1.19785	0.46838
C	0.30025	1.72599	0.49046
C	-1.04644	1.84443	-0.12959
C	-1.97138	0.70465	0.11645
C	-1.58618	-0.40494	0.84035
C	-0.23688	-0.52050	1.41372
C	0.65866	0.61387	1.25044
O	-1.37371	2.84653	-0.78229
Cl	-3.56070	0.86588	-0.55869
Cl	-2.65697	-1.73658	1.13520
O	0.17130	-1.58485	1.98224
C	1.93420	0.53599	1.89199
N	2.97692	0.48994	2.42784
C	1.19012	2.82984	0.32265
N	1.92925	3.73060	0.17762
H	0.93472	-2.48151	1.02809
B	1.56130	-2.96938	-0.07389
H	2.66966	-3.25243	0.32343
H	0.81154	-3.86545	-0.40065

**C-Attack-TS (DDQ 1a + 2t)**

O	-0.43010	-1.08962	2.20967
C	-0.01384	-0.18608	1.46764
C	1.39811	-0.22403	0.92382
Cl	2.35131	-1.56536	1.44938
C	1.90501	0.74762	0.09961

Cl	3.53921	0.74432	-0.47857
C	1.08580	1.93242	-0.28777
O	1.54876	2.91552	-0.85316
C	-0.39768	1.83240	0.04485
C	-1.16609	3.02400	-0.23172
C	-0.83302	0.95341	1.06892
C	-2.12875	1.06167	1.63965
N	-1.80432	3.97934	-0.45937
N	-3.19654	1.15537	2.12419
H	-0.60747	1.09772	-1.34089
B	-0.83280	0.22223	-2.35946
H	0.20361	0.20528	-2.97947
H	-1.79461	0.75767	-2.86577
C	-0.81817	-2.95328	-0.30693
C	-2.09263	-2.49691	-0.04915
N	-2.25686	-1.33966	-0.77115
C	-1.12049	-1.04912	-1.48549
N	-0.23980	-2.05689	-1.17138
C	1.08144	-2.23079	-1.79519
H	-0.29006	-3.82408	0.05899
H	0.95358	-2.60710	-2.81750
H	1.65050	-2.94823	-1.19727
H	1.59747	-1.26777	-1.82288
H	-2.87333	-2.89542	0.58549
C	-3.52912	-0.60451	-0.85508
H	-3.89606	-0.40989	0.15787
H	-4.25260	-1.21377	-1.41149
H	-3.35602	0.33719	-1.38072

#### 4.6 References:

- (1) (a) Becker, H.-D. in *The Chemistry of the Quinoid Compounds, Part I*; Patai, S., Ed.; Wiley: Chichester, UK, 1974; pp 335–423. (b) Becker, H.-D.; Turner, A. B. in *The Chemistry of the Quinoid Compounds Vol. 2*; Patai, S., Rappoport, Z., Eds.; Wiley: Chichester, UK, 1988; pp 1351–1384.
- (2) For the series of papers, see: (a) Braude, E. A.; Jackman, L. M. and Linstead, R. P. *J. Chem. Soc.* **1954**, 3548-3563. (b) Braude, E. A.; Jackman, L. M. and Linstead, R. P. *J. Chem. Soc.* **1954**, 3564-3568. (c) Braude, E. A.; Brook, A. G. and Linstead, R. P. *J. Chem. Soc.* **1954**, 3569-3574. (d) Braude, E. A.; Linstead, R. P. and Wooldridge, K. R. *J. Chem. Soc.* **1956**, 3070-3074. (e) Barnard, J. R. and Jackman, L. M. *J. Chem. Soc.* **1960**, 3110-3115. (f) Braude, E. A.; Jackman, L. M.; Linstead, R. P. and Shannon, J. S. *J. Chem. Soc.* **1960**, 3116-3122. (g) Braude, E. A.; Jackman, L. M.; Linstead, R. P. and Lowe, G. J. *J. Chem. Soc.* **1960**, 3123-3132. (h) Braude, E. A.; Jackman, L. M.; Linstead, R. P. and Lowe, G. J. *J. Chem. Soc.* **1960**, 3133-3138. For a review, see: (i) Jackman, L. M. in *Advances in Organic Chemistry, Methods and Results Vol. 2*; Raphael, R. A., Taylor, E. C., and Wynberg, H., Eds.; Interscience Publishers, Inc., New York, 1960.

- (3) (a) *Cytochrome P450: Structure, Mechanism, and Biochemistry*, 3rd ed.; Ortiz de Montellano, P. R., Ed.; Kluwer Academic/Plenum Publishers, New York, 2005. (b) Lai, W.; Li, C.; Chen, H.; Shaik, S. *Angew. Chem., Int. Ed.* **2012**, *51*, 5556–5578. (c) Shaik, S.; Cohen, S.; Wang, Y.; Chen, H.; Kumar, D.; Thiel, W. *Chem. Rev.* **2010**, *110*, 949–1017.
- (4) (a) Trost, B. M. *J. Am. Chem. Soc.* **1967**, *89*, 1847–1851. (b) Müller, P. and Roček, J. *J. Am. Chem. Soc.* **1972**, *94*, 2716–2719. (c) Stoos, F. and Roček, J. *J. Am. Chem. Soc.* **1972**, *94*, 2719–2723. (d) Thummel, R. P.; Cravey, W. E. and Cantu, D. B. *J. Org. Chem.* **1980**, *45*, 1633–1637. (e) Müller, P. *Helv. Chim. Acta.* **1973**, *56*, 1243–1251. (f) Müller, P. and Joly, D. *Helv. Chim. Acta.* **1983**, *66*, 1110–1118. (g) Carlson, B. W. and Miller, L. L. *J. Am. Chem. Soc.* **1985**, *107*, 479–485. (h) Fukuzumi, S.; Koumitsu, S.; Hironaka, K. and Tanaka, T. *J. Am. Chem. Soc.* **1987**, *109*, 305–316. (i) Zaman, K. M.; Yamamoto, S.; Nishimura, N.; Maruta, J. and Fukuzumi, S. *J. Am. Chem. Soc.* **1994**, *116*, 12099–12100. (j) Batista, V. S.; Crabtree, R. H.; Konezny, S. J.; Luca, O. R. and Praetorius, J. M. *New J. Chem.* **2012**, *36*, 1141–1144.
- (5) (a) Thiele, J.; Günther, F. *Liebigs Ann. Chem.* **1906**, *349*, 45–66. (b) Walker, D.; Hiebert, J. D. *Chem. Rev.* **1967**, *67*, 153–195. (c) Buckle, D. R. in *Encyclopedia of Reagents for Organic Synthesis Vol. 3* Paquette, L. A., Ed.; Wiley: Chichester, UK, 1995; p 1699.
- (6) (a) Zhang, Y.; Li, C. *J. Angew. Chem., Int. Ed.* **2006**, *45*, 1949–1952. (b) Zhang, Y.; Li, C. *J. Am. Chem. Soc.* **2006**, *128*, 4242–4243. (c) Tu, W.; Floreancig, P. E. *Angew. Chem., Int. Ed.* **2009**, *48*, 4567–4571. (d) Liu, L.; Floreancig, P. E. *Angew. Chem. Int. Ed.* **2010**, *49*, 3069–3072. (e) Guo, C.; Song, J.; Luo, S. W.; Gong, L. Z. *Angew. Chem. Int. Ed.* **2010**, *49*, 5558–5562. (f) Y. Hayashi, T. Itoh, H. Ishikawa, *Angew. Chem., Int. Ed.* **2011**, *50*, 3920–3924. (g) Tsang, A. S.-K.; Jensen, P.; Hook, J. M.; Hashmi, A. S. K.; Todd, M. H. *Pure Appl. Chem.* **2011**, *83*, 655–665. (h) Alagiri, K.; Devadig, P.; Prabhu, K. R. *Chem. Eur. J.* **2012**, *18*, 5160–5164. (i) Rohlmann, R.; Garcia Mancheño, O. *Synlett.* **2013**, *24*, 6–10.
- (7) Guo, X.; Mayr, H. *J. Am. Chem. Soc.* **2013**, *135*, 12377–12387.
- (8) (a) Mayr, H.; Patz, M. *Angew. Chem., Int. Ed. Engl.* **1994**, *33*, 938–957. (b) Mayr, H.; Ofial, A. R. *Pure Appl. Chem.* **2005**, *77*, 1807–1821. (c) Mayr, H.; Ofial, A. R. *J. Phys. Org. Chem.* **2008**, *21*, 584–595. (d) Mayr, H.; Kempf, B.; Ofial, A. R. *Acc. Chem. Res.* **2003**, *36*, 66–77.
- (9) For a comprehensive database of nucleophilicity parameters  $N$  and  $s_N$  as well as electrophilicity parameters  $E$ , see <http://www.cup.lmu.de/oc/mayr/DBintro.html>.

- (10) Horn, M.; Schappele, L. H.; Lang-Wittkowski, G.; Mayr, H.; Ofial, A. R. *Chem. Eur. J.* **2013**, *19*, 249-263.
- (11) Carlsson, D. J. and Ingold, K. U. *J. Am. Chem. Soc.* **1968**, *90*, 7047-7055.
- (12) Klingler, R. J.; Mochida, K. and Kochi, J. K. *J. Am. Chem. Soc.* **1979**, *101*, 6626-6637.
- (13) Heyes, D.; Menon, R. S.; Watt, C. I. F.; Wiseman, J. and Kubinski, P. *J. Phys. Org. Chem.* **2002**, *15*, 689-700.
- (14) (a) Wigfield, D. C.; Phelps, D. J. *Can. J. Chem.* **1972**, *50*, 388-394; (b) Yamataka, H.; Hanafusa, T. *J. Am. Chem. Soc.* **1986**, *108*, 6643-6646.
- (15) Mayr, H.; Bug, T.; Gotta, M. F.; Hering, N.; Irrgang, B.; Janker, B.; Kempf, B.; Loos, R.; Ofial, A. R.; Remennikov, G.; Schimmel, H. *J. Am. Chem. Soc.* **2001**, *123*, 9500-9512.
- (16) Davis, R. E.; Brown, A. E.; Hopmann, R.; Kibby, C. L. *J. Am. Chem. Soc.* **1963**, *85*, 487-487.
- (17) Colter and coworkers have previously reported that no excess deuterium was observed in the hydroquinone isolated from the reaction of 9-deuterated *N*-methylacridan with benzoquinone, which supports O attack mechanism. Colter, A. K.; Saito, G. and Sharom, F. J. *Can. J. Chem.* **1977**, *55*, 2741-2751.
- (18) Frisch, M. J.; Trucks, G. W.; Schlegel, H.; Scuseria, G. E.; Robb, M. A.; Cheeseman, J. R.; Scalmani, G.; Barone, V.; Mennucci, B.; Petersson, G. A.; Nakatsuji, H.; Caricato, M.; Li, X.; Hratchian, H. P.; Izmaylov, A. F.; Bloino, J.; Zheng, G.; Sonnenberg, J. L.; Hada, M.; Ehara, M.; Toyota, K.; Fukuda, R.; Hasegawa, J.; Ishida, M.; Nakajima, T.; Honda, Y.; Kitao, O.; Nakai, H.; Vreven, T.; Montgomery, J. A.; Peralta, J. E.; Ogliaro, F.; Bearpark, M.; Heyd, J. J.; Brothers, E.; Kudin, K. N.; Staroverov, V. N.; Kobayashi, R.; Normand, J.; Raghavachari, K.; Rendell, A.; Burant, J. C.; Iyengar, S. S.; Tomasi, J.; Cossi, M.; Rega, N.; Millam, J. M.; Klene, M.; Knox, J. E.; Cross, J. B.; Bakken, V.; Adamo, C.; Jaramillo, J.; Gomperts, R.; Stratmann, R. E.; Yazyev, O.; Austin, A. J.; Cammi, R.; Pomelli, C.; Ochterski, J. W.; Martin, R. L.; Morokuma, K.; Zakrzewski, V. G.; Voth, G. A.; Salvador, P.; Dannenberg, J. J.; Dapprich, S.; Daniels, A. D.; Farkas, Foresman, J. B.; Ortiz, J. V.; Cioslowski, J.; Fox, D. J. *Gaussian 09*, Revision A.02; Gaussian, Inc.: Wallingford CT, 2009.
- (19) Marenich, A. V.; Cramer, C. J.; Truhlar, D. G. *J. Phys. Chem. B* **2009**, *113*, 6378-6396.
- (20) For **2c**, similar rates for O- and C-attack were calculated.
- (21) (a) Nagase S.; Morokuma, K.; *J. Am. Chem. Soc.* **1978**, *100*, 1666-1672; (b) Ess, D. H.; Houk, K. N. *J. Am. Chem. Soc.* **2007**, *129*, 10646-10647. (c) Ess, D. H.; Houk, K. N. *J. Am. Chem. Soc.* **2008**, *130*, 10187-10198. (d) Ess, D. H.; Jones, G. O.; Houk, K. N. *Org.*

- Lett.* **2008**, *10*, 1633-1636. (e) Bickelhaupt, F. M. *J. Comput. Chem.* **1999**, *20*, 114-128. (f) Diefenbach, A.; Bickelhaupt, F. M. *J. Chem. Phys.* **2001**, *115*, 4030-4040. (g) Diefenbach, A.; Bickelhaupt, F. M. *J. Phys. Chem. A* **2004**, *108*, 8460-8466.
- (22) Krapcho, A. P.; Bothner-By, A. A. *J. Am. Chem. Soc.* **1959**, *81*, 3658-3666.
- (23) Roberts, R. M. G.; Ostovic, D.; Kreevoy, M. M. *Faraday Discuss. Chem. Soc.* **1982**, *74*, 257-265.
- (24) Mauserall, D.; Westheimer, F. H. *J. Am. Chem. Soc.* **1955**, *77*, 2261-2264.
- (25) (a) Ueng, S.-H.; Makhlof Brahmi, M.; Derat, E.; Fensterbank, L.; Lacôte, E.; Malacria, M.; Curran, D. P. *J. Am. Chem. Soc.* **2008**, *130*, 10082-10083. (b) Walton, J. C.; Makhlof Brahmi, M.; Fensterbank, L.; Lacôte, E.; Malacria, M.; Chu, Q.; Ueng, S.-H.; Solovyeu, A.; Curran, D. P. *J. Am. Chem. Soc.* **2010**, *132*, 2350-2358
- (26) Cowley, R. E.; Eckert, N. A.; Vaddadi, S.; Figg, T. M.; Cundari, T. R. and Holland, P. L. *J. Am. Chem. Soc.* **2011**, *133*, 9796-9811.
- (27) López-Alvarado, P.; Avendaño, C.; Menéndez, J. C. *Synth. Commun.* **2002**, *32*, 3233-3239.





---

## Curriculum Vitae

### Personal information

Name: Guo, Xingwei  
Citizenship: Chinese  
Gender: Male  
Date of birth: Jan, 28, 1985  
Place of birth: Qinhuangdao, Hebei, China

### Education

Ph.D. in Organic Chemistry: (2010-2014): Department Chemie und Biochemie  
Ludwig-Maximilians-Universität München, Germany  
Thesis Supervisor: Prof. Dr. Herbert Mayr  
Thesis Title: Kinetic and mechanistic studies on the reactions of quinones: SET vs. polar reactions

Master of Science: (2007-2010) Department of Chemistry  
Renmin University of China, China  
Thesis Supervisor: Prof. Dr. Zhiping Li  
Thesis Title: Iron-catalyzed C-H bond functionalizations

Bachelor of Science: (2003-2007) Department of Applied Chemistry,  
Hebei University of Technology, China  
Thesis Supervisor: Prof. Dr. Wenjun Zhang  
Thesis Title: New screening algorithms for QSAR studies

### Fellowship

Ph.D fellowship by the China Scholarship Council (2010-2013)